

**STUDIES ON CORROSION INHIBITION
OF 18% Ni M 250 GRADE MARAGING
STEEL UNDER WELD AGED CONDITION
IN ACIDIC MEDIA**

Thesis

submitted in partial fulfillment of the requirements for the degree of

DOCTOR OF PHILOSOPHY

by

SANATKUMAR B. S.

(Reg. No. CY09F02)



**DEPARTMENT OF CHEMISTRY
NATIONAL INSTITUTE OF TECHNOLOGY
KARNATAKA**

SURATHKAL, MANGALORE - 575 025

JUNE, 2013

DECLARATION

by the Ph.D. Research Scholar

I hereby *declare* that the Research Thesis entitled “**Studies on corrosion inhibition of 18% Ni M 250 grade maraging steel under weld aged condition in acidic media**” which is being submitted to the **National Institute of Technology Karnataka, Surathkal** in partial fulfillment of the requirements for the award of the Degree of **Doctor of Philosophy in Chemistry** is a *bonafide report of the research work carried out by me*. The material contained in this Research Thesis has not been submitted to any University or Institution for the award of any degree.

(Signature of the Research Scholar)

Name: **SANATKUMAR B. S.**

Reg. No: **CY09F02**

Department: **CHEMISTRY**

Place: **NITK - SURATHKAL**

Date: **21th JUNE, 2012**

C E R T I F I C A T E

This is to certify that the Research Thesis entitled “**Studies on corrosion inhibition of 18% Ni M 250 grade maraging steel under weld aged condition in acidic media**” submitted by **Sanatkumar B. S.** (Register Number: **CY09F02**) as the record of the research work carried out by him, is accepted as the Research Thesis submission in partial fulfillment of the requirements for the award of degree of **Doctor of Philosophy.**

Dr. A. Nityananda Shetty

Dr. Jagannatha Nayak

Research Guides

(Name and Signature with date and seal)

Chairman - DRPC

(Signature with date and seal)

I dedicate this thesis to my parents and my research guides to say thank you for everything.

ACKNOWLEDGEMENT

I owe my deepest gratitude to my research supervisor Dr. A. Nityananda Shetty, Professor Department of Chemistry, National Institute of Technology Karnataka, Surathkal, for giving me an opportunity to carry out research in corrosion studies under his able guidance. It has been an honour to be his research student. I appreciate all his contributions of time and ideas to make my research experience productive and stimulating.

I wish to express my gratitude to my research supervisor Dr. Jagannath Nayak, Professor, Department of Metallurgical and Materials Engineering, National Institute of Technology Karnataka, Surathkal, for his continued encouragement and invaluable suggestions during this work. His guidance on the techniques of corrosion study enabled me to develop an understanding of the subject.

I remain ever grateful to both my supervisors who have made this thesis possible.

I would like to thank the members of RPAC, Dr. A. O. Surendranathan, Professor, Metallurgical and Materials Engineering and Dr. Darshak R. Trivedi, Assistant Professor, Department of Chemistry, National Institute of Technology Karnataka, Surathkal, for their valuable suggestions throughout this work.

I am grateful to Dr. A. C. Hegde, Head, Department of Chemistry, National Institute of Technology Karnataka, Surathkal for providing me required experimental facilities of the department. I am thankful to faculty of the Department of Chemistry, National Institute of Technology Karnataka, Surathkal, Dr. A. V. Adhikari, Dr. D. Krishna Bhat, Dr. Arun M. Isloor, Dr. B. Ramachandra Bhat, Dr. Uday Kumar D and Dr. Darshak R. Trivedi for their suggestions and support. I am ever grateful to the Department of Chemistry, NITK for all the laboratory facility and Department of Metallurgical and Materials Engineering, NITK for SEM facility.

I am indebted to the nonteaching staff, Department of Chemistry NITK, Mrs. Kasturi Rohidas for her help in official work, Mr. Prashant, Mr. Pradeep Crasta, Mr. Ashoka and Mr. Harish for their assistance in the laboratory.

It is a pleasure to thank my fellow research scholars, Dr. Poornima , Dr. Reena Kiran, Dr. Geetha, Dr. Aarti, Mr. Pradeep Kumar, Mr. Mahesh Padaki, Mr. Vijayaganapathi Karanth, Mr. Garuda, Mr. Yathish Ullal, Mr. Subramanya B., Mr. Sreekanth Jois, Mrs. Pavithra, Dr. Santhosh, Mr. Srinivasa Murthi and all others for making my stay at NITK during research a memorable one.

I gratefully acknowledge the cooperation and encouragement given by the Principal, Dr. V. Mariappan, Agnel Institute of Technology and Design, Goa.

At this point of time I must acknowledge my chemistry teachers at graduate and postgraduate levels who inspired me to take up chemistry as my career.

Lastly and most importantly, I wish to thank my parents, research guides and friends for their cooperation, care and love. To them I dedicate this thesis.

SANATKUMAR B. S.

ABSTRACT

The corrosion behaviour of 18 % Ni M250 grade maraging steel under weld aged conditions in two different acid media, namely, hydrochloric acid and sulphuric acid in various concentrations and temperatures have been studied by Tafel polarization and electrochemical impedance spectroscopy techniques. The corrosion rate in the sulphuric acid medium was higher than in the hydrochloric acid medium.

Five organic inhibitors were synthesized and characterized using spectral and elemental analysis. The five inhibitors were 1(2E)-1-(4-aminophenyl)-3-(2-thienyl) prop-2-en-1-one (ATPI), 2-(4-chlorophenyl)-2-oxoethyl benzoate (CPOB), 2-(4-bromophenyl)-2-oxoethyl-4-chlorobenzoate (CPOM), (E)-1-(2,4-dinitrophenyl)-2-[1-(2-nitrophenyl) ethylidene] hydrazine (DNPH) and 5-diethylamino-2-[[2-(2,4-dinitrophenyl) hydrazin-1-ylidene]methyl] - phenol (DDPM). The results pertaining to the corrosion inhibition studies of five inhibitors in two different acid media at different temperatures in the presence of varying concentrations of inhibitors are reported in the thesis. Activation parameters for the corrosion of the alloy and thermodynamic parameters for the adsorption of the inhibitors have been calculated and the results have been analysed.

The adsorption of first four inhibitors on the alloy was through both physisorption and chemisorption, with predominant physisorption in both the media. The mode of adsorption for the DDPM predominantly chemisorption in both the media. The adsorption of all the five inhibitors on alloy surfaces follows Langmuir adsorption isotherm. The inhibition efficiencies of first four inhibitors decrease with the increase in temperature, the inhibition efficiency of DDPM increases with the increase in temperature.

Key Words: Maraging steel, Corrosion, Inhibitor, Adsorption.

CONTENTS

Page No.

CHAPTER - 1	INTRODUCTION	
1.1	IMPORTANCE OF CORROSION	1
1.2	NEED FOR CORROSION STUDY	2
1.3	ELECTROCHEMICAL THEORY OF CORROSION	4
1.4	CLASSIFICATION OF CORROSION	6
1.4.1	Forms of Corrosion	7
1.4.4.1	Uniform corrosion	7
1.4.4.2	Galvanic corrosion	7
1.4.4.3	Crevice corrosion	8
1.4.4.4	Pitting corrosion	8
1.4.4.5	Intergranular corrosion	8
1.4.4.6	Selective leaching	9
1.4.4.7	Erosion corrosion	9
1.4.4.8	Stress corrosion cracking (SCC)	9
1.4.4.9	Hydrogen embrittlement	10
1.4.4.10	Corrosion fatigue	10
1.5	FACTORS AFFECTING CORROSION RATE	10
1.5.1	Nature of the metal	10
1.5.2	Difference in potential between anodic and cathodic region	11
1.5.3	Nature of the corrosion product	11
1.5.4	Ratio of anodic to cathodic area	11
1.5.5	Hydrogen overvoltage	11
1.5.6	Temperature	12
1.5.7	pH	12
1.5.8	Presence of oxidising agents	12
1.5.9	Polarization at anodic and cathodic region	12
1.5.10	Effect of dissolved oxygen	12
1.5.11	Effect of velocity of the medium	13
1.5.12	Effect of other ions present in the solution	13

1.6 THERMODYNAMICS OF CORROSION	13
1.7 KINETICS OF CORROSION	16
1.8 MIXED POTENTIAL THEORY	19
1.9 ELECTROCHEMICAL CORROSION TESTING	21
1.9.1 DC Electrochemical monitoring techniques:	21
1.9.2 AC Electrochemical monitoring techniques	27
1.10 METHODS TO CONTROL CORROSION	34
1.11 CORROSION INHIBITORS	35
1.11.1 Classification of corrosion inhibitors	37
1.11.1.1 Environmental conditioners (Scavengers)	37
1.11.1.2 Interface inhibitors	38
1.12 EXAMPLES OF CORROSION INHIBITORS	41
1.13 CORROSION INHIBITION MECHANISM	42
1.14 MARAGING STEELS	45
1.14.1 Uses of maraging steel	49
1.13.2 Role of alloying elements in maraging steel	50
1.14.3 Weld aged maraging steel	51
1.15 LITERATURE REVIEW	52
1.15.1 Corrosion of maraging steels	52
1.15.2 Organic inhibitors for the corrosion inhibition of iron and iron alloys in aqueous media	55
1.16 SCOPE AND OBJECTIVES	62
1.17 OUTLINE OF THE THESIS	63
CHAPTER – 2 MATERIALS AND METHODS	
2.1 MATERIALS	64
2.1.1 18 % Ni M250 grade maraging steel	64
2.1.2 Material Conditions	64
2.1.3 Material preparation	65
2.2 MEDIA	65
2.2.1 Preparation of standard hydrochloric acid solution	65

2.2.2 Preparation of standard sulphuric acid solution	65
2.3 INHIBITORS	66
2.3.1 Synthesis of 1(2E)-1-(4-aminophenyl)-3-(2-thienyl) prop-2-en-1-one (ATPI)	66
2.3.2 Synthesis of 2-(4-chlorophenyl)-2-oxoethyl benzoate (CPOB)	66
2.3.3 Synthesis of 2-(4-bromophenyl)-2-oxoethyl-4-chlorobenzoate (CPOM)	67
2.3.4 Synthesis of (E)-1-(2,4-dinitrophenyl)-2-[1-(2-nitrophenyl) ethylidene] hydrazine (DNPH)	68
2.3.5 Synthesis of 5-diethylamino-2-[[2-(2,4-dinitrophenyl) hydrazin-1-ylidene]methyl]-phenol (DDPM)	68
2.4 METHODS	69
2.4.1 Potentiodynamic polarization measurements	69
2.4.2 Electrochemical impedance spectroscopy (EIS) studies	71
2.4.3 Scanning electron microscopic (SEM) studies and EDS analysis	72
2.5 CALCULATION OF CORROSION RATE	72
2.6 CALCULATION OF INHIBITION EFFICIENCY	73
2.7 ACTIVATION PARAMETERS	74
2.8 ADSORPTION ISOTHERMS	75
2.9 THERMODYNAMIC PARAMETERS	76

CHAPTER – 3 RESULTS AND DISCUSSION

3.1 CORROSION OF 18% Ni M250 GRADE MARAGING STEEL UNDER WELD AGED CONDITION IN HYDROCHLORIC ACID MEDIUM	78
3.1.1 Potentiodynamic polarization studies	78
3.1.2 Electrochemical impedance spectroscopy (EIS) studies	80
3.1.3 Effect of temperature	83
3.1.4 SEM/EDS studies	87
3.2 CORROSION OF 18% Ni M250 GRADE MARAGING STEEL	93

UNDER WELD AGED CONDITION IN SULPHURIC ACID
MEDIUM

3.2.1 Potentiodynamic polarization studies	93
3.2.2 Electrochemical impedance spectroscopy (EIS) studies	94
3.2.3 Effect of temperature	95
3.2.4 SEM/EDS studies	98
3.3 1(2E)-1-(4-AMINOPHENYL)-3-(2-THIENYL)PROP-2-EN - 1- ONE (ATPI) AS INHIBITOR FOR THE CORROSION OF WELD AGED MARAGING STEEL IN HYDROCHLORIC ACID MEDIUM	103
3.3.1 Potentiodynamic polarization studies	103
3.3.2 Electrochemical impedance spectroscopy	105
3.3.3 Effect of temperature	109
3.3.4 Effect of hydrochloric acid concentration	112
3.3.5 Adsorption isotherm	112
3.3.6 Mechanism of corrosion inhibition	115
3.3.7 SEM/EDS studies	117
3.4 2-(4-CHLOROPHENYL)-2-OXOETHYL BENZOATE (CPOB) AS INHIBITOR FOR THE CORROSION OF WELD AGED MARAGING STEEL IN HYDROCHLORIC ACID MEDIUM	133
3.4.1 Potentiodynamic polarization studies	133
3.4.2 Electrochemical impedance spectroscopy	134
3.4.3 Effect of temperature	136
3.4.4 Effect of hydrochloric acid concentration	138
3.4.5 Adsorption isotherm	138
3.4.6 Mechanism of corrosion inhibition	139
3.4.7 SEM/EDS studies	140
3.5 2-(4-BROMOPHENYL) -2-OXOETHYL- 4-CHLOROBENZOATE (CPOM) AS INHIBITOR FOR THE CORROSION OF WELD AGED MARAGING STEEL IN HYDROCHLORIC ACID MEDIUM	155
3.5.1 Potentiodynamic polarization studies	155
3.5.2 Electrochemical impedance spectroscopy	156

3.5.3 Effect of temperature	158
3.5.4 Effect of hydrochloric acid concentration	160
3.5.5 Adsorption isotherm	160
3.5.6 Mechanism of corrosion inhibition	161
3.5.7 SEM/EDS studies	161
3.6 (E)-1-(2,4-DINITROPHENYL)-2-[1-(2-NITROPHENYL) THYLIDENE] HYDRAZINE (DNPH) AS INHIBITOR FOR THE CORROSION OF WELD AGED MARAGING STEEL IN HYDROCHLORIC ACID MEDIUM	176
3.6.1 Potentiodynamic polarization studies	176
3.6.2 Electrochemical impedance spectroscopy	177
3.6.3 Effect of temperature	179
3.6.4 Effect of hydrochloric acid concentration	180
3.6.5 Adsorption isotherm	181
3.6.6 Mechanism of corrosion inhibition	181
3.6.7 SEM/EDS studies	182
3.7 5-DIETHYLAMINO-2-2-[(2-(2,4-DINITROPHENYL) HYDRAZIN-1-YLIDENE] METHYL PHENOL (DDPM) AS INHIBITOR FOR CORROSION OF WELD AGED MARAGING STEEL IN HYDROCHLORIC ACID MEDIUM	197
3.7.1 Potentiodynamic polarization studies	197
3.7.2 Electrochemical impedance spectroscopy	198
3.7.3 Effect of temperature	200
3.7.4 Effect of hydrochloric acid concentration	202
3.7.5 Adsorption isotherm	202
3.7.6 Mechanism of corrosion inhibition	203
3.7.7 SEM/EDS studies	203
3.8 1(2E)-1-(4-AMINOPHENYL)-3-(2-THIENYL) PROP-2-EN- 1-ONE (ATPI) AS INHIBITOR FOR THE CORROSION OF WELD AGED MARAGING STEEL IN SULPHURIC ACID MEDIUM	218
3.8.1 Potentiodynamic polarization studies	218

3.8.2 Electrochemical impedance spectroscopy	219
3.8.3 Effect of temperature	222
3.8.4 Effect of hydrochloric acid concentration	224
3.8.5 Adsorption isotherm	225
3.8.6 Mechanism of corrosion inhibition	226
3.8.7 SEM/EDS studies	228
3.9 2-(4-CHLOROPHENYL)-2-OXOETHYL BENZOATE (CPOB) AS INHIBITOR FOR THE CORROSION OF WELD AGED MARAGING STEEL IN SULPHURIC ACID MEDIUM	244
3.9.1 Potentiodynamic polarization studies	244
3.9.2 Electrochemical impedance spectroscopy	245
3.9.3 Effect of temperature	247
3.9.4 Effect of sulphuric acid concentration	249
3.9.5 Adsorption isotherm	249
3.9.6 Mechanism of corrosion inhibition	250
3.9.7 SEM/EDS studies	250
3.10 2-(4-BROMOPHENYL)-2-OXOETHYL-4-CHLOROBENZOATE (CPOM) AS INHIBITOR FOR THE CORROSION OF WELD AGED MARAGING STEEL IN SULPHURIC ACID MEDIUM	265
3.10.1 Potentiodynamic polarization studies	265
3.10.2 Electrochemical impedance spectroscopy	266
3.10.3 Effect of temperature	268
3.10.4 Effect of sulphuric acid concentration	269
3.10.5 Adsorption isotherm	270
3.10.6 Mechanism of corrosion inhibition	270
3.10.7 SEM/EDS studies	271
3.11 (E)-1-(2,4-DINITROPHENYL)-2-[1-(2-NITROPHENYL) THYLIDENE] HYDRAZINE (DNPH) AS INHIBITOR FOR THE CORROSION OF WELD AGED MARAGING STEEL IN SULPHURIC ACID MEDIUM	286
3.11.1 Potentiodynamic polarization studies	286

3.11.2 Electrochemical impedance spectroscopy	287
3.11.3 Effect of temperature	289
3.11.4 Effect of sulphuric acid concentration	290
3.11.5 Adsorption isotherm	291
3.11.6 Mechanism of corrosion inhibition	291
3.11.7 SEM/EDS studies	292
3.12 5-DIETHYLAMINO-2-[2-(2,4-DINITROPHENYL) HYDRAZIN-1-YLIDENE]METHYL - PHENOL (DDPM) AS INHIBITOR FOR THE CORROSION OF WELD AGED MARAGING STEEL IN SULPHURIC ACID MEDIUM	309
3.12.1 Potentiodynamic polarization studies	307
3.12.2 Electrochemical impedance spectroscopy	308
3.12.3 Effect of temperature	310
3.12.4 Effect of sulphuric acid concentration	311
3.12.5 Adsorption isotherm	312
3.12.6 Mechanism of corrosion inhibition	312
3.12.7 SEM/EDS studies	313
CHAPTER – 4 SUMMARY AND CONCLUSIONS	
4.1 SUMMARY	328
4.2 CONCLUSIONS	328
4.3 SCOPE FOR THE FUTURE WORK	329
REFERENCES	330
LIST OF PUBLICATIONS	345
BIO DATA	346

LIST OF FIGURES

Fig. No.	Caption	Page No.
1.1	The corrosion cycle of steel.	1
1.2	The electrochemical cell set up between anodic and cathodic sites on a metal surface undergoing corrosion.	5
1.3	Pourbaix diagram for iron/water/dissolved oxygen system.	15
1.4	Electrode kinetic behaviour of pure iron in acid solution (schematic).	20
1.5	Plot of the current density versus potential showing the extrapolation of the Potentiodynamic regions to the corrosion potential, E_{corr} to yield the corrosion current, i_{corr} .	23
1.6	Determination of corrosion current density by extrapolation of linear parts of the polarization curves.	24
1.7	Linear polarization curve.	27
1.8	Nyquist plot.	31
1.9	Bode plot.	31
1.10	Classification of inhibitors.	37
1.11	Evans diagrams showing the effect of addition of a) anodic inhibitor, b) cathodic inhibitor, c) mixed inhibitor.	41
3.1	Potentiodynamic polarization curves for the corrosion of weld aged maraging steel in different concentrations of hydrochloric acid at 30 °C.	78
3.2	Nyquist plots for the corrosion of weld aged maraging steel in different concentrations of hydrochloric acid at 30 °C.	81
3.3	The equivalent circuit model used to fit the experimental data for the corrosion of the specimen in 2.0 M hydrochloric acid solution at 30 °C.	82
3.4	Potentiodynamic polarisation curves for the corrosion of weld aged maraging steel at different temperatures in 0.5 M hydrochloric acid.	84

3.5	Nyquist plots for the corrosion of weld aged maraging steel in 0.5 M hydrochloric acid at different temperatures.	85
3.6	Arrhenius plots for the corrosion of weld aged maraging steel in hydrochloric acid.	86
3.7	Plots of $\ln(v_{\text{corr}}/T)$ vs $1/T$ for the corrosion of weld aged maraging steel in hydrochloric acid.	86
3.8	SEM images of (a) freshly polished surface (b) corroded surface	87
3.9 (a)	EDS spectra of the freshly polished surface of weld aged maraging steel.	88
3.9 (b)	EDS spectra of the weld aged maraging steel after immersion in 2.0 M hydrochloric acid.	89
3.10	Potentiodynamic polarisation curves for the corrosion of weld aged maraging steel in different concentrations of sulphuric acid at 30 °C.	93
3.11	Nyquist plots for weld aged maraging steel in different concentrations of sulphuric acid at 30 °C.	94
3.12	Potentiodynamic polarisation curves for the corrosion of weld aged maraging steel at different temperatures in 1.0 M sulphuric acid.	96
3.13	Nyquist plots for the corrosion of weld aged maraging steel in 1.0 M sulphuric acid at different temperatures.	96
3.14	Arrhenius plots for the corrosion of weld aged sample of maraging steel in sulphuric acid.	97
3.15	Plots of $\ln(v_{\text{corr}}/T)$ vs $1/T$ for the corrosion of weld aged sample of maraging steel in sulphuric acid.	97
3.16	SEM images of (a) freshly polished surface (b) corroded surface	98
3.17 (a)	EDS spectra of the freshly polished surface of weld aged maraging steel.	99
3.17 (b)	EDS spectra of the weld aged maraging steel after immersion	99

	in 1.0 M sulphuric acid.	
3.18	Potentiodynamic polarization curves for the corrosion of weld aged maraging steel in 1.5 M hydrochloric acid containing different concentrations of ATPI at 30 °C.	103
3.19	Nyquist plots for the corrosion of weld aged maraging steel in 1.5 M hydrochloric acid containing different concentrations of ATPI at 30 °C.	106
3.20	Equivalent circuit used to fit the experimental EIS data for the corrosion of weld aged maraging steel in hydrochloric acid in the presence of different concentration of ATPI.	108
3.21	Bode plots for the corrosion of weld aged maraging steel in 1.5 M hydrochloric acid containing different concentrations of ATPI at 30 °C.	109
3.22	Arrhenius plots for the corrosion of weld aged maraging steel in 1.5 M hydrochloric acid containing different concentrations of ATPI.	111
3.23	Plots of $\ln(v_{\text{corr}}/T)$ versus $1/T$ for the corrosion of weld aged maraging steel in 1.5 M hydrochloric acid containing different concentrations of ATPI.	111
3.24	Langmuir adsorption isotherms for the adsorption of ATPI on weld aged maraging steel in 1.5 M hydrochloric acid at different temperatures.	114
3.25	SEM images of the weld aged maraging steel after immersion in 1.5 M hydrochloric acid a) in the absence and b) in the presence of ATPI.	118
3.26 (a)	EDS spectra of the weld aged maraging steel after immersion in 1.5 M hydrochloric acid in the absence of ATPI.	119
3.26 (b)	EDS spectra of the weld aged maraging steel after immersion in 1.5 M hydrochloric acid in the presence of ATPI.	119
3.27	Potentiodynamic polarization curves for the corrosion of weld aged maraging steel in 0.5 M hydrochloric acid containing	133

	different concentrations of CPOB at 30 °C.	
3.28	Nyquist plots for the corrosion of weld aged maraging steel in 0.5 M hydrochloric acid containing different concentrations of CPOB at 30 °C.	135
3.29	Bode plots for the corrosion of weld aged maraging steel in 0.5 M hydrochloric acid containing different concentrations of CPOB at 30 °C.	136
3.30	Arrhenius plots for the corrosion of weld aged maraging steel in 0.5 M hydrochloric acid containing different concentrations of CPOB.	137
3.31	Plots of $\ln(v_{\text{corr}}/T)$ versus $1/T$ for the corrosion of weld aged maraging steel in 0.5 M hydrochloric acid containing different concentrations of CPOB.	137
3.32	Langmuir adsorption isotherms for the adsorption of CPOB on weld aged maraging steel in 0.5 M hydrochloric acid at different temperatures.	139
3.33	SEM images of the weld aged maraging steel after immersion in 0.5 M hydrochloric acid a) in the absence and b) in the presence of CPOB.	140
3.34	EDS spectra of the weld aged maraging steel after immersion in 0.5 M hydrochloric acid in the presence of CPOB.	141
3.35	Potentiodynamic polarization curves for the corrosion of weld aged maraging steel in 2.0 M hydrochloric acid containing different concentrations of CPOM at 30 °C.	155
3.36	Nyquist plots for the corrosion of weld aged maraging steel in 2.0 M hydrochloric acid containing different concentrations of CPOM at 30 °C.	156
3.37	Bode plots for the corrosion of weld aged maraging steel in 2.0 M hydrochloric acid containing different concentrations of CPOM at 30 °C.	157
3.38	Arrhenius plots for the corrosion of weld aged maraging steel	159

	in 2.0 M hydrochloric acid containing different concentrations of CPOM.	
3.39	Plots of $\ln(v_{\text{corr}}/T)$ versus $1/T$ for the corrosion of weld aged maraging steel in 2.0 M hydrochloric acid containing different concentrations of CPOM.	159
3.40	Langmuir adsorption isotherms for the adsorption of CPOM on weld aged maraging steel in 2.0 M hydrochloric acid at different temperatures.	160
3.41	SEM images of the weld aged maraging steel after immersion in 2.0 M hydrochloric acid a) in the absence and b) in the presence of CPOM.	162
3.42	EDS spectra of the weld aged maraging steel after immersion in 2.0 M hydrochloric acid in the presence of CPOM.	162
3.43	Potentiodynamic polarization curves for the corrosion of weld aged maraging steel in 1.5 M hydrochloric acid containing different concentrations of DNPH at 30 °C.	176
3.44	Nyquist plots for the corrosion of weld aged maraging steel in 1.5 M hydrochloric acid containing different concentrations of DNPH at 30 °C.	177
3.45	Bode plots for the corrosion of weld aged maraging steel in 1.5 M hydrochloric acid containing different concentrations of DNPH at 30 °C.	178
3.46	Arrhenius plots for the corrosion of weld aged maraging steel in 1.5 M hydrochloric acid containing different concentrations of DNPH.	179
3.47	Plots of $\ln(v_{\text{corr}}/T)$ versus $1/T$ for the corrosion of weld aged maraging steel in 1.5 M hydrochloric acid containing different concentrations of DNPH.	180
3.48	Langmuir adsorption isotherms for the adsorption of DNPH on weld aged maraging steel in 1.5 M hydrochloric acid at different temperatures.	181

3.49	SEM images of the weld aged maraging steel after immersion in 1.5 M hydrochloric acid a) in the absence and b) in the presence of DNPH.	182
3.50	EDS spectra of the weld aged maraging steel after immersion in 1.5 M hydrochloric acid in the presence of DNPH.	183
3.51	Potentiodynamic polarization curves for the corrosion of weld aged maraging steel in 1.0 M hydrochloric acid containing different concentrations of DDPM at 30 °C.	197
3.52	Nyquist plots for the corrosion of weld aged maraging steel in 1.0 M hydrochloric acid containing different concentrations of DDPM at 30 °C.	198
3.53	Bode plots for the corrosion of weld aged maraging steel in 1.5 M hydrochloric acid containing different concentrations of DDPM at 30 °C.	199
3.54	Arrhenius plots for the corrosion of weld aged maraging steel in 1.0 M hydrochloric acid containing different concentrations of DDPM.	200
3.55	Plots of $\ln(v_{\text{corr}}/T)$ versus $1/T$ for the corrosion of weld aged maraging steel in 1.0 M hydrochloric acid containing different concentrations of DDPM.	201
3.56	Langmuir adsorption isotherms for the adsorption of DDPM on weld aged maraging steel in 1.0 M Hydrochloric acid at different temperatures.	202
3.57	SEM images of the weld aged maraging steel after immersion in 1.0 M hydrochloric acid a) in the absence and b) in the presence of DDPM.	204
3.58	EDS spectra of the weld aged maraging steel after immersion in 1.0 M hydrochloric acid in the absence of DDPM.	204
3.59	Potentiodynamic polarization curves for the corrosion of weld aged maraging steel in 1.0 M sulphuric acid containing different concentrations of ATPI at 30 °C.	218

3.60	Nyquist plots for the corrosion of weld aged maraging steel in 1.0 M sulphuric acid containing different concentrations of ATPI at 30 °C.	220
3.61	Bode plots for the corrosion of weld aged maraging steel in 1.0 M sulphuric acid containing different concentrations of ATPI at 30 °C.	222
3.62	Arrhenius plots for the corrosion of weld aged maraging steel in 1.0 M sulphuric acid containing different concentrations of ATPI.	223
3.63	Plots of $\ln(v_{\text{corr}}/T)$ versus $1/T$ for the corrosion of weld aged maraging steel in 1.0 M sulphuric acid containing different concentrations of ATPI.	224
3.64	Langmuir adsorption isotherms for the adsorption of ATPI on weld aged maraging steel in 1.0 M sulphuric acid at different temperatures.	225
3.65	SEM images of the weld aged maraging steel after immersion in 1.0 M sulphuric a) in the absence and b) in the presence of ATPI.	229
3.66 (a)	EDS spectra of the weld aged maraging steel after immersion in 1.0 M sulphuric in the absence of ATPI.	230
3.66 (b)	EDS spectra of the weld aged maraging steel after immersion in 1.0 M sulphuric in the presence of ATPI.	230
3.67	Potentiodynamic polarization curves for the corrosion of weld aged maraging steel in 0.5 M sulphuric acid containing different concentrations of CPOB at 30 °C.	244
3.68	Nyquist plots for the corrosion of weld aged maraging steel in 0.5 M sulphuric acid containing different concentrations of CPOB at 30 °C.	245
3.69	Bode plots for the corrosion of weld aged maraging steel specimen in 0.5 M sulphuric acid containing different concentrations of CPOB at 30 °C.	246

3.70	Arrhenius plots for the corrosion of weld aged maraging steel in 0.5 M sulphuric acid containing different concentrations of CPOB.	248
3.71	Plots of $\ln(v_{\text{corr}}/T)$ versus $1/T$ for the corrosion of weld aged maraging steel in 0.5 M sulphuric acid containing different concentrations of CPOB.	248
3.72	Langmuir adsorption isotherms for the adsorption of CPOB on weld aged maraging steel in 0.5 M sulphuric acid at different temperatures.	249
3.73	SEM images of the weld aged maraging steel after immersion in 0.5 M sulphuric acid a) in the absence and b) in the presence of CPOB.	251
3.74	EDS spectra of the weld aged maraging steel after immersion in 0.5 M sulphuric acid in the presence of CPOB.	251
3.75	Potentiodynamic polarization curves for the corrosion of weld aged maraging steel in 2.0 M sulphuric acid containing different concentrations of CPOM at 30 °C.	265
3.76	Nyquist plots for the corrosion of weld aged maraging steel in 2.0 M sulphuric acid containing different concentrations of CPOM at 30 °C.	266
3.77	Bode plots for the corrosion of weld aged maraging steel in 2.0 M sulphuric acid containing different concentrations of CPOM at 30 °C.	267
3.78	Arrhenius plots for the corrosion of weld aged maraging steel in 2.0 M sulphuric acid containing different concentrations of CPOM.	268
3.79	Plots of $\ln(v_{\text{corr}}/T)$ versus $1/T$ for the corrosion of weld aged maraging steel in 2.0 M sulphuric acid containing different concentrations of CPOM.	269
3.80	Langmuir adsorption isotherms for the adsorption of CPOM on weld aged maraging steel in 2.0 M sulphuric acid at different	270

	temperatures.	
3.81	SEM images of the weld aged maraging steel after immersion in 2.0 M sulphuric acid a) in the absence and b) in the presence of CPOM.	271
3.82	EDS spectra of the weld aged maraging steel after immersion in 2.0 M sulphuric acid in the presence of CPOM.	272
3.83	Potentiodynamic polarization curves for the corrosion of weld aged maraging steel in 0.5 M sulphuric acid containing different concentrations of DNPH at 30 °C.	286
3.84	Nyquist plots for the corrosion of weld aged maraging steel in 0.5 M sulphuric acid containing different concentrations of DNPH at 30 °C.	288
3.85	Bode plots for the corrosion of weld aged maraging steel in 0.5 M sulphuric acid containing different concentrations of DNPH at 30 °C.	288
3.86	Arrhenius plots for the corrosion of weld aged maraging steel in 0.5 M sulphuric acid containing different concentrations of DNPH.	289
3.87	Plots of $\ln(v_{\text{corr}}/T)$ versus $1/T$ for the corrosion of weld aged maraging steel in 0.5 M sulphuric acid containing different concentrations of DNPH.	290
3.88	Langmuir adsorption isotherms for the adsorption of DNPH on weld aged maraging steel in 0.5 M sulphuric acid at different temperatures.	291
3.89	SEM images of the weld aged maraging steel after immersion in 0.5 M sulphuric acid a) in the absence and b) in the presence of DNPH.	292
3.90	EDS spectra of the weld aged maraging steel after immersion in 0.5 M sulphuric acid in the absence of DNPH.	293
3.91	Potentiodynamic polarization curves for the corrosion of weld aged maraging steel in 0.1 M sulphuric acid containing	307

	different concentrations of DDPM at 30 °C.	
3.92	Nyquist plots for the corrosion of weld aged maraging steel specimen in 0.1 M sulphuric acid containing different concentrations of DDPM at 30 °C.	308
3.93	Bode plots for the corrosion of weld aged maraging steel specimen in 0.1 M sulphuric acid containing different concentrations of DDPM at 30 °C.	309
3.94	Arrhenius plots for the corrosion of weld aged maraging steel in 0.1 M sulphuric acid containing different concentrations of DDPM.	310
3.95	Plots of $\ln(v_{\text{corr}}/T)$ versus $1/T$ for the corrosion of weld aged maraging steel in 0.1 M sulphuric acid containing different concentrations of DDPM.	311
3.96	Langmuir adsorption isotherms for the adsorption of DDPM on weld aged maraging steel in 0.1 M sulphuric acid at different temperatures.	312
3.97	SEM images of the weld aged maraging steel after immersion in 0.1 M sulphuric a) in the absence and b) in the presence of DDPM.	313
3.98	EDS spectra of the weld aged maraging steel after immersion in 0.1 M sulphuric acid in the absence of DDPM.	314

Table	LIST OF TABLES	Page
No.		No.
1.1	Common anchoring organic groups	42
1.2	Nominal compositions (wt%) and the respective strength of commercial maraging steels (Inco).	47
1.3	Role of alloying elements in maraging steel.	50
1.4	Some important organic inhibitors studied for iron and iron alloys	55
2.1	Composition of 18 % Ni M250 grade maraging steel (weight %).	64
2.2	Adsorption isotherms to characterise the adsorption of inhibitors on the metal surface.	74
3.1	Results of Potentiodynamic polarisation studies for the corrosion of weld aged maraging steel in different concentrations of hydrochloric acid at different temperatures.	90
3.2	Results of EIS studies for the corrosion of weld aged maraging steel in different concentrations hydrochloric acid at different temperatures.	91
3.3	Activation parameters for the corrosion of weld aged maraging steel in hydrochloric acid.	92
3.4	Results of Potentiodynamic polarisation studies for the corrosion of weld aged maraging steel in different concentrations of sulphuric acid at different temperatures.	100
3.5	Results of EIS studies for the corrosion of weld aged maraging steel in different concentrations sulphuric acid at different temperatures.	101
3.6	Activation parameters for the corrosion of weld aged maraging steel in sulphuric acid.	102
3.7	Results of Potentiodynamic polarization studies for the corrosion of weld aged maraging steel in 0.1 M hydrochloric acid containing different concentrations of ATPI.	120
3.8	Results of Potentiodynamic polarization studies for the corrosion of weld aged maraging steel in 0.5 M hydrochloric acid containing different concentrations of ATPI.	121

3.9	Results of Potentiodynamic polarization studies for the corrosion of weld aged maraging steel in 1.0 M hydrochloric acid containing different concentrations of ATPI.	122
3.10	Results of Potentiodynamic polarization studies for the corrosion of weld aged maraging steel in 1.5 M hydrochloric acid containing different concentrations of ATPI.	123
3.11	Results of Potentiodynamic polarization studies for the corrosion of weld aged maraging steel in 2.0 M hydrochloric acid containing different concentrations of ATPI.	124
3.12	EIS data for the corrosion of weld aged maraging steel in 0.1 M hydrochloric acid containing different concentrations of ATPI.	125
3.13	EIS data for the corrosion of weld aged maraging steel in 0.5 M hydrochloric acid containing different concentrations of ATPI.	126
3.14	EIS data for the corrosion of weld aged maraging steel in 1.0 M hydrochloric acid containing different concentrations of ATPI.	127
3.15	EIS data for the corrosion of weld aged maraging steel in 1.5 M hydrochloric acid containing different concentrations of ATPI.	128
3.16	EIS data for the corrosion of weld aged maraging steel in 2.0 M hydrochloric acid containing different concentrations of ATPI.	129
3.17	Comparison of maximum attainable inhibition efficiencies by the Potentiodynamic method and EIS method for the corrosion of weld aged maraging steel in hydrochloric acid solutions of different concentrations in the presence of ATPI at 30 °C.	130
3.18	Activation parameters for the corrosion of weld aged maraging steel in hydrochloric acid containing different concentrations of ATPI.	131
3.19	Thermodynamic parameters for the adsorption of ATPI on weld aged maraging steel surface in hydrochloric acid at different temperatures.	132
3.20	Results of Potentiodynamic polarization studies for the corrosion of weld aged maraging steel in 0.1 M hydrochloric acid containing different concentrations of CPOB.	142
3.21	Results of Potentiodynamic polarization studies for the corrosion of	143

	weld aged maraging steel in 0.5 M hydrochloric acid containing different concentrations of CPOB.	
3.22	Results of Potentiodynamic polarization studies for the corrosion of weld aged maraging steel in 1.0 M hydrochloric acid containing different concentrations of CPOB.	144
3.23	Results of Potentiodynamic polarization studies for the corrosion of weld aged maraging steel in 1.5 M hydrochloric acid containing different concentrations of CPOB.	145
3.24	Results of Potentiodynamic polarization studies for the corrosion of weld aged maraging steel in 2.0 M hydrochloric acid containing different concentrations of CPOB.	146
3.25	EIS data for the corrosion of weld aged maraging steel in 0.1 M hydrochloric acid containing different concentrations of CPOB.	147
3.26	EIS data for the corrosion of weld aged maraging steel in 0.5 M hydrochloric acid containing different concentrations of CPOB.	148
3.27	EIS data for the corrosion of weld aged maraging steel in 1.0 M hydrochloric acid containing different concentrations of CPOB.	149
3.28	EIS data for the corrosion of weld aged maraging steel in 1.5 M hydrochloric acid containing different concentrations of CPOB.	150
3.29	EIS data for the corrosion of weld aged maraging steel in 2.0 M hydrochloric acid containing different concentrations of CPOB.	151
3.30	Comparison of maximum attainable inhibition efficiencies by the Potentiodynamic method and EIS method for the corrosion of weld aged maraging steel in hydrochloric acid solutions of different concentrations in the presence of CPOB at 30 °C.	152
3.31	Activation parameters for the corrosion of weld aged maraging steel in hydrochloric acid containing different concentrations of CPOB.	153
3.32	Thermodynamic parameters for the adsorption of CPOB on weld aged maraging steel surface in hydrochloric acid at different temperatures.	154
3.33	Results of Potentiodynamic polarization studies for the corrosion of	163

	weld aged maraging steel in 0.1 M hydrochloric acid containing different concentrations of CPOM.	
3.34	Results of Potentiodynamic polarization studies for the corrosion of weld aged maraging steel in 0.5 M hydrochloric acid containing different concentrations of CPOM.	164
3.35	Results of Potentiodynamic polarization studies for the corrosion of weld aged maraging steel in 1.0 M hydrochloric acid containing different concentrations of CPOM.	165
3.36	Results of Potentiodynamic polarization studies for the corrosion of weld aged maraging steel in 1.5 M hydrochloric acid containing different concentrations of CPOM.	166
3.37	Results of Potentiodynamic polarization studies for the corrosion of weld aged maraging steel in 2.0 M hydrochloric acid containing different concentrations of CPOM.	167
3.38	EIS data for the corrosion of weld aged maraging steel in 0.1 M hydrochloric acid containing different concentrations of CPOM.	168
3.39	EIS data for the corrosion of weld aged maraging steel in 0.5 M hydrochloric acid containing different concentrations of CPOM.	169
3.40	EIS data for the corrosion of weld aged maraging steel in 1.0 M hydrochloric acid containing different concentrations of CPOM.	170
3.41	EIS data for the corrosion of weld aged maraging steel in 1.5 M hydrochloric acid containing different concentrations of CPOM.	171
3.42	EIS data for the corrosion of weld aged maraging steel in 2.0 M hydrochloric acid containing different concentrations of CPOM.	172
3.43	Comparison of maximum attainable inhibition efficiencies by the Potentiodynamic method and EIS method for the corrosion of weld aged maraging steel in hydrochloric acid solutions of different concentrations in the presence of CPOM at 30 °C.	173
3.44	Activation parameters for the corrosion of weld aged maraging steel in hydrochloric acid containing different concentrations of CPOM.	174
3.45	Thermodynamic parameters for the adsorption of CPOM on weld	175

	aged maraging steel surface in hydrochloric acid at different temperatures.	
3.46	Results of Potentiodynamic polarization studies for the corrosion of weld aged maraging steel in 0.1 M hydrochloric acid containing different concentrations of DNPH.	184
3.47	Results of Potentiodynamic polarization studies for the corrosion of weld aged maraging steel in 0.5 M hydrochloric acid containing different concentrations of DNPH.	185
3.48	Results of Potentiodynamic polarization studies for the corrosion of weld aged maraging steel in 1.0 M hydrochloric acid containing different concentrations of DNPH.	186
3.49	Results of Potentiodynamic polarization studies for the corrosion of weld aged maraging steel in 1.5 M hydrochloric acid containing different concentrations of DNPH.	187
3.50	Results of Potentiodynamic polarization studies for the corrosion of weld aged maraging steel in 2.0 M hydrochloric acid containing different concentrations of DNPH.	188
3.51	EIS data for the corrosion of weld aged maraging steel in 0.1 M hydrochloric acid containing different concentrations of DNPH.	189
3.52	EIS data for the corrosion of weld aged maraging steel in 0.5 M hydrochloric acid containing different concentrations of DNPH.	190
3.53	EIS data for the corrosion of weld aged maraging steel in 1.0 M hydrochloric acid containing different concentrations of DNPH.	191
3.54	EIS data for the corrosion of weld aged maraging steel in 1.5 M hydrochloric acid containing different concentrations of DNPH.	192
3.55	EIS data for the corrosion of weld aged maraging steel in 2.0 M hydrochloric acid containing different concentrations of DNPH.	193
3.56	Comparison of maximum attainable inhibition efficiencies by the Potentiodynamic method and EIS method for the corrosion of weld aged maraging steel in hydrochloric acid solutions of different concentrations in the presence of DNPH at 30 °C.	194

3.57	Activation parameters for the corrosion of weld aged maraging steel in hydrochloric acid containing different concentrations of DNPH.	195
3.58	Thermodynamic parameters for the adsorption of DNPH on weld aged maraging steel surface in hydrochloric acid at different temperatures.	196
3.59	Results of Potentiodynamic polarization studies for the corrosion of weld aged maraging steel in 0.1 M hydrochloric acid containing different concentrations of DDPM.	205
3.60	Results of Potentiodynamic polarization studies for the corrosion of weld aged maraging steel in 0.5 M hydrochloric acid containing different concentrations of DDPM.	206
3.61	Results of Potentiodynamic polarization studies for the corrosion of weld aged maraging steel in 1.0 M hydrochloric acid containing different concentrations of DDPM.	207
3.62	Results of Potentiodynamic polarization studies for the corrosion of weld aged maraging steel in 1.5 M hydrochloric acid containing different concentrations of DDPM.	208
3.63	Results of Potentiodynamic polarization studies for the corrosion of weld aged maraging steel in 2.0 M hydrochloric acid containing different concentrations of DDPM.	209
3.64	EIS data for the corrosion of weld aged maraging steel in 0.1 M hydrochloric acid containing different concentrations of DDPM.	210
3.65	EIS data for the corrosion of weld aged maraging steel in 0.5 M hydrochloric acid containing different concentrations of DDPM.	211
3.66	EIS data for the corrosion of weld aged maraging steel in 1.0 M hydrochloric acid containing different concentrations of DDPM.	212
3.67	EIS data for the corrosion of weld aged maraging steel in 1.5 M hydrochloric acid containing different concentrations of DDPM.	213
3.68	EIS data for the corrosion of weld aged maraging steel in 2.0 M hydrochloric acid containing different concentrations of DDPM.	214
3.99	Comparison of maximum attainable inhibition efficiencies by the	215

	Potentiodynamic method and EIS method for the corrosion of weld aged maraging steel in hydrochloric acid solutions of different concentrations in the presence of DDPM at 30 °C.	
3.70	Activation parameters for the corrosion of weld aged maraging steel in hydrochloric acid containing different concentrations of DDPM.	216
3.71	Thermodynamic parameters for the adsorption of DDPM on weld aged maraging steel surface in hydrochloric acid at different temperatures.	217
3.72	Results of Potentiodynamic polarization studies for the corrosion of weld aged maraging steel in 0.1 M sulphuric acid containing different concentrations of ATPI.	231
3.73	Results of Potentiodynamic polarization studies for the corrosion of weld aged maraging steel in 0.5 M sulphuric acid containing different concentrations of ATPI.	232
3.74	Results of Potentiodynamic polarization studies for the corrosion of weld aged maraging steel in 1.0 M sulphuric acid containing different concentrations of ATPI.	233
3.75	Results of Potentiodynamic polarization studies for the corrosion of weld aged maraging steel in 1.5 M sulphuric acid containing different concentrations of ATPI.	234
3.76	Results of Potentiodynamic polarization studies for the corrosion of weld aged maraging steel in 2.0 M sulphuric acid containing different concentrations of ATPI.	235
3.77	EIS data for the corrosion of weld aged maraging steel in 0.1 M sulphuric acid containing different concentrations of ATPI.	236
3.78	EIS data for the corrosion of weld aged maraging steel in 0.5 M sulphuric acid containing different concentrations of ATPI.	237
3.79	EIS data for the corrosion of weld aged maraging steel in 1.0 M sulphuric acid containing different concentrations of ATPI.	238
3.80	EIS data for the corrosion of weld aged maraging steel in 1.5 M sulphuric acid containing different concentrations of ATPI.	239

3.81	EIS data for the corrosion of weld aged maraging steel in 2.0 M sulphuric acid containing different concentrations of ATPI.	240
3.82	Comparison of maximum attainable inhibition efficiencies by the Potentiodynamic method and EIS method for the corrosion of weld aged maraging steel in sulphuric acid solutions of different concentrations in the presence of ATPI at 30 °C.	241
3.83	Activation parameters for the corrosion of weld aged maraging steel in sulphuric acid containing different concentrations of ATPI.	242
3.84	Thermodynamic parameters for the adsorption of ATPI on weld aged maraging steel surface in sulphuric acid at different temperatures.	243
3.85	Results of Potentiodynamic polarization studies for the corrosion of weld aged maraging steel in 0.1 M sulphuric acid containing different concentrations of CPOB.	252
3.86	Results of Potentiodynamic polarization studies for the corrosion of weld aged maraging steel in 0.5 M sulphuric acid containing different concentrations of CPOB.	253
3.87	Results of Potentiodynamic polarization studies for the corrosion of weld aged maraging steel in 1.0 M sulphuric acid containing different concentrations of CPOB.	254
3.88	Results of Potentiodynamic polarization studies for the corrosion of weld aged maraging steel in 1.5 M sulphuric acid containing different concentrations of CPOB.	255
3.90	Results of Potentiodynamic polarization studies for the corrosion of weld aged maraging steel in 2.0 M sulphuric acid containing different concentrations of CPOB.	256
3.91	EIS data for the corrosion of weld aged maraging steel in 0.1 M sulphuric acid containing different concentrations of CPOB.	257
3.92	EIS data for the corrosion of weld aged maraging steel in 0.5 M sulphuric acid containing different concentrations of CPOB.	258
3.92	EIS data for the corrosion of weld aged maraging steel in 1.0 M sulphuric acid containing different concentrations of CPOB.	259

3.93	EIS data for the corrosion of weld aged maraging steel in 1.5 M sulphuric acid containing different concentrations of CPOB.	260
3.94	EIS data for the corrosion of weld aged maraging steel in 2.0 M sulphuric acid containing different concentrations of CPOB.	261
3.95	Comparison of maximum attainable inhibition efficiencies by the Potentiodynamic method and EIS method for the corrosion of weld aged maraging steel in sulphuric acid solutions of different concentrations in the presence of CPOB at 30 °C.	262
3.96	Activation parameters for the corrosion of weld aged maraging steel in sulphuric acid containing different concentrations of CPOB.	263
3.97	Thermodynamic parameters for the adsorption of CPOB on weld aged maraging steel surface in sulphuric acid at different temperatures.	264
3.98	Results of Potentiodynamic polarization studies for the corrosion of weld aged maraging steel in 1.0 M sulphuric acid containing different concentrations of CPOM	273
3.99	Results of Potentiodynamic polarization studies for the corrosion of weld aged maraging steel in 0.5 M sulphuric acid containing different concentrations of CPOM.	274
3.100	Results of Potentiodynamic polarization studies for the corrosion of weld aged maraging steel in 1.0 M sulphuric acid containing different concentrations of CPOM.	275
3.101	Results of Potentiodynamic polarization studies for the corrosion of weld aged maraging steel in 1.5 M sulphuric acid containing different concentrations of CPOM.	276
3.102	Results of Potentiodynamic polarization studies for the corrosion of weld aged maraging steel in 2.0 M sulphuric acid containing different concentrations of CPOM.	277
3.103	EIS data for the corrosion of weld aged maraging steel in 0.1 M sulphuric acid containing different concentrations of CPOM.	278
3.104	EIS data for the corrosion of weld aged maraging steel in 0.5 M	279

	sulphuric acid containing different concentrations of CPOM.	
3.105	EIS data for the corrosion of weld aged maraging steel in 1.0 M sulphuric acid containing different concentrations of CPOM.	280
3.106	EIS data for the corrosion of weld aged maraging steel in 1.5 M sulphuric acid containing different concentrations of CPOM.	281
3.107	EIS data for the corrosion of weld aged maraging steel in 2.0 M sulphuric acid containing different concentrations of CPOM.	282
3.108	Comparison of maximum attainable inhibition efficiencies by the Potentiodynamic method and EIS method for the corrosion of weld aged maraging steel in sulphuric acid solutions of different concentrations in the presence of CPOM at 30 °C.	283
3.109	Activation parameters for the corrosion of weld aged maraging steel in sulphuric acid containing different concentrations of CPOM.	284
3.110	Thermodynamic parameters for the adsorption of CPOM on weld aged maraging steel surface in sulphuric acid at different temperatures.	285
3.111	Results of Potentiodynamic polarization studies for the corrosion of weld aged maraging steel in 0.1 M sulphuric acid containing different concentrations of DNPH	294
3.112	Results of Potentiodynamic polarization studies for the corrosion of weld aged maraging steel in 0.5 M sulphuric acid containing different concentrations of DNPH.	295
3.113	Results of Potentiodynamic polarization studies for the corrosion of weld aged maraging steel in 1.0 M sulphuric acid containing different concentrations of DNPH.	296
3.114	Results of Potentiodynamic polarization studies for the corrosion of weld aged maraging steel in 1.5 M sulphuric acid containing different concentrations of DNPH.	297
3.115	Results of Potentiodynamic polarization studies for the corrosion of weld aged maraging steel in 2.0 M sulphuric acid containing different concentrations of DNPH.	298

3.116	EIS data for the corrosion of weld aged maraging steel in 0.1 M sulphuric acid containing different concentrations of DNPH.	299
3.117	EIS data for the corrosion of weld aged maraging steel in 0.5 M sulphuric acid containing different concentrations of DNPH.	300
3.118	EIS data for the corrosion of weld aged maraging steel in 1.0 M sulphuric acid containing different concentrations of DNPH.	301
3.119	EIS data for the corrosion of weld aged maraging steel in 1.5 M sulphuric acid containing different concentrations of DNPH.	302
3.12	EIS data for the corrosion of weld aged maraging steel in 2.0 M sulphuric acid containing different concentrations of DNPH.	303
3.121	Comparison of maximum attainable inhibition efficiencies by the Potentiodynamic method and EIS method for the corrosion of weld aged maraging steel in sulphuric acid solutions of different concentrations in the presence of DNPH at 30 °C.	304
3.122	Activation parameters for the corrosion of weld aged maraging steel in sulphuric acid containing different concentrations of DNPH.	305
3.123	Thermodynamic parameters for the adsorption of DNPH on weld aged maraging steel surface in sulphuric acid at different temperatures.	306
3.124	Results of Potentiodynamic polarization studies for the corrosion of weld aged maraging steel in 0.1 M sulphuric acid containing different concentrations of DDPM	315
3.125	Results of Potentiodynamic polarization studies for the corrosion of weld aged maraging steel in 0.5 M sulphuric acid containing different concentrations of DDPM.	316
3.126	Results of Potentiodynamic polarization studies for the corrosion of weld aged maraging steel in 1.0 M sulphuric acid containing different concentrations of DDPM.	317
3.127	Results of Potentiodynamic polarization studies for the corrosion of weld aged maraging steel in 1.5 M sulphuric acid containing different concentrations of DDPM.	318

3.128	Results of Potentiodynamic polarization studies for the corrosion of weld aged maraging steel in 2.0 M sulphuric acid containing different concentrations of DDPM.	319
3.129	EIS data for the corrosion of weld aged maraging steel in 0.1 M sulphuric acid containing different concentrations of DDPM.	320
3.130	EIS data for the corrosion of weld aged maraging steel in 0.5 M sulphuric acid containing different concentrations of DDPM.	321
3.131	EIS data for the corrosion of weld aged maraging steel in 1.0 M sulphuric acid containing different concentrations of DDPM.	322
3.132	EIS data for the corrosion of weld aged maraging steel in 1.5 M sulphuric acid containing different concentrations of DDPM.	323
3.133	EIS data for the corrosion of weld aged maraging steel in 2.0 M sulphuric acid containing different concentrations of DDPM.	324
3.134	Comparison of maximum attainable inhibition efficiencies by the Potentiodynamic method and EIS method for the corrosion of weld aged maraging steel in sulphuric acid solutions of different concentrations in the presence of DDPM at 30 °C.	325
3.135	Activation parameters for the corrosion of weld aged maraging steel in sulphuric acid containing different concentrations of DDPM.	326
3.136	Thermodynamic parameters for the adsorption of DDPM on weld aged maraging steel surface in sulphuric acid at different temperatures.	327

LIST OF ABBREVIATIONS

Abbreviations	Nomenclature
DNPH	(E)-1-(2,4-dinitrophenyl)-2-[1-(2-nitrophenyl) ethylidene] hydrazine
ATPI	1(2E)-1-(4-aminophenyl)-3-(2-thienyl) prop-2-en-1-one
CPOM	2-(4-bromophenyl)-2-oxoethyl 4-chlorobenzoate
CPOB	2-(4-chlorophenyl)-2-oxoethyl benzoate
DDPM	5-diethylamino-2-[[2-(2,4-dinitrophenyl) hydrazin-1-ylidene]methyl - phenol
bcc	Body centred cubic structure
EIS	Electrochemical impedance spectroscopy
e.m.f	Electromotive force
Fig.	Figure
HF	High frequency
LF	Low frequency
M250	Maraging steel 250 grade
OCP	Open circuit potential
SCE	Saturated calomel electrode
SEM	Scanning electron microscopic
SCC	Stress Corrosion Cracking
VPI	Vapour phase inhibitor
ZCP	Zero charge potential

LIST OF SYMBOLS

Symbol	Definition
T	Absolute temperature
E _a	Activation energy
η _{act}	Activation overpotential
E ₀	Amplitude of the signal
ω	Angular frequency
Z(ω)	Angular frequency (ω) dependent impedance
b _a	Anodic Potentiodynamic slope
W _i	Atomic weight of the i th element in the alloy
C _f	Capacitance of the inhibitor film
b _c	Cathodic Potentiodynamic slope
E	Cell potential
R _{ct}	Charge transfer resistance
C _{inh}	Concentration of the inhibitor
η _{conc}	Concentration overpotential
B	Constant
K	Constant
Q	Constant phase element
R ²	Correlation coefficient
i _{corr}	Corrosion current density
i _{corr(inh)}	Corrosion current density in the presence of inhibitor
E _{corr}	Corrosion potential
v _{corr}	Corrosion rate
C _{dl}	Double layer capacitance
EDS	Energy dispersive X-ray spectroscopy
EW	Equivalent weight
F	Faraday constant
R _f	Film resistance
R	Gas constant

Z''	Imaginary part impedance
Inh	Inhibitor
η	inhibition efficiency
l	Length
ϵ	Local dielectric constant
f_i	Mass fraction of the i^{th} element in the alloy
IR	Ohmic drop
a_{ox}	Oxidized species
ϵ°	Permittivity of the air
pH diagrams	Pourbaix diagrams
Z'	Real part of impedance
a_{red}	Reduced species
ρ	Resistivity of the solution
SEM	Scanning electron microscope
χ	Size ratio
R_s	Solution resistance
E°	Standard cell potential
$\Delta H_{\text{ads}}^{\circ}$	Standard enthalpy of adsorption
$\Delta S_{\text{ads}}^{\circ}$	Standard entropy of adsorption
$\Delta G_{\text{ads}}^{\circ}$	Standard free energy of adsorption
θ	Surface coverage
S	surface of the electrode
d	Thickness of the film
t	Time
n_i	Valence of the i^{th} element of the alloy
$\Psi_{\text{z.ch}}$	Zero charge potential

CHAPTER 1

INTRODUCTION

1.1 IMPORTANCE OF CORROSION

The deterioration of materials due to reactions with their environments is the currently accepted broad definition of corrosion. The term corrosion has its origin in Latin. The Latin term “rodere” means ‘gnawing’ and “corrodere” means ‘gnawing to pieces’ (Sastri et al. 2007). The process of corrosion is the transformation of pure metal into its undesired metallic compounds. Corrosion degrades the useful properties of materials and structures including strength, appearance and permeability to liquids and gases. The life of a metal gets shortened by corrosion process (Uhlig 1948, Bardal 2003). The corrosion can be a fast or a slow process depending upon the metal and the environment in which it is undergoing corrosion (Fontana 1987). It occurs with all metals except the least active noble metals such as gold and platinum (Banerjee 1985).

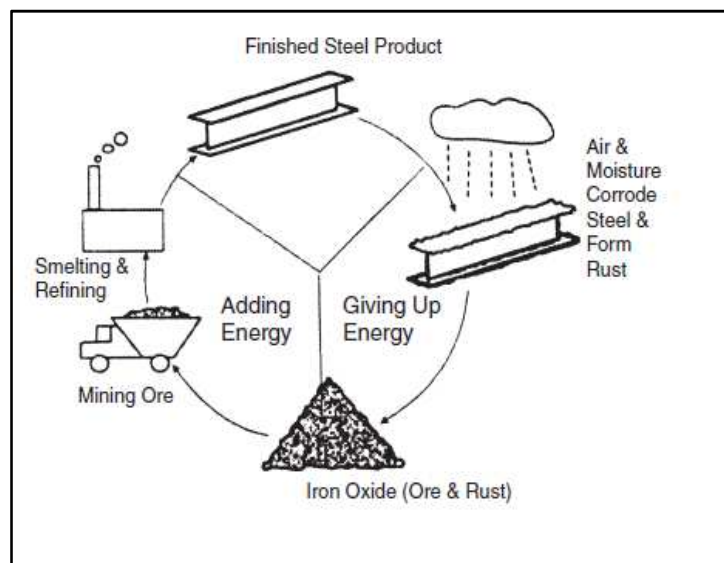


Fig. 1.1: The corrosion cycle of steel.

Most of the metals occur in combined state except the noble metals. Pure metal is extracted from their ores by metallurgical process, energy being supplied in the form of heat or electrical energy (Pierre 2008). The obtained pure metals are relatively at higher energy state compared to their corresponding ores, and they have a natural tendency to

revert back to their combined state. Thus corrosion of metals can be considered as extractive metallurgy in reverse (Fontana 1987, Davis 2000). Fig. 1 illustrates the corrosion life cycle of a steel product (Davis 2000). Fortunately, the rate at which most of these processes progress is slow enough to provide useful building materials. Only inert atmospheres and vacuums can be considered free of corrosion for most metallic materials (Philip 1996).

1.2 NEED FOR CORROSION STUDY

Corrosion is all around us. It shows itself in rust-stained structures that are falling down with age. Corrosion processes cost billions of dollars each year in maintenance and repair. Corrosion is relentless and patient, and inevitable. There are three primary reasons for concern about and the study of corrosion - safety, economics and conservation. Corrosion is an economic problem associated closely with the loss of capital assets and business profits. Corrosion control provides most advantageous course of avoiding such losses. Emergence of rust holes in body panel of new automobile, aircrafts, failure of weapons in defence, outdoor rusting of steel households, rusting of steel bars in concrete bridges, expensive repair and replacement of plumbing systems, water heaters are common experiences. Petroleum industry, chemical processing plants, deterioration of concrete bridges, electric power generation plants, electronic equipments, ships and other concrete structures etc., are facing devastating corrosion costs (Fontana 1987, Sastri et al. 2007, Philip 2007). The scientist studies corrosion mechanism to improve

- The understanding of the causes of corrosion.
- The ways to prevent or minimize damage caused by corrosion.
- The understanding of mechanism of corrosion and the possible methods and mechanism of control.

1.2.1 Some of the economic consequences are as follows

- Replacement of corroded equipments.
- Overdesign to allow for corrosions.
- Preventive maintenance, for example, painting.
- Shutdown of equipment due to corrosion failure.
- Contamination of a product.
- Loss of efficiency.
- Decrease in the heat-transfer rate in heat exchangers.
- Loss of valuable product (Fontana 1987, Davis 2000, McCafferty 2010).

1.2.2 Still other consequences are social. These can involve the following issues

- Safety, for example, sudden failure can cause fire, explosion, release of toxic product and construction collapse.
- Health, for example, pollution due to escaping product from corroded equipment or due to a corrosion product itself.
- Depletion of natural resources, including metals and the fuels used to manufacture them.
- Appearance as when corroded material is unpleasing to the eye (Davis 2000, Philip 2007).

Another aspect of concern is the limit of resources in the world. We have reached a level of maturity to be able to recognize that our natural resources are limited and finite in our world, and that methods to conserve these resources by recycling and other methods have a prominent role to play. Corrosion prevention and protection arrests the degradation of metals/materials and contributes in a significant way to the conservation of resources with minimum damage to the ecosystems. Since materials are prone to corrosion it is useful to know the factors both direct and indirect, which affect the choice of materials and their related corrosion resistance in the design of an engineering structure (Sastri et al. 2007).

1.3 ELECTROCHEMICAL THEORY OF CORROSION (Fontana 1987, Bardal 2004, Gadag and Shetty 2006, Einar 2004, Pierre 2008)

The corrosion of a metal in the environment is an electrochemical process. According to electrochemical theory, corrosion of a metal in aqueous solution involves oxidation and reduction with the formation of anodic and cathodic regions on the metal surface. These regions together form corrosion cells. At anodic region oxidation reaction takes place (i.e., liberation of free electrons) and the metal is converted into its ions (M^{n+}). Consequently, metal undergoes corrosion at the anodic region. Thus anodic metal is destroyed by either dissolution of the metal to form soluble ionic products or an insoluble compound of the metal, usually an oxide. There are several cathodic reactions, which are frequently encountered in metallic corrosion depending on the type of reducible species present in the environment. At cathodic site, reduction reaction (i.e., gain of electrons) takes place. Since metal cannot be reduced further metal atoms at the cathodic region are unaffected by the cathodic reaction. The electrons liberated at the anodic region migrate to the cathodic region constituting corrosion current. The metal ions liberated at the anode and some anions formed at cathode diffuse towards each other through the conducting medium and form a corrosion product somewhere between anode and cathode. Since anodic and cathodic reactions occur simultaneously and at the same rate on metal surface, they create an electrochemical cell. The basic corrosion process in acid medium is represented in Fig. 1.2.

The anodic reaction in every corrosion reaction is the oxidation of a metal to its ion. This can be written in the general form:



The number of electrons produced is equal to the valency of the metal. The possible anodic reaction during corrosion of iron can be represented as follows,



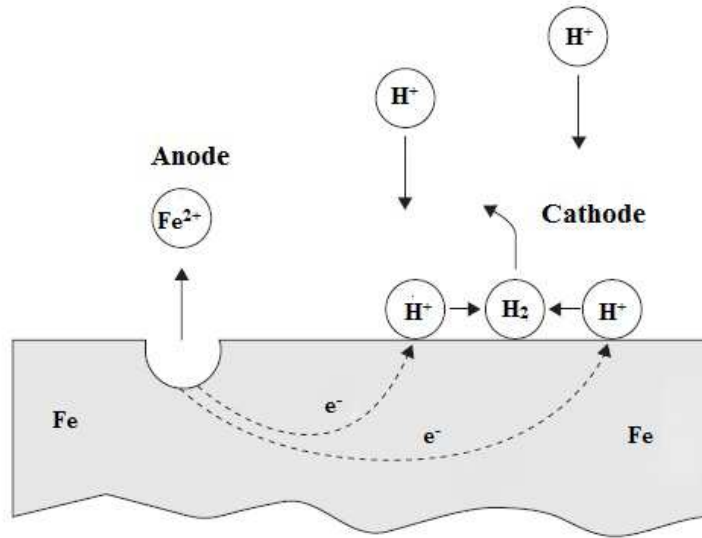


Fig. 1.2: The electrochemical cell set up between anodic and cathodic sites on a metal surface undergoing corrosion.

There are several cathodic reactions, which are frequently encountered, in metallic corrosion. The most common cathodic reactions are;

Hydrogen evolution (acid solutions):



Hydrogen evolution (neutral or basic solutions):



Oxygen reduction (acid solutions):



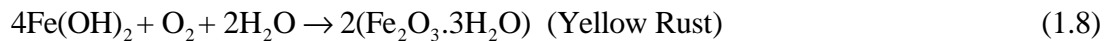
Oxygen reduction (neutral or basic solutions):



Rusting of iron in neutral aqueous solution in the presence of atmospheric oxygen is a common example of corrosion. Corrosion of iron produces Fe^{2+} ions and OH^- ions at the anode and cathode sites, respectively. These ions diffuse towards each other. Since smaller Fe^{2+} ions diffuse more rapidly than OH^- ions, their combination occurs more commonly near the cathodic region to produce insoluble $\text{Fe}(\text{OH})_2$.



If enough oxygen is present, ferrous hydroxide is readily oxidized to hydrated ferric oxide.



In the presence of limited oxygen, ferrous hydroxide is converted into magnetic oxide of iron (Fe_3O_4) and known as black rust.



1.4 CLASSIFICATION OF CORROSION

Corrosion has been classified in many different ways. Classification is usually based on one of three factors (Jones 1996, Philip 1996, Davis et al. 2003).

No.	Factor	Types	Characteristics
1.	Nature of the corrodent	1. Wet corrosion	Electrochemical attack in the presence of moisture
		2. Dry corrosion	Direct chemical attack in the absence of moisture

2.	Mechanism of corrosion	1. Electrochemical corrosion	Destruction by electrolytes
		2. Chemical corrosion	Direct chemical attack
3.	Appearance of the corroded metal	1. Uniform corrosion	Corrodes at the same rate over the entire surface
		2. Localized corrosion	Metal corrodes only at small areas

1.4.1 Forms of Corrosion (Fontana 1987, Jones 1996, Philip 1996)

The classification is based on the appearance of corroded material. Some of the types of corrosion cases observed are discussed below.

1.4.4.1 Uniform corrosion

It is one of the most easily measured and predictable forms of corrosion. The corrosion corresponds to the corrosion attack with the greatest weight loss of the metal. It is the uniform thinning of the metal without any localized attack, thereby causing an eventual failure of the material. Uniform corrosion is generally thought of in terms of metal loss due to chemical attack or dissolution of the metallic component into metallic ions.

1.4.4.2 Galvanic corrosion

It refers to corrosion damage induced when two dissimilar metals are coupled in a corrosive electrolyte. When two different metallic materials are electrically connected and placed in a conductive solution, the potential difference between the two will provide a stronger driving force for the dissolution of the less noble (more electrically negative) material. The less noble metal will suffer from oxidation while the more noble metal acts as the cathode. Example: steel screws in copper sheet.

1.4.4.3 Crevice corrosion

Crevice corrosion is a localized type of corrosion occurring within or adjacent to narrow gaps or openings formed by metal-to-metal-to-nonmetal contact. It results from local differences in oxygen concentrations, associated deposits on the metal surface, gaskets, lap joints, or crevices under a bolt or around rivet heads where small amounts of liquid can collect and become stagnant. Crevice corrosion may take place on any metal and in any corrosive environment. The material responsible for forming the crevice need not be metallic. Wood, plastic, rubber, glass, concrete, asbestos, wax, and living organisms have been reported to cause crevice corrosion. After the attack begins within the crevice, its progress is very rapid. Example: corrosion of steel in an industrial environment resulting from wetted area within crevice.

1.4.4.4 Pitting corrosion

It is a localized and intense form of corrosion that results in holes in the metal, where the bulk of the surface remains unattacked. Pitting occurs only when a small area of a metal becomes anodic with respect to the rest of the surface. In the extreme case, it appears as a deep, tiny hole. The depth of the pit eventually leads to a thorough perforation or a massive undercut in the thickness of the metal part. This form of attack is most commonly found in those materials of which passive films have broken down. Example: stainless steel exposed to chloride containing water.

1.4.4.5 Intergranular corrosion

As the name suggests, this particular corrosion attacks those sites where individual grains within a metallic material touch each other. It is a localized attack at and adjacent to grain boundaries, with relatively little corrosion of the grains. These boundaries are natural regions of higher energy due to the greater frequency of dislocations of atoms from the natural order of the material's structure. Grain boundary material of limited area, acting as anode is in contact with large areas of grain acting as

cathode. Example: Depletion of chromium in the grain boundary regions results in intergranular corrosion of stainless steels.

1.4.4.6 Selective leaching

It is the process whereby a specific element is removed from an alloy due to an electrochemical interaction with the environment. It is the preferential dissolution of one element from an alloy. The result of this corrosion is that of leaving a porous and usually brittle shadow of the original component. Examples: i) Dezincification of brass alloys is the most familiar example of this type of corrosion. ii) Selective loss of aluminium in aluminium-copper alloys and the loss of iron in cast iron-carbon steels.

1.4.4.7 Erosion corrosion

It is a type of corrosion resulting from the increased rate of corrosion attack which is due to the movement of a corrodent over a metal surface. The movement of the corrodent can be associated with mechanical wear. The increase in corrosion due to the erosion process is usually related to the removal or damage of the protective surface film. The mechanism is usually identified by localized corrosion which exhibits a pattern that follows the flow of the corrodent. A type of corrosion familiar to pump impellers, this form of attack is caused by the formation and collapse of tiny vapour bubbles near a metallic surface in the presence of a corrodent. The protective surface film is again damaged, in this case by the high pressures caused by the collapse of the bubbles.

1.4.4.8 Stress corrosion cracking (SCC)

In this type of corrosion, the cracking is induced from the combined influence of tensile stress and a corrosive environment. During stress corrosion, the metal or alloy is virtually unattacked over most of its surface, while fine cracks progress through it normal to the direction of tensile stress. In this type of corrosion, stressed part of the metal acts as anode and the stress free part acts as cathode. It can lead to unexpected sudden failure of normally ductile metals subjected to a tensile stress, especially at elevated temperature in

the case of metals. SCC often progresses rapidly, and is more common among alloys than pure metals. Season cracking of brass and caustic embrittlement of steel are two classic cases of stress corrosion.

1.4.4.9 Hydrogen embrittlement

Atomic hydrogen generated during pickling, plating, welding or corrosion; diffuses into the metal or alloys through the grain boundaries and combine at the crystal imperfections to form molecules. The equilibrium pressure of molecular hydrogen in contact with atomic hydrogen exerts very large pressure. Therefore high internal stresses are induced which cause stress corrosion and thus failure of equipment. Hydrogen blistering, hydrogen embrittlement and decarburization are caused because of hydrogen damage.

1.4.4.10 Corrosion fatigue

Corrosion fatigue is defined as the reduction of fatigue resistance due to the presence of a corrosive medium. Thus corrosion fatigue is not defined in terms of the appearance of failure but in terms of mechanical properties as there is degradation in these. There is usually a large area covered with corrosion products and small roughened area resulting from the final brittle fracture. Corrosion fatigue can be viewed as special case of stress corrosion cracking.

1.5 FACTORS AFFECTING CORROSION RATE

Some of the important factors which influence the rate of corrosion are discussed below (Speller 1951, Jones 1996, Gadag and Shetty 2006).

1.5.1 Nature of the metal

The tendency of a metal to undergo corrosion in aqueous solution depends upon its electrode potential, which is variable, subject to other conditions such as temperature, pressure and concentration. In general, the metals with lower electrode potential values

are more reactive than the metals with higher electrode potential values. The metals with lower electrode potential are more susceptible for corrosion than the ones with higher electrode potentials. However there are exceptions to this general trend as some metals show passivity.

1.5.2 Difference in potential between anodic and cathodic region

Larger the potential difference between the anodic region and cathodic region of the corrosion cell, higher is the corrosion rate.

1.5.3 Nature of the corrosion product

The corrosion product formed on the surface of the metal may or may not act as protective film. If the corrosion product deposited is insoluble, stable, uniform, nonporous and adherent it acts as a protective film. A thin, invisible, impervious, continuous film formed on the surface acts as a barrier between the fresh metal surface and the corrosion environment.

1.5.4 Ratio of anodic to cathodic area

The rate of corrosion is greatly influenced by the relative sizes of anodic and cathodic areas. If a metal has a small anodic area and large cathodic area, then the corrosion is more intensive at the anodic region because electrons released at the anode are rapidly consumed at the cathode. If cathode is smaller than anode, the consumption of electrons at the cathode will be slower and lower will be the corrosion rate.

1.5.5 Hydrogen overvoltage

Hydrogen overpotential is an important factor of corrosion where hydrogen evolution is the cathodic reaction. Under the given environmental conditions of temperature, pressure and flow rate of medium, each metal exhibits its own characteristic resistance (hydrogen overpotential) to hydrogen evolution reaction. Higher the hydrogen overvoltage, more difficult is the liberation of hydrogen on the metal surface. Hence any

factor, which increases hydrogen over potential, will considerably retard the corrosion rate.

1.5.6 Temperature

In general, corrosion rate increases with the increase in temperature, probably due to the increase in conductance of the medium, decrease in polarization effects, solubility of corrosion products, breakdown of protective film, etc.

1.5.7 pH

Depending on the pH of the medium and the nature of the metal, either hydrogen evolution or oxygen reduction reaction predominates. In general, lower the pH of the corrosion medium, higher is the corrosion rate. However, some metals like Al, Zn, etc., undergo fast corrosion in highly alkaline solution.

1.5.8 Presence of oxidising agents

The presence of oxidising agents increases the corrosion rate of the metal. Even noble metals undergo corrosion in the presence of oxidising agents.

1.5.9 Polarization at anodic and cathodic region

During the process of corrosion, the polarization of the anode and the cathode decreases the corrosion rate substantially. Polarization at the electrodes is due to: (i) change in concentration at the vicinity of the electrode (ii) overvoltage or (iii) presence of surface films on the electrodes.

1.5.10 Effect of dissolved oxygen

Amount of dissolved oxygen in the corrosion medium plays a significant role in cathodic reaction of the corrosion. In many cases, irrespective of the pH of the solution, corrosion occurs at relatively slow rate involving oxygen as the depolarizer. Differential aeration or oxygen concentration cell is formed on the metal surface, when it is exposed

to the environment having different oxygen concentrations. Oxygen rich area becomes cathodic whereas oxygen deficient area becomes anodic. In some cases the metal oxide formed acts as a passive barrier between metal and the environment.

1.5.11 Effect of velocity of the medium

If the corrosion is due to presence of stagnant zone of corrosive fluid or due to formation of shielded area, increase in velocity will decrease the corrosion rate. If the corrosive ions are supplied because of velocity, the corrosion rate will increase. Increase in velocity can also increase the corrosion rate where the corrosion resistance is due to formation of less strong surface film.

1.5.12 Effect of other ions present in the solution

The rate of corrosion process is affected by the presence of certain ions like Cl^- , SO_4^{2-} , NO_3^- , etc. For instance in the formation of protective film on the metals such as aluminium, iron, copper etc., chloride ions will interfere and can cause extensive damage. Similar effects with less severity were also observed in the presence of sulphate ions. Sometimes the intermediate corrosion products become predominant in controlling the rate of corrosion process.

1.6 THERMODYNAMICS OF CORROSION (Fontana1987, Davis 2003, Philip 2007, Winston et al. 2008).

Thermodynamic approach of energy changes involved in the electrochemical reactions of corrosion provides the information about the driving force and the spontaneous direction of the reaction. The change in free energy ΔG is a direct measure of the work capacity or maximum electric energy available from a system. If the change in free energy accompanying the transition of a system from one state to another state is negative, this indicates a loss in free energy and also the spontaneous reaction of the system. It is not possible to predict accurately the velocity of a reaction from change in free energy. This parameter reflects only the direction of reaction by its sign, and any

predictions of velocity based on the magnitude of the change in free energy may be erroneous.

The free energy change accompanying an electrochemical reaction can be calculated by the following equation.

$$\Delta G = - nFE \quad (1.10)$$

where ΔG is the free energy change, n is the number of electrons involved in the reaction, F is the Faraday constant and E is the cell potential.

To determine the potential of a system in which the reactants are not at unit activity, the Nernst equation can be employed, that is,

$$E = E^0 + 2.303 \frac{RT}{nF} \log \frac{a_{\text{ox}}}{a_{\text{red}}} \quad (1.11)$$

where E is the cell potential, E^0 the standard cell potential, R is the gas constant, T is absolute temperature, n is the number of electrons transferred, F is the Faraday constant, a_{ox} and a_{red} are the activities of oxidized and reduced species. Thus, there is a definite relation between the free energy change and the cell potential of an electrochemical reaction. In any electrochemical reaction, the most negative or active half-cell tends to be oxidized, and most positive or noble half-cell tends to be reduced. Electrode potentials are very useful in predicting corrosion behaviour. All metals with reversible potentials more active than hydrogen will tend to be corroded by acid solutions. Hence, electrode potentials can be used to state a criterion for corrosion.

Potential/pH diagrams (Pourbaix diagrams) graphically represent the stability of a metal and its corrosion products as a function of the potential and pH of an aqueous solution. The pH is shown on the horizontal axis and the potential on the vertical axis. The main uses of these diagrams are, i) Predicting the spontaneous direction of reactions, ii) Estimating the composition of corrosion products, iii) Predicting the environmental changes that will prevent or reduce corrosive attack.

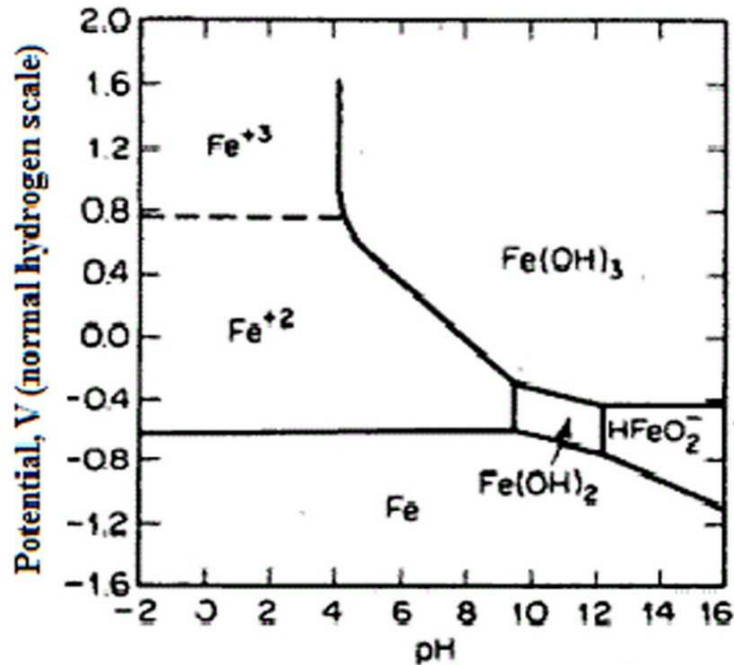


Fig. 1.3: Pourbaix diagram for iron/water/dissolved oxygen system.

From a corrosion engineering perspective, the value of Pourbaix diagrams is their usefulness in identifying potential – pH domains where corrosion does not occur - that is, where the metal itself is the stable phase. By controlling potential (e.g., by cathodic protection) and/or by adjusting the pH in specific domains identified using Pourbaix diagrams, it may be possible to prevent corrosion from taking place.

A typical Pourbaix diagram for iron is shown in Fig. 1.3. As shown, it is possible to delineate areas in which iron, iron hydroxide, ferrous iron etc., thermodynamically stable. That is these forms represent states of lowest free energy. Thermodynamics does not predict how fast the corrosion reaction will occur. To understand the kinetics of corrosion, examination of a number of electrochemical principles for example, mixed potential behaviour, polarization behaviour, and the concept of exchange currents, are required. Some useful terms used to explain electrochemical kinetics of corrosion are explained in the following sections.

1.7 KINETICS OF CORROSION (Robert et al. 2003, Nestor 2004, Philip 2007, Pierre 2008)

Electrochemical reaction kinetics is essential in determining the rate of corrosion of a metal exposed to a corrosive medium (electrolyte). On the other hand, thermodynamics predicts the possibility of corrosion, but it does not provide information on how slow or fast corrosion occurs. The kinetics of a reaction on an electrode surface depends on the electrode potential. Thus, a reaction rate strongly depends on the rate of electron flow to or from a metal-electrolyte interface. If the electrochemical system (electrode and electrolyte) is at equilibrium, then the net rate of reaction is zero. In comparison, reaction rates are governed by chemical kinetics, while corrosion rates are primarily governed by electrochemical kinetics.

Electrochemical kinetics of a corroding metal can be characterized by determining at least three polarization parameters, such as corrosion current density (i_{corr}) corrosion potential (E_{corr}) and Tafel slopes (b_a and/or b_c). Then the corrosion behaviour can be disclosed by a polarization curve (E vs. $\log i$). Evaluation of these parameters leads to the determination of the polarization resistance and the corrosion rate which is often converted into Faradaic corrosion rate C_R having units of mm y^{-1} . In reality, polarization effects control the cathodic and anodic currents that are integral components of corrosion processes.

To develop a current in either a galvanic or electrolytic cell, a driving force in the form of a potential is required to overcome the resistance of ions to movement toward the anode and the cathode. Just as metallic conduction, this force follows ohm's law and equal to the product of I in A and R in Ω . The force is generally referred to as ohmic potential, or IR drop. The net effect of IR drop is to increase the potential required to operate an electrolytic cell and to decrease measured potential of a galvanic cell. Therefore, the IR drop is always subtracted from the theoretical cell potential, that is,

$$E_{\text{cell}} = E_{\text{cathode}} - E_{\text{anode}} - IR \quad (1.12)$$

The equation 1.12 predicts that at constant electrode potentials, a linear relationship should exist between the cell voltage and the current. In fact, departures from linearity are often encountered and under these circumstances, the cell is said to be polarized. The polarization may arise at one or both electrodes.

The degree of polarization of electrode is measured by the overvoltage or overpotential η , which is the difference between the actual electrode potential E and the thermodynamic or equilibrium potential E_{eq} , where $E < E_{eq}$, but in the case of anodic polarisation this equation will be opposite ($E > E_{eq}$). It is important to realize that polarization always reduces the electrode potential for a system. The polarization is said to be anodic when the anodic processes on the electrode are accelerated by moving the potential in the positive (noble) direction or cathodic when the cathodic processes are accelerated by moving the potential in the negative (active) direction. There are three distinct types of polarization and these are additive, as expressed in Eq. (1.13):

$$\eta_{total} = \eta_{act} + \eta_{conc} + IR \quad (1.13)$$

where, i) η_{act} is the activation overpotential, a complex function describing the charge transfer kinetics of an electrochemical reaction. η_{act} is always present and the main polarization component at small polarization currents or voltages.

ii) η_{conc} is the concentration overpotential, a function describing the mass transport limitations associated with electrochemical processes. η_{conc} is dominant at larger polarization currents or voltages.

iii) IR is the ohmic drop. This function takes into account the electrolytic resistivity of an environment when the anodic and cathodic elements of a corrosion reaction are separated by this environment while still electrically coupled.

Electrochemical polarizations are divided into three main types.

a) Activation polarization

Activation polarization is usually the controlling factor during corrosion in strong acids since both η_{conc} and IR are relatively small. Activation polarization is caused by the resistance against the reaction itself at the metal-electrolyte interface. In other words activation polarization is caused by a slow electrode reaction because the reaction at the electrode requires activation energy. Both anodic and cathodic reactions can be under activation polarization. A reaction for which activation polarization dominates is referred to as activation controlled.

b) Concentration polarization

Concentration polarization is observed when the reaction rates are controlled by the diffusion of the specific species in the bulk electrolyte to the metal electrolyte interface. When a chemical species participating in a corrosion process is in short supply, the mass transport of that species to the corroding surface can become rate controlling. Concentration polarization usually predominates when the concentration of the active species is low; for example, in dilute acids or in aerated waters where the active component, dissolved oxygen, is only present at very low levels.

c) Ohmic polarization

Solutions of electrolytes have rather poor conductivity compared to metals, particularly in dilute solutions. In corrosion systems, if the metal surface is covered by paints or other films of insulating material or if the electrolyte surrounding the electrode has high resistance, it will give rise to a potential drop through either a portion of electrolyte or through the film on the metal surface or both, which is known as resistance polarization. If resistance polarization dominates a reaction, it is referred as resistance or IR controlled. The ohmic drop will become an extremely important factor when studying corrosion phenomena for which there is a clear separation of the anodic and cathodic corrosion sites, for example, crevice corrosion.

1.8 MIXED POTENTIAL THEORY

According to this theory (Wagner and Truad 1938), any electrochemical reaction can be divided into two or more oxidation and reduction reactions, and there can be no accumulation of electrical charge during the reaction. Two basic premises underlie mixed-potential theory. First, the anodic current in an electrochemical cell must equal the cathodic current. This is a requirement of the conservation of electrical charge. The number of electrons generated by the total of all oxidation reactions must be exactly equal to the number of electrons consumed by the total of all reduction reactions. Second, for the purpose of examination and definition of the electrochemical cell, the anodic (oxidation) and cathodic (reduction) reactions can be defined, written, and treated independently. Oxidation reactions occurring at the anode liberates electrons as given by equation (1.1) to (1.2). The mixed potential theory proposes that all the electrons generated by anodic reactions are consumed by corresponding reduction reactions. The more common cathodic reactions encountered in aqueous corrosion are given in equations (1.3) to (1.6).

During corrosion more than one anodic and more than one cathodic reaction may be operative. The mixed potential itself, which is commonly referred to as the corrosion potential (E_{corr}), is the potential at which the total rates of all the anodic reactions are equal to the total rates of all the cathodic reactions. The current density at E_{corr} is called the corrosion current density, i_{corr} , and is a measure of the corrosion rate. When a metal such as iron is corroding in an acid solution, both the half-cell reactions occur simultaneously on the surface.



The corrosion behaviour of iron in dilute mineral acid solution (HCl) can be taken to illustrate the importance of kinetic factor in determining the rate of corrosion. The

electrochemical characteristics of the system can be represented by the modified Evan's diagram schematically shown in Fig.1.4.

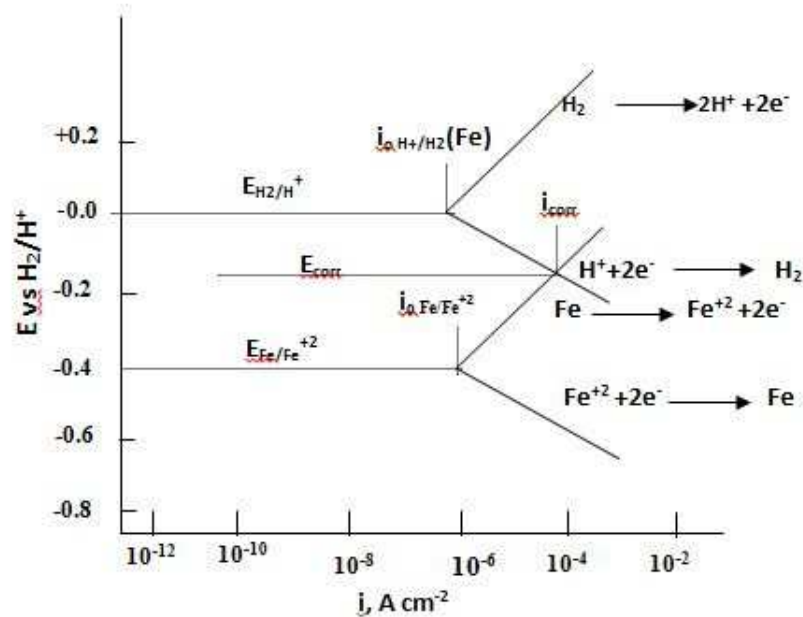


Fig. 1.4: Electrode kinetic behaviour of pure iron in acid solution (schematic).

Each electrode has its own half-cell electrode potential and exchange current density, as shown in Fig. 1.4. However, the two half-cell electrode potentials $E_{\text{Fe}/\text{Fe}^{2+}}$ and $E_{\text{H}^+/\text{H}_2}$ cannot coexist separately on an electrically conductive surface. Each must polarise or change potential to a common intermediate value, E_{corr} , (corrosion potential) which is also referred to as a mixed potential since it is a combination or mixture of the half-cell electrode potentials for reaction (1.14) and (1.15) (Jones 1996, Fontana 1987).

If an iron piece is dipped in HCl containing some ferrous ions, the electrode cannot remain at either of these two reversible potentials but must lie at some other potential. Iron is metallic and a good conductor of electricity and therefore the entire surface must be at a constant potential. The total rates of oxidation and reduction reactions are equal at the intersection of polarization curves for the two processes represented by E_{corr} . The rate of hydrogen evolution and the rate of iron dissolution will

be equal and this is expressed in terms of i_{corr} , corrosion current density. For most of the metals the corrosion current density of $1\mu\text{A}/\text{cm}^2$ will be equal to the corrosion rate of 0.025 mm y^{-1} .

1.9 ELECTROCHEMICAL CORROSION TESTING

Corrosion of metal occurs through electrochemical reactions at the metal-solution interface. Understanding the electrochemical phenomenon of a corrosion process will help to monitor and mitigate corrosion reaction. By using electrochemical methods, it is possible to monitor as well as understand the actual electrochemical process taking place on the metal surface. Unlike weight loss or gravimetric methods, electrochemical methods are fast in determining and analysing the electrochemical properties (Davis 2003, Robert 2003). The electrochemical methods used for this study are described in the following sub-sections.

1.9.1 DC Electrochemical monitoring techniques:

DC polarization test is a potential dynamic corrosion testing technique. When an electrode is polarized, it can cause current to flow via electrochemical reactions that occur at the electrode surface. The amount of current generated is controlled by the kinetics of the reactions and the diffusion of reactants both towards and away from the electrode. In a cell where an electrode undergoes uniform corrosion at open circuit, the open circuit potential is controlled by the equilibrium between the two different electrochemical reactions. One of the reactions generates cathodic current and the other anodic current. The open circuit potential is also the potential at which the cathodic and anodic currents are equal. It is referred to as a mixed potential. The value of the current for either of the reactions is known as the corrosion current. Mixed potential control also occurs in cells where the electrode is not corroding.

1.9.1.1 Tafel Polarization technique for estimating corrosion current (Fontana 1987, Jones 1996, Bardal 2004, Winston 2008)

The Tafel plots are generated by applying a potential of 250 mV in both the positive and negative directions from the open circuit potential against reference electrode. The current density is measured and usually plotted on a logarithmic scale. The corrosion potential (E_{corr}) and the corrosion current density (i_{corr}) are obtained from the Tafel plots. The corrosion potential (E_{corr}) or the open-circuit potential is the potential a metal will assume when placed in contact with a conductive medium. E_{corr} is a characteristic of the corroding system and is unrelated with the electrochemical instrumentation. The Tafel plot provides a direct measure of corrosion current, which can be used to calculate the corrosion rate.

A typical Tafel plot consists of an anodic and a cathodic branch, the intersection of these branches can be projected on the X and Y axes to get the i_{corr} and the E_{corr} values. Tangents are drawn to the anodic and cathodic regions of the Tafel curve, the intersection of these provide the values of E_{corr} and i_{corr} when projected on the corresponding axes. If the electrode potential is plotted against the logarithm of applied current density the plot as given in Fig 1.5 is obtained. The slopes of the linear portions of this plot are called the Tafel constants, which are used to calculate the polarization resistance using the Stern-Geary equation.

$$R_p = \frac{B}{i_{\text{corr}}} = \left(\frac{\Delta E}{\Delta i} \right) \Delta E \rightarrow 0 \quad (1.16)$$

where, i is the total current at a potential E , E_{corr} is the open circuit potential.

$$B = \frac{b_a b_c}{2.303(b_a + b_c)} \quad (1.17)$$

b_a & b_c are the Tafel proportionality constants for the anodic and the cathodic reactions; respectively. The corrosion rate is calculated using the following equation.

The corrosion rate (v_{corr}) can be expressed as (in mm y^{-1}):

$$\text{Corrosion rate } (v_{\text{corr}}) = K \frac{i_{\text{corr}}}{\rho} EW \quad (1.18)$$

where i_{corr} = corrosion current density in $\mu\text{A}/\text{cm}^2$

ρ = Density of corroding material in g/cm^3

EW = Equivalent weight of corroding material (atomic weight/oxidation number)

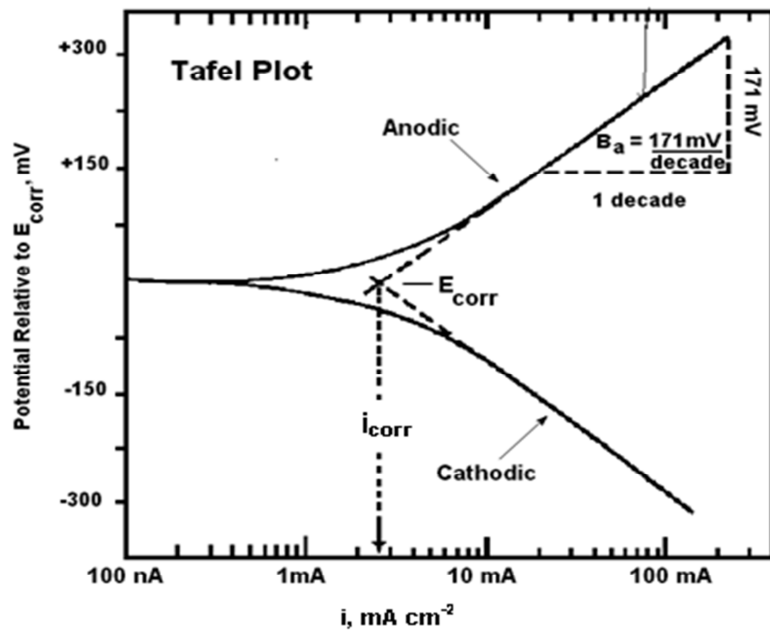


Fig. 1.5: Plot of the current density versus potential showing the extrapolation of the Tafel regions to the corrosion potential, E_{corr} to yield the corrosion current, i_{corr} .

It is usually assumed that the process of oxidation is uniform and does not occur selectively to any component of the alloy. Equivalent weight (EW) for alloys was calculated from following equation:

$$EW = \frac{1}{\sum \frac{n_i f_i}{W_i}} \quad (1.19)$$

where f_i is the mass fraction of the i^{th} element in the alloy, W_i is the atomic weight of the i^{th} element in the alloy and n_i is the valence of the i^{th} element of the alloy (Dean 1999).

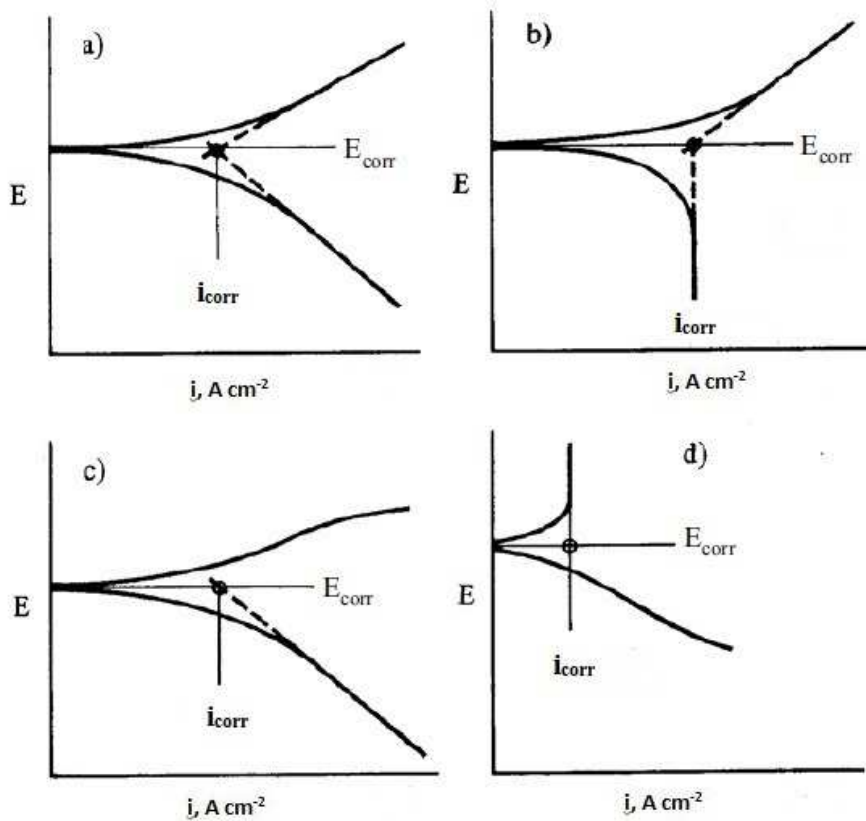


Fig. 1.6: Determination of corrosion current density by extrapolation of linear parts of the polarization curves. a) Both the cathodic and the anodic reaction are under activation control (the overvoltage curves are Tafel lines). b) The cathodic reaction is diffusion controlled and the anodic reaction activation controlled. c) The cathodic reaction is activation controlled, the anodic curve is irregular. d) The cathodic curve is irregular, the metal is passive, i.e. the corrosion current equals the passive current.

The intersection point between the extrapolated Tafel regions, in other words the overvoltage curves, gives the corrosion current. Unfortunately, the overvoltage curves are not always pure Tafel curves. But if either the anodic or the cathodic overvoltage curve

has a sufficiently long linear part around the corrosion potential, the necessary basis for the determination of corrosion rate is present: the linear part of the actual polarization curve can be extrapolated to the corrosion potential. Thus, the corrosion rate is determined regardless of the other polarization curve. In Fig. 1.6 four different cases are shown, in which the corrosion rate is determined by extrapolating linear parts of both or one of the polarization curves.

Advantages of Tafel polarization method:

- With this method it is possible to measure very low corrosion rates.
- It can be used, to continuously monitor corrosion rate of a system.
- This technique is more rapid than the conventional weight loss methods.
- The Tafel constants b_a and b_c can be used with linear polarization data.

Disadvantages of Tafel polarization method:

- This method can be applied only to systems containing one reduction process, since Tafel region is distorted if more than one reduction process occurs.
- To ensure reasonable accuracy, Tafel region must extend over a current range of at least one order of magnitude but this cannot be achieved because of interference from concentration polarization and other extraneous effects.
- Due to polarization of material under test by several hundred mV from corrosion potential, the system gets disturbed.

1.9.1.2 Linear polarization method (Fontana 1987, Jones 1996)

The main advantage linear polarization has over the Tafel polarization measurement method is its potential spectrum is so small, that it is essentially a non – destructive test. Consequently, linear polarization measurements can be repeatedly made

on the same test electrode, allowing it to be used for other applications. Over a small potential range (< 20 mV), it is observed that the applied current density is a linear function of the electrode potential. The applied potentials are more positive than the corrosion potential result in anodic current, whereas potentials that are more negative than the corrosion potential result in cathodic current to the specimen. At potentials that are further away from the corrosion potential, the linear relationship between potential and current is no longer obeyed. The usefulness of this measurement is that the slope of potential versus current plot, i.e., $\Delta E/\Delta i_{\text{app}}$. The relationship of the slope of the linear polarization curve to the corrosion current density, the anodic and the cathodic Tafel slopes are,

$$\frac{\Delta E}{\Delta i_{\text{app}}} = \frac{b_a b_c}{2.303 i_{\text{corr}} (b_a + b_c)} \quad (1.20)$$

where, $\Delta E/\Delta i_{\text{app}}$ is the slope of the linear portion of the curve, b_a and b_c is the anodic and cathodic slope and i_{corr} is the corrosion current density. The typical linear polarization graph is shown in the Fig. 1.7.

Advantages of linear polarization technique:

- The method permits rapid corrosion rate measurement and can be used to monitor corrosion rate in various process streams.
- It is used for measuring very low corrosion rates in nuclear, pharmaceutical and food processing industries, which are difficult and tedious to perform by conventional methods.
- This method is non-destructive since the potential applied to the sample is very small.

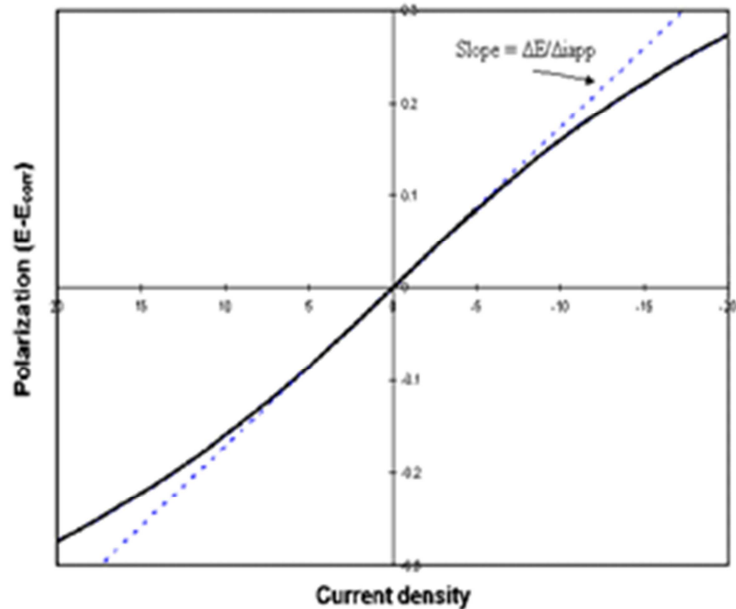


Fig. 1.7: Linear polarization curve

Disadvantages of linear polarization technique:

- The main demerit of this technique is that it needs Tafel data to calculate corrosion rate, which must be obtained either from literature or from other experiments.
- If solution resistance is very high, corrosion rates would be erroneously underestimated.

1.9.2 AC Electrochemical monitoring techniques:

1.9.2.1 Electrochemical Impedance Spectroscopy (EIS)

Electrochemical Impedance Spectroscopy (EIS) also known as AC impedance spectroscopy is a nondestructive electrochemical method that is used to evaluate the electrochemical properties of electrode and electrode/electrolyte interface. EIS has found its application in the field of electrochemistry due to the vital information that is extracted

about the electrode surface and the interfacial properties with an electrically conducting electrode. Corrosion is one such field where EIS plays a major role in analysing the kinetic properties and the mechanism. Knowing and understanding the basic electrochemical reactions at the electrode surface and electrode/electrolyte interface is the key factor in understanding the corrosion mechanisms and its properties. Electrochemical impedance is usually measured by applying an AC potential to an electrochemical cell and measuring the current through the cell. The data obtained is then modeled as equivalent electrical circuits and a variety of information like the charge transfer resistance, film capacitance, double layer capacitance, coating resistance, number of defects and life-time durability of the system can be obtained (Robert et al. 2003, Nestor 2004, Barsoukov and Macdonald 2005).

1.9.2.2 Principle of the EIS technique (Winston Revie 2000, Venkatasubramanian 2009, Gamry instruments 2009)

EIS is based on Ohm's law on electrical circuits which defines resistance as the ratio of voltage over current.

$$R = \frac{E}{I} \quad (1.21)$$

where, R is the resistance, I is the current through the resistor and E is the voltage across the resistor.

The ability of a conducting material to resist the flow of current in an electrical circuit is called resistance and the material is called a resistor. For ideal resistors, the resistance value is independent of frequency at all current and voltage values. Impedance is the general term similar to resistance and is used where complex behaviour of one or more electrical circuit elements exists. In EIS a small AC voltage (1-10 mV) is applied to the electrochemical system over a wide range of frequencies and the response to the input signal i.e., current, is measured. The response current signal usually has a phase difference with the applied potential signal. The change in output potential with phase

difference when an AC current is applied to a system is called overvoltage. When an electrochemical system is stimulated by a potential signal it causes various fundamental processes such as electron transfer within the electrode and at the electrode/electrolyte interface to and from, from a charged species. Each electrode / electrolyte interface will behave uniquely when the system is disturbed by an electrical signal. By measuring this unique transient response it is possible to extract various properties of that electrochemical system with a single measurement.

The rate of transfer of charged particles within the electrolyte, electrode and at electrode/electrolyte interface depends on the resistance of the electrolyte, electrode and on the rate of reaction at the interface. Surface structural defects, crystallographic orientation, inclusion of foreign species can also influence the local electric field. EIS always applies a small potential disturbance in order to maintain the pseudo linearity in the cell's response. For small electrical signals the response is always pseudo linear with a small change in phase between the applied and response signal.

Consider an AC sinusoidal potential signal as the input to the electrochemical system:

$$E = E_0 \sin(\omega t) \quad (1.22)$$

where, E is the potential at time t , E_0 is the amplitude of the signal. ω and t are radial frequency and time respectively. The response to the above sinusoidal potential signal will be a sinusoidal current signal which has the same frequency with different amplitude and a phase shift. It is given as

$$I = I_0 \sin(\omega t + \phi) \quad (1.23)$$

where, I_0 is the amplitude and I is the current response at time t with a phase change ϕ .

By applying Ohm's law on electrical circuits to the above input and response signal we can calculate the impedance as below.

$$Z = \frac{E}{I} \quad (1.24)$$

$$Z = \frac{E_0 \sin(\omega t)}{I_0 \sin(\omega t + \phi)} \quad (1.25)$$

$$Z = Z_0 \frac{\sin(\omega t)}{\sin(\omega t + \phi)} \quad (1.26)$$

where $Z_0 = E_0/I_0$ is the amplitude of the impedance.

By applying Euler's rule of complex functions for the above relation, it is possible to express impedance in the form of complex function with both real and imaginary parts as given below

$$Z = Z_0(\cos\phi + j \sin\phi) \quad (1.27)$$

The complex function is expressed in one or both of the two graphical representations called Bode and Nyquist plots. If the real part of the impedance is plotted against the imaginary part of the impedance on abscissa and ordinate axes, respectively, we get a Nyquist plot. From the Nyquist plot it is possible to extract few electrochemical parameters such as solution resistance, polarization resistance and total resistance. Also it is possible to determine the number of time constants involved in the electrochemical reaction by looking at the shape of the Nyquist plot. Each semicircle in the Nyquist plot is characteristic of a time constant involved in the electrochemical process. The impedance behaviour of an electrode may be expressed in Nyquist plots of $-Z''_{\text{img}}$ as a function of Z'_{re} as in Fig. 1.8.

A Nyquist plot does not show any frequency value although some definite frequency was used to get the impedance at each data point. To overcome this shortcoming, a Bode plot was developed to indicate exactly what frequency was used to create a data point. Thus a Bode plot is plotted with frequency on the abscissa axis and

the absolute value of impedance and the phase angle on the ordinate axes. A typical Bode plot is shown in Fig. 1.9.

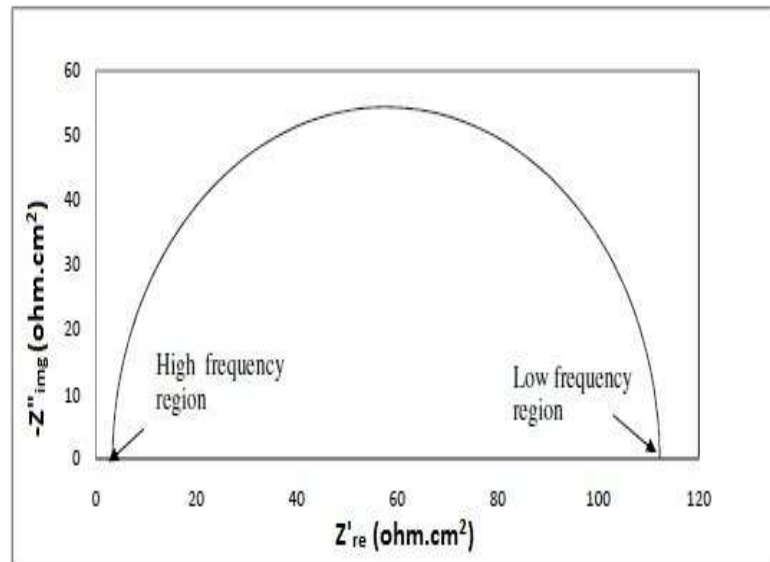


Fig. 1.8: Nyquist plot

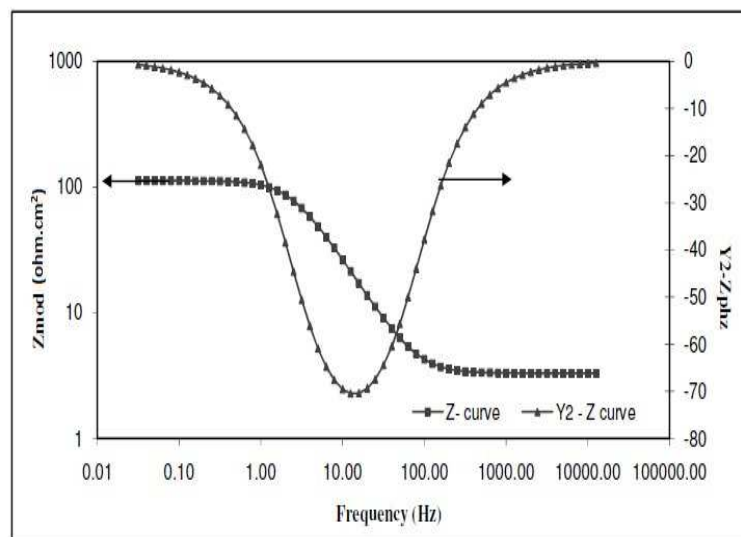


Fig. 1.9: Bode plot

From the Bode plot it is possible to read impedance with respect to frequency and also the involvement of capacitance and resistance in the electrochemical reaction from the phase angle and frequency.

1.9.2.3 Equivalent electric circuit models

The analysis of Nyquist and Bode plots from experimental data is done by fitting the experimental curves to an equivalent electrical circuit consisting of common electrical circuit elements such as resistors, capacitors, and inductors. These circuit elements should have some physical relationship to the electrochemical parameters of the reaction. For example a resistor can be used in places where there are possible conductive paths in the electrochemical reaction. Therefore electrochemical parameters such as solution resistance (between the reference electrode and the working electrode) and polarization resistance are represented by an equivalent resistor in the model circuit. Capacitors and inductors are used where there are possible space charge polarization region in the electrochemical process. The impedance of a capacitor has inverse relationship with frequency and the current through a capacitor leads the voltage across the capacitor by 90 degrees. These electric circuit elements are connected in a fashion that represents the actual electrochemical process taking place. Since electrical circuit models can be made in different configurations with different elements to give the same output, there could be more than one possible circuit model for a particular electrochemical reaction (Deepika 2003, Venkatasubramaniyan 2009, Gamry instruments 2009).

1.9.2.4 EIS modeling parameters (Stansbury 2000, Deepika 2003, Robert 2003, Nestor 2004)

While fitting the EIS data to electrical circuits, some important parameters need to be considered.

Electrolyte Resistance (R_s)

Electrolyte Resistance or Solution resistance is often a significant factor in the impedance of an electrochemical cell. A modern 3 electrode potentiostat compensates for

the solution resistance between the counter and reference electrodes. However, any solution resistance between the reference electrode and the working electrode must be considered when the system is modelled. The resistance of an ionic solution depends on the ionic concentration, type of ions, temperature and the geometry of the area in which current is carried. In a bounded area with area A and length l carrying a uniform current the resistance is defined as:

$$R = \rho \frac{l}{A} \quad (1.28)$$

Where, ρ is the resistivity of the solution.

Double Layer Capacitance (C_{dl})

An electrical double layer exists at the interface between an electrode and its surrounding electrolyte. This double layer is formed as ions from the solution stick on to the electrode surface. Charges in the electrode are separated from the charges of these ions. The separation is very small, of the order of angstroms. The value of the double layer capacitance depends on many variables including electrode potential, temperature, ionic concentrations, types of ions, oxide layers, electrode roughness, impurity adsorption, etc.

Charge Transfer Resistance (R_{ct})

The charge transfer resistance is formed by a single kinetically controlled electrochemical reaction. In this case, there is a single reaction at equilibrium. Consider a metal substrate in contact with an electrolyte. The metal molecules can electrolytically dissolve into the electrolyte, according to:



or more generally:



In the forward reaction in the first equation, electrons enter the metal and metal ions diffuse into the electrolyte. Charge is being transferred. This charge transfer reaction has a certain speed, which is dependent on the kind of reaction, the temperature, the concentration of the reaction products and the potential.

Film Capacitance (C_f) or coating capacitance

A capacitor is formed when two conducting plates are separated by a non-conducting media, called the dielectric. The value of the capacitance depends on the size of the plates, the distance between the plates and the properties of the dielectric. The relationship is:

$$C_{\text{dl}} = \frac{\epsilon^{\circ}\epsilon}{d}S \quad (1.31)$$

where d is the thickness of the film, S the surface of the electrode, ϵ° the permittivity of the air and ϵ is the local dielectric constant. Whereas the electrical permittivity is a physical constant, the relative electrical permittivity depends on the material.

1.10. METHODS TO CONTROL CORROSION

Corrosion is both costly and dangerous. Billions of dollars are spent annually for the replacement of corroded structures, machinery, and components, including metal roofing, condenser tubes, pipelines, and many other items. The corrosion can be better understood with the basic knowledge of electrochemistry and thereby a suitable and more appropriate corrosion control method could be developed. Understanding of the corrosion process in general and chemical reaction involved in particular leads to more information about corrosion control and prevention methods. It is the practical experience for many corrosion engineers that adoption of simple control methods has enhanced the service life

of a particular component, thereby finally increasing the life of the equipment (Davis 2003, Bardal 2004, Sastri et al. 2007, Pierre 2008).

The control methods listed below can be selected by understanding the corrosion process.

- Altering the nature of metal
- Changing the nature of environment of the metal
- Painting, electroplating, surface modification
- Neutralizing the corrosion agents of the environment
- Anodic and cathodic protection
- Alloying.
- Addition of inhibitors.

1.11 CORROSION INHIBITORS (Revie 2000, Davis 2003, Pierre 2008, Revie and Uhlig 2008)

An inhibitor is a substance, which when added in small concentrations to a corrosion environment decreases the corrosion rate. The inhibitors reduce the corrosion rate either by reducing the probability of its occurrence or by reducing the rate of attack or by doing both. Inhibitor forms thin film on the metal surface by adsorbing themselves. Inhibitors protect the metal surface from the attack of the constituents of environment. Corrosion inhibitors are widely used in the industry to control corrosion. They find major use in closed environment systems that have good circulation, so that an adequate and controlled concentration of inhibitor is ensured.

Inhibitors are used in a wide range of applications such as oil pipe lines, domestic central heating systems, industrial water cooling systems, acid pickling and metal extraction plants. Inhibitors are also commonly added to coolants, fuels, hydraulic fluids,

boiler water and many other fluids used in industry. Some of the most effective inorganic inhibitors are chromates, nitrites, silicates, carbonates, phosphates, and arsenates. There are plenty of organic inhibitors, they include amines, heterocyclic nitrogen compounds, sulphur compounds (such as thioethers, thioalcohols, thiourea, thiosemicarbazones), some natural compounds (such as glue, plant extracts, honey) and mixture of two or more compounds. An efficient inhibitor is compatible with the environment, is economical for application, and produces the desired effect when present in small concentrations.

A corrosion inhibitor may act in a number of ways:

- It may restrict the rate of the anodic process or the cathodic process by simply blocking active sites on the metal surface.
- It may act by increasing the potential of the metal surface so that the metal enters the passivation region where a natural oxide film forms.
- The mode of action of some inhibitors is that the inhibiting compound contributes to the formation of a thin layer on the surface, which stifles the corrosion process.

Inhibitors are often easy to use and offer the advantage of in-situ application without causing any significant disruption to the process. However, there are several considerations when choosing an inhibitor.

- Cost of the inhibitor can be sometimes very high when the material involved is expensive or when the amount needed is huge.
- Toxicity of the inhibitor can cause jeopardizing effects on human beings and other living species.
- Availability of the inhibitor will determine the selection. If the availability is low, the material is often expensive.
- Environmental friendliness.

A good inhibitor is selected based on the considerations of cost, toxicity, availability, environmental friendliness and green approach availability for the synthesis of environmental friendly inhibitors, etc.

1.11.1 Classification of corrosion inhibitors

Inhibitor selection is based on the metal and the environment. A qualitative classification of inhibitors is presented in Fig. 1.10. Inhibitors can be classified into environmental conditioners (Scavengers) and interface inhibitors (Revie 2000 and Davis 2003).

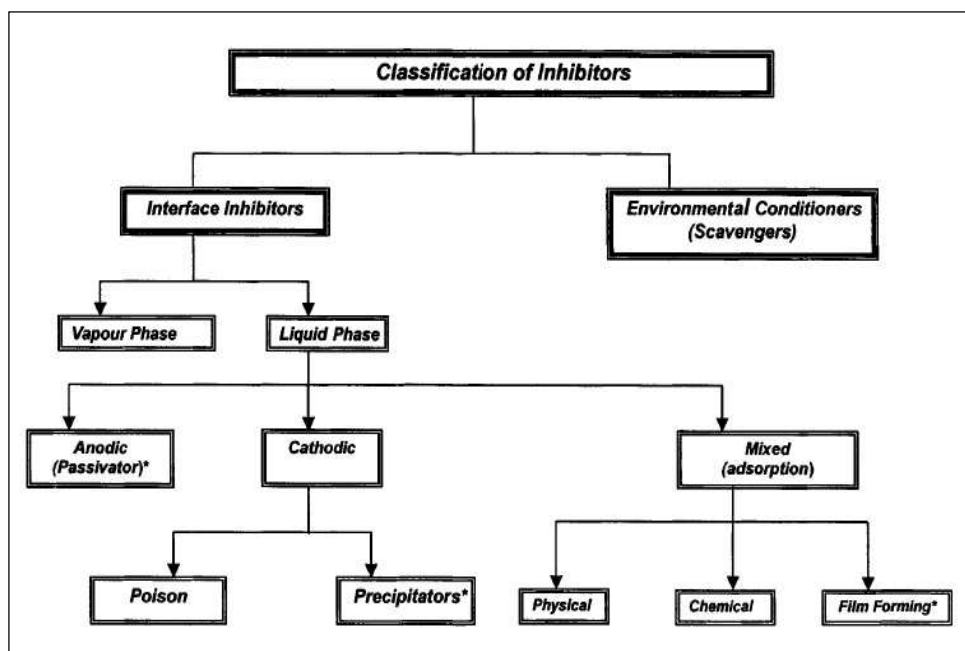


Fig 1.10: Classification of inhibitors

1.11.1.1 Environmental conditioners (Scavengers)

These substances act by removing corrosive agents from the solution. It is apparent that these inhibitors will work very effectively in solutions where oxygen reduction is the controlling cathodic reaction but will not be effective in strong acid solutions. Examples of this type of inhibitor are sodium sulphite and hydrazine, which remove dissolved oxygen from aqueous solutions as indicated in the following equations:



1.11.1.2 Interface inhibitors

Interface inhibitors control the corrosion by forming film at the metal/environment interface. Interface inhibitors can be classified into liquid and vapour phase inhibitors.

a) Liquid phase inhibitor

Liquid phase inhibitors are classified as anodic, cathodic and mixed inhibitors, depending on whether they inhibit anodic, cathodic or both electrochemical reactions.

Anodic (passivating) inhibitors

Anodic inhibitors are those substances which reduce the anodic reaction rate by acting on the anodic sites and polarize the anodic reaction. They displace the corrosion potential (E_{corr}) in the positive direction and reduces corrosion current (i_{corr}), there by retard anodic reaction and suppress the corrosion rate. Anodic inhibitors are generally effective in the pH range of 6.5 - 10.5 (near neutral to basic). Basically, oxyanions such as chromates, molybdates, tungstates and also sodium nitrite are very effective anodic inhibitors. Oxidation of metal is the reaction that occurs at anodic sites during corrosion. The anodic inhibitors combine with metal ions formed at the anodic region, forming the sparingly soluble respective salts. These compounds formed are deposited on the anodic sites forming the protective films, which acts as barrier between fresh metal surface and corrosive medium, thereby preventing further anodic reaction. Anodic inhibitors are found to be effective only when sufficient amount of the inhibitor is added into the corrosion medium. When concentration of an anodic inhibitor is not sufficient, corrosion may be accelerated rather than inhibited. The effect of anodic inhibitors on polarization curves is shown in Fig. 1.11 (a).

Cathodic inhibitors

These are the substances which reduce the cathodic reaction rate and polarize the cathodic reaction. They displace the corrosion potential in the negative direction and reduce corrosion current, there by retard cathodic reaction and suppress the corrosion rate. Cathodic inhibitors may divide into three categories viz. (i) those that absorb oxygen (deaerators or oxygen scavengers), (ii) those that reduce the area of cathode, and (iii) those that increase the hydrogen over potential of cathodic process. Cathodic inhibitors inhibit the hydrogen evolution in acidic solutions or the reduction of oxygen in neutral or alkaline solutions. It is also observed that the cathodic polarization curve is affected when a cathodic inhibitor is added to a system. Substances with high overpotential for hydrogen in acidic solutions and those that form insoluble products in alkaline solutions are generally effective cathodic inhibitors. Some examples of such inhibitors are inorganic phosphates, silicates or borates in alkaline solutions which inhibit the oxygen reduction at the cathodic sites. Substances such as carbonates of calcium and magnesium, due to limited solubility, block the cathodic sites. Cathodic inhibitors can provide inhibition by two different mechanisms: (1) as cathodic poisons, (2) as cathodic precipitators. The effect of cathodic inhibitors on polarization curves is shown in Fig. 1.11 (b).

Cathodic poisons:

The cathodic inhibitors which reduce corrosion by slowing the reduction reaction rate of the electrochemical corrosion are called cathodic poisons. The cathodic poisons such as sulphides and selenides are adsorbed on the metal surface whereas compounds of arsenic, bismuth and antimony are reduced at the cathode and form a metallic layer. They reduce the rate of hydrogen reduction. These inhibitors are effective in acid solutions but are ineffective in environments where other reduction processes such as oxygen reduction are the controlling cathodic reactions.

Cathodic precipitators:

The other types of cathodic inhibitors either slow the cathodic reaction by selectively precipitating on cathodic areas to increase the surface impedance and limit the diffusion of reducible species to these areas. For example calcium, magnesium and zinc ions precipitate as their respective hydroxides on cathodic sites.

Mixed inhibitors

About 80% of the inhibitors are organic compounds that cannot be designated specifically as anodic or cathodic inhibitors and are called mixed inhibitors. In these compounds the electron density distribution causes the molecules to be attracted to both anodic and cathodic sites. They are adsorbed onto the metal surface, forming a layer, which influences the electrochemical activity at both the anode and cathode. These inhibitors are more desirable because of their universal effect on the corrosion process equally or unequally, depending on the concentration of the inhibitor. The corrosion potential remains unaffected but the corrosion current density decreases. These inhibitors suppress the rate of both anodic and cathodic reactions by adsorption on the metal surface. The effect of mixed inhibitors on polarization curves is shown in Fig. 1.11 (c).

b) Vapour-phase inhibitor

These inhibitors have relatively high vapour pressures and that adsorb on the metal surfaces. They are organic compounds characterized by small vapour pressures from 0.013 to 66.66 Pa. They include inhibitors for steam and vapour zones in a closed system. On contact with metal surface, vapour of these inhibitors condenses and moisture hydrolyses it to liberate protective ions. Temporary protection against atmospheric corrosion, particularly in closed environments can be achieved using vapour-phase inhibitors (VPI). Substances having low but significant pressure of vapour with inhibiting properties are effective. The VPIs are used by impregnating wrapping paper or by placing them loosely inside a closed container. The slow vaporization of the inhibitor protects against air and moisture. In general, VPIs are more effective for ferrous than non-ferrous metals (Revie 2000, Banerjee 1985).

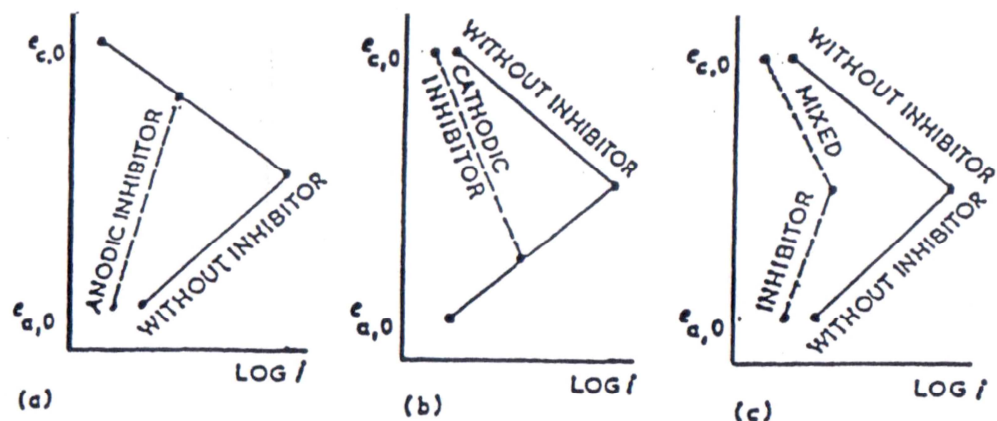


Fig. 1.11: Evans diagrams showing the effect of addition of a) anodic inhibitor, b) cathodic inhibitor, c) mixed inhibitor.

1.12 EXAMPLES OF CORROSION INHIBITORS (Jones 1996, Revie 2000, Bardal 2004, Philip 2007)

Application of corrosion inhibitors is the most economical and practical method to mitigate electrochemical corrosion. Several groups of organic compounds have been reported to exert inhibitive effects on the corrosion of Iron and Iron alloys. Inhibitors are rarely used as pure substances. They are usually mixtures. Commercial inhibitor packages contain, in addition to active inhibitor other chemicals like surfactants, deemulsifiers, carriers and biocides. The active ingredient of organic inhibitors invariably contain one or more functional groups containing one or more heteroatoms, N, O, S, P or Se through which the inhibitors anchor to the metal surface. Some common anchoring organic groups are given in the Table 1.1. These groups are attached to a parent chain (backbone), which increases the ability of the inhibitor molecule to cover a large surface area. The backbone may contain additional molecules, or substituent groups, to enhance

the electronic bonding strength of the anchoring group on the metal and/or to enhance the surface coverage.

Table 1.1: Common anchoring organic groups

Structure	Name	Structure	Name
-OH	Hydroxyl	-CONH ₂	Amide
-C≡C-	-yne	-SH	Thiol
-C-O-C-	Epoxy	-S-	Sulphide
-COOH	Carboxy	-S=O-	Sulphoxide
-C-N-C-	Amine	-C=S-	Thio
-NH ₂	Amino	-P=O	Phosphonium
-NH	Imino	-P-	Phospho
-NO ₂	Nitro	-As-	Arseno
-N=N-N-	Triazole	-Se-	Seleno

1.13 CORROSION INHIBITION MECHANISM

The primary event on the inhibiting action of a compound is adsorption. Thus it is very important to predict which substances will be adsorbed on a metal and at what potential region the adsorption will occur. If the adsorption is electrostatic in nature, then it will depend on the charge of the metal surface, that is the adsorbate, and the charge of the adsorbent, that is the inhibitor. Thus it is very important to know the electrical properties of both of the components participating in the process. Then it is possible to predict the type of the compounds which will be preferentially adsorbed on the metal surface at the corrosion potential. The effectiveness of organic inhibitor is related to the extent to which they adsorb and cover the metal surface. The extent of adsorption of an inhibitor depends on many factors such as the nature and the surface charge of the metal; the mode of adsorption of the inhibitor; the inhibitor's chemical structure; and the type of the aggressive solution. The presence of hetero atoms (oxygen, nitrogen, sulphur, and phosphorus), triple bonds, and aromatic rings in the inhibitor's chemical structure

enhances the adsorption process. It has been reported that the order of the inhibitor efficiency of heterocyclic organic compounds follows the sequence: oxygen < nitrogen < sulphur < phosphorus (Morad 1997, Abd El-Rehim 1999, Khaled 2004).

The zero charge potential ($\psi_{z.ch}$) is defined as the metal potential measured against the reference electrode under conditions of zero charge on the metal. At the zero charge potential the ionic double layer is absent at the electrode, At the zero charge potential an electrode is best able to adsorb substances dissolved in the electrolyte. The ability of an electrode to adsorb organic molecules is reduced in the presence of potential difference at the ionic double layer. This is because the field pulls in water molecules having high dielectric constant, dislodging organic molecules from the surface. Thus the adsorption capacity of an electrode is a maximum close to the zero charge potential. Antropove (1963) proposes a special scale of potential, the initial value of which is the zero charge potential of the surface $\psi_{z.ch}$. Then the potential ψ on this scale will be the difference between the steady state potential ψ_{st} of the electrode and the zero charge potential

$$\Psi = \psi_{st} - \psi_{z.ch} \quad (1.34)$$

For $\psi > 0$ the metal will be positively charged relative to the electrolyte. In this case a layer consisting primarily of anions will be adjacent to the metal surface on the side of the solution. For $\psi < 0$, the metal will be negatively charged relative to the solution; in this case the double layer on the side of the solution is made up of cations. Knowledge of the zero charge potentials of metals and the steady state potentials in a given medium can facilitate considerably the selection of suitable corrosion inhibitor. If the zero charge potential is higher than the steady state potential of the metal in a given electrolyte $\psi_{z.ch} > \psi_{st}$, the metal surface is negatively charged, then the adsorption of cations or positively charged colloid particles will be most likely. For $\psi_{z.ch} < \psi_{st}$, the metal surface is positively charged, the adsorption of anions and negatively charged colloid particles is most likely (Papavinas 2000, Abd El - Maksoud 2008).

Inhibitors protect the metal in three possible ways (Jones 1996, Revie 2000, Bardal 2004, Philip 2007)

- i) Physical adsorption
- ii) Chemical adsorption
- iii) Film formation

i) Physical adsorption

Physical (or electrostatic) adsorption is a result of electrostatic attraction between the inhibitor and the metal surface. The metal surface can be either positively charged or negatively charged. When a metal surface is positively charged negatively charged (anionic) inhibitor is adsorbed on the metal surface. Positively charged molecules acting in combination with a negatively charged intermediate can inhibit a positively charged metal. On the other hand, cationic species would not be adsorbed on a positively charged metal surface. Physically adsorbed species can be removed from the surface by physical force such as increased temperature and increased velocity.

Physical adsorption depends on

- Structural parameters, such as hydrocarbon chain length and the nature and position of substituent in aromatic ring.
- Electrical characteristics of inhibitors i.e. charge of the hydrophilic group.
- Type of ions present in the solution.
- Potential of the metal.

ii) Chemical adsorption

The most effective inhibitors are those that chemically adsorb (chemisorb), a process that involves charge sharing or charge transfer between the inhibitor molecules and the metal surface. Chemisorption takes place more slowly than physical adsorption.

This results in a strong binding of the inhibitors with the metal surface. As temperature increases, adsorption and inhibition also increase. This phenomenon is caused by sharing of charges or charge transfer between inhibitor species and the metal surface.

iii) Film formation

During the chemical adsorption adsorbed inhibitor molecules may undergo surface reactions producing films. The properties of films are dependent upon its thickness, composition, solubility temperature and other physical forces. Some adsorbed inhibitor molecules produce polymeric films. Corrosion protection increases markedly as the films grow from nearly two-dimensional adsorbed layers to three-dimension films up to several hundred angstroms thick. Inhibition is effective only when the films are adherent, are insoluble, and prevent access of the solution to the metal.

1.14 MARAGING STEELS

Maraging steel was developed in 1950s for applications requiring ultrahigh strength in combination with good fracture toughness. These alloys are low carbon steels that classically contain about 18 wt % Ni, substantial amounts of Co and Mo together with small additions of Ti. However, depending on the demands dedicated by the application, the composition of the material can be modified (Stiller et al. 1996). The initial development of these steels is attributed largely to the work by Bieber of Inco (International Nickel Company) in the late 1950s. This work resulted in the first two grades of maraging steel being introduced. These steels contained 20 per cent and 25 per cent nickel, respectively, with small additions of aluminum, titanium and niobium. Further development by Decker, Eash and Goldman illustrated the very effective hardening produced in Fe-Ni martensites by cobalt and molybdenum (Sha and Guo 2009). In the early 1960s various grades of 18Ni maraging steel (200, 250, 300) having cobalt and molybdenum were developed (Sagar et al. 2006). The name maraging derives from “martensite-aging,” referring to the heat treatment carried out to induce the precipitation of intermetallics in the Fe - Ni martensitic matrix, responsible for the

excellent mechanical properties (Menapace et al. 2010, Poornima et al. 2010). The strength of Fe-Ni alloys can be increased by the addition of cobalt and molybdenum, whereas alloying with aluminium and titanium forms intermetallics with other elements, in particular with Mo and Ni (Nayak 2004, Grum and Slabe 2006).

Maraging steels are a special class of ultrahigh strength steels that differ from other steels in that they are not hardened by carbon. In fact, carbon is considered as an impurity element in these steels and is kept as low as is commercially practicable. Instead of relying on carbide precipitation, these steels are hardened by the precipitation of intermetallic compounds. The absence of carbon in the steels confers significantly better hardenability, formability, and a combination of strength and toughness. A number of grades of maraging steels have been optimised to provide specific yield strength levels. The compositions of some common grades developed by International Nickel Ltd. (Inco) are shown in Table 1.2. Typically, these steels contain high levels of nickel, cobalt and molybdenum (Nayak 2004, Sha and Guo 2009).

Maraging steels are basically martensitic in structure in the solution annealed condition and in this condition are easily machined (Rohrbach and Schmidt 1990). It has been known that Fe-Ni alloys of 5-25% Ni transform from austenite to martensite when cooled to room temperature. However, the Fe-Ni martensite so formed, unlike the more familiar Fe-C martensite, is relatively soft and ductile. The strength of this basic system is increased primarily by addition of Co and Mo whilst Ti and Al form intermetallic compounds with other alloying elements, enabling age hardening to take place. Increasing Ti content progressively increases strength though toughness may be reduced. Hardening occurs by ageing this martensitic structure (hence the term maraging) at a temperature in the range of 450 °C to 500 °C. During aging heat treatment, high strength is achieved by precipitation of a high amount of intermetallic compounds (like Fe₂Mo, Ni₂Mo, Ni₃Mo, Ni₃Ti, Fe₇Mo, etc.; depending upon the alloying elements and aging treatment) dispersed in a carbonless martensitic matrix supersaturated with alloying elements.

Table 1.2: Nominal compositions (wt%) and the respective strength of commercial maraging steels (Inco).

Alloy designation	Ni	Mo	Co	Ti	Al	Y _s (MPa)
18Ni (200)	18	3.3	8.5	0.2	0.1	1400
18Ni (250)	18	5.0	8.5	0.4	0.1	1700
18Ni (300)	18	5.0	9.0	0.7	0.1	2000
18Ni (350)	18	4.2	12.5	1.6	0.1	2400
18Ni (cast)	17	4.6	10.0	0.3	0.1	1650

During this stage, the metastable martensite in the steels decomposes. Fortunately, the precipitation hardening occurs much more rapidly than the reversion reactions producing austenite and ferrite. Thus, substantial hardening can be produced before reversion occurs. Austenite reversion, or the prevention of it in most cases, is important to ageing, because austenite is a stable phase at room temperature for maraging steel compositions. The hardening alloying elements include titanium, vanadium, aluminium, beryllium, manganese, molybdenum, tungsten, niobium, tantalum, silicon and copper. When heat-treated, the alloy has very little dimensional change, so it is often machined to its final dimensions. They can be finely polished and easily fabricated. Nearly 30 grades of maraging steel including Ni-Cr, Ni-Co-Mo and Ni-Co-Mo-Cr type have been developed during past several years. Maraging steels generally contain less than 0.03% carbon, 5-25% Ni, 7-9% Co, 4.5-5% Mo, 0.1-1.4% Ti, 0.1-0.3% Al, 0.1-0.4% Nb, 0.1%Be, 0.1-0.2% Cu and W and V up to 6 % in special cases (Stiller et al. 1996, Pereloma et al. 2004, Sha and Guo 2009).

Maraging steels are characterized by a large number of alloying elements and, consequently, they are expensive materials compared with many other engineering alloys. The compositions shown in Table 1.1 may be compared with carbon steels with typically 0.04 – 1.7% C and 0.8% Mn. The resulting ultrahigh strength (Y_s) in maraging steels (the last column of Table 1.2, compared to standard yield strength grades of 275 and 355 MPa for carbon structural steels) is accompanied by a much higher cost in producing them.

The maraging alloy development is significantly influenced by the availability and price of the alloying elements. For instance, the development of a family of cobalt-free maraging steels in the late 1970s was solely due to the sharp rise in cobalt pricing. Although the manufacturing of maraging steels requires special processes, their ageing heat treatment is very simple, resulting in minimum distortion (Grum and Slabe 2006, Sha and Guo 2009).

The automobile manufacturers and corresponding component suppliers of all over the world have been looking for ultra-high-strength materials for weight reduction or other reasons, in which maraging steel with super-high strength can be considered as a new choice. Maraging steels have been extensively used in a variety of applications due to their attractive combination of properties such as high strength, moderate toughness and good weldability (Grum et al. 2006, Rao et al. 2009). Due to the low carbon content, maraging steels have good machinability. Maraging steels are iron alloys which are known for possessing superior strength and toughness without losing malleability, although they cannot hold a good cutting edge. They have higher modulus of elasticity and lower thermal expansion coefficient. Another important property is its better thermal conductivity, which reduces surface temperature during thermal loading and lowers thermal stresses (Klobcar et al. 2008). Over the past half a century, two major types of maraging steels have been developed (He et al. 2002c), the 18Ni maraging steels and the cobalt-free maraging steels. Between the two types, the 18Ni maraging steels are in a more advanced and mature stage of development and applications, with maximum strength levels reaching 2400 MPa accompanied by good toughness and ductility. However, these steels contain an expensive alloying element, cobalt, at levels as high as 8 – 13%. This keeps the steels rather expensive, preventing wider selection and application. Therefore, developing cobalt-free maraging steel with reduced quantities of expensive alloying elements in order to lower the production cost has been an important direction of maraging steels research. Over the past two decades, enormous advancement has been achieved in the development of cobalt-free maraging steels, to a strength level of 2000 MPa (He et al. 2002c).

1.14.1 Uses of maraging steel (Razek et al. 1997, Nayak 2004, Ohue et al. 2007, Nedjad et al. 2008, Poornima et al. 2010, Wang et al. 2010).

Maraging steels have been extensively used in a variety of applications due to their attractive combination of high strength, moderate toughness and good weldability (Menapace et al. 2010).

- ❖ Maraging steel's strength and malleability allows it to be formed into thinner rocket and missile skins, allowing more room for payload while still possessing sufficient strength for the application.
- ❖ Maraging steels are suited to engine component applications such as crankshafts and gears that work at 'warm' temperatures and the firing pins of automatic weapons that cycle from hot to cool repeatedly while under substantial loads and impacts.
- ❖ Their uniform expansion and easy machinability, carried out before aging makes maraging steel useful in high wear portions of assembly lines, as well as in the manufacture of dies.
- ❖ In sporting use, for the construction of bicycle frames, fencing blades and golf club heads.
- ❖ In surgical components and hypodermic syringes.
- ❖ Maraging steel is used in creating gas centrifuges for uranium enrichment, nuclear bomb casing due to its extremely high strength and balance. Nations importing maraging steel often find themselves receiving a great deal of attention (Nedjad et al. 2008).

1.14.2 Role of alloying elements in maraging steel

Nickel maraging steels have been extensively used in a variety of applications due to their attractive combination of high strength, moderate toughness and good weldability. Although Fe-Ni system, particularly at Fe-18 % Ni level, offered a number of technological advantages including moderately strong and very tough martensite on solution annealing, the negligible dimensional changes, insensitivity of the transformation product to cooling rate, etc., there was a need to strengthen the Fe-Ni martensite with various alloying elements to a level of engineering interests without affecting the toughness. The important alloying elements in the Fe based maraging steel are nickel, molybdenum, cobalt, titanium and aluminium. The residual elements should be kept as low as possible as they adversely affect the properties of maraging steels. Common residual elements present are carbon, sulphur, silicon, manganese, aluminium, hydrogen, oxygen and nitrogen (Gupta et al. 1996, Avadhani 2001, Nayak 2004). Table 1.3 gives the effect of alloying elements in maraging steel.

Table 1.3: Role of alloying elements in maraging steel.

Element	Effect
Ni	Fe-Ni martensite is quite tough and soft, is a well suited host for age hardenable elements. Nickel is also responsible for high toughness by promoting cross slip during deformation.
Mo	Increases strength by solid solution hardening. Forms intermetallic compounds Fe_2Mo , Ni_3Mo . Improves toughness by reducing grain boundary segregation.
Co	Enhances martensite formation by elevating $*M_s$ temperature. Reduces the solubility of Mo and increases volume fraction of precipitates.

Ti	Improves age hardening characteristics by forming Ni ₃ Ti precipitate.
Al	Elevates Ms temperature slightly. Increases strength by solid solution hardening and age hardening. Strong deoxidiser.
C	Ties up with Ti and Mo to form their respective carbides which reduce the strength as well as ductility
S	Forms, particularly in welds, low melting titanium sulphide promoting hot shortness.
Si	Lowers impact properties.
Mn	Lowers impact properties.
H	More than 3 ppm induces cracking tendency
O	Forms oxides and reduces ductility and toughness.
N	Forms nitrides and reduces ductility and toughness.

*M_s temperature is a temperature at which martensite starts to transform from austenite.

1.14.3 Weld aged maraging steel

Maraging steels exhibit superior combination properties including high specific strength, excellent fracture toughness and good weldability (Grum and Slabe 2006). For many of the applications of these steels, welding is the important means of fabrication. The unique property of being weldable in solutionised condition followed by a low temperature (480° C) post - weld maraging treatment makes these steel attractive for fabrication of large structures (Klobcar et al. 2008). Several welding process have been recommended for steels. Though with low heat input processes like electron beam

welding, high joint efficiencies can be achieved, in common practice, gas tungsten - arc welding [GTAW] is widely employed in view of the consistency of weld quality and overall economy. During welding the metal will be in liquid state (fusion zone) which will be subsequently cooled to room temperature. Hence the principal microstructure change in the weld fusion zone is transformation of austenite to martensite on cooling. It was reported by Shamantha et al. (2000) that the use of filler material similar in composition to the maraging steel base material results in segregation of alloying elements, particularly molybdenum and titanium, at the substrate boundaries in the weld fusion zone (Schnitzer et al. 2010).

During aging of the weld metal the well-known precipitation reaction occurs leading to hardening. It is generally believed that initial precipitation in an 18 Ni (250) steel at 480° C occurs as Ni₃Mo, which on prolonged aging is replaced by either Fe₂Mo or the σ phase. If the alloy additionally contains titanium as a supplemental hardener, the precipitation of Ni₃Ti is also possible; alternatively, a part of the titanium may be present in the molybdenum precipitate, i.e. as (Mo, Ti). Hardening of maraging steel takes place in two stages namely formation of martensitic structure during cooling and subsequent aging of martensite (Stiller et al. 1996). The hardness and the tensile strength increases with the progression of precipitation reaction. During ageing, sub microscopic domains enriched with alloying elements and intermetallics like NiAl, NiBe, NiMn, Ni₃Ti and Ni₃Al are formed. The material under investigation is weld - aged maraging steel. Its strength and resistance to extreme temperatures makes it a truly effective material in a wide range of atmospheres. After maraging steel has undergone heat treatment, it demonstrates excellent mechanical properties (Pereloma et al. 2004, Nayak 2004, Sha and Guo 2009).

1.15 LITERATURE REVIEW

1.15.1 Corrosion of maraging steels

The corrosion of maraging steel is of fundamental, academic and industrial concern that has received a considerable amount of attention. In most of the industries

like fertilizers & chemicals, oil refineries, nuclear power plants etc., the maraging steel is used for making containers, steam generators, liquid carrying pipes and so on. In steel and ferrous alloy industries, the hydrochloric acid is used as a pickling agent. Moisture, micro dust particles, acids & bases and other agents of the environment influence the extent of corrosion taking place in these industries. It is inevitable to expose the surface of the maraging steel to different industrial environments while in use. A search of the literature reveals only a few reports on the corrosion studies of 18 Ni 250 grade maraging steel, which is entirely in martensitic phase (Nayak 2004, Poornima et al. 2010).

According to available literature, atmospheric exposure of 18 Ni maraging steel leads to corrosion in a uniform manner and gets completely rust covered (Kirk et al. 1968). Pit depths tend to be shallower than in high strength steels (Dean 1965 and Copson 1965). Bellanger et al. (1996) have studied the effect of slightly acid pH with or without chloride in radioactive water on the corrosion of maraging steel and have reported that corrosion behaviour of maraging steel at the corrosion potential depends on pH and intermediates remaining on maraging steel surface in the active region, favouring the passivity. The effect of carbonate ions in slightly alkaline medium on the corrosion of maraging steel was studied by Bellanger (1994), and reported that the corrosion potential did not change with carbonate ions at constant pH. With carbonate ions and at a low scan rate, the break down trans passive potentials were displaced towards more positive potentials and the passive potential region was broader, while at a high scan rate these potentials are displaced towards more negative values. After the beginning of the reverse scans, the current was again positive. These suggested that the corrosion kinetics was not the same.

Maraging steels were found to be less susceptible to hydrogen embrittlement than common high strength steels owing to significantly low diffusion of hydrogen in them (Rezek et al. 1997). The corrosion rates of maraging steels in acid solutions such as sulphuric, hydrochloric, formic and stearic acid are substantial although lower than those of the low alloy high-strength steels. Polarization studies indicate that maraging steels

exhibit active - passive behaviour in 1.0 N and 0.1 N sulphuric acids. The corrosion potential, critical current density, primary passivation potential and passive current density are all affected by variations in aging treatment. The critical and passive current densities increase as the structure is varied from fully annealed to fully aged. Stress corrosion of maraging steel may also occur in acid environments (Dautovich 1976).

Poornima et al. (2010) have studied the corrosion behaviour of 18 Ni 250 grade maraging steel in a phosphoric acid medium and reported that the corrosion rate of the annealed sample is less than that of the aged sample. Similar observations also have been reported for the corrosion of 18 Ni 250 grade maraging steel in sulphuric acid medium. The corrosion rate for both maraging steel and the low alloy steels in sea water are similar initially, but from about 1 year onwards the maraging steels tend to corrode more slowly as indicated by (Kenyon et al. 1971). The corrosion rates for both low alloy and maraging steel increase with water velocity (Kirk et al. 1968). During sea water exposure the initial attack was confined to local anodic areas, whereas other areas (cathodic) remained almost free from attack, the later were covered with a calcareous deposit typical of cathodic areas in sea water exposure. In time, the anodic rust areas covered the entire surface (Dean et al. 1965). Polarization tests (Stavros et al. 1971) indicate that maraging steel does not exhibit passive behaviour in 3% NaCl, and that the polarization curves are unaffected by changes in heat treatment.

The corrosion rate of maraging steel in acid solutions such as sulphuric acid, hydrochloric acid formic acid and stearic acid are substantial. Polarization studies show that maraging steels exhibit active passive behaviour in 1.0 N and 0.1N H₂SO₄. Heat treatment affects corrosion rate. Critical and passive current densities increase as the structure is varied from fully annealed to fully aged (Data bulletin on 18%Ni maraging steel 1964). Investigations on electrochemical corrosion behaviour of 350 grade maraging steel in 1.0 N H₂SO₄, 1.0 N HCl and in artificial sea water showed passive behaviour in 1N H₂SO₄ but not in 1N HCl and in artificial sea water (Iqbal et al. 1993)

Nayak (2004) has studied corrosion behaviour of 18Ni 250 grade maraging steel in aqueous medium and reported that, the rate of corrosion decreases as pH increases and near neutral region corrosion rate is independent of pH, corrosion rate increases with increase in temperature, aged samples show higher rate of corrosion than annealed samples and mechanism of corrosion was found to be due to anodic dissolution at the grain boundary and pitting corrosion was also observed.

Literature is saturated with corrosion inhibitors for different metals and alloys. But very less work seems to be available regarding the corrosion inhibition of maraging steel.

1.15.2 Organic inhibitors for the corrosion inhibition of iron and iron alloys in aqueous media.

A large number of investigations were carried out using organic compounds as corrosion inhibitors for pure iron and iron alloys in various aqueous media. Organic inhibitors play a major role as they cover the maximum surface area of the metal. Hence small amount of the inhibitor is sufficient to cover the large surface area. However, limited literatures reported the corrosion inhibition of maraging steel. Some of the important inhibitors used for iron and iron alloys are given in Table 1.4.

1.4: Some important organic inhibitors studied for Iron and Iron alloys.

Inhibitor	Medium	Remarks	References
Hydrazide derivatives	Mild Steel in HCl	Langmuir adsorption isotherm	Shanbhag et al. 2008
3-Anilino-5-imino-4-phenyl-1,2,4-thiadiazoline	Mild steel in HCl	Mixed inhibitors	Quraishi and Sardar 2003

Thioacetamide, Thiourea and Thiobenzamide	Mild steel in H ₂ SO ₄	Thiobenzamide most efficient and thioacetamide the least inhibition efficiency	Ozacan and Dehri 2004
1,2,3-Benzotriazole	Stainless steel in H ₂ SO ₄	Physical interaction, Langmuir isotherm.	Satpati and Ravindran 2008
Zenthoxylum alatum plant extract	Mild steel in H ₃ PO ₄	XPS and FT-IR show inhibitor layer containing compounds present in plant extract, iron oxide and iron phosphate.	Gunasekaran and Chauhan 2004
Propargyl alcohol (PA)	Mild steel in H ₃ PO ₄	PA inhibits the cathodic corrosion reaction by adsorption onto steel surface via triple-bond carbon atoms.	Morad 1999
Methionine	Mild steel in H ₂ SO ₄	Temkin and modified Langmuir isotherm	Oguzie et al. 2007
4-Phynylazo-3-methyl-2-pyrazolon-5-one and its derivatives	C-steel in HCl	Frumkin's adsorption isotherm	Fouda et al. 2006

Benzimidazole derivatives	Mild steel in H_2SO_4	Both by physical and chemical adsorption.	Popova et al. 2003
2-Amino-4-(p-tolyl)thiazole (APT), 2-Methoxy-1,3-thiazole (MTT) Thiazole-4-carboxaldehyde (TCA)	Mild steel in H_2SO_4	Mixed inhibitor	Khaled and Mohammed 2009
2-Amino-5-phenyl-1,3,4-thiadiazole	Iron in H_2SO_4	Mixed inhibitor, Langmuir isotherm	Yongming et al. 2009
N-Alkyl quaternary ammonium salt	Carbon steel in H_2SO_4	Mixed inhibitor, Langmuir isotherm, both physical and chemical adsorption	Fuchs-Godec 2006
Triazole derivatives	Mild steel in H_3PO_4	Mixed type	Wang 2006
Imidazole derivatives	Mild steel in H_3PO_4	Flory-Huggins adsorption isotherm	Ghanbari et al. 2010
Methylthiourea (MTU), Phenylthiourea (PTU) and	Mild steel in H_2SO_4	Efficient at 30 °C, 40 °C and 50 °C	Dehri and Ozcan 2006

Thiobenzamide (TBA)			
N, N-Dipropoxy methyl amine trimethyl phosphonate	Iron in H ₂ SO ₄	Mixed inhibitor, Frumkin and Flory-Huggins isotherm	Tianbao Du et al. 2001
Polyacrylamide (PA)	Mild steel H ₂ SO ₄	El-Awady, chemisorptions mechanism, synergistic effect observed between PA and KI	Umoren et al. 2010
Natural honey	C-steel in highly saline water	Langmuir adsorption isotherm	El-Etre et al. 2000
2-Naphthalenesulfonic acid, 2,7-Naphthalenedisulfonic acid, 2-Naphthol-3,6-disulfonic acid	Iron in H ₂ SO ₄	Frumkin isotherm, physical as well as chemical adsorption.	Vracar and Drazic 2002
6-Benzylaminopurine	Cold rolled steel in H ₂ SO ₄	Mixed inhibitor, Temkin isotherm	Xianghong et al. 2009
1-Methyl- 3- pyridine- 2-	Mild steel in	Mixed inhibitor,	Hosseini and

yl-thiourea	H ₂ SO ₄	Langmuir isotherm	Azimi 2009
Sodium dodecylbenzenesulphonate (SDBS), Hexamethylenetetramine (HA)	Mild steel in H ₂ SO ₄	Adsorption of SDBS follows Frumkin isotherm, HA follows Langmuir isotherm	Hosseini et al. 2003
Barbituric acid, Thiobarbituric acid, 5,5-Diethylbarbituric acid sodium salt.	Mild steel in H ₃ PO ₄	Physical adsorption, Langmuir isotherm, addition of I-improved inhibition efficiency.	Muzaffer et al. 2008
Phenacyl dimethylsulfonium bromide and p-substituted derivatives.	Iron-base metallic glass alloy in H ₃ PO ₄	Mixed inhibitors, Hammet equation was used to correlate, inhibition efficiency and p-substitution.	Arab and Al-Turkustani 2006
2,5-Bis(n-pyridyl)-1,3,4-thiadiazoles	Mild steel in H ₂ SO ₄	Mixed inhibitor Langmuir isotherm	El-Azhar et al. 2001
Hexamethylpararosaniline chloride	Mild steel in H ₂ SO ₄	Adsorption of protonated inhibitor, Langmuir isotherm	Oguzie et al. 2008

Caffeic acid as green inhibitor	Iron in H_2SO_4	Chemisorption	De Souza and Spinelli et al. 2009
O- substituted anilines	Iron in in HCl	Langmuir adsorption isotherm	Khaled and Hackerman 2003
Quinol-2-thione	Mild steel in HCl	Langmuir adsorption isotherm	Prabhu et al. 2008
2 -Mercaptobenzimidazole	Mild steel in H_3PO_4	Langmuir behaviour was not observed suggesting that surface attachment is not due to simple chemisorption.	Wang 2001
2,3- Diphenylbenzoquinoxaline	Mild steel in H_2SO_4	Langmuir adsorption isotherm	Obot et al. 2010
Cefazolin	Mild steel in HCl	Langmuir adsorption model	Singh and Quraishi 2010
Thiourea	Mild steel in HCl	Langmuir adsorption model	Benali et al. 2009
Pyrrrole and	Ground	Mixed type inhibitors	Gopi et al.

Thienylcarbonyl benzotriazoles	water		2009
Lasianthera Africana	Mild steel in H ₂ SO ₄	Langmuir and Temkin adsorption models.	Eddy et al. 2009
Piperazine derivatives	Mild steel in HCl	Langmuir adsorption model	Ousslim et al. 2009
Thiadiazole derivatives	Mild steel in H ₂ SO ₄	Langmuir's adsorption	Fouda et al. 2009

Nayak (2004) has studied mercapto compound, 4-mercapto-8-trifluoromethyl quinoline as an inhibitor for 18Ni 250 grade maraging steel and reported an efficiency of 97.2% at 200 ppm concentration of inhibitor and inhibition efficiency was less for aged sample when compared to annealed sample. Inhibition behaviour follows Temkin's adsorption model.

The effect of 3, 4-dimethoxybenzaldehyde thiosemicarbazone in 0.5 M H₂SO₄ medium on corrosion of aged maraging steel was studied by Poornima et al. and reported good inhibitor efficiency.

Poornima et al. have studied effect diacetylmonoxime thiosemicarbazone on the corrosion of annealed 18 Ni 250 grade maraging steel in phosphoric acid solution, reported higher inhibition efficiency.

Poornima et al. (2012) have also studied Effect of 4-(N,N-diethylamino)benzaldehyde thiosemicarbazone on the corrosion of aged 18 Ni 250 grade

maraging steel in phosphoric acid solution. Inhibition behaviour follows Langmuir adsorption model.

1.16 SCOPE AND OBJECTIVES

Maraging steels have been extensively used in a variety of applications due to their attractive combination of properties such as high strength, moderate toughness and good weldability. Due to variety of applications maraging steel frequently come in contact with acid during cleaning, pickling, descaling, acidizing, etc. Hence studying their corrosion behaviour in acid medium and finding out a suitable corrosion inhibitor is of prime importance. A review of literature has revealed large number of corrosion inhibitors for various metals and alloys. But very less study appears to be done in the area of corrosion behaviour and corrosion inhibition of weld aged maraging steel. So it is planned specifically to study the corrosion behaviour of weld aged maraging steel in a medium of hydrochloric acid and sulphuric acid and then use suitable inhibitors having necessary structural requirements of a good inhibitor.

The objectives of the research work are listed as under:

- Investigation of the corrosion behaviour of 18% Ni M 250 grade maraging steel under weld aged condition in hydrochloric acid and sulphuric acid media of different concentrations at different temperatures.
- Investigation of the corrosion inhibition performance of some organic compounds on the corrosion of the weld aged maraging steel in hydrochloric acid and sulphuric acid media.
- Investigation of the effect of parameters such as acid concentration, temperature and inhibitor concentration on the inhibition efficiency.
- Evaluation of the activation parameters of corrosion reaction in the presence of inhibitors.

- Evaluation of the thermodynamic parameters for the adsorption of inhibitor molecules on the surface of the alloys and to arrive at the type of adsorption of the inhibitor molecules in the alloy surface.

1.17 OUTLINE OF THE THESIS

The present investigation has been documented in the thesis under 4 different chapters. **Chapter 1** includes the introduction to, corrosion, theoretical concepts of electrochemistry of corrosion, corrosion rate measurement techniques, corrosion inhibitors, maraging steels and the literature survey on the corrosion and corrosion inhibition of maraging steel. The chapter also explains the scope and objectives of the study.

In **Chapter 2**, the materials, medium, inhibitors, methods and calculation of various corrosion parameters, used for the present investigation have been discussed.

Chapter 3 presents the results and discussion on the work carried out. The results of investigation on the corrosion behaviour of weld aged maraging steel in hydrochloric acid medium and sulphuric acid medium have been discussed in section 3.1 and 3.2, respectively. The sections 3.3 – 3.12 describe the inhibition effect of the five compounds, ATPI, CPOB, CPOM, DNPH and DDPM on the corrosion of weld aged maraging steel in the hydrochloric acid medium and sulphuric acid medium. The effect of temperature, concentration of the medium, and concentration of the inhibitor on the inhibition efficiency is discussed in the chapter. The type of adsorption and mechanism of inhibition in each case is explained in the chapter.

Chapter 4 summarizes the work included in the thesis and also lists the conclusions drawn on the basis of experimental evidences and discussions.

CHAPTER 2

MATERIALS AND METHODS

2.1 MATERIALS

2.1.1 18 % Ni M250 grade maraging steel

The 18 % Ni M250 grade maraging steel samples in different conditions were obtained from National Institute of Interdisciplinary Science and Technology (NIIST), Thiruvananthapuram. The composition of the maraging steel used in the present investigation is given in Table 2.1.

Table 2.1: Composition of 18 % Ni M250 grade maraging steel (weight %).

Element	Composition	Element	Composition
C	0.015%	Ti	0.3-0.6%
Ni	17-19%	Al	0.005-0.15%
Mo	4.6-5.2%	Mn	0.1%
Co	7-8.5%	P	0.01%
Si	0.1%	S	0.01%
O	30 ppm	N	30 ppm
H	2.0 ppm	Fe	Balance

2.1.2 Material Conditions

Investigations were carried out on maraging steel (18% Ni M250 grade) specimen under weld aged condition. The maraging steel plates of composition as mentioned in Table 2.1 were welded by GTAW-DCSP, with 5 passes using filler material of composition as given in Table 2.2. The weld specimens were taken from the all weld regions of the weld maraging steel. The specimen was taken from the plates which were welded as per above and aged at 480 ± 5 °C for three hours followed by air cooling.

Table 2.2: Composition of the filler material used for welding (% by weight)

Element	Composition	Element	Composition
C	0.015%	Ti	0.015%
Ni	17%	Al	0.4%
Mo	2.55%	Mn	0.1%
Co	12%	Si	0.1%
Fe	Balance		

2.1.3 Material preparation

Cylindrical test coupons were cut from the plate and sealed with epoxy resin in such a way that, the area exposed to the medium was constant (0.64 cm^2). These coupons were polished as per standard metallographic practice, belt grinding followed by polishing on emery papers of 180, 400, 600, 800, 1000, 1200, 1500 and 2000 grades, finally on polishing wheel using levigated alumina to obtain mirror finish. It was then degreased with acetone, washed with double distilled water and dried before immersing in the corrosion medium.

2.2 MEDIA

The media used for the investigation were standard hydrochloric acid and sulphuric acid at five levels of concentrations. Experiments were carried out at temperatures 30°C , 35°C , 40°C , 45°C and 50°C ($\pm 0.5^\circ\text{C}$) using calibrated thermostat.

2.2.1 Preparation of standard hydrochloric acid solution

A stock solution of hydrochloric acid was prepared by diluting a known volume of 37 % analar grade hydrochloric acid to an appropriate volume. The solution was standardized by titrimetry. Solutions of different concentrations (0.1 M, 0.5 M, 1.0 M, 1.5 M and 2.0 M) were prepared by the appropriate dilution of the stock solution.

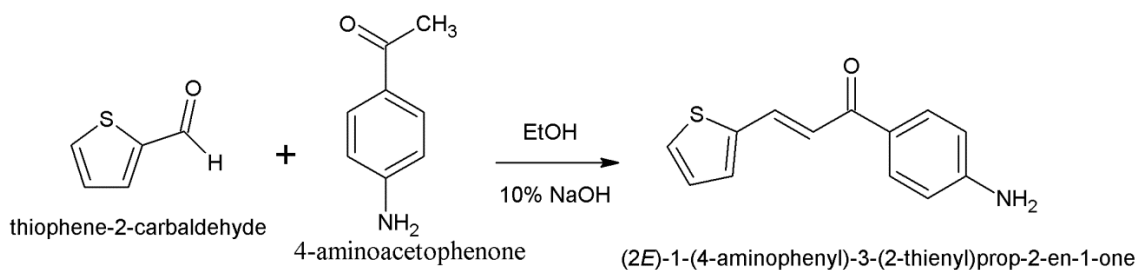
2.2.2 Preparation of standard sulphuric acid solution

A stock solution of sulphuric acid was prepared by diluting a known volume of 98 % analar grade sulphuric acid to an appropriate volume. The solution was standardized by titrimetry. Solutions of different concentrations (0.1 M, 0.5 M, 1.0 M, 1.5 M and 2.0 M) were prepared by the appropriate dilution of the stock solution.

2.3 INHIBITORS

2.3.1 Synthesis of 1(2E)-1-(4-aminophenyl)-3-(2-thienyl)prop-2-en-1-one (ATPI)

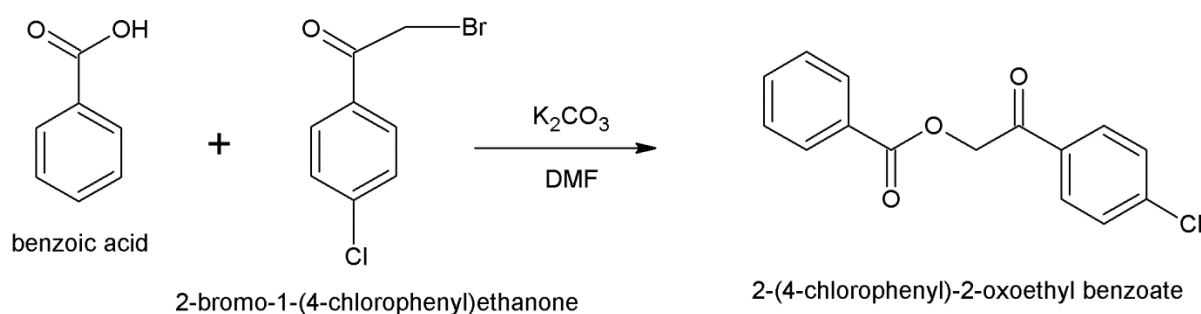
The inhibitor 1(2E)-1-(4-aminophenyl)-3-(2-thienyl) prop-2-en-1-one (ATPI) was synthesized as per the reported procedure (Hoong-Kun et al. 2009) in one-step reaction of 4-aminoacetophenone (0.40 g, 3 mmol) with thiophene-2-carboxaldehyde (0.28 ml, 3 mmol) in ethanol (30 ml) in the presence of 10% NaOH (aq) (5 ml). The reaction mixture was stirred for 2 hr at room temperature. The resulting yellow solid was collected by filtration, washed with distilled water and dried. The product was purified by recrystallization from acetone and was identified by melting point (105 – 106 °C), elemental analysis and infrared spectra. The molecular weight of the compound is 229.29. The synthesis scheme is given below.



2.3.2 Synthesis of 2-(4-chlorophenyl)-2-oxoethyl benzoate (CPOB)

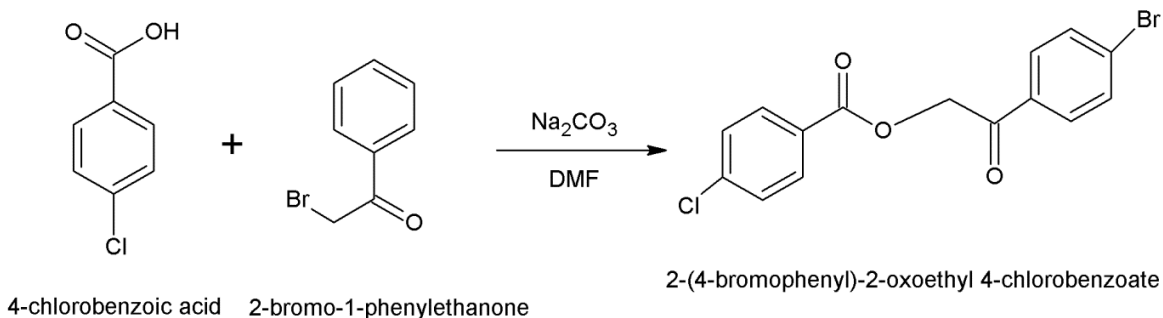
The inhibitor CPOB was synthesized as reported in the literature (Fun et al. 2011). A mixture of benzoic acid (1.0 g, 0.0081 mol), potassium carbonate (1.23 g, 0.0089 mol) and 2-bromo-1-(4-chlorophenyl) ethanone (1.81 g, 0.0081 mol) in

dimethylformamide (10 ml) was stirred at room temperature for 2h. On cooling, colorless needle-shaped crystals of 2-(4-chlorophenyl)-2-oxoethyl benzoate began to separate out. The crude product was filtered off and re-crystallized from ethanol. The product was characterized by elemental analyses, melting point (119-120 °C) and infrared spectra (Fun et al. 2010). The synthesis scheme is shown below.



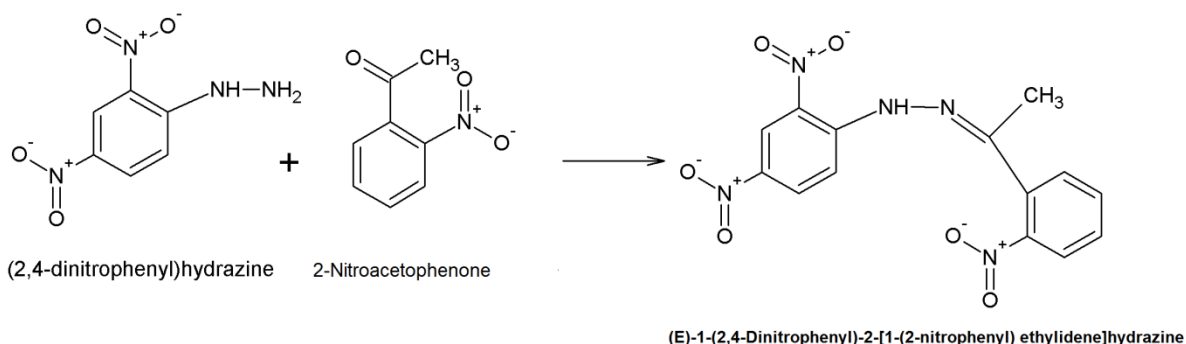
2.3.3 Synthesis of 2-(4-bromophenyl)-2-oxoethyl 4-chlorobenzoate (CPOM)

The inhibitor 2-(4-bromophenyl)-2-oxoethyl 4-chlorobenzoate (CPOM) was synthesized as per the reported procedure (Fun et al. 2011). A mixture of 4-chlorobenzoic acid (1.0 g, 0.0063 mol), sodium carbonate (0.744 g, 0.0070 mol) and 2-bromo-1-phenylethanone (1.94 g, 0.0070 mol) in dimethylformamide (10 ml) was stirred at room temperature for 2 h. On cooling, colourless needle-shaped crystals of 2-(4-bromophenyl)-2-oxoethyl 4-chlorobenzoate separated. The product was collected by filtration. The product was purified by recrystallization from ethanol and was identified by melting point (127 – 128 °C), elemental analysis and infrared spectra. The molecular weight of the compound is 353.59 (Fun et al. 2011). The synthesis scheme is given below.



2.3.4 Synthesis of (E)-1-(2,4-dinitrophenyl)-2-[1-(2-nitrophenyl) ethylidene] hydrazine (DNPH)

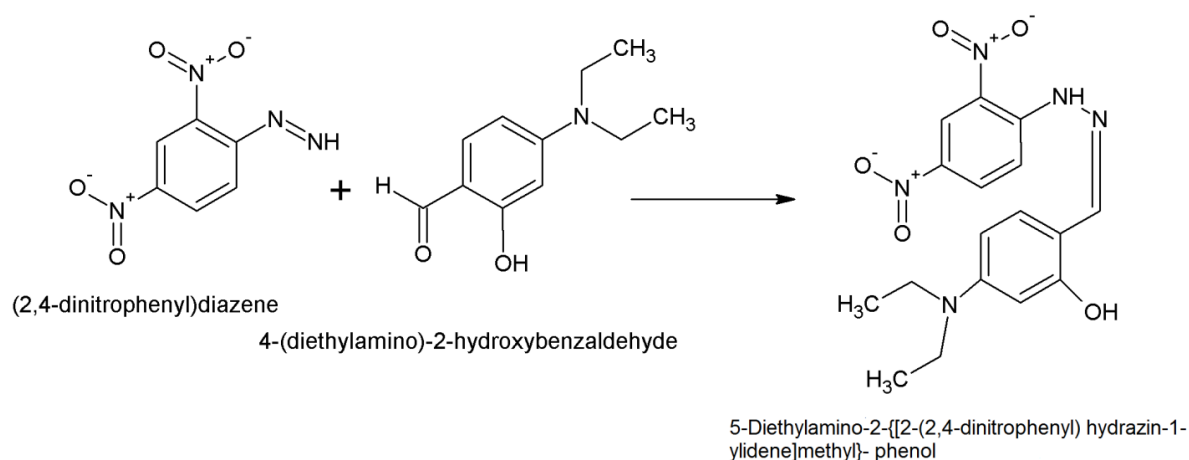
The title compound was synthesized by dissolving 2,4-dinitrophenylhydrazine (0.40 g, 2 mmol) in ethanol (10.00 ml), and H_2SO_4 (98%, 0.50 ml) was slowly added with stirring. 2 Nitroacetophenone (0.27 ml, 2 mmol) was then added to the solution with continuous stirring. The solution was refluxed for 1 h yielding a yellow solid, which was filtered off and washed with methanol. Yellow block-shaped single crystals of the title compound were recrystallized from ethanol by slow evaporation of the solvent at room temperature over several days. M.p. 170 - 171 °C (Nilwanna et al. 2011).



2.3.5 Synthesis of 5-diethylamino-2-[[2-(2,4-dinitrophenyl) hydrazin-1-ethylidene]methyl]- phenol (DDPM)

2,4-dinitrophenylhydrazine (1 mmol, 0.198 g) was dissolved in anhydrous ethanol (10 ml), H_2SO_4 (98%, 0.5 ml) was then added and the mixture was stirred for several

minutes at 78 °C, 4-(Diethylamino)-2-hydroxybenzaldehyde (1 mmol, 0.193 g) in ethanol (10 mm l) was added drop wise and the mixture was stirred at refluxing temperature for 2 h. The product was purified by recrystallization from DMF and was identified by melting point (127 – 128 °C), elemental analysis and infrared spectra. The molecular weight of the compound is 373.37 (Lin et al. 2011). The synthesis scheme is given below.



2.4 METHODS

Electrochemical measurements were carried out using an electrochemical workstation, Gill AC having ACM instrument Version 5 software. A three electrode compartment cell was used for the electrochemical measurements. The working electrode was made of weld aged maraging steel. A saturated calomel electrode (SCE) and a platinum electrode were used as the reference and the counter electrode, respectively. Electrode potentials were measured with respect to saturated calomel electrode (SCE).

2.4.1 Potentiodynamic polarisation measurements

Finely polished maraging steel specimens were exposed to corrosion medium of hydrochloric acid and sulphuric acid in the presence and absence of studied inhibitors at temperatures 30 °C, 35 °C, 40 °C, 45 °C, 50 °C and allowed to establish a steady state open

circuit potential. The potentiodynamic current-potential curves were recorded by polarizing the specimen to -250 mV cathodically and +250 mV anodically with respect to open circuit potential (OCP) at a scan rate of 1 mV s^{-1} . Electrochemical polarisation parameters were evaluated from the Tafel plots.

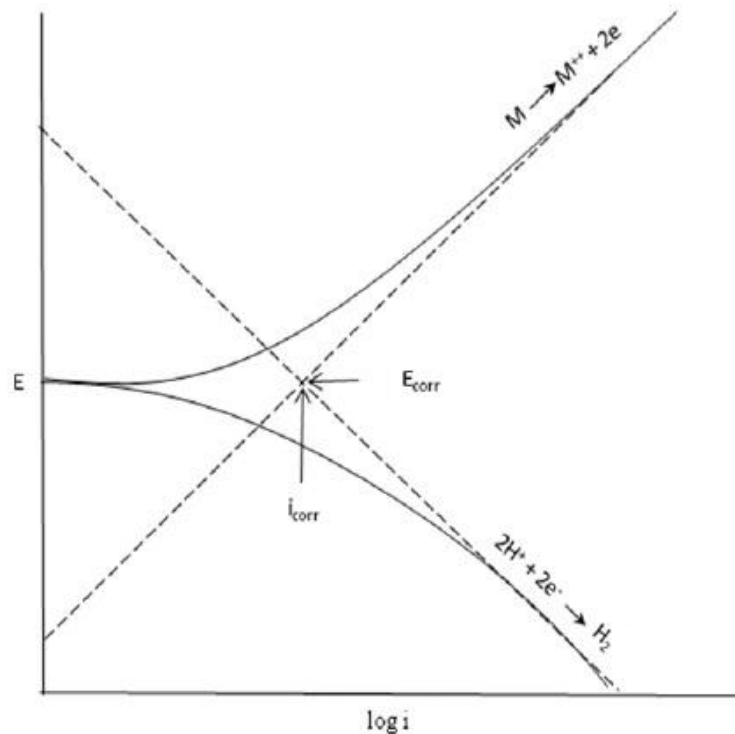


Fig 2.1: Polarization behavior of a metal in acid solution

In the Fig. 2.1 the total anodic and cathodic polarization curves corresponding to hydrogen evolution and metal dissolution are superimposed as dotted lines. It can be seen that at relatively high-applied current densities, the applied current density and that corresponding to hydrogen evolution have become virtually identical. To determine the corrosion rate from such polarization measurements, the Tafel region is extrapolated to the corrosion potential, as shown in Fig. 2.1. Extrapolation of cathodic and anodic Tafel slopes back to the corrosion potential (E_{corr}) are shown. Intersection point corresponds to

corrosion current density (i_{corr}), from which corrosion rate is calculated. At least one decade of linearity in Tafel extrapolation is desirable to ensure good accuracy. At the corrosion potential, E_{corr} , rate of cathodic reduction is equal to rate of anodic reaction (metal corrosion). Tafel constants (b_a and b_c) are calculated from the anodic and cathodic slopes.

Potentiodynamic polarisation parameters were extracted by Tafel fitment method. At first the Tafel ruler tool was selected, which was inbuilt in the instrument data analysis software. The rulers were kept on the Tafel plot and adjusted in such a way that rulers should overlap both anodic and cathodic slopes, and central line of the ruler should coincide with the rest potential. Auto scale function re-scales the graph to the maximum scaling. The quality of the fitting is judged by how well the Tafel rulers overlap the Tafel slope.

In all the above measurements, at least three similar results were considered, and their average values are reported. The deviations from mean of test results obtained under reproducibility conditions are also included.

2.4.2 Electrochemical impedance spectroscopy (EIS) studies

In EIS technique, a small amplitude ac signal of 10 mV was applied to the electrochemical system over a wide range of frequencies (10 kHz to 0.01 Hz) at the OCP and the response to the input signal was measured. The double-layer capacitance (C_{dl}), the charge-transfer resistance (R_{ct}), film capacitance (C_f) and film resistance (R_f) were calculated from the Nyquist plot.

In EIS studies data were analysed using Nyquist plots. The EIS instrument records the real (resistance) and imaginary (capacitance) components of the impedance response of the system. Depending upon the shape of the EIS spectrum, a circuit model or circuit description code and initial circuit parameters were assumed and input by the operator. The value of R_{ct} was extracted from the diameter of semi-circular Nyquist plots. Circle fit is the specific method to analyse Nyquist graphs. At first the cursor tool was

selected, which was inbuilt in the instrument data analysis software and the cursors were kept on the arc of the semicircle. Then the circle fit was done by using the mouse pointer as the third point of the circle, adjusting it until the circle best fits the data and by clicking the mouse button the results were calculated. The quality of the fitting is judged by how well the fitting curve overlaps the original spectrum. By fitting the EIS data it is possible to obtain a set of parameters which can be correlated with the corrosion of the alloy substrate.

In all the above measurements, at least three similar results were considered, and their average values are reported. The deviations from mean of test results obtained under reproducibility conditions are also included. The circuit fitment was done by ZSimpWin software of version 3.21, the best fit was obtained within in the error range of 4 - 5.5%.

2.4.3 Scanning electron microscopic (SEM) studies and EDS analysis

The scanning electron microscopic images and EDS spectra of the samples were recorded using JEOL JSM-6380L Analytical scanning electron microscope. The surface morphology of the weld aged maraging steel specimen immersed in hydrochloric acid and sulphuric acid solution in the presence and absence of inhibitor were compared by recording the SEM images of the samples. Energy dispersive X-ray spectroscopy (EDS) investigations were carried out in order to identify the elemental composition of the species formed on the metal surface after its immersion in acid in the presence and absence of inhibitor.

2.5 CALCULATION OF CORROSION RATE

The corrosion rates (v_{corr}), in mm y^{-1} , were calculated from the values of corrosion current density (i_{corr}) using the expression 1.18 given in section 1.9 (Dean 1999).

$$\text{Corrosion rate } (v_{\text{corr}}) = K \frac{i_{\text{corr}}}{\rho} EW \quad (1.18)$$

where K is 3.27×10^{-3} , $\text{mm g}/\mu\text{A cm y}$, a constant that defines the unit for the corrosion

rate, i_{corr} is current density in A cm^{-2} , ρ density is in g cm^{-3} and EW is equivalent weight of the alloy. Equivalent weight for alloys was calculated using expression 1.19 given in section 1.9 (Dean 1999):

$$EW = \frac{1}{\sum \frac{n_i f_i}{W_i}} \quad (1.19)$$

where f_i is the mass fraction of the i^{th} element in the alloy, W_i is the atomic weight of the i^{th} element in the alloy and n_i is the valence of the i^{th} element of the alloy (Dean 1999).

2.6 CALCULATION OF INHIBITION EFFICIENCY

From the Tafel polarisation study, the inhibition efficiency of the inhibitor was determined from the i_{corr} value using following equation (2.1).

$$\eta(\%) = \frac{i_{\text{corr}} - i_{\text{corr(inh)}}}{i_{\text{corr}}} \times 100 \quad (2.1)$$

where i_{corr} and $i_{\text{corr(inh)}}$ signify the corrosion current density in the absence and presence of inhibitors, respectively.

From the EIS study, the inhibition efficiency of the inhibitor was determined from the R_{ct} value using following equation (2.2).

$$\eta(\%) = \frac{R_{\text{ct(inh)}} - R_{\text{ct}}}{R_{\text{ct(inh)}}} \times 100 \quad (2.2)$$

where $R_{\text{ct(inh)}}$ and R_{ct} are the charge-transfer resistances obtained in inhibited and uninhibited solutions, respectively.

The surface coverage (θ) was calculated from potentiodynamic polarization data using the equation (2.3).

$$\theta = \frac{\eta(\%)}{100} \quad (2.3)$$

where η (%) is the percentage inhibition efficiency.

2.7 ACTIVATION PARAMETERS

Activation parameters such as activation energy (E_a), enthalpy of activation (ΔH^\ddagger) and entropy of activation (ΔS^\ddagger) for the corrosion of the metal in the studied acid media in the absence and presence of different concentrations of inhibitors were calculated from Arrhenius equation and transition state theory equation.

Arrhenius equation:

$$\ln(v_{\text{corr}}) = B - \frac{E_a}{RT} \quad (2.4)$$

where B is a constant which depends on the metal type and R is the universal gas constant, v_{corr} is corrosion rate, E_a is the activation energy, T is absolute temperature. The plot of $\ln(v_{\text{corr}})$ versus reciprocal of absolute temperature ($1/T$) gives a straight line with slope = $-E_a / R$, from which, the activation energy values for the corrosion process were calculated.

$$\text{Slope} = \frac{-E_a}{R} \quad (2.5)$$

Transition state theory equation:

The entropy of activation (ΔS^\ddagger) and enthalpy of activation (ΔH^\ddagger) for the corrosion of alloy were calculated from the transition state theory Equation.

$$v_{\text{corr}} = \frac{RT}{Nh} \exp\left(\frac{\Delta S^\ddagger}{R}\right) \exp\left(\frac{-\Delta H^\ddagger}{R}\right) \quad (2.6)$$

where h is Plank's constant, and N is Avagadro's number. A plot of $\ln(v_{\text{corr}}/T)$ vs $1/T$ gives straight line with slope given by equation (2.7) and intercept given by equation (2.8).

$$\text{Slope} = \frac{-\Delta H^\#}{R} \quad (2.7)$$

$$\text{Intercept} = \ln\left(\frac{R}{Nh}\right) + \frac{\Delta S^\#}{R} \quad (2.8)$$

$\Delta H^\#$ and $\Delta S^\#$ values were calculated using equation (2.7) and (2.8) respectively.

2.8 ADSORPTION ISOTHERMS

The information on the interaction between the inhibitor molecules and the metal surface can be provided by adsorption isotherm. To evaluate the nature and strength of adsorption of inhibitor on the alloy surface, the experimental data are fitted to the isotherm, and from the best fit, the thermodynamic data for adsorption are evaluated. The adsorption strength can be deduced from the adsorption isotherm, which shows the equilibrium relationship between concentrations of inhibitors on the surface and in the bulk of the solution.

In the present study attempts were made to fit the degree of surface coverage (θ) values obtained for the weld aged maraging steel specimen in different concentrations of hydrochloric acid and sulphuric acid in the presence of different concentrations of inhibitor to various isotherms including Langmuir, Temkin, Frumkin, Freundlich and Flory- Huggins isotherms. Various adsorption isotherms used to characterize the adsorption of inhibitor on the metal surface are presented in Table 2.3.

Table 2.3: Adsorption isotherms to characterise the adsorption of inhibitors on the metal surface.

Name	Isotherm	Verification plot
Langmuir	$\theta / 1-\theta = \beta c$	$\theta / 1-\theta$ Vs $\log c$
Temkin	$\theta = 1 / f (\ln Kc)$	θ Vs $\log c$
Frumkin	$(\theta / 1-\theta) e^{f\theta} = \beta c$	θ Vs $\log c$
Bockris- Swinkels	$\theta / (1-\theta)^n [\theta + n (1-\theta)_{n-1}/n^n] = c.e^{-\beta/55.4}$	$\theta / 1-\theta$ Vs $\log c$
Virial Parson	$\theta.e^{2f\theta} = \beta.c$	θ Vs $\log \theta / c$
Flory Huggins	$\log(\theta/c) = \log mK + m\log (1- \theta)$	$\log (\theta/c)$ vs $\log(1- \theta)$
Freundlich	$\theta = Kc^m$	$\log \theta$ /vs $\log c$
El – Awady	$\log[\theta/(1- \theta)] = \log K + y \log c$	$\log[\theta/(1- \theta)]$ vs $\log c$.

where θ - surface coverage; $\beta = \Delta G/2.303RT$; ΔG - free energy of adsorption; R – gas constant; T - temperature; c - bulk inhibitor concentration; m - number of water molecules; f - inhibitor interaction parameter (0, no interaction; +, attraction; -, repulsion); K, y - constants; (Papavinasam 2006).

In order to obtain the isotherm, the linear relation between surface coverage (θ) value and inhibitor concentration (c) must be found. Attempts were made to fit the θ and c values to various isotherms, listed in the Table 2.2.

2.9 THERMODYNAMIC PARAMETERS

The standard free energy of adsorption of the inhibitor molecules on the metal surface, ΔG^0_{ads} was calculated using the relation (2.9).

$$K_{ads} = \frac{1}{55.5} \exp\left(\frac{-\Delta G^0_{ads}}{RT}\right) \quad (2.9)$$

where the value 55.5 is the concentration of water in solution in mol dm⁻³, R is the universal gas constant and T is absolute temperature. K

Standard enthalpy of adsorption (ΔH_{ads}^0) and standard entropy of adsorption (ΔS_{ads}^0) were calculated from Gibbs–Helmholtz equation.

$$\Delta G_{\text{ads}}^0 = \Delta H_{\text{ads}}^0 - T\Delta S_{\text{ads}}^0 \quad (2.10)$$

The variation of ΔG_{ads}^0 with T gives a straight line with an intercept equals to ΔH_{ads}^0 and slope equals to ΔS_{ads}^0 .

CHAPTER 3

RESULTS AND DISCUSSION

3.1 CORROSION OF 18% Ni M250 GRADE MARAGING STEEL UNDER WELD AGED CONDITION IN HYDROCHLORIC ACID MEDIUM

3.1.1 Potentiodynamic polarization studies

The corrosion behaviour of the weld aged maraging steel specimen was investigated in 0.1 M, 0.5 M, 1.0 M, 1.5 M and 2.0 M hydrochloric acid at 30 °C, 35 °C, 40 °C, 45 °C and 50 °C temperatures using potentiodynamic polarization technique. Fig. 3.1 represents the potentiodynamic polarization curves for the corrosion of weld aged maraging steel in hydrochloric solutions of different concentrations at 30 °C. Similar results were obtained at other temperatures also. The potentiodynamic polarization parameters like corrosion potential (E_{corr}), corrosion current density (i_{corr}), anodic and cathodic slopes (b_a and b_c) and corrosion rate (v_{corr}) were calculated from potentiodynamic polarization plots and are tabulated in Table 3.1.

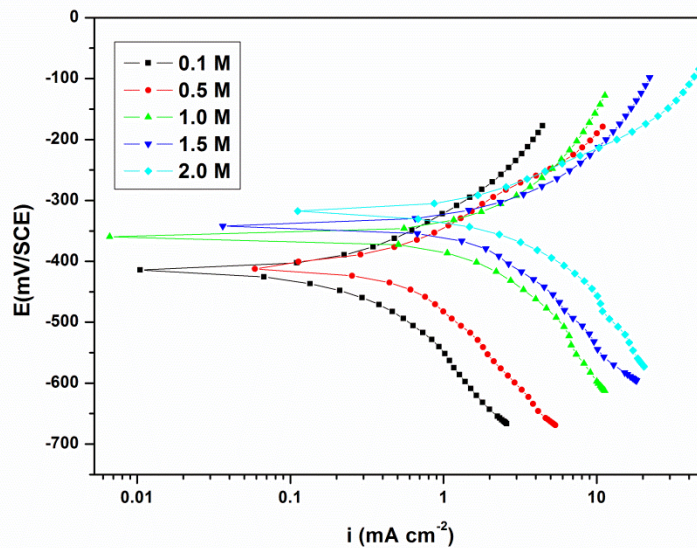
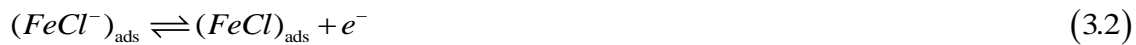


Fig. 3.1: Potentiodynamic polarization curves for the corrosion of weld aged maraging steel in different concentrations of hydrochloric acid at 30 °C.

It is seen from the figure that the polarization curves are shifted to the high current density region as the concentration of hydrochloric acid is increased, indicating the increase in the corrosion rate with the increase in hydrochloric acid concentration. It is clear from the data presented in Table 3.1 that the corrosion rate of weld aged maraging steel specimen increases with increase in the concentration of hydrochloric acid in the solution. It is also observed from the results that the corrosion potential is shifted towards less negative values as the concentration of hydrochloric acid is increased. The positive shift in the corrosion potential (E_{corr}) indicates that the anodic process is much more affected by the acid concentration than the cathodic process (Touhamia et al. 2000, Machnikova et al. 2008). This observation is in accordance with Muralidharan et al. (1979) who proposed dependence of E_{corr} and i_{corr} on solution parameters. There is no significant change in the values of b_a and b_c with the change in concentration of acid, which implies that, there is no change in corrosion reaction mechanism with change in acid concentration. This fact is supported by similar shapes of polarization curves at different concentrations of acid.

The corrosion of steel in acid medium normally proceeds via two partial reactions in acid solutions. The partial anodic reaction involves the oxidation of metal and formation of soluble Fe^{2+} ions, while the partial cathodic reaction involves the evolution of hydrogen gas (Kriaa et al. 2009). In hydrochloric acid solution, the following mechanism is proposed for the corrosion of iron and steel. In the anodic reaction, the dissolution of iron takes place as follows (Ashish Kumar et al. 2010):



In the cathodic reaction, hydrogen evolution takes place as follows:



3.1.2 Electrochemical impedance spectroscopy (EIS) studies

The impedance spectra recorded are displayed as Nyquist plots for the specimen. Fig. 3.2 represents Nyquist plots for the corrosion of weld aged maraging steel in different concentrations of hydrochloric acid at 30 °C. Similar plots were obtained at other temperatures also. The point where the semi-circle of the Nyquist plot intersects the real axis at high frequency (close to the origin) yields solution resistance (R_s). The intercept on real axis at the other end of the semicircle (low frequency) gives the sum of solution resistance and the charge transfer resistance (R_{ct}). Hence the charge transfer resistance value is simply the diameter of the semicircle (Prabhu et al. 2008). The diagonal region in between the high frequency and low frequency region has a negative slope due to the capacitive behaviour of the electrochemical double layer. R_{ct} is inversely proportional to the corrosion current and was used to calculate the corrosion rate.

From Fig. 3.2 it is clear that the diameter of the semicircle decreases with the increase in the concentration of hydrochloric acid, indicating the decrease in R_{ct} value and increase in corrosion rate. The fact that impedance diagrams have semi-circular appearance shows that the corrosion of weld aged maraging steel is mainly controlled by a charge transfer process and the mechanism of dissolution of metal in hydrochloric acid is not altered with the change in the hydrochloric acid concentration (Larabi et al. 2005). As seen from the figure, the Nyquist plots are not perfect semicircles. The deviation has been attributed to frequency dispersion. The “depressed” semicircles have a centre under

the real axis, and can be seen as depressed capacitive loops. Such phenomena often correspond to surface heterogeneity which may be the result of surface roughness, dislocations, distribution of the active sites or adsorption of molecules (Li et al. 2008).

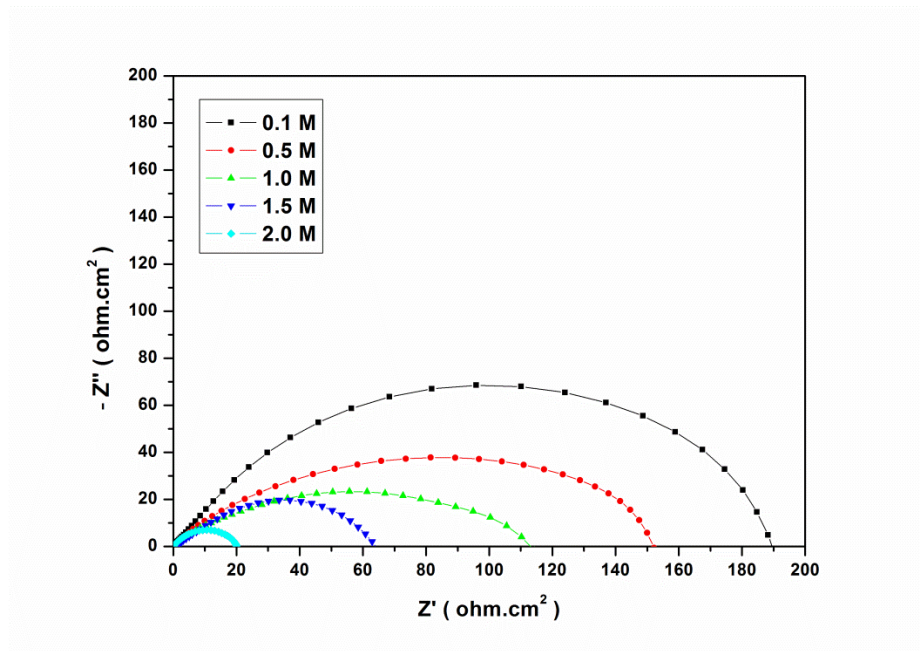


Fig. 3.2: Nyquist plots for the corrosion of weld aged maraging steel in different concentrations of hydrochloric acid at 30 °C.

The results obtained can be interpreted in terms of the equivalent circuit of the electrical double layer. The circuit fitment was done by ZSimpWin software of version 3.21. The impedance data of weld aged maraging steel in hydrochloric acid were analysed using the circuit fitment shown in Fig. 3.3 in which R_s represents the solution resistance and R_{ct} the charge transfer resistance. The constant phase element (CPE) is substituted for the capacitive element to give a more accurate fit, as most capacitive loops are depressed semi circles rather than regular semi circles (Tang et al. 2008). The results of EIS measurement are summarized in Table 3.2. The impedance of constant phase (Z_{CPE}) is described by the expression:

$$Z_{CPE} = \frac{1}{Q} \times \frac{1}{(j\omega)^n} \quad (3.8)$$

where Q is the CPE coefficient, n the CPE exponent (phase shift), ω the angular frequency ($\omega = 2\pi f$, where f is the AC frequency), n is dependent on the surface morphology: $-1 \leq n \leq 1$ and j here is the imaginary unit. When the value of n is 1, the CPE behaves like an ideal double-layer capacitance (C_{dl}). The value of double layer capacitance (C_{dl}) can be obtained from the equation.

$$C_{dl} = Q (\omega_{max})^{n-1} \quad (3.9)$$

where ω is the frequency at which the imaginary part of the impedance ($-Z''$) is maximum (Tang et al. 2008 and Machnikova et al. 2008).

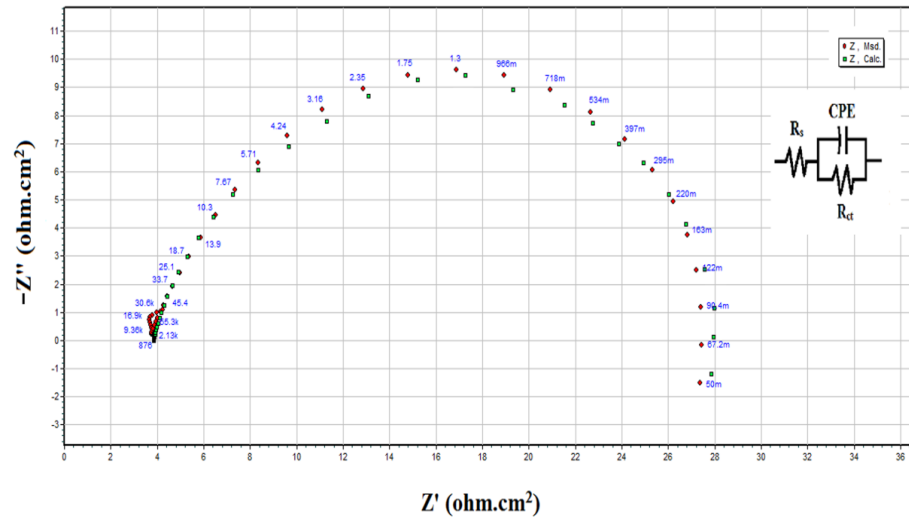


Fig. 3.3: The equivalent circuit model used to fit the experimental data for the corrosion of the specimen in 2.0 M hydrochloric acid solution at 30 °C.

The results show that charge transfer resistance (R_{ct}) value decreases and double layer capacitance (C_{dl}) increases with the increase in the concentration of hydrochloric acid. The increase in the C_{dl} value may be due to the desorption of the chloride ions at the

metal surface causing a change in the double layer structure (Abd Ei-Rehim et al. 1999). The Nyquist plots obtained in the real system represent a general behaviour where the double layer on the interface of metal/solution does not behave as a real capacitor. On the metal side electrons control the charge distribution whereas on the solution side it is controlled by ions. As ions are much larger than the electrons, the equivalent number of ions to the charge on the metal will occupy quite a large volume on the solution side of the double layer. Increase in the capacitance which can result from an increase in local dielectric constant and/or a decrease in the thickness of the electrical double layer, suggests that the chloride ions act by adsorption at the metal/solution interface (Prabhu et al. 2007).

3.1.3 Effect of temperature

It is clear from the data presented in Tables 3.1 and 3.2 that the corrosion rate of the weld aged maraging steel increases with increase in temperature of hydrochloric acid medium from 30 °C to 50 °C. Fig. 3.4 and Fig. 3.5 represent the potentiodynamic polarization curves and Nyquist plots respectively, for the corrosion of weld aged maraging steel in 0.5 M hydrochloric acid at different temperatures. Similar curves were obtained at other concentrations also. The increase in corrosion rate with temperature may be attributed to the fact that the hydrogen evolution overpotential decreases with the increase in temperature that leads to increase in cathodic reaction rate. The values of b_c and b_a change with the increase in acid concentration and also with the increase in temperature, which indicate the influence of acid concentration and temperature on the kinetics of hydrogen evolution and metal dissolution.

The variation of corrosion rate with the temperature follows Arrhenius equation which is utilized to calculate the activation energy (E_a). According to Arrhenius equation, the corrosion rate (v_{corr}) is given by given by the expression:

$$\ln(v_{\text{corr}}) = B - \frac{E_a}{RT} \quad (2.4)$$

where B is a constant which depends on the metal type and R is the universal gas constant, v_{corr} is corrosion rate, E_a is the activation energy, T is absolute temperature. A plot of $\ln(v_{\text{corr}})$ vs $1/T$ gives straight line with slope $-E_a/R$.

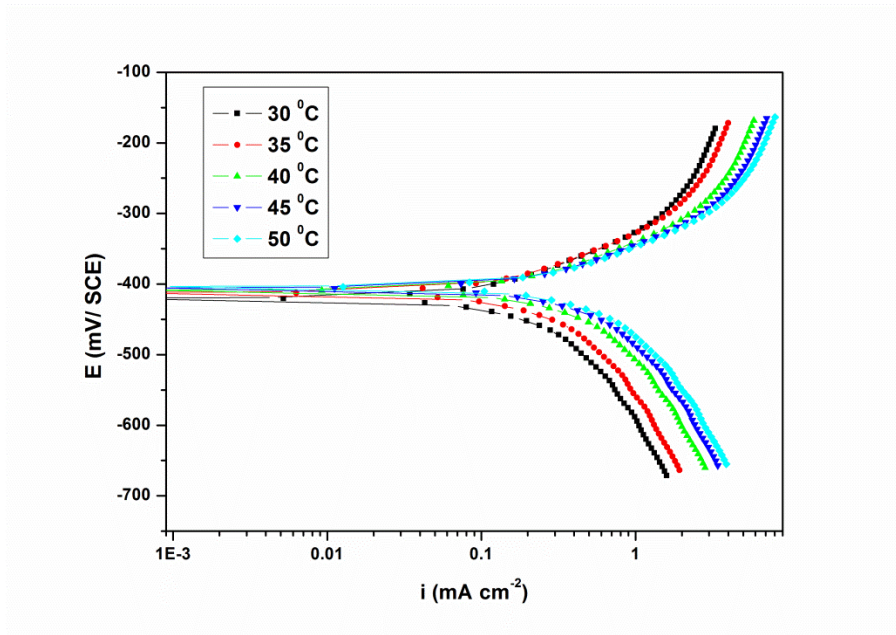


Fig. 3.4: Potentiodynamic polarization curves for the corrosion of weld aged maraging steel at different temperatures in 0.5 M hydrochloric acid.

Enthalpy of activation (ΔH^\ddagger) and the entropy of activation (ΔS^\ddagger) were calculated from transition state equation:

$$v_{\text{corr}} = \frac{RT}{Nh} \exp\left(\frac{\Delta S^\ddagger}{R}\right) \exp\left(\frac{-\Delta H^\ddagger}{R}\right) \quad (2.6)$$

where h is Plank's constant, and N is Avagadro's number. A plot of $\ln(v_{\text{corr}}/T)$ vs $1/T$ gives straight line with slope given by equation (2.7) and intercept given by equation (2.8).

$$\text{Slope} = \frac{-\Delta H^\ddagger}{R} \quad (2.7)$$

$$\text{Intercept} = \ln\left(\frac{R}{N_h}\right) + \frac{\Delta S^\ddagger}{R} \quad (2.8)$$

ΔH^\ddagger and ΔS^\ddagger values were calculated using equation (2.7) and (2.8), respectively.

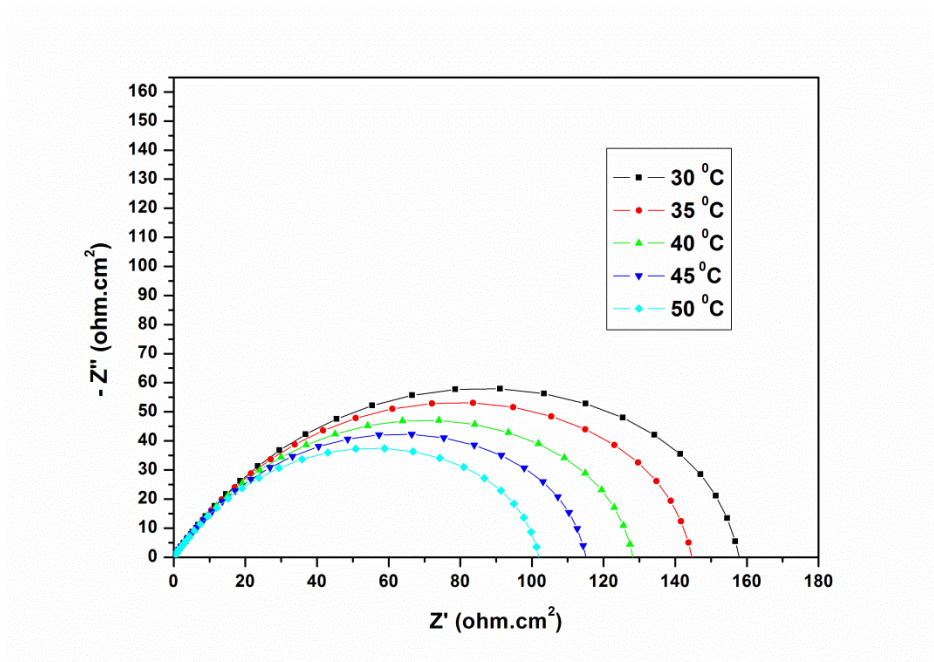


Fig. 3.5: Nyquist plots for the corrosion of weld aged maraging steel in 0.5 M hydrochloric acid at different temperatures.

The Arrhenius plots for the corrosion of weld aged specimen in hydrochloric acid are shown in the Fig. 3.6. The plots of $\ln(v_{\text{corr}}/T)$ vs $1/T$ are shown in the Fig. 3.7. The activation parameters are given in the Table 3.3. The activation energy values indicate that the corrosion of the alloy is controlled by surface reaction, since the values of activation energy for the corrosion process are greater than 20 kJ mol^{-1} (Bouklah et al. 2005). As seen from Table 3.3, the value of energy of activation (E_a) for the corrosion of the alloy decreases with the increase in acid concentration. This indicates that the formation of activated complex is slower in hydrochloric acid of lower concentration, becomes faster as the concentration of acid increases.

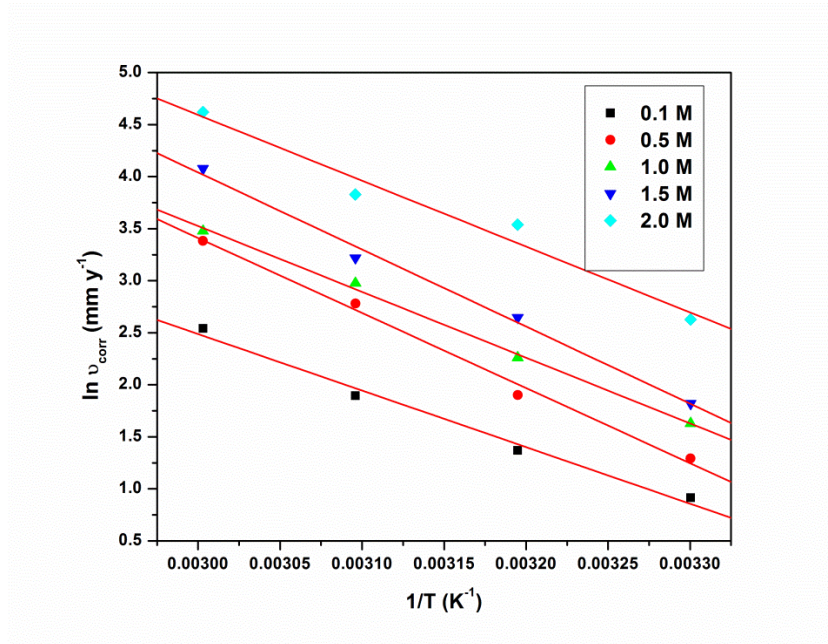


Fig. 3.6: Arrhenius plots for the corrosion of weld aged maraging steel in hydrochloric acid.

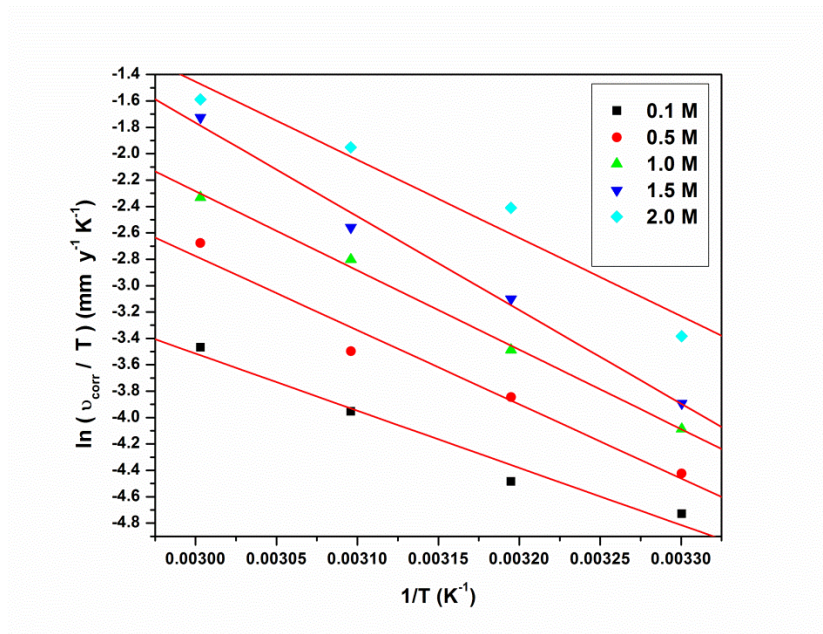


Fig. 3.7: Plots of $\ln(v_{\text{corr}}/T)$ vs $1/T$ for the corrosion of weld aged maraging steel in hydrochloric acid.

The variation in E_a values is in accordance with the observed trend that corrosion rate of the alloy increases with the increase in the concentration of hydrochloric acid. The variation of enthalpy of activation (ΔH^\ddagger) with the concentration of hydrochloric acid is similar to the variation of energy of activation (E_a). The entropy of activation is negative. This implies that the activated complex in the rate-determining step represents association rather than dissociation, indicating that a decrease in randomness takes place on going from reactants to the activated complex (Prabhu et al. 2007).

3.1.4 SEM/EDS studies

The scanning electron microscope images were recorded to establish the interaction of acid solution with the metal surface. The SEM image of a freshly polished surface of weld aged maraging steel sample is given in Fig. 3.8 (a), which shows the uncorroded surface with few scratches due to polishing. Fig. 3.8 (b) shows the SEM image of weld aged maraging steel surface after immersed for 3 h in 2.0 M hydrochloric acid. The SEM images reveal that the surface of the specimen immersed in 2.0 M hydrochloric acid is deteriorated due to the acid action. The corroded surface shows detachment of particles from the surface.

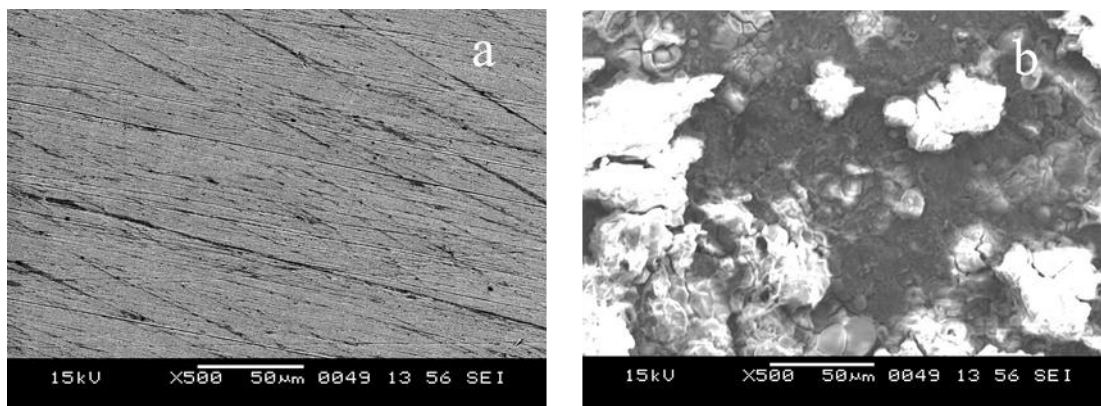


Fig. 3.8: SEM images of (a) freshly polished surface (b) corroded surface

EDS investigations were carried out in order to identify the composition of the freshly polished surface and corroded metal surface in 2.0 M hydrochloric acid. The

corresponding EDS profile analyses for the selected areas on the SEM images of Fig. 3.8 (a) and 3.8 (b) are shown in Fig. 3.9 (a) and 3.9 (b), respectively.

The atomic percentages of the elements found in the EDS profile of uncorroded metal surface were 66.5 % Fe, 17.2% Ni, 3.1% Mo, 6.7% Co, 0.07% Si and 0.22% Ti. The atomic percentages of corroded metal surface were 13.18% Fe, 4.53% Ni, 4.7% Cl, 3.18% Mo, 66.21% O and 3.2 % Co and indicated that iron oxide is existing in this area. These elemental compositions prove that the corrosion of weld aged maraging steel results in the formation of oxide layer on the surface. The elemental compositions mentioned above were mean values at different regions.

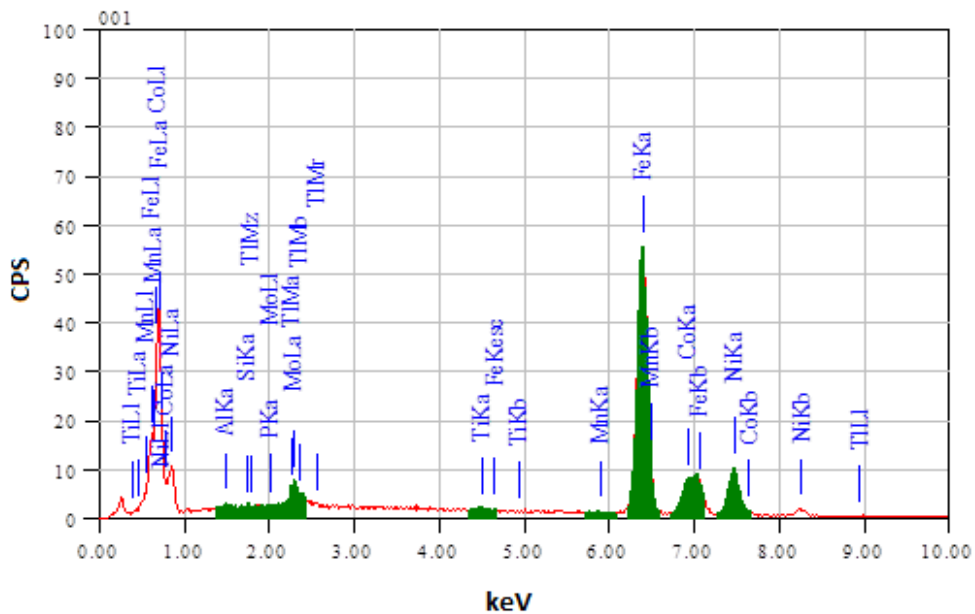


Fig. 3.9 (a): EDS spectra of the freshly polished surface of weld aged maraging steel.

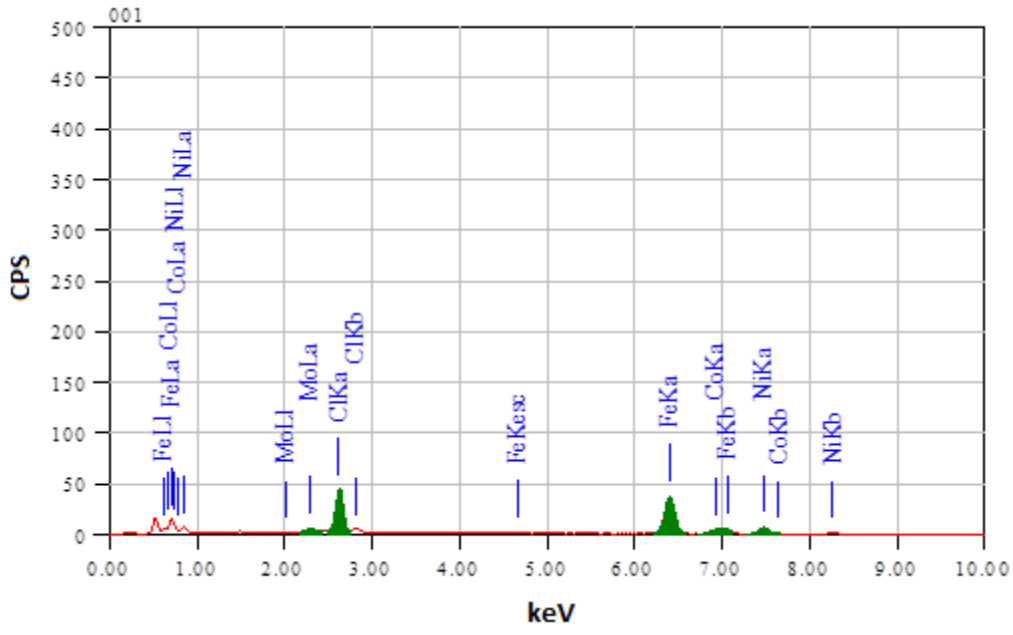


Fig. 3.9 (b): EDS spectra of the weld aged maraging steel after immersion in 2.0 M hydrochloric acid.

Table 3.1: Results of potentiodynamic polarization studies for the corrosion of weld aged maraging steel in different concentrations of hydrochloric acid at different temperatures.

Molarity of hydrochloric acid (M)	Temperature °C	E_{corr} (mV/ SCE)	b_a (mV)	$-b_c$ (mV)	i_{corr} (mA cm ⁻²)	v_{corr} (mm y ⁻¹)
0.1	30	-419±3	142±3	226±3	0.22±0.02	2.53±0.23
	35	-416±3	150±3	234±3	0.26±0.02	2.99±0.20
	40	-412±2	159±1	242±3	0.30±0.01	3.45±0.14
	45	-409±2	165±3	250±2	0.33±0.01	3.80±0.13
	50	-405±3	173±2	259±2	0.37±0.03	4.26±0.27
0.5	30	-413±2	148±2	247±2	0.27±0.02	3.11±0.24
	35	-411±2	156±2	254±1	0.35±0.02	4.03±0.19
	40	-408±2	165±1	262±2	0.42±0.02	4.83±0.21
	45	-406±3	172±1	269±2	0.52±0.01	5.87±0.14
	50	-404±4	183±4	277±1	0.59±0.03	6.79±0.26
1.0	30	-371±2	153±2	256±3	0.33±0.03	3.80±0.25
	35	-368±2	159±1	261±1	0.45±0.02	5.20±0.21
	40	-364±2	165±3	266±3	0.56±0.02	6.45±0.17
	45	-361±4	172±2	273±1	0.76±0.04	8.72±0.39
	50	-358±3	177±2	278±4	0.92±0.06	10.63±0.64
1.5	30	-342±3	158±1	267±1	0.70±0.02	8.05±0.18
	35	-339±3	165±4	276±3	0.82±0.03	9.45±0.26
	40	-337±4	173±4	282±3	0.94±0.02	10.85±0.19
	45	-334±3	179±1	286±2	1.53±0.06	17.60±0.65
	50	-332±4	185±1	292±2	1.61±0.11	18.57±1.36
2.0	30	-324±3	175±4	287±3	2.77±0.10	31.85±1.23
	35	-321±2	182±3	293±4	3.09±0.15	35.49±1.73
	40	-319±1	189±3	300±4	3.39±0.09	39.03±1.12
	45	-315±3	196±1	307±4	3.63±0.11	41.73±1.30
	50	-312±1	203±1	312±3	3.89±0.22	44.77±2.50

Table 3.2: Results of EIS studies for the corrosion of weld aged maraging steel in different concentrations hydrochloric acid at different temperatures.

Molarity of hydrochloric acid (M)	Temperature (°C)	R_{ct} (ohm. cm ²)	C_{dl} (mF cm ⁻²)	v_{corr} (mm y ⁻¹)
0.1	30	181.20±3.11	0.93±0.22	2.41±0.11
	35	158.00±3.06	1.10±0.15	2.89±0.23
	40	135.21±2.68	1.40±0.29	3.55±0.42
	45	127.54±2.55	1.55±0.25	3.89±0.18
	50	117.23±2.47	1.80±0.11	4.42±0.32
0.5	30	156.30±2.45	0.96±0.31	2.96±0.25
	35	139.27±3.05	1.17±0.33	3.47±0.62
	40	123.15±2.63	1.45±0.37	4.11±0.29
	45	107.56±2.43	1.74±0.37	4.87±0.26
	50	90.34±3.39	1.83±0.30	6.09±0.37
1.0	30	116.20±2.52	1.68±0.22	4.12±0.19
	35	97.32±2.07	1.75±0.27	5.07±0.25
	40	82.68±2.31	2.15±0.47	6.16±0.18
	45	65.24±2.84	2.36±0.42	8.09±0.91
	50	53.86±2.41	2.79±0.64	10.04±0.83
1.5	30	64.30±2.88	3.01±0.27	7.71±0.25
	35	58.75±2.29	3.38±0.35	8.78±0.36
	40	53.42±3.09	3.74±0.23	10.03±0.64
	45	36.89±2.85	4.13±0.33	14.91±0.12
	50	32.05±2.74	4.59±0.80	17.65±0.67
2.0	30	20.21±3.10	5.75±0.52	26.87±0.18
	35	17.34±3.26	8.26±1.24	32.35±0.27
	40	15.01±4.83	13.22±1.58	38.59±0.55
	45	12.89±4.85	15.87±1.38	46.36±0.24
	50	11.67±3.28	18.95±1.20	52.65±0.37

Table 3.3: Activation parameters for the corrosion of weld aged maraging steel in hydrochloric acid.

Molarity of hydrochloric acid (M)	E_a (kJ mol ⁻¹)	ΔH^\ddagger (kJ mol ⁻¹)	ΔS^\ddagger (J mol ⁻¹ K ⁻¹)
0.1	39.12	41.61	-94.90
0.5	36.56	38.51	-103.71
1.0	35.70	34.98	-108.66
1.5	32.08	30.55	-117.80
2.0	30.33	31.24	-122.37

3.2 CORROSION OF 18% Ni M250 GRADE MARAGING STEEL UNDER WELD AGED CONDITION IN SULPHURIC ACID MEDIUM

3.2.1 Potentiodynamic polarization studies

Fig. 3.10 represents the potentiodynamic polarization curves for the corrosion of weld aged sample of maraging steel in sulphuric acid solutions of different concentrations at 30 °C. Similar plots were obtained at other temperatures also. The potentiodynamic polarization parameters are summarized in the Table 3.4. These results predict substantial corrosion of the weld aged maraging steel in sulphuric acid at all the studied temperatures and concentrations. The corrosion rate increases with the increase in concentration of sulphuric acid.

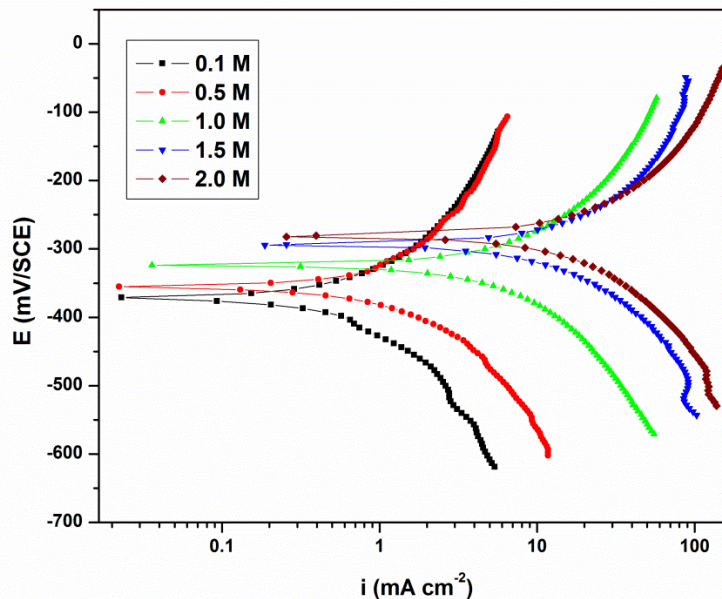


Fig. 3.10: Potentiodynamic polarisation curves for the corrosion of weld aged maraging steel in different concentrations of sulphuric acid at 30 °C.

As can be seen from the polarisation curves, the corrosion potential is shifted in the positive direction, when the concentration of sulphuric acid is increased. This observation is similar to the one discussed in the section 3.1.4 and hence same discussion holds good here. There is no significant change in the values of b_a and b_c for weld aged specimen implies that, there is no change in corrosion reaction mechanism with change in acid concentration.

3.2.2 Electrochemical impedance spectroscopy (EIS) studies

Nyquist plots for the corrosion of weld aged maraging steel in different concentrations of sulphuric acid at 30 °C are shown in Fig. 3.11. Similar plots were obtained at other temperatures also. The similar semi-circular appearance of the impedance diagrams shows that the corrosion of weld aged maraging steel is controlled by a charge transfer process and the mechanism of dissolution of the metal is not affected by the variation in the concentration of sulphuric acid (Larabi et al., 2005).

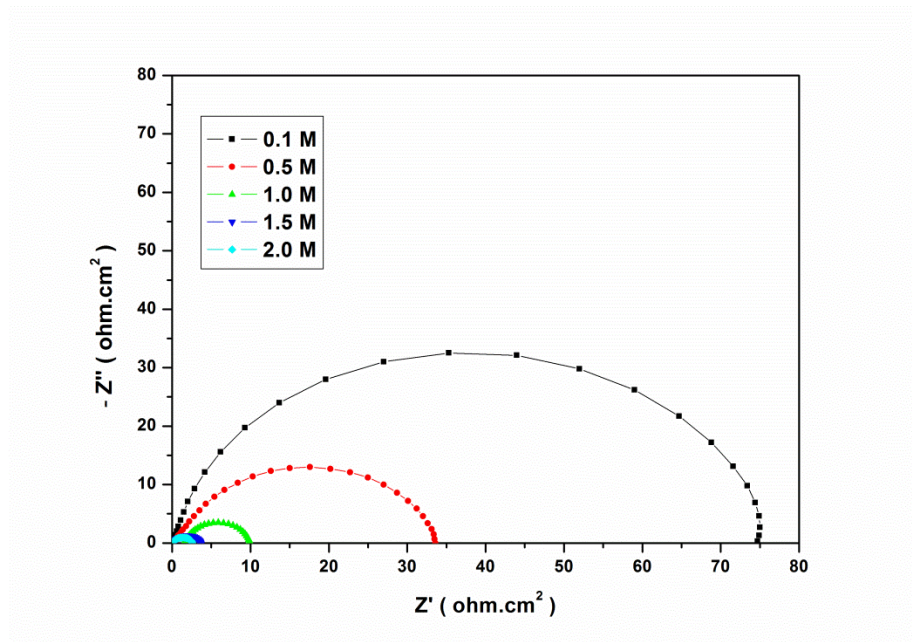


Fig. 3.11: Nyquist plots for the corrosion of weld aged maraging steel in different concentrations of sulphuric acid at 30 °C.

The equivalent circuit shown in the Fig. 3.3 (Section 3.1.2) is used to fit the experimental data. The impedance plots are analysed as discussed in the section 3.1.2. The calculated values of R_{ct} and C_{dl} are listed in Table 3.5. The CPE element is used to explain the depression of the capacitance semi-circle, which corresponds to surface heterogeneity resulting from surface roughness, impurities, dislocations, grain boundaries, adsorption of ions, formation of porous layers etc (Wei-hua et al. 2008). The EIS results also show substantial corrosion of the weld aged maraging steel specimen in sulphuric acid medium. The results show that charge transfer resistance (R_{ct}) value decreases and double layer capacitance (C_{dl}) increases with the increase in the concentration of sulphuric acid. This indicates that the rate of corrosion increases with the increase in the concentration of sulphuric acid. This is in agreement with the results obtained from potentiodynamic polarisation studies.

3.2.3 Effect of temperature

The Fig. 3.12 and 3.13 represents the potentiodynamic polarisation curves and Nyquist plots, respectively, for the corrosion of weld aged maraging steel in 1.0 M sulphuric acid medium at different temperatures. Similar plots are obtained at other concentrations also. The electrochemical polarisation parameters and EIS parameters have already been tabulated in table 3.4 and 3.5, respectively.

It is clear from the Fig. 3.12 and 3.13 and the data presented in the Tables 3.4 and 3.5 that the corrosion rate of weld aged maraging steel increases with the increase in the temperature of sulphuric acid medium. This may be attributed to the fact that the hydrogen evolution overpotential decreases with the increase in temperature, that leads to increase in cathodic reaction rate (Bellanger and Rameau, 1996). The values of b_c and b_a change with the increase in temperature, which indicates the influence of solution temperature on the kinetics of hydrogen evolution and metal dissolution processes. The activation parameters for the corrosion of weld aged maraging steel in sulphuric acid medium were calculated from the Arrhenius plots (Fig. 3.14) and from the plots of $\ln(v_{corr}/T)$ vs $(1/T)$ (Fig. 3.15). These values are listed in the Table 3.6. The variation of activation parameters are similar to that obtained in hydrochloric acid medium.

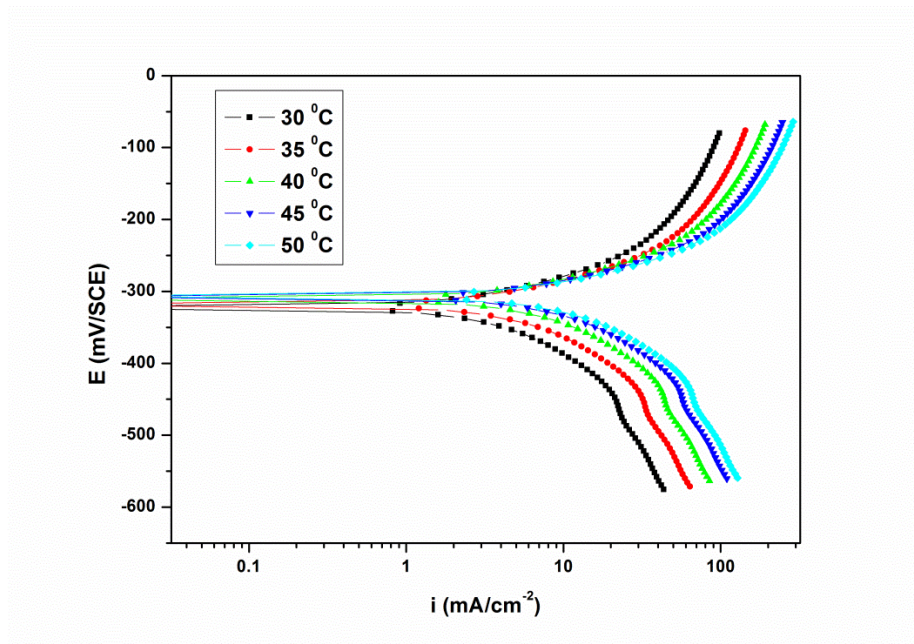


Fig. 3.12: Potentiodynamic polarisation curves for the corrosion of weld aged maraging steel specimen at different temperatures in 1.0 M sulphuric acid.

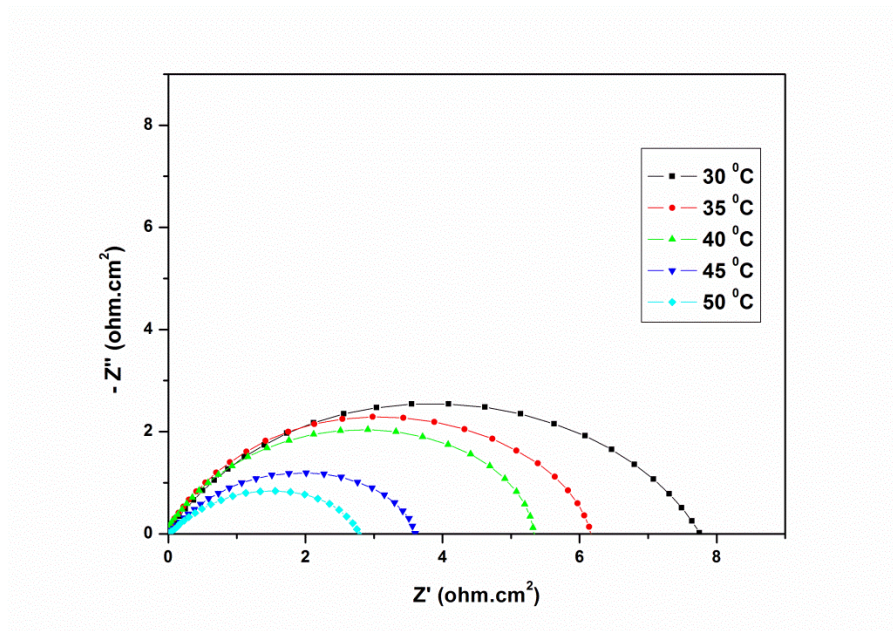


Fig. 3.13: Nyquist plots for the corrosion of weld aged Maraging Steel in 1.0 M sulphuric acid at different temperatures.

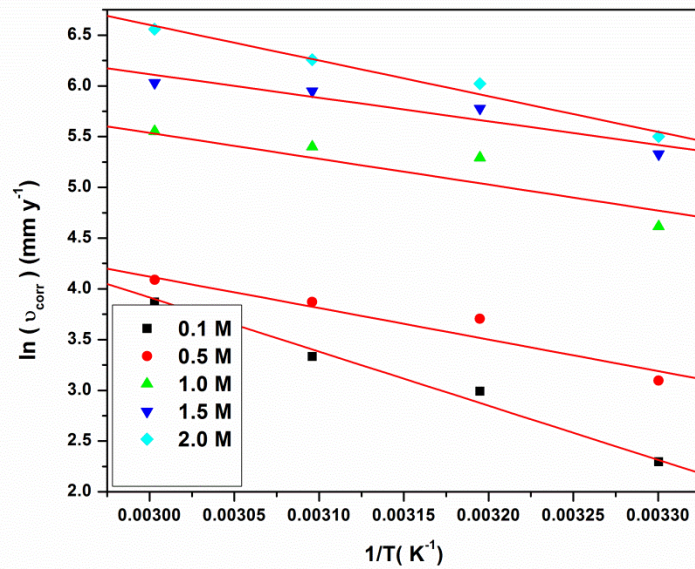


Fig. 3.14: Arrhenius plots for the corrosion of weld aged sample of maraging steel in sulphuric acid.

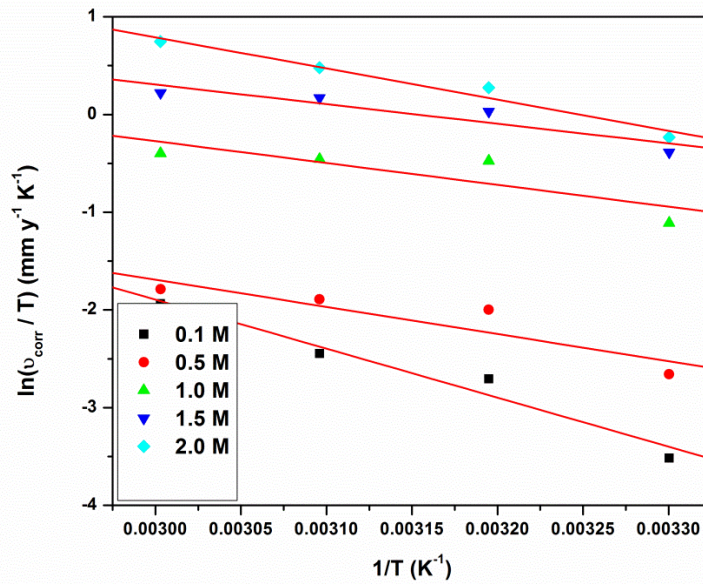


Fig. 3.15: Plots of $\ln(v_{\text{corr}}/T)$ vs $1/T$ for the corrosion of weld aged sample of maraging steel in sulphuric acid.

The correlation coefficient (R^2) was used to choose the isotherm that best fit the experimental data. The plots are linear, with an average correlation coefficient of 0.9691.

3.2.4 SEM/EDS studies

The surface morphology of the weld aged maraging steel specimen immersed in 1.0 M sulphuric acid solution was compared with that of the non-corroded specimen by recording their SEM images. The SEM image of a freshly polished surface of the weld aged maraging steel sample is given in Fig. 3.16 (a), which shows the non-corroded surface with few scratches due to polishing. Fig. 3.16 (b) shows the SEM image of weld aged maraging steel surface after immersion for 3 h in 1.0 M sulphuric acid, with a deteriorated surface due to the acid action.

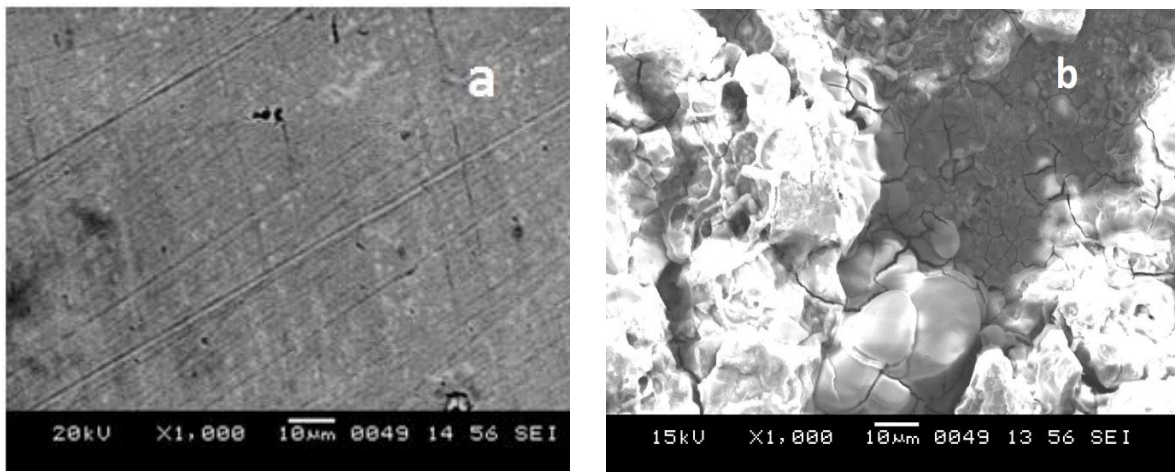


Fig. 3.16: SEM images of (a) freshly polished surface (b) corroded surface

EDS investigations were carried out in order to identify the composition of the freshly polished surface and corroded metal surface in 1.0 M sulphuric acid. The corresponding EDS profile analyses for the selected areas on the freshly polished surface and corroded surface are shown in Fig. 3.17 (a) and 3.17 (b), respectively. The atomic percentages of the elements found in the EDS profile of uncorroded metal surface were 66.5 % Fe, 17.2% Ni, 3.1% Mo, 6.7% Co, 0.07% Si and 0.22% Ti. The atomic percentages found in the EDS profile of corroded metal surface were 16.24% Fe, 7.66%

Ni, 6.52% S, 2.79% Mo, 59.21% O and 4.17 % Co and indicated that iron oxide is existing in this area. These elemental composition prove that the corrosion of weld aged maraging steel through the formation of oxide layer. The elemental compositions mentioned above were mean values of different regions.

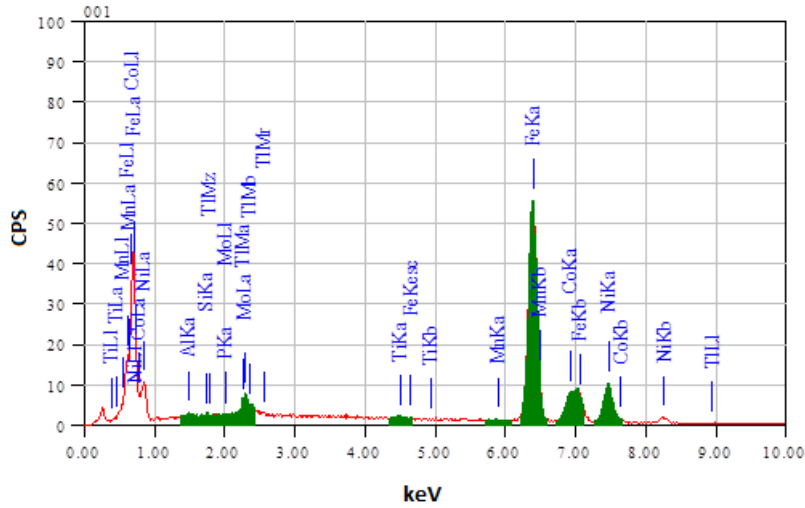


Fig. 3.17 (a): EDS spectra of the freshly polished surface of weld aged maraging steel.

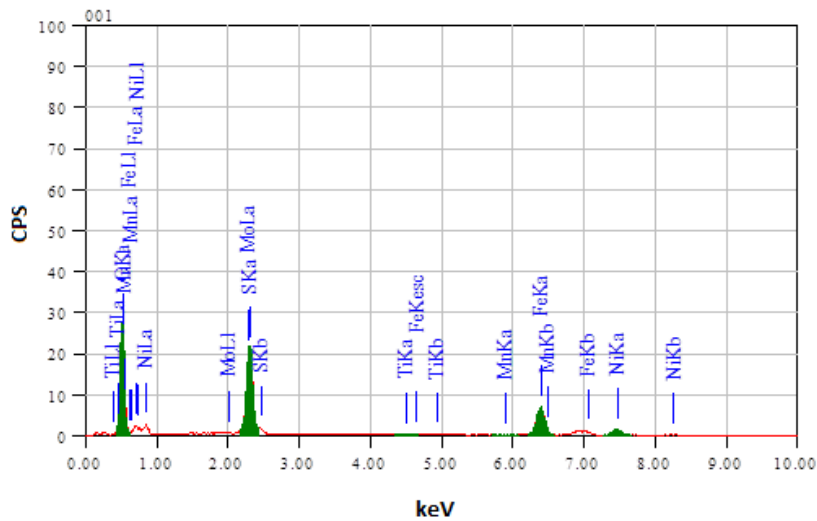


Fig. 3.17 (b): EDS spectra of the weld aged maraging steel after immersion in 1.0 M sulphuric acid.

Table 3.4: Results of potentiodynamic polarisation studies for the corrosion of weld aged maraging steel in different concentrations of sulphuric acid at different temperatures.

Molarity of sulphuric acid (M)	Temperature ($^{\circ}\text{C}$)	E_{corr} (mV/SCE)	b_a (mV)	$-b_c$ (mV)	i_{corr} (mA cm^{-2})	v_{corr} (mm y^{-1})
0.1	30	-371 \pm 2	221 \pm 1	266 \pm 1	0.78 \pm 0.03	8.99 \pm 0.31
	35	-368 \pm 3	257 \pm 1	283 \pm 1	1.27 \pm 0.11	14.64 \pm 1.12
	40	-365 \pm 1	289 \pm 3	296 \pm 3	1.99 \pm 0.21	22.95 \pm 2.27
	45	-362 \pm 2	295 \pm 2	317 \pm 1	2.21 \pm 0.23	25.48 \pm 2.26
	50	-359 \pm 2	298 \pm 2	321 \pm 1	2.47 \pm 0.22	28.48 \pm 2.58
0.5	30	-356 \pm 2	235 \pm 1	268 \pm 2	1.80 \pm 0.17	20.71 \pm 1.79
	35	-353 \pm 2	257 \pm 1	276 \pm 1	2.41 \pm 0.19	27.73 \pm 2.21
	40	-350 \pm 1	279 \pm 1	288 \pm 1	3.83 \pm 0.11	44.07 \pm 1.44
	45	-348 \pm 2	296 \pm 2	297 \pm 3	4.44 \pm 0.15	46.21 \pm 1.87
	50	-346 \pm 3	315 \pm 3	306 \pm 2	4.60 \pm 0.33	49.47 \pm 3.64
1.0	30	-323 \pm 2	247 \pm 1	301 \pm 3	8.56 \pm 0.38	98.41 \pm 3.85
	35	-318 \pm 2	276 \pm 1	303 \pm 2	12.82 \pm 0.30	147.28 \pm 3.01
	40	-309 \pm 2	292 \pm 2	305 \pm 1	16.92 \pm 0.22	194.46 \pm 2.20
	45	-307 \pm 3	298 \pm 2	307 \pm 1	19.42 \pm 0.32	223.23 \pm 3.17
	50	-305 \pm 3	312 \pm 1	311 \pm 1	22.10 \pm 0.41	253.15 \pm 4.13
1.5	30	-295 \pm 3	252 \pm 2	260 \pm 1	17.02 \pm 0.28	195.54 \pm 2.79
	35	-291 \pm 3	253 \pm 1	272 \pm 2	23.64 \pm 0.25	271.53 \pm 2.53
	40	-288 \pm 2	254 \pm 2	276 \pm 2	28.05 \pm 0.58	332.15 \pm 5.83
	45	-285 \pm 2	266 \pm 3	283 \pm 1	30.34 \pm 0.46	348.61 \pm 4.60
	50	-283 \pm 2	272 \pm 3	296 \pm 1	33.05 \pm 0.35	379.67 \pm 3.54
2.0	30	-281 \pm 3	223 \pm 3	251 \pm 3	20.31 \pm 0.39	233.51 \pm 3.87
	35	-279 \pm 2	245 \pm 2	263 \pm 2	27.63 \pm 0.44	317.55 \pm 4.42
	40	-278 \pm 1	269 \pm 2	274 \pm 1	35.00 \pm 0.48	402.63 \pm 4.83
	45	-275 \pm 2	281 \pm 3	288 \pm 2	40.72 \pm 0.26	468.28 \pm 2.59
	50	-273 \pm 1	301 \pm 3	302 \pm 2	45.24 \pm 0.58	520.05 \pm 5.81

Table 3.5: Results of EIS studies for the corrosion of weld aged maraging steel in different concentrations sulphuric acid at different temperatures.

Molarity of sulphuric acid (M)	Temperature (°C)	R_{ct} (ohm. cm ²)	C_{dl} (mF cm ⁻²)	v_{corr} (mm y ⁻¹)
0.1	30	74.66±3.24	21.01±3.15	8.08±0.91
	35	51.17±3.47	26.57±3.99	13.15±1.23
	40	35.45±2.68	32.14±2.96	20.61±1.42
	45	33.36±2.54	36.48±2.87	22.88±1.18
	50	30.19±2.64	41.49±2.19	25.57±2.32
0.5	30	33.56±1.62	40.12±2.65	18.64±1.55
	35	26.64±4.82	65.92±2.91	24.96±1.62
	40	17.85±3.14	109.77±2.90	39.66±1.29
	45	17.84±4.29	125.60±3.51	41.52±2.26
	50	17.42±4.17	158.27±3.51	44.51±2.37
1.0	30	7.09±2.45	11.00±2.79	95.62±2.89
	35	5.05±2.38	11.83±1.86	142.89±2.16
	40	3.95±1.35	12.37±1.20	188.68±2.13
	45	3.49±2.08	15.26±1.69	216.46±3.22
	50	3.15±1.64	18.08±2.38	247.02±2.87
1.5	30	3.34±0.50	13.71±2.86	191.41±2.62
	35	2.46±1.85	14.52±2.56	266.20±2.93
	40	2.09±1.24	16.09±1.33	316.18±4.42
	45	2.01±0.98	18.30±1.15	340.81±3.45
	50	1.90±0.39	21.47±2.18	372.71±4.57
2.0	30	2.58±1.31	16.45±2.15	228.66±2.26
	35	2.04±1.16	17.21±2.27	310.63±3.13
	40	1.72±0.78	19.56±1.58	394.26±4.42
	45	1.55±0.53	23.82±2.18	458.43±3.41
	50	1.48±1.33	26.00±1.80	508.87±5.73

Table 3.6: Activation parameters of corrosion reaction of weld aged maraging steel specimen in sulphuric acid.

Molarity of sulphuric acid (M)	E_a (kJ mol ⁻¹)	ΔH^\ddagger (kJ mol ⁻¹)	ΔS^\ddagger (J mol ⁻¹ K ⁻¹)	R^2
0.1	44.31	43.16	-88.32	0.9532
0.5	35.50	37.48	-111.52	0.9431
1.0	32.79	28.11	-144.08	0.9775
1.5	25.24	23.69	-141.93	0.9861
2.0	21.20	22.58	-142.28	0.9842

3.3 1(2E)-1-(4-AMINOPHENYL)-3-(2-THIENYL)PROP-2-EN-1-ONE (ATPI) AS INHIBITOR FOR THE CORROSION OF WELD AGED MARAGING STEEL IN HYDROCHLORIC ACID MEDIUM

3.3.1 Potentiodynamic polarization studies

The potentiodynamic polarization curves for the corrosion of weld aged maraging steel specimen in 1.5 M hydrochloric acid in the presence of different concentrations of ATPI, at 30 °C are shown in the Fig. 3.18. Similar plots were obtained in the other four concentrations of hydrochloric acid at the different temperatures studied.

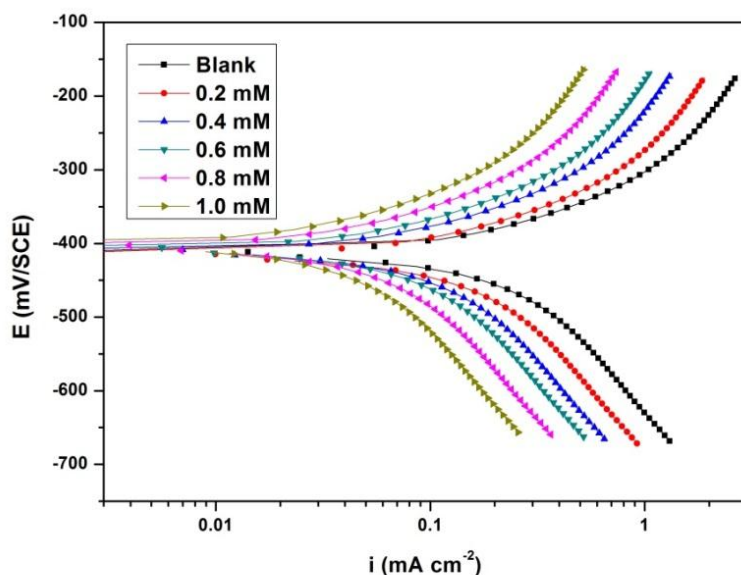


Fig. 3.18: Potentiodynamic polarization curves for the corrosion of weld aged maraging steel in 1.5 M hydrochloric acid containing different concentrations of ATPI at 30 °C.

The potentiodynamic polarization parameters such as corrosion potential (E_{corr}), cathodic and anodic Tafel slopes (b_c and b_a), corrosion current density (i_{corr}) and the inhibition efficiency values η (%) were calculated from Tafel plots in all the five studied

concentrations of hydrochloric acid in the presence of different concentrations of ATPI at different temperatures and are summarized in Tables 3.7 to 3.11.

In general, according to the results presented in Table 3.7 to Table 3.11 and also from polarization curves in Fig. 3.18, the corrosion current density (i_{corr}) decreased significantly even on the addition of a small concentration of ATPI and the inhibition efficiency ($\eta\%$) increases with the increase in the inhibitor concentration, up to an optimum value. Thereafter the increase in the inhibitor concentration resulted in negligible increase in inhibition efficiency.

It is seen from Tables 3.7 to 3.11, that the value of b_c does not change significantly with the increase in ATPI concentration, which indicates that the addition of ATPI does not change the hydrogen evolution reaction mechanism (Atta et al. 2011). The parallel cathodic Tafel curves indicate that the hydrogen evolution is activation controlled (Tao et al. 2011). Hydrogen evolution reaction has been reported to be generally the dominant local cathodic process in the corrosion of weld aged maraging steel alloy in aqueous acidic solutions, via H^+ ion or H_2O molecule reduction, respectively.

It is also seen from the data that the anodic slope b_a also does not change significantly on increasing the concentration of ATPI, indicating its non-interference in the mechanism of anodic reaction. This indicates that the inhibitive action of ATPI may be considered due to the adsorption and formation of barrier film on the electrode surface. The barrier film formed on the metal surface reduces the probability of both the anodic and cathodic reactions, which results in decrease in corrosion rate (Li et al. 2007 and Ferreira et al. 2004). The inhibition efficiency increases with the increase in inhibitor concentration, indicating increase in surface coverage and the inhibition efficiency reaching a maximum value of 94.6 % at 0.8 mM of ATPI in 0.1 M hydrochloric acid.

It can also be seen from Tables 3.7 to Table 3.11, that there is no appreciable shift in the corrosion potential value (E_{corr}) on the addition of ATPI to the corrosion medium and also on increasing the concentration of ATPI. If the displacement in corrosion

potential is more than ± 85 mV with respect to corrosion potential of the blank, then the inhibitor can be considered as a cathodic or anodic type. However, the maximum displacement in the present study is ± 20 mV, which indicates that ATPI is a mixed type inhibitor (Ferreira et al. 2004, Li et al. 2008, Poornima et al. 2011). According to Cao (1996) if the shift in E_{corr} is negligible, the inhibition is most probably caused by a geometric blocking effect of the adsorbed inhibitive species on the surface of the corroding metal. In the present study although there is no remarkable change (± 85 mV) in E_{corr} , the shift in E_{corr} is not negligible. This can be attributed to the difference in the active sites blocking effect of the inhibitor for the anodic and cathodic reactions, as it is impossible that the active sites on the metal surface are identical for both anodic and cathodic reactions of corrosion process.

As the concentration of the inhibitor increases, it is noticed that the corrosion potential shifts slightly toward more positive potential. This indicates that the inhibitor promotes passivation of weld aged maraging steel through adsorption (Larabi et al. 2005). The inhibitor ATPI can be considered as a mixed inhibitor with predominant anodic action. The increase in the inhibition efficiency with the increase in inhibitor concentration is attributed to the increased surface coverage by the inhibitor molecules as the concentration is increased (El- Sayed et al. 1997).

3.3.2 Electrochemical impedance spectroscopy

Fig. 3.19 shows the Nyquist plots for the corrosion of weld aged maraging steel in 1.5 M hydrochloric acid solution at 30 °C in the presence of different concentrations of ATPI. Similar plots were obtained in other concentrations of hydrochloric acid and also at other temperatures. The results of EIS studies for the corrosion of weld aged maraging steel are summarized in Tables 3.12 to 3.16.

As can be seen from Fig. 3.19 the Nyquist plots are semi-circular in the presence as well as in the absence of inhibitor. This indicates that the corrosion of weld aged maraging steel is controlled by a charge transfer process in the presence and absence of

the inhibitor (Tao et al. 2011). The presence of inhibitor increases the impedance indicating a decrease in the corrosion rate. It is also observed from the figure that a second time constant appears at the high frequency in the presence of inhibitor. The second time constant can be attributed to the inhibitor film formation by the adsorbed ATPI molecules. The increase in diameter of the semicircle with the increase in the ATPI concentration, indicating the increase in charge transfer resistance (R_{ct}) value and decrease in corrosion rate (v_{corr}).

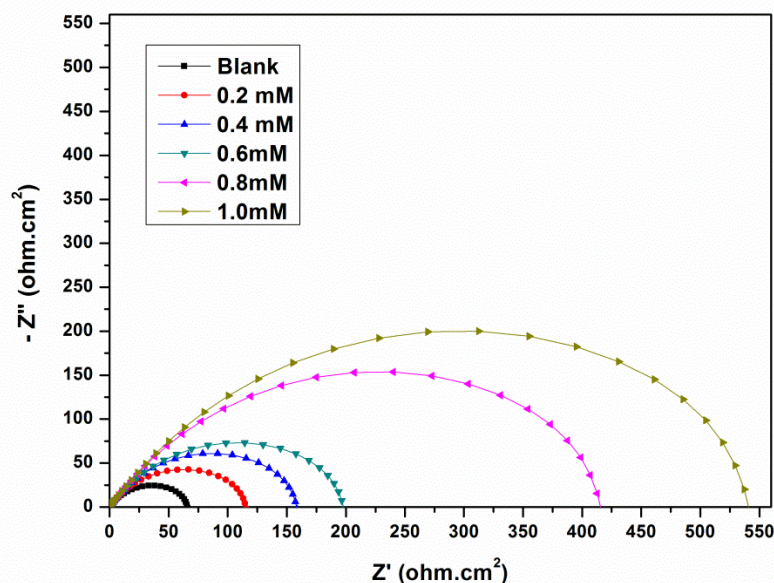


Fig. 3.19: Nyquist plots for the corrosion of weld aged maraging steel in 1.5 M hydrochloric acid containing different concentrations of ATPI at 30 °C.

In order to fit and analyse the EIS data, the experimental impedance results are simulated to pure electronic models that can verify or rule out mechanistic models and enable the calculation of numerical values corresponding to the physical and/or chemical properties of the electrochemical system under investigation. The equivalent circuit given in Fig. 3.3 was used to fit the experimental data for the corrosion of weld aged maraging steel in hydrochloric acid in the absence of ATPI. Hence the discussion in the section

3.1.2 on the equivalent circuit model for the corrosion of weld aged maraging steel in the absence of inhibitor holds good here also.

However, the impedance plots recorded for the corrosion of the alloy in the presence of ATPI were modelled by using the equivalent circuit depicted in Fig. 3.20 (best fit within the range of 4 – 5.5% error), which consists of the R_{ct} , C_{dl} , C_{pf} (film capacitance) and R_{pf} (film resistance). The R_{ct} , R_{pf} , C_{dl} and C_{pf} were determined by the analysis of Nyquist plots and their values are given in Table 3.12 to Table 3.16. The results show that the values of C_{dl} and C_{pf} decrease, while the values of R_{ct} and R_{pf} increase with the increase in the concentration of ATPI, suggesting that the amount of the inhibitor molecules adsorbed on the electrode surface increases as the concentration of ATPI increases (Amin et al. 2007). The decrease in C_{dl} and C_{pf} could be attributed to the decrease in local dielectric constant and/or an increase in the thickness of the electrical double layer, signifying that the ATPI molecules act by adsorption at the interface of metal/solution. The increase in R_{ct} and R_{pf} values is due to the gradual replacement of water molecules by the adsorption of inhibitor molecules on the surface to form an adherent film on the metal surface and thereby reducing the metal dissolution in the solution (Wang et al. 2010). The inhibitor molecule ATPI has the electron rich environment in phenyl group due to resonance of π -electrons of double bonds that can be adsorbed well on the sample surface. Also carbonyl groups are electron donating groups containing oxygen atom as an active site (Atta et al. 2011). ATPI inhibits the corrosion primarily through its adsorption and subsequent formation of a barrier film on the metal surface. This is accordance with the observations of Tafel polarization measurements.

In addition, the more the inhibitor is adsorbed, the more the thickness of the barrier layer is increased according to the expression of the Helmholtz model:

$$C_{dl} = \frac{\epsilon^{\circ}\epsilon}{d}S \quad (3.10)$$

where d is the thickness of the film, S the surface of the electrode, ϵ° the permittivity of the air and ϵ is the local dielectric constant.

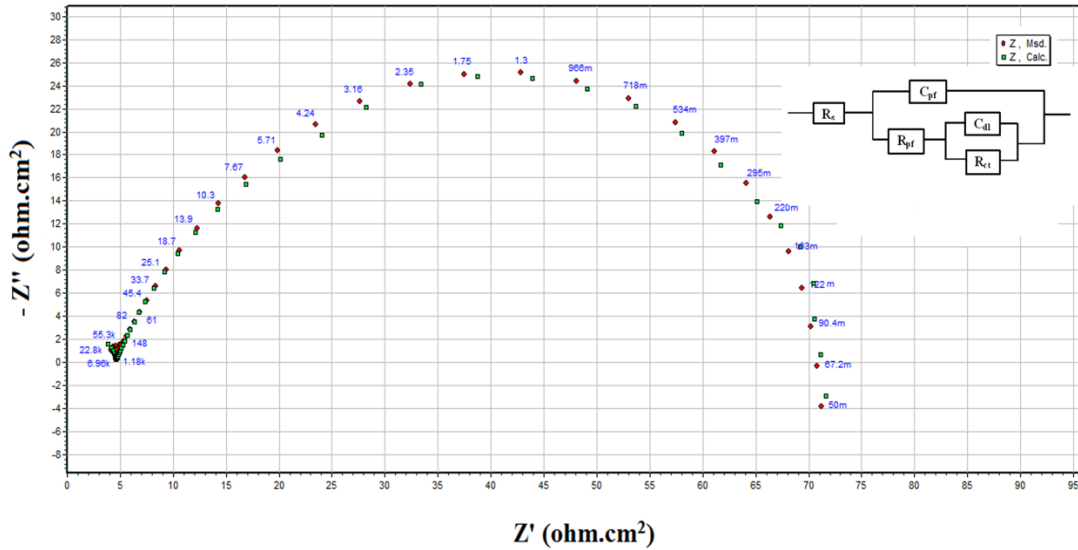


Fig. 3.20: Equivalent circuit used to fit the experimental EIS data for the corrosion of weld aged maraging steel specimen in hydrochloric acid in the presence of different concentration of ATPI.

The Bode plots for the corrosion of the alloy in the presence of different concentrations of ATPI are shown in Fig. 3.21. The frequency vs impedance plot shows the increase in impedance with the increase in the concentration of the inhibitor concentration, indicating the increase in corrosion resistance and inhibition efficiency. In the frequency vs phase angle plots the high frequency (HF) limits correspond to R_s , while the lower frequency (LF) limits correspond to $(R_{ct} + R_s)$, which are associated with the dissolution processes at the interface (Fouda et al. 2009). Phase angle increases with the increase in the concentrations of ATPI in hydrochloric acid. This might be attributed to the decrease in the capacitive behaviour on the metal surface due to the decrease in the dissolution rate of the metal. The difference between the HF limit and LF limit, corresponding to R_{ct} value for the inhibited system in the Bode plot increases with

increase in the concentration of ATPI (Elewady et al. 2008). The adsorption of ATPI on the metal surface modifies the interface between solution and metal surface and decreases its electrical capacity. This modification results in an increase of charge transfer resistance where the resulting adsorption films isolate the metal surface from the corrosive medium and decrease metal dissolution (Arab et al. 2008, Ozcan et al. 2004, Machnikova et al. 2008).

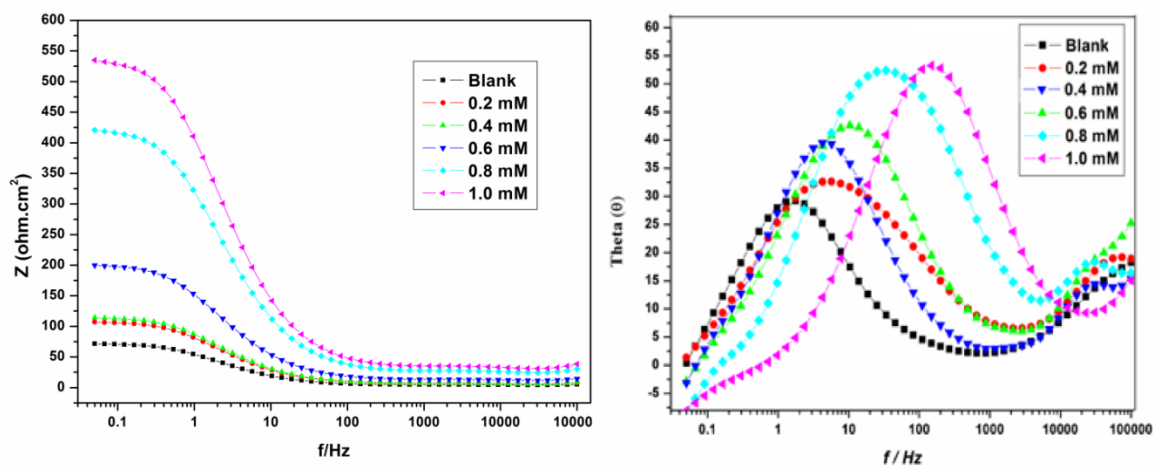


Fig. 3.21: Bode plots for the corrosion of weld aged maraging steel in 1.5 M hydrochloric acid containing different concentrations of ATPI at 30 °C.

A comparison of maximum attainable inhibition efficiencies by the Tafel method and EIS method, for the corrosion of weld aged maraging steel in hydrochloric acid solutions of different concentrations in the presence of ATPI at 30 °C are listed in Table 3.17. It is evident from Table that the inhibition efficiency values obtained by the two methods are in good agreement. Similar levels of agreement were obtained at other temperatures also.

3.3.3 Effect of temperature

The study on the effect of temperature on the corrosion rate and inhibition efficiency facilitates the calculation of kinetic and thermodynamic parameters for the

inhibition and the adsorption processes. These parameters are useful in interpreting the type of adsorption by the inhibitor. The results in Tables 3.7 to 3.16 indicate that the inhibition efficiency of ATPI decreases with the increase in temperature. It is also seen from the data in Tables 3.7 to 3.16, that the increase in solution temperature, does not alter the corrosion potential (E_{corr}), anodic Tafel slope (b_a) and cathodic Tafel slope (b_c) values significantly. This indicates that the increase in temperature does not change the mechanism of corrosion reaction (Poornima et al. 2011). However, i_{corr} and hence the corrosion rate of the specimen increases with the increase in temperature for both blank and inhibited solutions. The decrease in inhibition efficiency with the increase in temperature may be attributed to the higher dissolution rates of weld aged maraging steel at elevated temperature and also a possible desorption of adsorbed inhibitor due to the increased solution agitation resulting from higher rates of hydrogen gas evolution. The higher rate of hydrogen gas evolution may also reduce the ability of the inhibitor to be adsorbed on the metal surface. The decrease in inhibition efficiency with the increase in temperature is also suggestive of physisorption of the inhibitor molecules on the metal surface (Geetha et al. 2011).

The Arrhenius plots for the corrosion of weld aged maraging steel in the presence of different concentrations of ATPI in 1.5 M hydrochloric acid are shown in Fig. 3.22. The enthalpy and entropy of activation for the dissolution of the alloy, (ΔH^\ddagger & ΔS^\ddagger) were calculated from transition state theory equation as discussed in the section 2.7. The plots of $\ln(i_{\text{corr}}/T)$ versus $1/T$ for the corrosion of weld aged samples of maraging steel in the presence of different concentrations of ATPI in 1.5 M hydrochloric acid are shown in Fig. 3.23. The calculated values of activation parameters are recorded in Table 3.18. The results show that the value of E_a increases with the increase in the concentration of ATPI indicating that the energy barrier for the corrosion reaction increases. The extent of increase is proportional to the inhibitor concentration, indicating that the energy barrier for the corrosion reaction increases with the increase in ATPI concentration. It is also indicated that the whole process is controlled by surface reaction (Fouda et al. 2009), since the activation energies of the corrosion process are above 20 kJ mol^{-1} .

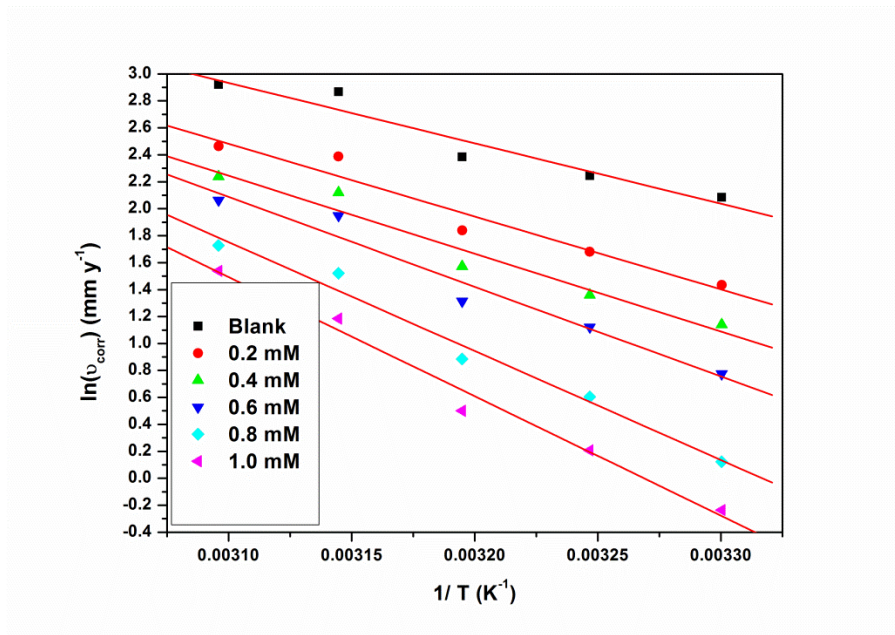


Fig. 3.22: Arrhenius plots for the corrosion of weld aged maraging steel in 1.5 M hydrochloric acid containing different concentrations of ATPI.

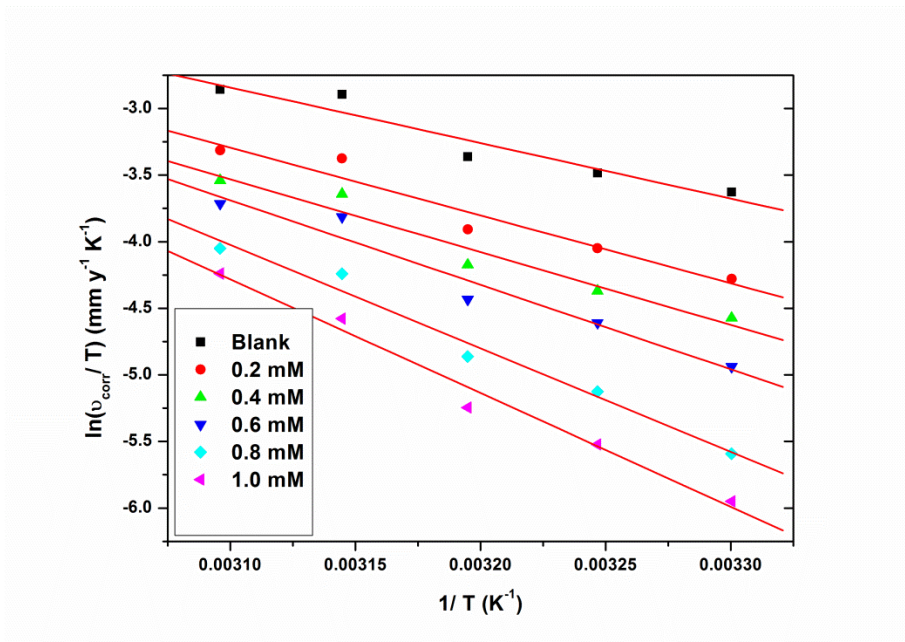


Fig. 3.23: Plots of $\ln(v_{\text{corr}}/T)$ versus $1/T$ for the corrosion of weld aged maraging steel in 1.5 M hydrochloric acid containing different concentrations of ATPI.

The adsorption of the inhibitor on the electrode surface leads to the formation of a physical barrier between the metal surface and the corrosion medium, blocking the charge transfer, and thereby reducing the metal reactivity in the electrochemical reactions of corrosion.

The entropy of activation values in the absence and the presence of ATPI are large and negative; this indicates that the activated complex formation in the rate-determining step represents an association rather than dissociation, decreasing the randomness on going from the reactants to the activated complex (Abd EI Rehim et al. 2003, Fekry et al. 2011).

3.3.4 Effect of hydrochloric acid concentration

It is evident from both polarization and EIS experimental results that, for a particular concentration of inhibitor, the inhibition efficiency decreases with the increase in hydrochloric acid concentration. The highest inhibition efficiency is observed at 0.1 M solution of hydrochloric acid. As the concentration of hydrochloric acid is increased, higher concentration of ATPI is required to achieve higher inhibition efficiency. Since the present investigation also aims at finding the optimum concentration of inhibitor required to get maximum inhibition efficiency, different concentrations of inhibitor have been used in different concentrations of hydrochloric acid instead of using same set of inhibitor concentration in all concentrations of hydrochloric acid. The decreased inhibition efficiency in solution of higher concentration of hydrochloric acid can be attributed to the higher corrosivity of the medium.

3.3.5 Adsorption isotherm

The information on the interaction between the inhibitor molecules and the metal surface can be provided by adsorption isotherm (Fekry et al. 2010). The adsorption of ATPI molecule on the metal surface can occur either through donor-acceptor interaction between the unshared electron pairs and/or π -electrons of inhibitor molecule and the vacant d-orbitals of the metal surface atoms or through electrostatic interaction of the

inhibitor molecules with already adsorbed chloride ions (Ashish Kumar et al. 2010). The adsorption bond strength is dependent on the composition of the metal, corrosive, inhibitor structure, concentration and orientation as well as temperature. The adsorption of an organic adsorbate at metal/solution interface can be presented as a substitution adsorption process between the organic molecules in aqueous solution (Inh_{aq}), and the water molecules on metallic surface ($\text{H}_2\text{O}_{\text{ads}}$), as given below (Tao et al. 2011):



where χ , the size ratio, is the number of water molecules displaced by one molecule of organic inhibitor. χ is assumed to be independent of coverage or charge on the electrode (Oguzie et al. 2008, Tao et al. 2010). In order to obtain an isotherm, the linear relation between the surface coverage (θ) value and concentration of the inhibitor (C_{inh}) must be found. The surface coverage θ is given by equation (2.3).

The values of θ at different concentrations of inhibitor in the solution (C_{inh}) were applied to various isotherms including Langmuir, Temkin, Frumkin and Florye - Huggins isotherms. It was found that the data fitted best with the Langmuir adsorption isotherm, which is given by the relation (Wang et al. 2010):

$$\frac{C_{\text{inh}}}{\theta} = C_{\text{inh}} + \frac{1}{K} \quad (3.12)$$

where K is the adsorption/desorption equilibrium constant, C_{inh} is the corrosion inhibitor concentration in the solution, and θ is the surface coverage. The plot of C_{inh}/θ versus C_{inh} gives a straight line with an intercept of $1/K$. The Langmuir adsorption isotherms for the adsorption of ATPI on the maraging steel surface are shown in Fig. 3.24. The plots are linear, with an average correlation coefficient (R^2) of 0.993.

The linear regression coefficients are close to unity and the slopes of straight lines are nearly unity, suggesting that the adsorption of ATPI obeys Langmuir's adsorption

isotherm and there is negligible interaction between the adsorbed molecules (Li et al. 2008). The high values of K_{ads} for the studied inhibitor indicate strong adsorption of inhibitor on the alloy surface. The values of standard free energy of adsorption (ΔG^0_{ads}) were calculated using equation 2.9. The standard enthalpy of adsorption (ΔH^0_{ads}) and standard entropy of adsorption (ΔS^0_{ads}) were calculated from the plots of (ΔG^0_{ads}) vs T as per the equation (2.10). The thermodynamic parameters for the adsorption of ATPI on the weld aged maraging steel are listed in Tables 3.19.

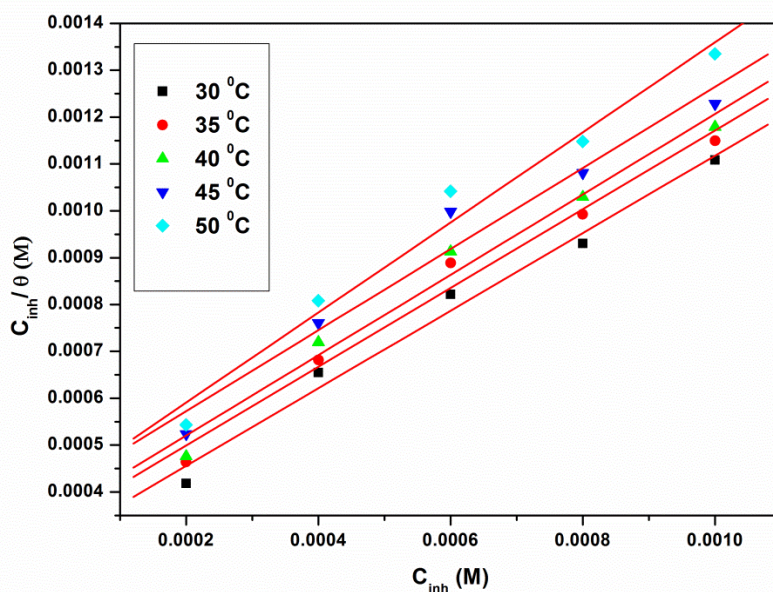


Fig. 3.24: Langmuir adsorption isotherms for the adsorption of ATPI on weld aged maraging steel in 1.5 M hydrochloric acid at different temperatures.

The negative values of ΔG^0_{ads} indicate the spontaneity of the adsorption process and the stability of the adsorbed layer on the metal surface (Tao et al. 2011). Generally the values of ΔG^0_{ads} less negative than -20 kJ mol^{-1} are consistent with physisorption, while those more negative than -40 kJ mol^{-1} are corresponding to chemisorptions (Fuchs et al. 2006). The calculated values of ΔG^0_{ads} obtained in this study range between $-29.5 \text{ kJ mol}^{-1}$ and $-36.4 \text{ kJ mol}^{-1}$, indicating both physical and chemical adsorption behaviour of

ATPI on the metal surface. These values indicate that the adsorption process may involve complex interactions involving both physical and chemical adsorption of the inhibitor (Hosseini et al. 2003, Machnikova et al. 2008). The fact that both ΔG_{ads}^0 and inhibition efficiency decrease with the increase in temperature, indicates that the adsorption of ATPI on the weld aged maraging steel surface in hydrochloric acid are not favoured at high temperature and hence can be considered to be predominantly physisorption.

The negative sign of ΔH_{ads}^0 in hydrochloric acid solution indicates that the adsorption of inhibitor molecules is an exothermic process. Generally, an exothermic adsorption process signifies either physisorption or chemisorptions while the endothermic process is attributable unequivocally to chemisorption. Typically, the enthalpy of a physisorption process is less negative than $-41.86 \text{ kJ mol}^{-1}$, while that of a chemisorption process approaches -100 kJ mol^{-1} (Martinez and Stern 2002). In the present study, the value of ΔH_{ads}^0 found to be less negative than $-41.86 \text{ kJ mol}^{-1}$, which shows that the adsorption of ATPI on weld aged maraging steel involves physisorption phenomena. From the values of both ΔG_{ads}^0 and ΔH_{ads}^0 it can be confirmed that the adsorption of ATPI on the alloy surface is mixed type with predominant physisorption.

The ΔS_{ads}^0 value is large and negative; indicating that decrease in disordering takes place on going from the reactant to the alloy adsorbed species. This can be attributed to the fact that adsorption is always accompanied by decrease in entropy (Ashish Kumar et al. 2010). It is also seen from the Table 3.19 that ΔS_{ads}^0 increases with the increase in inhibitor concentration. This could be the result of the adsorption of inhibitor molecules, which could be regarded as a quasi-substitution process between inhibitor molecule and water molecule at the electrode surface. In the present case the solvent entropy resulting from the desorption of water molecules from the metal surface overweighs the decrease in entropy due to the orderly arrangement of inhibitor molecule on the metal surface.

3.3.6 Mechanism of corrosion inhibition

The inhibitive effect of ATPI on the corrosion of weld aged maraging steel can be accounted for on the basis of its adsorption on the alloy surface. The adsorption of ATPI molecules on the metal surface can be attributed to the presence of electronegative elements like oxygen, nitrogen and sulphur and also to the presence of π -electron cloud in the benzene ring of the molecule. The adsorption mechanism for a given inhibitor depends on factors, such as the nature of the metal, the corrosive medium, the pH, and the concentration of the inhibitor as well as the functional groups present in its molecule, since different groups are adsorbed to different extents (Bilgic et al. 2003, Taner et al. 2009, Wang et al. 2010). Weld aged maraging steel consists of segregated alloying elements along the grain boundaries. Since these segregations have different composition, their electrochemical behaviour is expected to be different from that of the matrix. Also, the lattice mismatch between the precipitate and the matrix causes strain field around the segregated precipitates. These strain fields in combination with the galvanic effect due to the composition difference leads to the enhanced corrosion of weld aged maraging steel in acid medium. Considering the inhomogeneous nature, the surface of the alloy is generally characterized by multiple adsorption sites having different activation energies and enthalpies of adsorption. Inhibitor molecules may thus be adsorbed more readily at surface active sites having suitable adsorption enthalpies (Poornima et al. 2011).

On the other hand, iron is well known for its coordination affinity to ligands possessing heteroatom (Hackerman et al. 1996). Increase in inhibition efficiencies with increase in inhibitor concentration shows that the inhibition action is due to the adsorption on the maraging steel surface. Adsorption may take place by organic molecules at metal/solution interface due to electrostatic attraction between the charged molecules and charged metal, interaction of unshared electron pairs in the molecule with the metal, interaction of π - electrons with the metal or the combination of the above (Selim et al. 1996). To understand the mechanism of inhibition and the effect of inhibitor in aggressive acidic environment, some knowledge of interaction between the protective

compound and the metal surface is required. Many organic corrosion inhibitors have at least one polar unit with a heteroatom; this polar unit is regarded as the reaction centre for the adsorption process (Gao et al. 2009).

It is considered that in acidic solution the ATPI molecule can undergo protonation at its amino group and can exist as a protonated positive species. In a highly acidic medium like the one in the present investigation, the metal surface is positively charged. This would cause the negatively charged chloride ions to become adsorbed on the metal surface, making the metal surface negatively charged. The positively charged protonated ATPI molecules can interact electrostatically with the negatively charged chloride adsorbed metal surface, resulting in physisorption (Ekpe et al. 1995, Quraishi et al. 2003, Maayta et al. 2004). The negative charge centres of the ATPI molecules containing a lone pair of electrons and/or π electrons can electrostatically interact with the anodic sites on the metal surface and get adsorbed. The neutral inhibitor molecules may occupy the vacant adsorption sites on the metal surface through the chemisorption mode involving the displacement of water molecules from the metal surface and sharing of electrons by the hetero atoms like oxygen or nitrogen. Chemisorption is also possible by the donor - acceptor interactions between π electrons of the aromatic ring and the vacant d orbitals of iron, providing another mode of protection (El Azhar et al. 2001, Wang, et al. 2004, Barouni et al. 2008). The presence of ATPI in the protonated form and the presence of negative charge centres on the molecule are also responsible for the mutual interaction of inhibitor molecules on the alloy surface (Popova et al. 2004, Morad et al. 2006, Solmaz et al. 2008). This is reflected in the deviation of slopes of Langmuir adsorption isotherms as discussed in the previous section.

3.3.7 SEM/EDS studies

In order to differentiate between the surface morphology and to identify the composition of the species formed on the metal surface after its immersion in hydrochloric acid in the absence and in the presence of ATPI, SEM/EDS investigations were carried out. Fig. 3.25 (a) represents SEM image of the corroded weld aged maraging

steel sample. The corroded surface shows detachment of particles from the surface. The corrosion of the alloy may be predominantly attributed to the inter-granular corrosion assisted by the galvanic effect between the precipitates and the matrix, along the grain boundaries. Fig. 3.25 (b) represents SEM image of weld aged maraging steel after the corrosion tests in a medium of 1.5 M hydrochloric acid containing 1.0 mM of ATPI. The image clearly shows a smooth surface due to the adsorbed layer of inhibitor molecules on the alloy surface, thus protecting the metal from corrosion.

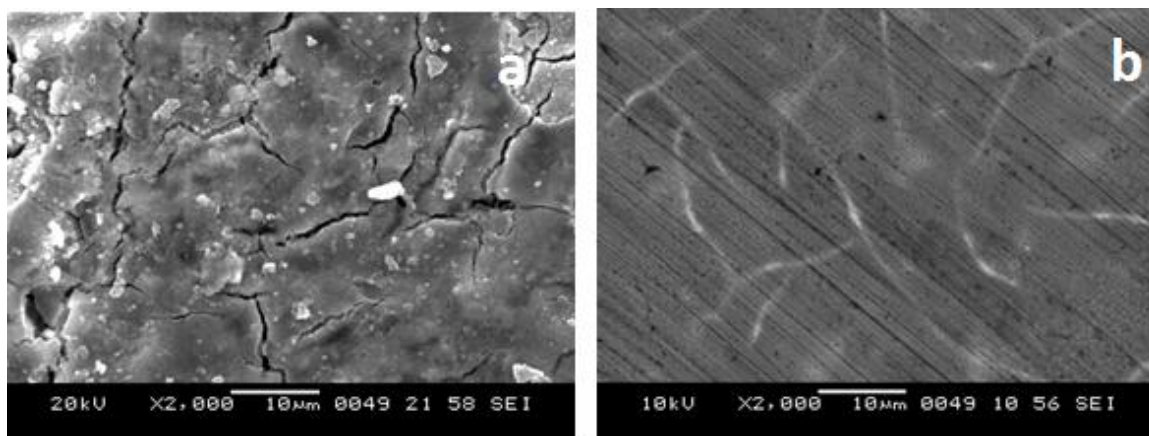


Fig. 3.25: SEM images of the weld aged maraging steel after immersion in 1.5 M hydrochloric acid a) in the absence and b) in the presence of ATPI.

EDS investigations were carried out in order to identify the composition of the species formed on the metal surface in 1.5 hydrochloric acid in the absence and presence of ATPI. The corresponding EDS profile analyses for the selected areas on the alloy sample in the absence and presence of ATPI are shown in Fig. 3.26 (a) and 3.26 (b), respectively, after immersion for 3 h in 1.5 M hydrochloric acid. The atomic percentages of the elements found in the EDS profile of the corroded metal surface were 13.18% Fe, 4.53 Ni, 3.18% Mo, 66.21% O and 3.2 % Co and indicated that iron oxide is existing in this area. The atomic percentages of the elements found in the EDS profile of the inhibited metal surface were 22.5 % Fe, 9.87% S, 7.2% Ni, 2.11% Mo, 30.1 % O, 9.4% N, 4.6% Co, 1.92 % Cl and 18.54 % C and indicated the formation of inhibitor film in

this area. The elemental compositions mentioned above were mean values of different regions.

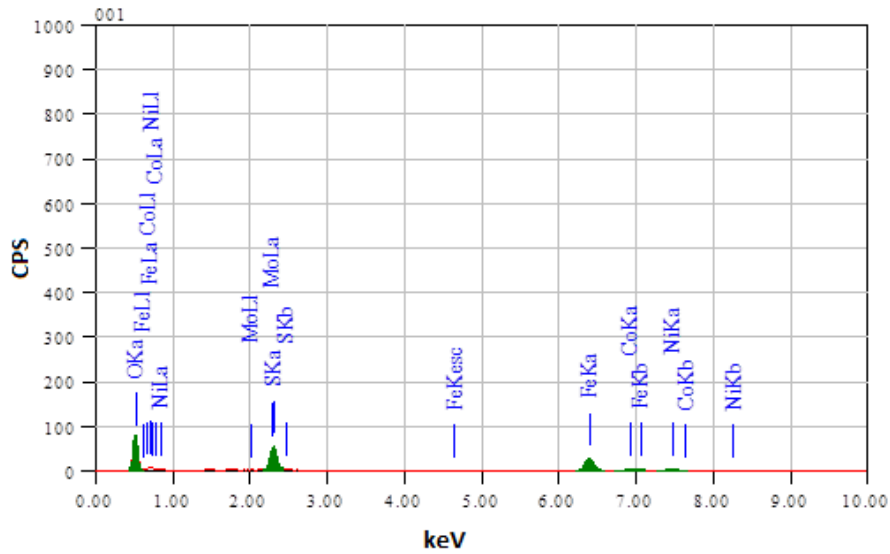


Fig. 3.26 (a): EDS spectra of the weld aged maraging steel after immersion in 1.5 hydrochloric acid in the absence of ATPI.

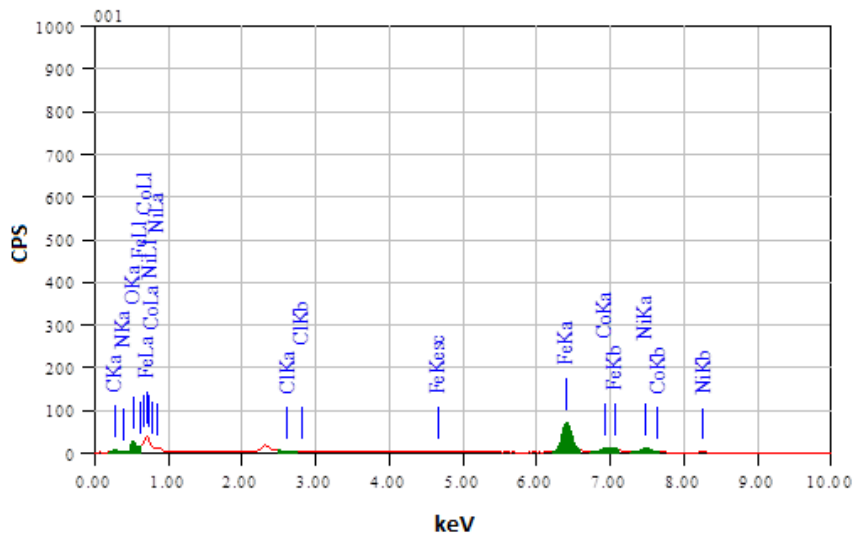


Fig. 3.26 (b): EDS spectra of the weld aged maraging steel after immersion in 1.5 M hydrochloric acid in the presence of ATPI.

Table 3.7: Results of potentiodynamic polarization studies for the corrosion of weld aged maraging steel in 0.1 M hydrochloric acid containing different concentrations of ATPI.

Temperature (°C)	Conc. of inhibitor (mM)	E_{corr} (mV /SCE)	b_a (mV dec ⁻¹)	$-b_c$ (mV dec ⁻¹)	i_{corr} (mA cm ⁻²)	v_{corr} (mm y ⁻¹)	η (%)
30	Blank	-419±3	142±3	226±3	0.22±0.02	2.53±0.23	
	0.1	-416±2	139±3	226±3	0.11±0.01	1.20±0.14	52.4
	0.2	-410±1	138±3	224±1	0.07±0.01	0.86±0.13	66.2
	0.4	-408±2	133±3	217±1	0.04±0.02	0.50±0.18	80.1
	0.6	-406±2	131±1	213±1	0.03±0.02	0.32±0.20	87.3
	0.8	-402±2	126±1	211±3	0.01±0.01	0.14±0.11	94.6
	35	Blank	-416±3	150±3	234±3	0.26±0.02	2.99±0.20
0.1		-415±2	151±3	233±1	0.15±0.01	1.77±0.12	40.9
0.2		-411±1	149±1	231±3	0.11±0.02	1.23±0.22	58.8
0.4		-410±2	142±1	225±3	0.07±0.03	0.79±0.25	73.7
0.6		-406±3	139±1	222±1	0.05±0.03	0.55±0.26	81.6
0.8		-401±1	135±1	221±3	0.03±0.01	0.32±0.10	89.2
40		Blank	-412±2	159±1	242±3	0.30±0.01	3.45±0.14
	0.1	-410±1	158±2	241±3	0.18±0.01	2.11±0.12	39.0
	0.2	-405±3	156±1	239±1	0.13±0.01	1.48±0.11	57.1
	0.4	-404±1	152±1	235±3	0.08±0.02	0.96±0.23	72.1
	0.6	-399±1	150±1	233±1	0.06±0.02	0.69±0.21	80.1
	0.8	-398±2	145±3	231±3	0.04±0.01	0.42±0.12	87.8
	45	Blank	-409±2	165±3	250±2	0.33±0.01	3.80±0.13
0.1		-403±3	161±1	251±1	0.21±0.02	2.44±0.20	35.7
0.2		-400±3	160±3	249±2	0.16±0.02	1.78±0.24	53.1
0.4		-401±1	153±1	244±3	0.11±0.01	1.23±0.11	67.5
0.6		-397±1	152±2	241±3	0.09±0.03	0.99±0.29	73.8
0.8		-391±1	149±1	240±1	0.05±0.02	0.62±0.24	83.6
50		Blank	-405±3	173±2	259±2	0.37±0.03	4.26±0.27
	0.1	-406±3	171±1	257±1	0.25±0.03	2.85±0.30	33.1
	0.2	-400±3	169±2	256±3	0.19±0.02	2.15±0.20	49.4
	0.4	-398±3	165±3	252±3	0.13±0.02	1.54±0.16	63.8
	0.6	-394±3	164±2	250±1	0.11±0.02	1.23±0.19	71.1
	0.8	-392±1	158±1	244±3	0.07±0.02	0.81±0.24	81.0

Table 3.8: Results of potentiodynamic polarization studies for the corrosion of weld aged maraging steel in 0.5 M hydrochloric acid containing different concentrations of ATPI.

Temperature (°C)	Conc. of inhibitor (mM)	E_{corr} (mV /SCE)	b_a (mV dec ⁻¹)	$-b_c$ (mV dec ⁻¹)	i_{corr} (mA cm ⁻²)	v_{corr} (mm y ⁻¹)	η (%)
30	Blank	-413±2	148±2	247±2	0.27±0.02	3.11±0.24	
	0.1	-414±3	140±4	242±3	0.13±0.01	1.54±0.11	50.4
	0.2	-408±3	135±4	235±3	0.10±0.02	1.15±0.18	63.1
	0.4	-406±3	130±3	232±2	0.06±0.03	0.69±0.27	77.7
	0.6	-403±3	127±1	229±1	0.04±0.01	0.45±0.14	85.6
	0.8	-401±2	124±3	227±4	0.02±0.01	0.23±0.11	92.5
35	Blank	-411±2	156±2	254±1	0.35±0.02	4.03±0.19	
	0.1	-410±3	147±4	252±1	0.18±0.02	2.08±0.22	48.3
	0.2	-406±2	140±4	247±3	0.14±0.01	1.57±0.11	61.1
	0.4	-407±2	137±2	244±2	0.08±0.02	0.97±0.21	75.9
	0.6	-403±3	134±1	241±2	0.06±0.03	0.65±0.25	83.9
	0.8	-398±2	132±1	239±2	0.03±0.02	0.36±0.24	91.3
40	Blank	-408±2	165±1	262±2	0.42±0.02	4.83±0.21	
	0.1	-404±2	159±2	257±3	0.23±0.02	2.62±0.20	45.8
	0.2	-400±2	152±4	250±3	0.17±0.02	2.00±0.18	58.7
	0.4	-398±1	149±4	247±4	0.11±0.03	1.27±0.29	73.7
	0.6	-394±1	146±4	244±4	0.08±0.03	0.88±0.28	81.7
	0.8	-393±4	144±1	242±3	0.05±0.01	0.54±0.12	88.9
45	Blank	-406±3	172±1	269±2	0.52±0.01	5.87±0.14	
	0.1	-399±2	164±3	265±1	0.29±0.02	3.39±0.22	42.2
	0.2	-396±1	157±2	260±3	0.23±0.03	2.63±0.28	55.2
	0.4	-397±2	154±3	257±4	0.15±0.01	1.74±0.11	70.4
	0.6	-392±1	151±1	254±1	0.11±0.02	1.26±0.18	78.5
	0.8	-387±4	149±4	252±4	0.07±0.02	0.84±0.23	85.7
50	Blank	-404±4	183±4	277±1	0.59±0.03	6.79±0.26	
	0.1	-400±3	175±3	275±2	0.36±0.02	4.16±0.16	38.6
	0.2	-394±1	168±3	270±1	0.29±0.02	3.27±0.20	51.7
	0.4	-393±3	165±4	267±1	0.19±0.02	2.24±0.15	67.1
	0.6	-388±4	162±3	264±2	0.15±0.02	1.68±0.23	75.3
	0.8	-385±3	160±3	262±2	0.10±0.03	1.18±0.28	82.5

Table 3.9: Results of potentiodynamic polarization studies for the corrosion of weld aged maraging steel in 1.0 M hydrochloric acid containing different concentrations of ATPI.

Temperature (°C)	Conc. of inhibitor (mM)	E_{corr} (mV /SCE)	b_a (mV dec ⁻¹)	$-b_c$ (mV dec ⁻¹)	i_{corr} (mA cm ⁻²)	v_{corr} (mm y ⁻¹)	η (%)
30	Blank	-371±2	153±2	256±3	0.33±0.03	3.80±0.25	
	0.2	-373±4	149±4	254±1	0.16±0.03	1.81±0.27	52.3
	0.4	-370±1	146±2	251±1	0.12±0.01	1.34±0.13	64.7
	0.6	-368±3	142±3	247±1	0.08±0.01	0.93±0.15	75.6
	0.8	-365±2	140±2	244±2	0.05±0.03	0.59±0.28	84.5
	1.0	-361±3	137±1	242±1	0.02±0.01	0.26±0.12	93.2
35	Blank	-368±2	159±1	261±1	0.45±0.02	5.20±0.21	
	0.2	-366±4	155±2	258±3	0.23±0.04	2.58±0.37	50.3
	0.4	-362±4	152±2	255±1	0.17±0.02	1.93±0.25	62.8
	0.6	-359±1	150±3	251±2	0.12±0.03	1.36±0.33	73.8
	0.8	-356±3	147±1	248±3	0.08±0.01	0.89±0.13	82.8
	1.0	-352±1	142±4	246±4	0.04±0.02	0.44±0.17	91.6
40	Blank	-364±2	165±3	266±3	0.56±0.02	6.45±0.17	
	0.2	-361±1	163±3	262±5	0.29±0.02	3.36±0.18	47.9
	0.4	-360±2	160±3	260±1	0.22±0.02	2.54±0.17	60.6
	0.6	-357±1	158±2	257±2	0.16±0.02	1.82±0.24	71.7
	0.8	-355±1	156±4	255±2	0.11±0.01	1.24±0.13	80.8
	1.0	-350±1	151±1.	252±1	0.06±0.02	0.66±0.15	89.7
45	Blank	-361±4	172±2	273±1	0.76±0.04	8.72±0.39	
	0.2	-359±4	170±2	270±3	0.42±0.01	4.80±0.12	44.9
	0.4	-356±1.	168±2	268±1	0.32±0.03	3.69±0.33	57.7
	0.6	-352±1	165±2	265±2	0.24±0.01	2.71±0.14	68.9
	0.8	-350±2	161±1	261±2	0.17±0.02	1.91±0.20	78.1
	1.0	-347±3	157±1	258±2	0.10±0.01	1.13±0.31	87.2
50	Blank	-358±3	177±2	278±3	0.92±0.02	10.63±0.24	
	0.2	-355±1	172±1	275±4	0.54±0.04	6.24±0.36	41.3
	0.4	-352±1	170±2	273±4	0.42±0.03	4.86±0.26	54.2
	0.6	-350±4	168±4	270±2	0.32±0.02	3.66±0.22	65.6
	0.8	-347±3	165±3	268±1	0.23±0.04	2.67±0.39	74.8
	1.0	-344±4	162±4	265±4	0.15±0.02	1.71±0.21	83.9

Table 3.10: Results of potentiodynamic polarization studies for the corrosion of weld aged maraging steel in 1.5 M hydrochloric acid containing different concentrations of ATPI.

Temperature (°C)	Conc. of inhibitor (mM)	E_{corr} (mV /SCE)	b_a (mV dec ⁻¹)	$-b_c$ (mV dec ⁻¹)	i_{corr} (mA cm ⁻²)	v_{corr} (mm y ⁻¹)	η (%)
30	Blank	-342±3	158±1	267±1	0.70±0.02	8.05±0.18	
	0.2	-339±3	153±4	262±3	0.37±0.02	4.20±0.18	47.8
	0.4	-334±2	146±3	255±1	0.27±0.03	3.13±0.29	61.1
	0.6	-330±3	143±2	252±1	0.19±0.02	2.17±0.16	73.1
	0.8	-326±2	140±4	249±4	0.10±0.03	1.13±0.31	86.3
	1.0	-322±3	138±4	247±4	0.07±0.01	0.79±0.12	90.3
	35	Blank	-339±3	165±4.	276±3	0.82±0.03	9.45±0.26
0.2		-333±3	163±4	277±3	0.47±0.02	5.37±0.22	43.1
0.4		-331±3	156±2	269±3	0.34±0.03	3.90±0.30	58.7
0.6		-330±2	153±2	266±4	0.27±0.02	3.07±0.15	67.5
0.8		-327±4	150±1	263±4	0.16±0.04	1.83±0.36	80.6
1.0		-321±1	148±4	261±1	0.11±0.02	1.23±0.23	87.1
40		Blank	-337±4	173±4	282±3	0.94±0.02	10.85±0.19
	0.2	-334±2	171±3	283±2	0.55±0.01	6.29±0.15	42.1
	0.4	-329±3	164±2	276±1	0.42±0.02	4.82±0.25	55.6
	0.6	-327±4	161±1	272±2	0.32±0.01	3.72±0.12	65.7
	0.8	-323±4	158±1	269±1	0.21±0.03	2.42±0.26	77.7
	1.0	-322±4	156±3	267±1	0.14±0.03	1.65±0.33	84.8
	45	Blank	-334±3	179±1	286±2	1.53±0.02	17.60±0.25
0.2		-327±1	174±2	281±3	0.95±0.03	10.88±0.33	38.2
0.4		-324±2	167±1	274±2	0.73±0.04	8.34±0.37	52.6
0.6		-324±4	164±2	271±1	0.61±0.01	7.02±0.10	60.1
0.8		-320±4	161±4	268±1	0.40±0.02	4.58±0.18	74.0
1.0		-326±2	159±2	266±3	0.29±0.04	3.27±0.37	81.4
50		Blank	-332±4	185±1	292±2	1.61±0.04	18.57±0.36
	0.2	-328±1	184±2	293±1	1.02±0.02	11.74±0.19	36.8
	0.4	-322±1	177±3	286±1	0.82±0.03	9.38±0.28	49.5
	0.6	-319±3	173±3	283±2	0.68±0.03	7.87±0.31	57.6
	0.8	-316±4	170±4	280±4	0.49±0.04	5.63±0.37	69.7
	1.0	-314±1	168±3	278±4	0.41±0.03	4.66±0.26	74.9

Table 3.11: Results of potentiodynamic polarization studies for the corrosion of weld aged maraging steel in 2.0 M hydrochloric acid containing different concentrations of ATPI.

Temperature (°C)	Conc. of inhibitor (mM)	E_{corr} (mV /SCE)	b_a (mV dec ⁻¹)	$-b_c$ (mV dec ⁻¹)	i_{corr} (mA cm ⁻²)	v_{corr} (mm y ⁻¹)	η (%)
30	Blank	-324±3	175±4	287±3	2.77±0.03	31.85±0.32	
	0.3	-319±1	167±2	288±2	1.62±0.03	18.58±0.25	41.5
	0.6	-315±3	160±1	281±3	1.24±0.01	14.29±0.12	55.1
	0.9	-313±1	157±4	278±1	0.89±0.03	10.23±0.27	67.8
	1.2	-309±4	154±1	274±4	0.69±0.04	7.97±0.36	74.9
	1.5	-308±4	152±1	272±2	0.46±0.04	5.33±0.40	83.2
	35	Blank	-321±1	182±3	293±4	3.09±0.02	35.49±0.23
0.3		-315±4	181±1	288±1	1.87±0.01	21.48±0.13	39.3
0.6		-311±4	173±1	281±4	1.45±0.03	16.64±0.29	53.3
0.9		-310±3	170±3	278±4	1.05±0.04	12.06±0.36	65.9
1.2		-307±4	167±3	275±2	0.83±0.01	9.52±0.15	73.1
1.5		-303±2	165±2	273±4	0.57±0.02	6.55±0.24	81.5
40		Blank	-319±1	189±3	300±4	3.39±0.01	39.03±0.11
	0.3	-314±3	184±4	301±3	2.48±0.01	28.48±0.11	36.8
	0.6	-310±1	177±3	294±3	1.94±0.03	22.26±0.35	50.6
	0.9	-309±3	174±1	291±4	1.42±0.02	16.37±0.20	63.7
	1.2	-303±4	171±2	288±3	1.14±0.03	13.11±0.30	70.9
	1.5	-302±2	169±4	286±1	0.81±0.04	9.29±0.35	79.4
	45	Blank	-315±4	196±1	307±4	3.63±0.03	41.73±0.30
0.3		-309±3	195±4	302±3	2.40±0.03	27.57±0.32	33.8
0.6		-305±3	188±2	295±1	1.89±0.01	21.78±0.11	47.7
0.9		-304±4	185±3	292±2	1.42±0.01	16.28±0.14	60.9
1.2		-301±1	182±4	289±4	1.15±0.03	13.24±0.34	68.2
1.5		-296±4	180±4	287±4	0.84±0.02	9.67±0.21	76.7
50		Blank	-312±1	203±1	312±3	3.89±0.02	44.77±0.20
	0.3	-309±1	202±4	313±3	2.71±0.02	31.20±0.24	30.3
	0.6	-304±4	195±2	306±3	2.16±0.02	24.90±0.17	44.3
	0.9	-302±1	192±3	303±4	1.65±0.03	18.94±0.29	57.6
	1.2	-296±3	189±3	300±2	1.36±0.04	15.63±0.39	65.6
	1.5	-297±1	187±4	298±2	1.02±0.01	11.77±0.15	73.7

Table 3.12: EIS data for the corrosion of weld aged maraging steel in 0.1 M hydrochloric acid containing different concentrations of ATPI.

Temperature (°C)	Conc. of inhibitor (mM)	R_{ct} (ohm. cm ²)	C_{dl} (mF cm ⁻²)	R_{pf} (ohm. cm ²)	C_{pf} (mF cm ⁻²)	η (%)
30	Blank	181.20±3.11	0.93±0.22			
	0.1	395.98±2.99	0.70±0.14	26.28±2.41	0.23±0.07	54.2
	0.2	569.45±4.52	0.56±0.14	36.95±2.82	0.19±0.09	68.2
	0.4	1019.12±3.54	0.41±0.15	64.62±2.24	0.15±0.04	82.2
	0.6	1724.07±4.60	0.33±0.12	107.99±2.78	0.13±0.09	89.5
	0.8	5789.14±4.59	0.26±0.06	358.09±3.87	0.11±0.08	96.9
	35	Blank	158.00±3.06	1.10±0.15		
0.1		273.97±2.08	0.94±0.19	18.78±1.78	0.30±0.10	42.3
0.2		399.90±3.92	0.71±0.28	26.52±1.63	0.24±0.06	60.5
0.4		644.63±4.51	0.53±0.14	41.58±2.01	0.18±0.05	75.5
0.6		954.68±2.89	0.43±0.10	60.66±1.26	0.16±0.05	83.5
0.8		1795.45±3.69	0.33±0.07	112.38±3.27	0.13±0.04	91.2
40		Blank	135.21±2.68	1.40±0.29		
	0.1	225.91±4.56	1.16±0.19	15.82±1.35	0.36±0.06	40.2
	0.2	325.73±3.14	0.88±0.19	21.96±2.86	0.28±0.07	58.5
	0.4	513.13±2.76	0.64±0.23	33.49±2.75	0.22±0.07	73.7
	0.6	738.45±2.37	0.51±0.11	47.35±1.91	0.18±0.06	81.7
	0.8	1290.17±3.09	0.39±0.05	81.30±4.52	0.15±0.08	89.5
	45	Blank	127.54±2.55	1.55±0.25		
0.1		200.95±3.90	1.33±0.24	14.28±1.47	0.41±0.08	36.5
0.2		277.68±2.81	1.02±0.23	19.00±2.50	0.32±0.06	54.1
0.4		407.09±4.31	0.77±0.12	26.97±1.46	0.25±0.09	68.7
0.6		509.96±2.84	0.66±0.19	33.29±1.34	0.22±0.06	75.0
0.8		844.08±4.30	0.49±0.09	53.85±3.13	0.17±0.09	84.9
50		Blank	117.23±2.47	1.80±0.11		
	0.1	177.27±3.70	1.56±0.17	12.83±1.70	0.47±0.06	33.9
	0.2	236.30±3.08	1.23±0.20	16.46±2.24	0.38±0.06	50.4
	0.4	333.89±3.07	0.93±0.22	22.46±1.16	0.30±0.08	64.9
	0.6	422.15±4.88	0.79±0.21	27.89±1.22	0.26±0.07	72.2
	0.8	659.71±3.39	0.58±0.11	42.51±2.61	0.20±0.04	82.2

Table 3.13: EIS data for the corrosion of weld aged maraging steel in 0.5 M hydrochloric acid containing different concentrations of ATPI.

Temperature (°C)	Conc. of inhibitor (mM)	R_{ct} (ohm. cm ²)	C_{dl} (mF cm ⁻²)	R_{pf} (ohm. cm ²)	C_{pf} (mF cm ⁻²)	η (%)
30	Blank	156.30±2.45	0.96±0.31			
	0.1	328.50±3.70	0.74±0.31	22.13±2.01	0.24±0.12	52.4
	0.2	448.49±2.79	0.60±0.27	29.51±3.55	0.20±0.08	65.2
	0.4	781.50±3.31	0.44±0.15	50.00±2.16	0.16±0.06	80.1
	0.6	1300.33±5.18	0.35±0.12	81.92±3.91	0.13±0.07	88.0
	0.8	3157.58±4.21	0.28±0.07	196.19±3.03	0.11±0.05	95.1
35	Blank	139.27±3.05	1.17±0.33			
	0.1	277.87±3.27	0.85±0.23	19.01±3.20	0.27±0.06	49.9
	0.2	373.78±2.93	0.69±0.22	24.92±2.91	0.23±0.09	62.7
	0.4	625.65±3.34	0.50±0.17	40.41±3.43	0.18±0.06	77.7
	0.6	980.77±3.48	0.40±0.13	62.26±2.72	0.15±0.03	85.8
	0.8	1972.66±5.79	0.31±0.10	123.29±3.78	0.12±0.01	92.9
40	Blank	123.15±2.63	1.45±0.37			
	0.1	232.62±2.34	1.01±0.29	16.23±2.02	0.32±0.06	47.1
	0.2	308.26±2.05	0.82±0.27	20.88±2.71	0.27±0.04	60.1
	0.4	496.57±3.15	0.59±0.15	32.47±3.22	0.20±0.05	75.2
	0.6	739.20±4.82	0.47±0.16	47.40±2.17	0.17±0.08	83.3
	0.8	1304.56±5.13	0.37±0.11	82.18±2.69	0.14±0.06	90.6
45	Blank	107.56±2.43	1.74±0.37			
	0.1	190.17±2.48	1.20±0.23	13.62±2.06	0.37±0.03	43.4
	0.2	247.66±3.90	0.98±0.29	17.16±3.16	0.31±0.04	56.6
	0.4	382.37±3.55	0.71±0.27	25.44±2.69	0.24±0.09	71.9
	0.6	540.50±5.30	0.57±0.13	35.17±3.94	0.20±0.09	80.1
	0.8	852.30±3.90	0.44±0.10	54.36±2.29	0.16±0.07	87.4
50	Blank	90.34±3.39	1.83±0.30			
	0.1	150.07±3.62	1.40±0.38	11.15±2.81	0.43±0.09	39.8
	0.2	192.42±3.58	1.14±0.37	13.76±2.77	0.36±0.06	53.1
	0.4	286.88±2.89	0.84±0.33	19.57±3.59	0.27±0.11	68.5
	0.6	389.73±4.16	0.68±0.14	25.90±3.43	0.23±0.06	76.8
	0.8	571.05±3.80	0.53±0.12	37.05±3.70	0.18±0.10	84.2

Table 3.14: EIS data for the corrosion of weld aged maraging steel in 1.0 M hydrochloric acid containing different concentrations of ATPI.

Temperature (°C)	Conc. of inhibitor (mM)	R_{ct} (ohm. cm ²)	C_{dl} (mF cm ⁻²)	R_{pf} (ohm. cm ²)	C_{pf} (mF cm ⁻²)	η (%)
30	Blank	116.20±2.52	1.68±0.22			
	0.2	253.93±2.08	1.09±0.24	17.54±2.89	0.34±0.19	54.2
	0.4	349.68±4.36	0.85±0.35	23.43±2.57	0.27±0.11	66.8
	0.6	522.95±5.57	0.64±0.22	34.09±2.50	0.22±0.10	77.8
	0.8	878.31±3.98	0.47±0.20	55.96±4.90	0.17±0.05	86.8
	1.0	2617.12±5.83	0.31±0.10	162.94±4.37	0.12±0.05	95.6
	35	Blank	97.32±2.07	1.75±0.27		
0.2		202.79±3.15	1.17±0.21	14.40±3.83	0.36±0.15	52.0
0.4		275.48±4.38	0.92±0.38	18.87±3.10	0.29±0.12	64.7
0.6		402.07±2.87	0.70±0.21	26.66±3.93	0.23±0.10	75.8
0.8		643.52±4.73	0.52±0.23	41.51±3.34	0.18±0.06	84.9
1.0		1559.29±5.49	0.35±0.12	97.85±4.96	0.13±0.04	93.8
40		Blank	82.68±2.31	2.15±0.47		
	0.2	163.14±2.14	1.44±0.39	11.96±2.11	0.44±0.20	49.4
	0.4	218.29±3.21	1.13±0.26	15.35±3.78	0.35±0.13	62.2
	0.6	310.41±3.19	0.86±0.23	21.02±3.50	0.28±0.10	73.4
	0.8	473.90±5.21	0.64±0.21	31.08±3.13	0.22±0.14	82.6
	1.0	976.36±4.22	0.43±0.12	61.99±4.37	0.16±0.09	91.5
	45	Blank	65.24±2.84	2.36±0.42		
0.2		115.51±2.14	1.72±0.35	9.03±3.60	0.52±0.15	45.9
0.4		151.74±3.62	1.36±0.23	11.25±2.94	0.42±0.18	58.8
0.6		209.38±3.63	1.05±0.33	14.80±2.38	0.33±0.15	70.2
0.8		303.55±5.66	0.79±0.30	20.59±3.42	0.26±0.13	79.4
1.0		542.06±5.78	0.54±0.15	35.27±3.23	0.19±0.07	88.5
50		Blank	53.86±2.41	2.79±0.44		
	0.2	93.18±3.02	2.01±0.33	7.65±3.22	0.60±0.11	42.3
	0.4	120.38±5.71	1.60±0.26	9.33±2.57	0.49±0.17	55.3
	0.6	161.95±3.30	1.25±0.24	11.88±3.42	0.39±0.10	66.8
	0.8	225.39±5.07	0.96±0.18	15.79±3.70	0.31±0.12	76.1
	1.0	365.49±4.48	0.68±0.15	24.41±3.69	0.23±0.10	85.3

Table 3.15: EIS data for the corrosion of weld aged maraging steel in 1.5 M hydrochloric acid containing different concentrations of ATPI.

Temperature (°C)	Conc. of inhibitor (mM)	R_{ct} (ohm. cm ²)	C_{dl} (mF cm ⁻²)	R_{pf} (ohm. cm ²)	C_{pf} (mF cm ⁻²)	η (%)
30	Blank	64.30±2.88	3.01±0.27			
	0.2	113.16±4.75	2.14±0.35	8.88±3.58	0.64±0.19	43.1
	0.4	155.58±3.40	1.62±0.37	11.49±3.59	0.49±0.11	58.6
	0.6	200.94±5.73	1.30±0.35	14.28±3.49	0.40±0.19	68.0
	0.8	425.55±5.20	0.73±0.21	28.10±3.77	0.24±0.17	84.8
	1.0	537.18±5.13	0.63±0.18	34.97±2.79	0.21±0.08	88.0
35	Blank	58.75±2.29	3.38±0.35			
	0.2	101.29±2.64	2.43±0.27	8.15±2.27	0.72±0.18	42.0
	0.4	126.62±3.46	1.99±0.38	9.71±2.21	0.59±0.21	53.6
	0.6	155.34±5.41	1.66±0.37	11.48±2.16	0.50±0.27	62.1
	0.8	236.23±5.04	1.17±0.24	16.45±3.77	0.36±0.22	75.1
	1.0	336.68±5.07	0.89±0.15	22.63±3.97	0.29±0.08	82.5
40	Blank	53.42±3.09	3.74±0.23			
	0.2	90.54±3.03	2.70±0.36	7.49±2.48	0.79±0.23	41.1
	0.4	113.03±2.89	2.21±0.22	8.87±3.30	0.66±0.13	52.7
	0.6	139.11±3.24	1.84±0.27	10.48±2.07	0.55±0.10	61.6
	0.8	191.47±4.87	1.40±0.32	13.70±3.03	0.43±0.28	72.1
	1.0	285.67±5.22	1.01±0.24	19.49±2.24	0.32±0.05	81.3
45	Blank	36.89±2.85	4.13±0.33			
	0.2	61.48±3.59	3.01±0.26	5.70±2.41	0.88±0.29	40.0
	0.4	65.99±3.74	2.82±0.30	5.98±3.98	0.83±0.10	44.1
	0.6	81.45±2.87	2.33±0.35	6.93±3.93	0.69±0.17	54.7
	0.8	113.51±5.54	1.73±0.27	8.90±3.13	0.52±0.15	67.5
	1.0	154.61±4.69	1.33±0.15	11.43±1.42	0.41±0.11	76.1
50	Blank	32.05±2.74	4.59±0.20			
	0.2	48.71±4.40	3.61±0.35	4.92±1.24	1.05±0.26	34.2
	0.4	60.24±4.11	2.96±0.24	5.63±2.29	0.87±0.29	46.8
	0.6	69.22±3.05	2.61±0.36	6.18±3.37	0.77±0.11	53.7
	0.8	88.29±4.84	2.09±0.26	7.35±3.60	0.62±0.13	63.7
	1.0	116.63±5.67	1.64±0.10	9.09±1.36	0.50±0.09	72.5

Table 3.16: EIS data for the corrosion of weld aged maraging steel in 2.0 M hydrochloric acid containing different concentrations of ATPI.

Temperature (°C)	Conc. of inhibitor (mM)	R_{ct} (ohm. cm ²)	C_{dl} (mF cm ⁻²)	R_{pf} (ohm. cm ²)	C_{pf} (mF cm ⁻²)	η (%)
30	Blank	20.21±3.10	5.75±0.52			
	0.3	37.13±4.11	3.68±0.29	4.20±1.26	1.07±0.15	45.6
	0.6	49.15±2.93	3.02±0.55	4.94±2.00	0.88±0.11	58.9
	0.9	68.94±3.34	2.44±0.34	6.16±2.27	0.72±0.24	70.7
	1.2	124.69±3.54	1.79±0.21	9.59±3.34	0.54±0.15	83.8
	1.5	178.76±4.07	1.55±0.11	12.92±2.79	0.47±0.10	82.7
35	Blank	17.34±3.26	8.26±1.24			
	0.3	29.34±4.51	5.63±0.40	3.72±3.98	1.62±0.16	40.9
	0.6	39.86±4.52	4.40±0.35	4.37±2.19	1.27±0.11	56.5
	0.9	49.97±4.81	3.71±0.36	4.99±2.18	1.08±0.09	65.3
	1.2	80.28±3.61	2.68±0.27	6.86±3.89	0.79±0.18	78.4
	1.5	114.08±4.51	2.18±0.14	8.94±2.50	0.65±0.12	84.8
40	Blank	15.01±4.83	13.22±1.58			
	0.3	24.85±3.32	8.84±0.47	3.45±2.62	2.52±0.12	39.6
	0.6	32.07±4.93	7.07±0.31	3.89±2.01	2.02±0.17	53.2
	0.9	40.90±2.34	5.76±0.21	4.44±2.96	1.65±0.20	63.3
	1.2	61.77±2.04	4.15±0.23	5.72±3.47	1.20±0.21	75.7
	1.5	85.28±2.58	3.28±0.15	7.17±2.01	0.96±0.14	82.4
45	Blank	12.89±4.85	15.87±1.38			
	0.3	20.08±3.91	9.95±0.31	3.15±3.89	2.83±0.28	35.8
	0.6	25.88±3.30	7.95±0.40	3.51±2.46	2.27±0.28	50.2
	0.9	30.47±4.38	6.90±0.31	3.79±2.28	1.97±0.11	57.7
	1.2	45.39±2.54	4.96±0.27	4.71±3.19	1.43±0.13	71.6
	1.5	61.38±2.88	3.92±0.15	5.70±2.44	1.14±0.11	79.1
50	Blank	11.67±3.28	18.95±1.20			
	0.3	17.79±2.23	12.12±0.33	3.01±2.61	3.44±0.29	34.4
	0.6	22.06±3.60	9.97±0.31	3.28±2.19	2.83±0.19	47.1
	0.9	26.05±3.58	8.59±0.26	3.52±2.62	2.45±0.24	55.2
	1.2	35.69±4.00	6.54±0.28	4.11±2.66	1.87±0.17	67.3
	1.5	42.44±4.23	5.66±0.13	4.53±2.69	1.62±0.10	72.5

Table 3.17: Comparison of maximum attainable inhibition efficiencies by the Tafel method and EIS method for the corrosion of weld aged maraging steel in hydrochloric acid solutions of different concentrations in the presence of ATPI at 30 °C.

Molarity of hydrochloric acid	Conc. of ATPI (mM)	η (%)	
		Tafel	EIS
0.1	0.8	94.6	96.8
0.5	0.8	92.5	95.0
1.0	1.0	93.2	95.5
1.5	1.0	90.3	88.0
2.0	1.5	83.2	82.7

Table 3.18: Activation parameters for the corrosion of weld aged maraging steel in hydrochloric acid containing different concentrations of ATPI.

Molarity of hydrochloric acid (M)	Conc. of inhibitor (mM)	E_a ($\text{kJ}^{-1} \text{mol}^{-1}$)	ΔH^\ddagger ($\text{kJ}^{-1} \text{mol}^{-1}$)	ΔS^\ddagger ($\text{J mol}^{-1} \text{K}^{-1}$)
0.1	0.0	39.12	41.60	-94.97
	0.1	43.03	45.76	-85.22
	0.2	47.73	50.75	-69.72
	0.4	52.42	55.74	-61.01
	0.6	56.25	59.82	-43.58
	0.8	60.24	64.06	-20.34
	0.5	0.0	36.56	38.51
0.1		40.22	42.36	-93.12
0.2		44.60	46.98	-76.19
0.4		48.99	51.60	-66.66
0.6		52.57	55.38	-47.62
0.8		56.30	59.31	-22.22
1.0		0.0	35.70	34.98
	0.2	39.27	38.48	-96.98
	0.4	43.55	42.68	-79.35
	0.6	47.84	46.87	-69.43
	0.8	51.34	50.30	-49.59
	1.0	54.98	53.87	-33.14
	1.5	0.0	32.08	30.55
0.2		35.29	33.61	-105.78
0.4		39.14	37.27	-86.55
0.6		42.99	40.94	-75.73
0.8		46.13	43.93	-54.09
1.0		49.40	47.05	-40.24
2.0		0.0	30.33	31.24
	0.3	33.36	34.36	-109.82
	0.6	37.00	38.11	-89.85
	0.9	40.64	41.86	-78.62
	1.2	43.61	44.92	-56.16
	1.5	46.71	48.11	-46.21

Table 3.19: Thermodynamic parameters for the adsorption of ATPI on weld aged maraging steel surface in hydrochloric acid at different temperatures.

Molarity of hydrochloric acid (M)	Temperature (°C)	$-\Delta G_{\text{ads}}^{\circ}$ (kJ mol ⁻¹)	$\Delta H_{\text{ads}}^{\circ}$ (kJ mol ⁻¹)	$\Delta S_{\text{ads}}^{\circ}$ (J mol ⁻¹ K ⁻¹)
0.1	30	36.45	- 11.67	-69.63
	35	36.05		
	40	35.91		
	45	35.74		
	50	35.56		
0.5	30	35.39	-18.23	-55.93
	35	33.84		
	40	33.70		
	45	33.54		
	50	33.38		
1.0	30	32.72	-26.35	-47.61
	35	32.59		
	40	32.43		
	45	32.27		
	50	32.12		
1.5	30	31.42	-33.21	-33.67
	35	31.80		
	40	32.33		
	45	33.48		
	50	32.82		
2.0	30	30.08	-40.22	-23.19
	35	29.96		
	40	29.81		
	45	29.67		
	50	29.52		

3.4 2-(4-CHLOROPHENYL)-2-OXOETHYL BENZOATE (CPOB) AS INHIBITOR FOR THE CORROSION OF WELD AGED MARAGING STEEL IN HYDROCHLORIC ACID MEDIUM

3.4.1 Potentiodynamic polarization studies

The potentiodynamic polarization curves for the corrosion of weld aged maraging steel specimen in 0.5 M hydrochloric acid in the presence of different concentrations of CPOB, at 30 °C are shown in Fig. 3.27. Similar plots were obtained in the other four concentrations of hydrochloric acid at the different temperatures studied.

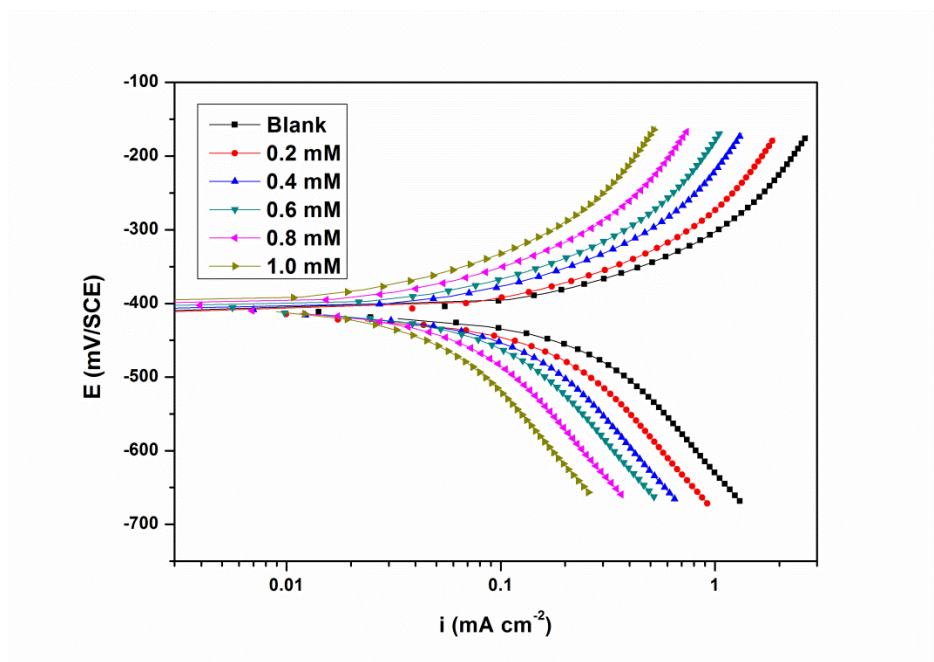


Fig. 3.27: Potentiodynamic polarization curves for the corrosion of weld aged maraging steel in 0.5 M hydrochloric acid containing different concentrations of CPOB at 30 °C.

The potentiodynamic polarization parameters (E_{corr} , b_c , b_a , i_{corr} and η (%)) were calculated from Tafel plots in all the five studied concentrations of hydrochloric acid in the presence of different concentrations of CPOB at different temperatures and are summarized in Tables 3.20 to 3.24. The data in the Tables clearly show that the corrosion

current density (i_{corr}) decreased significantly even on the addition of a small concentration of CPOB and the inhibition efficiency ($\eta\%$) increases with the increase in the inhibitor concentration for the weld aged maraging steel at all the studied concentrations of hydrochloric acid. CPOB shows similar inhibition behaviour as that of ATPI and hence the discussion regarding the inhibition behaviour of ATPI for the corrosion of weld aged maraging steel in hydrochloric acid medium, under the section 3.3.1 holds good for CPOB also. According to the observed E_{corr} values presented in Tables 3.20 to 3.24 CPOB can be regarded as mixed type inhibitor with predominant anodic inhibition effect. CPOB shows slightly lower inhibition efficiency than that of ATPI for the corrosion of weld aged maraging steel in hydrochloric acid.

3.4.2 Electrochemical impedance spectroscopy (EIS) studies

The Nyquist plots obtained for the corrosion of weld aged samples of maraging steel specimen in 0.5 M hydrochloric acid in the presence of different concentrations of CPOB at 30 °C is shown in Fig. 3.28. Similar plots were obtained in other concentrations of hydrochloric acid and also at other temperatures. The electrochemical parameters obtained from the EIS studies are summarized in Tables 3.25 to 3.29. The plots are similar to those obtained in the presence of ATPI as discussed in the section 3.3.2. From Fig. 3.28, it can be observed that the impedance spectra show a single semicircle and the diameter of semicircle increases with increasing inhibitor concentration. The semicircle in all cases corresponds to a capacitive loop and the semicircle radii depend on the inhibitor concentration. The increase in diameter of the semicircle with the increase in the CPOB concentration, indicating the increase in charge transfer resistance (R_{ct}) value and decrease in corrosion rate (v_{corr}).

The equivalent circuit given in Fig. 3.20 is used to fit the experimental data for the corrosion of weld aged maraging steel in hydrochloric acid in the presence of CPOB. Hence the discussion in the section 3.3.2 on the equivalent circuit model for the corrosion of weld aged maraging steel in the presence ATPI holds good here also. As can be seen from the Tables 3.25 to 3.29, R_{ct} , R_{pf} values increases and C_{dl} , C_{pf} values decreases with

the increase in the concentration of CPOB. The inhibitor molecule CPOB has the electron rich environment in phenyl group due to resonance of π -electrons of double bonds that can be adsorbed well on the sample surface. Also carbonyl groups are electron donating groups containing oxygen atom as an active site (Atta et al. 2011).

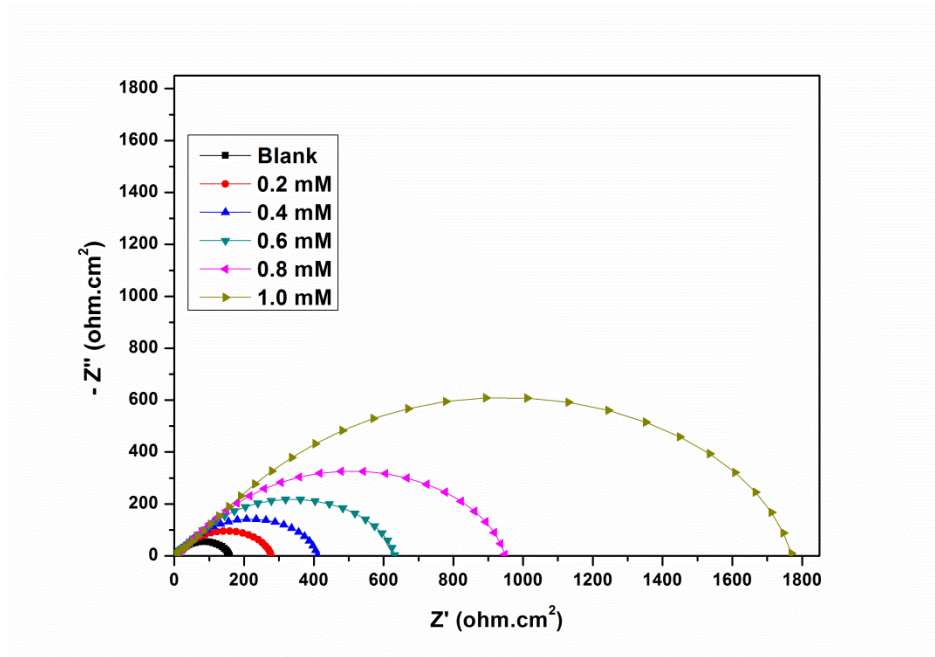


Fig. 3.28: Nyquist plots for the corrosion of weld aged maraging steel specimen in 0.5 M hydrochloric acid containing different concentrations of CPOB at 30 °C.

The Bode plots for the corrosion of the alloy in the presence of different concentrations of CPOB are shown in Fig. 3.29. They are similar to the ones shown in Fig. 3.21. Hence the discussion regarding the Bode plots under the section 3.3.2 holds good for CPOB also.

A comparison of maximum attainable inhibition efficiencies by the Tafel method and EIS method, in the presence of CPOB for the corrosion of weld aged maraging steel in hydrochloric acid solutions of different concentrations at 30 °C are listed in Table 3.30. It is evident from the table that the η (%) values obtained by the two methods are in good agreement. Similar levels of agreement were obtained at other temperatures also.

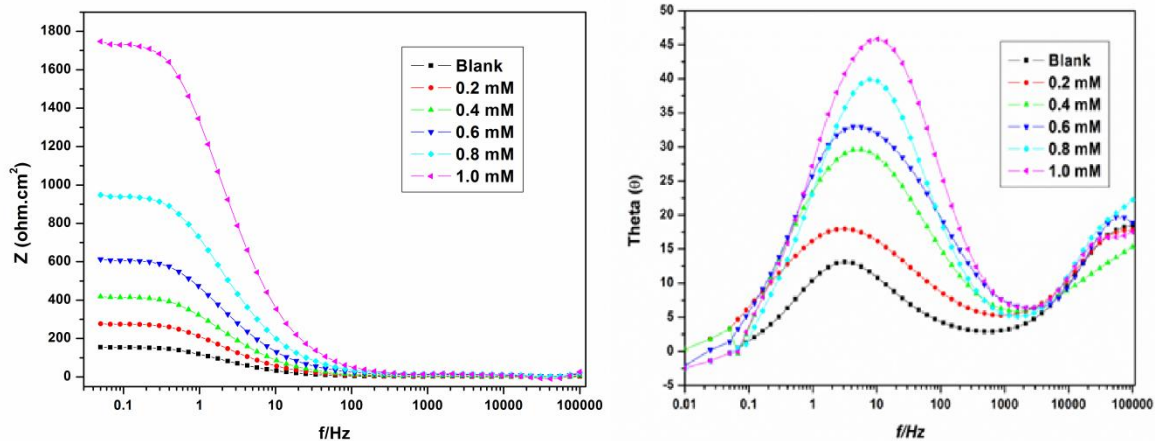


Fig. 3.29: Bode plots for the corrosion of weld aged maraging steel in 0.5 M hydrochloric acid containing different concentrations of CPOB at 30 °C.

3.4.3 Effect of temperature

The Tafel and EIS results pertaining to different temperatures in different concentrations of hydrochloric acid have already been listed in Tables 3.20 to 3.29. The effect of temperature on corrosion inhibition behaviour of CPOB is similar to that of ATPI on weld aged maraging steel as discussed in the section 3.3.3. The decrease in the inhibition efficiency of CPOB with the increase in temperature on weld aged maraging steel surface may be attributed to the physisorption of CPOB. The Arrhenius plots for the corrosion of weld aged maraging steel in 0.5 M hydrochloric acid in the presence of different concentrations of CPOB are shown in Fig. 3.30. The plots of $\ln(u_{\text{corr}}/T)$ vs $(1/T)$ are shown in Fig. 3.31.

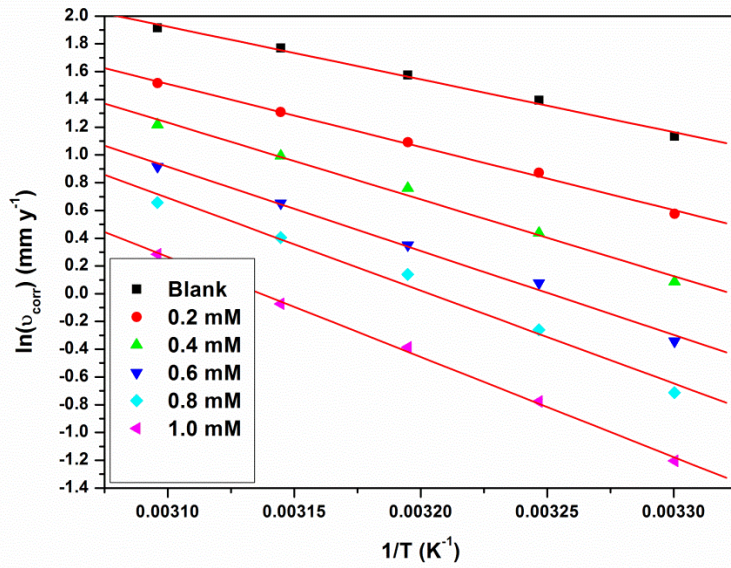


Fig. 3.30: Arrhenius plots for the corrosion of weld aged maraging steel in 0.5 M hydrochloric acid containing different concentrations of CPOB.

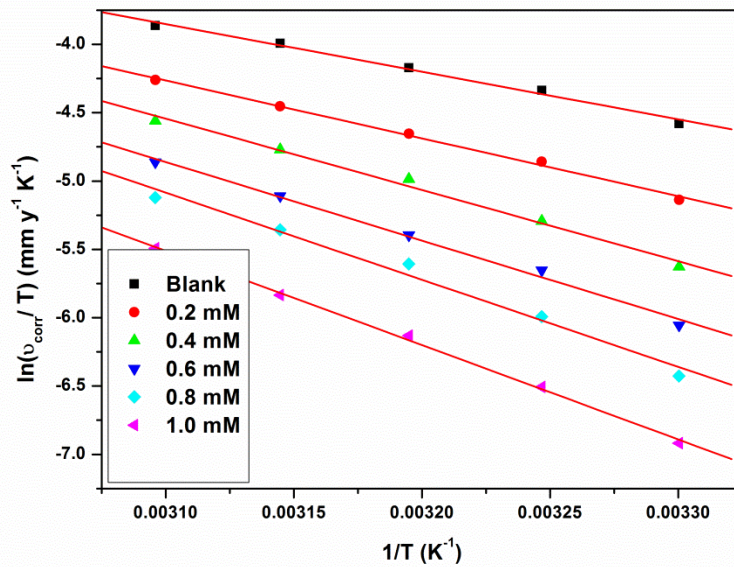


Fig. 3.31: Plots of $\ln(v_{\text{corr}}/T)$ versus $1/T$ for the corrosion of weld aged maraging steel in 0.5 M hydrochloric acid containing different concentrations of CPOB.

The calculated values of activation parameters are given in Table 3.31. The observations are similar to the ones obtained in the presence of ATPI. The value of E_a for the dissolution of weld aged maraging steel is greater in the presence of CPOB than that in the absence of CPOB in the hydrochloric acid medium. The increase in the E_a values with the increase in CPOB concentration indicates the increase in energy barrier for the corrosion reaction. The entropy of activation in the absence and presence of CPOB is large and negative for the corrosion of alloy. This implies that the activated complex in the rate determining step represents an association rather than dissociation step, indicating that a decrease in disordering takes place on going from reactants to activated complex (Marsh 1988, Gomma and Wahdan 1995).

3.4.4 Effect of hydrochloric acid concentration

It is evident from both the polarization and EIS experimental results that, for a particular concentration of the CPOB, the inhibition efficiency decreases with the increase in hydrochloric acid concentration on weld aged maraging steel. The maximum inhibition efficiency is observed in 0.1 M solution of hydrochloric acid.

3.4.5 Adsorption isotherms

The adsorption of CPOB on the surfaces of weld aged maraging steel was found to obey Langmuir adsorption isotherm. The Langmuir adsorption isotherms for the adsorption of CPOB on weld aged maraging steel in 0.5 M hydrochloric acid are shown in Fig. 3.32. The thermodynamic parameters for the adsorption of CPOB on weld aged maraging steel are tabulated in Tables 3.32. These data also reveal similar inhibition behaviour of CPOB as that of ATPI as discussed in section 3.3.5. The high values of K_{ads} and negative values of ΔG^0_{ads} for the studied inhibitor indicate strong and spontaneous adsorption of inhibitor on the alloy surface. The ΔG^0_{ads} values obtained for the adsorption of CPOB on weld aged maraging steel in all the studied concentrations of hydrochloric acid are in the range of -32.11 to -35.95 kJ mol⁻¹ indicating both physisorption and chemisorption on the alloy surface.

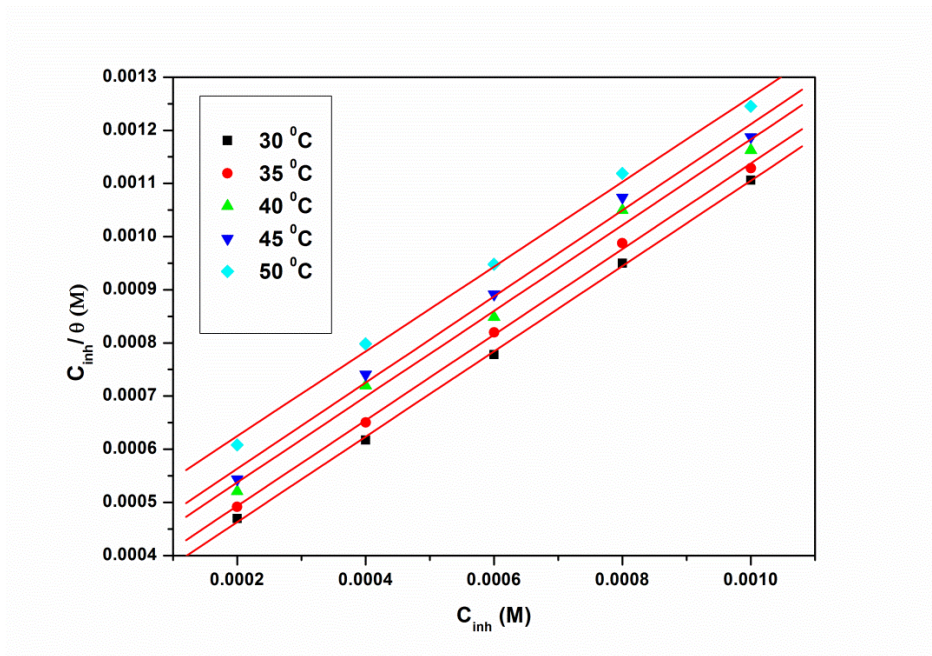


Fig. 3.32: Langmuir adsorption isotherms for the adsorption of CPOB on weld aged maraging steel in 0.5 M hydrochloric acid at different temperatures.

The ΔH_{ads}^0 values on weld aged maraging steel is negative with the absolute value below $-41.86 \text{ kJ mol}^{-1}$, suggesting physisorption. Therefore it can be concluded that the adsorption of CPOB, on weld aged maraging steel is predominantly physisorption. The ΔS_{ads}^0 value is large and negative; indicating that decrease in disordering takes place on going from the reactant to the alloy adsorbed species. This can be attributed to the fact that adsorption is always accompanied by decrease in entropy (Ashish Kumar et al. 2010).

3.4.6 Mechanism of corrosion inhibition

The mechanism of corrosion inhibition of weld aged maraging steel in the presence of CPOB is similar to that in the presence of ATPI as discussed under section 3.3.6. It is considered that in acidic solution the CPOB molecule can undergo protonation at its free oxygen and carbonyl group and can exist as a protonated positive species. The protonated species gets adsorbed on the cathodic sites of the metal surface through

electrostatic interaction, thereby decreasing the rate of the cathodic reaction. The physisorption of CPOB may be considered through electrostatic attraction between the protonated CPOB and negatively charged chloride ions already adsorbed on the alloy surface. CPOB shows slightly higher inhibition efficiency than that of ATPI for the corrosion of weld aged maraging steel in hydrochloric acid medium at lower concentration of hydrochloric acid.

3.4.7 SEM/EDS studies

The surface morphology of alloy was examined by SEM immediately after the samples were subjected to corrosion tests in hydrochloric acid in the absence and presence of inhibitor. Fig. 3.33 (a) represents SEM image of the corroded weld aged maraging steel sample in 0.5 M hydrochloric acid, which shows the facets due to the attack of hydrochloric acid on the metal surface with cracks and rough surfaces Fig. 3.33 (b) represents SEM image of weld aged maraging steel after the corrosion tests in a medium of 0.5 M hydrochloric acid containing 0.8 mM of CPOB. It can be seen that the alloy surface is smooth without any visible corrosion attack. Thus, it can be concluded that CPOB protects the alloy from corrosion by forming a uniform film on the alloy surface.

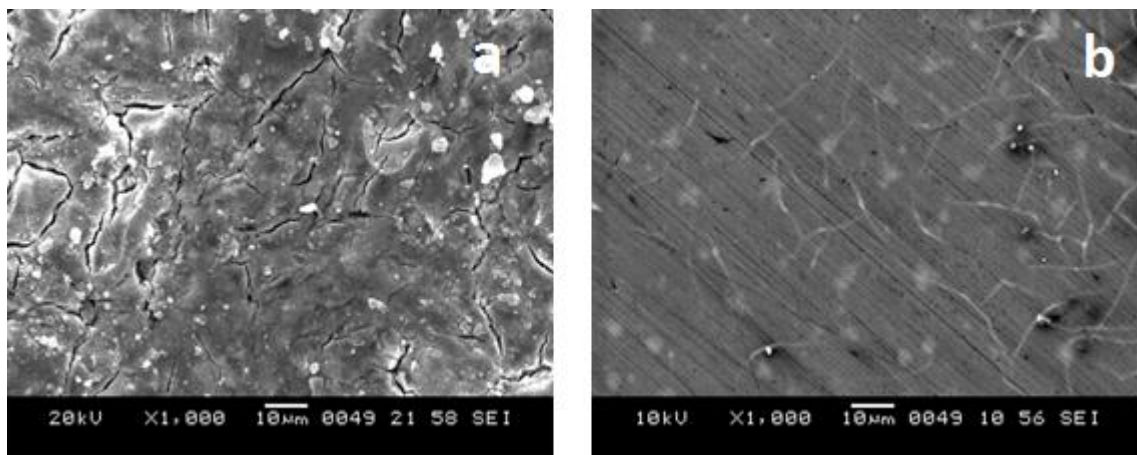


Fig. 3.33: SEM images of the weld aged maraging steel after immersion in 0.5 M hydrochloric acid a) in the absence and b) in the presence of CPOB.

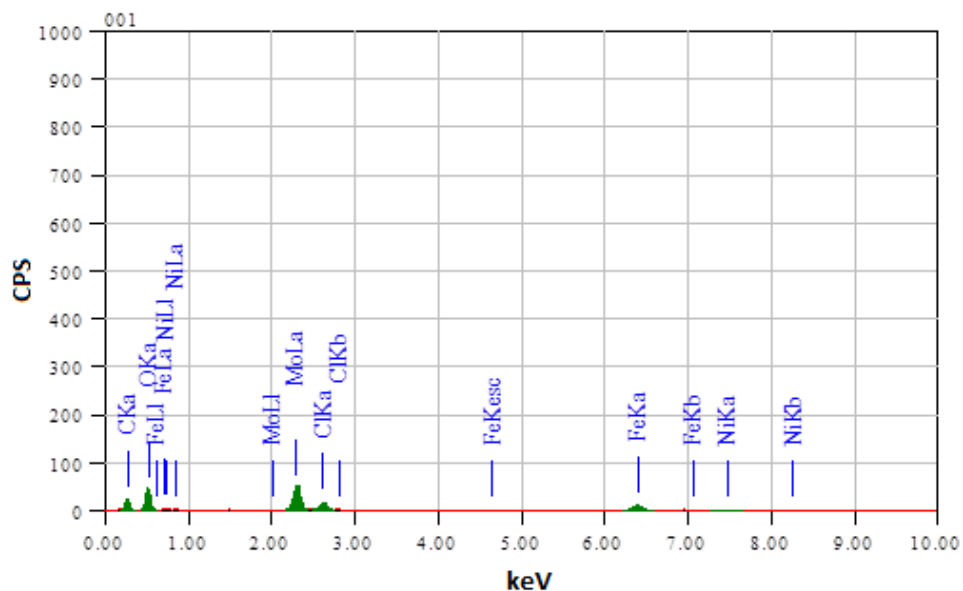


Fig. 3.34: EDS spectra of the weld aged maraging steel after immersion in 0.5 M hydrochloric acid in the presence of CPOB.

EDS investigations were carried out in order to identify the composition of the species formed on the metal surface in hydrochloric acid in the absence and presence of CPOB. The EDS profile analyses for the corrosion of weld aged maraging steel in hydrochloric acid has been already discussed under section 3.3.7. The EDS profile analyses of the corroded surface of the alloy in the presence of CPOB is shown in Fig. 3.34. The atomic percentages of the elements found in the EDS profile were 4.07 % Fe, 0.62% Ni, 1.85% Mo, 52.90% O, 2.03% Cl and 34.21% C, which indicated the formation of inhibitor film on the surface of alloy.

Table 3.20: Results of potentiodynamic polarization studies for the corrosion of weld aged maraging steel in 0.1 M hydrochloric acid containing different concentrations of CPOB.

Temperature (°C)	Conc. of inhibitor (mM)	E_{corr} (mV /SCE)	b_a (mV dec ⁻¹)	$-b_c$ (mV dec ⁻¹)	i_{corr} (mA cm ⁻²)	v_{corr} (mm y ⁻¹)	η (%)
30	Blank	-419±2	142±4	226±3	0.22±0.02	2.53±0.22	
	0.1	-417±3	138±4	223±2	0.12±0.02	1.38±0.21	44.3
	0.2	-413±3	135±3	220±4	0.08±0.02	0.92±0.23	63.5
	0.4	-410±4	131±4	216±4	0.05±0.02	0.58±0.19	77.8
	0.6	-406±3	127±3	234±2	0.03±0.01	0.35±0.12	85.9
	0.8	-408±1	124±1	230±1	0.02±0.01	0.23±0.11	92.1
	35	Blank	-416±2	150±4	234±1	0.26±0.03	2.99±0.25
0.1		-418±2	148±2	230±3	0.15±0.01	1.73±0.14	42.5
0.2		-415±3	145±2	227±3	0.10±0.02	1.19±0.15	60.3
0.4		-412±2	141±3	224±1	0.07±0.02	0.75±0.18	75.0
0.6		-408±4	137±3	220±4	0.05±0.01	0.52±0.11	82.8
0.8		-405±4	135±1	217±1	0.03±0.01	0.29±0.08	90.4
40		Blank	-412±2	159±2	242±2	0.30±0.03	3.45±0.29
	0.1	-411±3	157±3	238±2	0.18±0.01	2.05±0.11	40.6
	0.2	-408±4	153±2	235±1	0.13±0.03	1.46±0.28	57.8
	0.4	-406±4	150±3	234±4	0.08±0.02	0.93±0.22	72.9
	0.6	-403±2	146±3	231±4	0.06±0.01	0.71±0.12	79.4
	0.8	-400±3	143±3	227±4	0.04±0.01	0.40±0.15	88.2
	45	Blank	-409±4	165±3	250±1	0.33±0.02	3.80±0.17
0.1		-406±3	163±2	248±2	0.20±0.02	2.34±0.22	38.4
0.2		-404±4	160±2	245±3	0.15±0.02	1.69±0.15	55.6
0.4		-401±3	156±3	243±2	0.10±0.03	1.14±0.28	69.9
0.6		-399±3	153±3	239±3	0.08±0.03	0.91±0.28	76.1
0.8		-395±1	150±3	236±1	0.05±0.02	0.54±0.11	85.8
50		Blank	-405±1	173±1	259±2	0.37±0.02	4.26±0.15
	0.1	-407±1	170±2	256±2	0.24±0.03	2.72±0.27	36.1
	0.2	-403±2	166±1	253±4	0.18±0.01	2.02±0.12	52.3
	0.4	-400±4	163±2	250±4	0.12±0.03	1.43±0.28	66.5
	0.6	-398±2	160±2	246±3	0.10±0.03	1.12±0.26	73.7
	0.8	-396±2	156±1	242±3	0.06±0.02	0.70±0.18	83.5

Table 3.21: Results of potentiodynamic polarization studies for the corrosion of weld aged maraging steel in 0.5 M hydrochloric acid containing different concentrations of CPOB.

Temperature (°C)	Conc. of inhibitor (mM)	E_{corr} (mV /SCE)	b_a (mV dec ⁻¹)	$-b_c$ (mV dec ⁻¹)	i_{corr} (mA cm ⁻²)	v_{corr} (mm y ⁻¹)	η (%)
30	Blank	-413±2	148±4	247±4	0.27±0.02	3.11±0.23	
	0.2	-415±2	144±4	243±1	0.16±0.01	1.78±0.14	42.6
	0.4	-411±3	142±3	240±3	0.10±0.03	1.09±0.29	64.8
	0.6	-408±3	138±1	236±1	0.06±0.02	0.71±0.25	77.1
	0.8	-405±1	135±2	233±2	0.04±0.02	0.49±0.19	84.2
	1.0	-403±2	131±1	229±3	0.03±0.01	0.30±0.12	90.4
	35	Blank	-411±4	156±2	254±3	0.35±0.02	4.03±0.19
0.2		-413±3	154±1	250±2	0.21±0.02	2.39±0.19	40.7
0.4		-410±4	150±2	246±4	0.14±0.01	1.55±0.13	61.5
0.6		-408±1	148±4	242±1	0.09±0.02	1.08±0.15	73.2
0.8		-405±3	144±4	240±3	0.07±0.01	0.77±0.11	81.1
1.0		-402±3	141±3	237±2	0.04±0.02	0.46±0.18	88.6
40		Blank	-408±1	165±3	262±1	0.42±0.02	4.83±0.21
	0.2	-405±1	163±3	258±1	0.26±0.02	2.98±0.16	38.4
	0.4	-403±2	160±1	255±2	0.19±0.03	2.14±0.27	55.6
	0.6	-400±1	156±1	251±3	0.12±0.02	1.42±0.15	70.7
	0.8	-398±3	152±2	248±2	0.10±0.03	1.15±0.26	76.2
	1.0	-395±1	149±2	245±4	0.06±0.01	0.68±0.11	86.0
	45	Blank	-406±2	172±2	269±3	0.51±0.03	5.87±0.26
0.2		-402±1	168±4	265±2	0.33±0.02	3.84±0.16	34.5
0.4		-400±2	166±3	261±2	0.24±0.01	2.80±0.13	52.3
0.6		-398±4	162±1	258±4	0.17±0.02	1.97±0.18	66.5
0.8		-394±4	159±3	255±2	0.13±0.01	1.54±0.13	73.7
1.0		-391±4	154±3	251±1	0.09±0.01	1.05±0.12	82.1
50		Blank	-404±2	183±1	277±4	0.59±0.02	6.79±0.21
	0.2	-401±3	180±3	273±2	0.40±0.03	4.56±0.26	32.9
	0.4	-397±2	176±3	270±2	0.29±0.01	3.38±0.13	50.1
	0.6	-395±3	173±2	268±2	0.22±0.01	2.50±0.14	63.3
	0.8	-392±3	169±4	264±3	0.17±0.01	1.93±0.14	71.5
	1.0	-390±4	165±2	261±4	0.12±0.02	1.33±0.27	80.3

Table 3.22: Results of potentiodynamic polarization studies for the corrosion of weld aged maraging steel in 1.0 M hydrochloric acid containing different concentrations of CPOB.

Temperature (°C)	Conc. of inhibitor (mM)	E_{corr} (mV /SCE)	b_a (mV dec ⁻¹)	$-b_c$ (mV dec ⁻¹)	i_{corr} (mA cm ⁻²)	v_{corr} (mm y ⁻¹)	η (%)
30	Blank	-371±2	153±3	256±3	0.33±0.01	3.80±0.12	
	0.3	-373±4	149±2	254±2	0.19±0.01	2.24±0.11	40.9
	0.6	-370±3	146±3	251±4	0.12±0.03	1.44±0.25	62.1
	0.9	-368±2	142±3	247±2	0.08±0.01	0.97±0.11	74.4
	1.2	-365±3	140±1	244±1	0.06±0.02	0.70±0.16	81.5
	1.5	-361±2	137±3	242±2	0.04±0.01	0.47±0.14	87.7
	35	Blank	-368±2	159±4	261±4	0.45±0.04	5.20±0.43
0.3		-366±1	155±4	258±3	0.28±0.03	3.22±0.31	38.1
0.6		-362±1	152±2	255±1	0.18±0.03	2.14±0.34	58.9
0.9		-359±2	150±1	251±4	0.13±0.04	1.53±0.35	70.6
1.2		-356±2	147±1	248±4	0.09±0.04	1.13±0.36	78.4
1.5		-352±3	142±4	246±3	0.06±0.02	0.72±0.16	86.0
40		Blank	-364±3	165±3	266±3	0.56±0.06	6.45±0.64
	0.3	-361±1	163±2	262±2	0.36±0.02	4.14±0.17	35.9
	0.6	-360±4	160±3	260±4	0.26±0.02	3.03±0.21	53.1
	0.9	-357±4	158±4	257±1	0.17±0.02	2.05±0.22	68.2
	1.2	-355±2	156±2	255±1	0.14±0.01	1.70±0.11	73.7
	1.5	-352±4	151±1	252±4	0.09±0.01	1.07±0.19	83.5
	45	Blank	-361±4	172±1	273±2	0.75±0.12	8.72±1.25
0.3		-359±3	170±4	270±4	0.49±0.03	5.71±0.30	34.5
0.6		-356±4	168±3	268±4	0.36±0.02	4.21±0.19	51.7
0.9		-352±3	165±3	265±3	0.26±0.04	3.05±0.38	65.3
1.2		-350±4	161±4	261±4	0.21±0.03	2.43±0.30	72.2
1.5		-347±2	157±3	258±3	0.13±0.03	1.58±0.34	81.9
50		Blank	-358±4	177±3	278±3	0.92±0.14	10.63±1.15
	0.3	-355±3	172±4	275±3	0.62±0.09	7.16±1.00	32.7
	0.6	-352±4	170±2	273±2	0.48±0.06	5.53±0.60	47.9
	0.9	-350±4	168±3	270±1	0.35±0.02	4.13±0.21	61.1
	1.2	-347±2	165±1	268±3	0.28±0.03	3.27±0.27	69.3
	1.5	-344±4	162±1	265±4	0.20±0.02	2.32±0.15	78.1

Table 3.23: Results of potentiodynamic polarization studies for the corrosion of weld aged maraging steel in 1.5 M hydrochloric acid containing different concentrations of CPOB.

Temperature (°C)	Conc. of inhibitor (mM)	E_{corr} (mV /SCE)	b_a (mV dec ⁻¹)	$-b_c$ (mV dec ⁻¹)	i_{corr} (mA cm ⁻²)	v_{corr} (mm y ⁻¹)	η (%)
30	Blank	-342±2	158±2	267±3	0.70±0.03	8.05±0.33	
	0.4	-340±3	155±3	265±1	0.36±0.02	4.20±0.22	47.8
	0.8	-337±3	150±4	262±2	0.27±0.03	3.13±0.31	61.1
	1.2	-332±4	146±2	259±2	0.18±0.03	2.17±0.27	73.0
	1.6	-330±1	144±2	256±2	0.09±0.02	1.13±0.17	86.2
	2.0	-328±2	141±4	252±2	0.06±0.02	0.79±0.20	90.2
	35	Blank	-339±4	165±2	276±4	0.82±0.04	9.45±0.36
0.4		-336±2	162±2	273±4	0.46±0.04	5.37±0.38	43.1
0.8		-335±2	160±1	271±1	0.33±0.03	3.90±0.34	58.7
1.2		-331±4	157±4	267±2	0.26±0.04	3.07±0.38	67.5
1.6		-329±4	153±4	263±2	0.15±0.03	1.83±0.27	80.6
2.0		-325±1	151±1	259±4	0.10±0.03	1.23±0.33	87.0
40		Blank	-337±3	173±2	282±2	0.94±0.02	10.85±0.19
	0.4	-335±1	170±2	280±3	0.54±0.02	6.29±0.17	42.2
	0.8	-332±2	168±3	276±2	0.41±0.03	4.82±0.26	55.6
	1.2	-329±4	164±3	273±1	0.32±0.01	3.72±0.12	65.7
	1.6	-327±3	161±1	272±3	0.21±0.03	2.42±0.31	77.7
	2.0	-324±4	157±1	268±2	0.14±0.04	1.65±0.39	84.8
	45	Blank	-334±4	179±4	286±3	1.53±0.02	17.60±0.29
0.4		-330±3	177±4	285±4	0.94±0.02	10.88±0.19	38.2
0.8		-328±4	172±2	281±2	0.72±0.03	8.34±0.28	52.6
1.2		-325±1	170±3	278±2	0.61±0.02	7.02±0.17	60.1
1.6		-322±4	168±1	275±2	0.39±0.04	4.58±0.38	74.3
2.0		-330±3	165±4	270±3	0.28±0.01	3.28±0.11	81.4
50		Blank	-332±3	185±2	292±2	1.61±0.04	18.57±0.36
	0.4	-329±4	181±2	290±4	1.02±0.01	11.75±0.12	36.8
	0.8	-325±2	179±3	287±1	0.81±0.03	9.39±0.26	49.5
	1.2	-321±2	175±1	284±1	0.68±0.03	7.88±0.28	57.6
	1.6	-320±2	171±3	280±1	0.48±0.02	5.63±0.18	69.7
	2.0	-316±1	169±3	276±2	0.40±0.01	4.66±0.11	74.9

Table 3.24: Results of potentiodynamic polarization studies for the corrosion of weld aged maraging steel in 2.0 M hydrochloric acid containing different concentrations of CPOB.

Temperature (°C)	Conc. of inhibitor (mM)	E_{corr} (mV /SCE)	b_a (mV dec ⁻¹)	$-b_c$ (mV dec ⁻¹)	i_{corr} (mA cm ⁻²)	v_{corr} (mm y ⁻¹)	η (%)
30	Blank	-324±2	175±1	287±3	2.76±0.12	31.85±1.14	
	0.4	-320±4	172±4	285±4	1.54±0.09	17.80±1.05	44.1
	0.8	-318±1	168±1	281±2	1.17±0.08	13.57±0.80	57.4
	1.2	-315±3	165±2	278±4	0.85±0.04	9.81±0.42	69.2
	1.6	-313±4	161±3	274±4	0.48±0.04	5.64±0.41	82.3
	2.0	-310±3	157±2	271±4	0.37±0.02	4.30±0.20	86.5
35	Blank	-321±1	182±1	293±4	3.08±0.09	35.49±0.10	
	0.4	-318±2	180±4	291±2	1.87±0.08	21.52±0.84	39.4
	0.8	-315±4	177±4	287±2	1.38±0.04	15.97±0.43	55.1
	1.2	-311±2	175±1	285±1	1.11±0.04	12.85±0.35	63.8
	1.6	-309±2	171±4	283±1	0.71±0.01	8.20±0.14	76.9
	2.0	-307±4	168±4	280±2	0.51±0.04	5.93±0.44	83.3
40	Blank	-319±3	189±4	300±4	3.39±0.04	39.03±0.40	
	0.4	-315±2	187±1	297±4	2.09±0.04	24.08±0.39	38.3
	0.8	-313±1	185±2	295±2	1.63±0.03	18.78±0.33	51.9
	1.2	-311±2	181±1	291±2	1.28±0.03	14.83±0.32	62.1
	1.6	-307±3	178±2	287±2	0.88±0.02	10.15±0.21	74.2
	2.0	-304±1	174±4	285±2	0.64±0.04	7.38±0.39	81.1
45	Blank	-315±3	196±4	307±2	3.62±0.14	41.73±1.51	
	0.4	-312±3	193±3	302±3	2.37±0.08	27.34±0.82	34.5
	0.8	-309±3	191±4	300±3	1.85±0.06	21.32±0.64	48.9
	1.2	-305±2	188±3	298±1	1.58±0.05	18.19±0.46	56.4
	1.6	-303±3	185±4	295±2	1.07±0.03	12.39±0.31	70.3
	2.0	-300±4	181±3	291±2	0.80±0.02	9.31±0.15	77.7
50	Blank	-312±1	203±3	312±4	3.89±0.23	44.77±2.27	
	0.4	-310±4	200±2	308±3	2.60±0.12	29.95±1.21	33.1
	0.8	-307±1	197±1	304±3	2.10±0.10	24.27±1.04	45.8
	1.2	-304±1	194±1	302±1	1.79±0.08	20.64±0.87	53.9
	1.6	-300±3	190±1	299±4	1.32±0.05	15.22±0.67	66.1
	2.0	-299±3	188±4	296±2	1.12±0.02	12.90±0.16	71.2

Table 3.25: EIS data for the corrosion of weld aged maraging steel in 0.1 M hydrochloric acid containing different concentrations of CPOB.

Temperature (°C)	Conc. of inhibitor (mM)	R_{ct} (ohm. cm ²)	C_{dl} (mF cm ⁻²)	R_{pf} (ohm. cm ²)	C_{pf} (mF cm ⁻²)	η (%)
30	Blank	181.20±3.05	0.93±0.24			
	0.1	318.45±2.66	0.51±0.14	22.11±2.13	0.12±0.04	43.1
	0.2	469.43±3.63	0.33±0.09	32.54±2.01	0.08±0.03	61.4
	0.4	696.92±4.16	0.20±0.11	52.02±3.95	0.05±0.02	74.1
	0.6	1104.88±5.54	0.13±0.04	80.57±2.69	0.04±0.01	83.6
	0.8	1948.39±6.31	0.07±0.03	142.01±4.83	0.03±0.01	90.7
35	Blank	158.00±3.36	1.10±0.21			
	0.1	267.80±2.68	0.63±0.24	19.04±3.73	0.15±0.03	41.0
	0.2	410.39±3.23	0.44±0.15	26.54±3.21	0.10±0.02	61.5
	0.4	589.55±4.53	0.27±0.08	40.79±3.56	0.06±0.03	73.2
	0.6	802.03±5.48	0.19±0.06	58.25±2.19	0.04±0.02	80.3
	0.8	1423.42±5.06	0.10±0.03	102.55±4.96	0.03±0.01	88.9
40	Blank	135.21±3.40	1.40±0.20			
	0.1	211.93±2.81	0.82±0.16	16.16±2.28	0.19±0.04	36.2
	0.2	306.60±3.33	0.58±0.27	21.82±3.52	0.14±0.02	55.9
	0.4	452.21±4.37	0.37±0.13	32.69±2.89	0.09±0.02	70.1
	0.6	609.05±4.99	0.28±0.11	42.28±2.31	0.07±0.02	77.8
	0.8	958.94±5.35	0.16±0.03	72.09±3.61	0.04±0.01	85.9
45	Blank	127.54±2.03	1.55±0.18			
	0.1	200.53±3.55	0.95±0.25	14.91±2.55	0.22±0.03	36.4
	0.2	271.36±3.88	0.68±0.12	19.80±2.57	0.16±0.04	53.2
	0.4	384.16±3.38	0.46±0.16	28.11±3.05	0.11±0.01	66.8
	0.6	520.57±5.77	0.36±0.13	34.80±2.94	0.09±0.02	75.5
	0.8	763.71±6.63	0.21±0.09	57.01±4.98	0.05±0.02	83.3
50	Blank	117.23±2.11	1.80±0.21			
	0.1	178.98±2.34	1.14±0.29	13.47±2.24	0.27±0.05	34.5
	0.2	235.40±3.03	0.85±0.17	17.27±3.29	0.20±0.03	50.2
	0.4	332.10±3.03	0.60±0.22	23.61±3.51	0.14±0.04	64.7
	0.6	402.85±4.18	0.47±0.27	29.45±3.25	0.11±0.02	70.9
	0.8	626.90±5.15	0.29±0.05	45.57±3.24	0.07±0.02	81.3

Table 3.26: EIS data for the corrosion of weld aged maraging steel in 0.5 M hydrochloric acid containing different concentrations of CPOB.

Temperature (°C)	Conc. of inhibitor (mM)	R_{ct} (ohm. cm ²)	C_{dl} (mF cm ⁻²)	R_{pf} (ohm. cm ²)	C_{pf} (mF cm ⁻²)	η (%)
30	Blank	156.30±3.15	0.96±0.17			
	0.2	275.66±2.58	0.54±0.24	19.09±2.06	0.13±0.03	43.3
	0.4	416.80±3.56	0.35±0.14	27.69±3.45	0.08±0.02	62.5
	0.6	620.24±4.54	0.24±0.10	40.08±3.97	0.06±0.03	74.8
	0.8	914.04±6.15	0.16±0.05	57.97±3.12	0.04±0.02	82.9
	1.0	1756.18±6.17	0.08±0.02	109.27±4.63	0.03±0.01	91.1
35	Blank	139.27±3.46	1.11±0.29			
	0.2	240.12±2.69	0.63±0.27	16.93±2.23	0.15±0.03	42.0
	0.4	355.28±2.63	0.43±0.13	23.94±3.70	0.10±0.03	60.8
	0.6	525.55±5.90	0.29±0.15	34.31±2.70	0.07±0.01	73.5
	0.8	740.80±6.92	0.20±0.10	47.42±3.74	0.05±0.02	81.2
	1.0	1378.91±7.90	0.11±0.03	86.29±3.26	0.04±0.01	89.9
40	Blank	123.15±2.64	1.33±0.17			
	0.2	202.55±3.08	0.80±0.30	14.64±1.18	0.19±0.03	39.2
	0.4	282.45±3.20	0.58±0.17	19.50±2.18	0.13±0.03	56.4
	0.6	432.11±5.34	0.37±0.21	28.62±2.85	0.09±0.03	71.5
	0.8	559.77±5.49	0.29±0.10	36.40±2.82	0.07±0.01	78.1
	1.0	867.25±6.58	0.18±0.08	55.12±3.06	0.04±0.02	85.8
45	Blank	107.56±3.46	1.55±0.24			
	0.2	166.76±3.41	0.96±0.13	12.46±2.53	0.22±0.02	35.5
	0.4	227.40±2.99	0.70±0.11	16.15±2.62	0.16±0.03	52.7
	0.6	325.94±3.11	0.49±0.15	22.15±3.70	0.11±0.03	67.1
	0.8	433.71±4.97	0.36±0.10	28.72±2.30	0.09±0.03	75.2
	1.0	629.01±5.90	0.25±0.08	40.61±3.78	0.06±0.02	82.9
50	Blank	90.34±3.69	1.74±0.26			
	0.2	137.29±2.40	1.11±0.28	10.66±2.04	0.26±0.03	34.2
	0.4	182.14±3.39	0.83±0.28	13.39±2.65	0.19±0.01	50.4
	0.6	255.20±3.34	0.59±0.23	17.84±2.34	0.14±0.01	64.6
	0.8	332.13±4.16	0.46±0.10	22.53±2.84	0.11±0.02	72.8
	1.0	465.67±5.55	0.32±0.08	30.66±3.89	0.08±0.03	80.6

Table 3.27: EIS data for the corrosion of weld aged maraging steel in 1.0 M hydrochloric acid containing different concentrations of CPOB.

Temperature (°C)	Conc. of inhibitor (mM)	R_{ct} (ohm. cm ²)	C_{dl} (mF cm ⁻²)	R_{pf} (ohm. cm ²)	C_{pf} (mF cm ⁻²)	η (%)
30	Blank	117.37±3.29	1.68±0.18			
	0.3	200.30±3.30	1.28±0.26	14.38±3.69	0.52±0.12	41.4
	0.6	297.88±2.28	0.96±0.16	20.26±2.82	0.44±0.19	60.6
	0.9	433.13±4.70	0.75±0.12	28.42±3.53	0.39±0.25	72.9
	1.2	617.78±5.22	0.62±0.10	39.55±3.25	0.36±0.15	81.1
	1.5	1086.77±6.28	0.48±0.07	67.83±2.21	0.33±0.10	89.2
35	Blank	98.28±2.56	1.75±0.10			
	0.3	163.23±2.98	1.32±0.12	12.14±2.85	0.53±0.28	39.8
	0.6	237.37±3.59	1.00±0.21	16.61±3.09	0.45±0.15	58.6
	0.9	342.42±4.12	0.79±0.23	22.95±2.12	0.40±0.23	71.3
	1.2	467.98±4.72	0.66±0.28	30.52±2.80	0.37±0.21	79.1
	1.5	799.09±5.27	0.51±0.11	50.49±2.68	0.34±0.12	87.7
40	Blank	83.43±2.11	2.15±0.22			
	0.3	133.23±3.49	1.64±0.26	10.33±2.99	0.60±0.16	37.4
	0.6	183.74±2.47	1.27±0.28	13.38±2.58	0.52±0.13	54.6
	0.9	275.35±3.76	0.95±0.21	18.90±2.27	0.44±0.18	69.7
	1.2	350.61±4.09	0.81±0.16	23.44±2.59	0.41±0.28	76.2
	1.5	521.52±4.66	0.64±0.13	33.75±2.90	0.37±0.11	84.2
45	Blank	65.86±2.22	2.36±0.29			
	0.3	98.89±3.36	1.83±0.25	8.26±3.65	0.65±0.18	33.4
	0.6	133.33±3.60	1.43±0.20	10.34±2.84	0.55±0.14	50.6
	0.9	187.68±3.77	1.10±0.29	13.62±2.71	0.48±0.16	64.9
	1.2	244.85±3.30	0.92±0.22	17.06±3.28	0.43±0.21	73.1
	1.5	343.03±4.99	0.74±0.15	22.98±3.57	0.39±0.12	80.8
50	Blank	54.34±2.78	2.79±0.10			
	0.3	80.40±3.06	2.10±0.18	7.15±2.29	0.71±0.11	32.4
	0.6	105.76±3.21	1.67±0.21	8.68±3.94	0.61±0.16	48.6
	0.9	146.06±3.81	1.29±0.28	11.11±2.04	0.52±0.16	62.8
	1.2	187.37±2.07	1.07±0.15	13.60±2.79	0.47±0.22	71.2
	1.5	256.36±3.15	0.86±0.11	17.76±2.80	0.42±0.18	78.8

Table 3.28: EIS data for the corrosion of weld aged maraging steel in 1.5 M hydrochloric acid containing different concentrations of CPOB.

Temperature (°C)	Conc. of inhibitor (mM)	R_{ct} (ohm. cm ²)	C_{dl} (mF cm ⁻²)	R_{pf} (ohm. cm ²)	C_{pf} (mF cm ⁻²)	η (%)
30	Blank	64.30±3.36	3.01±0.21			
	0.4	113.16±2.13	1.97±0.21	9.19±2.29	0.68±0.22	43.1
	0.8	155.58±3.77	1.50±0.29	11.78±3.94	0.57±0.28	58.6
	1.2	200.94±3.75	1.23±0.30	14.54±3.62	0.51±0.21	68.3
	1.6	425.55±2.38	0.72±0.36	28.22±2.89	0.39±0.16	84.8
	2.0	537.18±5.54	0.63±0.24	35.02±2.55	0.37±0.08	88.0
35	Blank	58.75±2.89	3.38±0.33			
	0.4	101.29±3.55	2.16±0.31	8.47±3.28	0.72±0.24	42.1
	0.8	126.62±2.83	1.78±0.38	10.01±2.30	0.63±0.17	53.6
	1.2	155.34±2.15	1.50±0.36	11.76±3.27	0.57±0.21	62.1
	1.6	236.23±3.57	1.08±0.35	16.69±3.15	0.47±0.24	75.1
	2.0	336.68±3.18	0.84±0.21	22.81±3.72	0.42±0.11	82.5
40	Blank	53.42±2.65	3.74±0.27			
	0.4	90.54±2.36	2.44±0.25	7.81±2.27	0.79±0.12	41.3
	0.8	113.03±2.27	2.00±0.38	9.18±3.19	0.69±0.14	52.7
	1.2	139.11±3.97	1.68±0.30	10.77±2.04	0.61±0.22	61.6
	1.6	191.47±2.13	1.29±0.31	13.96±2.76	0.52±0.25	72.1
	2.0	285.67±4.74	0.96±0.29	19.70±2.80	0.44±0.13	81.3
45	Blank	36.89±2.42	4.13±0.37			
	0.4	61.48±2.05	2.67±0.40	6.04±2.46	0.84±0.23	40.2
	0.8	65.99±3.15	2.51±0.34	6.32±3.64	0.80±0.23	44.1
	1.2	81.45±2.28	2.08±0.29	7.26±2.81	0.70±0.18	54.7
	1.6	113.51±3.67	1.57±0.22	9.21±3.39	0.59±0.12	67.5
	2.0	154.61±3.56	1.22±0.36	11.72±3.48	0.50±0.08	76.1
50	Blank	32.05±2.46	4.59±0.30			
	0.4	48.71±2.62	3.23±0.23	5.27±2.19	0.97±0.24	34.2
	0.8	60.24±3.15	2.66±0.36	5.97±2.80	0.84±0.30	46.8
	1.2	69.22±3.96	2.35±0.23	6.52±3.19	0.77±0.25	53.7
	1.6	88.29±2.87	1.90±0.34	7.68±2.55	0.66±0.27	63.7
	2.0	116.63±3.30	1.50±0.33	9.40±2.01	0.57±0.11	72.5

Table 3.29: EIS data for the corrosion of weld aged maraging steel in 2.0 M hydrochloric acid containing different concentrations of CPOB.

Temperature (°C)	Conc. of inhibitor (mM)	R_{ct} (ohm. cm ²)	C_{dl} (mF cm ⁻²)	R_{pf} (ohm. cm ²)	C_{pf} (mF cm ⁻²)	η (%)
30	Blank	20.21±3.51	5.75±1.31			
	0.4	37.13±2.33	3.68±0.22	4.96±1.41	1.10±0.19	45.6
	0.8	49.15±2.88	3.02±0.23	5.69±2.85	0.92±0.29	58.9
	1.2	68.94±2.48	2.44±0.38	6.90±2.90	0.79±0.28	70.7
	1.6	124.69±3.30	1.79±0.24	10.29±2.61	0.64±0.27	83.8
	2.0	178.76±4.49	1.55±0.21	13.59±3.95	0.58±0.14	88.7
35	Blank	17.34±2.55	8.26±1.32			
	0.4	29.34±2.34	5.63±0.58	4.49±1.07	1.55±0.11	40.9
	0.8	39.86±2.30	4.40±0.21	5.13±2.79	1.25±0.23	56.5
	1.2	49.97±2.64	3.71±0.31	5.74±2.67	1.08±0.26	65.3
	1.6	80.28±3.83	2.68±0.28	7.59±3.63	0.84±0.28	78.4
	2.0	114.08±3.06	2.18±0.34	9.65±2.08	0.73±0.12	84.8
40	Blank	15.01±3.21	13.22±1.21			
	0.4	24.85±2.97	8.84±0.78	4.21±1.81	2.30±0.12	39.6
	0.8	32.07±3.53	7.07±0.27	4.65±2.49	1.87±0.16	53.2
	1.2	40.90±2.48	5.76±0.31	5.19±3.03	1.56±0.16	63.3
	1.6	61.77±2.53	4.15±0.29	6.46±3.86	1.19±0.23	75.7
	2.0	85.28±3.52	3.28±0.32	7.89±2.38	0.98±0.17	82.4
45	Blank	12.89±3.38	15.87±1.38			
	0.4	20.08±3.41	9.95±0.55	3.92±0.92	2.56±0.17	35.8
	0.8	25.88±2.78	7.95±0.32	4.28±1.29	2.07±0.22	50.2
	1.2	30.47±3.45	6.90±0.37	4.56±2.42	1.83±0.28	57.7
	1.6	45.39±2.29	4.96±0.35	5.46±2.40	1.38±0.24	71.6
	2.0	61.38±3.92	3.92±0.36	6.44±3.87	1.13±0.18	79.0
50	Blank	11.67±2.83	18.95±1.23			
	0.4	17.79±2.27	12.12±1.29	3.78±1.23	3.06±0.29	34.4
	0.8	22.06±2.59	9.97±0.27	4.04±1.99	2.54±0.21	47.1
	1.2	26.05±2.55	8.59±0.37	4.29±1.42	2.22±0.18	55.2
	1.6	35.69±2.06	6.54±0.21	4.87±2.26	1.74±0.17	67.3
	2.0	42.44±2.11	5.66±0.34	5.28±2.63	1.54±0.23	72.4

Table 3.30: Comparison of maximum attainable inhibition efficiencies by the Tafel method and EIS method for the corrosion of weld aged maraging steel in hydrochloric acid solutions of different concentrations in the presence of CPOB at 30 °C.

Molarity of hydrochloric acid	Conc. of CPOB (mM)	η (%)	
		Tafel	EIS
0.1	0.8	92.1	90.7
0.5	1.0	90.4	91.1
1.0	1.5	87.7	89.2
1.5	2.0	90.2	88.0
2.0	2.0	86.5	88.7

Table 3.31: Activation parameters for the corrosion of weld aged maraging steel in hydrochloric acid containing different concentrations of CPOB.

Molarity of hydrochloric acid (M)	Conc. of inhibitor (mM)	E_a ($\text{kJ}^{-1} \text{mol}^{-1}$)	ΔH^\ddagger ($\text{kJ}^{-1} \text{mol}^{-1}$)	ΔS^\ddagger ($\text{J mol}^{-1} \text{K}^{-1}$)
0.1	0.0	39.12	41.60	-94.92
	0.1	46.94	49.92	-75.53
	0.2	55.55	59.07	-64.88
	0.4	65.33	69.47	-58.10
	0.6	67.29	71.55	-38.73
	0.8	70.81	75.30	-16.46
	0.5	0.0	36.56	38.51
0.2		43.87	46.21	-82.54
0.4		51.92	54.68	-70.90
0.6		61.06	64.31	-63.49
0.8		62.88	66.24	-42.33
1.0		66.17	69.70	-17.99
1.0		0.0	35.70	34.98
	0.3	42.84	41.98	-86.12
	0.6	50.69	49.67	-73.97
	0.9	59.62	58.42	-66.24
	1.2	61.40	60.17	-44.16
	1.5	64.62	63.31	-18.77
	1.5	0.0	32.08	30.55
0.4		38.50	36.66	-93.76
0.8		45.55	43.38	-80.54
1.2		53.57	51.02	-72.12
1.6		55.18	52.55	-48.08
2.0		58.06	55.30	-20.43
2.0		0.0	30.33	31.24
	0.4	36.40	37.49	-97.34
	0.8	43.07	44.36	-83.61
	1.2	50.65	52.17	-74.88
	1.6	52.17	53.73	-49.92
	2.0	54.90	56.54	-21.22

Table 3.32: Thermodynamic parameters for the adsorption of CPOB on weld aged maraging steel surface in hydrochloric acid at different temperatures.

Molarity of hydrochloric acid (M)	Temperature (°C)	$-\Delta G^{\circ}_{\text{ads}}$ (kJ mol ⁻¹)	$\Delta H^{\circ}_{\text{ads}}$ (kJ mol ⁻¹)	$\Delta S^{\circ}_{\text{ads}}$ (J mol ⁻¹ K ⁻¹)
0.1	30	34.04	- 18.33	-55.31
	35	33.90		
	40	33.74		
	45	33.57		
	50	33.41		
0.5	30	32.74	-27.12	-43.35
	35	32.61		
	40	32.45		
	45	32.29		
	50	32.14		
1.0	30	33.36	-35.70	-36.12
	35	33.23		
	40	33.07		
	45	32.91		
	50	32.75		
1.5	30	35.95	-43.01	-24.10
	35	35.81		
	40	35.64		
	45	35.46		
	50	35.29		
2.0	30	32.71	-48.99	-12.08
	35	32.58		
	40	32.42		
	45	32.26		
	50	32.11		

3.5 2-(4-BROMOPHENYL)-2-OXOETHYL-4-CHLOROBENZOATE (CPOM) AS INHIBITOR FOR THE CORROSION OF WELD AGED MARAGING STEEL IN HYDROCHLORIC ACID MEDIUM

3.5.1 Potentiodynamic polarization studies

The potentiodynamic polarization curves for the corrosion of weld aged maraging steel specimen in 2.0 M hydrochloric acid in the presence of different concentrations of CPOM, at 30 °C are shown in Fig. 3.35. Similar plots were obtained in the other four concentrations of hydrochloric acid at the different temperatures studied.

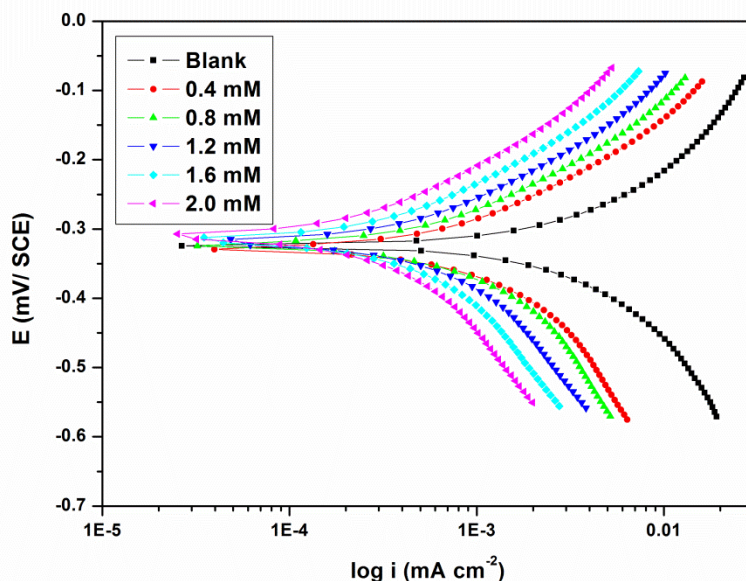


Fig. 3.35: Potentiodynamic polarization curves for the corrosion of weld aged maraging steel in 2.0 M hydrochloric acid containing different concentrations of CPOM at 30 °C.

The potentiodynamic polarization parameters (E_{corr} , b_c , b_a , i_{corr} and η (%)) are summarized in Tables 3.33 to 3.37. It is seen from the Tables that the i_{corr} decreases and the inhibition efficiency ($\eta\%$) increases with the increase in the inhibitor concentration.

The presence of CPOM shifts E_{corr} slightly towards positive direction. However, the maximum displacement in the present study is ± 25 mV, therefore it can be concluded that CPOM acts as a mixed type inhibitor on weld aged maraging steel. The rest of the discussion is similar to the one already discussed under section 3.3.1. CPOM shows slightly higher inhibition efficiency than that of ATPI and CPOB for the corrosion of weld aged maraging steel in hydrochloric acid.

3.5.2 Electrochemical impedance spectroscopy

Fig. 3.36 represents Nyquist plots for the corrosion of weld aged maraging steel in 2.0 M hydrochloric acid in the presence of different concentrations of CPOM at 30 °C. Similar plots were obtained in other concentrations of hydrochloric acid and also at other temperatures.

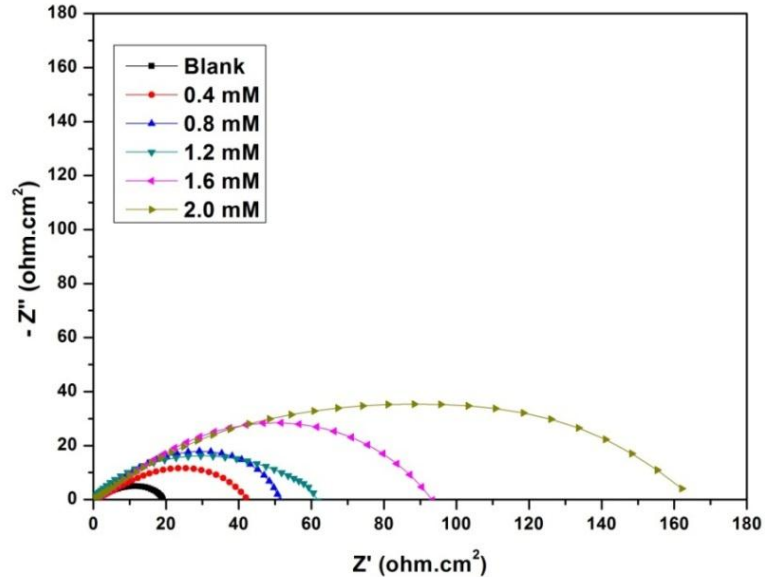


Fig. 3.36: Nyquist plots for the corrosion of weld aged maraging steel in 2.0 M hydrochloric acid containing different concentrations of CPOM at 30 °C.

The impedance parameters derived from the EIS studies are summarized in Tables 3.38 to 3.42. It is clear from Fig. 3.36 that the shapes of the impedance plots for the corrosion of weld aged maraging steel in the presence of inhibitor are not substantially different from those of the uninhibited one. The plots are similar to those obtained in the presence of ATPI as discussed in the section 3.3.2. The equivalent circuit given in Fig. 3.20 is used to fit the experimental data for the corrosion of weld aged maraging steel in hydrochloric acid in the presence of CPOM. As can be seen from the Tables 3.38 to 3.42, R_{ct} , R_{pf} values increase and C_{dl} , C_{pf} values decrease with the increase in the concentration of CPOM. The inhibitor molecule CPOM has the electron rich environment in phenyl group due to resonance of π -electrons of double bonds that can be adsorbed well on the sample surface. Also carbonyl groups are electron donating groups containing oxygen atom as an active site (Atta et al. 2011).

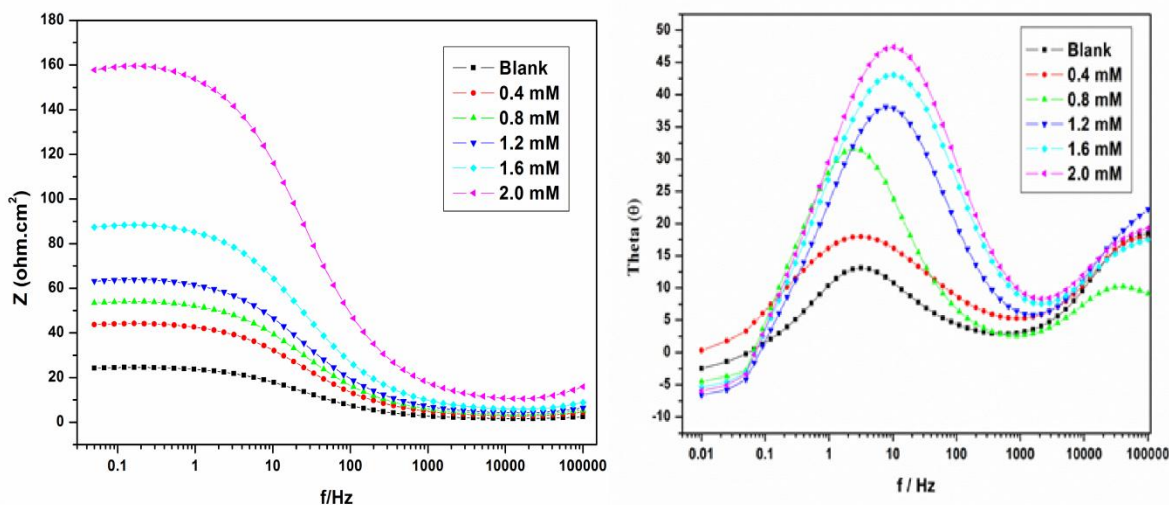


Fig. 3.37: Bode plots for the corrosion of weld aged maraging steel in 2.0 M hydrochloric acid containing different concentrations of CPOM at 30 °C.

The Bode plots for the corrosion of the alloy in the presence of different concentrations of CPOM are shown in Fig. 3.37. They are similar to the ones shown in

Fig. 3.21. Hence the discussion regarding the Bode plot under the section 3.3.2 holds good for CPOM also.

A comparison of maximum attainable inhibition efficiencies by the Tafel method and EIS method, in the presence of CPOM for the corrosion of weld aged maraging steel in hydrochloric acid solutions of different concentrations at 30 °C are listed in Table 3.43. It is evident from the table that the η (%) values obtained by the two methods are in good agreement. Similar levels of agreement were obtained at other temperatures also.

3.4.3 Effect of temperature

The Tafel and EIS results pertaining to different temperatures in different concentrations of hydrochloric acid have already been listed in Tables 3.33 to 3.42. The effect of temperature on corrosion inhibition behaviour of CPOM is similar to that of ATPI and CPOB on weld aged maraging steel as discussed in the earlier sections. The decrease in the inhibition efficiency of CPOM with the increase in temperature on weld aged maraging steel surface may be attributed to the physisorption of CPOM. The Arrhenius plots for the corrosion of weld aged maraging steel in 2.0 M hydrochloric acid in the presence of different concentrations of CPOM are shown in Fig. 3.38. The plots of $\ln(v_{\text{corr}}/T)$ vs $(1/T)$ are shown in Fig. 3.39. The calculated values of activation parameters are given in Table 3.44. The observations are similar to the ones obtained in the presence of ATPI and CPOB.

The increase in the E_a values with the increase in CPOM concentration indicates the increase in energy barrier for the corrosion reaction as discussed in earlier sections. The entropy of activation in the absence and presence of CPOM is large and negative for the corrosion of alloy. This implies that the activated complex in the rate determining step represents an association rather than dissociation step, indicating that a decrease in disordering takes place on going from reactants to activated complex (Marsh 1988, Gomma and Wahdan 1995).

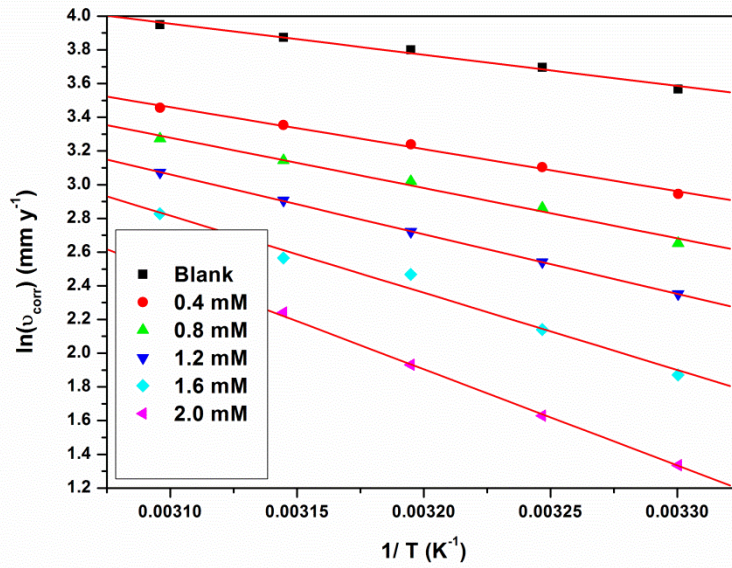


Fig. 3.38: Arrhenius plots for the corrosion of weld aged maraging steel in 2.0 M hydrochloric acid containing different concentrations of CPOM.

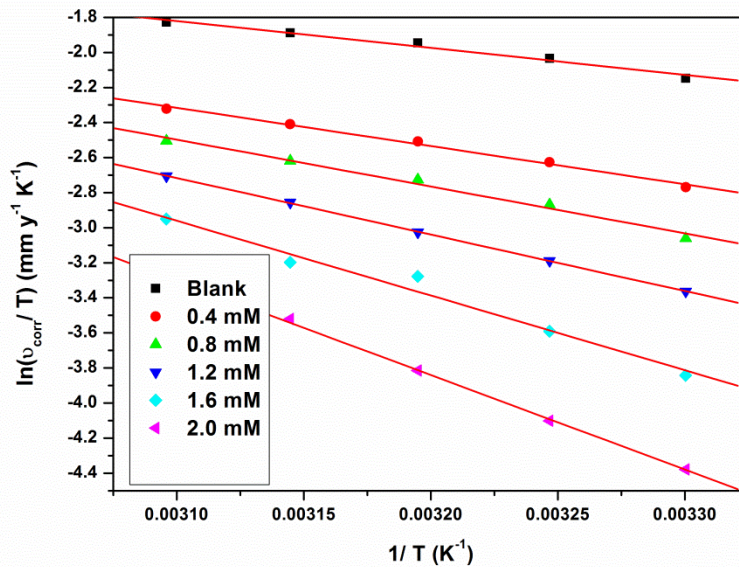


Fig. 3.39: Plots of $\ln(v_{\text{corr}}/T)$ versus $1/T$ for the corrosion of weld aged maraging steel in 2.0 M hydrochloric acid containing different concentrations of CPOM.

3.5.4 Effect of hydrochloric acid concentration

It is evident from both the polarization and EIS experimental results that, for a particular concentration of the CPOM, the inhibition efficiency decreases with the increase in hydrochloric acid concentration. The maximum inhibition efficiency is observed in 0.1 M solution of hydrochloric acid.

3.5.5 Adsorption isotherms

The adsorption of CPOM on the surfaces of weld aged maraging steel was found to obey Langmuir adsorption isotherm as shown in Fig. 3.40. The thermodynamic parameters obtained for the adsorption of CPOM on weld aged maraging steel are tabulated in Tables 3.45. These data also reveal similar inhibition behaviour of CPOM as that of ATPI as discussed in section 3.3.5.

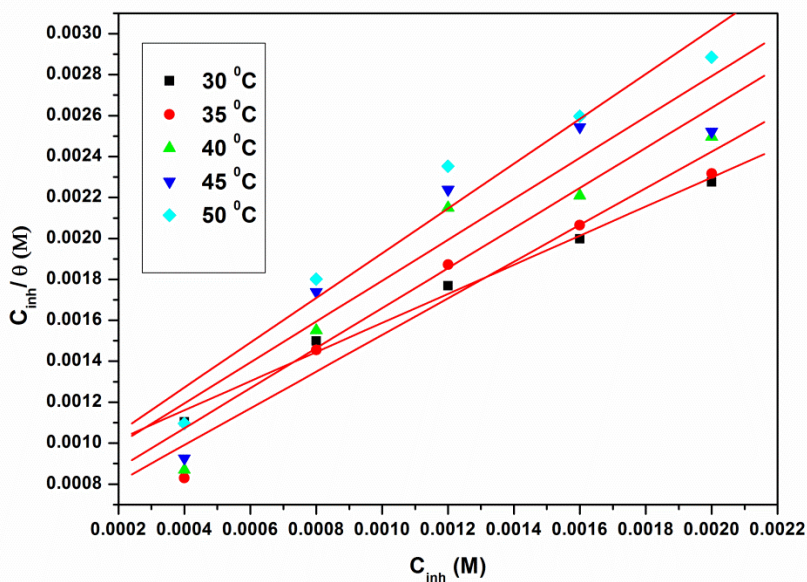


Fig. 3.40: Langmuir adsorption isotherms for the adsorption of CPOM on weld aged maraging steel in 2.0 M hydrochloric acid at different temperatures.

The values of ΔG_{ads}^0 and ΔH_{ads}^0 suggest both physisorption and chemisorption of CPOM on weld aged maraging steel with predominant physisorption. The ΔS_{ads}^0 value indicates the increase in randomness on going from the reactants to the metal adsorbed species.

3.5.6 Mechanism of corrosion inhibition

The mechanism of corrosion inhibition of weld aged maraging steel in the presence of CPOM is similar to that of ATPI as discussed under section 3.3.6. The protonated CPOM is responsible for physisorption and neutral CPOM molecule with lone pair of electrons on oxygen and π - electrons of benzene rings are responsible for the chemisorption of CPOM on the alloy surfaces, as discussed in earlier sections. CPOM shows slightly better inhibition efficiency than that of ATPI and CPOB for the corrosion of weld aged maraging steel in hydrochloric acid medium. This can be attributed to the fact that the presence of methoxy groups and chlorine and bromine group in the inhibitor moiety increases electron density at the binding sites in CPOM. Hence CPOM can adsorb on the alloy surface more strongly than ATPI and CPOB. Hence CPOM covers the alloy surface more effectively.

3.5.7 SEM/EDS studies

Fig. 3.41 (a) represents SEM image of the corroded weld aged maraging steel sample which shows the facets due to the attack of hydrochloric acid on the metal surface with cracks and rough surfaces. Fig. 3.41 (b) shows the SEM image of the sample after immersion in 2.0 M hydrochloric acid in the presence of CPOM. It can be seen that the alloy surface is smooth without any visible corrosion attack. Thus, it can be concluded that CPOM protects the alloy from corrosion by forming a uniform film on the alloy surface.

The EDS profile analyses for the corrosion of weld aged maraging steel in hydrochloric acid is already discussed under section 3.3.7. The EDS profile of the corroded surface of the alloy in the presence of CPOM is shown in Fig. 3.42. The atomic

percentages of the elements found in the EDS profile were 5.20 % Fe, 0.62% Ni, 1.20% Mo, 15.19% O, 2.66% Cl, 70.56% C and 4.37% Br and indicated the formation of inhibitor film on the surface of alloy.

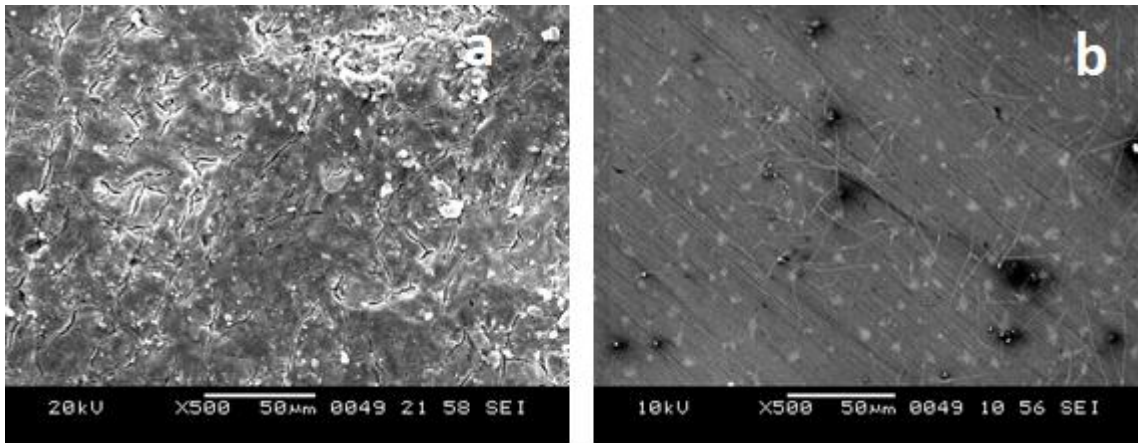


Fig. 3.41: SEM images of the weld aged maraging steel after immersion in 2.0 M hydrochloric acid a) in the absence and b) in the presence of CPOM.

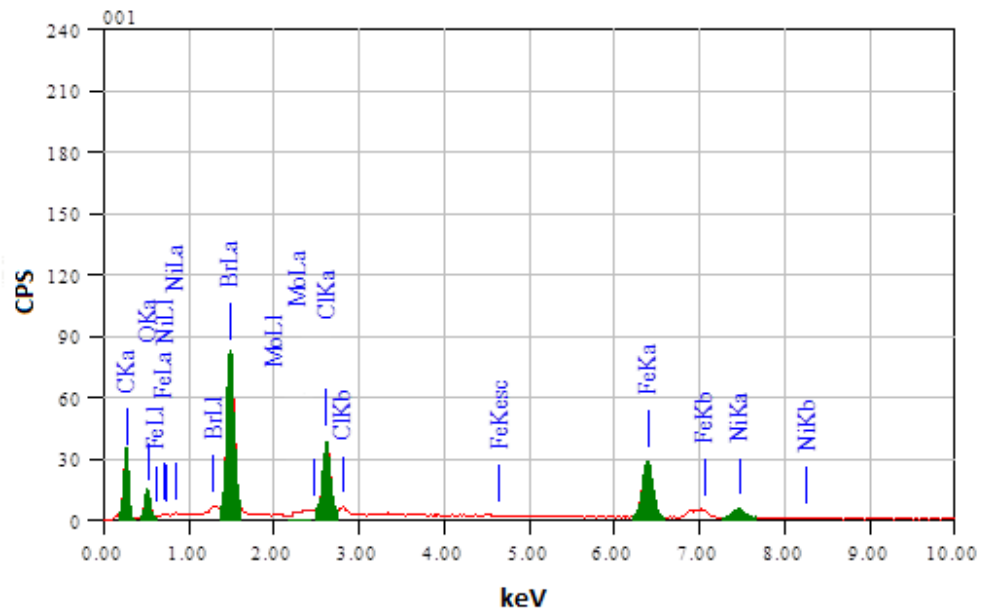


Fig. 3.42: EDS spectra of the weld aged maraging steel after immersion in 2.0 M hydrochloric acid in the presence of CPOM.

Table 3.33: Results of potentiodynamic polarization studies for the corrosion of weld aged maraging steel in 0.1 M hydrochloric acid containing different concentrations of CPOM.

Temperature (°C)	Conc. of inhibitor (mM)	E_{corr} (mV /SCE)	b_a (mV dec ⁻¹)	$-b_c$ (mV dec ⁻¹)	i_{corr} (mA cm ⁻²)	v_{corr} (mm y ⁻¹)	η (%)
30	Blank	-419±1	142±3	226±2	0.22±0.03	2.53±0.26	
	0.1	-415±3	138±3	221±4	0.12±0.02	1.35±0.20	46.5
	0.2	-411±3	135±2	219±3	0.08±0.02	0.88±0.23	65.2
	0.4	-408±1	132±3	216±3	0.05±0.03	0.56±0.25	77.7
	0.6	-406±4	129±4	212±2	0.03±0.02	0.29±0.12	88.4
	0.8	-403±3	125±2	210±4	0.01±0.01	0.13±0.10	97.8
35	Blank	-416±4	150±3	234±1	0.26±0.01	2.99±0.12	
	0.1	-413±2	146±3	232±3	0.15±0.03	1.68±0.27	44.1
	0.2	-411±1	142±3	230±3	0.10±0.02	1.11±0.18	62.9
	0.4	-407±3	140±4	227±1	0.06±0.03	0.73±0.29	75.6
	0.6	-405±3	137±1	225±2	0.04±0.02	0.41±0.20	86.4
	0.8	-402±4	133±2	221±4	0.01±0.01	0.15±0.11	95.9
40	Blank	-412±2	159±3	242±3	0.30±0.02	3.45±0.18	
	0.1	-410±1	155±1	239±1	0.17±0.02	1.94±0.23	41.5
	0.2	-408±3	152±4	236±3	0.11±0.03	1.28±0.27	60.6
	0.4	-405±1	150±3	234±3	0.07±0.03	0.85±0.27	73.4
	0.6	-401±1	148±2	232±2	0.04±0.03	0.47±0.28	84.3
	0.8	-399±1	144±2	229±3	0.01±0.01	0.14±0.13	93.9
45	Blank	-409±3	165±4	250±1	0.33±0.01	3.80±0.13	
	0.1	-405±3	163±3	247±4	0.20±0.02	2.33±0.17	38.7
	0.2	-400±4	161±4	242±2	0.14±0.01	1.59±0.13	58.2
	0.4	-398±3	158±3	240±4	0.10±0.02	1.10±0.24	70.9
	0.6	-395±3	155±4	236±1	0.06±0.02	0.69±0.22	81.9
	0.8	-393±1	151±2	233±1	0.03±0.02	0.32±0.19	91.6
50	Blank	-405±2	173±2	259±3	0.37±0.02	4.26±0.21	
	0.1	-400±1	170±1	255±1	0.24±0.02	2.73±0.22	35.9
	0.2	-398±3	166±1	251±4	0.17±0.02	1.90±0.23	55.4
	0.4	-395±3	164±3	247±2	0.12±0.02	1.35±0.17	68.4
	0.6	-393±3	161±2	244±4	0.08±0.01	0.87±0.11	79.5
	0.8	-391±2	158±2	241±3	0.04±0.02	0.46±0.28	89.3

Table 3.34: Results of potentiodynamic polarization studies for the corrosion of weld aged maraging steel in 0.5 M hydrochloric acid containing different concentrations of CPOM.

Temperature (°C)	Conc. of inhibitor (mM)	E_{corr} (mV /SCE)	b_a (mV dec ⁻¹)	$-b_c$ (mV dec ⁻¹)	i_{corr} (mA cm ⁻²)	v_{corr} (mm y ⁻¹)	η (%)
30	Blank	-413±1	148±1	247±3	0.27±0.02	3.11±0.16	
	0.2	-417±3	144±1	245±2	0.14±0.01	1.61±0.12	48.7
	0.4	-415±4	141±1	242±2	0.10±0.02	1.14±0.23	63.5
	0.6	-410±1	140±3	239±4	0.07±0.02	0.74±0.15	76.2
	0.8	-407±2	138±2	236±3	0.03±0.02	0.33±0.22	89.3
	1.0	-402±1	135±1	231±1	0.01±0.01	0.14±0.10	95.4
35	Blank	-411±1	156±1	254±1	0.35±0.02	4.03±0.22	
	0.2	-407±4	152±2	250±3	0.19±0.03	2.22±0.29	45.0
	0.4	-409±3	150±3	248±3	0.14±0.01	1.59±0.15	60.6
	0.6	-405±1	148±4	245±4	0.09±0.02	1.08±0.22	73.2
	0.8	-401±2	144±4	241±3	0.05±0.02	0.58±0.18	85.7
	1.0	-399±2	140±1	238±2	0.02±0.01	0.26±0.14	93.5
40	Blank	-408±1	165±2	262±4	0.42±0.02	4.83±0.23	
	0.2	-406±3	161±4	258±2	0.24±0.02	2.76±0.15	43.2
	0.4	-404±2	158±1	255±1	0.18±0.01	2.08±0.12	57.3
	0.6	-402±3	155±2	252±2	0.12±0.01	1.37±0.12	71.9
	0.8	-398±1	152±4	248±3	0.07±0.02	0.85±0.23	82.6
	1.0	-395±4	150±3	244±2	0.03±0.02	0.39±0.21	91.9
45	Blank	-406±2	172±2	269±3	0.52±0.01	5.87±0.13	
	0.2	-404±2	170±3	266±2	0.30±0.02	3.47±0.16	41.6
	0.4	-401±4	166±2	264±1	0.23±0.01	2.69±0.11	54.8
	0.6	-403±4	162±4	261±3	0.16±0.02	1.89±0.17	68.3
	0.8	-400±3	160±2	258±1	0.11±0.02	1.23±0.23	79.3
	1.0	-398±2	157±4	254±1	0.07±0.01	0.83±0.14	86.1
50	Blank	-404±2	183±4	277±2	0.59±0.01	6.79±0.14	
	0.2	-406±4	179±2	275±3	0.36±0.01	4.11±0.12	39.5
	0.4	-403±3	176±2	271±4	0.29±0.01	3.29±0.14	51.6
	0.6	-401±2	173±1	268±1	0.20±0.02	2.34±0.18	65.5
	0.8	-398±3	170±3	264±1	0.14±0.03	1.60±0.27	76.4
	1.0	-395±2	168±2	261±2	0.10±0.03	1.11±0.28	83.6

Table 3.35: Results of potentiodynamic polarization studies for the corrosion of weld aged maraging steel in 1.0 M hydrochloric acid containing different concentrations of CPOM.

Temperature (°C)	Conc. of inhibitor (mM)	E_{corr} (mV /SCE)	b_a (mV dec ⁻¹)	$-b_c$ (mV dec ⁻¹)	i_{corr} (mA cm ⁻²)	v_{corr} (mm y ⁻¹)	η (%)
30	Blank	-371±2	153±4	256±3	0.33±0.04	3.80±0.37	
	0.3	-375±2	149±2	251±1	0.16±0.02	1.86±0.17	50.9
	0.6	-372±4	144±2	246±1	0.12±0.02	1.36±0.21	64.1
	0.9	-368±2	141±2	243±4	0.07±0.04	0.85±0.36	77.5
	1.2	-366±3	139±3	241±2	0.04±0.02	0.51±0.22	86.7
	1.5	-362±4	136±1	237±3	0.02±0.01	0.24±0.19	93.5
35	Blank	-368±4	159±4	261±3	0.45±0.01	5.20±0.13	
	0.3	-363±2	158±3	255±3	0.23±0.03	2.65±0.31	49.1
	0.6	-365±3	155±1	251±3	0.18±0.03	2.02±0.27	61.3
	0.9	-362±4	151±4	248±4	0.12±0.02	1.43±0.17	72.6
	1.2	-360±4	148±4	246±2	0.08±0.03	0.87±0.29	83.1
	1.5	-357±3	144±3	242±2	0.04±0.03	0.45±0.17	91.4
40	Blank	-364±2	165±3	266±1	0.56±0.04	6.45±0.36	
	0.3	-360±4	162±3	263±1	0.30±0.01	3.42±0.12	47.1
	0.6	-362±2	160±1	260±1	0.23±0.03	2.68±0.32	58.4
	0.9	-359±2	156±4	258±4	0.17±0.02	1.93±0.17	70.1
	1.2	-357±3	154±4	256±3	0.11±0.02	1.30±0.19	79.9
	1.5	-354±2	151±4	252±3	0.06±0.03	0.74±0.35	88.6
45	Blank	-361±3	172±1	273±3	0.76±0.02	8.72±0.24	
	0.3	-363±4	170±3	271±1	0.42±0.03	4.84±0.35	44.5
	0.6	-365±1	167±2	268±4	0.33±0.04	3.84±0.39	55.9
	0.9	-362±4	163±1	266±4	0.26±0.03	2.95±0.30	66.2
	1.2	-357±1	161±3	263±2	0.17±0.02	2.00±0.20	77.1
	1.5	-355±1	158±4	261±3	0.12±0.01	1.35±0.14	84.5
50	Blank	-358±4	177±2	278±3	0.92±0.04	10.63±0.37	
	0.3	-355±3	172±2	275±2	0.53±0.03	6.09±0.29	42.7
	0.6	-351±2	170±1	271±4	0.44±0.01	5.02±0.12	52.8
	0.9	-348±2	168±3	269±4	0.35±0.02	4.00±0.18	62.3
	1.2	-346±3	164±3	266±3	0.24±0.03	2.76±0.25	74.2
	1.5	-342±2.	161±1	262±3	0.18±0.02	2.04±0.21	80.8

Table 3.36: Results of potentiodynamic polarization studies for the corrosion of weld aged maraging steel in 1.5 M hydrochloric acid containing different concentrations of CPOM.

Temperature (°C)	Conc. of inhibitor (mM)	E_{corr} (mV /SCE)	b_a (mV dec ⁻¹)	$-b_c$ (mV dec ⁻¹)	i_{corr} (mA cm ⁻²)	v_{corr} (mm y ⁻¹)	η (%)
30	Blank	-342±2	158±4	267±3	0.70±0.03	8.05±0.31	
	0.3	-344±1	155±2	263±2	0.36±0.03	4.15±0.37	48.5
	0.6	-341±3	152±4	260±3	0.27±0.03	3.08±0.34	61.7
	0.9	-338±2	149±2	257±3	0.17±0.03	2.00±0.28	75.1
	1.2	-335±1	146±4	254±1	0.11±0.04	1.27±0.39	84.3
	1.5	-331±2	142±1	252±4	0.06±0.03	0.71±0.25	91.1
35	Blank	-339±1	165±4	276±3	0.82±0.03	9.45±0.35	
	0.3	-338±1	163±4	273±3	0.44±0.01	5.04±0.15	46.7
	0.6	-340±2	160±1	270±2	0.34±0.03	3.91±0.33	58.6
	0.9	-338±3	158±1	268±1	0.25±0.03	2.82±0.27	70.2
	1.2	-334±4	155±3	264±2	0.16±0.02	1.82±0.22	80.7
	1.5	-330±4	151±3	261±3	0.09±0.02	1.04±0.26	89.1
40	Blank	-337±2	173±4	282±2	0.94±0.04	10.85±0.36	
	0.3	-340±1	171±4	280±1	0.52±0.03	5.99±0.33	44.7
	0.6	-336±2	168±1	278±4	0.42±0.04	4.77±0.36	56.1
	0.9	-332±2	165±2	274±1	0.31±0.02	3.51±0.21	67.7
	1.2	-330±4	161±4	270±3	0.21±0.02	2.44±0.19	77.5
	1.5	-328±3	157±2	268±4	0.13±0.02	1.50±0.12	86.2
45	Blank	-334±1	179±3	286±3	1.53±0.03	17.60±0.32	
	0.3	-330±2	175±3	283±3	0.89±0.04	10.19±0.40	42.1
	0.6	-327±4	172±4	280±3	0.71±0.03	8.18±0.29	53.5
	0.9	-324±4	168±1	278±4	0.55±0.01	6.37±0.12	63.8
	1.2	-321±3	165±1	275±4	0.39±0.02	4.45±0.15	74.7
	1.5	-320±2	161±2	271±4	0.27±0.02	3.15±0.23	82.1
50	Blank	-332±4	185±1	292±3	1.61±0.03	18.57±0.34	
	0.3	-330±2	181±4	290±4	0.96±0.04	11.09±0.36	40.3
	0.6	-327±4	178±2	288±1	0.80±0.01	9.22±0.12	50.4
	0.9	-324±2	175±4	285±2	0.65±0.03	7.44±0.30	59.9
	1.2	-321±3	172±2	282±1	0.46±0.03	5.27±0.26	71.6
	1.5	-318±2	170±1	278±4	0.35±0.02	4.02±0.21	78.4

Table 3.37: Results of potentiodynamic polarization studies for the corrosion of weld aged maraging steel in 2.0 M hydrochloric acid containing different concentrations of CPOM.

Temperature (°C)	Conc. of inhibitor (mM)	E_{corr} (mV /SCE)	b_a (mV dec ⁻¹)	$-b_c$ (mV dec ⁻¹)	i_{corr} (mA cm ⁻²)	v_{corr} (mm y ⁻¹)	η (%)
30	Blank	-324±2	175±3	287±3	3.08±0.12	35.44±1.23	
	0.4	-327±3	173±4	291±3	1.65±0.15	19.02±1.67	46.4
	0.8	-322±3	168±4	285±3	1.24±0.01	14.21±0.15	59.6
	1.2	-318±3	170±3	282±1	0.92±0.04	10.51±0.40	70.2
	1.6	-315±2	165±2	278±4	0.57±0.03	6.51±0.33	81.2
	2.0	-310±1	159±1	274±3	0.33±0.02	3.80±0.17	89.2
35	Blank	-325±4	189±4	307±3	3.50±0.15	40.34±1.17	
	0.4	-323±1	193±4	305±2	1.94±0.14	22.32±1.44	44.6
	0.8	-319±4	186±1	303±2	1.52±0.04	17.52±0.43	56.5
	1.2	-320±1	183±4	299±2	1.11±0.02	12.71±0.24	68.1
	1.6	-316±3	178±3	295±3	0.74±0.04	8.51±0.43	78.6
	2.0	-313±2	175±1	293±3	0.45±0.04	5.11±0.45	86.9
40	Blank	-321±3	192±2	325±4	3.88±0.24	44.74±2.36	
	0.4	-324±1	188±2	322±2	2.22±0.14	25.53±1.44	42.8
	0.8	-320±2	185±2	317±1	1.78±0.01	20.52±0.14	54.1
	1.2	-318±4	181±1	319±2	1.32±0.05	15.22±0.47	65.8
	1.6	-315±3	176±3	312±3	1.03±0.02	11.81±0.23	75.6
	2.0	-310±1	170±2	309±1	0.60±0.04	6.91±0.42	84.3
45	Blank	-322±1	206±4	332±1	4.18±0.22	48.15±2.51	
	0.4	-318±2	208±3	330±1	2.49±0.13	28.63±1.28	40.2
	0.8	-320±1	203±1	335±3	2.02±0.05	23.22±0.49	51.6
	1.2	-317±4	198±3	327±1	1.59±0.02	18.32±0.19	61.9
	1.6	-314±3	195±4	323±4	1.13±0.01	13.01±0.14	72.8
	2.0	-309±1	191±3	319±2	0.82±0.02	9.41±0.23	80.2
50	Blank	-319±1	224±3	340±4	4.51±0.21	51.95±2.36	
	0.4	-322±2	227±3	337±1	2.76±0.11	31.73±1.14	38.6
	0.8	-324±1	221±3	332±3	2.30±0.04	26.43±0.41	48.7
	1.2	-321±1	218±4	335±5	1.88±0.05	21.62±0.46	58.2
	1.6	-315±4	214±2	330±2	1.47±0.03	16.92±0.32	67.3
	2.0	-307±4	211±3	326±3	1.05±0.03	12.01±0.32	76.7

Table 3.38: EIS data for the corrosion of weld aged maraging steel in 0.1 M hydrochloric acid containing different concentrations of CPOM.

Temperature (°C)	Conc. of inhibitor (mM)	R_{ct} (ohm. cm^2)	C_{dl} (mF cm^{-2})	R_{pf} (ohm. cm^2)	C_{pf} (mF cm^{-2})	η (%)
30	Blank	181.20±2.35	0.93±0.11			
	0.1	367.62±3.63	0.74±0.08	24.99±1.34	0.24±0.06	50.7
	0.2	527.66±4.68	0.58±0.07	34.94±2.93	0.20±0.08	65.7
	0.4	842.01±7.84	0.45±0.13	54.48±3.39	0.16±0.06	78.5
	0.6	2188.41±9.25	0.31±0.10	138.16±3.80	0.12±0.10	91.7
	0.8	8547.17±11.97	0.25±0.08	533.37±2.54	0.11±0.04	97.9
35	Blank	156.30±3.28	0.96±0.13			
	0.1	296.42±3.06	0.79±0.19	20.57±1.78	0.26±0.10	47.3
	0.2	422.78±4.64	0.62±0.18	28.42±2.27	0.21±0.11	63.1
	0.4	644.80±6.21	0.49±0.15	42.22±2.77	0.17±0.11	75.8
	0.6	1345.09±5.19	0.35±0.08	85.74±2.56	0.13±0.08	88.4
	0.8	3868.81±7.53	0.27±0.07	242.60±3.83	0.12±0.05	96.3
40	Blank	116.20±4.46	1.68±0.16			
	0.1	213.02±4.54	1.25±0.20	15.38±2.17	0.39±0.10	45.5
	0.2	288.34±3.68	0.98±0.15	20.06±2.81	0.31±0.10	59.7
	0.4	454.62±5.88	0.71±0.19	30.40±3.38	0.24±0.06	74.4
	0.6	787.80±7.27	0.50±0.19	51.11±3.96	0.18±0.13	85.3
	0.8	2053.00±10.48	0.33±0.14	129.74±3.11	0.13±0.10	94.3
45	Blank	64.30±3.60	3.01±0.22			
	0.1	113.46±2.01	2.19±0.17	9.19±2.09	0.65±0.08	43.3
	0.2	148.40±2.20	1.73±0.08	11.37±3.56	0.52±0.11	56.7
	0.4	216.50±3.81	1.25±0.07	15.60±3.36	0.39±0.11	70.3
	0.6	345.88±4.28	0.87±0.19	23.64±2.79	0.28±0.07	81.4
	0.8	548.63±6.04	0.63±0.07	36.24±3.69	0.21±0.14	88.3
50	Blank	20.21±3.73	5.75±0.50			
	0.1	34.38±4.42	3.98±0.07	4.28±1.40	1.15±0.12	41.2
	0.2	43.40±3.36	3.20±0.14	4.84±2.59	0.93±0.14	53.4
	0.4	62.13±4.12	2.30±0.06	6.00±2.23	0.68±0.18	67.5
	0.6	93.91±3.64	1.60±0.12	7.98±2.11	0.49±0.17	78.5
	0.8	141.92±4.20	1.14±0.07	10.96±2.66	0.36±0.12	85.8

Table 3.39: EIS data for the corrosion of weld aged maraging steel in 0.5 M hydrochloric acid containing different concentrations of CPOM.

Temperature (°C)	Conc. of inhibitor (mM)	R_{ct} (ohm. cm ²)	C_{dl} (mF cm ⁻²)	R_{pf} (ohm. cm ²)	C_{pf} (mF cm ⁻²)	η (%)
30	Blank	156.30±2.83	0.96±0.26			
	0.2	317.10±2.50	0.76±0.11	21.85±1.48	0.25±0.11	48.8
	0.4	455.15±3.88	0.59±0.18	30.43±2.47	0.20±0.14	63.8
	0.6	726.30±3.87	0.46±0.20	47.28±3.95	0.17±0.12	76.6
	0.8	1887.68±7.12	0.31±0.12	119.47±2.69	0.12±0.19	89.8
	1.0	7372.64±9.21	0.25±0.12	460.37±3.75	0.10±0.03	96.0
35	Blank	139.27±4.73	1.11±0.24			
	0.2	264.12±3.79	0.88±0.19	18.56±2.02	0.28±0.12	45.4
	0.4	376.71±4.60	0.68±0.15	25.56±2.80	0.23±0.19	61.1
	0.6	574.55±5.54	0.52±0.11	37.85±2.21	0.18±0.16	73.9
	0.8	1198.54±8.63	0.37±0.15	76.63±3.47	0.14±0.15	86.5
	1.0	3447.28±11.66	0.27±0.05	216.40±2.09	0.11±0.04	94.1
40	Blank	123.15±4.82	1.33±0.28			
	0.2	225.76±4.24	1.00±0.16	16.17±3.01	0.32±0.16	43.6
	0.4	305.58±3.23	0.80±0.10	21.14±3.08	0.26±0.13	57.8
	0.6	481.81±4.59	0.59±0.15	32.09±2.39	0.20±0.12	72.5
	0.8	834.92±7.83	0.43±0.13	54.03±3.20	0.16±0.17	83.4
	1.0	2175.80±9.61	0.31±0.08	137.37±3.52	0.12±0.10	92.4
45	Blank	107.56±2.28	2.55±0.37			
	0.2	189.80±4.90	1.17±0.19	13.94±2.53	0.36±0.10	41.4
	0.4	248.23±3.48	0.95±0.20	17.57±2.06	0.30±0.11	54.8
	0.6	362.15±2.86	0.72±0.11	24.65±2.66	0.24±0.12	68.4
	0.8	578.59±4.08	0.54±0.14	38.10±2.03	0.19±0.19	79.5
	1.0	917.75±6.54	0.42±0.06	59.18±3.79	0.15±0.11	86.4
50	Blank	90.34±3.82	3.74±0.59			
	0.2	153.67±2.50	2.34±0.15	11.69±2.13	0.41±0.19	39.3
	0.4	193.99±3.79	1.11±0.18	14.20±3.37	0.35±0.11	51.5
	0.6	277.71±2.43	0.84±0.11	19.40±3.32	0.27±0.14	65.6
	0.8	419.80±3.50	0.63±0.15	28.23±3.18	0.21±0.13	76.6
	1.0	634.41±4.71	0.50±0.04	41.57±3.62	0.18±0.09	83.9

Table 3.40: EIS data for the corrosion of weld aged maraging steel in 1.0 M hydrochloric acid containing different concentrations of CPOM.

Temperature (°C)	Conc. of inhibitor (mM)	R_{ct} (ohm. cm^2)	C_{dl} (mF cm^{-2})	R_{pf} (ohm. cm^2)	C_{pf} (mF cm^{-2})	η (%)
30	Blank	116.21±2.67	1.68±0.17			
	0.3	242.59±3.84	1.19±0.24	17.48±2.60	0.52±0.30	52.1
	0.6	337.79±3.97	0.97±0.11	23.27±3.00	0.45±0.15	65.6
	0.9	530.59±4.10	0.76±0.29	35.02±2.77	0.40±0.27	78.1
	1.2	937.10±6.01	0.60±0.29	59.78±2.40	0.36±0.29	87.6
	1.5	2112.73±8.03	0.48±0.20	131.38±3.11	0.33±0.11	94.5
35	Blank	97.32±3.94	1.75±0.18			
	0.3	195.77±2.81	1.23±0.28	14.62±3.02	0.53±0.12	50.3
	0.6	252.07±3.00	1.04±0.12	18.05±2.59	0.46±0.19	61.4
	0.9	363.06±2.39	0.84±0.13	24.81±3.58	0.42±0.22	73.2
	1.2	640.13±5.75	0.65±0.23	41.69±2.12	0.37±0.23	84.8
	1.5	1216.25±6.45	0.53±0.17	76.78±2.45	0.34±0.19	92.2
40	Blank	82.61±2.57	2.15±0.45			
	0.3	160.39±3.42	1.49±0.22	12.47±2.07	0.59±0.11	48.5
	0.6	201.96±3.47	1.26±0.19	15.00±3.08	0.51±0.19	59.1
	0.9	291.87±3.96	0.99±0.15	20.48±3.14	0.45±0.28	71.7
	1.2	444.09±3.03	0.79±0.22	29.75±3.42	0.40±0.28	81.4
	1.5	764.81±4.55	0.62±0.20	49.28±3.25	0.36±0.11	89.2
45	Blank	65.22±2.70	2.36±0.35			
	0.3	120.52±3.37	1.57±0.25	10.04±1.91	0.61±0.24	45.9
	0.6	148.86±2.32	1.35±0.12	11.77±3.71	0.53±0.19	56.2
	0.9	200.00±3.44	1.10±0.23	14.88±2.65	0.48±0.19	67.4
	1.2	291.07±4.83	0.88±0.25	20.43±3.26	0.43±0.13	77.6
	1.5	449.66±5.02	0.71±0.14	30.09±3.55	0.39±0.14	85.5
50	Blank	53.86±2.31	2.79±0.25			
	0.3	96.94±3.21	1.87±0.23	8.60±1.60	0.68±0.16	44.5
	0.6	117.72±3.24	1.61±0.23	9.87±2.60	0.60±0.30	54.3
	0.9	148.21±3.86	1.36±0.28	11.73±3.12	0.54±0.28	63.7
	1.2	223.24±2.98	1.03±0.16	16.30±2.69	0.46±0.18	75.9
	1.5	309.20±4.69	0.85±0.22	21.53±2.00	0.42±0.17	82.6

Table 3.41: EIS data for the corrosion of weld aged maraging steel in 1.5 M hydrochloric acid containing different concentrations of CPOM.

Temperature (°C)	Conc. of inhibitor (mM)	R_{ct} (ohm. cm ²)	C_{dl} (mF cm ⁻²)	R_{pf} (ohm. cm ²)	C_{pf} (mF cm ⁻²)	η (%)
30	Blank	64.30±2.83	3.01±0.45			
	0.3	119.74±3.22	2.60±0.11	9.99±3.07	0.85±0.12	46.3
	0.6	176.16±2.97	2.08±0.18	13.43±2.04	0.70±0.16	63.5
	0.9	278.35±3.92	1.68±0.16	19.65±3.10	0.61±0.26	76.9
	1.2	462.59±4.01	1.41±0.20	30.88±2.55	0.55±0.19	86.1
	1.5	905.63±6.23	1.20±0.25	57.86±3.68	0.50±0.12	92.9
35	Blank	58.75±3.13	3.38±0.52			
	0.3	106.43±3.06	2.83±0.21	9.18±2.24	0.90±0.18	44.8
	0.6	135.68±2.57	2.43±0.15	10.96±2.93	0.79±0.16	56.7
	0.9	185.33±3.13	2.05±0.11	13.99±3.06	0.70±0.30	68.3
	1.2	277.12±4.72	1.70±0.11	19.58±3.99	0.62±0.20	78.8
	1.5	455.43±5.23	1.42±0.16	30.44±2.31	0.55±0.18	87.1
40	Blank	53.42±3.47	3.74±0.36			
	0.3	93.39±2.62	3.11±0.22	8.39±3.33	0.96±0.20	42.8
	0.6	116.38±3.81	2.69±0.27	9.79±2.84	0.85±0.20	54.1
	0.9	156.20±2.84	2.26±0.11	12.21±2.18	0.75±0.16	65.8
	1.2	218.93±3.68	1.90±0.15	16.03±3.58	0.66±0.28	75.6
	1.5	340.25±3.65	1.57±0.21	23.42±3.43	0.59±0.12	84.3
45	Blank	36.89±2.08	4.13±0.72			
	0.3	61.48±2.26	3.47±0.18	6.44±2.19	1.05±0.21	40.2
	0.6	75.91±3.43	3.00±0.29	7.32±2.88	0.92±0.29	51.4
	0.9	96.32±2.79	2.57±0.25	8.57±2.41	0.82±0.13	61.7
	1.2	134.64±2.12	2.12±0.22	10.90±2.35	0.71±0.11	72.6
	1.5	184.45±3.03	1.82±0.16	13.93±3.41	0.64±0.20	80.1
50	Blank	32.05±3.44	5.75±0.40			
	0.3	51.86±3.39	4.54±0.27	5.86±2.67	1.30±0.30	38.2
	0.6	61.99±2.62	3.96±0.29	6.48±2.70	1.14±0.29	48.3
	0.9	75.95±2.14	3.42±0.26	7.33±2.88	1.02±0.18	57.8
	1.2	105.08±2.21	2.74±0.16	9.10±2.15	0.86±0.19	69.5
	1.5	135.23±3.88	2.35±0.17	10.94±3.21	0.77±0.11	76.3

Table 3.42: EIS data for the corrosion of weld aged maraging steel in 2.0 M hydrochloric acid containing different concentrations of CPOM.

Temperature (°C)	Conc. of inhibitor (mM)	R_{ct} (ohm. cm ²)	C_{dl} (mF cm ⁻²)	R_{pf} (ohm. cm ²)	C_{pf} (mF cm ⁻²)	η (%)
30	Blank	20.02±2.98	5.71±0.35			
	0.4	39.04±3.28	3.13±0.16	1.90±0.22	0.82±0.27	48.7
	0.8	48.05±3.84	2.84±0.12	2.80±0.74	0.64±0.16	58.4
	1.2	61.06±3.41	2.11±0.20	3.60±1.04	0.46±0.15	67.2
	1.6	87.09±2.55	1.56±0.28	4.90±2.69	0.33±0.11	77.3
	2.0	157.16±4.88	0.83±0.20	8.80±2.75	0.21±0.16	87.2
35	Blank	18.02±2.28	8.25±0.24			
	0.4	33.03±2.33	5.23±0.30	1.60±0.16	1.36±0.13	45.4
	0.8	41.04±2.83	4.79±0.16	2.50±0.80	0.89±0.27	56.1
	1.2	54.45±3.62	3.67±0.19	3.30±1.51	0.63±0.19	65.9
	1.6	74.27±2.60	2.98±0.13	4.40±2.46	0.52±0.21	75.7
	2.0	116.12±4.30	2.05±0.19	7.90±2.95	0.31±0.10	84.4
40	Blank	15.52±2.65	13.21±0.29			
	0.4	27.03±3.42	7.44±0.29	1.52±0.36	1.89±0.26	42.5
	0.8	33.33±2.11	5.35±0.26	2.20±0.93	1.22±0.23	53.4
	1.2	41.54±2.49	4.76±0.21	3.10±1.42	0.92±0.16	62.6
	1.6	57.46±3.80	4.11±0.29	4.00±1.55	0.78±0.15	72.9
	2.0	89.39±3.74	3.05±0.25	6.80±2.93	0.45±0.12	82.6
45	Blank	13.21±2.15	15.74±0.88			
	0.4	21.52±3.68	10.64±0.11	1.30±0.39	2.40±0.48	38.6
	0.8	26.43±3.28	7.02±0.22	1.90±0.58	1.73±0.17	50.5
	1.2	32.63±3.79	5.89±0.23	2.80±1.79	1.45±0.24	59.5
	1.6	44.84±3.43	4.35±0.23	3.70±1.38	0.92±0.28	70.5
	2.0	73.27±2.57	3.23±0.20	6.00±2.73	0.61±0.22	81.9
50	Blank	11.01±2.55	16.31±0.50			
	0.4	17.12±2.80	12.72±0.24	0.90±0.29	3.16±0.37	35.6
	0.8	20.12±2.23	9.52±0.29	1.50±1.39	2.62±0.10	46.2
	1.2	24.82±2.01	7.76±0.27	2.30±1.62	1.99±0.25	55.6
	1.6	32.43±3.77	6.10±0.24	3.10±1.85	1.35±0.22	66.5
	2.0	51.05±2.28	4.24±0.18	5.40±1.78	0.91±0.15	78.4

Table 3.43: Comparison of maximum attainable inhibition efficiencies by the Tafel method and EIS method for the corrosion of weld aged maraging steel in hydrochloric acid solutions of different concentrations in the presence of CPOM at 30 °C.

Molarity of hydrochloric acid	Conc. of CPOM (mM)	η (%)	
		Tafel	EIS
0.1	0.8	97.8	94.5
0.5	1.0	95.4	96.8
1.0	1.5	93.5	94.5
1.5	1.5	91.1	92.9
2.0	2.0	89.0	87.2

Table 3.44: Activation parameters for the corrosion of weld aged maraging steel in hydrochloric acid containing different concentrations of CPOM.

Molarity of hydrochloric acid (M)	Conc. of inhibitor (mM)	E_a ($\text{kJ}^{-1} \text{mol}^{-1}$)	ΔH^\ddagger ($\text{kJ}^{-1} \text{mol}^{-1}$)	ΔS^\ddagger ($\text{J mol}^{-1} \text{K}^{-1}$)
0.1	0.0	39.12	41.60	-94.92
	0.1	51.64	54.91	-71.66
	0.2	55.16	58.66	-60.04
	0.4	66.11	70.30	-56.17
	0.6	70.42	74.88	-33.89
	0.8	73.55	78.21	-21.62
0.5	0.0	36.56	38.51	-103.7
	0.2	48.26	50.83	-78.30
	0.4	51.55	54.30	-65.61
	0.6	61.79	65.08	-61.37
	0.8	65.81	69.32	-37.04
	1.0	68.73	72.40	-16.70
1.0	0.0	35.70	34.98	-108.26
	0.3	47.12	46.17	-81.70
	0.6	50.34	49.32	-68.45
	0.9	60.33	59.12	-64.04
	1.2	64.26	62.96	-38.64
	1.5	67.12	65.76	-13.25
1.5	0.0	32.08	30.55	-117.83
	0.3	42.35	40.33	-88.95
	0.6	45.23	43.08	-74.53
	0.9	54.22	51.63	-69.72
	1.2	57.74	54.99	-42.07
	1.5	60.31	57.43	-14.42
2.0	0.0	30.33	31.24	-122.31
	0.4	40.04	41.24	-92.35
	0.8	42.77	44.05	-77.37
	1.2	51.26	52.80	-72.38
	1.6	54.59	56.23	-43.68
	2.0	57.02	58.73	-14.98

Table 3.45: Thermodynamic parameters for the adsorption of CPOM on weld aged maraging steel surface in hydrochloric acid at different temperatures.

Molarity of hydrochloric acid (M)	Temperature (°C)	$-\Delta G^{\circ}_{\text{ads}}$ (kJ mol ⁻¹)	$\Delta H^{\circ}_{\text{ads}}$ (kJ mol ⁻¹)	$\Delta S^{\circ}_{\text{ads}}$ (J mol ⁻¹ K ⁻¹)
0.1	30	35.59	-9.53	-67.21
	35	35.45		
	40	35.27		
	45	35.10		
	50	34.93		
0.5	30	35.43	-15.21	-50.25
	35	35.29		
	40	35.12		
	45	34.95		
	50	34.78		
1.0	30	35.82	-21.43	-40.06
	35	35.67		
	40	35.50		
	45	35.33		
	50	35.16		
1.5	30	36.00	-29.08	-31.22
	35	35.86		
	40	35.69		
	45	35.51		
	50	35.34		
2.0	30	34.65	-35.06	-24.05
	35	34.51		
	40	34.34		
	45	34.18		
	50	34.01		

3.6 (E)-1-(2,4-DINITROPHENYL)-2-[1-(2-NITROPHENYL) THYLIDENE] HYDRAZINE (DNPH) AS INHIBITOR FOR THE CORROSION OF WELD AGED MARAGING STEEL IN HYDROCHLORIC ACID MEDIUM

3.6.1 Potentiodynamic polarization studies

The potentiodynamic polarization curves for the corrosion of weld aged maraging steel specimen in 1.5 M hydrochloric acid in the presence of different concentrations of DNPH, at 30 °C are shown in Fig. 3.43. Similar plots were obtained in the other four concentrations of hydrochloric acid at the different temperatures studied. The potentiodynamic polarization parameters (E_{corr} , b_c , b_a , i_{corr} and η (%)) are summarized in Tables 3.46 to 3.50.

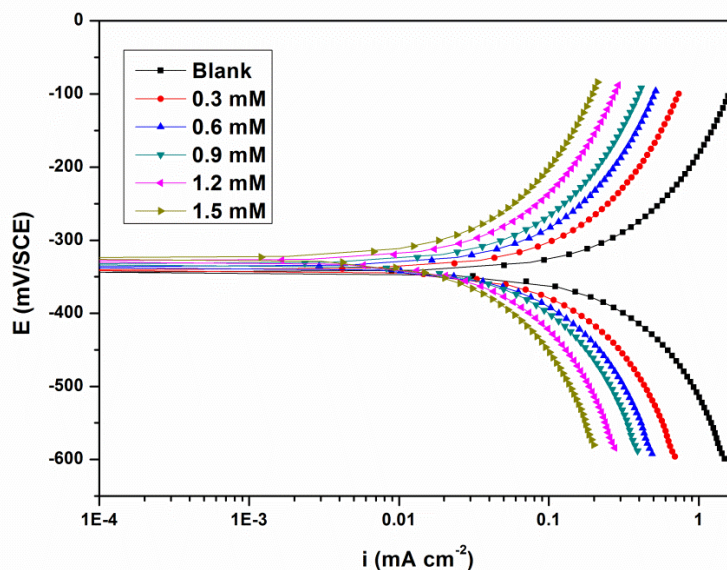


Fig. 3.43: Potentiodynamic polarization curves for the corrosion of weld aged maraging steel in 1.5 M hydrochloric acid containing different concentrations of DNPH at 30 °C.

According to the observed E_{corr} , b_a and b_c values presented in Tables 3.46 to 3.50 DNPH can be regarded as a mixed type inhibitor with predominant anodic inhibition

effect as discussed earlier in the section 3.3.1. DNPH shows lower inhibition efficiency than that of ATPI, CPOB and CPOM for the corrosion of weld aged maraging steel in hydrochloric acid medium.

3.6.2 Electrochemical impedance spectroscopy

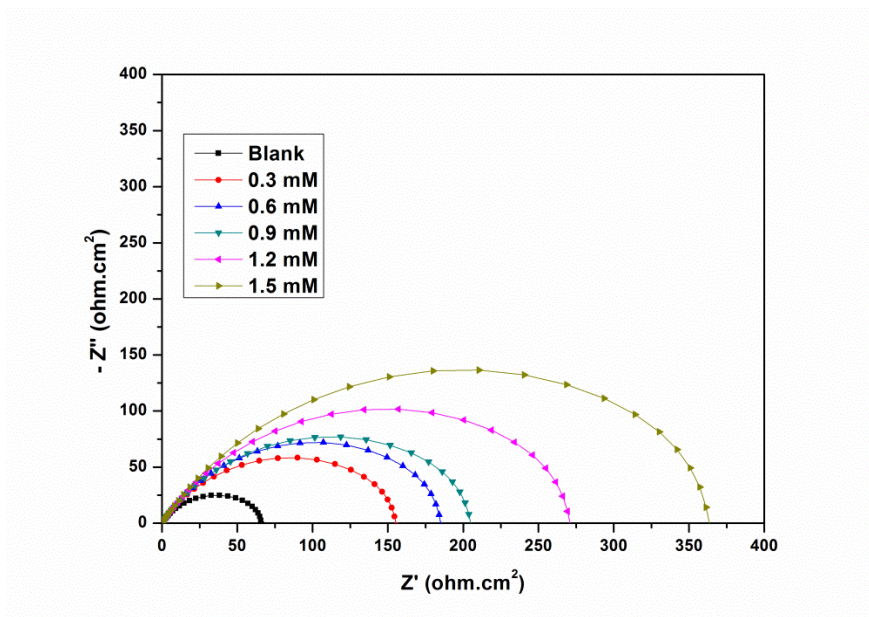


Fig. 3.44: Nyquist plots for the corrosion of weld aged maraging steel in 1.5 M hydrochloric acid containing different concentrations of DNPH at 30 °C.

The Nyquist plots obtained for the corrosion of weld aged samples of maraging steel specimen in 1.5 M hydrochloric acid in the presence of different concentrations of DNPH at 30 °C are shown in Fig. 3.44. Similar plots were obtained in other concentrations of hydrochloric acid and also at other temperatures. The electrochemical parameters obtained from the EIS studies are summarized in Tables 3.51 to 3.55. From Fig. 3.44, it can be observed that the impedance spectra show a single semicircle and the diameter of semicircle increases with increasing inhibitor concentration, indicating the increase in charge transfer resistance (R_{ct}) value and decrease in corrosion rate (v_{corr}). The plots are similar to those obtained in the presence of CPOB as discussed in the

section 3.3.2. The equivalent circuit given in Fig. 3.20 is used to fit the experimental data for the corrosion of weld aged maraging steel in hydrochloric acid in the presence of DNPH. Hence the discussion in the section 3.3.2 on the equivalent circuit model for the corrosion of weld aged maraging steel in the presence of CPOB holds good here also. The results show that the values of C_{dl} and C_{pf} decreases, while the values of R_{ct} and R_{pf} increase with the increase in the concentration of DNPH, suggesting that the amount of the inhibitor molecules adsorbed on the electrode surface increases as the concentration of DNPH increases (Amin et al. 2007).

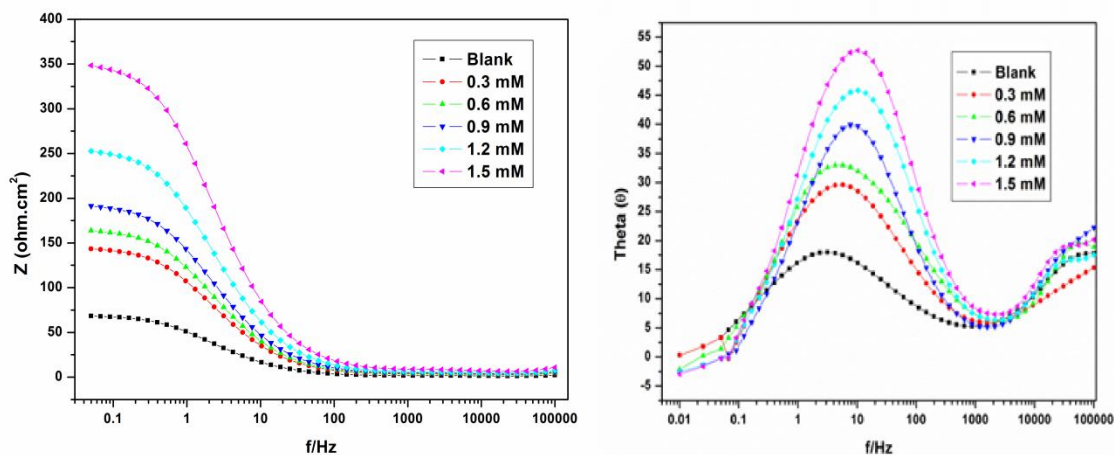


Fig. 3.45: Bode plots for the corrosion of weld aged maraging steel in 1.5 M hydrochloric acid containing different concentrations of DNPH at 30 °C.

The Bode plots for the corrosion of the alloy in the presence of different concentrations of DNPH are shown in Fig. 3.45. They are similar to the ones shown in Fig. 3.21. Hence the discussion regarding the Bode plot under the section 3.3.2 holds good for DNPH also.

A comparison of maximum attainable inhibition efficiencies by the Tafel method and EIS method, in the presence of DNPH for the corrosion of weld aged maraging steel in hydrochloric acid solutions of different concentrations at 30 °C are listed in Table 3.56.

It is evident from the table that the η (%) values obtained by the two methods are in good agreement. Similar levels of agreement were obtained at other temperatures also.

3.6.3 Effect of temperature

The Tafel and EIS results pertaining to different temperatures in different concentrations of hydrochloric acid have already been listed in Tables 3.46 to 3.55. The effect of temperature on corrosion inhibition behaviour of DNPH is similar to that of ATPI, CPOB and CPOM on weld aged maraging steel as discussed in the earlier section. The decrease in the inhibition efficiency of DNPH with the increase in temperature on weld aged maraging steel surface may be attributed to the physisorption of DNPH. The Arrhenius plots for the corrosion of weld aged maraging steel in 1.5 M hydrochloric acid in the presence of different concentrations of DNPH are shown in Fig. 3.46. The plots of $\ln(v_{\text{corr}}/T)$ vs $(1/T)$ are shown in Fig. 3.47.

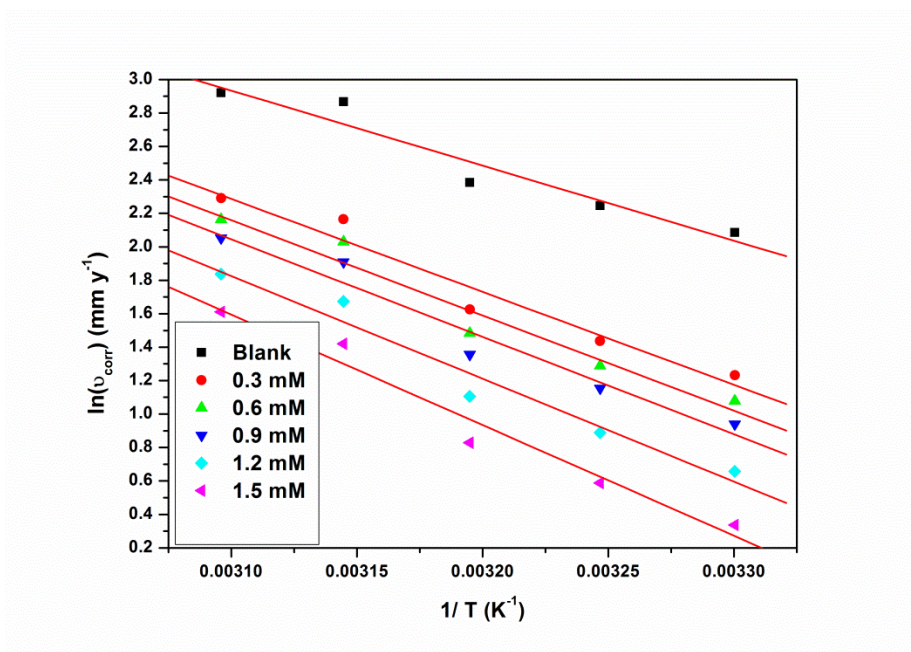


Fig. 3.46: Arrhenius plots for the corrosion of weld aged maraging steel in 1.5 M hydrochloric acid containing different concentrations of DNPH.

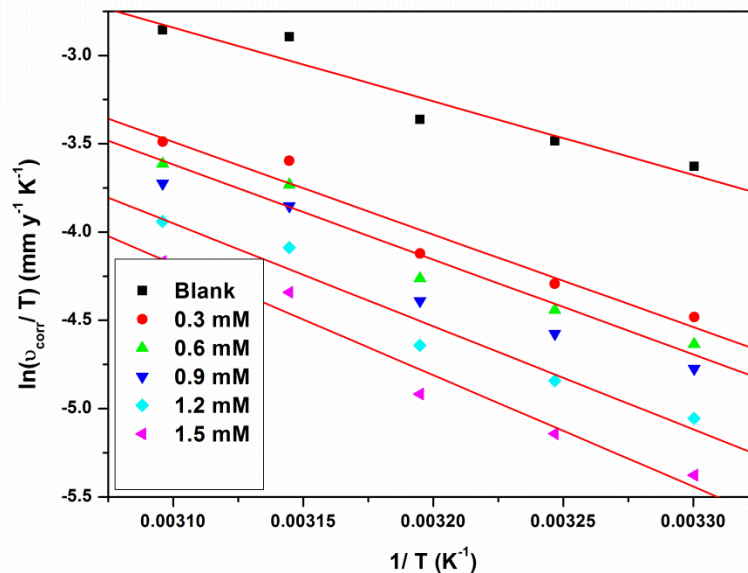


Fig. 3.47: Plots of $\ln(v_{\text{corr}}/T)$ versus $1/T$ for the corrosion of weld aged maraging steel in 1.5 M hydrochloric acid containing different concentrations of DNPH.

The calculated values of activation parameters are given in Table 3.57. The observations are similar to the ones obtained in the presence of ATPI. The increase in the activation energy for the corrosion of weld aged maraging steel in the presence of DNPH indicates the increase in energy barrier for the corrosion reaction. The entropies of activation in the absence and presence of the inhibitor are large and negative. This implies that the activated complex in the rate determining step represents an association resulting in decrease in randomness on going from the reactants to the activated complex (Gomma and Wahdan 1995, Marsh 1988).

3.6.4 Effect of hydrochloric acid concentration

It is evident from both the polarization and EIS experimental results that, for a particular concentration of the DNPH, the inhibition efficiency decreases with the increase in hydrochloric acid concentration on weld aged maraging steel. The maximum inhibition efficiency is observed at 1.0 M solution of hydrochloric acid.

3.6.5 Adsorption isotherms

The adsorption of DNPH on the surfaces of weld aged maraging steel was found to obey Langmuir adsorption isotherm. The Langmuir adsorption isotherms for the adsorption of DNPH on weld aged maraging steel in 1.5 M hydrochloric acid are shown in Fig. 3.48.

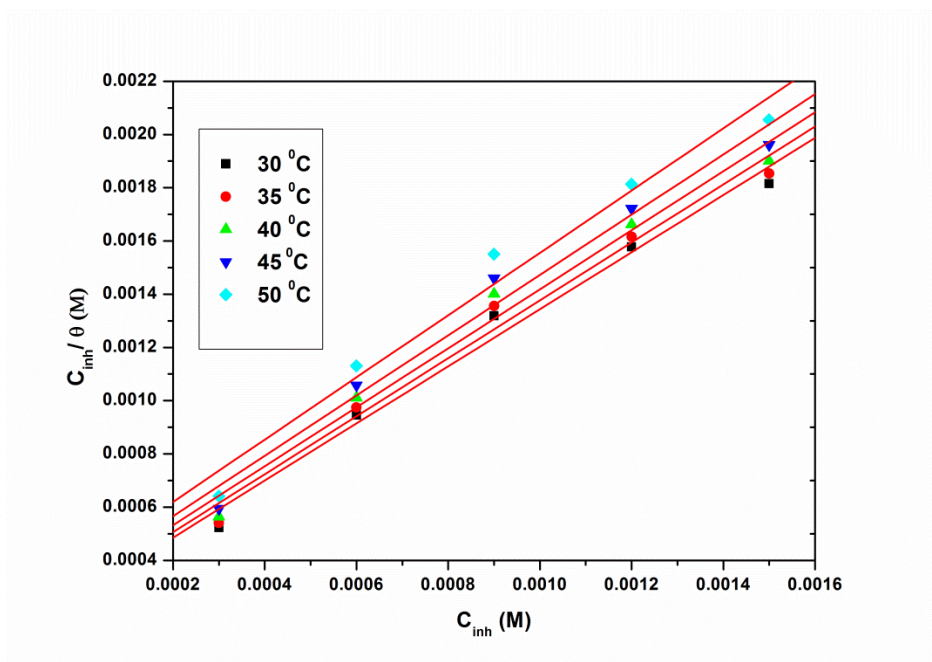


Fig. 3.48: Langmuir adsorption isotherms for the adsorption of DNPH on weld aged maraging steel in 1.5 M hydrochloric acid at different temperatures.

The thermodynamic parameters for the adsorption of DNPH on weld aged maraging steel are tabulated in Tables 3.58. These data also reveal similar inhibition behaviour of DNPH as that of ATPI as discussed in section 3.3.5. The values of ΔG^0_{ads} and ΔH^0_{ads} indicate both physisorption and chemisorption of DNPH on weld aged maraging steel with predominant physisorption.

3.6.6 Mechanism of corrosion inhibition

The mechanism of corrosion inhibition of weld aged maraging steel in the presence of DNPH is similar to that in the presence of ATPI as discussed under section

3.3.6. It is considered that in acidic solution the DNPH molecule can undergo protonation at amino group and can exist as a protonated positive species. The physisorption of DNPH may be considered through electrostatic attraction between the protonated DNPH and negatively charged chloride ions already adsorbed on the alloy surface.

DNPH shows slightly lesser inhibition efficiency than that of ATPI, CPOB and CPOM for the corrosion of weld aged maraging steel in hydrochloric acid medium.

3.6.7 SEM/EDS studies

Fig. 3.49 (a) represents SEM image of the corroded weld aged maraging steel sample which shows the facets due to the attack of hydrochloric acid on the metal surface with cracks and rough surfaces. Fig. 3.49 (b) shows the SEM image of the sample after immersion in 1.5 M hydrochloric acid in the presence of DNPH. It can be seen that the alloy surface is smooth without any visible corrosion attack. Thus, it can be concluded that DNPH protects the alloy from corrosion by forming a uniform film on the alloy surface.

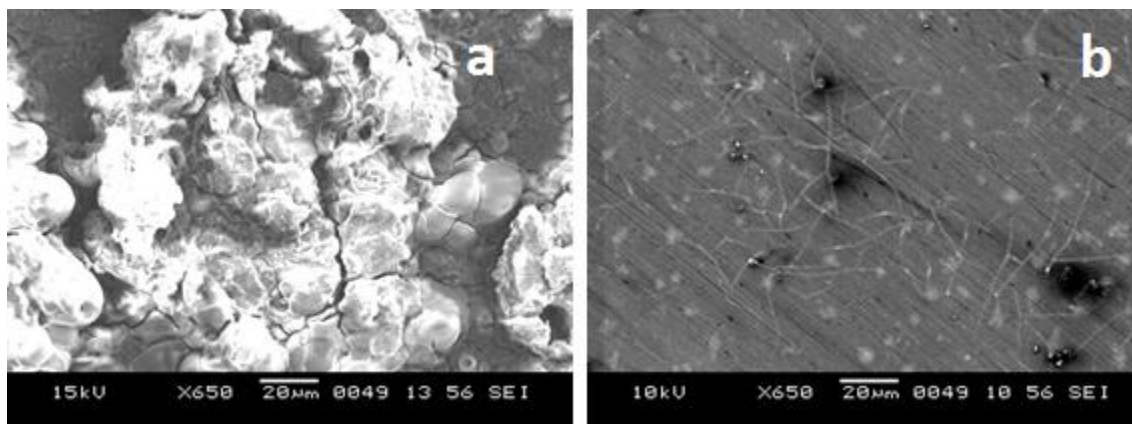


Fig. 3.49: SEM images of the weld aged maraging steel after immersion in 1.5 M hydrochloric acid a) in the absence and b) in the presence of DNPH.

The EDS profile analyses of the corroded surface of the alloy in the presence of DNPH is shown in Fig. 3.50. The atomic percentages of the elements found in the EDS

profile were 6.20 % Fe, 0.86% Ni, 2.71% Mo, 22.37% O, 3.01% Cl, 62.44% C and 6.23 N and indicated the formation of inhibitor film on the surface of alloy.

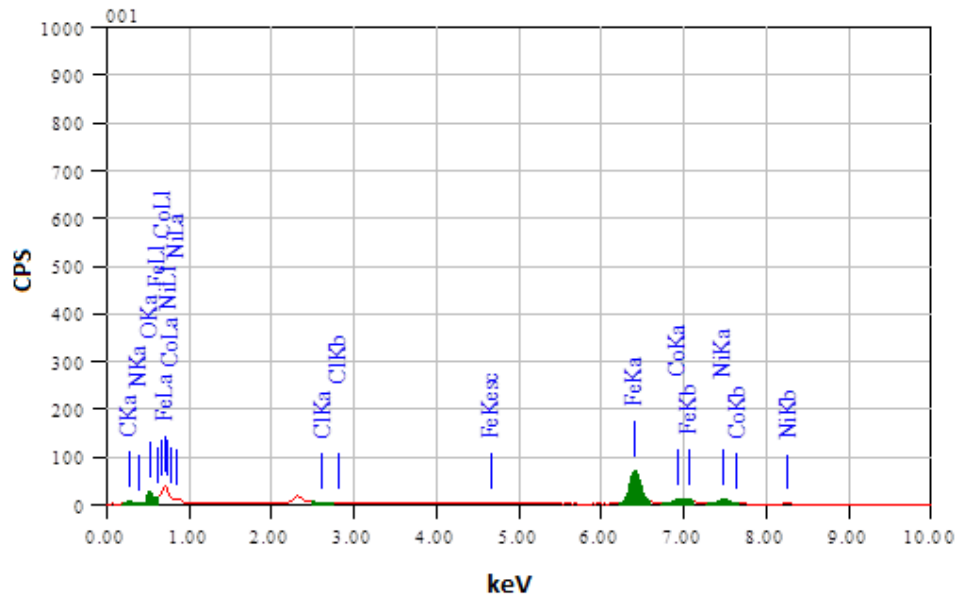


Fig. 3.50 (a): EDS spectra of the weld aged maraging steel after immersion in 1.5 hydrochloric acid in the presence of DNPH.

Table 3.46: Results of potentiodynamic polarization studies for the corrosion of weld aged maraging steel in 0.1 M hydrochloric acid containing different concentrations of DNPH.

Temperature (°C)	Conc. of inhibitor (mM)	E_{corr} (mV /SCE)	b_a (mV dec ⁻¹)	$-b_c$ (mV dec ⁻¹)	i_{corr} (mA cm ⁻²)	v_{corr} (mm y ⁻¹)	η (%)
30	Blank	-419±2	142±3	226±4	0.22±0.02	2.53±0.22	
	0.1	-418±3	137±4	223±3	0.10±0.03	1.10±0.26	56.7
	0.2	-414±2	131±2	217±3	0.08±0.01	0.95±0.11	62.5
	0.4	-411±4	127±2	212±1	0.07±0.02	0.83±0.19	67.1
	0.6	-407±1	124±4	208±2	0.06±0.02	0.64±0.16	74.6
	0.8	-401±2	120±3	205±4	0.04±0.02	0.48±0.08	80.9
	35	Blank	-416±2	150±2	234±2	0.26±0.02	2.99±0.23
0.1		-412±1	147±1	230±4	0.12±0.02	1.37±0.18	54.2
0.2		-410±3	141±2	227±4	0.10±0.01	1.19±0.15	60.1
0.4		-405±3	135±2	221±2	0.09±0.02	1.06±0.20	64.7
0.6		-400±1	130±1	216±4	0.07±0.02	0.83±0.18	72.3
0.8		-397±4	126±2	210±3	0.06±0.03	0.64±0.16	78.7
40		Blank	-412±2	159±4	242±4	0.30±0.01	3.45±0.14
	0.1	-413±2	155±4	238±1	0.15±0.02	1.67±0.22	51.8
	0.2	-409±2	148±1	232±2	0.13±0.02	1.46±0.21	57.8
	0.4	-407±3	144±3	229±3	0.11±0.03	1.30±0.26	62.4
	0.6	-403±1	140±1	224±1	0.09±0.03	1.04±0.29	70.1
	0.8	-396±2	136±4	220±4	0.07±0.01	0.81±0.28	76.6
	45	Blank	-409±2	165±3	250±3	0.33±0.02	3.80±0.18
0.1		-408±3	161±4	245±2	0.17±0.01	1.93±0.11	49.1
0.2		-405±4	154±1	240±1	0.15±0.02	1.70±0.21	55.2
0.4		-400±1	150±4	237±1	0.13±0.02	1.53±0.18	59.8
0.6		-397±2	144±4	233±3	0.11±0.03	1.23±0.29	67.6
0.8		-395±3	140±2	231±2	0.09±0.02	0.98±0.17	74.1
50		Blank	-405±4	173±1	259±4	0.37±0.02	4.26±0.22
	0.1	-402±2	169±1	255±2	0.20±0.01	2.29±0.11	46.1
	0.2	-396±4	165±3	250±4	0.18±0.02	2.03±0.20	52.2
	0.4	-392±2	160±3	244±4	0.16±0.01	1.83±0.11	56.9
	0.6	-390±4	156±3	240±3	0.13±0.01	1.50±0.15	64.7
	0.8	-387±1	152±2	235±4	0.11±0.01	1.22±0.13	71.3

Table 3.47: Results of potentiodynamic polarization studies for the corrosion of weld aged maraging steel in 0.5 M hydrochloric acid containing different concentrations of DNPH.

Temperature (°C)	Conc. of inhibitor (mM)	E_{corr} (mV /SCE)	b_a (mV dec ⁻¹)	$-b_c$ (mV dec ⁻¹)	i_{corr} (mA cm ⁻²)	v_{corr} (mm y ⁻¹)	η (%)
30	Blank	-413±1	148±2	247±3	0.27±0.02	3.11±0.20	
	0.1	-415±4	145±4	242±4	0.13±0.02	1.46±0.17	53.5
	0.2	-410±2	139±2	237±1	0.11±0.02	1.27±0.20	59.4
	0.4	-407±2	132±3	230±1	0.10±0.03	1.12±0.28	64.1
	0.6	-402±1	129±3	225±2	0.08±0.01	0.88±0.12	71.7
	0.8	-398±1	125±4	221±1	0.06±0.03	0.68±0.28	78.2
35	Blank	-411±2	156±2	254±1	0.35±0.02	4.03±0.22	
	0.1	-409±1	151±1	252±1	0.18±0.02	2.02±0.17	50.1
	0.2	-404±3	147±4	247±2	0.15±0.02	1.77±0.19	56.1
	0.4	-400±4	139±3	241±1	0.14±0.02	1.58±0.19	60.9
	0.6	-398±2	135±1	235±1	0.11±0.03	1.26±0.29	68.7
	0.8	-392±4	129±3	231±1	0.09±0.02	1.00±0.15	75.3
40	Blank	-408±2	165±4	262±2	0.42±0.03	4.83±0.27	
	0.1	-405±3	161±2	258±4	0.23±0.01	2.60±0.14	46.5
	0.2	-401±3	155±3	251±3	0.20±0.01	2.30±0.13	52.7
	0.4	-396±3	151±1	244±2	0.18±0.02	2.07±0.20	57.6
	0.6	-392±4	147±1	239±4	0.15±0.01	1.68±0.13	65.5
	0.8	-390±3	143±4	235±4	0.12±0.01	1.35±0.12	72.2
45	Blank	-406±1	172±4	269±2	0.51±0.02	5.87±0.15	
	0.1	-402±2	167±3	267±4	0.29±0.02	3.39±0.23	43.0
	0.2	-400±3	162±3	260±3	0.26±0.02	3.03±0.22	49.1
	0.4	-397±4	155±2	254±3	0.24±0.01	2.73±0.11	54.1
	0.6	-393±4	146±1	250±3	0.20±0.03	2.24±0.28	62.3
	0.8	-390±1	143±4	246±3	0.16±0.01	1.84±0.14	69.1
50	Blank	-404±1	183±2	277±3	0.59±0.01	6.79±0.14	
	0.1	-400±1	180±3	273±3	0.36±0.02	4.12±0.24	39.4
	0.2	-397±3	175±1	267±1	0.32±0.02	3.70±0.18	45.6
	0.4	-393±3	168±3	262±2	0.29±0.02	3.35±0.23	50.6
	0.6	-390±4	163±4	254±3	0.24±0.03	2.79±0.26	58.9
	0.8	-387±3	160±1	250±4	0.20±0.03	2.31±0.28	65.9

Table 3.48: Results of potentiodynamic polarization studies for the corrosion of weld aged maraging steel in 1.0 M hydrochloric acid containing different concentrations of DNPB.

Temperature (°C)	Conc. of inhibitor (mM)	E_{corr} (mV /SCE)	b_a (mV dec ⁻¹)	$-b_c$ (mV dec ⁻¹)	i_{corr} (mA cm ⁻²)	v_{corr} (mm y ⁻¹)	η (%)
30	Blank	-371±1	153±4	256±1	0.33±0.01	3.80±0.10	
	0.2	-370±2	149±4	252±1	0.13±0.02	1.48±0.17	61.1
	0.4	-367±3	144±2	245±3	0.11±0.03	1.25±0.26	67.0
	0.6	-365±3	138±4	238±4	0.09±0.02	1.07±0.17	71.8
	0.8	-362±4	134±4	233±2	0.07±0.02	0.78±0.18	79.5
	1.0	-358±4	130±3	228±1	0.05±0.03	0.53±0.30	86.2
	35	Blank	-368±4	159±4	261±3	0.45±0.02	5.20±0.16
0.2		-364±1	154±2	259±4	0.19±0.03	2.13±0.33	59.0
0.4		-360±4	147±2	255±4	0.16±0.01	1.81±0.13	65.1
0.6		-355±1	142±2	248±1	0.14±0.02	1.56±0.20	70.1
0.8		-351±2	135±2	244±1	0.10±0.02	1.15±0.16	77.8
1.0		-347±4	132±3	242±1	0.07±0.04	0.81±0.39	84.5
40		Blank	-364±2	165±1	266±4	0.56±0.03	6.45±0.26
	0.2	-362±3	161±3	263±1	0.24±0.04	2.81±0.37	56.4
	0.4	-360±1	155±3	256±1	0.21±0.02	2.41±0.24	62.7
	0.6	-354±1	152±4	249±4	0.18±0.02	2.09±0.24	67.6
	0.8	-350±1	148±2	244±2	0.14±0.03	1.57±0.30	75.7
	1.0	-345±4	143±1	239±3	0.10±0.04	1.13±0.36	82.4
	45	Blank	-361±4	172±1	273±1	0.75±0.03	8.72±0.31
0.2		-356±1	167±4	271±1	0.35±0.02	4.05±0.20	53.5
0.4		-352±2	160±3	265±4	0.30±0.02	3.50±0.17	59.9
0.6		-350±1	155±4	262±2	0.27±0.04	3.06±0.37	64.9
0.8		-345±4	149±1	256±2	0.20±0.01	2.35±0.11	73.1
1.0		-341±2	142±1	251±1	0.15±0.04	1.74±0.35	80.0
50		Blank	-358±2	177±1	278±1	0.92±0.02	10.63±0.18
	0.2	-353±1	174±1	275±3	0.46±0.03	5.28±0.32	50.3
	0.4	-350±4	167±1	267±2	0.40±0.03	4.59±0.34	56.8
	0.6	-349±3	163±3	262±2	0.35±0.01	4.05±0.10	61.9
	0.8	-344±1	158±3	256±3	0.27±0.03	3.16±0.32	70.3
	1.0	-340±2	153±3	252±2	0.21±0.03	2.41±0.26	76.4

Table 3.49: Results of potentiodynamic polarization studies for the corrosion of weld aged maraging steel in 1.5 M hydrochloric acid containing different concentrations of DNPH.

Temperature (°C)	Conc. of inhibitor (mM)	E_{corr} (mV /SCE)	b_a (mV dec ⁻¹)	$-b_c$ (mV dec ⁻¹)	i_{corr} (mA cm ⁻²)	v_{corr} (mm y ⁻¹)	η (%)
30	Blank	-342±1	158±1	267±3	0.70±0.04	8.05±0.39	
	0.3	-340±4	154±2	262±4	0.30±0.03	3.43±0.32	57.4
	0.6	-336±1	148±1	256±4	0.26±0.01	2.94±0.10	63.4
	0.9	-332±3	143±3	250±2	0.22±0.04	2.56±0.35	68.2
	1.2	-328±4	139±3	244±3	0.17±0.03	1.93±0.28	76.0
	1.5	-324±3	136±3	240±4	0.12±0.03	1.40±0.28	82.6
35	Blank	-339±1	165±3	276±2	0.82±0.05	9.45±0.46	
	0.3	-335±1	160±4	274±2	0.37±0.03	4.21±0.27	55.5
	0.6	-332±3	154±1	268±4	0.32±0.02	3.63±0.22	61.6
	0.9	-330±4	148±2	263±4	0.28±0.03	3.17±0.28	66.4
	1.2	-327±1	142±2	259±3	0.21±0.02	2.43±0.24	74.3
	1.5	-322±1	138±4	256±3	0.16±0.01	1.80±0.11	80.9
40	Blank	-337±4	173±4	282±1	0.94±0.09	10.85±0.89	
	0.3	-341±1	169±2	277±4	0.44±0.02	5.08±0.21	53.2
	0.6	-332±1	163±1	271±4	0.38±0.01	4.41±0.14	59.4
	0.9	-330±1	158±2	265±1	0.34±0.03	3.88±0.30	64.2
	1.2	-325±4	154±3	259±2	0.26±0.03	3.02±0.27	72.2
	1.5	-320±3	151±3	255±1	0.20±0.03	2.29±0.26	78.9
45	Blank	-334±2	179±2	286±2	1.53±0.08	17.60±0.73	
	0.3	-331±2	174±2	285±2	0.76±0.03	8.72±0.32	50.5
	0.6	-326±1	168±4	279±1	0.66±0.03	7.62±0.34	56.7
	0.9	-321±4	162±4	273±2	0.59±0.02	6.75±0.22	61.7
	1.2	-318±4	156±3	269±2	0.46±0.03	5.33±0.32	69.7
	1.5	-316±1	152±2	266±4	0.36±0.01	4.14±0.10	76.5
50	Blank	-332±2	185±4	292±3	1.61±0.09	18.57±0.85	
	0.3	-328±2	182±4	287±1	0.86±0.03	9.88±0.29	46.8
	0.6	-322±3	176±3	281±3	0.76±0.02	8.71±0.17	53.1
	0.9	-320±3	170±2	275±2	0.68±0.02	7.79±0.20	58.4
	1.2	-318±3	166±3	269±4	0.55±0.02	6.28±0.17	66.2
	1.5	-312±2	163±3	265±2	0.44±0.03	5.01±0.29	73.0

Table 3.50: Results of potentiodynamic polarization studies for the corrosion of weld aged maraging steel in 2.0 M hydrochloric acid containing different concentrations of DNPH.

Temperature (°C)	Conc. of inhibitor (mM)	E_{corr} (mV /SCE)	b_a (mV dec ⁻¹)	$-b_c$ (mV dec ⁻¹)	i_{corr} (mA cm ⁻²)	v_{corr} (mm y ⁻¹)	η (%)
30	Blank	-324±1	175±3	287±1	3.08±0.23	35.48±2.25	
	0.3	-326±3	171±3	283±1	1.44±0.13	16.54±1.04	53.3
	0.6	-320±2	165±1	278±1	1.25±0.08	14.38±0.81	59.4
	0.9	-315±3	161±1	275±4	1.10±0.02	12.66±0.20	64.3
	1.2	-311±4	157±3	267±4	0.86±0.02	9.87±0.23	72.2
	1.5	-307±2	153±2	265±4.	0.65±0.01	7.51±0.12	78.8
35	Blank	-325±3	189±1	307±2	3.50±0.12	40.31±1.01	
	0.3	-321±4	184±1	304±4	1.71±0.09	19.64±0.91	51.2
	0.6	-318±1	178±2	298±3	1.49±0.02	17.15±0.17	57.4
	0.9	-322±3	174±1	295±2	1.32±0.03	15.19±0.31	62.3
	1.2	-317±1	169±2	292±4	1.04±0.03	11.98±0.34	70.3
	1.5	-311±4	164±1	288±4	0.81±0.01	9.27±0.13	77.0
40	Blank	-321±1	192±3	325±1	3.88±0.22	44.72±2.13	
	0.3	-322±2	188±3	320±4	1.98±0.14	22.80±1.12	48.9
	0.6	-317±3	184±4	316±1	1.74±0.08	20.02±0.94	55.2
	0.9	-315±2	179±3	312±4	1.55±0.02	17.82±0.20	60.1
	1.2	-312±2	174±2	305±3	1.24±0.03	14.22±0.25	68.1
	1.5	-306±2	170±2	301±3	0.97±0.02	11.20±0.16	74.9
45	Blank	-322±4	206±3	332±4	4.18±0.23	48.14±2.28	
	0.3	-319±2	202±2	328±3	2.29±0.12	26.32±0.11	45.3
	0.6	-321±3	195±3	324±1	2.02±0.08	23.29±0.82	51.6
	0.9	-315±3	190±2	320±3	1.82±0.04	20.89±0.44	56.6
	1.2	-312±3	185±2	318±1	1.48±0.02	16.98±0.17	64.7
	1.5	-305±2	181±3	315±1	1.19±0.05	13.69±0.48	71.5
50	Blank	-319±2	224±4	340±4	4.51±0.24	51.91±2.29	
	0.3	-315±2	220±4	335±2	2.62±0.05	30.20±0.47	41.8
	0.6	-311±3	216±4	329±2	2.34±0.04	26.90±0.43	48.2
	0.9	-309±2	212±1	324±2	2.11±0.04	24.29±0.37	53.2
	1.2	-306±2	208±4	321±4	1.74±0.02	20.03±0.18	61.4
	1.5	-301±4	205±2	317±4	1.43±0.05	16.44±0.49	68.3

Table 3.51: EIS data for the corrosion of weld aged maraging steel in 0.1 M hydrochloric acid containing different concentrations of DNPH.

Temperature (°C)	Conc. of inhibitor (mM)	R_{ct} (ohm. cm ²)	C_{dl} (mF cm ⁻²)	R_{pf} (ohm. cm ²)	C_{pf} (mF cm ⁻²)	η (%)
30	Blank	181.20±2.48	0.93±0.31			
	0.1	449.40±3.35	0.65±0.23	29.57±2.43	0.22±0.08	59.7
	0.2	529.67±5.16	0.58±0.48	34.51±2.59	0.20±0.07	65.8
	0.4	616.96±4.62	0.53±0.41	39.88±2.09	0.18±0.06	70.6
	0.6	843.97±8.69	0.45±0.21	53.84±2.45	0.16±0.09	78.5
	0.8	1221.02±10.91	0.38±0.16	77.04±2.37	0.14±0.08	85.2
35	Blank	156.30±5.00	0.96±0.26			
	0.1	358.98±4.42	0.69±0.33	24.01±2.71	0.23±0.07	56.5
	0.2	417.91±3.18	0.63±0.48	27.63±2.24	0.21±0.06	62.6
	0.4	479.45±4.56	0.58±0.24	31.42±2.54	0.20±0.05	67.4
	0.6	633.05±8.99	0.49±0.25	40.87±2.96	0.17±0.07	75.3
	0.8	867.37±9.73	0.42±0.15	55.28±2.37	0.15±0.05	82.1
40	Blank	116.20±4.76	1.68±0.31			
	0.1	249.36±2.34	1.10±0.36	17.26±2.09	0.34±0.07	53.4
	0.2	287.55±4.67	0.99±0.31	19.61±2.93	0.31±0.08	59.6
	0.4	325.76±2.31	0.90±0.44	21.96±2.37	0.29±0.05	64.3
	0.6	419.04±5.43	0.75±0.36	27.70±2.56	0.25±0.08	72.3
	0.8	552.54±9.91	0.62±0.20	35.91±2.15	0.21±0.07	79.0
45	Blank	64.30±3.24	3.01±0.75			
	0.1	128.86±2.99	2.12±0.23	9.85±2.31	0.63±0.07	50.1
	0.2	147.24±2.26	1.89±0.35	10.98±2.45	0.57±0.08	56.3
	0.4	164.96±3.53	1.71±0.21	12.07±2.45	0.52±0.09	61.2
	0.6	207.29±3.36	1.40±0.21	14.67±2.04	0.43±0.07	69.0
	0.8	263.63±4.61	1.15±0.39	18.14±2.74	0.36±0.08	75.6
50	Blank	20.21±2.27	5.75±0.81			
	0.1	37.83±2.81	3.49±0.37	4.25±2.97	1.02±0.07	46.6
	0.2	42.75±3.12	3.12±0.22	4.55±2.56	0.91±0.07	52.7
	0.4	47.52±3.84	2.83±0.31	4.84±2.72	0.83±0.07	57.5
	0.6	58.33±4.30	2.34±0.36	5.51±2.87	0.69±0.08	65.4
	0.8	72.23±2.69	1.94±0.32	6.36±2.56	0.58±0.09	72.2

Table 3.52: EIS data for the corrosion of weld aged maraging steel in 0.5 M hydrochloric acid containing different concentrations of DNPH.

Temperature (°C)	Conc. of inhibitor (mM)	R_{ct} (ohm. cm ²)	C_{dl} (mF cm ⁻²)	R_{pf} (ohm. cm ²)	C_{pf} (mF cm ⁻²)	η (%)
30	Blank	156.30±2.56	0.96±0.36			
	0.1	359.31±4.54	0.69±0.24	24.03±1.80	0.23±0.09	56.5
	0.2	417.25±2.48	0.63±0.39	27.59±1.61	0.21±0.08	62.5
	0.4	478.42±4.25	0.58±0.23	31.35±1.86	0.20±0.07	67.3
	0.6	628.47±4.98	0.49±0.42	40.59±1.64	0.17±0.08	75.1
	0.8	853.63±5.73	0.42±0.11	54.44±2.00	0.15±0.06	81.7
35	Blank	139.27±3.69	1.11±0.22			
	0.1	293.94±3.24	0.81±0.23	20.00±2.45	0.26±0.07	52.6
	0.2	337.95±2.40	0.74±0.35	22.71±2.81	0.24±0.08	58.8
	0.4	383.35±4.02	0.68±0.21	25.50±1.46	0.23±0.05	63.7
	0.6	490.91±3.42	0.58±0.27	32.12±2.65	0.20±0.06	71.6
	0.8	642.98±4.70	0.49±0.15	41.48±2.52	0.17±0.05	78.3
40	Blank	123.15±2.31	1.33±0.50			
	0.1	239.45±4.32	0.99±0.31	16.65±1.76	0.31±0.09	48.6
	0.2	272.82±3.93	0.90±0.38	18.70±1.63	0.29±0.06	54.9
	0.4	306.72±2.52	0.82±0.37	20.79±1.61	0.27±0.06	59.9
	0.6	384.48±2.94	0.70±0.29	25.57±2.97	0.23±0.09	68.1
	0.8	488.88±4.25	0.60±0.18	32.00±2.68	0.20±0.05	74.8
45	Blank	107.56±3.63	1.55±0.32			
	0.1	194.33±3.74	1.18±0.32	13.88±2.01	0.37±0.04	44.7
	0.2	219.33±4.12	1.07±0.37	15.41±2.51	0.34±0.08	51.0
	0.4	244.73±4.97	0.99±0.31	16.98±1.38	0.31±0.04	56.1
	0.6	301.71±4.97	0.84±0.24	20.48±2.86	0.27±0.04	64.4
	0.8	375.03±3.39	0.72±0.14	24.99±2.06	0.24±0.05	71.3
50	Blank	90.34±3.14	1.74±0.26			
	0.1	151.99±4.10	1.38±0.26	11.27±1.68	0.42±0.08	40.6
	0.2	170.10±4.32	1.26±0.24	12.38±2.26	0.39±0.08	46.9
	0.4	188.52±4.39	1.16±0.50	13.52±1.40	0.36±0.03	52.1
	0.6	229.00±2.66	0.99±0.34	16.01±1.36	0.31±0.08	60.6
	0.8	279.34±3.58	0.85±0.20	19.11±1.33	0.27±0.05	67.7

Table 3.53: EIS data for the corrosion of weld aged maraging steel in 1.0 M hydrochloric acid containing different concentrations of DNPH.

Temperature (°C)	Conc. of inhibitor (mM)	R_{ct} (ohm. cm^2)	C_{dl} (mF cm^{-2})	R_{pf} (ohm. cm^2)	C_{pf} (mF cm^{-2})	η (%)
30	Blank	116.25±2.66	1.68±0.40			
	0.2	303.24±4.11	0.93±0.38	20.58±2.10	0.30±0.05	61.7
	0.4	361.43±2.06	0.82±0.15	24.16±2.46	0.27±0.05	67.9
	0.6	426.11±3.63	0.73±0.20	28.14±2.58	0.24±0.05	72.7
	0.8	602.07±3.87	0.58±0.19	38.96±2.63	0.20±0.05	80.7
	1.0	922.22±4.47	0.46±0.07	58.66±1.84	0.17±0.04	87.4
35	Blank	97.35±2.28	1.75±0.35			
	0.2	227.76±4.54	1.06±0.17	15.93±2.37	0.33±0.08	57.3
	0.4	266.14±3.52	0.94±0.33	18.29±2.48	0.30±0.08	63.4
	0.6	307.23±3.70	0.85±0.22	20.82±3.00	0.27±0.05	68.3
	0.8	410.55±3.93	0.69±0.18	27.18±2.68	0.23±0.03	76.3
	1.0	572.35±5.82	0.56±0.19	37.13±2.92	0.19±0.03	83.2
40	Blank	82.62±2.90	2.15±0.21			
	0.2	177.98±4.61	1.34±0.22	12.87±1.08	0.41±0.08	53.6
	0.4	211.09±2.74	1.16±0.38	14.91±2.38	0.36±0.07	60.9
	0.6	241.94±4.43	1.04±0.20	16.80±2.68	0.33±0.05	65.9
	0.8	317.57±4.33	0.85±0.13	21.46±1.13	0.27±0.06	74.3
	1.0	430.88±2.91	0.68±0.09	28.43±1.03	0.23±0.04	80.8
45	Blank	65.27±4.72	2.36±0.15			
	0.2	134.52±2.44	1.45±0.13	10.20±2.62	0.44±0.04	51.5
	0.4	155.02±2.57	1.29±0.23	11.46±1.77	0.40±0.03	57.9
	0.6	176.36±2.60	1.16±0.37	12.77±1.44	0.36±0.06	63.4
	0.8	227.34±2.49	0.95±0.28	15.91±2.40	0.30±0.08	71.3
	1.0	300.46±2.38	0.77±0.14	20.40±2.54	0.25±0.03	78.3
50	Blank	53.86±3.22	2.79±0.14			
	0.2	104.06±4.34	1.82±0.18	8.32±2.85	0.55±0.09	48.3
	0.4	119.16±2.69	1.62±0.37	9.25±1.46	0.49±0.05	54.9
	0.6	134.63±2.61	1.46±0.36	10.20±1.28	0.45±0.07	60.0
	0.8	170.85±2.02	1.20±0.19	12.43±2.39	0.37±0.04	68.5
	1.0	212.06±2.80	1.01±0.17	14.97±1.97	0.32±0.07	73.1

Table 3.54: EIS data for the corrosion of weld aged maraging steel in 1.5 M hydrochloric acid containing different concentrations of DNPH.

Temperature (°C)	Conc. of inhibitor (mM)	R_{ct} (ohm. cm ²)	C_{dl} (mF cm ⁻²)	R_{pf} (ohm. cm ²)	C_{pf} (mF cm ⁻²)	η (%)
30	Blank	64.30±2.56	3.01±0.27			
	0.3	145.34±2.17	1.72±0.42	10.86±1.91	0.52±0.03	55.8
	0.6	168.59±2.77	1.51±0.14	12.29±3.95	0.46±0.04	61.9
	0.9	193.09±2.65	1.35±0.23	13.80±2.67	0.42±0.09	66.7
	1.2	253.05±2.44	1.08±0.44	17.49±3.36	0.34±0.08	74.6
	1.5	342.39±3.27	0.86±0.16	22.98±1.04	0.28±0.05	81.2
35	Blank	58.75±2.10	3.38±0.11			
	0.3	126.29±2.52	1.93±0.28	9.69±2.10	0.58±0.09	53.5
	0.6	145.64±3.99	1.70±0.49	10.88±3.15	0.51±0.04	59.7
	0.9	165.68±3.42	1.52±0.20	12.11±3.88	0.46±0.08	64.5
	1.2	213.71±2.51	1.23±0.27	15.07±2.07	0.38±0.09	72.5
	1.5	282.59±2.51	0.99±0.16	19.31±1.96	0.31±0.08	79.2
40	Blank	53.42±3.81	3.74±0.16			
	0.3	109.00±2.15	2.25±0.35	8.63±1.93	0.67±0.05	51.1
	0.6	124.87±2.70	1.99±0.32	9.60±1.68	0.59±0.07	57.2
	0.9	141.14±3.99	1.79±0.24	10.60±3.78	0.54±0.03	62.2
	1.2	179.26±2.75	1.45±0.28	12.95±1.72	0.44±0.06	70.2
	1.5	232.06±3.75	1.17±0.33	16.20±3.10	0.36±0.07	77.0
45	Blank	36.89±3.70	4.13±0.14			
	0.3	71.02±3.22	2.56±0.19	6.29±3.18	0.75±0.09	48.1
	0.6	80.83±2.08	2.28±0.17	6.89±3.88	0.68±0.04	54.4
	0.9	90.73±3.53	2.05±0.46	7.50±2.04	0.61±0.06	59.3
	1.2	113.40±3.10	1.69±0.49	8.90±1.29	0.51±0.07	67.5
	1.5	143.60±3.63	1.38±0.15	10.75±2.22	0.42±0.07	74.3
50	Blank	32.05±3.79	5.75±0.37			
	0.3	57.32±2.08	3.80±0.33	5.45±1.56	1.10±0.07	44.1
	0.6	64.68±3.36	3.39±0.42	5.90±3.78	0.99±0.08	50.5
	0.9	71.99±2.03	3.07±0.36	6.35±3.78	0.90±0.04	55.5
	1.2	88.29±2.85	2.55±0.40	7.35±1.48	0.75±0.06	63.7
	1.5	109.05±3.50	2.10±0.16	8.63±1.97	0.63±0.04	70.6

Table 3.55: EIS data for the corrosion of weld aged maraging steel in 2.0 M hydrochloric acid containing different concentrations of DNPH.

Temperature (°C)	Conc. of inhibitor (mM)	R_{ct} (ohm. cm ²)	C_{dl} (mF cm ⁻²)	R_{pf} (ohm. cm ²)	C_{pf} (mF cm ⁻²)	η (%)
30	Blank	20.00±2.76	5.71±0.83			
	0.3	44.82±2.50	3.08±0.57	4.68±0.67	0.90±0.26	55.4
	0.6	52.02±3.40	2.69±0.74	5.12±0.84	0.79±0.23	61.6
	0.9	59.58±3.52	2.37±0.91	5.58±0.85	0.70±0.10	66.4
	1.2	78.13±2.91	1.86±0.70	6.73±0.79	0.56±0.30	74.4
	1.5	105.88±3.39	1.43±0.41	8.43±0.86	0.44±0.36	81.1
35	Blank	18.00±2.67	8.23±0.76			
	0.3	38.35±3.64	4.44±0.80	4.28±0.51	1.28±0.25	53.1
	0.6	44.22±2.41	3.88±0.73	4.64±0.76	1.13±0.29	59.3
	0.9	50.32±2.26	3.44±0.51	5.02±0.96	1.00±0.28	64.2
	1.2	64.94±2.95	2.72±0.70	5.91±1.08	0.80±0.35	72.3
	1.5	85.96±2.53	2.11±0.65	7.21±1.01	0.63±0.32	79.1
40	Blank	15.50±3.18	13.22±0.79			
	0.3	31.27±2.12	7.23±0.97	3.84±0.69	2.07±0.24	50.4
	0.6	35.81±3.27	6.34±0.62	4.12±0.53	1.82±0.19	56.7
	0.9	40.48±2.47	5.64±0.91	4.41±0.72	1.62±0.14	61.7
	1.2	51.39±2.18	4.49±1.00	5.08±0.63	1.30±0.24	69.8
	1.5	66.50±2.35	3.52±0.56	6.01±0.81	1.02±0.15	76.7
45	Blank	13.20±3.35	15.73±0.56			
	0.3	24.73±3.75	9.08±0.81	3.44±1.07	2.58±0.13	46.6
	0.6	28.07±2.71	8.03±0.59	3.65±0.74	2.29±0.14	53.1
	0.9	31.44±3.95	7.19±0.86	3.85±1.07	2.05±0.18	58.4
	1.2	39.09±2.87	5.83±0.61	4.32±1.01	1.67±0.32	66.2
	1.5	49.16±3.90	4.68±0.87	4.94±0.83	1.35±0.11	73.2
50	Blank	11.00±3.63	16.32±0.98			
	0.3	19.23±2.80	10.51±0.86	3.10±0.60	2.99±0.29	42.8
	0.6	21.66±2.69	9.35±1.00	3.25±0.55	2.66±0.40	49.2
	0.9	24.07±2.97	8.44±0.53	3.40±0.77	2.41±0.29	54.3
	1.2	29.41±2.62	6.95±1.05	3.73±0.86	1.99±0.27	62.6
	1.5	36.17±2.92	5.69±0.66	4.14±0.66	1.63±0.18	69.6

Table 3.56: Comparison of maximum attainable inhibition efficiencies by the Tafel method and EIS method for the corrosion of weld aged maraging steel in hydrochloric acid solutions of different concentrations in the presence of DNPH at 30 °C.

Molarity of hydrochloric acid	Conc. of DNPH (mM)	η (%)	
		Tafel	EIS
0.1	0.8	80.9	85.1
0.5	0.8	78.1	81.6
1.0	1.0	85.9	87.4
1.5	1.5	82.6	81.2
2.0	1.5	78.8	81.1

Table 3.57: Activation parameters for the corrosion of weld aged maraging steel in hydrochloric acid containing different concentrations of DNPH.

Molarity of hydrochloric acid (M)	Conc. of inhibitor (mM)	E_a ($\text{kJ}^{-1} \text{mol}^{-1}$)	ΔH^\ddagger ($\text{kJ}^{-1} \text{mol}^{-1}$)	ΔS^\ddagger ($\text{J mol}^{-1} \text{K}^{-1}$)
0.1	0.0	39.12	41.60	-94.98
	0.1	43.81	46.59	-67.79
	0.2	53.59	56.99	-56.17
	0.4	60.64	64.48	-51.32
	0.6	67.68	71.97	-38.73
	0.8	71.59	76.13	-22.27
	0.5	0.0	36.56	38.51
0.1		40.95	43.13	-74.07
0.2		50.09	52.76	-61.37
0.4		56.67	59.69	-56.08
0.6		63.25	66.62	-42.33
0.8		66.90	70.47	-24.34
1.0		0.0	35.70	34.98
	0.2	39.98	39.18	-77.29
	0.4	48.91	47.92	-64.04
	0.6	55.34	54.22	-58.52
	0.8	61.76	60.52	-44.16
	2.0	65.33	64.01	-28.39
	1.5	0.0	32.08	30.55
0.3		35.93	34.22	-84.14
0.6		43.95	41.85	-69.72
0.9		49.72	47.35	-63.71
1.2		55.50	52.85	-48.08
1.5		58.71	55.91	-32.65
2.0		0.0	30.33	31.24
	0.4	33.97	34.99	-87.36
	0.8	41.55	42.80	-72.38
	1.2	47.01	48.42	-66.14
	1.6	52.47	54.05	-49.92
	2.0	55.50	57.17	-36.70

Table 3.58: Thermodynamic parameters for the adsorption of DNPH on weld aged maraging steel surface in hydrochloric acid at different temperatures.

Molarity of hydrochloric acid (M)	Temperature (°C)	$-\Delta G^{\circ}_{\text{ads}}$ (kJ mol ⁻¹)	$\Delta H^{\circ}_{\text{ads}}$ (kJ mol ⁻¹)	$\Delta S^{\circ}_{\text{ads}}$ (J mol ⁻¹ K ⁻¹)
0.1	30	38.99	- 8.65	-43.67
	35	38.84		
	40	38.65		
	45	38.46		
	50	38.27		
0.5	30	38.16	-11.45	-38.08
	35	38.01		
	40	37.82		
	45	37.64		
	50	37.46		
1.0	30	37.68	-19.04	-32.16
	35	37.53		
	40	37.34		
	45	37.16		
	50	36.98		
1.5	30	37.53	-26.76	-24.05
	35	37.38		
	40	37.20		
	45	37.01		
	50	36.83		
2.0	30	36.54	-31.32	-15.19
	35	36.39		
	40	36.22		
	45	36.04		
	50	35.86		

3.7 5-DIETHYLAMINO-2-[2-(2,4-DINITROPHENYL) HYDRAZIN-1-YLIDENE] METHYL PHENOL (DDPM) AS INHIBITOR FOR CORROSION OF WELD AGED MARAGING STEEL IN HYDROCHLORIC ACID MEDIUM

3.7.1 Potentiodynamic polarization studies

The potentiodynamic polarization curves for the corrosion of weld aged maraging steel specimen in 1.0 M hydrochloric acid in the presence of different concentrations of DDPM, at 30 °C are shown in Fig. 3.51. Similar plots were obtained in the other four concentrations of hydrochloric acid at the different temperatures studied. The potentiodynamic polarization parameters (E_{corr} , b_c , b_a , i_{corr} and η (%)) are summarized in Tables 3.59 to 3.63.

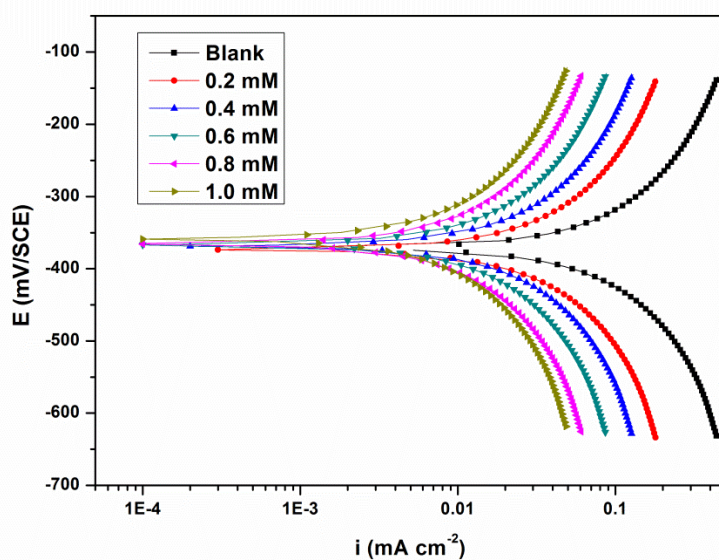


Fig. 3.51: Potentiodynamic polarization curves for the corrosion of weld aged maraging steel in 1.0 M hydrochloric acid containing different concentrations of DDPM at 30 °C.

According to the observed E_{corr} , b_a and b_c values presented in Tables 3.59 to 3.63 DDPM can be regarded as a mixed type inhibitor with predominant anodic inhibition

effect as discussed earlier in the section 3.3.1. DDPM shows lower inhibition efficiency than that of ATPI, CPOB, CPOM and DNPH for the corrosion of weld aged maraging steel in hydrochloric acid medium.

3.7.2 Electrochemical impedance spectroscopy

The Nyquist plots obtained for the corrosion of weld aged samples of maraging steel specimen in 1.0 M hydrochloric acid in the presence of different concentrations of DDPM at 30 °C are shown in Fig. 3.52. Similar plots were obtained in other concentrations of hydrochloric acid and also at other temperatures. The electrochemical parameters obtained from the EIS studies are summarized in Tables 3.64 to 3.68.

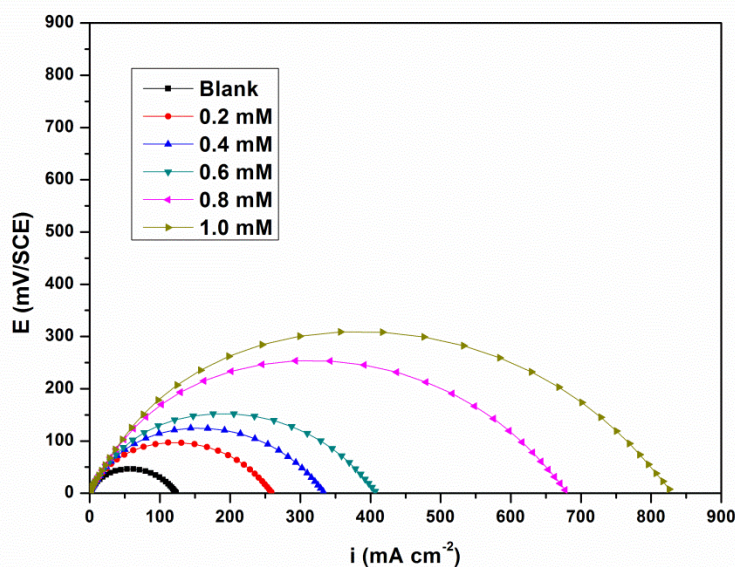


Fig. 3.52: Nyquist plots for the corrosion of weld aged maraging steel in 1.0 M hydrochloric acid containing different concentrations of DDPM at 30 °C.

From Fig. 3.52, it can be observed that the impedance spectra show a single semicircle and the diameter of semicircle increases with increasing inhibitor concentration, indicating the increase in charge transfer resistance (R_{ct}) value and

decrease in corrosion rate (v_{corr}). The plots are similar to those obtained in the presence of CPOB as discussed in the section 3.3.2. The equivalent circuit given in Fig. 3.20 is used to fit the experimental data for the corrosion of weld aged maraging steel in hydrochloric acid in the presence of DDPM. Hence the discussion in the section 3.3.2 on the equivalent circuit model for the corrosion of weld aged maraging steel in the presence of CPOB holds good here also. The results show that the values of C_{dl} and C_{pf} decrease, while the values of R_{ct} and R_{pf} increase with the increase in the concentration of DDPM, suggesting that the amount of the inhibitor molecules adsorbed on the electrode surface increases as the concentration of DDPM increases (Amin et al. 2007).

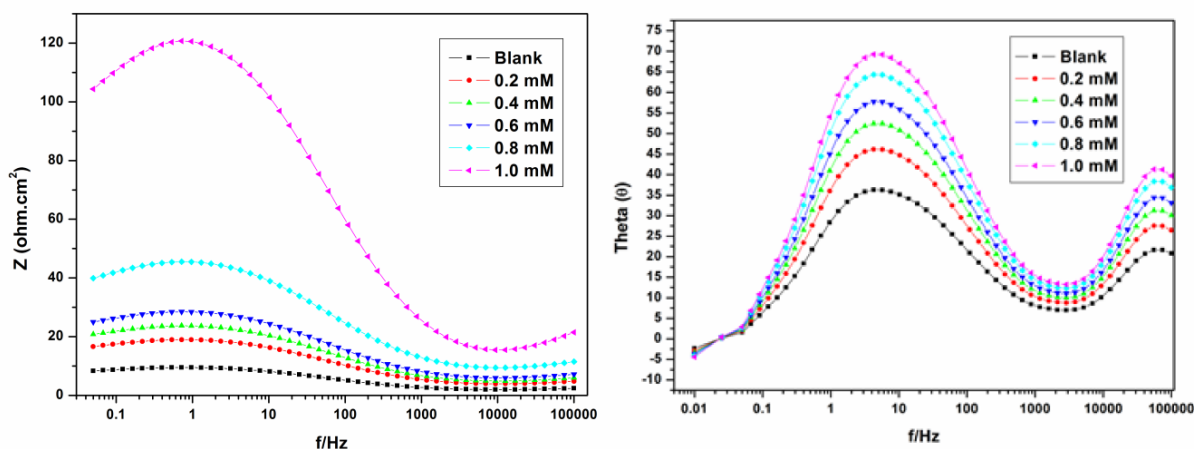


Fig. 3.53: Bode plots for the corrosion of weld aged maraging steel in 1.5 M hydrochloric acid containing different concentrations of DDPM at 30 °C.

The Bode plots for the corrosion of the alloy in the presence of different concentrations of DDPM are shown in Fig. 3.53. They are similar to the ones shown in Fig. 3.21. Hence the discussion regarding the Bode plot under the section 3.3.2 holds good for DDPM also.

A comparison of maximum attainable inhibition efficiencies by the Tafel method and EIS method, in the presence of DDPM for the corrosion of weld aged maraging steel in hydrochloric acid solutions of different concentrations at 30 °C are listed in Table 3.69.

It is evident from the table that the η (%) values obtained by the two methods are in good agreement. Similar levels of agreement were obtained at other temperatures also.

3.7.3 Effect of temperature

The data in Tables 3.59 to 3.68 reveal that, the inhibition efficiency of DDPM on weld aged maraging steel increases slightly with the increase in temperature. This can be probably attributed to the chemisorption of DDPM on the alloy surface (Szauer and Brand 1981, Sankarapavinasam et al. 1991). According to Singh et al. (1979) with the increase in temperature, leading to the increase in the electron densities at the adsorption centres of the molecule, thereby causing an improvement in inhibition efficiency.

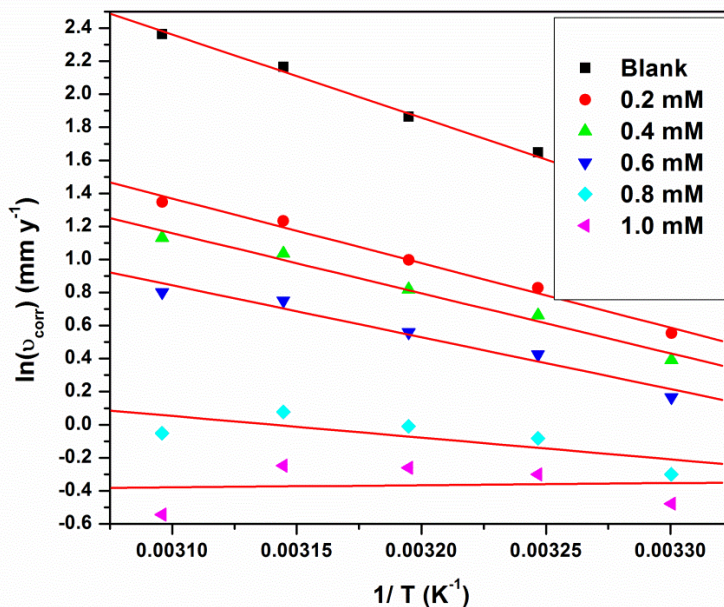


Fig. 3.54: Arrhenius plots for the corrosion of weld aged maraging steel in 1.0 M hydrochloric acid containing different concentrations of DDPM.

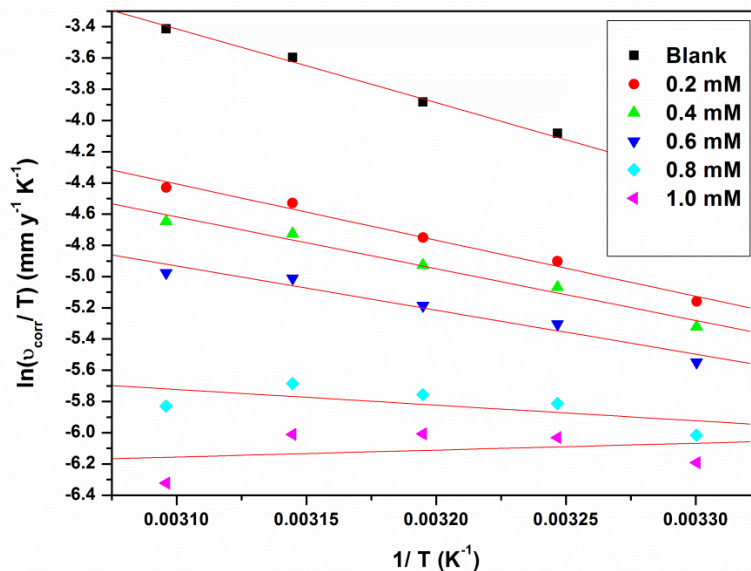


Fig. 3.55: Plots of $\ln(v_{\text{corr}}/T)$ versus $1/T$ for the corrosion of weld aged maraging steel in 1.0 M hydrochloric acid containing different concentrations of DDPM.

The Arrhenius plots for the corrosion of weld aged maraging steel in 1.0 M hydrochloric acid in the presence of different concentrations of DDPM are shown in Fig. 3.54. The plots of $\ln(v_{\text{corr}}/T)$ vs $(1/T)$ are shown in Fig. 3.55. The calculated values of activation parameters are given in Table 3.70.

The increase in the activation energy for the corrosion of weld aged maraging steel in the presence of DDPM indicates the increase in energy barrier for the corrosion reaction. The entropies of activation in the absence and presence of the inhibitor are large and negative. This implies that the activated complex in the rate determining step represents an association resulting in decrease in randomness on going from the reactants to the activated complex (Gomma and Wahdan 1995, Marsh 1988).

3.7.4 Effect of hydrochloric acid concentration

It is evident from both the polarization and EIS experimental results that, for a particular concentration of the DDPM, the inhibition efficiency decreases with the increase in hydrochloric acid concentrations. The maximum inhibition efficiency is observed at 1.0 M solution of hydrochloric acid.

3.7.5 Adsorption isotherms

The adsorption of DDPM on the surfaces of weld aged maraging steel was found to obey Langmuir adsorption isotherm. The Langmuir adsorption isotherms for the adsorption of DDPM on weld aged maraging steel in 1.0 M hydrochloric acid are shown in Fig. 3.56. The thermodynamic parameters for the adsorption of DDPM on weld aged maraging steel are tabulated in Tables 3.71.

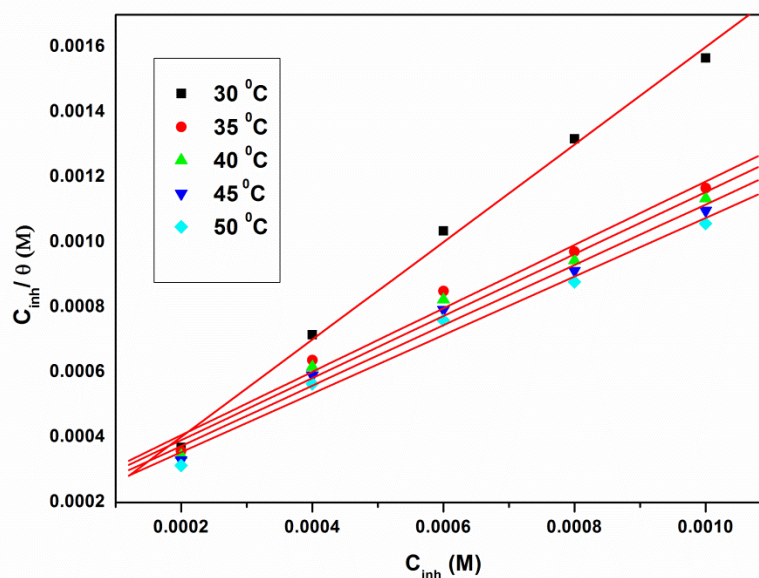


Fig. 3.56: Langmuir adsorption isotherms for the adsorption of DDPM on weld aged maraging steel in 1.0 M Hydrochloric acid at different temperatures.

The values of ΔG_{ads}^0 and ΔH_{ads}^0 indicate both physisorption and chemisorption of DDPM on weld aged maraging steel. The increase in inhibition efficiency with the increase in

temperature indicates predominant chemisorption. The ΔS_{ads}^0 value values indicate increase in randomness on going from the reactants to the metal adsorbed species.

3.7.6 Mechanism of corrosion inhibition

The mechanism of corrosion inhibition of weld aged maraging steel in the presence of DDPM is similar to that in the presence of ATPI as discussed under section 3.3.6. The chemisorption is attributed to be due to the chemical nature of interaction between inhibitor molecule and the alloy surface as reported by Lagrenee et al. (2002). DDPM can adsorb on the alloy surface through physisorption by the electrostatic interaction of protonated DDPM with the negatively charged chloride ions already adsorbed on the alloy surface. The free electron pairs on nitrogen and oxygen atoms of neutral DDPM can interact with the vacant d orbitals of iron (Satpati and Ravindran 2008), resulting in the chemisorption of DDPM on the alloy surface.

DDPM shows slightly lesser inhibition efficiency at lower temperature and higher inhibition efficiency at higher temperatures than that of ATPI, CPOB CPOM and DNPH for the corrosion of weld aged maraging steel in hydrochloric acid medium.

3.7.7 SEM/EDS studies

Fig. 3.57 (a) represents the SEM image of the corroded weld aged maraging steel sample. Fig. 3.57 (b) represents the SEM image of weld aged maraging steel after the corrosion tests in a medium of 1.0 M hydrochloric acid containing 1.5 mM of DDPM. The image clearly shows a smooth surface due to the adsorbed layer of inhibitor molecules on the alloy surface, thus protecting the metal from corrosion.

The EDS profile analyses of the corroded surface of the alloy in the presence of DNPH is shown in Fig. 3.58. The atomic percentages of the elements found in the EDS profile were 7.18 % Fe, 2.45% Ni, 2.99% Mo, 30.64% O, 4.26 % Cl, 50.09 % C and 5.42 N and indicated the formation of inhibitor film on the surface of alloy.

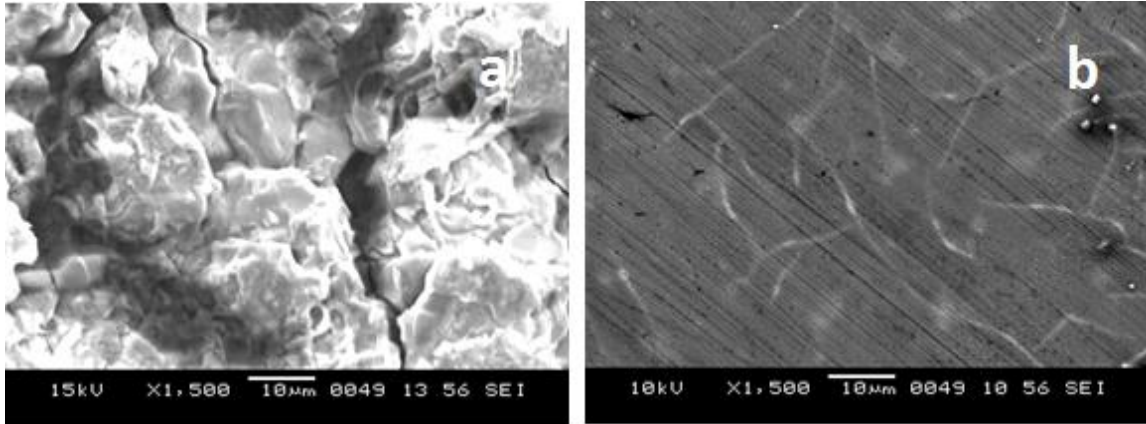


Fig. 3.57: SEM images of the weld aged maraging steel after immersion in 1.0 M hydrochloric acid a) in the absence and b) in the presence of DDPM.

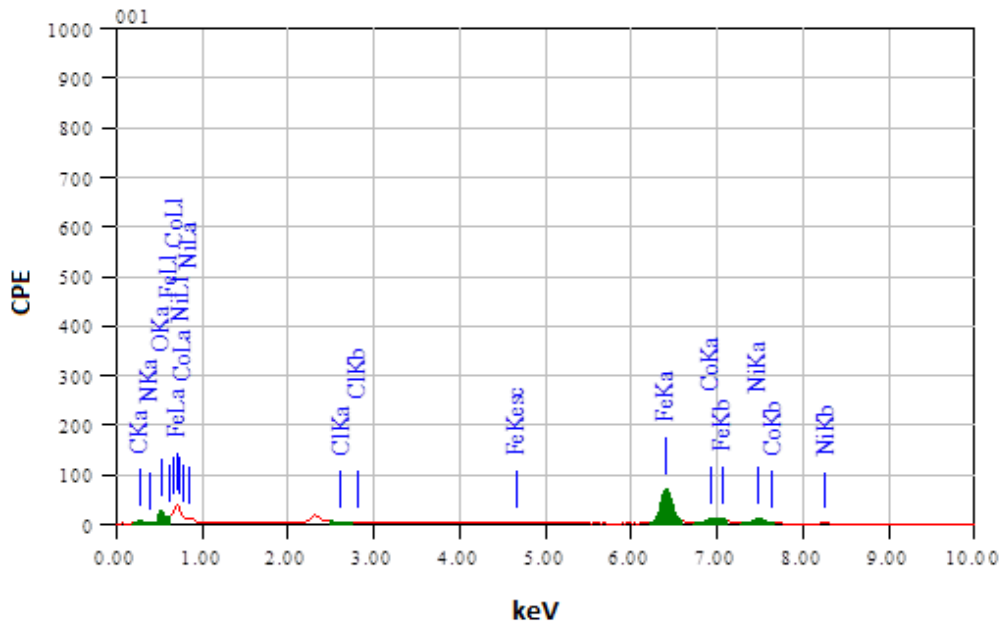


Fig. 3.58: EDS spectra of the weld aged maraging steel after immersion in 1.0 M hydrochloric acid in the absence of DDPM.

Table 3.59: Results of potentiodynamic polarization studies for the corrosion of weld aged maraging steel in 0.1 M hydrochloric acid containing different concentrations of DDPM.

Temperature (°C)	Conc. of inhibitor (mM)	E_{corr} (mV /SCE)	b_a (mV dec ⁻¹)	$-b_c$ (mV dec ⁻¹)	i_{corr} (mA cm ⁻²)	v_{corr} (mm y ⁻¹)	η (%)
30	Blank	-419±2	142±2	226±2	0.22±0.01	2.53±0.12	
	0.1	-414±3	140±2	220±3	0.15±0.02	1.68±0.21	33.5
	0.2	-409±2	133±2	216±1	0.12±0.02	1.33±0.23	47.6
	0.4	-409±2	130±1	212±1	0.10±0.03	1.13±0.27	55.2
	0.6	-404±2	127±3	204±2	0.07±0.03	0.79±0.27	68.7
	0.8	-404±1	124±3	203±3	0.03±0.02	0.30±0.16	83.1
	35	Blank	-416±2	150±1	234±1	0.26±0.02	2.99±0.15
0.1		-417±1	145±1	229±2	0.17±0.01	1.92±0.11	35.1
0.2		-412±3	138±3	222±1	0.13±0.02	1.49±0.16	49.2
0.4		-410±3	135±3	219±3	0.11±0.02	1.26±0.20	56.9
0.6		-404±3	132±2	216±3	0.07±0.03	0.85±0.28	70.5
0.8		-403±2	130±1	214±2	0.02±0.01	0.27±0.12	85.1
40		Blank	-412±2	159±2	242±2	0.30±0.02	3.45±0.25
	0.1	-408±3	153±2	242±2	0.18±0.01	2.09±0.14	36.8
	0.2	-404±3	149±3	235±3	0.14±0.02	1.59±0.21	51.2
	0.4	-405±1	145±1	232±2	0.12±0.03	1.33±0.29	59.0
	0.6	-401±2	137±2	229±1	0.07±0.02	0.85±0.16	72.7
	0.8	-396±1	136±2	227±3	0.01±0.01	0.17±0.07	87.4
	45	Blank	-409±2	165±3	250±2	0.33±0.02	3.80±0.25
0.1		-403±2	163±2	244±1	0.20±0.02	2.30±0.20	39.3
0.2		-400±3	156±2	240±1	0.15±0.01	1.75±0.12	53.8
0.4		-400±3	153±3	236±3	0.12±0.02	1.45±0.21	61.7
0.6		-397±1	150±1	228±1	0.08±0.02	0.93±0.23	75.6
0.8		-391±3	148±1	227±1	0.03±0.01	0.36±0.15	90.4
50		Blank	-405±1	173±2	259±1	0.37±0.02	4.26±0.22
	0.1	-404±3	168±3	259±3	0.21±0.01	2.46±0.11	42.2
	0.2	-399±1	161±2	252±2	0.15±0.01	1.83±0.13	56.9
	0.4	-399±2	158±1	249±3	0.13±0.01	1.50±0.11	64.8
	0.6	-396±2	155±3	246±3	0.07±0.02	0.90±0.20	78.9
	0.8	-392±1	153±1	244±3	0.02±0.01	0.26±0.12	93.9

Table 3.60: Results of potentiodynamic polarization studies for the corrosion of weld aged maraging steel in 0.5 M hydrochloric acid containing different concentrations of DDPM.

Temperature (°C)	Conc. of inhibitor (mM)	E_{corr} (mV /SCE)	b_a (mV dec ⁻¹)	$-b_c$ (mV dec ⁻¹)	i_{corr} (mA cm ⁻²)	v_{corr} (mm y ⁻¹)	η (%)
30	Blank	-413±3	148±1	247±4	0.27±0.03	3.11±0.29	
	0.2	-414±4	143±1	239±2	0.11±0.02	1.33±0.23	57.2
	0.4	-408±4	136±1	235±1	0.09±0.02	1.12±0.20	63.9
	0.6	-406±2	133±2	231±4	0.07±0.02	0.88±0.25	71.6
	0.8	-401±4	130±1	223±3	0.04±0.01	0.52±0.11	83.1
	1.0	-401±4	128±4	222±4	0.03±0.01	0.42±0.10	86.4
	35	Blank	-411±1	156±4	254±2	0.35±0.01	4.03±0.12
0.2		-410±4	154±2	247±4	0.14±0.01	1.64±0.10	59.3
0.4		-406±2	147±3	240±4	0.11±0.01	1.37±0.12	66.1
0.6		-407±3	144±2	237±2	0.09±0.01	1.05±0.10	74.0
0.8		-403±3	141±2	234±1	0.05±0.01	0.58±0.11	85.7
1.0		-398±2	139±2	232±2	0.03±0.02	0.44±0.17	89.1
40		Blank	-408±1	165±4	262±1	0.42±0.06	4.83±0.59
	0.2	-404±4	159±1	260±2	0.16±0.01	1.88±0.12	61.2
	0.4	-400±3	155±3	253±1	0.13±0.03	1.54±0.29	68.1
	0.6	-398±2	151±3	250±3	0.10±0.02	1.15±0.22	76.2
	0.8	-394±1	143±3	247±3	0.05±0.01	0.57±0.15	88.1
	1.0	-393±2	142±3	245±4	0.03±0.02	0.40±0.16	91.7
	45	Blank	-406±2	172±2	269±3	0.51±0.01	5.87±0.10
0.2		-399±4	167±2	261±3	0.18±0.02	2.16±0.22	63.1
0.4		-396±2	160±3	257±3	0.15±0.03	1.75±0.28	70.2
0.6		-397±4	157±2	253±3	0.11±0.01	1.27±0.13	78.4
0.8		-392±4	154±1	245±1	0.04±0.01	0.55±0.11	90.6
1.0		-387±1	152±1	244±3	0.03±0.02	0.39±0.22	93.3
50		Blank	-404±3	183±1	277±3	0.59±0.01	6.79±0.10
	0.2	-400±3	182±1	274±3	0.20±0.01	2.38±0.13	65.1
	0.4	-394±1	174±1	267±4	0.16±0.03	1.89±0.25	72.2
	0.6	-393±3	171±3	264±3	0.11±0.03	1.32±0.29	80.6
	0.8	-388±2	168±3	261±2	0.04±0.01	0.47±0.11	93.0
	1.0	-388±3	166±1	259±3	0.02±0.01	0.28±0.12	95.9

Table 3.61: Results of potentiodynamic polarization studies for the corrosion of weld aged maraging steel in 1.0 M hydrochloric acid containing different concentrations of DDPM.

Temperature (°C)	Conc. of inhibitor (mM)	E_{corr} (mV /SCE)	b_a (mV dec ⁻¹)	$-b_c$ (mV dec ⁻¹)	i_{corr} (mA cm ⁻²)	v_{corr} (mm y ⁻¹)	η (%)
30	Blank	-371±3	153±4	256±2	0.33±0.02	3.80±0.22	
	0.2	-372±1	149±3	250±1	0.15±0.02	1.74±0.18	54.2
	0.4	-368±2	142±2	243±2	0.12±0.02	1.48±0.17	61.0
	0.6	-367±4	139±3	240±3	0.10±0.01	1.18±0.11	68.8
	0.8	-364±3	136±2	237±4	0.06±0.02	0.74±0.17	80.4
	1.0	-358±2	134±3	235±2	0.05±0.03	0.62±0.28	83.7
35	Blank	-368±4	159±2	261±1	0.45±0.13	5.20±0.11	
	0.2	-362±4	153±2	260±2	0.19±0.02	2.29±0.18	55.9
	0.4	-362±1	147±4	253±3	0.16±0.02	1.94±0.23	62.7
	0.6	-360±1	143±2	250±3	0.13±0.02	1.53±0.22	70.6
	0.8	-356±3	135±4	247±4	0.08±0.02	0.92±0.17	82.3
	1.0	-355±3	134±1	245±3	0.06±0.02	0.74±0.19	85.7
40	Blank	-364±3	165±4	266±3	0.56±0.06	6.45±0.62	
	0.2	-357±4	160±2	259±4	0.23±0.02	2.71±0.18	58.0
	0.4	-358±1	153±1	255±3	0.19±0.02	2.27±0.21	64.9
	0.6	-358±4	150±1	251±3	0.15±0.03	1.75±0.26	72.8
	0.8	-355±2	147±4	243±2	0.08±0.02	0.99±0.22	84.7
	1.0	-350±1	145±3	242±2	0.06±0.03	0.77±0.28	88.1
45	Blank	-361±3	172±3	273±4	0.75±0.11	8.72±1.43	
	0.2	-362±3	163±4	268±3	0.29±0.02	3.43±0.24	60.7
	0.4	-362±1	159±3	261±2	0.24±0.02	2.82±0.23	67.7
	0.6	-360±4	155±2	258±2	0.18±0.02	2.12±0.23	75.4
	0.8	-353±3	147±1	255±1	0.09±0.02	1.08±0.19	87.5
	1.0	-353±3	146±2	253±3	0.06±0.02	0.78±0.15	91.1
50	Blank	-358±2	177±1	278±2	0.92±0.09	10.63±0.87	
	0.2	-352±4	176±1	276±4	0.33±0.06	3.85±0.59	63.8
	0.4	-347±2	168±2	268±2	0.26±0.04	3.10±0.39	70.9
	0.6	-347±3	165±1	265±1	0.19±0.02	2.23±0.24	79.2
	0.8	-344±2	162±1	262±3	0.08±0.02	0.95±0.23	91.1
	1.0	-338±3	160±2	260±3	0.05±0.02	0.58±0.16	96.6

Table 3.62: Results of potentiodynamic polarization studies for the corrosion of weld aged maraging steel in 1.5 M hydrochloric acid containing different concentrations of DDPM.

Temperature (°C)	Conc. of inhibitor (mM)	E_{corr} (mV /SCE)	b_a (mV dec ⁻¹)	$-b_c$ (mV dec ⁻¹)	i_{corr} (mA cm ⁻²)	v_{corr} (mm y ⁻¹)	η (%)
30	Blank	-342±3	158±3	267±4	0.70±0.12	8.05±1.56	
	0.3	-339±2	153±1	261±3	0.35±0.08	3.97±0.91	50.8
	0.6	-334±2	146±2	257±1	0.30±0.03	3.41±0.32	57.7
	0.9	-330±1	143±4	253±1	0.24±0.02	2.77±0.17	65.6
	1.2	-325±3	140±4	245±2	0.16±0.02	1.82±0.20	77.5
	1.5	-326±4	138±4	244±4	0.13±0.03	1.54±0.35	80.9
	Blank	-339±4	165±4	276±1	0.82±0.03	9.45±0.29	
35	0.3	-333±2	163±2	270±1	0.40±0.01	4.55±0.10	51.8
	0.6	-331±1	156±4	263±1	0.34±0.02	3.90±0.20	58.8
	0.9	-330±3	153±2	260±3	0.27±0.03	3.14±0.31	66.8
	1.2	-327±3	150±3	257±2	0.18±0.03	2.01±0.31	78.7
	1.5	-321±3	148±1	255±4	0.15±0.03	1.68±0.25	82.2
	Blank	-337±2	173±3	282±3	0.94±0.01	10.85±0.12	
	0.3	-334±1	167±4	283±3	0.44±0.03	5.03±0.32	53.6
40	0.6	-329±2	163±4	276±4	0.37±0.03	4.26±0.27	60.7
	0.9	-327±1	159±1	272±1	0.29±0.01	3.37±0.14	68.9
	1.2	-323±4	151±2	269±4	0.18±0.04	2.05±0.40	81.1
	1.5	-322±4	150±3	267±3	0.15±0.02	1.67±0.23	84.6
	Blank	-334±2	179±2	286±3	1.53±0.03	17.60±0.27	
	0.3	-327±2	178±4	280±2	0.68±0.01	7.81±0.15	55.7
	0.6	-324±2	170±3	273±1	0.57±0.02	6.53±0.19	62.9
45	0.9	-324±1	167±4	270±4	0.44±0.02	5.06±0.22	71.3
	1.2	-320±4	164±3	267±3	0.25±0.03	2.86±0.35	83.7
	1.5	-326±1	162±1	265±4	0.19±0.01	2.23±0.10	87.3
	Blank	-332±4	185±3	292±3	1.61±0.01	18.57±0.12	
	0.3	-326±3	179±2	293±3	0.68±0.02	7.81±0.22	57.9
	0.6	-321±4	175±2	286±2	0.56±0.02	6.44±0.20	65.3
	0.9	-320±4	171±4	283±4	0.42±0.02	4.85±0.17	73.9
50	1.2	-318±1	163±4	280±2	0.22±0.02	2.50±0.18	86.6
	1.5	-312±4	162±4	278±3	0.16±0.02	1.82±0.22	90.2

Table 3.63: Results of potentiodynamic polarization studies for the corrosion of weld aged maraging steel in 2.0 M hydrochloric acid containing different concentrations of DNPH.

Temperature (°C)	Conc. of inhibitor (mM)	E_{corr} (mV /SCE)	b_a (mV dec ⁻¹)	$-b_c$ (mV dec ⁻¹)	i_{corr} (mA cm ⁻²)	v_{corr} (mm y ⁻¹)	η (%)
30	Blank	-324±3	175±2	287±3	2.77±0.19	31.85±2.27	
	0.3	-317±2	171±2	283±2	1.49±0.11	17.13±1.41	46.2
	0.6	-314±1	167±1	279±4	1.27±0.05	14.59±0.50	54.2
	0.9	-314±4	163±3	276±2	0.99±0.04	11.40±0.38	64.2
	1.2	-311±2	155±3	272±1	0.80±0.01	9.18±0.12	71.2
	1.5	-306±4	154±4	270±2	0.68±0.04	7.76±0.46	75.6
35	Blank	-321±2	182±3	293±1	3.09±0.22	35.49±2.56	
	0.3	-317±1	179±3	288±3	1.59±0.11	18.28±1.47	48.5
	0.6	-312±3	171±3	281±4	1.34±0.02	15.40±0.18	56.6
	0.9	-309±4	168±3	278±3	1.02±0.04	11.77±0.41	66.9
	1.2	-305±3	165±2	275±3	0.80±0.02	9.24±0.21	74.2
	1.5	-305±3	163±3	273±1	0.66±0.03	7.63±0.26	78.5
40	Blank	-319±4	189±4	300±4	3.39±0.32	39.03±3.52	
	0.3	-312±1	186±2	294±1	1.65±0.10	19.00±1.33	51.3
	0.6	-309±3	179±4	290±4	1.37±0.06	15.76±0.90	59.6
	0.9	-310±4	176±2	286±3	1.02±0.03	11.69±0.28	70.1
	1.2	-305±2	172±2	278±1	0.77±0.01	8.86±0.14	77.3
	1.5	-300±3	170±2	277±1	0.61±0.03	7.05±0.32	81.9
45	Blank	-315±2	196±1	307±1	3.63±0.42	41.73±4.31	
	0.3	-311±3	192±1	300±2	1.65±0.04	18.94±0.38	54.6
	0.6	-306±3	185±3	293±3	1.34±0.01	15.41±0.11	63.1
	0.9	-303±3	181±2	290±1	0.95±0.02	10.97±0.22	73.7
	1.2	-299±1	173±4	287±1	0.68±0.01	7.87±0.12	81.1
	1.5	-298±1	172±4	285±4	0.51±0.02	5.90±0.22	85.9
50	Blank	-312±1	203±1	312±4	3.89±0.35	44.77±3.81	
	0.3	-307±3	202±2	308±4	1.65±0.11	18.95±1.46	57.7
	0.6	-303±4	195±2	304±1	1.31±0.01	15.09±0.13	66.3
	0.9	-303±2	192±3	300±2	0.89±0.04	10.23±0.44	77.2
	1.2	-298±1	189±3	292±2	0.60±0.01	6.84±0.15	84.7
	1.5	-295±3	187±2	291±4	0.41±0.02	4.68±0.16	89.6

Table 3.64: EIS data for the corrosion of weld aged maraging steel in 0.1 M hydrochloric acid containing different concentrations of DDPM.

Temperature (°C)	Conc. of inhibitor (mM)	R_{ct} (ohm. cm ²)	C_{dl} (mF cm ⁻²)	R_{pf} (ohm. cm ²)	C_{pf} (mF cm ⁻²)	η (%)
30	Blank	181.20±3.79	0.93±0.32			
	0.1	278.98±3.11	0.90±0.37	19.08±1.60	0.29±0.12	35.1
	0.2	357.33±2.45	0.75±0.28	23.90±2.65	0.25±0.09	49.3
	0.4	421.10±2.76	0.67±0.23	27.83±2.99	0.22±0.10	57.1
	0.6	616.54±5.99	0.53±0.20	39.85±2.47	0.18±0.06	70.6
	0.8	1220.20±6.52	0.38±0.15	76.99±2.84	0.14±0.06	85.2
35	Blank	158.01±2.19	1.10±0.38			
	0.1	248.08±2.51	1.01±0.20	17.18±2.20	0.32±0.15	36.3
	0.2	320.49±3.55	0.83±0.27	21.64±1.96	0.27±0.05	50.7
	0.4	380.26±3.09	0.74±0.18	25.31±1.76	0.24±0.03	58.5
	0.6	568.96±4.61	0.57±0.16	36.92±2.23	0.20±0.05	72.2
	0.8	1207.95±5.67	0.39±0.10	76.24±2.60	0.15±0.10	86.9
40	Blank	135.21±3.28	1.40±0.26			
	0.1	218.36±2.74	1.20±0.30	15.35±1.95	0.37±0.17	38.1
	0.2	285.31±4.61	0.97±0.33	19.47±2.60	0.31±0.11	52.6
	0.4	341.78±4.27	0.85±0.45	22.95±1.84	0.27±0.10	60.4
	0.6	527.34±5.72	0.63±0.48	34.36±2.56	0.21±0.04	74.4
	0.8	1250.79±6.18	0.38±0.17	78.87±3.69	0.14±0.04	89.2
45	Blank	127.54±2.96	1.55±0.26			
	0.1	213.85±3.26	1.26±0.40	15.08±2.35	0.39±0.15	40.4
	0.2	283.67±2.41	1.00±0.41	19.37±2.19	0.32±0.13	55.2
	0.4	344.33±3.17	0.87±0.39	23.10±2.08	0.28±0.18	63.0
	0.6	555.00±5.53	0.62±0.26	36.07±2.76	0.21±0.05	77.4
	0.8	1592.26±5.78	0.36±0.11	99.88±3.46	0.14±0.07	92.1
50	Blank	117.23±3.13	1.80±0.45			
	0.1	205.70±2.76	1.38±0.34	14.57±1.74	0.42±0.12	43.2
	0.2	278.06±2.56	1.08±0.39	19.03±2.76	0.34±0.11	57.8
	0.4	343.18±4.38	0.91±0.35	23.03±2.64	0.29±0.06	65.8
	0.6	587.32±5.15	0.63±0.25	38.05±2.55	0.21±0.05	80.1
	0.8	2422.11±7.57	0.32±0.17	150.94±3.54	0.13±0.03	95.2

Table 3.65: EIS data for the corrosion of weld aged maraging steel in 0.5 M hydrochloric acid containing different concentrations of DDPM.

Temperature (°C)	Conc. of inhibitor (mM)	R_{ct} (ohm. cm ²)	C_{dl} (mF cm ⁻²)	R_{pf} (ohm. cm ²)	C_{pf} (mF cm ⁻²)	η (%)
30	Blank	156.30±2.59	0.96±0.39			
	0.2	355.71±4.31	0.70±0.23	23.80±3.18	0.23±0.04	56.1
	0.4	420.50±4.79	0.62±0.44	27.79±2.40	0.21±0.06	62.8
	0.6	531.81±2.93	0.54±0.28	34.64±3.63	0.19±0.06	70.6
	0.8	879.08±2.51	0.42±0.15	56.00±2.18	0.15±0.06	82.2
	1.0	1082.41±5.91	0.38±0.11	68.51±2.25	0.14±0.04	85.6
35	Blank	139.27±4.13	1.11±0.22			
	0.2	331.20±4.90	0.74±0.21	22.30±3.52	0.24±0.06	58.0
	0.4	396.22±2.76	0.66±0.25	26.30±3.58	0.22±0.07	64.9
	0.6	511.83±3.90	0.56±0.26	33.41±2.46	0.19±0.04	72.8
	0.8	906.71±2.67	0.41±0.11	57.70±3.70	0.15±0.04	84.6
	1.0	1170.34±6.61	0.37±0.13	73.92±2.95	0.14±0.06	88.1
40	Blank	123.15±2.66	1.33±0.37			
	0.2	305.36±2.76	0.83±0.30	20.71±2.32	0.27±0.06	59.7
	0.4	369.93±3.21	0.72±0.20	24.68±2.57	0.24±0.05	66.7
	0.6	488.88±4.16	0.60±0.21	32.00±3.16	0.20±0.07	74.8
	0.8	940.08±8.56	0.42±0.10	59.76±2.89	0.15±0.05	86.9
	1.0	1294.95±9.81	0.37±0.19	81.59±3.39	0.14±0.05	90.5
45	Blank	107.56±3.70	1.55±0.25			
	0.2	278.82±2.69	0.89±0.31	19.07±3.57	0.29±0.05	61.4
	0.4	342.69±3.14	0.77±0.33	23.00±3.20	0.25±0.06	68.6
	0.6	465.27±2.59	0.63±0.21	30.54±3.52	0.21±0.07	76.9
	0.8	996.94±4.66	0.41±0.20	63.26±3.11	0.15±0.04	89.2
	1.0	1334.62±8.72	0.36±0.19	84.03±2.05	0.14±0.05	91.9
50	Blank	90.34±4.85	1.74±0.39			
	0.2	244.76±4.24	0.93±0.29	16.98±2.12	0.30±0.06	63.1
	0.4	305.31±2.57	0.79±0.32	20.70±3.97	0.26±0.04	70.4
	0.6	427.34±4.59	0.63±0.22	28.21±3.12	0.21±0.07	78.9
	0.8	1055.37±3.27	0.39±0.13	66.85±3.95	0.15±0.05	91.4
	1.0	1587.70±7.84	0.33±0.17	99.60±2.41	0.13±0.06	94.3

Table 3.66: EIS data for the corrosion of weld aged maraging steel in 1.0 M hydrochloric acid containing different concentrations of DDPM.

Temperature (°C)	Conc. of inhibitor (mM)	R_{ct} (ohm. cm ²)	C_{dl} (mF cm ⁻²)	R_{pf} (ohm. cm ²)	C_{pf} (mF cm ⁻²)	η (%)
30	Blank	116.21±2.67	1.68±0.17			
	0.2	260.19±3.11	1.07±0.10	17.93±2.46	0.34±0.05	55.3
	0.4	307.24±3.68	0.94±0.22	20.82±3.78	0.30±0.09	62.2
	0.6	387.85±4.75	0.79±0.19	25.78±3.79	0.26±0.07	70.3
	0.8	637.41±5.99	0.57±0.18	41.14±3.69	0.20±0.08	81.8
	1.0	781.97±7.04	0.50±0.15	50.03±2.93	0.18±0.07	85.1
35	Blank	97.34±3.18	1.75±0.20			
	0.2	227.44±4.13	1.16±0.13	15.91±1.82	0.36±0.06	57.2
	0.4	271.26±4.90	1.00±0.45	18.61±2.49	0.32±0.06	64.1
	0.6	348.37±4.67	0.81±0.15	23.35±3.79	0.26±0.06	72.1
	0.8	604.72±4.58	0.54±0.18	39.12±2.76	0.19±0.08	83.9
	1.0	767.35±4.66	0.46±0.15	49.13±1.98	0.17±0.09	87.3
40	Blank	82.64±4.47	2.15±0.14			
	0.2	204.30±2.80	1.17±0.23	14.49±3.04	0.36±0.07	59.6
	0.4	246.94±2.16	1.01±0.30	17.11±2.11	0.32±0.05	66.6
	0.6	324.81±4.10	0.82±0.40	21.90±3.00	0.27±0.07	74.6
	0.8	613.21±4.38	0.54±0.28	39.65±3.20	0.19±0.07	86.5
	1.0	823.53±3.90	0.46±0.12	52.59±3.48	0.16±0.06	90.2
45	Blank	65.26±2.27	2.36±0.31			
	0.2	173.45±2.29	1.19±0.29	12.59±2.04	0.37±0.05	62.4
	0.4	213.49±3.89	1.01±0.33	15.05±3.05	0.32±0.05	69.5
	0.6	290.68±3.90	0.80±0.37	19.80±3.92	0.26±0.07	77.6
	0.8	629.95±4.26	0.49±0.33	40.68±3.36	0.17±0.06	89.7
	1.0	947.67±7.02	0.40±0.19	60.22±3.91	0.15±0.08	93.1
50	Blank	53.82±3.65	2.79±0.27			
	0.2	158.19±2.14	1.24±0.10	11.65±2.50	0.38±0.06	66.0
	0.4	200.07±2.32	1.03±0.16	14.23±2.65	0.33±0.08	73.1
	0.6	287.55±3.87	0.78±0.25	19.61±3.32	0.26±0.05	81.3
	0.8	826.42±4.59	0.42±0.17	52.76±3.20	0.15±0.08	93.5
	1.0	1799.33±6.20	0.31±0.16	112.62±4.83	0.12±0.07	95.1

Table 3.67: EIS data for the corrosion of weld aged maraging steel in 1.5 M hydrochloric acid containing different concentrations of DDPM.

Temperature (°C)	Conc. of inhibitor (mM)	R _{ct} (ohm. cm ²)	C _{dl} (mF cm ⁻²)	R _{pf} (ohm. cm ²)	C _{pf} (mF cm ⁻²)	η (%)
30	Blank	64.30±2.70	3.01±0.22			
	0.3	132.25±2.68	1.86±0.21	10.06±3.05	0.56±0.05	51.4
	0.6	154.38±2.07	1.62±0.42	11.42±2.25	0.49±0.08	58.4
	0.9	191.20±3.38	1.35±0.23	13.68±3.48	0.42±0.06	66.4
	1.2	296.86±2.90	0.95±0.28	20.18±2.38	0.30±0.07	78.3
	1.5	353.10±4.44	0.84±0.13	23.64±2.22	0.27±0.09	81.8
35	Blank	58.75±2.97	3.38±0.28			
	0.3	123.79±2.29	1.96±0.35	9.54±2.72	0.59±0.09	52.5
	0.6	145.35±3.75	1.70±0.29	10.86±2.40	0.51±0.08	59.6
	0.9	181.78±2.01	1.41±0.30	13.10±2.69	0.43±0.10	67.7
	1.2	290.41±3.08	0.97±0.23	19.79±2.36	0.31±0.08	79.8
	1.5	350.54±5.54	0.84±0.12	23.49±3.32	0.27±0.09	83.2
40	Blank	53.42±3.05	3.74±0.40			
	0.3	118.40±3.25	2.09±0.39	9.20±3.92	0.62±0.08	54.9
	0.6	140.80±3.10	1.79±0.37	10.58±2.09	0.54±0.08	62.1
	0.9	180.05±3.65	1.45±0.27	13.00±3.71	0.44±0.06	70.3
	1.2	308.25±2.44	0.94±0.28	20.88±2.94	0.30±0.07	82.7
	1.5	387.38±7.43	0.79±0.14	25.75±2.91	0.26±0.05	86.2
45	Blank	36.89±3.68	4.13±0.47			
	0.3	86.11±3.69	2.16±0.42	7.22±3.03	0.64±0.08	57.2
	0.6	103.89±3.66	1.83±0.42	8.31±3.01	0.55±0.09	64.5
	0.9	136.33±2.47	1.45±0.22	10.31±2.47	0.44±0.06	72.9
	1.2	254.77±3.67	0.88±0.24	17.59±3.58	0.28±0.08	85.5
	1.5	339.69±4.48	0.72±0.12	22.82±3.32	0.24±0.09	89.1
50	Blank	32.05±2.76	4.59±0.29			
	0.3	77.49±3.15	2.35±0.42	6.69±3.45	0.70±0.09	58.6
	0.6	94.60±2.40	1.97±0.37	7.74±2.18	0.59±0.08	66.1
	0.9	126.88±2.86	1.53±0.29	9.73±3.81	0.47±0.06	74.7
	1.2	257.84±2.37	0.86±0.29	17.78±2.62	0.28±0.06	87.6
	1.5	366.70±5.44	0.67±0.22	24.48±3.01	0.22±0.06	91.3

Table 3.68: EIS data for the corrosion of weld aged maraging steel in 2.0 M hydrochloric acid containing different concentrations of DDPM.

Temperature (°C)	Conc. of inhibitor (mM)	R_{ct} (ohm. cm ²)	C_{dl} (mF cm ⁻²)	R_{pf} (ohm. cm ²)	C_{pf} (mF cm ⁻²)	η (%)
30	Blank	20.21±2.79	5.75±0.77			
	0.3	38.07±2.57	3.51±0.94	4.26±1.08	1.02±0.19	46.9
	0.6	44.88±3.31	3.01±0.85	4.68±1.49	0.88±0.11	55.2
	0.9	57.89±3.50	2.38±0.57	5.48±1.96	0.70±0.13	65.1
	1.2	72.52±3.83	1.95±0.60	6.38±1.87	0.58±0.10	72.1
	1.5	86.48±4.29	1.67±0.49	7.24±2.45	0.50±0.18	76.6
35	Blank	17.34±3.75	8.26±0.82			
	0.3	34.35±2.02	4.67±0.65	4.03±1.92	1.35±0.12	49.5
	0.6	41.02±3.46	3.95±0.90	4.44±1.58	1.14±0.17	57.7
	0.9	54.29±2.20	3.04±0.50	5.26±1.95	0.89±0.16	68.1
	1.2	70.03±2.02	2.41±0.54	6.23±2.07	0.71±0.17	75.2
	1.5	85.97±5.01	2.00±0.51	7.21±2.70	0.60±0.17	79.8
40	Blank	15.01±3.98	13.22±0.61			
	0.3	31.72±2.79	7.13±0.51	3.87±1.44	2.04±0.19	52.7
	0.6	38.54±3.56	5.91±0.56	4.29±1.88	1.70±0.19	61.1
	0.9	52.85±2.85	4.37±0.65	5.17±2.41	1.26±0.17	71.6
	1.2	71.24±4.00	3.30±0.49	6.30±1.55	0.96±0.12	78.9
	1.5	91.58±3.43	2.62±0.58	7.55±2.85	0.77±0.15	83.6
45	Blank	12.89±2.23	15.87±0.64			
	0.3	29.48±2.96	7.09±0.51	3.73±1.34	2.03±0.11	56.3
	0.6	36.64±2.72	5.74±0.99	4.17±1.42	1.65±0.16	64.8
	0.9	52.78±2.61	4.06±0.63	5.17±2.38	1.18±0.15	75.6
	1.2	76.09±2.62	2.88±0.65	6.60±1.44	0.84±0.19	83.1
	1.5	106.00±4.00	2.13±0.47	8.44±1.19	0.63±0.11	87.8
50	Blank	11.67±2.17	18.95±1.53			
	0.3	29.00±2.25	7.90±0.70	3.70±1.81	2.25±0.13	59.8
	0.6	37.02±2.28	6.23±0.50	4.20±1.61	1.78±0.11	68.5
	0.9	56.79±2.18	4.14±0.68	5.41±1.36	1.20±0.20	79.5
	1.2	90.40±3.47	2.69±0.50	7.48±1.80	0.79±0.11	87.1
	1.5	145.33±5.89	1.76±0.24	10.86±2.70	0.53±0.11	92.4

Table 3.69: Comparison of maximum attainable inhibition efficiencies by the Tafel method and EIS method for the corrosion of weld aged maraging steel in hydrochloric acid solutions of different concentrations in the presence of DDPM at 30 °C.

Molarity of hydrochloric acid	Conc. of DDPM (mM)	η (%)	
		Tafel	EIS
0.1	0.8	83.1	85.1
0.5	1.0	86.4	85.5
1.0	1.0	83.7	85.1
1.5	1.5	80.8	81.7
2.0	1.5	75.6	76.6

Table 3.70: Activation parameters for the corrosion of weld aged maraging steel in hydrochloric acid containing different concentrations of DDPM.

Molarity of hydrochloric acid (M)	Conc. of inhibitor (mM)	E_a (kJ ⁻¹ mol ⁻¹)	ΔH^\ddagger (kJ ⁻¹ mol ⁻¹)	ΔS^\ddagger (J mol ⁻¹ K ⁻¹)
0.1	0.0	39.12	41.60	-94.96
	0.1	58.68	62.40	-87.15
	0.2	63.47	67.49	-77.47
	0.4	71.05	75.56	-58.10
	0.6	76.64	81.50	-48.42
	0.8	87.82	93.39	-31.96
0.5	0.0	36.56	38.51	-103.73
	0.2	54.84	57.77	-95.23
	0.4	59.32	62.48	-84.65
	0.6	66.40	69.95	-63.49
	1.8	71.63	75.45	-52.91
	2.0	82.07	86.45	-34.92
1.0	0.0	35.70	34.98	-108.23
	0.2	53.55	52.47	-99.37
	0.4	57.92	56.75	-88.33
	0.6	64.84	63.54	-66.24
	1.8	69.94	68.53	-55.20
	2.0	80.14	78.53	-36.43
1.5	0.0	32.08	30.55	-117.82
	0.3	48.12	45.83	-108.18
	0.6	52.05	49.57	-96.16
	0.9	58.27	55.49	-72.12
	1.2	62.85	59.85	-60.10
	1.5	72.02	68.58	-39.67
2.0	0.0	30.33	31.24	-122.31
	0.3	45.50	46.86	-112.32
	0.6	49.21	50.69	-99.84
	0.9	55.09	56.74	-74.88
	1.2	59.42	61.20	-62.40
	1.5	68.09	70.13	-41.18

Table 3.71: Thermodynamic parameters for the adsorption of DDPM on weld aged maraging steel surface in hydrochloric acid at different temperatures.

Molarity of hydrochloric acid (M)	Temperature (°C)	$-\Delta G_{\text{ads}}^{\circ}$ (kJ mol ⁻¹)	$\Delta H_{\text{ads}}^{\circ}$ (kJ mol ⁻¹)	$\Delta S_{\text{ads}}^{\circ}$ (J mol ⁻¹ K ⁻¹)
0.1	30	46.76	- 27.28	-80.23
	35	46.62		
	40	46.44		
	45	46.27		
	50	46.10		
0.5	30	46.86	-32.12	-72.08
	35	46.71		
	40	46.54		
	45	46.37		
	50	46.19		
1.0	30	45.21	-43.92	-66.17
	35	45.08		
	40	44.91		
	45	44.75		
	50	44.58		
1.5	30	46.57	-48.70	-48.03
	35	46.43		
	40	46.25		
	45	46.08		
	50	45.91		
2.0	30	45.62	-54.32	-28.52
	35	45.48		
	40	45.31		
	45	45.15		
	50	44.98		

3.8 1(2E)-1-(4-AMINOPHENYL)-3-(2-THIENYL) PROP-2-EN-1-ONE (ATPI) AS INHIBITOR FOR THE CORROSION OF WELD AGED MARAGING STEEL IN SULPHURIC ACID MEDIUM

3.8.1 Potentiodynamic polarization studies

The potentiodynamic polarization curves for the corrosion of weld aged maraging steel specimen in 1.0 M sulphuric acid in the presence of different concentrations of ATPI, at 30 °C are shown in Fig. 3.59. Similar plots were obtained in the other four concentrations of sulphuric acid at the different temperatures studied. The potentiodynamic polarization parameters (E_{corr} , b_c , b_a , i_{corr} and η (%)) were calculated from Tafel plots in all the five studied concentrations of sulphuric acid in the presence of different concentrations of ATPI at different temperatures and are summarized in Tables 3.72 to 3.76.

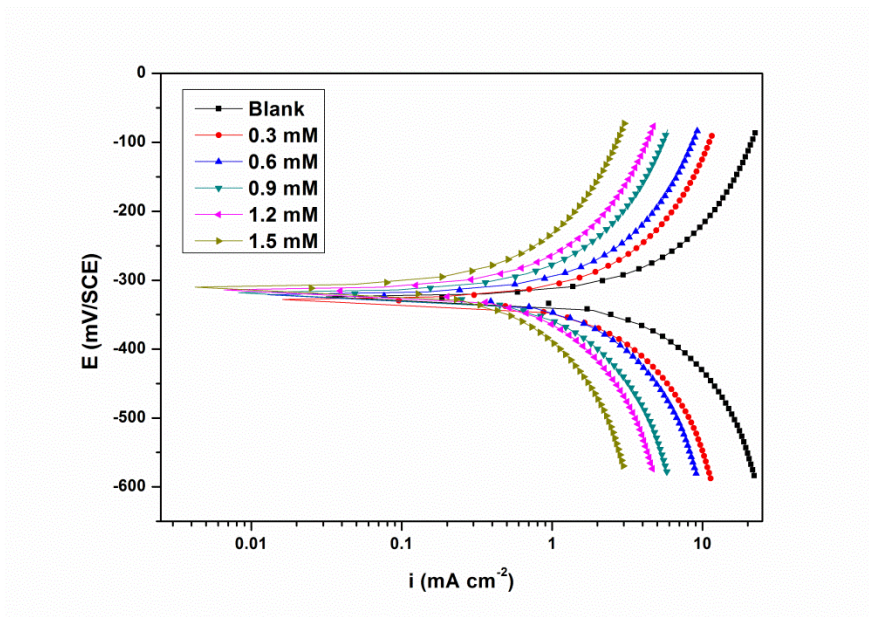


Fig. 3.59: Potentiodynamic polarization curves for the corrosion of weld aged maraging steel in 1.0 M sulphuric acid containing different concentrations of ATPI at 30 °C.

According to the results presented in Tables 3.72 to 3.76 and also from the polarization curves in Fig. 3.59, the corrosion current density (i_{corr}) decreases effectively even on the addition of small concentration of ATPI and the inhibition efficiency increases with the increase in the inhibitor concentration for the weld aged maraging steel at all the studied concentrations of sulphuric acid medium.

As can be seen from the polarization curves (Fig. 3.59) and Tables 3.72 to 3.76, the presence of inhibitor causes a slight anodic shift in E_{corr} values at all the studied temperatures and concentrations of sulphuric acid. The maximum displacement in this study is less than ± 25 mV, which indicates that ATPI is a mixed type inhibitor, affecting both anodic and cathodic reactions (Stanly and Parameswaran 2010). If the shift in E_{corr} is negligible, the inhibition is most probably caused by a geometric blocking effect of the adsorbed inhibitive species on the surface of the corroding metal (Cao 1996). In the present study although there is no remarkable change (± 85 mV) in E_{corr} , the shift in E_{corr} is not negligible. This can be attributed to the difference in the active sites blocking effect of the inhibitor for both the anodic and cathodic reaction. As the concentration of the inhibitor increases, it is noticed that the corrosion potential shifts slightly toward more positive potential. This indicates that the inhibitor promotes passivation of weld aged maraging steel through adsorption (Larabi et al. 2005). The inhibitor ATPI considered as a mixed type inhibitor with predominant anodic action. The increase in the inhibition efficiency with the increase in inhibitor concentration is attributed to the increased surface coverage by the inhibitor molecules as the concentration is increased (El- Sayed et al. 1997).

It is seen from Tables 3.72 to 3.76, that the anodic slope b_a and cathodic slope b_c do not change significantly on increasing the concentration of ATPI, indicating its non-interference in the mechanisms of anodic and cathodic reaction. This indicates that the inhibitive action of ATPI may be considered due to the adsorption and formation of barrier film on the electrode surface. The barrier film formed on the metal surface reduces the probability of both the anodic and cathodic reactions, which results in

decrease in the corrosion rate (Li et al. 2007 and Ferreira et al. 2004). The inhibition efficiency increases with the increase in inhibitor concentration, reaching a maximum value of 97.4 % at 1.0 mM of ATPI in 0.1 M sulphuric acid.

3.8.2 Electrochemical impedance spectroscopy

The Nyquist plots obtained for the corrosion of weld aged samples of maraging steel specimen in 1.0 M sulphuric acid in the presence of different concentrations of ATPI at 30 °C are shown in Fig. 3.60. Similar plots were obtained in other concentrations of sulphuric acid and also at other temperatures. The electrochemical parameters obtained from the EIS studies are summarized in Tables 3.77 to 3.81.

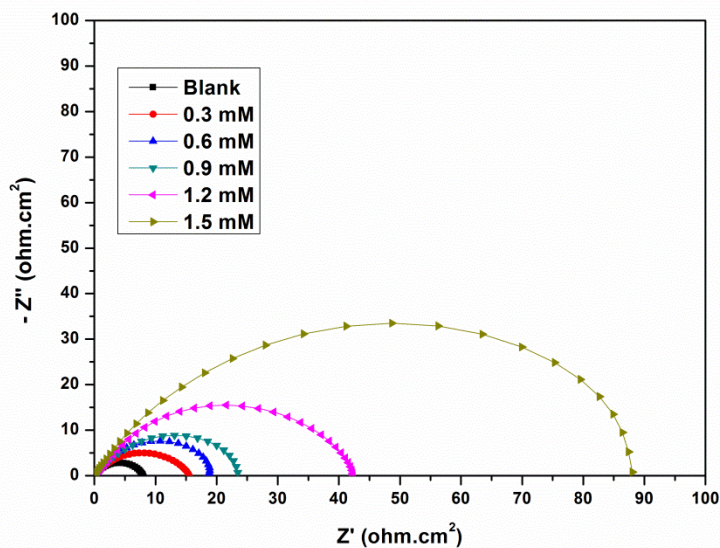


Fig. 3.60: Nyquist plots for the corrosion of weld aged maraging steel in 1.0 M sulphuric acid containing different concentrations of ATPI at 30 °C.

It is clear from Fig. 3.60 that the shapes of the impedance plots for the corrosion of the weld aged maraging steel in the presence of inhibitor are not substantially different from those of the uninhibited one. The presence of inhibitor increases the impedance but does not change other aspects of the behaviour. These results support the results of

polarization measurements. ATPI inhibits the corrosion primarily through its adsorption on the metal surface (Amin et al 2007) by active site blocking effect. The depressed semicircles in the impedance spectra are similar to the ones discussed earlier in Section 3.3.2 and the same explanations hold good in this case also. The equivalent circuit given in Fig. 3.20 (under Section 3.1.2) is used to fit the experimental data and to analyse the impedance spectra. The data in Tables 3.77 to 3.81 reveal that the charge transfer resistance (R_{ct}), increases with the increase in the inhibitor concentration, suggesting an hindrance to the charge transfer reaction (i.e., effective metal dissolution). The increase in R_{ct} values is due to the gradual replacement of water molecules by the adsorption of the inhibitor molecules on the metal surface to form an adherent film on the metal surface and thereby reducing the metal dissolution in the solution.

The data in Tables 3.77 to 3.81 also shows that the value of C_{dl} decreases with the increase in the concentration of ATPI. This decrease in C_{dl} could be due to the decrease in the local dielectric constant and/or an increase in the thickness of the electrical double layer as a result of the adsorption of ATPI molecules at the electrochemical interface and thereby thickening of the electrical double layer. ATPI inhibits the corrosion primarily through its adsorption and subsequent formation of a barrier film on the metal surface. This is in accordance with the observations of Tafel polarization measurements.

The Bode plots for the corrosion of the alloy in 1.0 M sulphuric acid containing different concentrations of ATPI at 30 °C are shown in Fig. 3.61. They are similar to the ones shown in Fig. 3.21. Hence the discussion regarding the Bode plot under the section 3.3.2 holds good for ATPI in sulphuric acid also.

A comparison of maximum attainable inhibition efficiencies by the Tafel method and EIS method, in the presence of ATPI for the corrosion of weld aged maraging steel in sulphuric acid solutions of different concentrations at 30 °C are listed in Table 3.82. It is evident from the table that the inhibition efficiency values obtained by the two methods are in good agreement. Similar levels of agreement were obtained at other temperatures also.

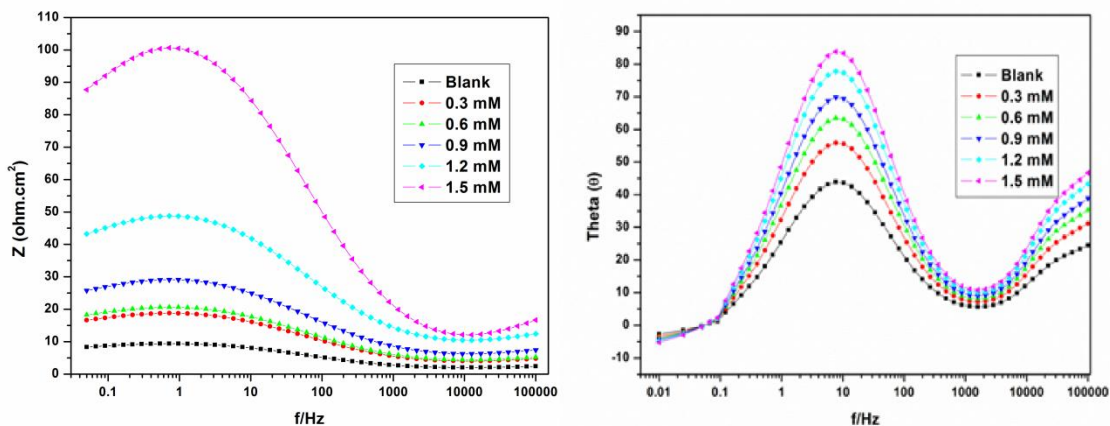


Fig. 3.61: Bode plots for the corrosion of weld aged maraging steel in 1.0 M sulphuric acid containing different concentrations of ATPI at 30 °C.

3.8.3 Effect of temperature

The Tafel and EIS results pertaining to different temperatures in different concentrations of sulphuric acid have already been listed in Tables 3.72 to 3.81. The results in Tables 3.72 to 3.81 indicate that the inhibition efficiency of ATPI decreases with increase in temperature. It is also seen from the data that the increase in solution temperature, does not alter the corrosion potential (E_{corr}), anodic Tafel slope (b_a) and cathodic Tafel slope (b_c) values significantly. This indicates that the increase in temperature does not change the mechanism of corrosion reaction (Poornima et al. 2011). The decrease in inhibition efficiency with the increase in temperature may be attributed to the higher dissolution rates of weld aged maraging steel at elevated temperature and also a possible desorption of adsorbed inhibitor due to the increased solution agitation resulting from higher rates of hydrogen gas evolution. The higher rate of hydrogen gas evolution may also reduce the ability of the inhibitor to be adsorbed on the metal surface. The decrease in inhibition efficiency with the increase in temperature is also suggestive of physisorption of the inhibitor molecules on the metal surface (Geetha et al. 2011).

The Arrhenius plots for the corrosion of weld aged maraging steel in the presence of different concentrations of ATPI in 1.0 M sulphuric acid are shown in Fig. 3.62. The enthalpy and entropy of activation for the dissolution of the alloy, (ΔH^\ddagger & ΔS^\ddagger) were calculated from transition state theory equation as discussed in the section 2.7. The plots of $\ln(v_{\text{corr}}/T)$ versus $1/T$ for the corrosion of weld aged samples of maraging steel in the presence of different concentrations of ATPI are shown in Fig. 3.63. The calculated values of activation parameters are recorded in Table 3.83.

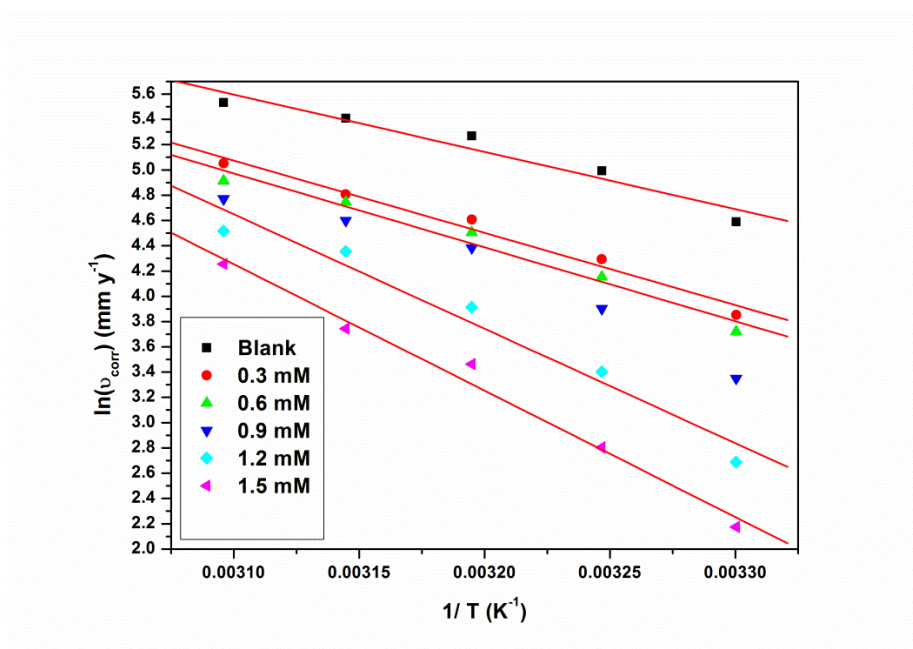


Fig. 3.62: Arrhenius plots for the corrosion of weld aged maraging steel in 1.0 M sulphuric acid containing different concentrations of ATPI.

According to the activation energy (E_a) values presented in the Table 3.83, E_a for the dissolution of specimen is greater in the presence of inhibitor than in the absence of inhibitor in the sulphuric acid medium. The extent of increase is proportional to the inhibitor concentration, indicating that the energy barrier for the corrosion reaction increases with the increase in ATPI concentration. The increase in the apparent activation energy E_a may be interpreted as due to the physical adsorption (Sherbini 1999) of the inhibitor, which results in the increase in surface coverage with the increase in the

concentration of the inhibitor. The values of entropy of activation in the absence and presence of inhibitor are large and negative. This implies that the activated complex in the rate determining step represents an association rather than dissociation, resulting in a decrease in randomness on going from the reactants to the activated complex (Marsh 1988, Gomma and Wahdan 1995).

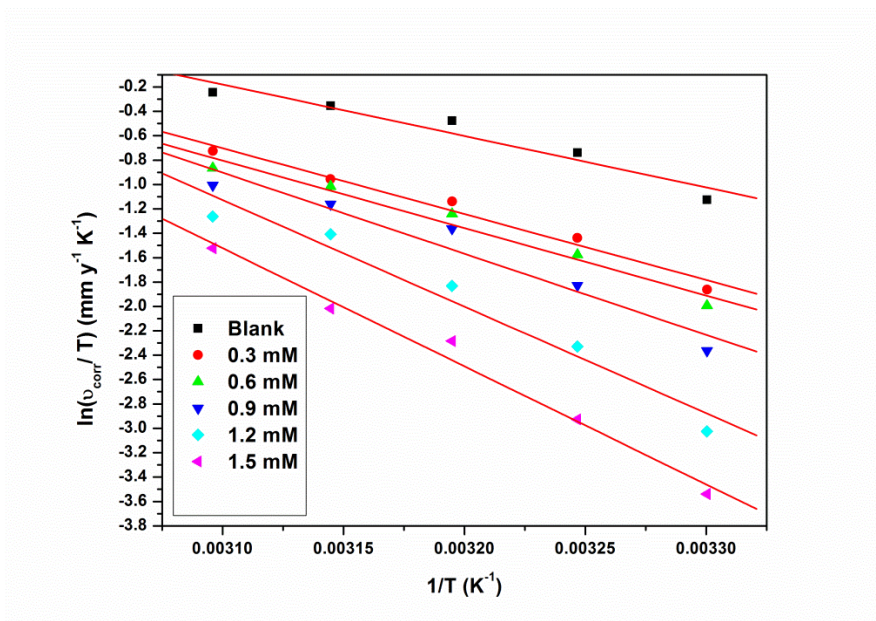


Fig. 3.63: Plots of $\ln(v_{\text{corr}}/T)$ versus $1/T$ for the corrosion of weld aged maraging steel in 1.0 M sulphuric acid containing different concentrations of ATPI.

3.8.4 Effect of sulphuric acid concentration

It is evident from both polarization and EIS experimental results that, for a particular concentration of inhibitor, the inhibition efficiency decreases with the increase in hydrochloric acid concentration. The maximum inhibition efficiency is observed in 0.1 M solution of sulphuric acid.

3.8.5 Adsorption isotherms

Attempts were made to fit the degree of surface coverage (θ) values obtained for weld aged maraging steel specimen in different concentrations of sulphuric acid in the presence of different concentrations of ATPI to various isotherms including Langmuir, Temkin, Frumkin and Flory - Huggins isotherms. By far the best fit was obtained with the modified Langmuir adsorption isotherm. The plots of (C_{inh}/θ) vs C_{inh} gives a straight line with intercept $(1/K_{ads})$. The Langmuir adsorption isotherm plots for the weld aged maraging steel in 1.0 M sulphuric acid in the presence of different concentrations of inhibitor are shown in Fig. 3.64.

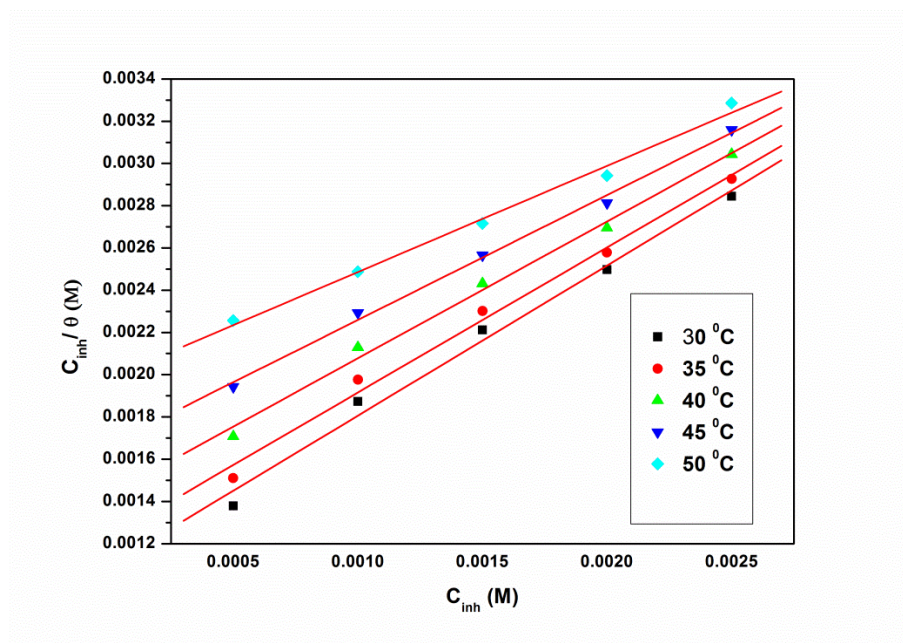


Fig. 3.64: Langmuir adsorption isotherms for the adsorption of ATPI on weld aged maraging steel in 1.0 M sulphuric acid at different temperatures.

The correlation coefficient (R^2) was used to choose the isotherm that best fits the experimental data (Bentiss et al. 2005). The linear regression coefficients are close to unity and the slopes of straight lines are nearly unity, suggesting that the adsorption of ATPI obeys Langmuir's adsorption isotherm and there is negligible interaction between

the adsorbed molecules (Li et al. 2008). The high value of K_{ads} for the studied inhibitor indicates strong and spontaneous adsorption of inhibitor on the alloy surface. The calculated values of thermodynamic parameters are listed in Tables 3.84.

The negative values of ΔG_{ads}^0 are characteristic feature of strong spontaneous adsorption for the studied compounds. Generally, the standard free energy values of -20 kJ mol^{-1} or less negative are associated with an electrostatic interaction between charged molecules and charged metal surface, resulting in physisorption and those of -40 kJ mol^{-1} or more negative involve charge sharing or transfer from the inhibitor molecules to the metal surface to form a coordinate covalent bond, resulting in chemisorption (Hosseini et al. 2003). The ΔG_{ads}^0 values obtained for the adsorption of ATPI on weld aged specimen of maraging steel at all the studied concentrations of sulphuric acid are in the range of -30.21 to $36.44 \text{ kJ mol}^{-1}$. These values predict both physical and chemical adsorption of the inhibitor (Singh and Quraishi 2010).

The values of ΔH_{ads}^0 are less negative than $-41.86 \text{ kJ mol}^{-1}$, indicating the adsorption of ATPI on the alloy surface to be physisorption. From the ΔG_{ads}^0 , ΔH_{ads}^0 values and decreasing inhibition efficiency trend with the temperature it can be concluded that the adsorption is mixed type, being predominantly physisorption. The ΔS_{ads}^0 value is large and negative; indicating that decrease in disordering takes place on going from the reactant to the alloy adsorbed species.

3.8.6 Mechanism of corrosion inhibition

To understand the mechanism of inhibition and the effect of inhibitor in aggressive acidic environment, some knowledge of interaction between the protective compound and the metal surface is required. The adsorption mechanism for a given inhibitor depends on factors, such as the nature of the metal, the corrosive medium, the pH, and the concentration of the inhibitor as well as the functional groups present in its molecule, since different groups are adsorbed to different extents. The corrosion inhibition mechanism of ATPI in sulphuric acid solution can be explained as follows: In

aqueous acidic solution, these inhibitors exist partly in the form of protonated species and partly as neutral molecules. Generally two modes of adsorption could be considered. It is well known that steel surface bears positive charge in acid solutions (Ahamad et al. 2010, Mu et al. 2004). In highly acidic medium the metal surface is positively charged. This would cause the adsorption of negatively charged sulphate ions on the metal surface, making metal surface negatively charged. The protonated ATPI molecule can electrochemically interact with the negatively charged sulphate ions, that adsorbed on the metal resulting in physisorption. The neutral inhibitor molecules may occupy the vacant adsorption sites on the metal surface through the chemisorption mode, involving the displacement of water molecules from the metal surface and sharing of electrons between the hetero atoms like nitrogen and sulphur with iron or by donor acceptor interactions between π electrons of the aromatic ring and vacant d orbitals of iron providing another mode of protection (Satpati and Ravindran 2008, Ahamad et al 2010).

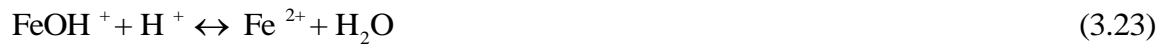
According to the mechanism for the dissolution of iron in acidic sulphate solution initially proposed by Bockris et al. 2000 and Obot et al. 2010, iron electro dissolution in acidic sulphate solution depends primarily on the adsorbed intermediate as follows:



The cathodic hydrogen evolution follows the steps



The following mechanism involving two adsorbed intermediates to account for the retardation of Fe anodic dissolution in the presence of an inhibitor:



where M represents the inhibitor species. According to the above detailed mechanism, displacement of some adsorbed water molecules on the metal surface by inhibitor species to yield the adsorbed intermediate FeM_{ads} reduces the amount of the species $\text{FeOH}_{\text{ads}}^-$ available for the rate determining steps and consequently retards the anodic dissolution of iron.

Since the adsorption of ATPI on the alloy surface is predominantly physisorption, the adsorption of protonated ATPI is the predominant process. The increase in inhibition efficiency with the increase in the ATPI concentration is in accordance with the mechanism.

3.8.7 SEM/EDS studies

Fig. 3.65 (a) represents SEM image of the corroded weld aged maraging steel sample. The corroded surface shows detachment of particles from the surface. The corrosion of the alloy may be predominantly attributed to the inter-granular corrosion assisted by the galvanic effect between the precipitates and the matrix along the grain

boundaries. Fig. 3.65 (b) represents SEM image of weld aged maraging steel after the corrosion tests in a medium of 1.0 M sulphuric acid containing 1.5 mM of ATPI. The image clearly shows a smooth surface due to the adsorbed layer of inhibitor molecules on the alloy surface, thus protecting the metal from corrosion.

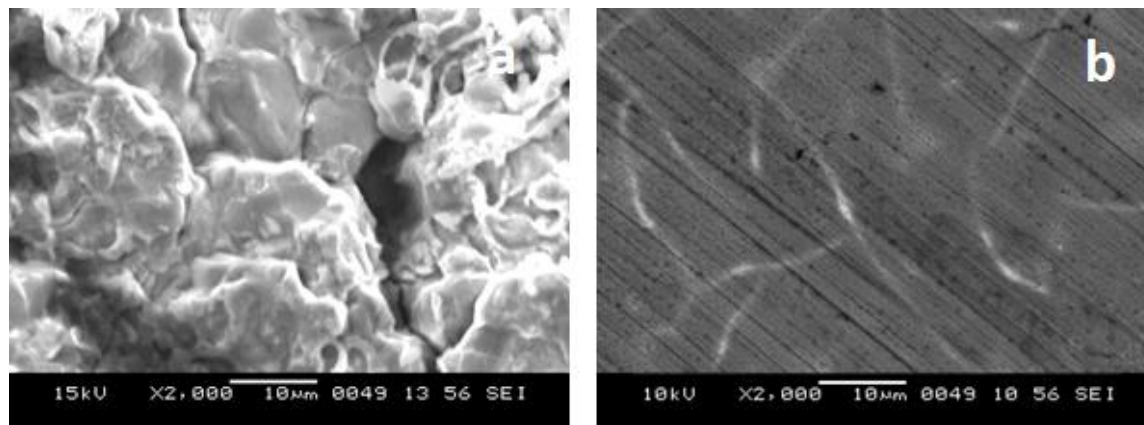


Fig. 3.65: SEM images of the weld aged maraging steel after immersion in 1.0 M sulphuric a) in the absence and b) in the presence of ATPI.

The EDS profiles of the corroded surface of the alloy in the absence and presence of ATPI are shown in Fig. 3.66 (a) and 3.66 (b), respectively. The atomic percentages of the elements found in the EDS profile for corroded metal surface were 17.22% Fe, 6.74 Ni, 2.75% Mo, 58.21% O, 3.51% S and 2.24 % Co and indicated the presence of iron oxide on the surface of alloy. The atomic percentages of the elements found in the EDS profile for inhibited metal surface were 31.5 % Fe, 5.28% S, 4.9% Ni, 4.16% Mo, 22.3 % O, 5.2% N, 3.9% Co, and 23.71 % C and indicated the formation of inhibitor film on the surface of the alloy.

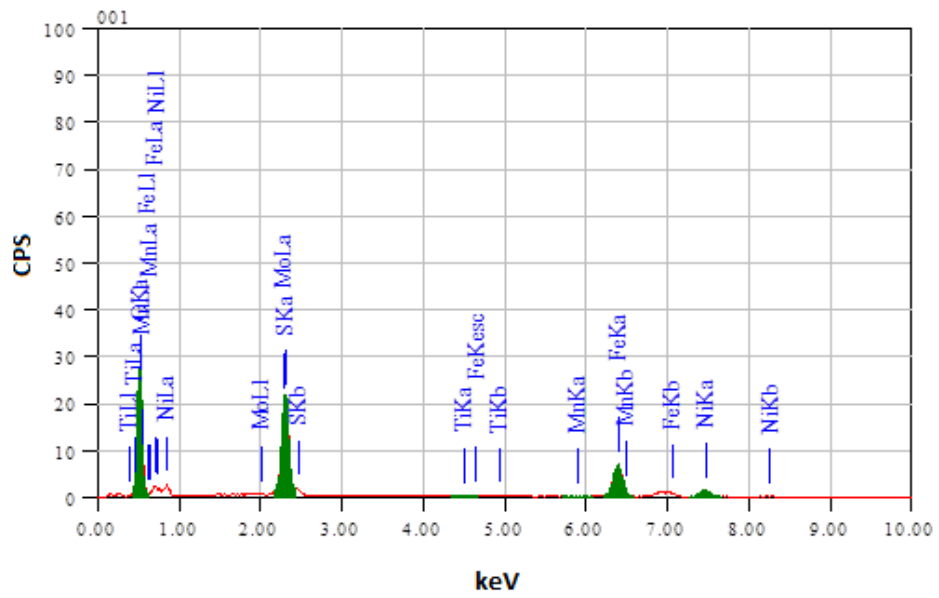


Fig. 3.66 (a): EDS spectra of the weld aged maraging steel after immersion in 1.0 M sulphuric in the absence of ATPI.

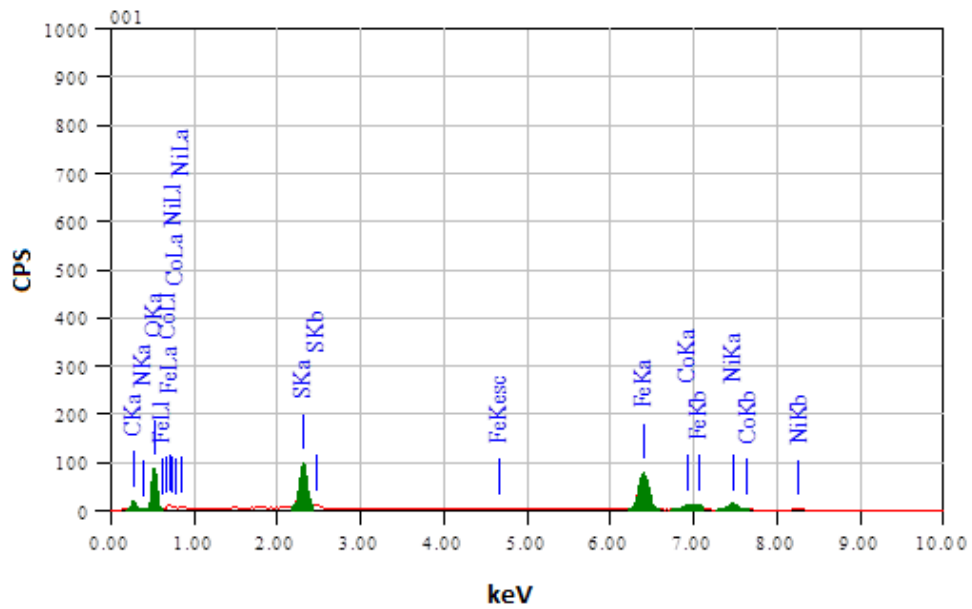


Fig. 3.66 (b): EDS spectra of the weld aged maraging steel after immersion in 1.0 M sulphuric in the presence of ATPI.

Table 3.72: Results of potentiodynamic polarization studies for the corrosion of weld aged maraging steel in 0.1 M sulphuric acid containing different concentrations of ATPI.

Temperature (°C)	Conc. of inhibitor (mM)	E_{corr} (mV /SCE)	b_a (mV dec ⁻¹)	$-b_c$ (mV dec ⁻¹)	i_{corr} (mA cm ⁻²)	v_{corr} (mm y ⁻¹)	η (%)
30	Blank	-371±2	221±2	266±1	0.78±0.03	8.99±0.31	
	0.2	-367±3	224±3	263±1	0.32±0.02	3.69±0.22	58.9
	0.4	-369±3	218±1	265±2	0.28±0.02	3.22±0.17	64.1
	0.6	-364±2	215±2	258±3	0.18±0.01	2.07±0.11	76.9
	0.8	-362±1	211±1	254±1	0.05±0.02	0.57±0.18	93.5
	1.0	-357±1	208±2	250±3	0.02±0.01	0.23±0.13	97.4
	35	Blank	-368±3	257±1	283±1	1.27±0.01	14.64±0.12
0.2		-371±2	254±1	279±3	0.56±0.02	6.45±0.21	55.9
0.4		-366±3	251±3	275±1	0.49±0.02	5.65±0.24	61.4
0.6		-362±3	248±1	273±3	0.35±0.01	4.03±0.14	72.4
0.8		-359±1	245±3	268±1	0.15±0.02	1.73±0.18	88.1
1.0		-355±1	241±3	266±1	0.09±0.02	1.03±0.21	93.7
40		Blank	-365±1	289±3	296±3	1.99±0.21	22.95±2.27
	0.2	-363±1	286±1	298±1	1.05±0.11	12.11±1.25	47.2
	0.4	-359±3	281±3	292±2	0.92±0.01	10.62±0.14	53.7
	0.6	-356±2	283±2	287±2	0.67±0.03	7.72±0.29	66.8
	0.8	-352±2	278±2	285±3	0.37±0.02	4.26±0.24	81.4
	1.0	-350±3	275±1	279±3	0.26±0.03	2.99±0.25	86.9
	45	Blank	-362±2	295±2	317±1	2.21±0.23	25.48±2.26
0.2		-360±1	291±2	311±1	1.30±0.03	14.99±0.26	41.1
0.4		-358±1	289±2	315±3	1.15±0.02	13.26±0.20	47.9
0.6		-355±1	285±2	309±2	0.88±0.02	10.14±0.21	60.1
0.8		-351±2	282±2	304±1	0.59±0.02	6.80±0.17	73.3
1.0		-349±3	279±1	298±3	0.43±0.03	4.95±0.28	80.5
50		Blank	-359±2	298±2	321±1	2.47±0.09	28.48±1.18
	0.2	-355±3	296±2	318±2	1.56±0.06	17.99±0.70	36.8
	0.4	-352±1	295±3	315±2	1.42±0.02	16.37±0.18	42.5
	0.6	-349±2	292±3	311±3	1.10±0.02	12.68±0.19	55.5
	0.8	-344±1	288±1	309±3	0.77±0.01	8.88±0.14	68.8
	1.0	-341±1	283±1	305±2	0.60±0.03	6.92±0.26	75.7

Table 3.73: Results of potentiodynamic polarization studies for the corrosion of weld aged maraging steel in 0.5 M sulphuric acid containing different concentrations of ATPI.

Temperature (°C)	Conc. of inhibitor (mM)	E_{corr} (mV /SCE)	b_a (mV dec ⁻¹)	$-b_c$ (mV dec ⁻¹)	i_{corr} (mA cm ⁻²)	v_{corr} (mm y ⁻¹)	η (%)
30	Blank	-356±2	235±1	268±2	1.80±0.17	20.71±1.79	
	0.2	-352±1	232±1	265±3	0.81±0.06	8.13±0.64	55.0
	0.4	-348±3	218±1	263±2	0.70±0.09	7.03±0.94	61.1
	0.6	-343±1	215±1	259±2	0.47±0.09	4.72±0.94	73.8
	0.8	-339±1	212±3	257±1	0.23±0.10	2.31±0.98	87.3
	1.0	-341±2	208±3	253±3	0.08±0.02	0.80±0.23	95.5
	35	Blank	-353±2	257±1	276±1	2.41±0.19	27.73±2.21
0.2		-356±3	255±2	272±2	1.15±0.09	11.55±0.90	52.2
0.4		-352±3	249±3	269±3	1.01±0.08	10.01±0.78	58.5
0.6		-349±1	244±1	266±1	0.76±0.06	7.63±0.60	68.4
0.8		-346±2	241±1	263±3	0.45±0.05	4.51±0.51	81.3
1.0		-342±2	237±3	259±1	0.18±0.06	1.80±0.58	92.5
40		Blank	-350±1	279±1	288±1	3.83±0.35	44.07±3.84
	0.2	-352±1	271±2	285±2	1.90±0.07	19.08±0.67	50.1
	0.4	-349±3	268±2	281±3	1.72±0.07	17.27±0.66	55.6
	0.6	-345±3	265±2	277±3	1.47±0.07	14.76±0.75	61.7
	0.8	-347±2	261±1	273±1	0.91±0.06	9.14±0.61	76.5
	1.0	-341±2	256±1	269±1	0.39±0.08	4.07±0.84	85.9
	45	Blank	-348±2	296±2	297±3	4.24±0.35	46.71±3.87
0.2		-349±2	293±3	293±3	4.01±0.26	42.14±2.89	47.6
0.4		-351±3	289±2	289±2	2.11±0.08	21.09±0.84	50.1
0.6		-347±2	286±1	286±1	1.94±0.07	19.08±0.70	57.6
0.8		-345±2	281±3	282±3	1.71±0.10	17.07±0.96	67.5
1.0		-342±2	276±1	279±1	0.54±0.10	5.42±0.88	79.5
50		Blank	-346±3	315±3	306±2	4.30±0.26	49.47±3.04
	0.2	-353±3	310±1	303±3	2.52±0.15	25.11±1.88	41.8
	0.4	-349±3	307±1	300±2	2.22±0.08	22.09±0.78	48.8
	0.6	-346±1	303±1	297±2	1.91±0.08	19.08±0.81	55.8
	0.8	-347±2	300±3	292±1	1.50±0.07	15.06±0.74	65.1
	1.0	-344±3	296±2	288±3	1.12±0.05	11.04±0.50	74.4

Table 3.74: Results of potentiodynamic polarization studies for the corrosion of weld aged maraging steel in 1.0 M sulphuric acid containing different concentrations of ATPI.

Temperature (°C)	Conc. of inhibitor (mM)	E_{corr} (mV /SCE)	b_a (mV dec ⁻¹)	$-b_c$ (mV dec ⁻¹)	i_{corr} (mA cm ⁻²)	v_{corr} (mm y ⁻¹)	η (%)
30	Blank	-323±2	247±1	301±3	8.56±0.38	98.41±3.85	
	0.3	-325±1	243±3	303±3	4.10±0.24	47.10±2.36	52.2
	0.6	-322±1	239±3	299±3	3.59±0.23	41.32±2.33	58.1
	0.9	-319±3	235±3	296±3	2.48±0.24	28.50±2.43	71.1
	1.2	-316±2	231±1	292±2	1.28±0.21	14.75±2.13	85.1
	1.5	-313±1	227±1	288±1	0.77±0.21	8.80±2.15	91.1
	35	Blank	-318±2	276±1	303±2	12.82±0.30	147.28±3.01
0.3		-315±1	278±3	302±1	6.36±0.28	73.18±2.76	50.4
0.6		-311±3	272±2	298±1	5.54±0.41	63.71±4.10	56.8
0.9		-313±2	269±3	295±2	4.31±0.29	49.50±2.95	66.4
1.2		-309±2	266±4	293±3	2.61±0.26	30.05±2.63	79.7
1.5		-305±2	262±2	289±3	1.44±0.18	16.50±2.10	88.8
40		Blank	-309±2	292±2	305±1	16.92±0.22	194.46±2.20
	0.3	-311±2	294±3	308±3	8.72±0.24	100.31±2.37	48.5
	0.6	-306±2	290±1	305±3	7.87±0.35	90.59±3.53	53.5
	0.9	-303±1	287±3	302±1	6.97±0.26	80.11±2.62	58.8
	1.2	-300±1	285±1	298±1	4.36±0.37	50.12±3.75	74.3
	1.5	-297±1	281±1	294±2	2.78±0.20	31.90±2.04	83.6
	45	Blank	-307±3	298±2	307±1	19.42±0.32	223.23±3.17
0.3		-305±2	295±3	305±2	10.63±0.36	122.31±3.56	45.3
0.6		-308±3	291±2	300±2	10.02±0.25	115.23±2.50	48.4
0.9		-303±1	288±1	297±2	8.65±0.31	99.56±3.15	55.5
1.2		-300±3	285±3	295±2	6.77±0.27	77.81±2.69	65.2
1.5		-298±1	281±3	292±1	3.68±0.18	42.30±1.76	81.1
50		Blank	-305±3	312±1	311±1	22.10±0.31	253.15±3.13
	0.3	-302±2	310±3	313±1	13.59±0.29	156.32±2.91	38.2
	0.6	-298±2	307±2	308±1	11.83±0.24	136.16±2.42	46.3
	0.9	-295±3	309±3	305±3	10.27±0.27	118.11±2.65	53.4
	1.2	-292±1	303±3	301±1	7.96±0.37	91.52±3.70	63.9
	1.5	-288±1	299±3	298±1	6.13±0.11	70.51±1.13	72.2

Table 3.75: Results of potentiodynamic polarization studies for the corrosion of weld aged maraging steel in 1.5 M sulphuric acid containing different concentrations of ATPI.

Temperature (°C)	Conc. of inhibitor (mM)	E_{corr} (mV /SCE)	b_a (mV dec ⁻¹)	$-b_c$ (mV dec ⁻¹)	i_{corr} (mA cm ⁻²)	v_{corr} (mm y ⁻¹)	η (%)
30	Blank	-295±3	252±2	260±1	17.02±0.28	195.54±2.79	
	0.4	-297±3	250±2	256±3	8.46±0.22	97.43±2.23	50.2
	0.8	-293±3	247±3	245±3	6.91±0.39	79.60±3.95	59.3
	1.2	-288±2	244±1	241±1	4.65±0.47	53.59±4.70	72.6
	1.6	-285±2	242±1	238±3	2.80±0.39	32.27±3.88	83.5
	2.0	-282±2	239±3	235±1	1.85±0.26	21.31±2.86	89.1
	35	Blank	-291±3	253±1	272±2	23.64±0.25	271.53±2.53
0.4		-288±3	255±3	270±2	12.15±0.36	139.83±3.63	48.5
0.8		-292±2	250±3	267±3	10.62±0.35	122.18±3.46	55.0
1.2		-285±2	248±2	263±2	8.40±0.34	96.66±3.45	64.4
1.6		-281±2	244±1	260±1	5.26±0.27	60.55±2.67	77.7
2.0		-279±3	241±3	258±3	3.30±0.23	38.01±2.27	86.1
40		Blank	-288±2	254±2	276±2	28.05±0.58	332.15±5.83
	0.4	-292±2	251±2	273±2	15.12±0.36	173.96±3.63	46.1
	0.8	-285±2	253±3	270±2	13.55±0.31	155.92±3.07	51.6
	1.2	-252±1	248±1	268±1	12.34±0.53	142.07±5.30	55.9
	1.6	-249±3	244±1	265±2	7.75±0.22	89.23±2.22	72.3
	2.0	-246±1	241±3	261±1	5.20±0.39	59.92±3.88	81.4
	45	Blank	-285±2	266±3	283±1	30.34±0.46	348.61±4.60
0.4		-281±3	263±1	279±3	17.24±0.57	198.35±5.73	43.1
0.8		-282±2	259±3	280±3	16.27±0.33	187.19±3.27	46.3
1.2		-277±3	255±1	276±3	14.24±0.25	163.83±2.53	53.3
1.6		-272±2	253±2	272±3	11.08±0.38	127.48±3.80	63.4
2.0		-269±2	249±2	269±3	6.21±0.23	71.44±2.31	79.5
50		Blank	-283±2	272±3	296±1	33.05±0.35	379.67±3.54
	0.4	-286±3	275±3	293±1	20.88±0.29	240.33±2.94	36.7
	0.8	-280±3	269±2	290±2	18.48±0.54	212.62±5.37	44.3
	1.2	-278±1	266±3	292±1	16.23±0.31	186.80±3.13	50.8
	1.6	-275±1	262±2	288±2	12.63±0.60	145.41±5.98	61.7
	2.0	-271±1	259±3	285±3	9.86±0.20	113.52±2.00	70.1

Table 3.76: Results of potentiodynamic polarization studies for the corrosion of weld aged maraging steel in 2.0 M sulphuric acid containing different concentrations of ATPI.

Temperature (°C)	Conc. of inhibitor (mM)	E_{corr} (mV /SCE)	b_a (mV dec ⁻¹)	$-b_c$ (mV dec ⁻¹)	i_{corr} (mA cm ⁻²)	v_{corr} (mm y ⁻¹)	η (%)
30	Blank	-281±3	223±3	251±3	20.31±0.39	233.51±3.87	
	0.5	-283±2	219±2	247±3	10.70±0.23	123.11±2.27	47.3
	1.0	-278±3	226±1	249±1	9.11±0.38	104.82±3.78	55.1
	1.5	-275±1	212±3	244±1	6.39±0.20	73.52±2.96	68.5
	2.0	-272±3	210±3	240±2	4.22±0.24	48.55±2.38	79.2
	2.5	-269±2	217±1	238±1	2.84±0.40	32.68±3.96	86.0
	35	Blank	-279±2	245±2	263±2	27.63±0.44	317.55±4.42
0.5		-281±2	241±1	260±3	15.21±0.48	175.00±4.80	44.9
1.0		-277±1	237±3	258±2	13.25±0.24	152.45±2.42	52
1.5		-274±2	234±1	255±1	10.54±0.31	121.27±3.06	61.8
2.0		-271±1	231±1	252±1	7.01±0.59	80.65±5.87	74.6
2.5		-268±1	228±1	249±3	4.77±0.38	54.88±3.78	82.7
40		Blank	-278±1	269±2	274±1	35.00±0.48	402.63±4.83
	0.5	-281±3	264±2	276±3	19.78±0.33	227.58±3.32	43.5
	1.0	-275±2	267±1	271±1	18.41±0.41	211.82±4.08	47.4
	1.5	-273±3	261±1	268±1	16.66±0.48	191.68±4.80	52.4
	2.0	-268±1	259±2	265±3	10.99±0.38	126.45±3.78	68.6
	2.5	-266±2	255±2	262±2	7.63±0.30	87.79±2.95	78.2
	45	Blank	-275±2	281±3	288±2	40.72±0.26	468.28±2.59
0.5		-272±2	277±1	285±3	24.79±0.35	285.22±3.53	39.1
1.0		-269±4	279±3	282±3	22.79±0.33	262.21±3.31	44.1
1.5		-266±1	275±4	279±3	20.68±0.22	237.93±2.17	49.2
2.0		-263±2	272±3	276±1	16.73±0.20	192.49±2.04	58.9
2.5		-259±3	269±2	273±2	9.24±0.38	106.31±3.82	77.3
50		Blank	-273±1	301±3	302±2	45.24±0.58	520.05±5.81
	0.5	-275±2	303±3	300±1	30.28±0.56	348.39±5.63	33.2
	1.0	-272±2	297±1	298±3	26.89±0.37	309.38±3.70	40.5
	1.5	-269±1	293±3	295±2	23.78±0.23	273.60±2.30	47.4
	2.0	-266±1	288±1	292±1	19.33±0.45	222.06±4.51	57.3
	2.5	-263±3	285±1	289±2	14.78±0.30	170.05±3.00	67.3

Table 3.77: EIS data for the corrosion of weld aged maraging steel in 0.1 M sulphuric acid containing different concentrations of ATPI.

Temperature (°C)	Conc. of inhibitor (mM)	R_{ct} (ohm. cm ²)	C_{dl} (mF cm ⁻²)	R_{pf} (ohm. cm ²)	C_{pf} (mF cm ⁻²)	η (%)
30	Blank	74.66±3.24	21.01±3.15			
	0.2	169.68±2.66	13.05±3.15	12.36±2.12	3.70±1.81	56.4
	0.4	191.93±2.72	9.18±2.83	13.73±2.73	2.61±1.49	61.1
	0.6	298.64±2.78	6.23±3.21	20.29±2.93	1.78±0.62	75.1
	0.8	1036.94±3.21	2.50±3.10	65.72±3.54	0.74±0.27	92.8
	1.0	2333.13±5.59	9.60±2.79	145.46±3.61	0.53±0.03	96.8
	35	Blank	51.17±3.47	26.57±3.99		
0.2		108.87±2.83	14.46±2.69	8.62±3.91	4.09±2.69	53.0
0.4		125.72±2.26	11.80±2.80	9.65±3.39	3.35±1.79	59.3
0.6		165.06±2.02	8.32±3.44	12.07±2.59	2.37±1.09	69.3
0.8		368.13±3.83	3.78±3.60	24.57±3.11	1.10±0.23	86.1
1.0		581.48±6.70	2.11±2.98	37.69±2.60	0.63±0.29	91.2
40		Blank	35.45±2.68	32.14±2.96		
	0.2	65.29±3.71	19.65±2.39	5.94±3.52	5.55±2.46	45.7
	0.4	73.85±3.56	17.41±3.94	6.46±2.57	4.92±1.58	52.1
	0.6	97.93±3.91	13.55±2.09	7.94±3.29	3.84±1.55	63.8
	0.8	168.81±2.75	7.45±2.27	12.31±2.27	2.13±0.84	79.2
	1.0	211.01±4.00	5.98±2.16	14.90±1.11	1.71±0.67	83.2
	45	Blank	33.36±2.54	36.48±2.87		
0.2		55.79±3.68	22.85±2.91	5.35±3.65	6.45±2.03	40.2
0.4		61.89±3.04	19.77±2.58	5.73±2.33	5.59±0.35	46.1
0.6		79.81±2.05	16.25±3.79	6.83±2.53	4.60±0.23	58.2
0.8		109.02±3.09	12.15±3.08	8.63±2.94	3.45±0.92	69.4
1.0		143.79±3.21	8.44±2.45	10.77±2.95	2.41±0.67	76.8
50		Blank	30.19±2.64	41.49±2.19		
	0.2	48.30±3.14	26.52±2.10	4.89±3.71	8.52±2.14	37.5
	0.4	51.17±2.14	23.21±3.29	5.07±2.22	6.21±1.16	41.0
	0.6	63.69±3.87	18.52±3.11	5.84±2.33	4.52±0.69	52.6
	0.8	85.52±3.40	13.25±3.10	7.18±3.95	4.25±0.96	64.7
	1.0	113.07±2.83	12.31±2.87	8.88±3.56	3.31±0.62	73.3

Table 3.78: EIS data for the corrosion of weld aged maraging steel in 0.5 M sulphuric acid containing different concentrations of ATPI.

Temperature (°C)	Conc. of inhibitor (mM)	R_{ct} (ohm. cm ²)	C_{dl} (mF cm ⁻²)	R_{pf} (ohm. cm ²)	C_{pf} (mF cm ⁻²)	η (%)
30	Blank	33.56±1.62	40.12±2.65			
	0.2	76.10±2.37	19.22±2.48	6.60±1.46	5.43±1.70	55.9
	0.4	85.61±4.59	16.91±3.51	7.19±1.28	4.78±1.53	60.8
	0.6	126.17±2.61	11.74±3.00	9.68±2.12	3.33±1.36	73.4
	0.8	262.19±3.30	6.30±2.65	18.05±1.62	1.80±0.27	87.2
	1.0	729.57±3.77	2.86±1.41	46.81±2.24	0.84±0.16	95.4
	35	Blank	26.64±1.82	65.92±2.91		
0.2		55.50±3.34	34.58±3.86	5.50±1.86	9.74±1.66	52.1
0.4		69.74±2.39	29.26±3.12	9.74±1.67	8.25±2.31	61.8
0.6		88.21±4.18	26.02±2.06	8.21±1.59	7.34±1.57	69.8
0.8		138.03±3.64	22.64±3.57	13.03±1.57	6.39±2.53	80.7
1.0		345.97±4.88	17.92±2.49	35.97±2.99	5.07±2.52	92.3
40		Blank	17.85±3.14	109.77±2.90		
	0.2	33.62±2.56	59.28±3.84	3.99±1.31	16.68±1.06	46.9
	0.4	39.49±3.40	50.60±2.13	4.35±2.62	14.24±2.37	54.8
	0.6	47.35±2.01	42.37±3.67	4.83±2.33	11.93±2.32	62.3
	0.8	71.69±3.20	28.32±3.99	6.33±1.51	7.99±1.74	75.1
	1.0	117.43±4.24	19.68±3.41	9.14±1.54	5.56±2.51	84.8
	45	Blank	17.84±1.29	125.60±3.51		
0.2		36.19±4.34	62.62±2.50	3.15±1.58	17.61±2.70	50.7
0.4		37.01±3.51	61.25±3.83	4.20±1.10	17.23±2.30	51.8
0.6		41.68±4.81	54.49±3.89	4.48±1.91	15.33±1.80	57.2
0.8		47.83±3.22	47.61±3.22	4.86±2.04	13.40±1.25	62.7
1.0		78.59±2.16	29.37±2.71	6.75±2.65	8.28±2.83	77.3
50		Blank	17.42±2.17	158.27±3.51		
	0.2	29.83±3.98	93.29±2.18	3.05±2.85	26.22±2.44	41.6
	0.4	35.41±4.70	78.72±3.54	4.10±1.21	22.13±1.52	50.8
	0.6	39.23±4.32	71.14±2.88	4.33±2.82	20.00±1.65	55.6
	0.8	49.35±3.32	56.77±2.07	4.96±2.62	15.97±1.26	64.7
	1.0	64.04±4.48	43.97±3.13	5.86±2.83	12.38±1.85	72.8

Table 3.79: EIS data for the corrosion of weld aged maraging steel in 1.0 M sulphuric acid containing different concentrations of ATPI.

Temperature (°C)	Conc. of inhibitor (mM)	R_{ct} (ohm. cm ²)	C_{dl} (mF cm ⁻²)	R_{pf} (ohm. cm ²)	C_{pf} (mF cm ⁻²)	η (%)
30	Blank	7.09±2.45	11.00±2.79			
	0.3	15.25±2.02	5.11±2.11	2.86±0.31	1.47±0.68	53.5
	0.6	16.30±2.04	4.01±1.06	2.92±1.08	1.16±0.54	56.5
	0.9	22.80±2.91	3.26±2.79	3.32±1.54	0.95±0.84	68.9
	1.2	42.71±2.36	1.53±1.16	4.55±1.88	0.47±0.65	83.4
	1.5	88.63±2.72	0.68±0.13	7.37±1.36	0.23±0.09	92.1
35	Blank	5.05±2.38	11.83±1.86			
	0.3	9.75±1.22	5.14±2.50	2.52±0.51	1.48±0.78	48.2
	0.6	11.22±1.37	4.78±1.31	2.61±1.14	1.38±0.51	55.0
	0.9	14.07±1.03	3.46±1.26	2.78±1.07	1.01±0.72	64.1
	1.2	22.44±2.77	1.87±0.36	3.30±1.17	0.56±0.17	77.5
	1.5	36.86±2.08	0.83±0.21	4.19±1.56	0.27±0.04	86.3
40	Blank	3.95±1.35	12.37±1.20			
	0.3	7.31±1.41	5.69±2.31	2.37±0.90	1.63±0.53	46.0
	0.6	8.16±1.54	5.00±2.18	2.42±1.11	1.44±0.31	51.6
	0.9	8.94±2.16	4.48±1.45	2.47±1.44	1.29±0.56	55.8
	1.2	14.31±1.12	2.42±1.93	2.80±1.14	0.72±0.17	72.4
	1.5	19.85±1.83	1.47±0.70	3.14±1.26	0.45±0.09	80.1
45	Blank	3.49±2.08	15.26±1.69			
	0.3	6.14±1.80	7.68±2.77	2.30±0.76	2.19±0.58	43.2
	0.6	6.46±2.73	9.26±2.96	2.32±1.83	2.64±0.84	46.3
	0.9	7.52±2.05	7.81±1.75	2.38±1.49	2.23±0.31	53.6
	1.2	9.41±1.11	6.05±1.27	2.50±1.95	1.73±0.22	62.9
	1.5	16.86±1.22	2.94±1.07	2.96±1.18	0.86±0.13	79.3
50	Blank	3.15±1.64	18.08±2.38			
	0.3	4.96±1.83	10.49±1.73	2.22±0.11	2.98±1.78	36.5
	0.6	5.67±2.95	13.67±2.56	2.27±1.46	3.87±0.84	44.4
	0.9	6.43±2.80	11.92±2.80	2.31±1.65	3.38±0.84	51.3
	1.2	8.20±1.06	9.13±1.19	2.42±1.91	2.60±0.61	61.6
	1.5	10.26±1.20	7.10±2.10	2.55±1.08	2.03±0.26	69.3

Table 3.80: EIS data for the corrosion of weld aged maraging steel in 1.5 M sulphuric acid containing different concentrations of ATPI.

Temperature (°C)	Conc. of inhibitor (mM)	R_{ct} (ohm. cm ²)	C_{dl} (mF cm ⁻²)	R_{pf} (ohm. cm ²)	C_{pf} (mF cm ⁻²)	η (%)
30	Blank	3.34±0.50	13.71±2.86			
	0.3	6.82±1.63	9.28±1.59	2.34±0.36	0.40±0.16	51.3
	0.6	7.21±1.94	7.77±0.50	2.36±1.88	2.22±0.93	53.7
	0.9	9.85±2.62	7.36±0.21	2.53±1.04	2.10±0.45	66.1
	1.2	16.95±1.74	5.45±1.56	2.96±1.14	1.57±0.25	80.3
	1.5	33.40±2.73	3.26±0.48	3.97±1.97	0.95±0.21	90.2
35	Blank	2.46±1.85	14.52±2.56			
	0.3	4.57±1.04	8.52±2.08	2.20±1.22	2.43±0.59	46.2
	0.6	5.06±2.84	7.71±1.34	2.23±1.18	2.20±0.66	51.4
	0.9	7.13±1.64	5.54±2.01	2.36±1.27	1.59±0.26	65.5
	1.2	11.34±2.42	3.57±2.54	2.62±1.34	1.04±0.35	78.3
	1.5	16.29±2.72	2.55±1.12	2.92±1.19	0.75±0.11	84.9
40	Blank	2.09±1.24	16.09±1.33			
	0.3	3.79±1.97	10.19±1.01	2.15±1.10	2.90±0.59	44.8
	0.6	4.14±1.85	9.35±2.39	2.17±1.37	2.66±1.38	49.5
	0.9	4.53±2.23	8.57±2.12	2.20±1.88	2.44±0.15	53.9
	1.2	6.97±2.96	5.65±1.13	2.35±1.33	1.62±0.10	70.2
	1.5	9.33±1.36	4.27±1.06	2.49±1.06	1.23±0.35	77.6
45	Blank	2.01±0.98	18.30±1.15			
	0.3	3.38±1.37	12.19±2.26	2.13±1.07	3.46±1.05	40.6
	0.6	3.62±1.75	11.40±2.01	2.14±1.49	3.24±0.91	44.5
	0.9	4.06±1.81	10.19±1.74	2.17±1.69	2.90±0.74	50.5
	1.2	5.06±1.56	8.22±1.15	2.23±1.50	2.34±1.04	60.3
	1.5	7.44±1.39	5.66±1.33	2.38±1.69	1.62±0.99	73.1
50	Blank	1.90±0.39	21.47±2.18			
	0.3	2.92±0.89	16.39±2.89	2.10±1.82	4.64±1.06	35.1
	0.6	3.30±2.46	14.53±1.30	2.12±1.48	4.11±1.41	42.5
	0.9	3.58±2.26	13.41±1.01	2.14±1.99	3.80±0.58	47.3
	1.2	4.55±2.94	10.60±2.06	2.20±1.51	3.01±0.57	58.2
	1.5	5.64±2.02	8.59±1.84	2.27±1.74	2.45±0.40	66.3

Table 3.81: EIS data for the corrosion of weld aged maraging steel in 2.0 M sulphuric acid containing different concentrations of ATPI.

Temperature (°C)	Conc. of inhibitor (mM)	R _{ct} (ohm. cm ²)	C _{dl} (mF cm ⁻²)	R _{pf} (ohm. cm ²)	C _{pf} (mF cm ⁻²)	η (%)
30	Blank	2.58±1.31	16.45±2.15			
	0.5	4.98±0.94	7.61±1.97	2.23±0.68	2.17±1.38	48.2
	1.0	5.21±0.53	7.23±2.19	2.24±0.97	2.07±0.81	50.5
	1.5	7.27±0.87	4.93±1.55	2.37±1.15	1.42±0.61	64.5
	2.0	11.62±1.39	2.75±1.40	2.63±1.33	0.81±0.24	77.8
	2.5	22.05±1.59	1.03±0.16	3.28±0.99	0.33±0.07	88.3
35	Blank	2.04±1.16	17.21±2.27			
	0.5	3.64±0.69	8.59±2.33	2.14±0.87	2.45±1.03	43.9
	1.0	3.95±1.16	7.83±1.93	2.16±1.12	2.23±1.07	48.4
	1.5	5.54±1.10	5.33±1.35	2.26±1.08	1.53±0.53	63.2
	2.0	8.54±0.56	3.15±2.18	2.44±1.41	0.92±0.29	76.1
	2.5	11.72±0.76	2.05±1.56	2.64±0.92	0.61±0.22	82.6
40	Blank	1.72±0.78	19.56±1.58			
	0.5	2.96±0.79	9.26±1.88	2.10±0.68	2.64±0.89	41.9
	1.0	3.28±0.53	8.29±1.32	2.12±0.67	2.36±1.16	47.5
	1.5	3.48±1.35	7.76±1.96	2.13±1.30	2.21±1.01	50.6
	2.0	5.21±1.48	4.89±2.28	2.24±1.00	1.41±0.30	67.1
	2.5	6.94±1.10	3.45±1.57	2.35±0.58	1.00±0.04	75.2
45	Blank	1.55±0.53	23.82±2.18			
	0.5	2.50±1.35	14.18±1.66	2.07±1.12	4.02±0.77	38.0
	1.0	2.67±0.73	13.27±2.03	2.08±1.03	3.76±0.62	41.9
	1.5	2.99±0.72	11.74±1.12	2.10±0.77	3.33±0.79	48.1
	2.0	3.72±0.81	9.25±2.23	2.15±1.17	2.63±0.85	58.3
	2.5	5.27±0.52	6.27±0.17	2.24±0.78	1.80±0.14	70.6
50	Blank	1.48±1.33	26.00±1.80			
	0.5	2.22±0.71	16.44±1.07	2.06±0.56	4.65±0.99	33.3
	1.0	2.46±1.49	14.74±2.40	2.07±1.38	4.17±1.31	39.8
	1.5	2.64±0.50	13.67±1.31	2.08±1.05	3.87±0.57	43.9
	2.0	3.34±0.53	10.64±1.97	2.12±1.27	3.02±0.16	55.7
	2.5	4.02±0.60	8.69±1.24	2.17±0.73	2.48±0.12	63.2

Table 3.82: Comparison of maximum attainable inhibition efficiencies by the Tafel method and EIS method for the corrosion of weld aged maraging steel in sulphuric acid solutions of different concentrations in the presence of ATPI at 30 °C.

Molarity of sulphuric acid	Conc. of ATPI (mM)	η (%)	
		Tafel	EIS
0.1	1.0	97.4	96.8
0.5	1.0	95.5	95.4
1.0	1.5	91.2	92.0
1.5	2.0	89.1	90.0
2.0	2.5	86.0	88.3

Table 3.83: Activation parameters for the corrosion of weld aged maraging steel in sulphuric acid containing different concentrations of ATPI.

Molarity of sulphuric acid	Conc. of inhibitor (mM)	E_a ($\text{kJ}^{-1} \text{mol}^{-1}$)	ΔH^\ddagger ($\text{kJ}^{-1} \text{mol}^{-1}$)	ΔS^\ddagger ($\text{J mol}^{-1} \text{K}^{-1}$)
0.1	0.0	44.31	43.16	-88.32
	0.2	50.19	50.02	-81.11
	0.4	67.37	67.14	-72.10
	0.6	80.48	80.21	-54.07
	1.8	86.81	86.52	-45.06
	2.0	99.47	99.13	-29.74
0.5	0.0	35.50	37.48	-111.52
	0.2	40.21	42.45	-102.42
	0.4	53.97	56.98	-91.04
	0.6	64.48	68.08	-68.28
	1.8	69.55	73.43	-56.90
	2.0	79.69	84.14	-37.55
1.0	0.0	32.79	28.11	-144.08
	0.3	37.14	31.84	-132.32
	0.6	49.85	42.74	-117.62
	0.9	59.56	51.06	-88.21
	1.2	64.24	55.07	-73.51
	1.5	73.61	63.10	-48.52
1.5	0.0	25.24	23.69	-141.93
	0.4	28.59	26.83	-130.34
	0.8	38.38	36.02	-115.86
	1.2	45.84	43.03	-86.90
	1.6	49.45	46.41	-72.41
	2.0	56.66	53.18	-47.79
2.0	0.0	21.20	22.58	-142.28
	0.5	24.01	25.58	-130.67
	1.0	32.23	34.33	-116.15
	1.5	38.51	41.01	-87.11
	2.0	41.53	44.24	-72.59
	2.5	47.59	50.69	-47.91

Table 3.84: Thermodynamic parameters for the adsorption of ATPI on weld aged maraging steel surface in sulphuric acid at different temperatures.

Molarity of sulphuric acid (M)	Temperature (°C)	$-\Delta G^{\circ}_{\text{ads}}$ (kJ mol ⁻¹)	$\Delta H^{\circ}_{\text{ads}}$ (kJ mol ⁻¹)	$\Delta S^{\circ}_{\text{ads}}$ (J mol ⁻¹ K ⁻¹)
0.1	30	36.38	- 17.22	-69.65
	35	36.24		
	40	36.06		
	45	35.88		
	50	35.71		
0.5	30	36.44	-21.09	-46.15
	35	36.30		
	40	36.12		
	45	35.94		
	50	35.77		
1.0	30	34.49	-27.65	-32.11
	35	34.35		
	40	34.19		
	45	34.02		
	50	33.85		
1.5	30	31.18	-33.45	-20.08
	35	31.05		
	40	30.90		
	45	30.75		
	50	30.60		
2.0	30	30.91	-39.53	-15.98
	35	30.79		
	40	30.64		
	45	30.49		
	50	30.34		

3.9 2-(4-CHLOROPHENYL)-2-OXOETHYL BENZOATE (CPOB) AS INHIBITOR FOR THE CORROSION OF WELD AGED MARAGING STEEL IN SULPHURIC ACID MEDIUM

3.9.1 Potentiodynamic polarization studies

The potentiodynamic polarization curves for the corrosion of weld aged maraging steel specimen in 0.5 M sulphuric acid in the presence of different concentrations of CPOB, at 30 °C are shown in Fig. 3.67. Similar plots were obtained in the other four concentrations of sulphuric acid at the different temperatures studied. The potentiodynamic polarization parameters (E_{corr} , b_c , b_a , i_{corr} and η (%)) were calculated from Tafel plots in all the five studied concentrations of sulphuric acid in the presence of different concentrations of CPOB at different temperatures and are summarized in Tables 3.85 to 3.89.

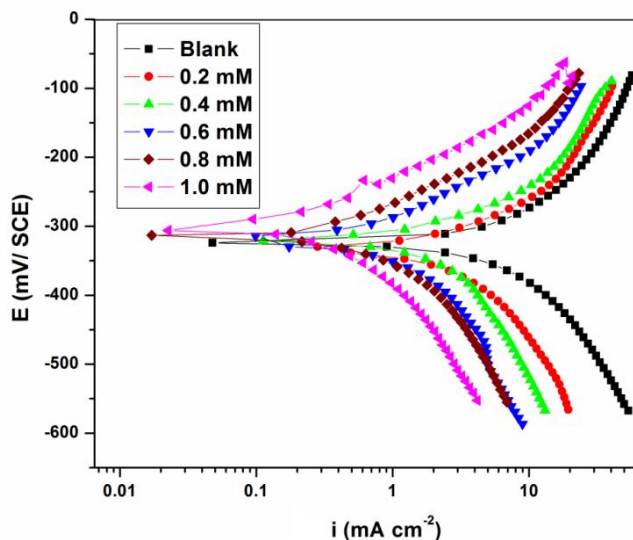


Fig. 3.67: Potentiodynamic polarization curves for the corrosion of weld aged maraging steel in 0.5 M sulphuric acid containing different concentrations of CPOB at 30 °C.

According to the results presented in Tables 3.85 to 3.89 and also from the polarization curves in Fig. 3.7, i_{corr} decreases on the addition of CPOB and the η % increases with the increase in the inhibitor concentration. CPOB shows similar inhibition behaviour as that of ATPI and hence the discussion regarding the inhibition behaviour of ATPI under the section 3.8.1 holds good for CPOB also. Based on the small positive shift in E_{corr} upon the addition of inhibitor, CPOB can be regarded as a mixed type inhibitor with predominant anodic control. CPOB shows slightly lower inhibition efficiency than that of ATPI for the corrosion of weld aged maraging steel in sulphuric acid.

3.9.2 Electrochemical impedance spectroscopy (EIS) studies

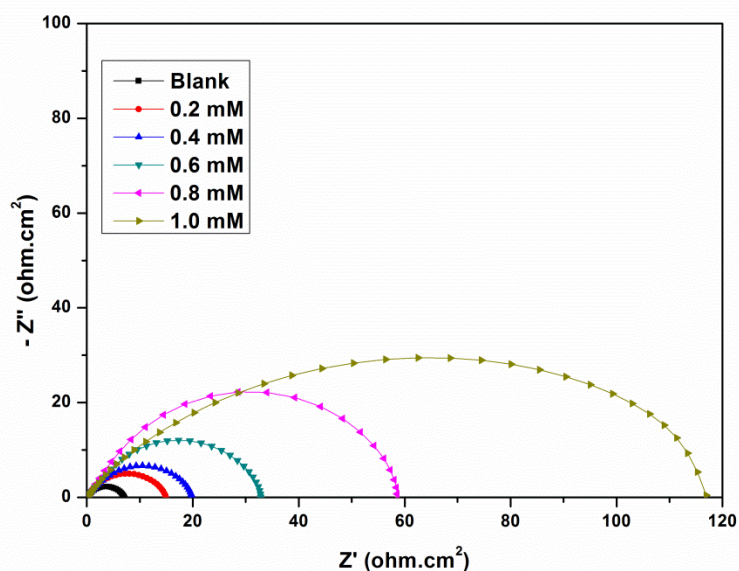


Fig. 3.68: Nyquist plots for the corrosion of weld aged maraging steel in 0.5 M sulphuric acid containing different concentrations of CPOB at 30 °C.

The Nyquist plots obtained for the corrosion of weld aged samples of maraging steel specimen in 0.5 M sulphuric acid in the presence of different concentrations of CPOB at 30 °C are shown in Fig. 3.68. Similar plots were obtained in other

concentrations of sulphuric acid and also at other temperatures. The electrochemical parameters obtained from the EIS studies are summarized in Tables 3.90 to 3.94. The increase in diameter of the semicircle with the increase in the CPOB concentration, indicating the increase in charge transfer resistance (R_{ct}) value and decrease in corrosion rate (v_{corr}). The plots are similar to the ones obtained in hydrochloric acid in the presence of CPOB. The equivalent circuit given in Fig. 3.20 is used to fit the experimental data for the corrosion of weld aged maraging steel in sulphuric acid in the presence of CPOB. Hence the discussion in the section 3.3.2 on the equivalent circuit model for the corrosion of weld aged maraging steel in the presence ATPI holds good here also. As can be seen from the Tables 3.90 to 3.94, R_{ct} , R_{pf} values increase and C_{dl} , C_{pf} values decreases with the increase in the concentration of CPOB, suggesting decrease in corrosion rate. The inhibitor molecule CPOB has the electron rich environment in phenyl group due to resonance of π -electrons of double bonds that can be adsorbed well on the sample surface. Also carbonyl groups are electron donating groups containing oxygen atom as an active site (Atta et al. 2011).

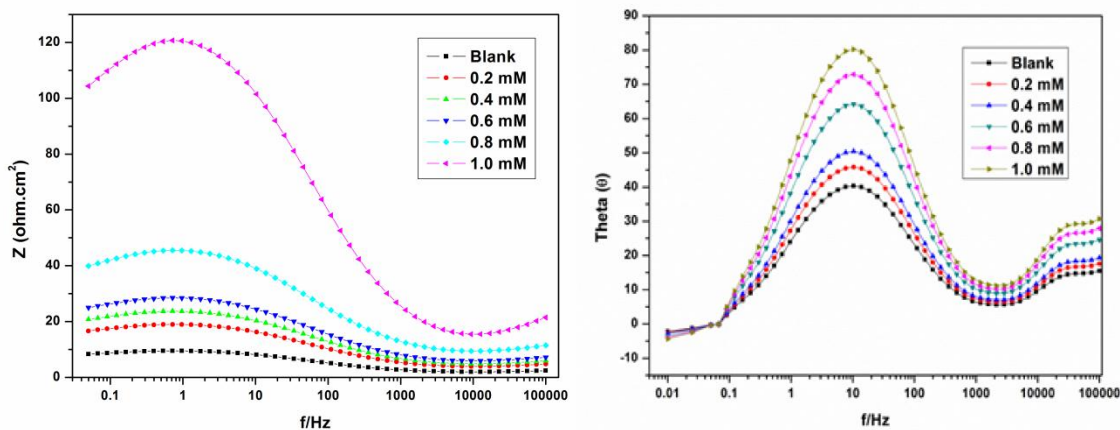


Fig. 3.69: Bode plots for the corrosion of weld aged maraging steel in 0.5 M sulphuric acid containing different concentrations of CPOB at 30 °C.

The Bode plots for the corrosion of the alloy in 0.5 M sulphuric acid containing different concentrations of CPOB at 30 °C are shown in Fig. 3.69. Phase angle increases

with the increase in the concentrations of CPOB in sulphuric acid, hence the discussion regarding the Bode plot under the section 3.3.2 holds good here also.

A comparison of maximum attainable inhibition efficiencies by the Tafel method and EIS method, in the presence of CPOB for the corrosion of weld aged maraging steel in sulphuric acid solutions of different concentrations at 30 °C are listed in Table 3.95. It is evident from the table that the η (%) values obtained by the two methods are in good agreement. Similar levels of agreement were obtained at other temperatures also.

3.9.3 Effect of temperature

The Tafel and EIS results pertaining to different temperatures in different concentrations of sulphuric acid have already been listed in Tables 3.85 to 3.89. The effect of temperature on corrosion inhibition behaviour of CPOB is similar to that of ATPI discussed in the section 3.8.3. The decrease in the inhibition efficiency of CPOB with the increase in temperature may be attributed to the physisorption of CPOB. The Arrhenius plots for the corrosion of weld aged maraging steel in 0.5 M sulphuric acid in the presence of different concentrations of CPOB are shown in Fig. 3.70. The plots of $\ln(v_{\text{corr}}/T)$ vs $(1/T)$ are shown in Fig. 3.71. The calculated values of activation parameters are given in Table 3.96.

According to the activation parameters presented in Table 3.96, E_a for the dissolution of weld aged specimen of maraging steel specimen is greater in the presence of inhibitor than in the absence of inhibitor and the extent of increase is proportional to the inhibitor concentration.

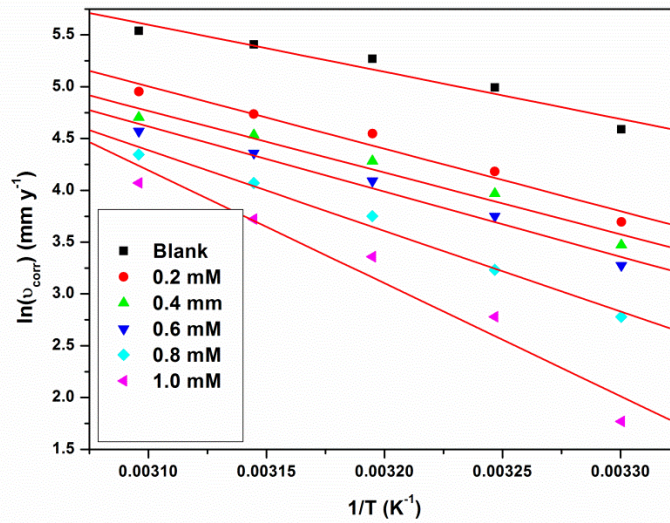


Fig. 3.70: Arrhenius plots for the corrosion of weld aged maraging steel in 0.5 M sulphuric acid containing different concentrations of CPOB.

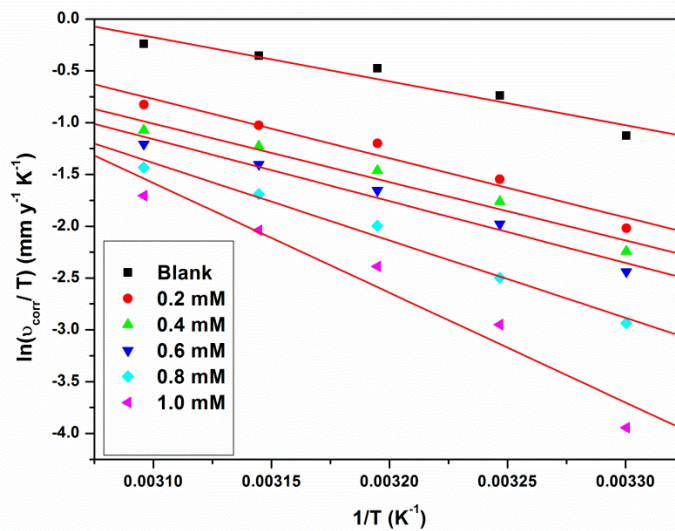


Fig. 3.71: Plots of $\ln(v_{\text{corr}}/T)$ versus $1/T$ for the corrosion of weld aged maraging steel in 0.5 M sulphuric acid containing different concentrations of CPOB.

The large negative entropy of activation implies that the activated complex in the rate determining step represents an association, resulting in a decrease in randomness on going from the reactants to the activated complex (Marsh 1988, Gomma and Wahdan 1995).

3.9.4 Effect of sulphuric acid concentration

It is evident from both the polarization and EIS experimental results that, for a particular concentration of the CPOB, the inhibition efficiency decreases with the increase in sulphuric acid concentration on weld aged maraging steel. The maximum inhibition efficiency is observed in 0.1 M solution of sulphuric acid.

3.9.5 Adsorption isotherm

The adsorption of CPOB on the surfaces of weld aged maraging steel was found to obey Langmuir adsorption isotherm. The Langmuir adsorption isotherms for the adsorption of CPOB on weld aged maraging steel in 0.5 M sulphuric acid are shown in Fig. 3.72.

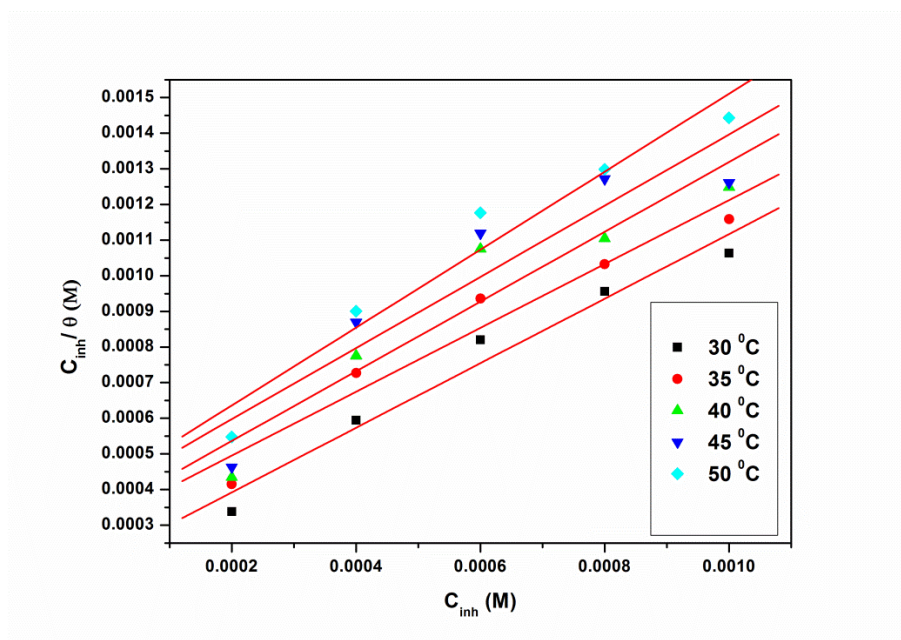


Fig. 3.72: Langmuir adsorption isotherms for the adsorption of CPOB on weld aged maraging steel in 0.5 M sulphuric acid at different temperatures.

The thermodynamic parameters for the adsorption of CPOB on weld aged maraging steel are tabulated in Tables 3.97. These data also reveal similar inhibition behaviour of CPOB as that of ATPI as discussed in section 3.8.5. The ΔG_{ads}^0 values obtained for the adsorption of CPOB on weld aged maraging steel in all the studied concentrations of sulphuric acid are in the range of -31.03 to -34.27 kJ mol⁻¹ indicating both physisorption and chemisorption on the alloy surface. The ΔH_{ads}^0 values on weld aged maraging steel is negative with the absolute value below -41.86 kJ mol⁻¹, suggesting physisorption. Therefore it can be concluded that the adsorption of CPOB, on weld aged maraging steel is mixed type with predominant physisorption. The ΔS_{ads}^0 value is large and negative; indicating that decrease in disordering takes place on going from the reactant to the alloy adsorbed species. This can be attributed to the fact that adsorption is always accompanied by decrease in entropy (Ashish Kumar et al. 2010).

3.9.6 Mechanism of corrosion inhibition

The corrosion inhibition mechanism of CPOB in sulphuric acid solution can be explained in the same lines as that of ATPI in the section 3.8.6. The inhibitor CPOB protects the alloy surface by adsorbing on it through predominant physisorption mode in which the protonated CPOB gets adsorbed on the alloy surface through electrostatic attraction and also to some extent through chemisorption mode involving neutral CPOB molecules as discussed in the section 3.8.6.

3.9.7 SEM/EDS studies

Fig. 3.73 (a) represents the SEM image of the corroded weld aged maraging steel sample. The corroded surface shows detachment of particles from the surface. Fig. 3.73 (b) represents SEM image of weld aged maraging steel after the corrosion tests in a medium of 0.5 M sulphuric containing 0.8 mM of CPOB. The image clearly shows a smooth surface due to the adsorbed layer of inhibitor molecules on the alloy surface, thus protecting the metal from corrosion.

The EDS profile of the corroded surface of the alloy in the presence of CPOB is shown in Fig. 3.74. The atomic percentages of the elements found in the EDS profile on the inhibited metal surface were 5.20 % Fe, 0.62% Ni, 1.20% Mo, 15.19% O, 2.66% S, 70.56% C and 4.37% Br and indicated the formation of inhibitor film on the surface of alloy.

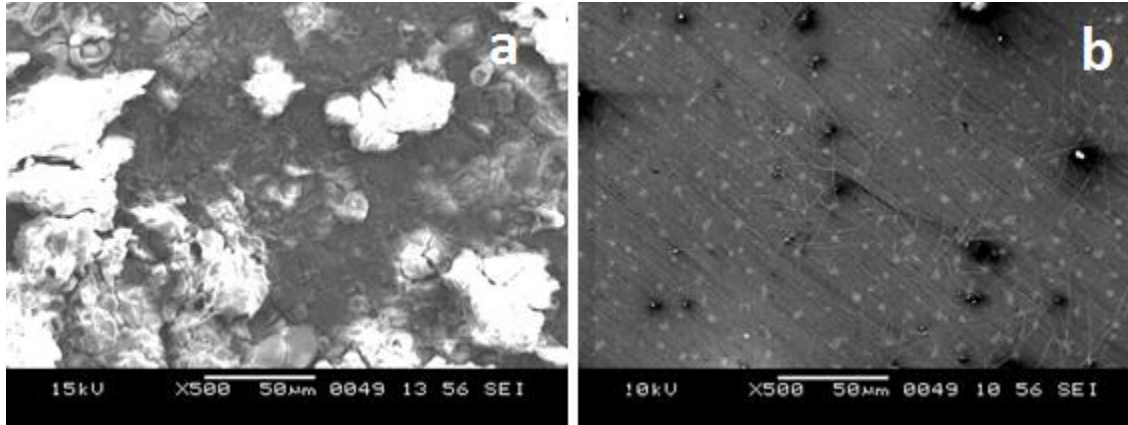


Fig. 3.73: SEM images of the weld aged maraging steel after immersion in 0.5 M sulphuric acid a) in the absence and b) in the presence of CPOB.

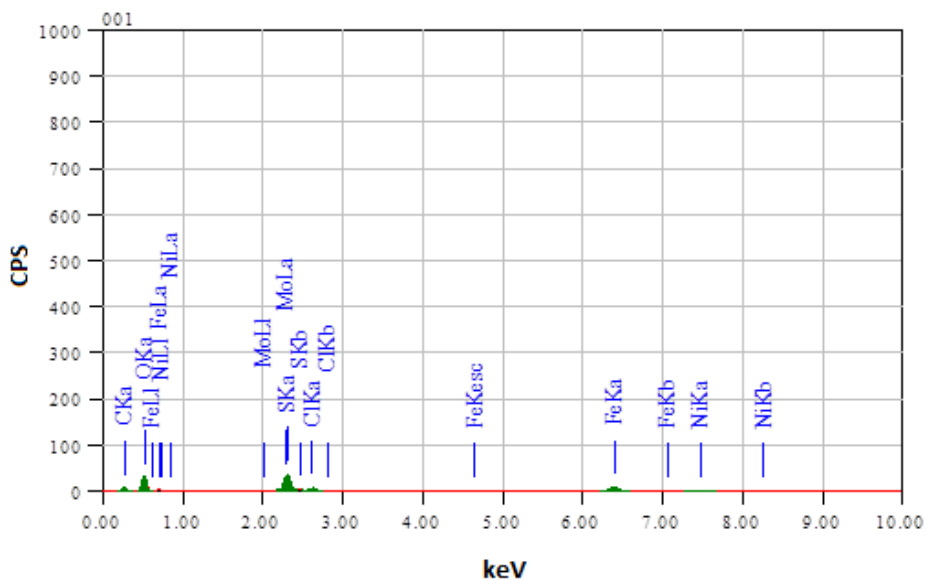


Fig. 3.74: EDS spectra of the weld aged maraging steel after immersion in 0.5 M sulphuric acid in the presence of CPOB.

Table 3.85: Results of potentiodynamic polarization studies for the corrosion of weld aged maraging steel in 0.1 M sulphuric acid containing different concentrations of CPOB.

Temperature (°C)	Conc. of inhibitor (mM)	E_{corr} (mV /SCE)	b_a (mV dec ⁻¹)	$-b_c$ (mV dec ⁻¹)	i_{corr} (mA cm ⁻²)	v_{corr} (mm y ⁻¹)	η (%)
30	Blank	-371±3	221±2	266±3	0.78±0.11	8.99±1.15	
	0.1	-373±1	218±1	264±2	0.36±0.07	4.14±0.77	53.2
	0.2	-370±1	216±3	261±2	0.27±0.03	3.11±0.33	65.9
	0.4	-368±3	212±1	259±1	0.20±0.02	2.30±0.28	74.4
	0.6	-365±1	208±2	255±1	0.10±0.01	1.15±0.12	86.6
	0.8	-362±1	205±3	252±1	0.01±0.01	0.12±0.10	98.3
	35	Blank	-368±1	257±3	283±2	1.27±0.14	14.64±1.41
0.1		-366±2	253±1	280±2	0.63±0.07	7.25±0.75	50.6
0.2		-362±1	250±3	278±1	0.46±0.08	5.29±0.85	63.9
0.4		-358±1	246±3	275±3	0.35±0.07	4.03±0.76	72.4
0.6		-355±1	244±2	269±1	0.21±0.67	2.42±0.72	83.7
0.8		-352±2	240±2	265±1	0.06±0.01	0.69±0.18	95.5
40		Blank	-365±1	289±2	296±1	1.99±0.20	22.95±2.56
	0.1	-367±1	285±1	292±3	1.03±0.14	11.85±1.42	48.3
	0.2	-362±2	280±2	290±1	0.77±0.07	8.86±0.75	61.3
	0.4	-359±2	277±3	286±2	0.59±0.05	6.79±0.54	70.3
	0.6	-357±3	275±1	282±3	0.40±0.04	4.60±0.38	80.1
	0.8	-352±1	272±3	277±1	0.16±0.03	1.84±0.37	92.4
	45	Blank	-362±1	295±3	317±1	2.21±0.21	25.48±2.08
0.1		-360±3	292±3	312±3	1.19±0.15	13.69±1.54	46.2
0.2		-355±1	289±1	310±2	0.94±0.13	10.82±1.30	57.7
0.4		-357±1	287±1	306±2	0.71±0.05	8.17±0.52	67.8
0.6		-351±3	285±3	302±1	0.49±0.04	5.64±0.34	77.6
0.8		-348±1	281±3	297±2	0.28±0.01	3.22±0.14	87.3
50		Blank	-359±1	298±3	321±3	2.47±0.14	28.48±1.78
	0.1	-358±1	295±1	319±3	1.41±0.11	16.22±1.39	43.1
	0.2	-354±1	292±2	314±1	1.15±0.08	13.23±0.90	53.4
	0.4	-351±2	290±1	310±1	0.90±0.03	10.36±0.37	63.4
	0.6	-347±3	289±2	306±3	0.63±0.02	7.25±0.24	74.6
	0.8	-344±2	285±1	301±2	0.39±0.01	4.49±0.10	84.1

Table 3.86: Results of potentiodynamic polarization studies for the corrosion of weld aged maraging steel in 0.5 M sulphuric acid containing different concentrations of CPOB.

Temperature (°C)	Conc. of inhibitor (mM)	E_{corr} (mV /SCE)	b_a (mV dec ⁻¹)	$-b_c$ (mV dec ⁻¹)	i_{corr} (mA cm ⁻²)	v_{corr} (mm y ⁻¹)	η (%)
30	Blank	-356±3	235±2	268±3	1.80±0.24	20.71±2.43	
	0.1	-353±2	232±1	262±3	0.79±0.18	9.09±1.83	56.2
	0.2	-350±3	230±3	258±1	0.64±0.17	7.36±1.74	64.4
	0.4	-346±3	227±1	255±2	0.41±0.11	4.72±1.10	77.2
	0.6	-348±1	222±3	251±3	0.28±0.05	3.22±0.55	84.3
	0.8	-342±2	218±3	249±1	0.07±0.02	0.81±0.28	96.4
	35	Blank	-353±2	257±2	276±3	2.41±0.28	27.73±2.75
0.1		-350±3	255±1	273±3	1.12±0.12	12.89±1.22	53.7
0.2		-347±1	251±2	271±1	0.91±0.15	10.47±1.51	62.2
0.4		-342±3	248±2	268±2	0.63±0.03	7.25±0.34	74.0
0.6		-340±2	243±3	266±1	0.44±0.02	5.06±0.27	81.9
0.8		-337±2	239±2	262±3	0.17±0.01	1.96±0.12	93.2
40		Blank	-350±3	279±2	288±3	3.83±0.23	44.07±2.32
	0.1	-347±1	276±3	284±1	1.90±0.16	21.86±1.59	50.5
	0.2	-343±2	274±3	282±1	1.53±0.19	17.60±1.92	60.0
	0.4	-340±1	271±3	279±1	1.14±0.04	13.12±0.41	70.3
	0.6	-336±3	268±1	276±1	0.87±0.04	10.01±0.45	77.4
	0.8	-333±3	264±2	271±1	0.37±0.02	4.26±0.25	90.3
	45	Blank	-348±2	296±3	297±1	4.01±0.25	46.14±2.47
0.1		-345±2	292±3	293±3	2.10±0.19	24.16±1.92	47.5
0.2		-340±1	288±3	289±1	1.68±0.17	19.33±1.72	58.2
0.4		-335±1	285±3	286±1	1.36±0.08	15.65±0.89	66.2
0.6		-332±1	282±2	282±1	0.98±0.03	11.28±0.34	75.5
0.8		-329±3	278±2	280±3	0.45±0.02	5.18±0.29	88.8
50		Blank	-346±2	315±1	306±2	4.30±0.38	49.47±3.83
	0.1	-343±3	311±2	304±1	2.36±0.27	27.15±2.71	45.0
	0.2	-341±3	309±1	301±3	1.91±0.20	21.98±2.01	55.5
	0.4	-339±2	305±3	298±3	1.61±0.19	18.52±1.92	62.5
	0.6	-335±3	303±3	295±3	1.18±0.17	13.58±1.73	72.6
	0.8	-332±1	300±2	291±1	0.59±0.19	6.79±1.93	86.2

Table 3.87: Results of potentiodynamic polarization studies for the corrosion of weld aged maraging steel in 1.0 M sulphuric acid containing different concentrations of CPOB.

Temperature (°C)	Conc. of inhibitor (mM)	E_{corr} (mV /SCE)	b_a (mV dec ⁻¹)	$-b_c$ (mV dec ⁻¹)	i_{corr} (mA cm ⁻²)	v_{corr} (mm y ⁻¹)	η (%)
30	Blank	-323±1	247±3	301±2	8.57±0.37	98.49±3.67	
	0.2	-327±3	243±3	303±2	3.50±0.24	40.27±2.45	59.1
	0.4	-319±3	238±2	298±1	2.80±0.25	32.22±2.53	67.3
	0.6	-314±3	240±1	291±3	2.30±0.29	26.46±2.87	73.1
	0.8	-312±1	235±3	288±2	1.40±0.21	16.11±2.10	83.6
	1.0	-309±3	231±3	285±2	0.51±0.20	5.87±2.02	94.1
35	Blank	-318±2	276±1	305±1	12.81±0.47	147.27±4.73	
	0.2	-314±2	271±2	301±2	5.71±0.12	65.58±1.15	55.5
	0.4	-312±1	274±3	297±1	4.60±0.25	52.93±2.46	64.1
	0.6	-315±2	267±2	302±1	3.70±0.21	42.57±2.06	71.1
	0.8	-309±3	259±2	291±2	2.20±0.38	25.31±3.80	82.2
	1.0	-302±3	263±2	287±2	1.40±0.10	16.11±1.01	89.1
40	Blank	-309±1	292±1	307±3	18.2±0.39	194.44±3.91	
	0.2	-311±2	287±2	310±3	8.21±0.32	94.35±3.20	51.5
	0.4	-306±2	279±2	299±2	6.31±0.33	72.49±3.25	62.7
	0.6	-302±2	283±3	292±2	5.21±0.27	59.83±2.70	69.2
	0.8	-299±3	274±2	295±1	3.70±0.39	42.57±3.88	78.1
	1.0	-295±2	270±3	288±1	2.50±0.19	28.76±1.94	85.2
45	Blank	-307±1	298±2	303±1	19.42±0.21	223.21±2.08	
	0.2	-305±3	295±1	299±1	9.91±0.56	113.91±5.62	49.1
	0.4	-309±2	287±1	301±3	8.11±0.26	93.20±2.58	58.2
	0.6	-311±3	291±4	295±3	6.81±0.22	78.24±2.20	64.9
	0.8	-308±3	283±3	287±3	5.11±0.33	58.68±3.28	73.7
	1.0	-293±3	278±2	282±3	3.60±0.18	41.42±1.80	81.4
50	Blank	-305±3	312±3	311±1	22.12±0.34	254.27±3.44	
	0.2	-303±1	314±3	306±2	12.31±0.37	141.52±3.73	44.3
	0.4	-300±2	307±3	309±2	9.61±0.24	110.45±2.37	56.6
	0.6	-297±3	302±1	303±1	8.41±0.24	96.65±2.38	62.0
	0.8	-292±3	297±1	300±1	6.71±0.27	77.09±2.67	69.7
	1.0	-288±1	294±2	291±2	5.11±0.17	58.68±1.71	76.9

Table 3.88: Results of potentiodynamic polarization studies for the corrosion of weld aged maraging steel in 1.5 M sulphuric acid containing different concentrations of CPOB.

Temperature (°C)	Conc. of inhibitor (mM)	E_{corr} (mV /SCE)	b_a (mV dec ⁻¹)	$-b_c$ (mV dec ⁻¹)	i_{corr} (mA cm ⁻²)	v_{corr} (mm y ⁻¹)	η (%)
30	Blank	-295±2	252±1	260±1	17.02±0.36	195.52±3.57	
	0.4	-296±1	249±2	257±1	7.71±0.25	88.59±2.50	54.7
	0.8	-292±1	246±3	255±1	6.28±0.32	72.14±3.22	63.1
	1.2	-289±2	242±3	252±3	4.86±0.24	55.92±2.36	71.4
	1.6	-286±3	239±2	249±2	3.35±0.25	38.54±2.53	80.3
	2.0	-283±3	235±2	245±1	1.43±0.15	16.45±1.49	91.6
	35	Blank	-291±1	253±2	272±2	23.62±0.40	271.53±3.96
0.4		-288±2	250±2	268±3	11.29±0.25	129.78±2.46	52.2
0.8		-290±1	248±1	265±2	9.10±0.22	104.59±2.21	61.5
1.2		-286±2	245±2	262±3	7.61±0.22	87.44±2.21	67.8
1.6		-283±1	244±1	259±3	5.20±0.37	59.71±3.65	78.0
2.0		-280±2	241±1	255±3	2.81±0.28	32.33±2.79	88.1
40		Blank	-288±2	254±3	276±2	28.03±0.23	332.15±2.30
	0.4	-290±2	253±2	272±2	13.98±0.25	160.73±2.53	50.1
	0.8	287±1	250±1	270±2	11.49±0.23	132.08±2.26	59.0
	1.2	-285±3	247±1	267±1	9.45±0.28	108.61±2.77	66.3
	1.6	-282±2	243±1	263±1	6.79±0.26	78.01±2.65	75.8
	2.0	-279±2	240±1	261±1	3.86±0.21	44.41±2.06	86.2
	45	Blank	-285±2	266±1	283±2	30.33±0.31	348.61±3.10
0.4		-281±3	264±1	281±2	15.69±0.28	180.29±2.85	48.3
0.8		-283±1	261±3	278±2	13.07±0.27	150.26±2.70	56.9
1.2		-279±1	258±3	276±2	10.86±0.27	124.84±2.70	64.2
1.6		-277±2	255±3	272±2	8.19±0.24	94.12±2.41	73.0
2.0		-273±1	251±1	270±3	5.01±0.20	57.53±2.98	83.5
50		Blank	-283±1	272±1	296±3	33.03±0.31	379.64±3.05
	0.4	-280±1	268±1	294±2	18.60±0.21	213.77±2.09	43.7
	0.8	-277±3	266±2	290±3	15.27±0.28	175.46±2.77	53.8
	1.2	-279±1	263±1	289±3	12.45±0.21	143.13±2.12	62.3
	1.6	-275±1	261±1	286±1	9.94±0.39	114.25±3.94	69.9
	2.0	-274±2	258±1	284±1	7.93±0.41	91.92±4.13	76.1

Table 3.89: Results of potentiodynamic polarization studies for the corrosion of weld aged maraging steel in 2.0 M sulphuric acid containing different concentrations of CPOB.

Temperature (°C)	Conc. of inhibitor (mM)	E_{corr} (mV /SCE)	b_a (mV dec ⁻¹)	$-b_c$ (mV dec ⁻¹)	i_{corr} (mA cm ⁻²)	v_{corr} (mm y ⁻¹)	η (%)
30	Blank	-281±2	223±2	251±1	20.31±0.31	233.51±3.05	
	0.5	-279±1	219±2	248±1	9.80±0.30	112.75±3.03	51.7
	1.0	-280±1	215±1	245±1	8.26±0.23	95.04±2.30	59.3
	1.5	-276±3	212±3	243±2	6.50±0.27	74.79±2.65	68.0
	2.0	-272±2	209±1	239±2	4.43±0.29	50.97±2.86	78.2
	2.5	-275±2	207±1	236±3	2.27±0.27	26.12±2.75	88.8
35	Blank	-279±2	245±3	263±2	27.63±0.22	317.55±2.19	
	0.5	-282±2	242±1	260±1	14.05±0.25	161.65±2.50	49.1
	1.0	-280±1	238±1	258±3	11.79±0.39	135.65±3.87	57.3
	1.5	-277±3	234±1	254±3	9.25±0.26	106.43±2.60	66.5
	2.0	-274±1	231±2	251±3	6.68±0.35	76.86±3.53	75.8
	2.5	-272±2	228±1	248±2	3.97±0.15	45.68±1.50	85.6
40	Blank	-278±3	269±2	274±3	35.04±0.33	402.63±3.34	
	0.5	-276±3	265±1	271±1	18.55±0.21	213.43±2.07	47.0
	1.0	-280±1	263±3	268±1	15.93±0.29	183.28±2.93	54.5
	1.5	-274±2	260±2	265±1	12.88±0.48	148.19±4.83	63.2
	2.0	-271±1	257±3	261±3	9.52±0.29	109.53±2.88	72.8
	2.5	-267±3	254±1	259±2	6.20±0.16	71.33±1.64	82.3
45	Blank	-275±3	281±1	288±3	40.71±0.26	468.28±2.65	
	0.5	-272±2	278±3	285±1	22.18±0.29	255.19±2.92	45.5
	1.0	-270±1	275±3	282±1	19.29±0.30	221.94±3.02	52.6
	1.5	-267±1	273±2	278±3	16.00±0.33	184.09±3.32	60.7
	2.0	-264±1	270±2	276±2	12.58±0.31	144.74±3.08	69.1
	2.5	-261±2	267±2	274±3	8.26±0.10	95.04±1.97	79.7
50	Blank	-273±3	301±3	302±2	45.27±0.47	520.05±4.65	
	0.5	-275±1	299±1	300±1	26.17±0.31	301.10±3.12	42.1
	1.0	-270±1	295±3	296±3	22.92±0.33	263.71±3.25	49.3
	1.5	-267±2	292±3	294±3	18.71±0.34	215.27±3.41	58.6
	2.0	-263±3	288±3	290±3	15.19±0.25	174.77±2.55	66.4
	2.5	-260±1	284±2	289±3	10.94±0.25	125.87±2.54	75.8

Table 3.90: EIS data for the corrosion of weld aged maraging steel in 0.1 M sulphuric acid containing different concentrations of CPOB.

Temperature (°C)	Conc. of inhibitor (mM)	R_{ct} (ohm. cm ²)	C_{dl} (mF cm ⁻²)	R_{pf} (ohm. cm ²)	C_{pf} (mF cm ⁻²)	η (%)
30	Blank	74.66±1.93	21.01±3.16			
	0.1	166.54±2.31	10.40±3.83	8.93±1.92	2.64±1.26	55.2
	0.2	210.43±2.86	8.44±2.90	11.30±2.52	2.19±1.91	64.5
	0.4	306.74±2.75	6.10±3.82	16.48±2.84	1.64±0.81	75.7
	0.6	574.75±2.29	3.72±1.21	30.91±1.76	1.09±0.31	87.1
	0.8	2400.64±3.54	1.64±0.29	129.23±1.69	0.60±0.09	96.9
35	Blank	51.17±2.20	26.57±3.40			
	0.1	106.89±2.87	13.09±2.49	6.74±2.00	3.27±1.19	52.1
	0.2	135.48±2.79	10.57±3.26	8.55±2.13	2.68±1.15	62.2
	0.4	189.52±3.95	7.88±3.87	11.97±2.67	2.06±0.97	73.2
	0.6	335.98±2.91	4.83±3.97	21.24±2.27	1.35±0.13	84.8
	0.8	960.04±2.04	2.34±0.37	60.76±1.72	0.77±0.08	94.7
40	Blank	35.45±3.66	32.14±2.15			
	0.1	70.41±2.70	13.38±2.70	5.06±0.58	3.34±1.41	49.7
	0.2	87.12±3.30	10.73±2.23	6.27±2.01	2.72±0.79	59.3
	0.4	125.27±3.27	7.91±3.80	9.03±1.73	2.19±0.77	71.7
	0.6	192.04±3.36	4.94±1.07	13.86±1.77	1.37±0.82	81.5
	0.8	452.75±3.68	2.37±0.57	32.72±2.85	0.81±0.17	92.2
45	Blank	33.36±2.04	36.48±2.78			
	0.1	61.63±2.44	17.06±2.86	4.02±0.81	4.19±1.26	45.9
	0.2	76.22±2.81	13.98±2.86	4.98±2.17	3.48±1.13	56.2
	0.4	102.68±3.86	10.02±2.25	6.72±2.76	2.55±0.74	67.5
	0.6	157.51±2.34	6.88±2.50	10.32±1.70	1.82±0.43	78.8
	0.8	288.83±2.60	3.49±0.38	18.95±1.96	1.03±0.20	88.5
50	Blank	30.19±2.61	41.49±2.22			
	0.1	52.69±3.43	24.48±2.66	3.26±0.70	5.92±1.26	42.7
	0.2	63.26±2.28	20.56±3.74	3.92±2.33	5.01±1.42	52.3
	0.4	85.02±2.19	15.55±3.23	5.28±2.58	3.84±0.90	64.5
	0.6	122.47±2.34	11.10±3.02	7.63±2.73	2.81±0.39	75.4
	0.8	202.75±2.12	7.10±2.19	12.65±2.78	1.87±0.18	85.1

Table 3.91: EIS data for the corrosion of weld aged maraging steel in 0.5 M sulphuric acid containing different concentrations of CPOB.

Temperature (°C)	Conc. of inhibitor (mM)	R_{ct} (ohm. cm ²)	C_{dl} (μF cm ⁻²)	R_{pf} (ohm. cm ²)	C_{pf} (mF cm ⁻²)	η (%)
30	Blank	33.56±2.12	40.12±3.87			
	0.1	74.33±2.20	19.10±2.40	4.81±0.92	4.67±2.46	54.9
	0.2	97.39±3.16	14.82±3.29	6.31±2.18	3.67±1.54	65.5
	0.4	139.95±2.87	10.61±2.11	9.09±2.22	2.69±1.69	76.0
	0.6	205.26±2.01	7.55±1.95	13.34±2.28	1.98±0.44	83.7
	0.8	795.26±2.39	2.68±0.64	51.78±2.21	0.84±0.23	95.8
35	Blank	26.64±3.34	65.92±3.85			
	0.1	56.12±2.37	31.27±2.31	3.37±0.72	7.51±2.57	52.5
	0.2	73.73±3.50	24.03±2.14	4.43±2.12	5.82±1.01	63.9
	0.4	105.01±3.52	17.17±2.30	6.33±2.58	4.22±0.74	74.6
	0.6	140.21±3.48	13.11±2.35	8.46±1.73	3.27±0.60	81.0
	0.8	373.63±3.75	5.54±2.49	22.61±2.88	1.51±0.46	92.9
40	Blank	17.85±2.03	109.77±2.93			
	0.1	35.17±2.42	54.45±3.69	2.45±0.96	12.91±1.44	49.2
	0.2	45.95±3.11	41.91±2.96	3.21±2.81	9.98±1.95	61.2
	0.4	62.99±2.87	30.84±2.92	4.42±2.51	7.40±1.50	71.7
	0.6	83.10±3.56	23.61±2.21	5.84±2.65	5.72±1.22	78.5
	0.8	191.32±3.25	10.82±1.10	13.48±2.41	2.74±0.43	90.7
45	Blank	17.84±2.96	125.60±2.35			
	0.1	33.39±3.54	66.46±3.93	1.71±0.44	15.70±1.28	46.6
	0.2	44.29±3.86	50.36±2.51	2.28±1.75	11.95±2.61	59.7
	0.4	54.27±2.81	41.27±2.00	2.80±2.51	9.83±1.69	67.1
	0.6	75.24±2.15	30.05±3.98	3.90±2.24	7.22±1.49	76.3
	0.8	143.29±2.81	16.25±2.21	7.45±2.49	4.01±0.47	87.6
50	Blank	17.42±3.73	158.27±3.26			
	0.1	31.24±3.71	88.23±2.34	1.07±0.25	20.78±2.32	44.2
	0.2	40.18±3.45	68.80±2.31	1.39±1.60	16.25±2.94	56.7
	0.4	47.52±2.19	58.34±3.02	1.65±2.31	13.81±1.48	63.3
	0.6	65.93±2.24	42.32±3.04	2.30±2.57	10.08±2.34	73.6
	0.8	121.39±3.68	23.44±2.77	4.25±2.31	5.68±1.92	85.7

Table 3.92: EIS data of weld aged maraging steel in 1.0 M sulphuric acid containing different concentrations of CPOB.

Temperature (°C)	Conc. of inhibitor (mM)	R _{ct} (ohm. cm ²)	C _{dl} (mF cm ⁻²)	R _{pf} (ohm. cm ²)	C _{pf} (mF cm ⁻²)	η (%)
30	Blank	7.09±1.24	11.00±1.85			
	0.2	16.64±2.56	5.58±2.91	1.67±0.56	1.32±0.28	57.4
	0.4	20.43±2.05	4.71±1.64	2.05±0.67	0.79±0.26	65.3
	0.6	24.70±3.45	4.05±1.33	2.48±0.78	0.58±0.20	71.3
	0.8	39.83±3.95	2.85±0.49	3.75±0.66	0.36±0.17	82.2
	1.0	102.75±3.95	1.65±0.23	5.11±0.44	0.16±0.12	93.1
35	Blank	5.05±1.07	11.83±2.73			
	0.2	11.15±2.40	6.25±2.67	1.23±0.70	1.69±0.72	54.7
	0.4	14.03±3.48	5.15±2.95	1.55±0.43	1.09±0.33	64
	0.6	16.95±2.32	4.41±2.70	1.87±0.58	0.83±0.75	70.2
	0.8	26.44±3.69	3.14±1.38	3.20±0.64	0.64±0.18	80.9
	1.0	40.08±2.06	2.38±0.28	3.68±0.34	0.57±0.13	87.4
40	Blank	3.95±1.48	12.37±2.04			
	0.2	7.82±1.71	7.09±1.60	0.84±0.15	2.37±0.78	49.5
	0.4	10.05±2.92	5.70±1.30	1.08±0.78	2.18±0.43	60.7
	0.6	12.70±3.27	4.71±1.40	1.36±0.42	1.34±0.12	68.9
	0.8	18.04±2.68	3.58±1.05	2.12±0.66	0.81±0.15	78.1
	1.0	28.62±3.08	2.58±0.68	3.07±0.56	0.62±0.11	86.2
45	Blank	3.49±1.53	15.26±3.04			
	0.2	6.72±3.43	8.81±2.73	0.68±0.51	2.66±0.79	48.1
	0.4	8.33±3.17	7.34±2.54	0.81±0.44	2.25±0.54	58.1
	0.6	10.54±2.54	5.94±2.39	1.03±0.37	1.86±0.33	66.9
	0.8	12.64±2.24	5.09±1.22	1.17±0.72	1.20±0.34	72.4
	1.0	19.50±2.69	3.61±1.57	1.91±0.39	0.84±0.26	82.1
50	Blank	3.15±1.63	18.08±3.27			
	0.2	5.93±2.63	10.48±2.97	0.55±0.14	3.18±0.27	46.9
	0.4	7.02±3.00	9.00±2.81	0.65±0.22	2.64±0.23	55.1
	0.6	8.63±2.26	7.48±1.14	0.80±0.24	2.24±0.77	63.5
	0.8	10.79±1.59	6.16±1.48	1.05±0.36	1.67±0.30	70.8
	1.0	13.94±3.53	4.97±1.67	1.29±0.41	1.47±0.04	77.4

Table 3.93: EIS data for the corrosion of weld aged maraging steel in 1.5 M sulphuric acid containing different concentrations of CPOB.

Temperature (°C)	Conc. of inhibitor (mM)	R_{ct} (ohm. cm ²)	C_{dl} (mF cm ⁻²)	R_{pf} (ohm. cm ²)	C_{pf} (mF cm ⁻²)	η (%)
30	Blank	3.34±0.21	13.71±2.01			
	0.4	7.52±0.85	7.07±2.27	0.65±0.18	1.87±0.57	55.6
	0.8	8.86±0.93	6.16±1.98	0.77±0.20	1.66±0.56	62.3
	1.2	12.15±1.60	4.76±1.62	1.07±0.17	1.33±0.58	72.5
	1.6	18.15±1.34	3.51±1.63	1.62±0.23	1.04±0.36	81.6
	2.0	46.39±1.03	1.98±0.66	4.19±0.51	0.68±0.19	92.8
35	Blank	2.46±0.69	14.52±2.61			
	0.4	5.23±1.50	7.84±2.53	0.42±0.14	2.04±0.65	53.2
	0.8	6.13±1.61	6.80±2.36	0.49±0.21	1.80±0.47	59.9
	1.2	7.83±1.26	5.54±1.31	0.64±0.23	1.51±0.51	68.6
	1.6	11.88±0.81	3.99±1.86	0.99±0.50	1.15±0.37	79.3
	2.0	24.36±1.02	2.45±0.55	2.07±0.20	0.79±0.12	89.9
40	Blank	2.09±0.43	16.09±1.61			
	0.4	4.31±1.04	8.75±2.10	0.23±0.17	2.26±0.38	51.5
	0.8	4.88±1.03	7.83±2.68	0.27±0.14	2.04±0.67	57.2
	1.2	6.08±0.98	6.50±2.03	0.34±0.19	1.73±0.44	65.6
	1.6	9.01±1.16	4.70±1.60	0.52±0.20	1.31±0.49	76.8
	2.0	14.82±1.29	3.25±0.83	0.87±0.19	0.98±0.40	85.9
45	Blank	2.01±0.59	18.30±2.80			
	0.4	3.84±1.24	10.57±1.70	0.19±0.03	2.68±0.36	47.6
	0.8	4.47±1.19	9.23±2.82	0.22±0.07	2.37±0.51	55.1
	1.2	5.42±1.57	7.78±1.13	0.28±0.12	2.03±0.36	62.9
	1.6	7.23±1.36	6.08±2.16	0.38±0.14	1.64±0.61	72.2
	2.0	11.62±0.79	4.16±0.19	0.64±0.11	1.19±0.50	82.7
50	Blank	1.90±0.13	21.47±2.90			
	0.4	3.42±1.11	12.66±1.94	0.15±0.06	3.17±0.72	44.5
	0.8	3.99±0.92	10.99±1.86	0.18±0.06	2.78±0.38	52.4
	1.2	4.76±0.92	9.37±2.02	0.23±0.16	2.40±0.62	60.1
	1.6	6.29±0.86	7.33±1.61	0.31±0.15	1.93±0.58	69.8
	2.0	8.88±1.00	5.49±0.94	0.45±0.23	1.50±0.52	78.6

Table 3.94: EIS data for the corrosion of weld aged maraging steel in 2.0 M sulphuric acid containing different concentrations of CPOB.

Temperature (°C)	Conc. of inhibitor (mM)	R_{ct} (ohm. cm ²)	C_{dl} (mF cm ⁻²)	R_{pf} (ohm. cm ²)	C_{pf} (mF cm ⁻²)	η (%)
30	Blank	2.58±0.25	16.41±2.17			
	0.5	5.02±0.62	7.43±1.38	0.32±0.12	1.95±0.51	48.6
	1.0	6.00±1.38	6.06±1.31	0.39±0.11	1.63±0.70	57.0
	1.5	7.54±1.90	4.62±1.88	0.50±0.20	1.30±0.66	65.8
	2.0	10.62±1.31	2.99±0.74	0.72±0.13	0.92±0.28	75.7
	2.5	19.69±2.26	1.16±0.21	1.36±0.18	0.49±0.15	86.9
35	Blank	2.04±0.87	17.25±1.17			
	0.5	3.79±0.28	8.27±1.64	0.24±0.04	2.15±0.58	46.2
	1.0	4.58±1.30	6.67±1.08	0.30±0.10	1.77±0.63	55.5
	1.5	5.64±1.83	5.24±1.84	0.37±0.13	1.44±0.91	63.8
	2.0	7.64±2.52	3.60±1.05	0.51±0.19	1.06±0.34	73.3
	2.5	13.60±2.24	1.59±0.31	0.94±0.22	0.59±0.21	85.0
40	Blank	1.72±1.00	19.56±2.30			
	0.5	3.09±2.77	9.84±1.52	0.15±0.07	2.51±0.93	44.4
	1.0	3.71±1.84	8.07±1.43	0.19±0.08	2.10±0.75	53.6
	1.5	4.43±1.30	6.58±1.36	0.23±0.07	1.75±0.38	61.2
	2.0	5.77±2.07	4.83±1.51	0.31±0.08	1.35±0.41	70.2
	2.5	10.00±1.26	2.37±0.28	0.57±0.16	0.77±0.15	82.8
45	Blank	1.55±1.20	23.83±1.35			
	0.5	2.68±1.84	12.74±1.70	0.11±0.04	3.19±0.96	42.2
	1.0	3.12±1.08	10.82±1.03	0.13±0.03	2.74±0.81	50.3
	1.5	3.73±1.45	8.90±2.70	0.16±0.05	2.29±0.65	58.4
	2.0	4.94±1.96	6.48±1.72	0.23±0.08	1.73±0.47	68.6
	2.5	8.03±1.38	3.61±0.91	0.39±0.15	1.06±0.25	80.7
50	Blank	1.48±0.79	26.01±2.67			
	0.5	2.48±1.76	14.55±1.65	0.07±0.02	3.61±0.65	40.4
	1.0	2.77±1.81	12.93±2.55	0.08±0.02	3.23±0.68	46.5
	1.5	3.30±1.76	10.70±2.43	0.10±0.02	2.71±0.77	55.1
	2.0	4.10±1.38	8.41±1.94	0.13±0.03	2.18±0.54	63.9
	2.5	5.44±2.06	6.09±0.53	0.19±0.03	1.64±0.32	72.8

Table 3.95: Comparison of maximum attainable inhibition efficiencies by the Tafel method and EIS method for the corrosion of weld aged maraging steel in sulphuric acid solutions of different concentrations in the presence of CPOB at 30 °C.

Molarity of sulphuric acid	Conc. of CPOB (mM)	η (%)	
		Tafel	EIS
0.1	0.8	98.27	96.89
0.5	0.8	96.38	95.78
1.0	1.0	94.04	93.1
1.5	2.0	91.6	92.8
2.0	2.5	88.8	86.9

Table 3.96: Activation parameters for the corrosion of weld aged maraging steel in sulphuric acid containing different concentrations of CPOB.

Molarity of sulphuric acid	Conc. of inhibitor (mM)	E_a ($\text{kJ}^{-1} \text{mol}^{-1}$)	ΔH^\ddagger ($\text{kJ}^{-1} \text{mol}^{-1}$)	ΔS^\ddagger ($\text{J mol}^{-1} \text{K}^{-1}$)
0.1	0.0	44.31	43.16	-88.32
	0.1	47.62	45.29	-76.60
	0.2	64.45	67.02	-69.39
	0.4	77.36	76.89	-59.48
	0.6	82.62	80.08	-49.57
	0.8	95.91	92.29	-38.75
	0.5	0.0	35.50	37.48
0.1		43.83	46.28	-96.73
0.2		57.60	60.81	-87.62
0.4		68.10	71.90	75.11
0.6		72.45	76.49	-62.59
0.8		83.32	87.96	-48.93
1.0		0.0	32.79	28.11
	0.2	40.49	34.71	-124.97
	0.4	53.20	45.61	-113.21
	0.6	62.90	53.93	-97.03
	0.8	66.92	57.37	-80.86
	1.0	76.96	65.97	-63.22
1.5	0.0	25.24	23.69	-141.93
	0.4	31.16	29.25	-123.10
	0.8	40.95	38.44	-111.52
	1.2	48.42	45.45	-95.59
	1.6	51.51	48.35	-79.65
	2.0	59.24	55.60	-62.28
2.0	0.0	21.20	22.58	-142.28
	0.5	26.18	27.88	-123.41
	1.0	34.40	36.63	-111.79
	1.5	40.67	43.32	-95.82
	2.0	43.27	46.08	-79.85
	2.5	49.76	52.99	-62.43

Table 3.97: Thermodynamic parameters for the adsorption of CPOB on weld aged maraging steel surface in sulphuric acid at different temperatures.

Molarity of sulphuric acid	Temperature (°C)	$-\Delta G^{\circ}_{\text{ads}}$ (kJ mol ⁻¹)	$\Delta H^{\circ}_{\text{ads}}$ (kJ mol ⁻¹)	$\Delta S^{\circ}_{\text{ads}}$ (J mol ⁻¹ K ⁻¹)	R ²
0.1	30	34.27	- 22.26	-38.14	0.9675
	35	34.14			
	40	33.97			
	45	33.80			
	50	33.64			
0.5	30	32.39	-28.14	-30.56	0.9742
	35	32.27			
	40	32.11			
	45	31.95			
	50	31.80			
1.0	30	32.78	-32.72	-22.06	0.9609
	35	32.65			
	40	32.49			
	45	32.33			
	50	32.17			
1.5	30	32.01	-36.09	-14.17	0.9821
	35	31.88			
	40	31.73			
	45	31.57			
	50	31.42			
2.0	30	31.61	-38.11	-9.34	0.9805
	35	31.49			
	40	31.33			
	45	31.18			
	50	31.03			

3.10 2-(4-BROMOPHENYL)-2-OXOETHYL-4-CHLOROBENZOATE (CPOM) AS INHIBITOR FOR THE CORROSION OF WELD AGED MARAGING STEEL IN SULPHURICACID MEDIUM

3.10.1 Potentiodynamic polarization studies

The potentiodynamic polarization curves plots for the corrosion of weld aged maraging steel specimen in 2.0 M sulphuric acid in the presence of different concentrations of CPOM, at 30 °C are shown in Fig. 3.75. Similar plots were obtained in the other four concentrations of sulphuric acid at the different temperatures studied. The potentiodynamic polarization parameters (E_{corr} , b_c , b_a , i_{corr} and η (%)) were calculated from Tafel plots in all the five studied concentrations of sulphuric acid in the presence of different concentrations of CPOM at different temperatures and are summarized in Tables 3.98 to 3.102.

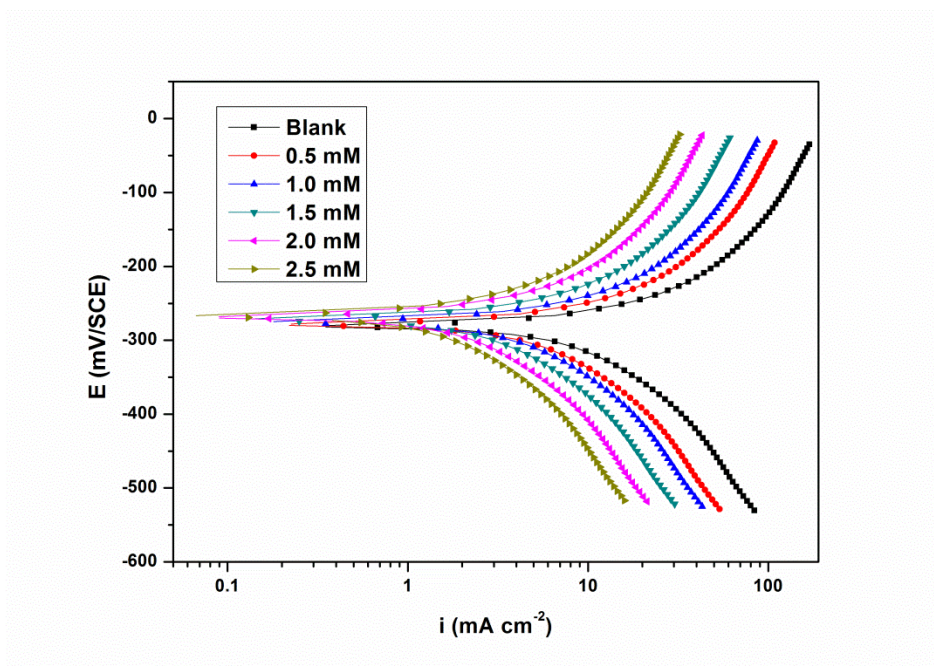


Fig. 3.75: Potentiodynamic polarization curves for the corrosion of weld aged maraging steel in 2.0 M sulphuric acid containing different concentrations of CPOM at 30 °C.

It is seen from the Tables that the i_{corr} decreases and the inhibition efficiency ($\eta\%$) increases with the increase in the inhibitor concentration. The presence of CPOM shifts E_{corr} slightly towards positive direction. Therefore it can be concluded that CPOM acts as a mixed type inhibitor on weld aged maraging steel. The rest of the discussion is similar to the discussion regarding the inhibition behaviour of ATPI, under the section 3.8.1. CPOM shows slightly lower inhibition efficiency than that of ATPI and CPOB for the corrosion of weld aged maraging steel in sulphuric acid.

3.10.2 Electrochemical impedance spectroscopy

Fig. 3.76 represents Nyquist plots for the corrosion of weld aged of maraging steel in 2.0 M sulphuric acid in the presence of different concentrations of CPOM at 30 °C. Similar plots were obtained in other concentrations of sulphuric acid and also at other temperatures. The impedance parameters derived from the EIS studies are summarized in Tables 3.103 to 3.107.

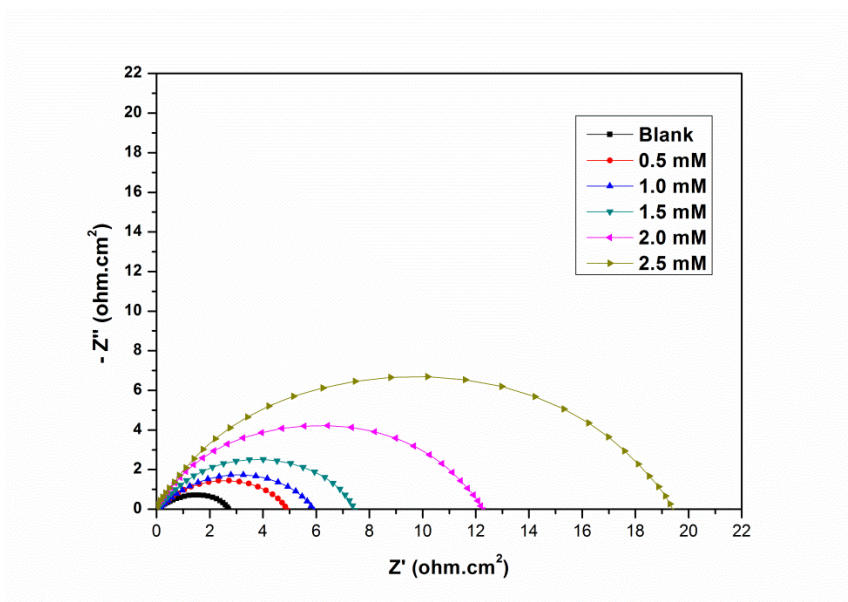


Fig. 3.76: Nyquist plots for the corrosion of weld aged maraging steel in 2.0 M sulphuric acid containing different concentrations of CPOM at 30 °C.

It is clear from Fig. 3.76 that the shapes of the impedance plots for the corrosion of weld aged maraging steel in the presence of inhibitor are not substantially different from those of the uninhibited one. The plots are similar to those obtained in the presence of CPOB as discussed in the earlier section 3.8.2. The equivalent circuit given in Fig. 3.20 is used to fit the experimental data for the corrosion of weld aged maraging steel in sulphuric acid in the presence of CPOM. As can be seen from the Tables, R_{ct} , R_{pf} values increase and C_{dl} , C_{pf} values decrease with the increase in the concentration of CPOM which suggests decrease in corrosion rate.

The Bode plots for the corrosion of the alloy in the presence of different concentrations of CPOM are shown in Fig. 3.77. Phase angle increases with the increase in the concentrations of CPOM in sulphuric acid. The discussion regarding the Bode plot under the section 3.3.2 holds good for CPOM also.

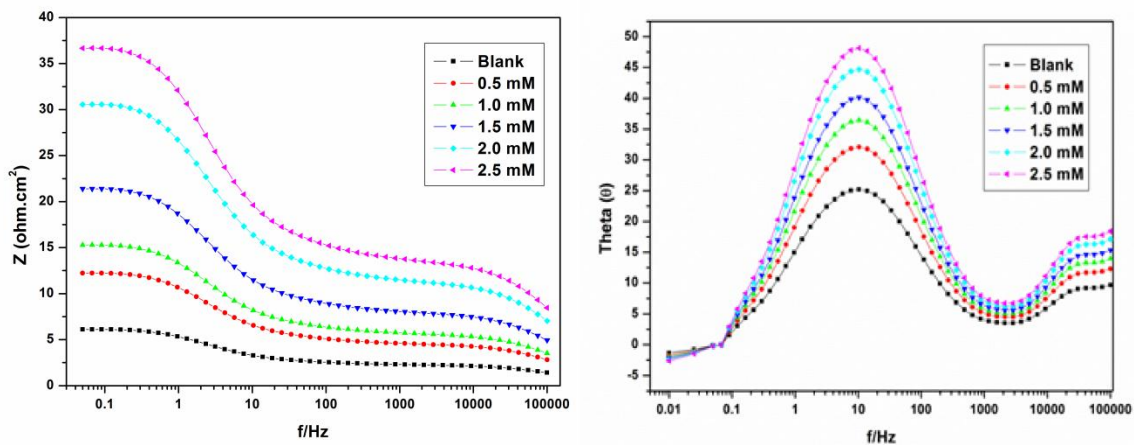


Fig. 3.77: Bode plots for the corrosion of weld aged maraging steel in 2.0 M sulphuric acid containing different concentrations of CPOM at 30 °C.

A comparison of maximum attainable inhibition efficiency by the Tafel method and EIS method, in the presence of CPOM for the corrosion of weld aged maraging steel in sulphuric acid solutions of different concentrations at 30 °C are listed in Table 3.108. It

is evident from the table that the η (%) values obtained by the two methods are in good agreement. Similar levels of agreement were obtained at other temperatures also.

3.10.3 Effect of temperature

The Tafel and EIS results pertaining to different temperatures in different concentrations of sulphuric acid have already been listed in Tables 3.98 to 3.107. The effect of temperature on corrosion inhibition behaviour of CPOM is similar to that of ATPI and CPOB on weld aged maraging steel as discussed in the earlier sections. The decrease in the inhibition efficiency of CPOM with the increase in temperature on weld aged maraging steel surface may be attributed to the physisorption of CPOM.

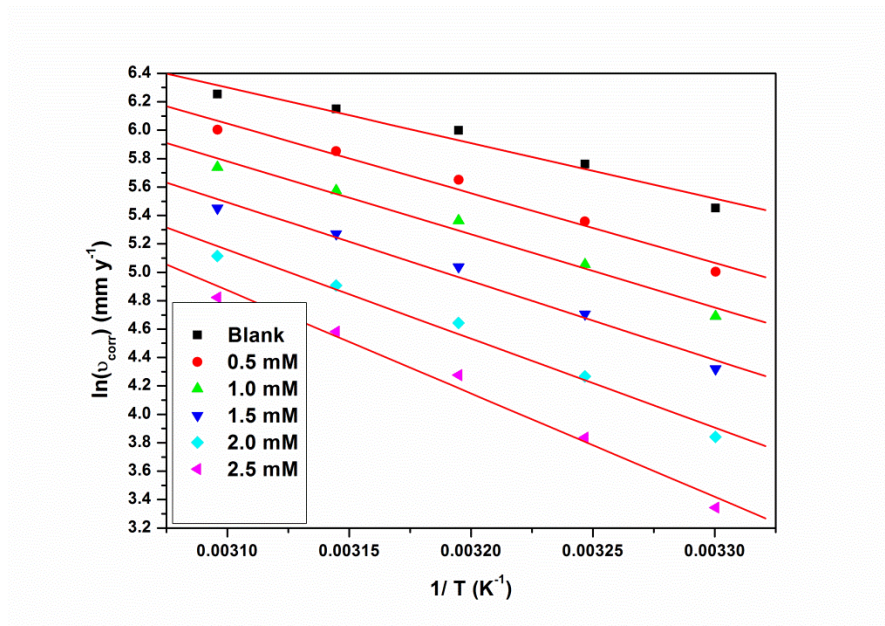


Fig. 3.78: Arrhenius plots for the corrosion of weld aged maraging steel in 2.0 M sulphuric acid containing different concentrations of CPOM.

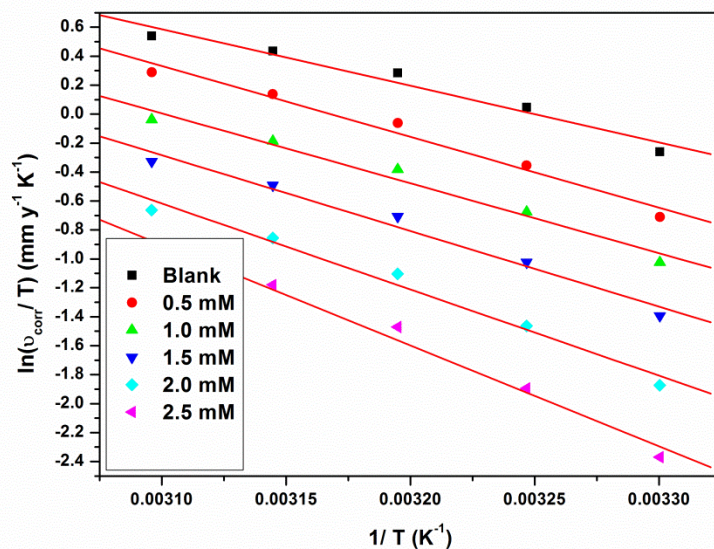


Fig. 3.79: Plots of $\ln(v_{\text{corr}}/T)$ versus $1/T$ for the corrosion of weld aged maraging steel in 2.0 M sulphuric acid containing different concentrations of CPOM.

The Arrhenius plots for the corrosion of weld aged maraging steel in 2.0 M sulphuric acid in the presence of different concentrations of CPOM are shown in Fig. 3.78. The plots of $\ln(v_{\text{corr}}/T)$ vs $(1/T)$ are shown in Fig. 3.79. The calculated values of activation parameters are given in Table 3.109.

The increase in the E_a values with the increase in CPOM concentration indicates the increase in energy barrier for the corrosion reaction as discussed in earlier sections. The entropy of activation in the absence and presence of CPOM is large and negative for the corrosion of alloy. This implies that the activated complex in the rate determining step represents an association rather than dissociation step, indicating that a decrease in disordering takes place on going from reactants to activated complex (Marsh 1988, Gomma and Wahdan 1995).

3.10.4 Effect of sulphuric acid concentration

It is evident from both the polarization and EIS experimental results that, for a particular concentration of the CPOM, the inhibition efficiency decreases with the

increase in sulphuric acid concentration on weld aged maraging steel. The maximum inhibition efficiency is observed in 0.1 M solution.

3.10.5 Adsorption isotherms

The adsorption of CPOM on the surfaces of weld aged maraging steel was found to obey Langmuir adsorption isotherm as shown in Fig. 3.80. The thermodynamic parameters obtained for the adsorption of CPOM are tabulated in Tables 3.110. These data also reveal similar inhibition behaviour of CPOM as that of ATPI as discussed in section 3.8.5. The values of ΔG_{ads}^0 and ΔH_{ads}^0 suggest both physisorption and chemisorption of CPOM on weld aged maraging steel with predominant physisorption. The ΔS_{ads}^0 value values indicate increase in randomness on going from the reactants to the metal adsorbed species.

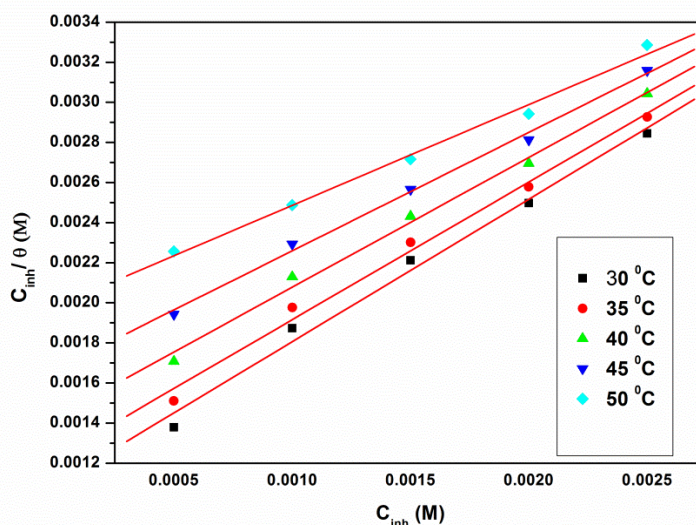


Fig. 3.80: Langmuir adsorption isotherms for the adsorption of CPOM on weld aged maraging steel in 2.0 M sulphuric acid at different temperatures.

3.10.6 Mechanism of corrosion inhibition

The mechanism of corrosion inhibition of weld aged maraging steel in the presence of CPOM is similar to that of ATPI as discussed under section 3.8.6. The

protonated CPOM is responsible for physisorption and neutral CPOM molecule with lone pair of electrons on oxygen and π - electrons of benzene rings are responsible for chemisorption of CPOM on the alloy surfaces, as discussed in earlier sections.

3.10.7 SEM/EDS studies

Fig. 3.81 (a) represents the SEM image of the corroded weld aged maraging steel sample which shows the facets due to the attack of sulphuric acid on the metal surface with cracks and rough surfaces. Fig. 3.81 (b) shows the SEM image of the sample after immersion in 2.0 M sulphuric acid in the presence of CPOM. It can be seen that the alloy surface is smooth without any visible corrosion attack. Thus, it can be concluded that CPOM protects the alloy from corrosion by forming a uniform film on the alloy surface.

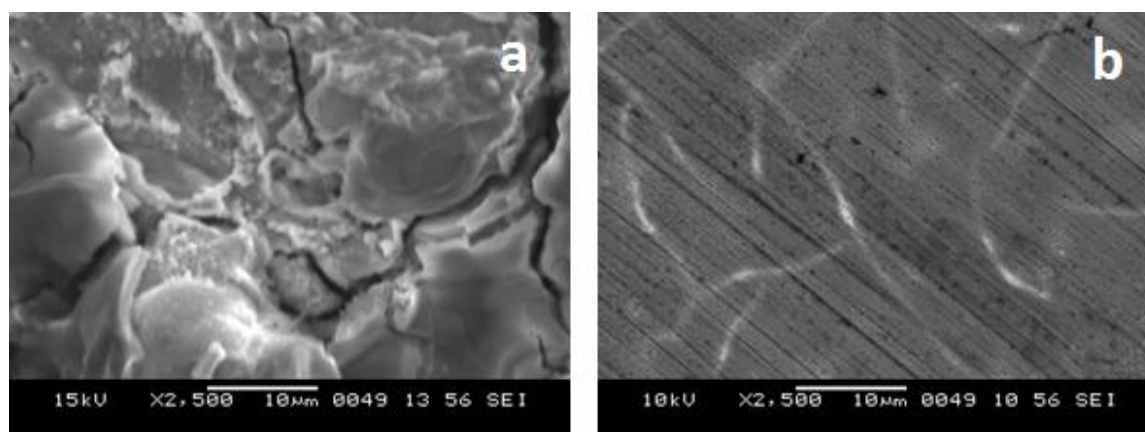


Fig. 3.81: SEM images of the weld aged maraging steel after immersion in 2.0 M sulphuric acid a) in the absence and b) in the presence of CPOM.

The EDS profile of the corroded surface of the alloy in the presence of CPOM is shown in Fig. 3.82. The atomic percentages of the elements found in the EDS profile for inhibited metal surface were 7.25 % Fe, 1.84% Ni, 2.33% Mo, 22.19% O, 2.66% Cl, 3.57% S, 66.58 % C and 4.09% Br and indicated the formation of inhibitor film on the surface of alloy.

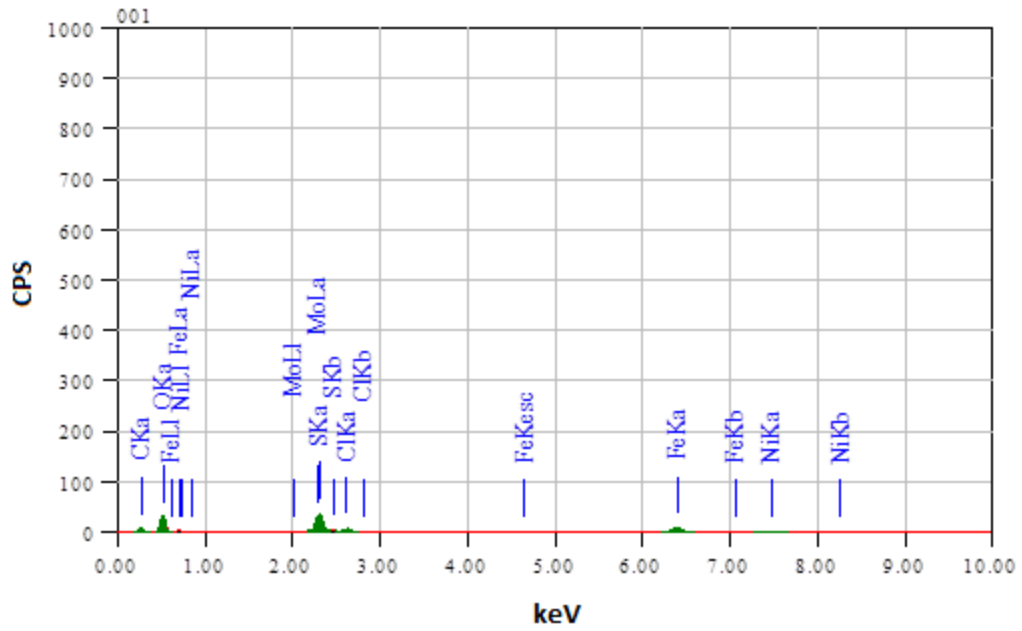


Fig. 3.82: EDS spectra of the weld aged maraging steel after immersion in 2.0 M sulphuric acid in the presence of CPOM.

Table 3.98: Results of potentiodynamic polarization studies for the corrosion of weld aged maraging steel in 0.1 M sulphuric acid containing different concentrations of CPOM.

Temperature (°C)	Conc. of inhibitor (mM)	E_{corr} (mV /SCE)	b_a (mV dec ⁻¹)	$-b_c$ (mV dec ⁻¹)	i_{corr} (mA cm ⁻²)	v_{corr} (mm y ⁻¹)	η (%)
30	Blank	-371±3	221±2	266±2	0.78±0.04	8.99±0.43	
	0.2	-370±3	216±2	262±3	0.45±0.04	5.13±0.39	42.8
	0.4	-372±3	214±2	257±3	0.32±0.02	3.72±0.20	58.6
	0.6	-369±1	210±2	254±1	0.22±0.01	2.52±0.11	71.9
	0.8	-367±1	207±1	251±1	0.13±0.04	1.51±0.41	83.2
	1.0	-364±3	202±3	248±1	0.07±0.02	0.86±0.22	90.4
35	Blank	-368±3	257±1	283±2	1.27±0.14	14.64±1.61	
	0.2	-369±3	255±2	279±2	0.75±0.01	8.68±0.13	40.6
	0.4	-365±1	250±3	274±2	0.56±0.03	6.44±0.34	55.9
	0.6	-361±3	248±1	271±2	0.41±0.04	4.66±0.40	68.1
	0.8	-358±2	245±3	267±1	0.25±0.02	2.82±0.15	80.7
	1.0	-354±2	242±3	262±2	0.15±0.05	1.68±0.46	88.5
40	Blank	-365±1	289±1	296±3	1.99±0.22	22.95±2.61	
	0.2	-362±3	287±2	293±2	1.23±0.01	14.10±0.11	38.4
	0.4	-360±3	282±1	289±2	0.92±0.03	10.62±0.26	53.6
	0.6	-357±1	279±2	284±3	0.68±0.05	7.78±0.48	66.0
	0.8	-354±3	274±1	280±2	0.44±0.02	5.06±0.18	77.9
	1.0	-350±2	269±3	275±3	0.27±0.01	3.16±0.11	86.2
45	Blank	-362±3	295±1	317±1	2.21±0.05	25.48±0.48	
	0.2	-364±1	290±2	314±2	1.40±0.02	16.07±0.22	36.8
	0.4	-359±1	287±2	312±1	1.09±0.02	12.59±0.23	50.5
	0.6	-355±2	285±1	307±1	0.81±0.02	9.31±0.17	63.4
	0.8	-352±1	281±3	303±3	0.55±0.05	6.31±0.47	75.2
	1.0	-347±3	278±3	299±2	0.38±0.01	4.32±0.15	83.0
50	Blank	-359±3	298±1	321±1	2.47±0.22	28.48±2.52	
	0.2	-356±2	294±1	316±1	1.66±0.02	19.13±0.16	32.7
	0.4	-353±2	290±3	312±2	1.30±0.04	14.95±0.39	47.4
	0.6	-350±3	287±1	310±1	0.98±0.02	11.31±0.24	60.2
	0.8	-346±3	285±1	305±2	0.68±0.03	7.79±0.33	72.6
	1.0	-342±2	281±1	299±2	0.49±0.05	5.63±0.50	80.2

Table 3.99: Results of potentiodynamic polarization studies for the corrosion of weld aged maraging steel in 0.5 M sulphuric acid containing different concentrations of CPOM.

Temperature (°C)	Conc. of inhibitor (mM)	E_{corr} (mV /SCE)	b_a (mV dec ⁻¹)	$-b_c$ (mV dec ⁻¹)	i_{corr} (mA cm ⁻²)	v_{corr} (mm y ⁻¹)	η (%)
30	Blank	-356±1	235±1	268±2	1.80±0.17	20.71±2.66	
	0.2	-355±1	230±2	262±2	1.10±0.15	12.60±1.52	39.1
	0.4	-352±1	227±3	260±3	0.80±0.18	9.19±1.84	55.6
	0.6	-348±1	225±3	257±3	0.55±0.06	6.32±0.60	69.4
	0.8	-345±3	222±1	255±2	0.34±0.17	3.89±1.71	81.2
	1.0	-341±3	220±2	251±3	0.20±0.10	2.33±1.15	88.7
	35	Blank	-353±1	257±3	276±3	2.41±0.12	27.73±1.17
0.2		-351±1	253±3	271±2	1.51±0.20	17.40±1.99	37.2
0.4		-347±3	250±3	269±1	1.12±0.07	12.93±0.68	53.3
0.6		-344±2	248±3	265±2	0.81±0.13	9.37±1.30	66.2
0.8		-340±3	244±2	262±1	0.50±0.08	5.70±0.82	79.4
1.0		-339±1	240±3	257±1	0.30±0.11	3.42±1.53	87.6
40		Blank	-350±3	279±1	288±2	3.83±0.11	44.07±1.27
	0.2	-348±1	273±2	282±3	2.49±0.18	28.67±1.75	34.9
	0.4	-344±1	270±1	280±3	1.88±0.12	21.62±1.21	50.9
	0.6	-341±1	267±2	277±2	1.38±0.17	15.87±1.75	63.9
	0.8	-339±3	265±1	274±3	0.90±0.20	10.35±1.97	76.5
	1.0	-334±2	260±1	271±2	0.56±0.17	6.50±1.73	85.2
	45	Blank	-348±1	296±3	297±3	4.01±0.28	46.14±2.47
0.2		-344±2	293±3	294±3	2.68±0.15	30.80±1.49	33.2
0.4		-341±3	290±3	290±1	2.10±0.06	24.14±0.64	47.6
0.6		-337±2	288±2	285±1	1.55±0.05	17.88±0.54	61.2
0.8		-336±1	286±2	281±3	1.06±0.11	12.15±1.09	73.6
1.0		-332±1	282±3	277±1	0.73±0.06	8.36±0.60	81.8
50		Blank	-346±3	315±1	306±3	4.30±0.18	49.47±1.82
	0.2	-344±1	310±3	301±2	3.06±0.16	35.16±1.61	28.9
	0.4	-342±3	298±3	297±3	2.39±0.18	27.50±1.82	44.4
	0.6	-339±2	294±2	295±1	1.81±0.16	20.84±1.61	57.8
	0.8	-337±2	291±1	291±2	1.25±0.13	14.38±1.32	70.9
	1.0	-335±3	288±3	289±3	0.91±0.06	10.42±0.63	78.9

Table 3.100: Results of potentiodynamic polarization studies for the corrosion of weld aged maraging steel in 1.0 M sulphuric acid containing different concentrations of CPOM.

Temperature (°C)	Conc. of inhibitor (mM)	E_{corr} (mV /SCE)	b_a (mV dec ⁻¹)	$-b_c$ (mV dec ⁻¹)	i_{corr} (mA cm ⁻²)	v_{corr} (mm y ⁻¹)	η (%)
30	Blank	-323±1	247±1	301±1	8.56±0.12	98.49±1.22	
	0.3	-319±1	242±3	299±1	5.01±0.23	57.62±2.31	41.9
	0.6	-314±3	240±2	294±3	3.59±0.24	41.30±2.37	58.7
	0.9	-312±3	239±1	292±2	2.37±0.20	27.26±2.00	72.8
	1.2	-310±1	235±3	290±1	1.36±0.21	15.60±2.06	84.8
	1.5	-308±1	233±3	288±2	0.64±0.17	7.42±1.67	92.5
	35	Blank	-318±1	276±1	303±1	12.80±0.21	147.27±2.10
0.3		-314±1	272±1	300±2	7.80±0.19	89.70±1.87	39.1
0.6		-311±2	270±3	297±1	5.63±0.17	64.74±1.67	56.1
0.9		-308±1	268±3	293±3	3.80±0.19	43.70±1.94	70.3
1.2		-306±1	266±1	290±3	2.25±0.18	25.83±1.78	82.5
1.5		-302±2	261±2	288±2	1.26±0.20	14.45±2.01	90.2
40		Blank	-309±1	292±3	305±3	16.93±0.29	194.44±2.93
	0.3	-304±2	288±2	300±3	10.70±0.23	123.16±2.29	36.7
	0.6	-301±2	286±1	298±2	7.81±0.14	89.87±1.41	53.8
	0.9	-300±2	282±2	296±1	5.37±0.24	61.81±2.45	68.2
	1.2	-298±3	280±3	294±3	3.30±0.23	37.99±2.32	80.5
	1.5	-296±1	279±1	290±1	1.98±0.12	22.81±1.22	88.3
	45	Blank	-307±2	298±2	307±3	19.40±0.38	223.21±3.77
0.3		-305±3	294±1	302±3	12.86±0.22	147.99±2.23	33.7
0.6		-300±2	291±3	300±1	9.51±0.23	109.39±2.29	51.2
0.9		-299±2	288±1	299±2	6.68±0.19	76.85±1.94	65.6
1.2		-295±2	285±2	295±2	4.28±0.14	49.24±1.37	77.9
1.5		-292±3	281±1	292±1	2.75±0.19	31.63±1.86	85.8
50		Blank	-305±2	312±1	311±3	22.15±0.23	253.12±2.25
	0.3	-300±2	308±3	309±3	15.27±0.14	175.68±1.35	30.9
	0.6	-298±1	305±1	305±3	11.41±0.24	131.28±2.37	48.4
	0.9	-294±3	302±1	301±1	8.15±0.12	93.83±1.23	63.1
	1.2	-290±2	300±1	299±3	5.39±0.15	62.04±1.48	75.6
	1.5	-288±1	299±1	296±1	3.63±0.15	41.78±1.46	83.6

Table 3.101: Results of potentiodynamic polarization studies for the corrosion of weld aged maraging steel in 1.5 M sulphuric acid containing different concentrations of CPOM.

Temperature (°C)	Conc. of inhibitor (mM)	E_{corr} (mV /SCE)	b_a (mV dec ⁻¹)	$-b_c$ (mV dec ⁻¹)	i_{corr} (mA cm ⁻²)	v_{corr} (mm y ⁻¹)	η (%)
30	Blank	-295±1	252±3	260±2	17.00±0.36	195.50±3.61	
	0.4	-290±2	245±2	256±2	10.34±0.39	118.94±3.86	39.2
	0.8	-287±2	241±2	252±1	7.46±0.35	85.79±3.52	56.1
	1.2	-284±3	238±1	248±3	5.03±0.28	57.84±2.80	70.4
	1.6	-281±1	235±1	245±2	2.96±0.34	34.09±3.44	82.6
	2.0	-278±2	233±3	242±3	1.65±0.18	18.99±1.83	90.3
	35	Blank	-291±2	253±2	272±2	23.60±0.21	271.53±2.06
0.4		-288±3	248±1	268±1	14.95±0.27	171.99±2.69	36.7
0.8		-285±3	244±3	265±2	10.91±0.28	125.50±2.76	53.8
1.2		-281±2	241±3	261±1	7.50±0.28	86.32±2.80	68.2
1.6		-277±2	238±1	255±1	4.61±0.32	53.03±3.22	80.5
2.0		-272±1	235±3	251±2	2.77±0.11	31.85±1.11	88.3
40		Blank	-288±1	254±2	276±2	28.00±0.25	332.15±2.55
	0.4	-285±2	249±2	272±2	18.56±0.36	213.59±3.57	33.7
	0.8	-281±2	244±2	268±2	13.72±0.30	157.89±2.96	51.1
	1.2	-277±1	241±3	263±3	9.64±0.39	110.92±3.93	65.6
	1.6	-273±1	238±2	260±3	6.17±0.29	71.04±2.87	78.0
	2.0	-270±1	235±2	257±1	3.97±0.22	45.65±2.20	85.8
	45	Blank	-285±3	266±1	283±2	30.30±0.26	348.61±2.58
0.4		-281±3	263±3	279±3	21.06±0.35	242.25±3.50	30.5
0.8		-278±3	260±2	275±1	15.77±0.34	181.39±3.39	48.1
1.2		-275±2	257±2	271±2	11.30±0.45	130.03±4.46	62.7
1.6		-271±3	252±2	268±2	7.51±0.22	86.46±2.25	75.2
2.0		-268±3	248±3	263±2	5.10±0.21	58.71±2.13	83.2
50		Blank	-283±2	272±2	296±1	33.01±0.49	379.62±2.88
	0.4	-280±1	268±3	293±1	24.13±0.34	277.62±3.35	26.9
	0.8	-278±2	265±2	290±3	18.31±0.45	210.65±4.47	44.5
	1.2	-274±3	262±3	288±1	13.40±0.46	154.19±4.64	59.4
	1.6	-270±1	258±1	285±1	9.23±0.37	106.24±3.72	72.2
	2.0	-267±1	252±2	281±3	6.58±0.26	75.71±2.60	80.1

Table 3.102: Results of Tafel polarization studies for the corrosion of weld aged maraging steel in 2.0 M sulphuric acid containing different concentrations of CPOM.

Temperature (°C)	Conc. of inhibitor (mM)	E_{corr} (mV /SCE)	b_a (mV dec ⁻¹)	$-b_c$ (mV dec ⁻¹)	i_{corr} (mA cm ⁻²)	v_{corr} (mm y ⁻¹)	η (%)
30	Blank	-281±2	223±3	251±1	20.31±0.31	233.54±3.14	
	0.5	-279±1	218±3	247±3	12.94±0.27	148.90±2.73	36.3
	1.0	-277±1	214±3	244±2	9.47±0.12	108.91±1.19	53.4
	1.5	-273±1	211±1	241±1	6.53±0.20	75.18±2.02	67.8
	2.0	-270±3	208±1	239±3	4.05±0.15	46.55±1.52	80.1
	2.5	-268±3	205±3	236±2	2.46±0.11	28.33±1.14	87.9
35	Blank	-279±1	245±2	263±2	27.65±0.35	317.55±3.54	
	0.5	-277±2	240±3	258±3	18.47±0.21	212.47±2.13	33.1
	1.0	274±4	238±3	255±3	13.64±0.35	156.90±3.48	50.6
	1.5	-271±1	236±3	251±3	9.62±0.25	110.64±2.50	65.2
	2.0	-269±2	234±3	248±2	6.20±0.38	71.29±3.75	77.6
	2.5	-265±1	230±3	246±2	4.02±0.18	46.30±1.76	85.4
40	Blank	-278±1	269±2	274±2	35.04±0.37	402.62±3.74	
	0.5	-275±1	265±1	270±2	24.75±0.55	284.79±3.51	29.3
	1.0	-272±2	262±2	267±2	18.56±0.51	213.59±3.14	47.1
	1.5	-270±1	260±2	265±3	13.41±0.40	154.31±4.01	61.7
	2.0	-266±2	258±2	262±3	9.03±0.28	103.94±2.83	74.2
	2.5	-262±3	255±2	259±3	6.25±0.43	71.92±1.30	82.1
45	Blank	-275±1	281±2	288±3	40.74±0.41	468.28±4.10	
	0.5	-271±1	278±2	284±2	30.22±0.27	347.74±2.69	25.7
	1.0	-268±3	274±1	280±3	22.95±0.36	264.11±3.61	43.6
	1.5	-265±1	271±1	278±1	16.91±0.29	194.52±2.95	58.5
	2.0	-261±1	269±3	277±3	11.76±0.46	135.33±4.59	71.1
	2.5	-258±2	266±2	272±2	8.49±0.18	97.73±1.78	79.1
50	Blank	-273±2	301±1	302±3	45.27±0.28	520.05±2.76	
	0.5	-269±3	297±3	298±2	35.18±0.20	404.81±2.99	22.2
	1.0	-265±3	292±2	296±1	27.03±0.46	310.99±4.63	40.2
	1.5	-261±3	288±1	294±1	20.25±0.30	232.93±3.97	55.2
	2.0	-257±3	283±1	291±2	14.47±0.23	166.52±2.29	68.0
	2.5	-255±1	280±1	289±1	10.81±0.19	124.34±1.88	76.1

Table 3.103: EIS data for the corrosion of weld aged maraging steel in 0.1 M sulphuric acid containing different concentrations of CPOM.

Temperature (°C)	Conc. of inhibitor (mM)	R _{ct} (ohm. cm ²)	C _{dl} (mF cm ⁻²)	R _{pf} (ohm. cm ²)	C _{pf} (mF cm ⁻²)	η (%)
30	Blank	74.66±2.75	21.01±2.84			
	0.2	133.08±2.85	13.17±2.03	9.46±1.48	3.73±1.12	43.9
	0.4	186.65±2.73	9.45±3.87	12.40±2.05	2.69±0.47	60.1
	0.6	282.80±3.95	6.31±3.13	17.68±3.15	1.81±0.86	73.6
	0.8	501.07±3.65	3.66±2.16	29.67±1.51	1.06±0.81	85.1
	1.0	995.47±2.01	1.95±0.51	56.84±2.63	0.58±0.15	92.5
35	Blank	51.17±2.17	26.57±2.85			
	0.2	87.02±3.69	16.95±3.82	7.77±1.02	4.79±0.62	41.2
	0.4	123.30±3.71	12.03±3.95	10.11±1.17	3.41±0.26	58.5
	0.6	179.54±2.65	8.33±2.12	13.75±3.39	2.37±0.71	71.5
	0.8	284.28±2.77	5.34±1.58	20.52±1.28	1.54±0.58	82.2
	1.0	511.70±2.45	3.07±0.24	35.21±2.32	0.90±0.33	90.0
40	Blank	35.45±2.38	32.14±3.45			
	0.2	58.02±2.66	21.66±2.87	6.43±1.80	6.12±1.27	38.9
	0.4	80.20±2.89	15.73±2.56	8.06±3.28	4.45±0.61	55.8
	0.6	108.41±2.29	11.69±3.71	10.14±2.83	3.32±0.78	67.3
	0.8	168.01±3.98	7.62±1.21	14.54±2.56	2.18±0.72	78.9
	1.0	283.60±2.38	4.60±1.57	23.08±2.53	1.33±0.45	87.5
45	Blank	33.36±3.90	36.48±3.21			
	0.2	51.88±3.89	25.65±3.76	5.62±2.85	7.24±1.34	35.7
	0.4	70.08±3.99	19.05±2.36	6.84±1.25	5.38±0.65	52.4
	0.6	91.40±2.86	14.65±2.63	8.27±3.25	4.15±1.09	63.5
	0.8	134.52±2.44	10.03±2.17	11.17±1.16	2.85±0.87	75.2
	1.0	222.40±2.76	6.15±1.46	17.06±2.56	1.76±0.43	85.2
50	Blank	30.19±3.30	41.49±3.85			
	0.2	45.47±2.12	30.13±2.57	5.04±2.34	8.49±1.15	33.6
	0.4	59.20±2.69	23.20±3.51	5.92±2.72	6.55±0.35	49.3
	0.6	76.43±3.47	18.02±3.63	7.02±1.80	5.09±0.67	60.5
	0.8	108.60±2.41	12.75±2.68	9.07±2.99	3.61±1.00	72.2
	1.0	167.72±3.38	8.33±1.30	12.85±1.80	2.37±0.26	82.0

Table 3.104: EIS data for the corrosion of weld aged maraging steel in 0.5 M sulphuric acid containing different concentrations of CPOM.

Temperature (°C)	Conc. of inhibitor (mM)	R_{ct} (ohm. cm ²)	C_{dl} (mF cm ⁻²)	R_{pf} (ohm. cm ²)	C_{pf} (mF cm ⁻²)	η (%)
30	Blank	33.56±2.84	4.01±1.82			
	0.2	57.76±3.77	2.51±0.95	5.78±1.48	0.74±0.27	41.9
	0.4	81.22±2.45	1.79±0.88	7.34±1.66	0.54±0.18	58.7
	0.6	123.52±3.84	1.19±0.50	10.15±2.46	0.37±0.04	72.8
	0.8	221.37±2.06	0.67±0.29	16.66±1.27	0.22±0.12	84.8
	1.0	446.87±3.06	0.34±0.15	31.65±2.70	0.13±0.05	92.5
35	Blank	26.64±2.21	6.59±2.62			
	0.2	44.36±3.24	4.23±1.41	4.68±1.46	1.22±0.34	40.1
	0.4	59.72±2.15	3.15±0.72	5.63±1.76	0.92±0.33	55.4
	0.6	87.32±2.63	2.16±0.70	7.34±1.88	0.64±0.47	69.5
	0.8	148.16±2.57	1.28±0.29	11.10±1.82	0.40±0.21	82.3
	1.0	251.32±2.23	0.77±0.08	17.48±2.66	0.25±0.16	89.4
40	Blank	17.85±3.55	10.98±2.94			
	0.2	28.60±3.34	7.24±2.65	4.00±1.12	2.07±0.33	37.6
	0.4	37.91±3.70	5.47±1.56	4.67±1.21	1.57±0.33	52.9
	0.6	54.47±2.41	3.81±1.87	5.86±2.54	1.11±0.22	67.2
	0.8	85.08±2.69	2.45±0.77	8.07±2.21	0.72±0.30	79.1
	1.0	136.57±3.08	1.54±0.25	11.78±1.85	0.47±0.19	86.9
45	Blank	17.84±2.86	12.56±1.66			
	0.2	27.82±3.55	8.51±1.84	3.42±1.05	2.42±0.49	35.9
	0.4	36.10±2.23	6.61±2.01	3.86±1.03	1.89±0.31	50.6
	0.6	50.17±3.07	4.82±1.06	4.61±1.11	1.39±0.22	64.4
	0.8	77.94±2.67	3.18±1.08	6.09±1.76	0.93±0.35	77.1
	1.0	115.02±3.85	2.22±0.60	8.07±1.93	0.66±0.23	84.5
50	Blank	17.42±3.34	15.83±1.86			
	0.2	25.80±2.05	11.63±2.52	2.87±0.51	3.30±0.35	32.5
	0.4	33.03±3.38	9.09±1.98	3.13±0.79	2.59±0.40	47.3
	0.6	44.67±2.18	6.73±1.72	3.55±1.53	1.93±0.36	61.3
	0.8	67.86±3.90	4.43±0.36	4.38±1.31	1.28±0.22	74.3
	1.0	94.11±2.58	3.20±0.43	5.33±2.01	0.93±0.17	81.5

Table 3.105: EIS data for the corrosion of weld aged maraging steel in 1.0 M sulphuric acid containing different concentrations of CPOM

Temperature (°C)	Conc. of inhibitor (mM)	R_{ct} (ohm. cm ²)	C_{dl} (mF cm ⁻²)	R_{pf} (ohm. cm ²)	C_{pf} (mF cm ⁻²)	η (%)
30	Blank	7.09±1.92	11.00±2.81			
	0.3	12.60±1.11	7.02±1.21	3.26±0.52	2.01±0.27	43.7
	0.6	18.04±1.38	4.97±1.27	3.84±0.07	1.43±0.23	60.7
	0.9	28.34±1.26	3.24±1.05	4.92±0.73	0.95±0.49	75
	1.2	55.00±1.15	1.78±0.76	7.73±1.85	0.54±0.20	87.1
	1.5	137.40±2.73	0.84±0.21	16.39±1.81	0.27±0.06	94.8
35	Blank	5.05±1.22	11.83±2.97			
	0.3	8.54±1.18	7.10±1.71	2.64±0.21	2.03±0.39	40.9
	0.6	12.03±1.70	5.11±1.58	2.93±0.31	1.47±0.26	58
	0.9	18.33±2.93	3.43±0.81	3.45±0.83	1.00±0.42	72.5
	1.2	33.03±2.49	2.00±0.41	4.66±0.89	0.60±0.26	84.7
	1.5	67.51±2.84	1.09±0.54	7.51±1.84	0.34±0.10	92.5
40	Blank	3.95±1.27	12.37±2.45			
	0.3	6.42±1.36	8.18±1.89	2.45±0.50	2.33±0.30	38.4
	0.6	8.92±1.74	5.94±0.83	2.65±0.74	1.70±0.43	55.7
	0.9	13.30±1.93	4.06±0.79	3.01±0.20	1.18±0.37	70.3
	1.2	22.82±2.10	2.46±0.80	3.77±0.93	0.73±0.21	82.7
	1.5	41.93±2.55	1.44±0.21	5.30±1.75	0.44±0.14	90.6
45	Blank	3.49±0.73	15.26±2.03			
	0.3	5.34±1.63	10.60±1.64	2.33±0.71	3.01±0.39	35.5
	0.6	7.33±1.25	7.79±1.96	2.48±0.24	2.22±0.35	52.9
	0.9	10.66±1.14	5.42±1.56	2.73±0.61	1.56±0.21	67.7
	1.2	17.37±2.66	3.41±1.04	3.22±0.77	0.99±0.27	80.1
	1.5	29.02±2.88	2.13±0.76	4.08±1.27	0.63±0.18	88.1
50	Blank	3.15±0.87	18.08±2.87			
	0.3	4.68±0.17	11.63±1.82	2.26±0.40	3.30±0.44	32.6
	0.6	6.33±1.40	8.65±1.36	2.38±0.51	2.46±0.31	50.3
	0.9	9.04±1.62	6.13±1.52	2.56±0.17	1.76±0.34	65.2
	1.2	14.18±1.39	3.99±1.75	2.92±0.55	1.16±0.33	77.8
	1.5	22.23±1.30	2.62±1.60	3.47±0.24	0.77±0.16	85.8

Table 3.106: EIS data for the corrosion of weld aged maraging steel in 1.5 M sulphuric acid containing different concentrations of CPOM.

Temperature (°C)	Conc. of inhibitor (mM)	R_{ct} (ohm. cm ²)	C_{dl} (mF cm ⁻²)	R_{pf} (ohm. cm ²)	C_{pf} (mF cm ⁻²)	η (%)
30	Blank	3.34±0.99	13.71±2.47			
	0.4	5.67±1.23	8.43±1.70	2.44±0.17	2.44±0.93	41.1
	0.8	7.99±1.16	6.13±1.58	2.66±0.82	2.29±0.09	58.2
	1.2	12.22±1.31	4.12±1.60	3.04±1.02	2.10±0.82	72.7
	1.6	22.15±1.86	2.43±0.53	3.96±1.64	2.01±0.41	84.9
	2.0	45.88±2.77	1.29±0.19	6.14±1.05	2.00±0.59	92.7
35	Blank	2.46±0.52	14.52±1.68			
	0.4	4.02±1.31	8.89±1.91	2.27±0.35	2.46±0.77	38.8
	0.8	5.60±1.40	6.35±1.21	2.41±0.60	2.30±0.31	56.1
	1.2	8.37±1.60	4.29±0.76	2.65±0.35	2.18±0.32	70.6
	1.6	14.47±2.47	2.52±0.35	3.19±0.27	2.07±0.58	83.0
	2.0	26.97±2.30	1.45±0.20	4.28±1.51	2.01±0.24	90.9
40	Blank	2.09±0.49	16.09±2.76			
	0.4	3.24±0.26	11.19±2.12	2.12±0.99	2.61±0.99	35.5
	0.8	4.44±1.40	8.21±1.64	2.20±0.28	2.42±0.41	52.9
	1.2	6.46±1.01	5.71±1.38	2.32±0.19	2.27±0.12	67.7
	1.6	10.53±1.89	3.59±0.46	2.58±0.58	2.14±0.73	80.2
	2.0	17.58±2.49	2.24±0.18	3.02±1.79	2.06±1.38	88.1
45	Blank	2.01±0.25	18.30±2.98			
	0.4	2.98±2.00	13.61±2.35	2.10±0.48	2.76±0.10	32.6
	0.8	4.04±2.48	10.13±1.80	2.16±0.71	2.54±0.44	50.3
	1.2	5.77±3.47	7.16±1.80	2.26±0.55	2.36±0.29	65.2
	1.6	9.05±2.67	4.65±0.84	2.45±0.78	2.21±0.09	77.8
	2.0	14.17±2.89	3.05±0.16	2.76±0.92	2.11±0.75	85.8
50	Blank	1.90±0.54	21.47±2.67			
	0.4	2.69±3.07	16.87±2.98	2.07±0.21	2.96±0.71	29.4
	0.8	3.60±2.34	12.68±2.92	2.12±0.67	2.70±0.68	47.2
	1.2	5.03±3.60	9.14±1.19	2.20±0.32	2.48±0.20	62.2
	1.6	7.59±2.95	6.13±0.52	2.34±0.22	2.30±0.58	75.3
	2.0	11.24±3.09	4.22±0.65	2.54±0.18	2.18±0.32	83.1

Table 3.107: EIS data for the corrosion of weld aged maraging steel in 2.0 M sulphuric acid containing different concentrations of CPOM.

Temperature (°C)	Conc. of inhibitor (mM)	R_{ct} (ohm. cm ²)	C_{dl} (mF cm ⁻²)	R_{pf} (ohm. cm ²)	C_{pf} (mF cm ⁻²)	η (%)
30	Blank	2.58±0.36	16.43±1.63			
	0.5	4.23±0.88	11.19±1.92	2.22±0.95	3.18±1.63	39.1
	1.0	5.91±1.27	8.08±1.51	2.34±0.00	2.30±0.42	56.3
	1.5	8.87±1.13	5.45±2.41	2.55±0.22	1.57±0.39	70.9
	2.0	15.45±1.35	3.23±1.93	3.02±0.37	0.94±0.26	83.3
	2.5	29.25±1.95	1.81±0.65	4.01±0.29	0.54±0.18	91.2
35	Blank	2.04±0.91	17.22±1.86			
	0.5	3.18±1.44	12.42±1.90	2.15±0.11	3.52±1.34	35.9
	1.0	4.39±1.30	9.06±2.57	2.24±0.40	2.58±0.85	53.5
	1.5	6.42±1.13	6.26±2.27	2.39±0.35	1.79±0.67	68.2
	2.0	10.60±1.32	3.88±1.96	2.69±0.81	1.13±0.11	80.8
	2.5	18.07±1.01	2.37±0.43	3.23±0.13	0.70±0.14	88.7
40	Blank	1.72±0.38	19.51±2.71			
	0.5	2.51±1.09	14.68±2.04	2.07±0.18	4.16±1.65	31.6
	1.0	3.40±1.37	10.90±2.56	2.13±0.40	3.10±0.41	49.5
	1.5	4.82±1.06	7.75±1.90	2.22±0.97	2.21±0.61	64.3
	2.0	7.47±1.27	5.08±2.72	2.38±0.95	1.46±0.48	77.0
	2.5	11.46±0.82	3.39±0.75	2.62±0.07	0.99±0.43	85.1
45	Blank	1.55±0.42	23.85±1.60			
	0.5	2.16±1.33	18.09±2.76	2.03±0.23	5.11±0.52	28.2
	1.0	2.88±1.08	13.61±2.08	2.07±0.30	3.86±0.51	46.3
	1.5	4.00±0.76	9.85±2.71	2.13±0.18	2.80±0.45	61.3
	2.0	5.97±1.14	6.69±2.62	2.24±0.20	1.91±0.14	74.7
	2.5	8.68±0.87	4.67±0.40	2.38±0.76	1.35±0.51	82.2
50	Blank	1.48±0.37	26.08±1.88			
	0.5	1.90±1.07	22.95±1.65	2.00±0.35	6.48±0.26	22.2
	1.0	2.47±1.09	17.68±2.20	2.02±0.63	5.00±0.86	40.2
	1.5	3.30±1.19	13.30±1.62	2.05±0.43	3.77±0.54	55.2
	2.0	4.62±1.06	9.58±1.08	2.11±0.35	2.73±0.71	68.8
	2.5	6.19±1.03	7.21±0.68	2.17±0.19	2.06±0.43	76.1

Table 3.108: Comparison of maximum attainable inhibition efficiencies by the Tafel method and EIS method for the corrosion of weld aged maraging steel in sulphuric acid solutions of different concentrations in the presence of CPOM at 30 °C.

Molarity of sulphuric acid (M)	Conc. of CPOM (mM)	η (%)	
		Tafel	EIS
0.1	1.0	90.4	92.5
0.5	1.0	88.7	92.4
1.0	1.5	92.4	94.8
1.5	2.0	90.2	92.7
2.0	2.5	87.7	91.1

Table 3.109: Activation parameters for the corrosion of weld aged maraging steel in sulphuric acid containing different concentrations of CPOM.

Molarity of sulphuric acid (M)	Conc. of inhibitor (mM)	E_a ($\text{kJ}^{-1} \text{mol}^{-1}$)	ΔH^\ddagger ($\text{kJ}^{-1} \text{mol}^{-1}$)	ΔS^\ddagger ($\text{J mol}^{-1} \text{K}^{-1}$)
0.1	0.0	44.31	43.16	-88.32
	0.2	51.04	53.46	-59.48
	0.4	63.70	66.79	-49.57
	0.6	76.36	74.12	-41.46
	0.8	82.69	80.28	-31.54
	1.0	94.99	92.29	-20.73
	0.5	0.0	35.50	37.48
0.2		48.90	59.46	-75.11
0.4		59.05	71.79	-62.59
0.6		69.19	84.12	-52.35
0.8		74.26	90.28	-39.83
1.0		83.32	101.29	-26.17
1.0		0.0	32.79	28.11
	0.3	45.17	38.72	-97.03
	0.6	54.54	46.75	-80.86
	0.9	63.91	54.79	-67.63
	1.2	68.59	58.80	-51.46
	1.5	76.96	65.97	-33.81
1.5	0.0	25.24	23.69	-141.93
	0.4	34.77	32.63	-95.59
	0.8	41.98	39.40	-79.65
	1.2	49.19	46.17	-66.62
	1.6	52.80	49.56	-50.69
	2.0	59.24	55.60	-33.31
2.0	0.0	21.20	22.58	-142.28
	0.5	29.20	31.11	-95.82
	1.0	35.26	37.56	-79.85
	1.5	41.32	44.01	-66.78
	2.0	44.35	47.23	-50.81
	2.5	49.76	52.99	-33.39

Table 3.110: Thermodynamic parameters for the adsorption of CPOM on weld aged maraging steel surface in sulphuric acid at different temperatures.

Molarity of Sulphuric acid	Temperature (°C)	$-\Delta G^{\circ}_{\text{ads}}$ (kJ mol ⁻¹)	$\Delta H^{\circ}_{\text{ads}}$ (kJ mol ⁻¹)	$\Delta S^{\circ}_{\text{ads}}$ (J mol ⁻¹ K ⁻¹)
0.1	30	38.19	- 20.56	-42.40
	35	38.04		
	40	37.85		
	45	37.67		
	50	37.49		
0.5	30	37.49	-27.22	-35.29
	35	37.34		
	40	37.16		
	45	36.98		
	50	36.80		
1.0	30	36.89	-33.63	-28.79
	35	36.75		
	40	36.57		
	45	36.39		
	50	36.21		
1.5	30	33.59	-38.44	-20.98
	35	33.46		
	40	33.29		
	45	33.13		
	50	32.97		
2.0	30	32.60	-44.32	-16.77
	35	32.47		
	40	32.31		
	45	32.16		
	50	32.00		

3.11 (E)-1-(2,4-DINITROPHENYL)-2-[1-(2-NITROPHENYL) ETHYLIDENE] HYDRAZINE (DNPH) AS INHIBITOR FOR THE CORROSION OF WELD AGED MARAGING STEEL IN SULPHURIC ACID MEDIUM

3.11.1 Potentiodynamic polarization studies

The potentiodynamic polarization curves for the corrosion of weld aged maraging steel specimen in 0.5 M sulphuric acid in the presence of different concentrations of DNPH, at 30 °C are shown in Fig. 3.83. Similar plots were obtained in the other four concentrations of sulphuric acid at the different temperatures studied. The potentiodynamic polarization parameters (E_{corr} , b_c , b_a , i_{corr} and η (%)) were calculated from Tafel plots in all the five studied concentrations of sulphuric acid in the presence of different concentrations of DNPH at different temperatures and are summarized in Tables 3.111 to 3.115.

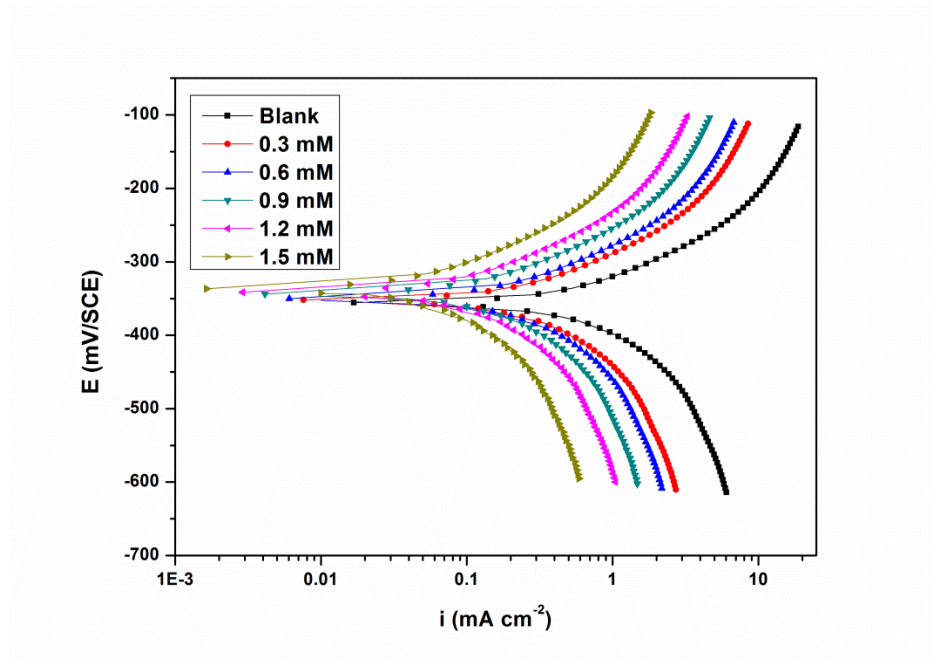


Fig. 3.83: Potentiodynamic polarization curves for the corrosion of weld aged maraging steel in 0.5 M sulphuric acid containing different concentrations of DNPH at 30 °C.

According to the observed E_{corr} , b_a and b_c values presented in Tables 3.114 to 3.115 DNPH can be regarded as a mixed type inhibitor with predominant anodic inhibition effect as discussed earlier in the section 3.8.1. DNPH shows lower inhibition efficiency than that of ATPI, CPOB and CPOM for the corrosion of weld aged maraging steel in sulphuric acid medium.

3.11.2 Electrochemical impedance spectroscopy

The Nyquist plots obtained for the corrosion of weld aged samples of maraging steel specimen in 0.5 M sulphuric acid in the presence of different concentrations of DNPH at 30 °C is shown in Fig. 3.84. Similar plots were obtained in other concentrations of sulphuric acid and also at other temperatures. The electrochemical parameters obtained from the EIS studies are summarized in Tables 3.116 to 3.120. From Fig. 3.84, it can be observed that the impedance spectra show a single semicircle and the diameter of semicircle increases with increasing inhibitor concentration, indicating the increase in charge transfer resistance (R_{ct}) value and decrease in corrosion rate (v_{corr}). The plots are similar to those obtained in the presence of CPOB as discussed in the section 3.8.2. The equivalent circuit given in Fig. 3.20 is used to fit the experimental data. The results show that the values of C_{dl} and C_{pf} decrease, while the values of R_{ct} and R_{pf} increase with the increase in the concentration of DNPH, suggesting that the amount of the inhibitor molecules adsorbed on the electrode surface increases as the concentration of DNPH increases (Amin et al. 2007).

The Bode plots for the corrosion of the alloy in the presence of different concentrations of DNPH is shown in Fig. 3.85. Phase angle increases with the increase in the concentrations of DNPH in sulphuric acid. The discussion regarding the Bode plot under the section 3.3.2 holds good for DNPH also.

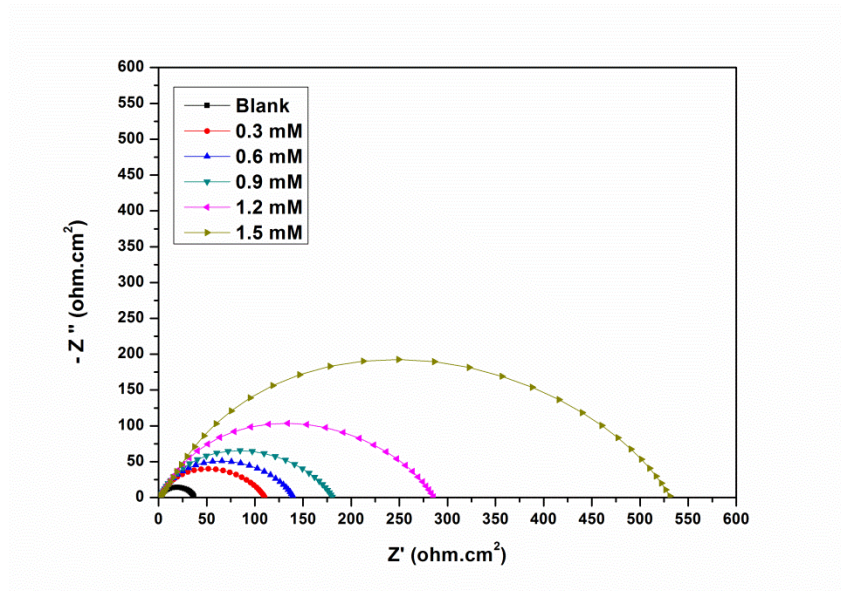


Fig. 3.84: Nyquist plots for the corrosion of weld aged maraging steel in 0.5 M sulphuric acid containing different concentrations of DNP at 30 °C.

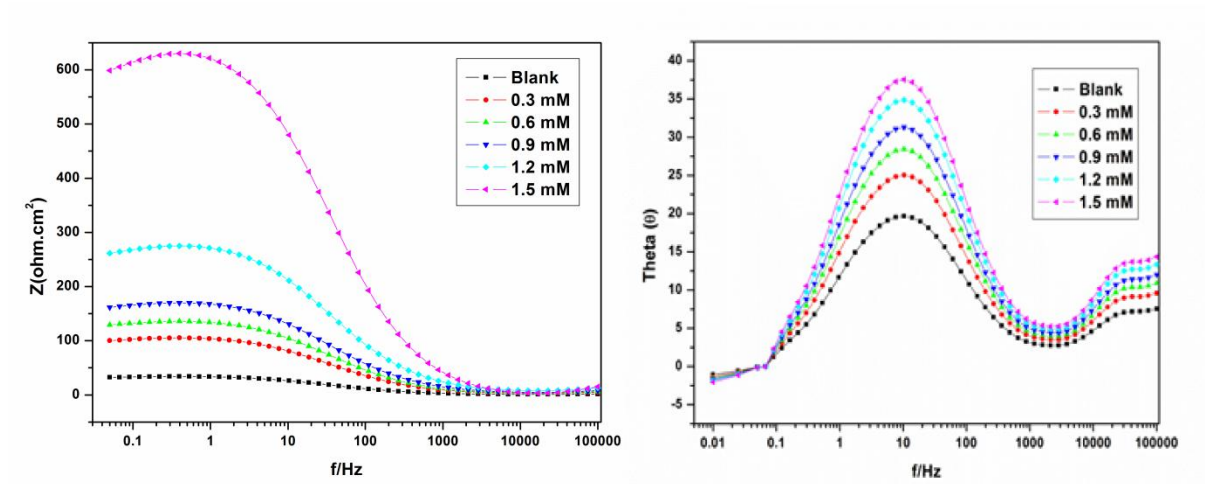


Fig. 3.85: Bode plots for the corrosion of weld aged maraging steel in 0.5 M sulphuric acid containing different concentrations of DNP at 30 °C.

A comparison of maximum attainable inhibition efficiencies by the Tafel method and EIS method, in the presence of DNP for the corrosion of weld aged maraging steel

in sulphuric acid solutions of different concentrations at 30 °C are listed in Table 3.121. It is evident from the table that the η (%) values obtained by the two methods are in good agreement. Similar levels of agreement were obtained at other temperatures also.

3.11.3 Effect of temperature

The Tafel and EIS results pertaining to different temperatures in different concentrations of sulphuric acid have already been listed in Tables 3.111 to 3.115. The effect of temperature on corrosion inhibition behaviour of DNPH is similar to that of ATPI, CPOB and CPOB on weld aged maraging steel as discussed in the section 3.8.3. The decrease in the inhibition efficiency of DNPH with the increase in temperature on weld aged maraging steel surface may be attributed to the physisorption of DNPH. The Arrhenius plots for the corrosion of weld aged maraging steel in 0.5 M sulphuric acid in the presence of different concentrations of DNPH are shown in Fig. 3.86. The plots of $\ln(v_{\text{corr}}/T)$ vs $(1/T)$ are shown in Fig. 3.87.

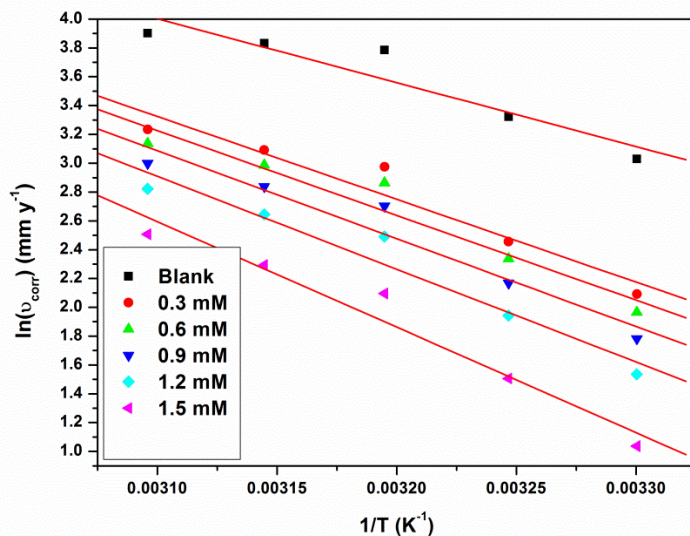


Fig. 3.86: Arrhenius plots for the corrosion of weld aged maraging steel in 0.5 M sulphuric acid containing different concentrations of DNPH.

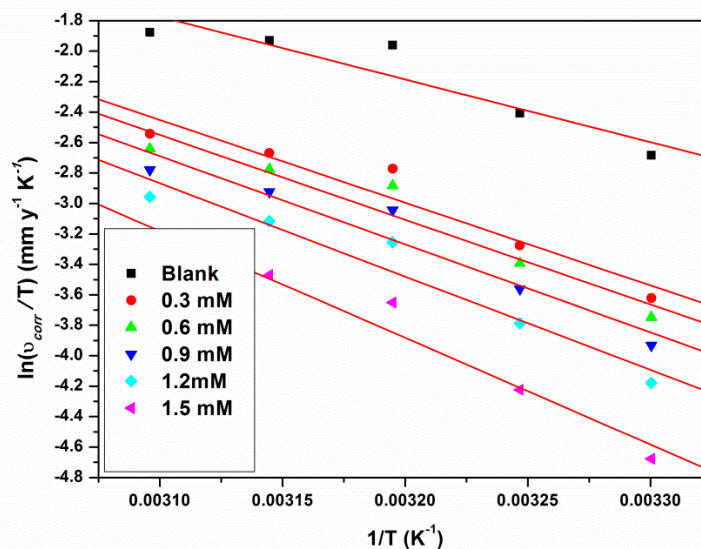


Fig. 3.87: Plots of $\ln(i_{\text{corr}}/T)$ versus $1/T$ for the corrosion of weld aged maraging steel in 0.5 M sulphuric acid containing different concentrations of DNPH.

The calculated values of activation parameters are given in Table 3.122. The observations are similar to the ones obtained in the presence of ATPI. The increase in the activation energy for the corrosion of weld aged maraging steel in the presence of DNPH indicates the increase in energy barrier for the corrosion reaction. The entropies of activation in the absence and presence of the inhibitor are large and negative. This implies that the activated complex in the rate determining step represents an association resulting in decrease in randomness on going from the reactants to the activated complex (Gomma and Wahdan 1995, Marsh 1988).

3.11.4 Effect of sulphuric acid concentration

It is evident from both the polarization and EIS experimental results that, for a particular concentration of the DNPH, the inhibition efficiency decreases with the increase in sulphuric acid concentration on weld aged maraging steel. The maximum inhibition efficiency is observed in 1.0 M solution of sulphuric acid.

3.11.5 Adsorption isotherms

The adsorption of DNPH on the surfaces of weld aged maraging steel was found to obey Langmuir adsorption isotherm. The Langmuir adsorption isotherms for the adsorption of DNPH on weld aged maraging steel in 0.5 M sulphuric acid are shown in Fig. 3.88. The thermodynamic parameters for the adsorption of DNPH on weld aged maraging steel are tabulated in Tables 3.123.

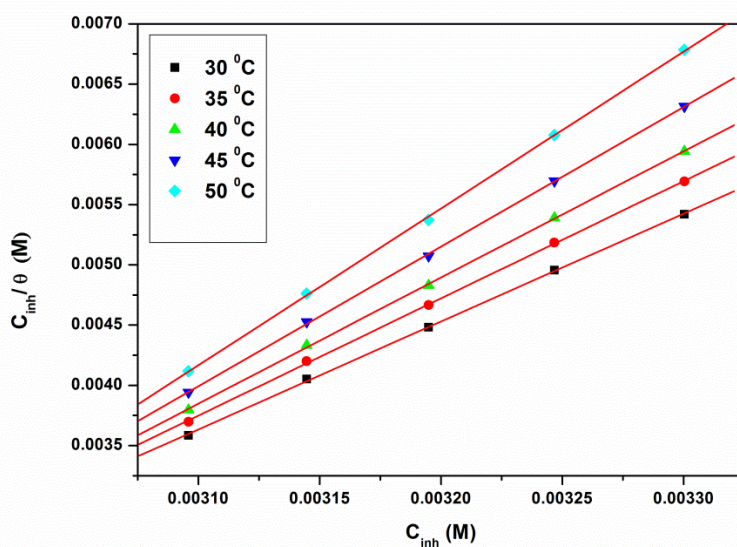


Fig. 3.88: Langmuir adsorption isotherms for the adsorption of DNPH on weld aged maraging steel in 0.5 M sulphuric acid at different temperatures.

These data reveal similar inhibition behaviour of DNPH as that of ATPI as discussed in section 3.8.5. The values of ΔG^0_{ads} and ΔH^0_{ads} indicate both physisorption and chemisorption of DNPH on weld aged maraging steel with predominant physisorption.

3.11.6 Mechanism of corrosion inhibition

The mechanism of corrosion inhibition of weld aged maraging steel in the presence of DNPH is similar to that in the presence of ATPI as discussed under section 3.8.6. It is considered that in acidic solution the DNPH molecule can undergo protonation

at amino group and can exist as a protonated positive species. The physisorption of DNPH may be considered through electrostatic attraction between the protonated DNPH and negatively charged chloride ions already adsorbed on the alloy surface.

DNPH shows slightly lesser inhibition efficiency than that of ATPI, CPOB and CPOM for the corrosion of weld aged maraging steel in sulphuric acid medium.

3.11.7 SEM/EDS studies

Fig. 3.89 (a) represents the SEM image of the corroded weld aged maraging steel sample which shows the facets due to the attack of sulphuric acid on the metal surface with cracks and rough surfaces. Fig. 3.89 (b) shows the SEM image of the sample after immersion in 0.5 M sulphuric acid in the presence of DNPH. It can be seen that the alloy surface is smooth without any visible corrosion attack. Thus, it can be concluded that DNPH protects the alloy from corrosion by forming a uniform film on the alloy surface.

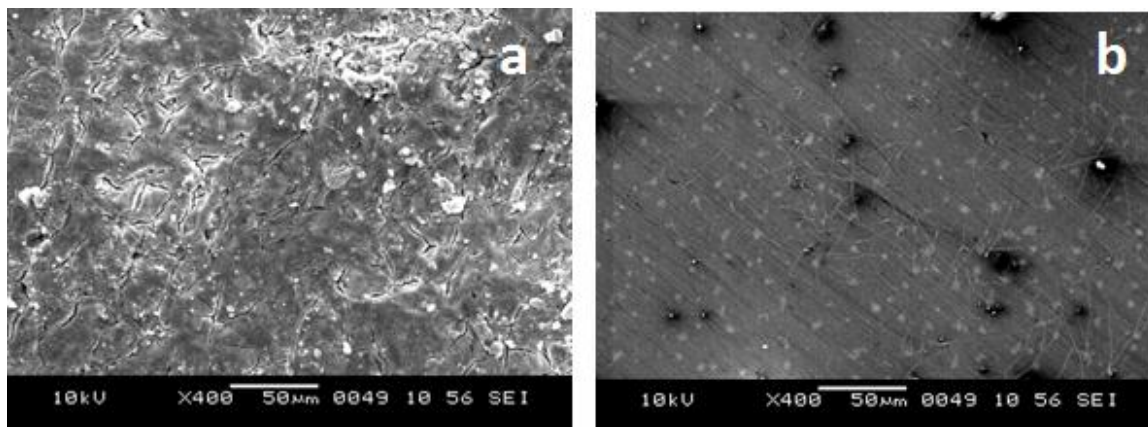


Fig. 3.89: SEM images of the weld aged maraging steel after immersion in 0.5 M sulphuric acid a) in the absence and b) in the presence of DNPH.

The EDS profile of the corroded surface of the alloy in the presence of DNPH is shown in Fig. 3.90. The atomic percentages of the elements found in the EDS profile for inhibited metal surface were 8.92 % Fe, 2.74% Ni, 2.66% Mo, 26.56% O, 3.39 % S,

55.01% C and 7.26% N and indicated the formation of inhibitor film on the surface of alloy.

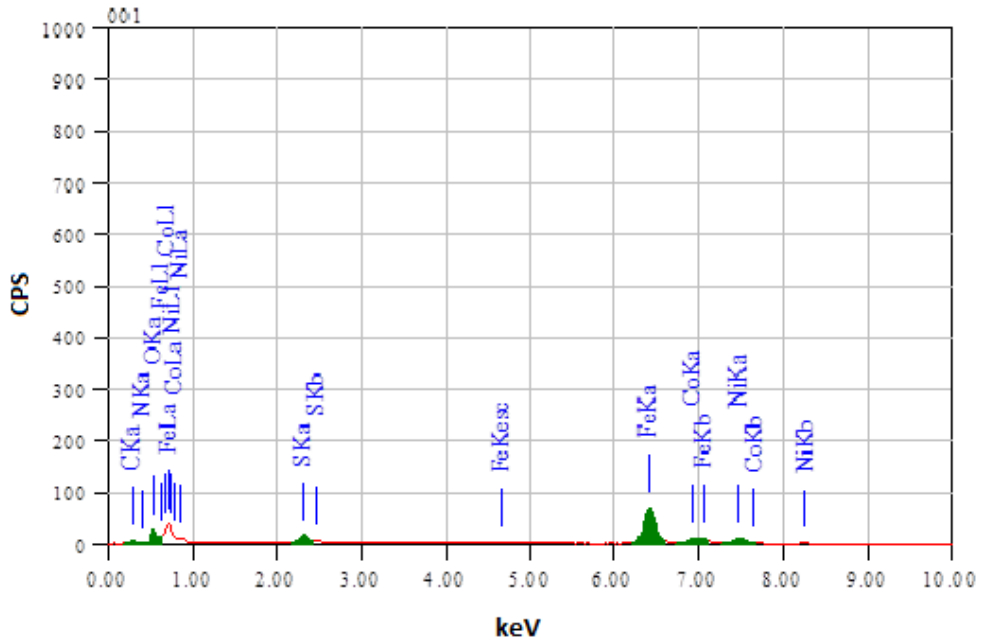


Fig. 3.90: EDS spectra of the weld aged maraging steel after immersion in 1.5 sulphuric acid in the absence of DNPH.

Table 3.111: Results of potentiodynamic polarization studies for the corrosion of weld aged maraging steel in 0.1 M sulphuric acid containing different concentrations of DNPH.

Temperature (°C)	Conc. of inhibitor (mM)	E_{corr} (mV /SCE)	b_a (mV dec ⁻¹)	$-b_c$ (mV dec ⁻¹)	i_{corr} (mA cm ⁻²)	v_{corr} (mm y ⁻¹)	η (%)
30	Blank	-371±1	221±3	266±2	0.78±0.02	8.99±0.23	
	0.3	-370±3	216±3	263±3	0.27±0.03	3.15±0.28	64.9
	0.6	-366±1	210±2	257±3	0.21±0.01	2.47±0.11	72.5
	0.9	-363±1	207±1	255±2	0.17±0.02	1.95±0.20	78.3
	1.2	-360±1	201±1	251±3	0.11±0.01	1.29±0.13	85.6
	1.5	-358±1	200±3	249±2	0.06±0.01	0.68±0.19	92.4
	35	Blank	-368±1	257±2	283±1	1.27±0.03	14.64±0.25
0.3		-362±3	254±1	278±3	0.47±0.01	5.41±0.15	63.0
0.6		-357±1	247±2	274±1	0.38±0.01	4.33±0.11	70.4
0.9		-354±2	245±2	268±3	0.30±0.02	3.47±0.16	76.3
1.2		-350±3	242±2	263±2	0.21±0.02	2.39±0.24	83.6
1.5		-348±2	240±3	262±1	0.12±0.02	1.39±0.21	90.5
40		Blank	-365±1	289±2	296±1	1.99±0.01	22.95±0.12
	0.3	-363±2	281±2	294±2	0.79±0.03	9.07±0.26	60.4
	0.6	-358±3	278±3	289±3	0.64±0.02	7.36±0.22	67.9
	0.9	-356±1	274±1	285±2	0.52±0.03	6.00±0.30	73.8
	1.2	-353±3	269±3	283±3	0.37±0.03	4.30±0.29	81.2
	1.5	-347±3	268±1	280±3	0.24±0.02	2.71±0.18	88.2
	45	Blank	-362±3	295±3	317±3	2.21±0.01	25.48±0.13
0.3		-355±2	287±1	312±1	0.93±0.02	10.65±0.23	58.1
0.6		-352±2	283±2	306±3	0.76±0.02	8.73±0.25	65.7
0.9		-353±3	279±1	302±2	0.63±0.03	7.21±0.30	71.7
1.2		-347±1	275±2	297±1	0.46±0.03	5.29±0.30	79.2
1.5		-342±3	273±2	293±2	0.31±0.03	3.51±0.26	86.2
50		Blank	-359±3	298±1	321±3	2.47±0.02	28.48±0.22
	0.3	-356±1	293±3	319±1	1.12±0.03	12.91±0.29	54.6
	0.6	-352±3	287±1	315±1	0.93±0.01	10.74±0.10	62.2
	0.9	-347±3	283±3	310±1	0.78±0.02	9.03±0.21	68.2
	1.2	-341±1	278±3	307±1	0.60±0.02	6.87±0.18	75.8
	1.5	-340±1	275±2	302±3	0.42±0.02	4.86±0.24	82.9

Table 3.112: Results of potentiodynamic polarization studies for the corrosion of weld aged maraging steel in 0.5 M sulphuric acid containing different concentrations of DNPH.

Temperature (°C)	Conc. of inhibitor (mM)	E_{corr} (mV /SCE)	b_a (mV dec ⁻¹)	$-b_c$ (mV dec ⁻¹)	i_{corr} (mA cm ⁻²)	v_{corr} (mm y ⁻¹)	η (%)
30	Blank	-356±2	235±3	268±1	1.80±0.03	20.71±0.30	
	0.3	-352±1	232±2	263±3	0.68±0.04	7.85±0.38	62.1
	0.6	-350±3	226±2	257±2	0.54±0.03	6.23±0.28	69.9
	0.9	-344±2	222±2	253±1	0.44±0.01	5.01±0.12	75.8
	1.2	-342±2	219±2	248±1	0.30±0.03	3.46±0.35	83.3
	1.5	-339±3	217±2	247±1	0.18±0.01	2.03±0.14	90.2
	35	Blank	-353±2	257±2	276±3	2.41±0.03	27.73±0.31
0.3		-348±1	252±1	273±1	0.96±0.02	11.04±0.22	60.2
0.6		-345±2	246±3	267±3	0.78±0.04	8.93±0.36	67.8
0.9		-340±3	242±1	264±3	0.63±0.02	7.26±0.22	73.8
1.2		-337±3	237±2	261±1	0.45±0.02	5.21±0.23	81.2
1.5		-337±3	236±1	259±2	0.28±0.03	3.24±0.31	88.3
40		Blank	-350±3	279±1	288±2	3.83±0.01	44.07±0.15
	0.3	-345±3	277±2	283±1	1.62±0.02	18.68±0.16	57.6
	0.6	-342±1	270±2	277±2	1.33±0.04	15.34±0.38	65.2
	0.9	-337±3	267±2	273±2	1.10±0.01	12.69±0.11	71.2
	1.2	-336±2	264±3	268±3	0.81±0.02	9.34±0.21	78.8
	1.5	-332±3	262±3	267±2	0.54±0.02	6.21±0.20	85.9
	45	Blank	-348±1	296±2	297±2	4.01±0.02	46.14±0.19
0.3		-341±3	291±1	295±3	1.80±0.02	20.67±0.21	55.2
0.6		-339±1	285±1	289±3	1.48±0.03	17.07±0.32	63.0
0.9		-333±3	281±3	286±3	1.24±0.02	14.26±0.19	69.1
1.2		-333±2	276±3	283±2	0.93±0.03	10.75±0.29	76.7
1.5		-330±3	275±3	281±1	0.65±0.03	7.43±0.34	83.9
50		Blank	-346±3	315±3	306±2	4.30±0.01	49.47±0.14
	0.3	-341±1	313±3	301±2	2.21±0.01	25.43±0.14	48.6
	0.6	-340±1	307±1	295±2	1.87±0.02	21.52±0.22	56.5
	0.9	-335±1	304±3	291±1	1.60±0.03	18.40±0.32	62.8
	1.2	-334±3	301±2	286±2	1.26±0.02	14.50±0.17	70.7
	1.5	-333±3	299±2	285±2	0.94±0.03	10.83±0.32	78.1

Table 3.113: Results of potentiodynamic polarization studies for the corrosion of weld aged maraging steel in 1.0 M sulphuric acid containing different concentrations of DNPH.

Temperature (°C)	Conc. of inhibitor (mM)	E_{corr} (mV /SCE)	b_a (mV dec ⁻¹)	$-b_c$ (mV dec ⁻¹)	i_{corr} (mA cm ⁻²)	v_{corr} (mm y ⁻¹)	η (%)
30	Blank	-323±3	247±1	301±1	8.56±0.24	98.41±2.40	
	0.4	-322±3	244±2	296±1	2.28±0.28	26.20±2.78	73.4
	0.8	-320±3	238±3	290±1	1.81±0.26	20.78±2.56	78.9
	1.2	-315±3	235±1	286±3	1.23±0.39	14.18±3.85	85.6
	1.6	-313±3	232±1	281±2	0.62±0.39	7.19±3.92	92.7
	2.0	-311±2	230±2	280±3	0.32±0.26	3.64±0.61	96.3
35	Blank	-318±3	276±2	303±2	12.81±0.22	147.27±2.22	
	0.4	-312±3	271±2	301±1	3.63±0.27	41.80±2.73	71.6
	0.8	-309±1	265±1	295±3	2.92±0.25	33.62±2.54	77.2
	1.2	-309±3	261±1	292±1	2.06±0.38	23.65±3.80	83.9
	1.6	-306±3	256±3	289±2	1.14±0.23	13.09±2.30	91.1
	2.0	-303±1	255±2	287±4	0.67±0.30	7.73±1.03	94.8
40	Blank	-309±3	292±2	305±2	16.49±0.35	194.44±3.54	
	0.4	-308±1	290±2	300±2	5.20±0.20	59.87±2.05	69.2
	0.8	-304±1	284±2	294±2	4.26±0.24	48.96±2.42	74.8
	1.2	-299±2	281±3	290±2	3.10±0.31	35.66±3.10	81.7
	1.6	-297±3	278±3	285±3	1.88±0.40	21.58±3.98	88.9
	2.0	-295±3	276±3	284±1	1.25±0.24	14.43±2.39	92.6
45	Blank	-307±2.	298±1	307±2	19.46±0.21	223.21±2.14	
	0.4	-302±3	293±1	305±1	6.52±0.27	75.06±2.75	66.4
	0.8	-306±1	287±2	299±3	5.42±0.29	62.41±2.95	72.0
	1.2	-299±3	283±1	296±2	4.08±0.35	46.99±3.46	79.0
	1.6	-297±2	278±2	293±1	2.67±0.31	30.67±3.12	86.3
	2.0	-296±3	277±3	291±1	1.94±0.35	22.37±1.47	90.0
50	Blank	-305±2	312±1	311±2	22.10±0.38	253.12±3.78	
	0.4	-299±2	310±3	306±1	8.11±0.37	93.32±3.70	63.3
	0.8	-296±2	304±1	300±1	6.84±0.35	78.75±3.46	69.0
	1.2	-291±3	301±3	296±1	5.30±0.27	61.00±2.74	76.2
	1.6	-289±1	298±1	291±2	3.67±0.24	42.23±2.35	83.4
	2.0	-286±1	296±2	290±2	2.84±0.37	32.67±1.66	87.2

Table 3.114: Results of potentiodynamic polarization studies for the corrosion of weld aged maraging steel in 1.5 M sulphuric acid containing different concentrations of DNPH.

Temperature (°C)	Conc. of inhibitor (mM)	E_{corr} (mV /SCE)	b_a (mV dec ⁻¹)	$-b_c$ (mV dec ⁻¹)	i_{corr} (mA cm ⁻²)	v_{corr} (mm y ⁻¹)	η (%)
30	Blank	-295±3	252±2	260±1	17.05±0.38	195.53±3.84	
	0.5	-293±2	247±3	257±3	5.15±0.31	59.27±3.14	69.7
	1.0	-289±2	241±3	251±1	4.22±0.22	48.51±2.16	75.2
	1.5	-286±2	237±1	248±2	3.08±0.47	35.40±4.67	81.9
	2.0	-283±3	232±1	245±2	1.87±0.30	21.52±2.98	89.0
	2.5	-280±3	231±2	243±1	1.26±0.13	14.47±1.28	92.6
	35	Blank	-291±2	253±2	272±2	23.63±0.39	271.53±3.92
0.5		-285±3	250±2	267±3	7.58±0.34	87.22±3.39	67.9
1.0		-287±3	244±3	261±3	6.27±0.46	72.15±4.63	73.4
1.5		-283±2	241±3	257±2	4.67±0.34	53.76±4.44	80.2
2.0		-280±2	238±2	252±2	2.98±0.28	34.29±2.79	87.4
2.5		-277±3	236±2	251±1	2.12±0.25	24.41±2.51	91.0
40		Blank	-288±1	254±1	276±3	28.02±0.45	332.15±4.46
	0.5	-288±3	249±2	273±1	9.62±0.44	110.69±4.42	65.6
	1.0	-291±3	243±3	267±2	8.05±0.49	92.65±4.87	71.2
	1.5	-282±1	239±2	264±2	6.14±0.31	70.62±3.12	78.1
	2.0	-280±2	234±2	261±1	4.11±0.35	47.29±3.51	85.3
	2.5	-278±2	233±1	259±1	3.08±0.26	35.44±2.55	89.0
	45	Blank	-285±1	266±1	283±3	30.31±0.26	348.61±2.61
0.5		-278±1	263±1	281±2	11.16±0.38	128.40±3.80	63.2
1.0		-280±2	257±2	274±1	9.44±0.30	108.66±3.05	68.8
1.5		-276±2	254±3	271±2	7.35±0.37	84.57±3.67	75.7
2.0		-274±1	251±1	268±2	5.14±0.46	59.09±4.59	83.1
2.5		-270±3	249±2	266±3	4.01±0.26	46.12±2.57	86.8
50		Blank	-283±3	272±1	296±1	33.08±0.35	379.65±3.47
	0.5	-278±3	267±3	291±2	12.98±0.39	149.29±3.91	60.7
	1.0	-273±3	261±2	285±3	11.09±0.25	127.61±2.46	66.4
	1.5	-276±1	257±1	281±1	8.79±0.47	101.11±4.70	73.4
	2.0	-273±1	252±2	276±2	6.35±0.32	73.05±3.17	80.8
	2.5	-271±2	251±2	275±2	5.11±0.17	58.77±1.65	84.5

Table 3.115: Results of potentiodynamic polarization studies for the corrosion of weld aged maraging steel in 2.0 M sulphuric acid containing different concentrations of DNPH.

Temperature (°C)	Conc. of inhibitor (mM)	E_{corr} (mV /SCE)	b_a (mV dec ⁻¹)	$-b_c$ (mV dec ⁻¹)	i_{corr} (mA cm ⁻²)	v_{corr} (mm y ⁻¹)	η (%)
30	Blank	-281±3	223±3	251±2	20.38±0.37	233.56±3.66	
	0.5	-278±3	219±2	246±2	7.34±0.29	84.46±2.90	63.8
	1.0	-277±1	213±2	240±3	6.21±0.36	71.49±3.58	69.4
	1.5	-274±3	210±1	236±1	4.84±0.28	55.68±2.79	76.2
	2.0	-268±3	207±1	231±1	3.38±0.12	38.93±1.23	83.3
	2.5	-273±2	205±1	230±2	2.65±0.19	30.43±1.93	87.0
35	Blank	-279±2	245±1	263±2	27.61±0.34	317.55±3.40	
	0.5	-279±1	240±3	260±2	10.39±0.29	119.53±2.87	62.4
	1.0	-276±1	234±1	254±3	8.84±0.32	101.71±3.16	68.0
	1.5	-276±1	230±2	251±1	6.95±0.20	79.99±2.99	74.8
	2.0	-272±1	225±1	248±3	4.95±0.21	57.00±2.07	82.1
	2.5	-268±3	224±3	246±1	3.94±0.19	45.31±1.95	85.7
40	Blank	-278±3	269±2	274±2	35.03±0.49	402.63±4.88	
	0.5	-275±2	264±3	266±2	13.94±0.36	160.43±3.63	60.2
	1.0	-277±3	258±3	260±3	11.96±0.37	137.60±3.71	65.8
	1.5	-272±3	254±1	257±1	9.54±0.36	109.77±3.61	72.7
	2.0	-267±3	249±2	254±2	6.98±0.38	80.34±3.80	80.1
	2.5	-265±3	248±2	252±3	5.68±0.21	65.36±2.07	83.8
45	Blank	-275±2	281±1	288±1	40.78±0.47	468.28±4.68	
	0.5	-269±2	279±3	283±1	17.65±0.33	203.09±3.29	56.6
	1.0	-266±2	272±3	277±2	15.32±0.29	176.31±2.88	62.4
	1.5	-266±1	269±3	273±2	12.48±0.56	143.62±5.61	69.3
	2.0	-262±2	266±3	268±1	9.47±0.31	109.01±3.12	76.7
	2.5	-257±3	264±3	267±1	7.95±0.38	91.45±3.84	80.5
50	Blank	-273±2	301±2	302±3	45.23±0.40	520.05±4.05	
	0.5	-274±1	299±3	297±1	20.76±0.22	238.86±2.24	54.1
	1.0	-267±3	293±1	291±2	18.15±0.44	208.80±4.41	59.9
	1.5	-265±2	290±1	287±2	14.96±0.60	172.14±5.96	66.9
	2.0	-259±2	287±1	282±3	11.59±0.58	133.34±5.76	74.4
	2.5	-258±2	285±1	281±1	9.88±0.20	113.63±2.03	78.2

Table 3.116: EIS data for the corrosion of weld aged maraging steel in 0.1 M sulphuric acid containing different concentrations of DNPH.

Temperature (°C)	Conc. of inhibitor (mM)	R_{ct} (ohm. cm ²)	C_{dl} (mF cm ⁻²)	R_{pf} (ohm. cm ²)	C_{pf} (mF cm ⁻²)	η (%)
30	Blank	74.66±3.52	21.01±2.11			
	0.3	224.00±3.66	8.02±2.17	15.70±1.02	2.29±0.85	66.7
	0.6	290.96±5.72	6.23±2.87	19.82±1.50	1.78±0.58	74.3
	0.9	377.07±3.49	4.86±2.67	25.12±2.21	1.40±0.39	80.2
	1.2	601.13±6.53	3.13±1.70	38.90±2.54	0.91±0.29	87.6
	1.5	1342.81±7.57	1.53±0.16	84.53±2.50	0.47±0.18	94.4
35	Blank	51.17±2.33	26.57±3.18			
	0.3	144.34±3.52	10.55±2.88	10.80±1.41	3.00±0.81	64.6
	0.6	182.95±3.72	8.37±2.03	13.18±1.63	2.39±1.15	72.0
	0.9	232.06±3.11	6.64±2.74	16.20±1.91	1.90±0.10	78.2
	1.2	350.48±4.83	4.48±1.85	23.48±2.82	1.29±0.42	85.4
	1.5	667.14±5.66	2.46±1.24	42.96±1.72	0.73±0.15	92.3
40	Blank	35.45±2.98	32.14±2.41			
	0.3	92.66±2.79	13.81±3.38	7.62±2.83	3.91±0.98	61.7
	0.6	115.47±3.50	11.12±2.75	9.02±1.32	3.16±0.60	69.3
	0.9	143.41±3.44	9.00±2.55	10.74±1.30	2.56±0.57	75.3
	1.2	206.22±2.84	6.33±2.73	14.61±2.14	1.81±0.29	82.8
	1.5	347.89±4.05	3.84±1.34	23.32±1.31	1.11±0.12	89.8
45	Blank	33.36±2.91	36.48±2.06			
	0.3	81.80±3.02	16.54±3.38	6.95±1.41	4.68±0.91	59.2
	0.6	100.69±3.69	13.48±2.23	8.11±2.09	3.82±0.57	66.9
	0.9	123.15±3.50	11.06±2.12	9.50±1.10	3.14±0.47	72.9
	1.2	171.16±2.10	8.02±2.54	12.45±1.80	2.29±0.63	80.5
	1.5	268.60±3.31	5.19±1.79	18.44±2.63	1.49±0.28	87.6
50	Blank	30.19±3.07	41.49±2.42			
	0.3	67.66±3.21	20.65±2.43	6.08±2.97	5.83±0.91	55.4
	0.6	81.82±2.89	17.12±3.19	6.95±1.86	4.84±0.56	63.1
	0.9	98.02±2.34	14.32±3.27	7.95±1.17	4.06±0.26	69.2
	1.2	130.58±2.87	10.81±2.06	9.95±2.05	3.07±0.38	76.9
	1.5	188.92±3.96	7.54±1.43	13.54±1.87	2.15±0.35	84.0

Table 3.117: EIS data for the corrosion of weld aged maraging steel in 0.5 M sulphuric acid containing different concentrations of DNPH.

Temperature (°C)	Conc. of inhibitor (mM)	R_{ct} (ohm. cm ²)	C_{dl} (mF cm ⁻²)	R_{pf} (ohm. cm ²)	C_{pf} (mF cm ⁻²)	η (%)
30	Blank	33.56±2.40	40.12±3.87			
	0.3	100.39±2.13	19.10±2.40	8.10±2.61	0.51±0.11	66.6
	0.6	130.28±3.89	14.82±3.29	9.93±1.89	0.42±0.15	74.2
	0.9	168.64±2.77	10.61±2.11	12.29±1.77	0.34±0.19	80.1
	1.2	267.84±3.98	7.55±1.95	18.40±2.85	0.26±0.17	87.5
	1.5	592.93±6.89	2.68±0.64	38.40±1.81	0.17±0.07	94.3
35	Blank	26.64±2.34	65.92±3.85			
	0.3	75.08±3.86	31.27±2.31	6.54±1.13	0.75±0.23	64.5
	0.6	95.14±2.76	24.03±2.14	7.77±2.14	0.62±0.15	72.1
	0.9	120.65±3.69	17.17±2.30	9.34±2.28	0.51±0.11	77.9
	1.2	182.09±4.72	13.11±2.35	13.12±1.02	0.37±0.15	85.4
	1.5	345.97±5.60	5.54±1.49	23.20±2.32	0.24±0.13	92.3
40	Blank	17.85±2.04	109.77±4.93			
	0.3	47.21±3.90	54.45±3.69	4.82±1.54	1.23±0.39	62.2
	0.6	59.03±3.92	41.91±2.96	5.55±1.88	1.01±0.37	69.8
	0.9	73.58±3.07	30.84±2.92	6.45±2.35	0.83±0.20	75.7
	1.2	106.63±4.10	23.61±1.21	8.48±1.32	0.60±0.15	83.3
	1.5	183.26±4.15	10.82±1.10	13.19±2.42	0.39±0.12	90.3
45	Blank	17.84±2.39	125.60±3.35			
	0.3	44.27±2.28	66.46±3.93	4.64±1.14	1.55±0.47	59.7
	0.6	54.62±3.38	50.36±2.51	5.28±2.94	1.28±0.71	67.3
	0.9	67.02±2.59	41.27±2.00	6.04±2.26	1.06±0.78	73.4
	1.2	93.80±3.41	30.05±1.98	7.69±2.45	0.79±0.21	81.4
	1.5	149.29±4.31	16.25±1.21	11.10±1.79	0.53±0.10	88.1
50	Blank	17.42±2.79	158.27±4.26			
	0.3	39.47±3.10	88.23±2.34	4.35±1.19	2.14±0.33	55.9
	0.6	47.84±2.30	68.80±2.31	4.86±1.87	1.78±0.78	63.6
	0.9	57.47±2.65	58.34±2.02	5.45±1.78	1.50±0.39	69.7
	1.2	76.94±2.91	42.32±1.04	6.65±1.45	1.14±0.34	77.4
	1.5	112.46±4.57	23.44±0.77	8.84±1.39	0.81±0.19	84.5

Table 3.118: EIS data for the corrosion of weld aged maraging steel in 1.0 M sulphuric acid containing different concentrations of DNPH.

Temperature (°C)	Conc. of inhibitor (mM)	R_{ct} (ohm. cm ²)	C_{dl} (mF cm ⁻²)	R_{pf} (ohm. cm ²)	C_{pf} (mF cm ⁻²)	η (%)
30	Blank	7.09±1.48	11.00±1.18			
	0.4	26.65±3.80	3.47±1.04	3.56±0.29	1.01±0.37	73.4
	0.8	33.60±3.17	2.80±0.62	3.99±0.54	0.82±0.16	78.9
	1.2	49.24±3.00	1.98±0.51	4.95±1.10	0.59±0.14	85.6
	1.6	97.12±3.73	1.12±0.43	7.89±1.22	0.35±0.19	92.7
	2.0	191.62±2.92	0.68±0.16	13.71±1.77	0.23±0.12	96.3
35	Blank	5.05±1.46	11.83±1.81			
	0.4	17.79±3.25	3.70±1.18	3.01±0.71	1.07±0.14	71.6
	0.8	22.12±3.58	3.02±0.66	3.28±0.91	0.88±0.31	77.2
	1.2	31.44±2.64	2.19±0.37	3.85±1.61	0.65±0.47	83.9
	1.6	56.81±3.36	1.31±0.52	5.41±1.13	0.40±0.25	91.1
	2.0	96.19±4.97	0.87±0.17	7.84±1.29	0.28±0.14	94.8
40	Blank	3.95±1.55	12.37±1.94			
	0.4	12.83±2.91	4.43±1.14	2.71±1.24	1.28±0.40	69.2
	0.8	15.69±3.06	3.66±0.83	2.88±1.95	1.06±0.32	74.8
	1.2	21.54±2.68	2.73±1.16	3.24±1.66	0.80±0.38	81.7
	1.6	35.59±2.83	1.74±0.44	4.11±1.16	0.52±0.23	88.9
	2.0	53.23±2.15	1.24±0.20	5.19±1.62	0.38±0.09	92.6
45	Blank	3.49±1.05	15.26±1.78			
	0.4	10.38±2.03	5.91±1.12	2.56±0.90	1.70±0.34	66.4
	0.8	12.48±3.52	4.95±0.99	2.69±1.92	1.43±0.48	72.2
	1.2	16.58±3.51	3.78±1.11	2.94±1.48	1.10±0.15	79.1
	1.6	25.40±2.35	2.55±0.79	3.48±1.50	0.75±0.34	86.3
	2.0	34.83±2.98	1.92±0.21	4.06±1.08	0.58±0.16	90.0
50	Blank	3.15±1.87	18.08±1.19			
	0.4	8.58±3.11	7.30±1.03	2.45±0.81	2.09±0.34	63.3
	0.8	10.17±2.78	6.19±1.19	2.54±1.88	1.77±0.21	69.0
	1.2	13.13±2.11	4.85±1.14	2.73±1.34	1.40±0.23	76.0
	1.6	18.96±2.56	3.42±0.15	3.09±1.44	1.00±0.38	83.4
	2.0	24.51±3.29	2.70±0.19	3.43±1.98	0.79±0.21	87.2

Table 3.119: EIS data for the corrosion of weld aged maraging steel in 1.5 M sulphuric acid containing different concentrations of DNPH.

Temperature (°C)	Conc. of inhibitor (mM)	R_{ct} (ohm. cm ²)	C_{dl} (mF cm ⁻²)	R_{pf} (ohm. cm ²)	C_{pf} (mF cm ⁻²)	η (%)
30	Blank	3.34±1.61	13.71±2.93			
	0.5	11.89±1.61	3.91±2.12	2.65±0.69	1.13±0.50	71.9
	1.0	14.84±2.12	3.18±1.71	2.83±0.64	0.93±0.43	77.5
	1.5	21.14±1.66	2.30±0.26	3.22±0.90	0.68±0.17	84.2
	2.0	38.84±1.16	1.35±0.14	4.31±0.72	0.42±0.18	91.4
	2.5	68.16±1.31	0.87±0.13	6.11±0.94	0.28±0.03	95.1
35	Blank	2.46±1.12	14.52±2.75			
	0.5	8.17±1.22	5.55±1.02	2.42±0.75	1.59±0.35	69.9
	1.0	10.04±1.76	4.56±1.80	2.54±0.72	1.32±0.23	75.5
	1.5	13.90±2.44	3.36±1.17	2.77±0.74	0.98±0.37	82.3
	2.0	23.65±1.05	2.07±0.95	3.37±0.61	0.62±0.12	89.6
	2.5	36.18±2.10	1.43±0.09	4.15±0.54	0.44±0.12	93.2
40	Blank	2.09±1.56	16.09±2.63			
	0.5	6.37±2.00	5.87±1.23	2.31±0.92	1.68±0.18	67.2
	1.0	7.71±2.08	4.89±1.67	2.39±0.72	1.41±0.29	72.9
	1.5	10.35±2.73	3.70±2.03	2.56±0.68	1.07±0.25	79.8
	2.0	16.20±1.90	2.44±0.69	2.92±0.88	0.72±0.19	87.1
	2.5	22.72±2.27	1.81±0.42	3.32±0.65	0.54±0.13	90.8
45	Blank	2.01±0.42	18.30±2.72			
	0.5	5.68±1.16	7.35±2.34	2.27±0.79	2.10±0.11	64.6
	1.0	6.77±2.82	6.20±1.11	2.34±0.54	1.78±0.41	70.3
	1.5	8.85±1.61	4.80±2.18	2.46±0.74	1.38±0.16	77.3
	2.0	13.05±2.29	3.32±1.63	2.72±0.86	0.97±0.16	84.6
	2.5	17.33±2.71	2.56±0.58	2.99±0.55	0.75±0.31	88.4
50	Blank	1.90±0.76	21.47±2.88			
	0.5	5.01±2.13	9.64±2.37	2.23±0.93	2.74±0.30	62.1
	1.0	5.90±2.03	8.22±2.88	2.28±0.68	2.34±0.23	67.8
	1.5	7.57±2.38	6.46±2.89	2.38±0.51	1.85±0.45	74.9
	2.0	10.73±2.49	4.62±2.03	2.58±0.65	1.33±0.33	82.3
	2.5	13.67±2.54	3.68±1.46	2.76±0.76	1.07±0.36	86.1

Table 3.120: EIS data for the corrosion of weld aged maraging steel in 2.0 M sulphuric acid containing different concentrations of DNPH.

Temperature (°C)	Conc. of inhibitor (mM)	R_{ct} (ohm. cm ²)	C_{dl} (mF cm ⁻²)	R_{pf} (ohm. cm ²)	C_{pf} (mF cm ⁻²)	η (%)
30	Blank	2.58±1.03	16.44±2.13			
	0.5	7.50±2.68	6.41±1.35	2.38±0.66	1.84±0.20	65.6
	1.0	8.96±2.38	5.40±1.74	2.47±0.76	1.55±0.24	71.2
	1.5	11.75±1.71	4.17±1.51	2.64±0.63	1.21±0.50	78.2
	2.0	17.53±2.21	2.87±1.10	3.00±0.58	0.84±0.49	85.3
	2.5	23.37±2.56	2.21±0.49	3.36±0.56	0.66±0.14	89.1
35	Blank	2.04±1.16	17.25±1.31			
	0.5	5.65±2.68	6.99±1.02	2.27±0.76	2.00±0.31	63.9
	1.0	6.71±2.68	5.92±1.44	2.33±0.96	1.70±0.34	69.6
	1.5	8.68±1.65	4.63±3.00	2.45±0.92	1.34±0.43	76.5
	2.0	12.60±1.79	3.26±2.97	2.69±0.51	0.95±0.13	83.8
	2.5	16.36±2.87	2.56±1.05	2.93±0.43	0.75±0.10	87.5
40	Blank	1.72±1.08	19.57±2.50			
	0.5	4.47±2.23	8.58±1.31	2.19±0.60	2.44±0.33	61.5
	1.0	5.25±2.64	7.34±2.58	2.24±0.78	2.10±0.10	67.2
	1.5	6.67±2.29	5.83±2.45	2.33±0.56	1.67±0.40	74.2
	2.0	9.34±2.79	4.22±2.95	2.49±0.58	1.22±0.18	81.6
	2.5	11.73±2.84	3.41±0.99	2.64±0.89	0.99±0.23	85.3
45	Blank	1.55±1.01	23.82±1.90			
	0.5	3.68±2.47	12.06±2.79	2.15±0.71	3.42±0.27	57.9
	1.0	4.27±3.03	10.42±1.98	2.18±0.84	2.96±0.35	63.7
	1.5	5.30±1.67	8.44±1.92	2.25±0.57	2.41±0.18	70.8
	2.0	7.12±1.66	6.34±1.87	2.36±0.56	1.82±0.21	78.2
	2.5	8.62±3.07	5.28±1.61	2.45±0.69	1.52±0.19	82.3
50	Blank	1.48±0.98	26.09±2.57			
	0.5	3.29±1.53	12.66±2.61	2.12±0.98	3.59±0.30	55.2
	1.0	3.78±2.45	11.04±1.82	2.15±0.76	3.13±0.48	60.9
	1.5	4.63±2.32	9.06±1.67	2.20±0.89	2.58±0.47	68.4
	2.0	6.05±1.52	6.98±2.73	2.29±0.66	2.00±0.19	75.5
	2.5	7.17±2.07	5.93±1.39	2.36±0.56	1.70±0.13	79.4

Table 3.122: Comparison of maximum attainable inhibition efficiencies by the Tafel method and EIS method for the corrosion of weld aged maraging steel in sulphuric acid solutions of different concentrations in the presence of DNPH at 30 °C.

Molarity of sulphuric acid	Conc. of DNPH (mM)	η (%)	
		Tafel	EIS
0.1	1.5	92.4	94.4
0.5	1.5	86.4	94.3
1.0	2.0	96.3	96.0
1.5	2.0	92.6	95.1
2.0	2.5	86.9	88.9

Table 3.122: Activation parameters for the corrosion of weld aged maraging steel in sulphuric acid containing different concentrations of DNPH.

Molarity of sulphuric acid	Conc. of inhibitor (mM)	E_a ($\text{kJ}^{-1} \text{mol}^{-1}$)	ΔH^\ddagger ($\text{kJ}^{-1} \text{mol}^{-1}$)	ΔS^\ddagger ($\text{J mol}^{-1} \text{K}^{-1}$)
0.1	0.0	44.31	43.16	-88.32
	0.1	48.83	47.56	-80.21
	0.2	50.64	49.33	-72.86
	0.4	55.61	54.17	-61.91
	0.6	63.30	61.66	-37.85
	0.8	72.34	70.47	-31.54
	0.5	0.0	35.50	37.48
0.1		39.12	41.30	-101.28
0.2		40.57	42.83	-92.00
0.4		44.56	47.04	-78.18
0.6		50.71	53.54	-47.79
0.8		57.96	61.19	-39.83
1.0		0.0	32.79	28.11
	0.2	36.14	30.98	-130.85
	0.4	37.47	32.13	-118.87
	0.6	41.15	35.28	-101.00
	0.8	46.84	40.16	-61.75
	1.0	53.53	45.89	-51.46
	1.5	0.0	25.24	23.69
0.4		27.82	26.11	-128.90
0.8		28.85	27.07	-117.09
1.2		31.68	29.73	-99.50
1.6		36.06	33.84	-60.83
2.0		41.21	38.68	-50.69
2.0		0.0	21.20	22.58
	0.5	23.36	24.88	-129.21
	1.0	24.23	25.81	-117.38
	1.5	26.61	28.34	-99.74
	2.0	30.29	32.26	-60.98
	2.5	34.61	36.87	-50.81

Table 3.123: Thermodynamic parameters for the adsorption of DNPH on weld aged maraging steel surface in sulphuric acid at different temperatures.

Molarity of sulphuric acid	Temperature (°C)	$-\Delta G^{\circ}_{\text{ads}}$ (kJ mol ⁻¹)	$\Delta H^{\circ}_{\text{ads}}$ (kJ mol ⁻¹)	$\Delta S^{\circ}_{\text{ads}}$ (J mol ⁻¹ K ⁻¹)
0.1	30	34.91	-14.32	-57.98
	35	34.77		
	40	34.60		
	45	34.43		
	50	34.26		
0.5	30	33.26	-25.02	-41.09
	35	33.13		
	40	32.97		
	45	32.81		
	50	32.65		
1.0	30	33.74	-32.50	-36.78
	35	33.61		
	40	33.44		
	45	33.28		
	50	33.12		
1.5	30	32.82	-36.78	-31.23
	35	32.69		
	40	32.53		
	45	32.37		
	50	32.21		
2.0	30	31.04	-39.01	-26.75
	35	30.92		
	40	30.76		
	45	30.61		
	50	30.47		

3.12 5-DIETHYLAMINO-2-[[2-(2,4-DINITROPHENYL) HYDRAZIN-1-ETHYLIDENE]METHYL PHENOL (DDPM) AS INHIBITOR FOR THE CORROSION OF WELD AGED MARAGING STEEL IN SULPHURIC ACID MEDIUM

3.12.1 Potentiodynamic polarization studies

The potentiodynamic polarization curves for the corrosion of weld aged maraging steel specimen in 0.1 M sulphuric acid in the presence of different concentrations of DDPM, at 30 °C are shown in Fig. 3.91. Similar plots were obtained in the other four concentrations of sulphuric acid at the different temperatures studied. The potentiodynamic polarization parameters (E_{corr} , b_c , b_a , i_{corr} and η (%)) were calculated from Tafel plots in all the five studied concentrations of sulphuric acid in the presence of different concentrations of DDPM at different temperatures and are summarized in Tables 3.124 to 3.128.

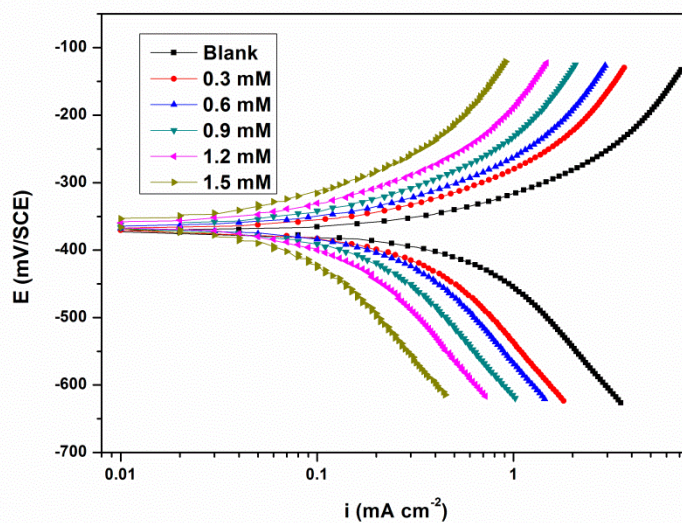


Fig. 3.91: Potentiodynamic polarization curves for the corrosion of weld aged maraging steel in 0.1 M sulphuric acid containing different concentrations of DDPM at 30 °C.

According to the observed E_{corr} , b_a and b_c values presented in Tables 3.124 to 3.128 DDPM can be regarded as a mixed type inhibitor with predominant anodic inhibition effect as discussed earlier in the section 3.8.1. DDPM shows lower inhibition efficiency than that of ATPI, CPOB, CPOM and DNPB for the corrosion of weld aged maraging steel in sulphuric acid medium.

3.12.2 Electrochemical impedance spectroscopy

The Nyquist plots obtained for the corrosion of weld aged samples of maraging steel specimen in 0.1 M sulphuric acid in the presence of different concentrations of DDPM at 30 °C is shown in Fig. 3.92. Similar plots were obtained in other concentrations of sulphuric acid and also at other temperatures. The electrochemical parameters obtained from the EIS studies are summarized in Tables 3.129 to 3.133.

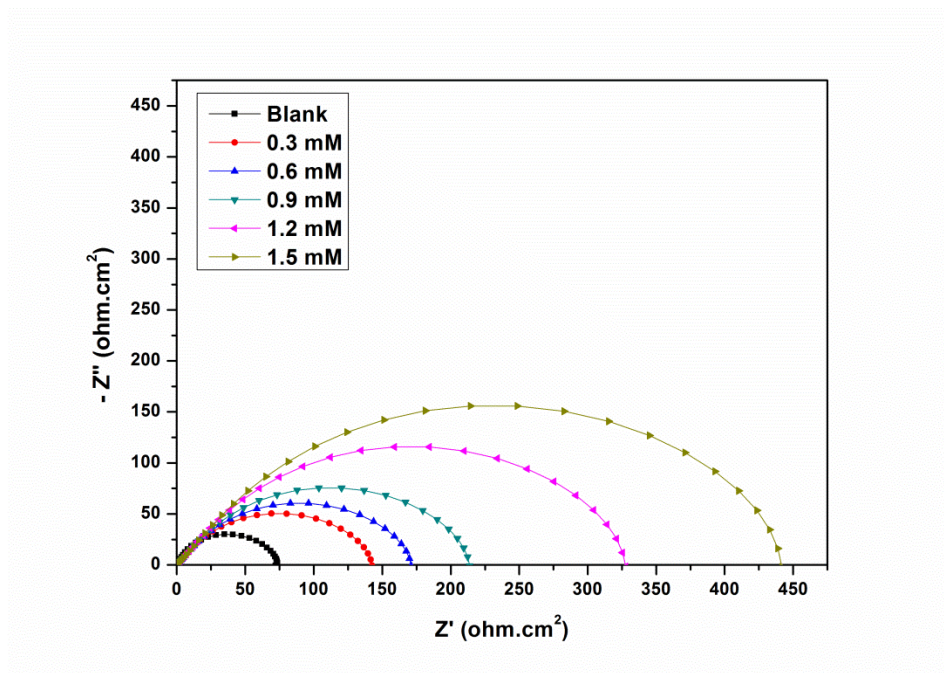


Fig. 3.92: Nyquist plots for the corrosion of weld aged maraging steel specimen in 0.1 M sulphuric acid containing different concentrations of DDPM at 30 °C.

EIS studies also revealed that inhibition behaviour of DDPM is similar to that of ATPI as discussed in the section 3.8.1. But DDPM shows slightly lower inhibition efficiency than that of ATPI. It is clear from the Fig. 3.92 that the shapes of the impedance plots for the corrosion weld aged maraging steel in the presence of inhibitor are not substantially different from those of the uninhibited one implying that, the presence of inhibitor increases the impedance but does not change other aspects of the behaviour. The equivalent circuit given in Fig. 3.20 (under Section 3.3.2) is used to fit the experimental data for the corrosion of weld aged maraging steel in sulphuric acid in the presence of DDPM. As can be seen from the Tables, R_{ct} and R_{pf} values increase and C_{dl} and C_{pf} values decrease with the increase in the concentration of DDPM. The Bode plots for the corrosion of the alloy in the presence of different concentrations of DDPM are shown in Fig. 3.93. Phase angle increases with the increase in the concentrations of DDPM in sulphuric acid.

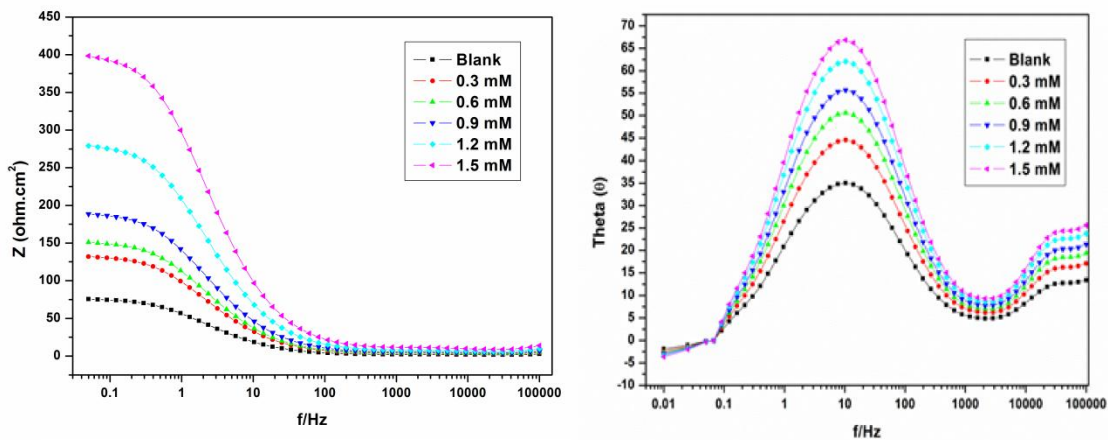


Fig. 3.93: Bode plots for the corrosion of weld aged maraging steel specimen in 0.1 M sulphuric acid containing different concentrations of DDPM at 30 °C.

A comparison of maximum attainable inhibition efficiencies in the presence of DDPM for the corrosion of weld aged maraging steel in the sulphuric acid solutions of different concentrations at 30 °C are listed in Table 3.134. It is evident from the table that

the inhibition efficiency values obtained by the two methods are in good agreement. Similar levels of agreement were obtained at other temperatures also.

3.12.3 Effect of temperature

The Tafel and EIS results pertaining to different temperatures in different concentrations of sulphuric acid have already been listed in Tables 3.124 to 3.133. The slight increase in inhibition efficiency with the increase in temperature on weld aged specimen may be the result of predominant chemisorption of DDPM on the alloy surface (Szauer and Brand 1981, Sankarapavinasam et al. 1991).

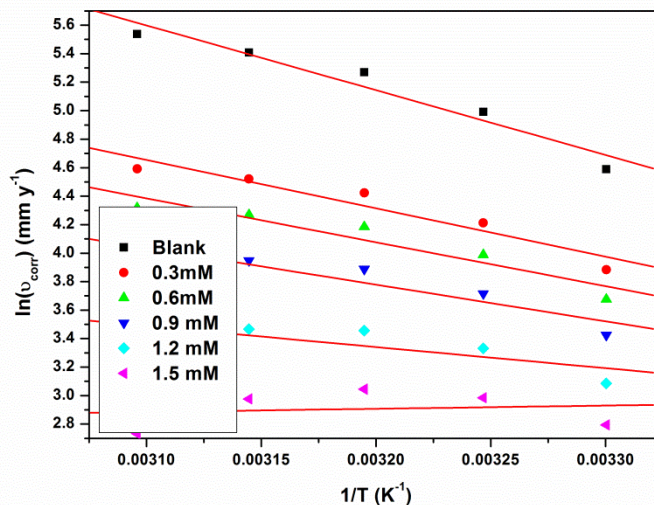


Fig. 3.94: Arrhenius plots for the corrosion of weld aged maraging steel in 0.1 M sulphuric acid containing different concentrations of DDPM.

According to Singh et al. (1979) with the increase in temperature some chemical changes occur in the inhibitor molecules, leading to the increase in the electron densities at the adsorption centres of the molecule, thereby causing an improvement in inhibition efficiency. The Arrhenius plots for the corrosion of weld aged maraging steel in 0.1 M sulphuric acid in the presence of different concentrations of DDPM are shown in Fig.

3.94. The plots of $\ln(v_{\text{corr}}/T)$ vs $(1/T)$ are shown in Fig. 3.95. The calculated values of activation parameters are given in Table 3.135.

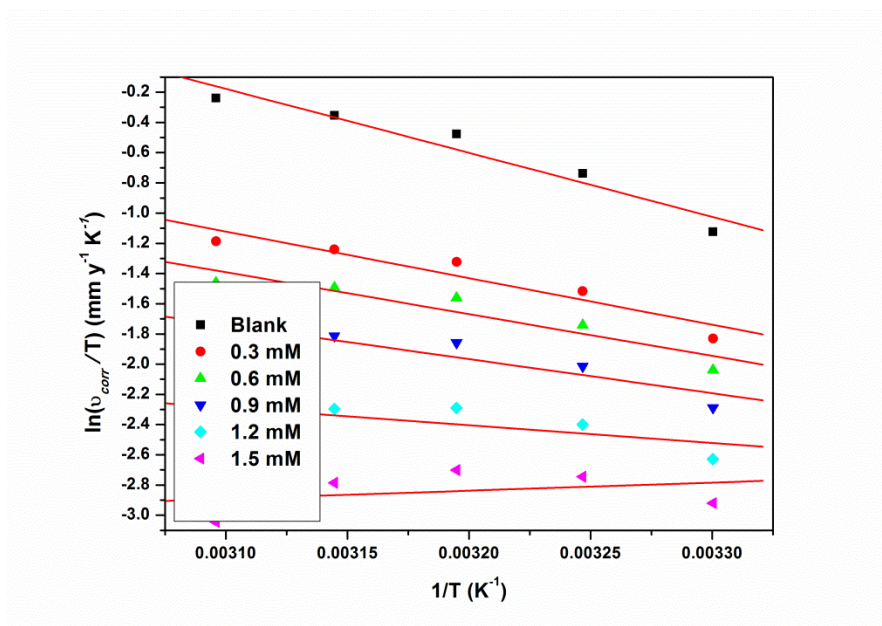


Fig. 3.95: Plots of $\ln(v_{\text{corr}}/T)$ versus $1/T$ for the corrosion of weld aged maraging steel in 0.1 M sulphuric acid containing different concentrations of DDPM.

The increase in the activation energy for the corrosion of weld aged maraging steel in the presence of DDPM indicates the increase in energy barrier for the corrosion reaction. The entropies of activation in the absence and presence of the inhibitor are large and negative. This implies that the activated complex in the rate determining step represents an association resulting in decrease in randomness on going from the reactants to the activated complex (Marsh 1988, Gomma and Wahdan 1995).

3.12.4 Effect of sulphuric acid concentration

It is evident from both the polarization and EIS experimental results that, for a particular concentration of the DDPM, the inhibition efficiency decreases with the increase in sulphuric acid concentration on weld aged maraging steel. The maximum inhibition efficiency is observed in 1.0 M solution.

3.12.5 Adsorption isotherms

The adsorption of DDPM on the surfaces of weld aged maraging steel was found to obey Langmuir adsorption isotherm. The Langmuir adsorption isotherms for the adsorption of DDPM on weld aged maraging steel in 0.1 M sulphuric acid are shown in Fig. 3.96. The thermodynamic parameters for the adsorption of DDPM on weld aged maraging steel are tabulated in Tables 3.136. The values of ΔG^0_{ads} and ΔH^0_{ads} indicate both physisorption and chemisorption of DDPM on weld aged maraging steel with predominant chemisorption. The ΔS^0_{ads} value values indicate increase in randomness on going from the reactants to the metal adsorbed species.

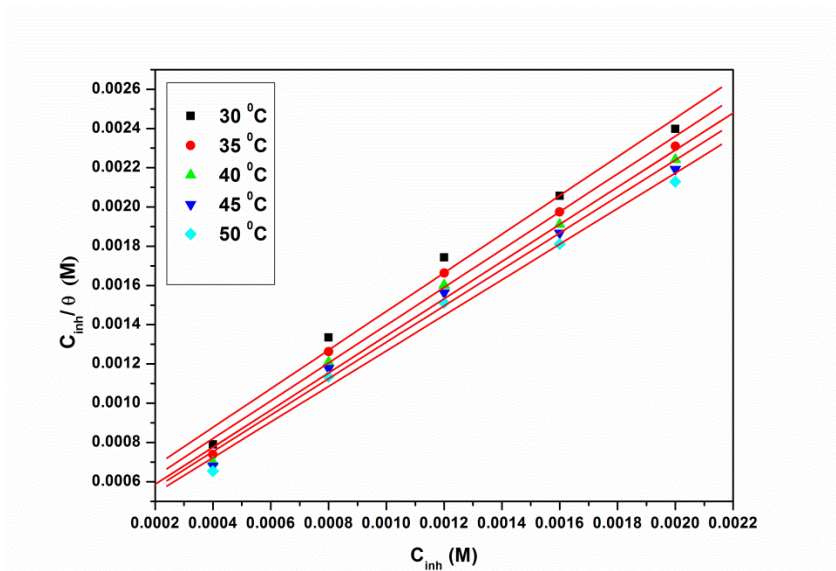


Fig. 3.96: Langmuir adsorption isotherms for the adsorption of DDPM on weld aged maraging steel in 0.1 M sulphuric acid at different temperatures.

3.12.6 Mechanism of corrosion inhibition

The mechanism of corrosion inhibition of weld aged maraging steel in the presence of DDPM is similar to that in the presence of ATPi as discussed under section 3.8.6. It is considered that in acidic solution the DDPM molecule can undergo protonation at amino group and can exist as a protonated positive species. The protonated

species gets adsorbed on the cathodic sites of the metal surface through electrostatic interaction, thereby decreasing the rate of the cathodic reaction. The chemisorption is attributed to be due to the chemical nature of interaction between inhibitor molecule and the alloy surface as reported by Lagrenee et al. (2002).

3.12.7 SEM/EDS studies

Fig. 3.97 (a) represents SEM image of the corroded weld aged maraging steel sample which shows the facets due to the attack of sulphuric acid on the metal surface with cracks and rough surfaces. Fig. 3.97 (b) shows the SEM image of the sample after immersion in 0.1 M sulphuric acid in the presence of DDPM.

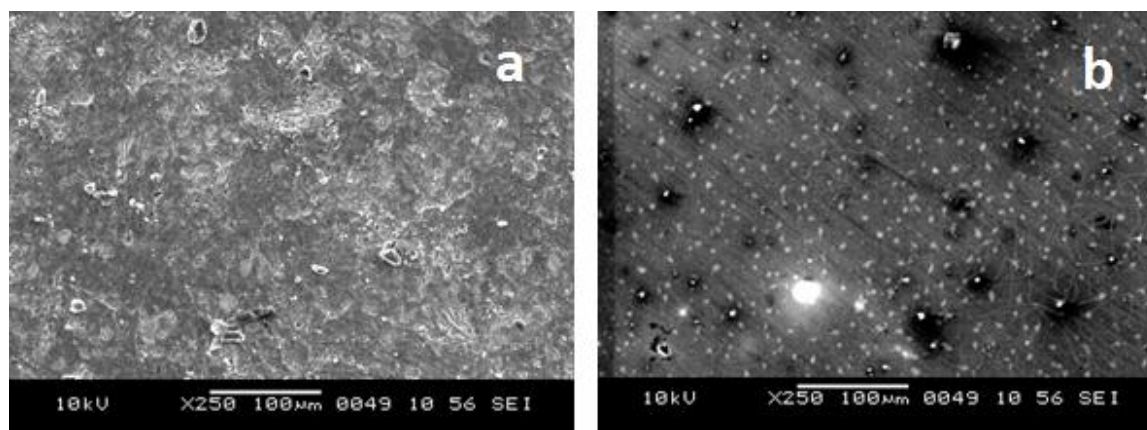


Fig. 3.97: SEM images of the weld aged maraging steel after immersion in 0.1 M sulphuric acid a) in the absence and b) in the presence of DDPM.

It can be seen that the alloy surface is smooth without any visible corrosion attack. Thus, it can be concluded that DDPM protects the alloy from corrosion by forming a uniform film on the alloy surface. The EDS profile of the corroded surface of the alloy in the presence of CPOM is shown in Fig. 3.98. The atomic percentages of the elements found in the EDS profile for inhibited metal surface were 6.05 % Fe, 3.11% Ni, 1.98% Mo, 34.25% O, 5.21 % S, 45.67 % C and 4.75 N and indicated the formation of inhibitor film on the surface of alloy.

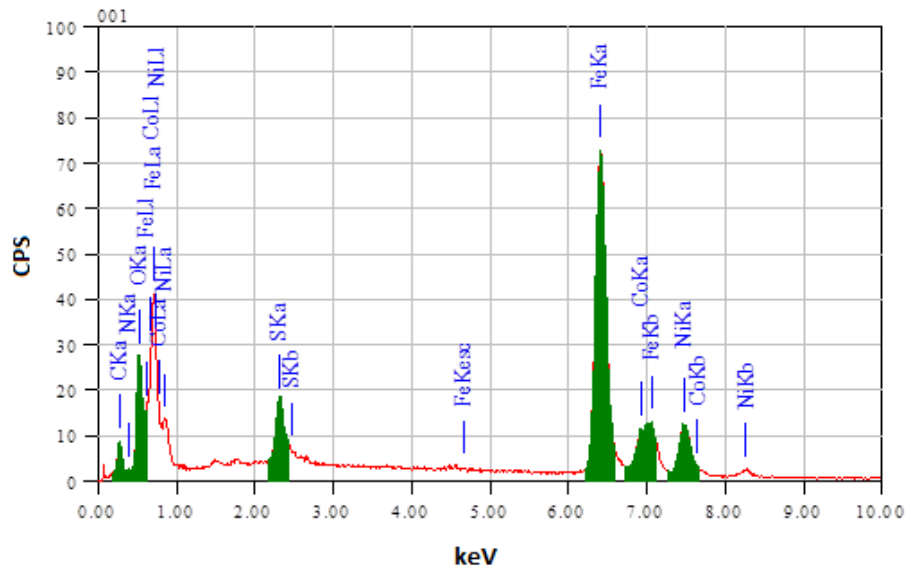


Fig. 3.98: EDS spectra of the weld aged maraging steel after immersion in 0.1 M sulphuric acid in the absence of DDPM.

Table 3.124: Results of potentiodynamic polarization studies for the corrosion of weld aged maraging steel in 0.1 M sulphuric containing different concentrations of DDPM.

Temperature (°C)	Conc. of inhibitor (mM)	E_{corr} (mV /SCE)	b_a (mV dec ⁻¹)	$-b_c$ (mV dec ⁻¹)	i_{corr} (mA cm ⁻²)	v_{corr} (mm y ⁻¹)	η (%)
30	Blank	-371±1	221±3	266±3	0.78±0.02	8.99±0.15	
	0.3	-370±3	219±2	262±1	0.43±0.01	5.00±0.13	44.3
	0.6	-366±2	211±1	258±3	0.36±0.01	4.18±0.14	53.4
	0.9	-365±3	208±2	253±3	0.29±0.02	3.35±0.17	62.7
	1.2	-362±1	205±1	249±1	0.19±0.03	2.20±0.30	75.5
	1.5	-360±2	203±1	246±2	0.14±0.02	1.56±0.18	82.6
	35	Blank	-368±3	257±3	283±2	1.27±0.03	14.64±0.26
0.3		-362±1	253±2	281±3	0.68±0.03	7.78±0.26	46.7
0.6		-360±3	249±2	273±2	0.56±0.02	6.43±0.16	56.1
0.9		-355±2	244±1	270±3	0.44±0.02	5.04±0.17	65.5
1.2		-352±3	240±3	267±2	0.27±0.03	3.13±0.30	78.6
1.5		-350±3	237±3	265±3	0.18±0.02	2.07±0.16	85.8
40		Blank	-365±2	289±1	296±3	1.99±0.02	22.95±0.21
	0.3	-362±3	293±1	300±3	1.00±0.02	11.49±0.24	49.8
	0.6	-358±2	285±2	292±1	0.81±0.02	9.32±0.23	59.3
	0.9	-356±1	282±2	289±3	0.62±0.02	7.10±0.21	69.2
	1.2	-354±3	279±3	286±1	0.35±0.01	4.05±0.14	82.3
	1.5	-350±3	277±2	284±2	0.21±0.02	2.36±0.20	89.7
	45	Blank	-362±2	295±3	317±2	2.22±0.03	25.48±0.25
0.3		-356±1	291±1	313±1	1.03±0.02	11.85±0.18	53.4
0.6		-353±1	287±1	309±1	0.82±0.03	9.39±0.27	63.1
0.9		-354±2	282±1	304±3	0.60±0.01	6.88±0.13	73.3
1.2		-348±3	278±2	300±3	0.30±0.02	3.42±0.22	86.6
1.5		-346±1	275±1	297±1	0.13±0.02	1.50±0.18	94.1
50		Blank	-359±3	298±2	321±1	2.47±0.02	28.48±0.18
	0.3	-356±3	302±2	326±1	1.08±0.02	12.41±0.25	56.3
	0.6	-350±2	294±3	317±1	0.84±0.02	9.61±0.23	66.2
	0.9	-348±4	291±1	314±1	0.59±0.02	6.74±0.23	76.3
	1.2	-344±3	288±3	311±3	0.24±0.01	2.80±0.11	90.2
	1.5	-342±1	286±1	309±2	0.05±0.03	0.61±0.30	97.9

Table 3.125: Results of potentiodynamic polarization studies for the corrosion of weld aged maraging steel in 0.5 M sulphuric containing different concentrations of CPOB.

Temperature (°C)	Conc. of inhibitor (mM)	E_{corr} (mV /SCE)	b_a (mV dec ⁻¹)	$-b_c$ (mV dec ⁻¹)	i_{corr} (mA cm ⁻²)	v_{corr} (mm y ⁻¹)	η (%)
30	Blank	-356±1	235±1	268±3	1.80±0.08	20.71±0.91	
	0.3	-353±1	231±3	266±3	1.07±0.02	12.30±0.19	40.6
	0.6	-350±2	227±2	258±3	0.90±0.03	10.40±0.34	49.8
	0.9	-346±1	222±3	255±3	0.74±0.02	8.45±0.19	59.2
	1.2	-348±1	218±3	252±1	0.50±0.02	5.77±0.15	72.1
	1.5	-342±3	215±3	250±3	0.37±0.04	4.29±0.36	79.3
35	Blank	-353±2	257±2	276±2	2.41±0.07	27.73±0.81	
	0.3	-350±1	255±1	272±3	1.38±0.02	15.85±0.24	42.8
	0.6	-347±1	247±3	268±3	1.15±0.02	13.28±0.18	52.1
	0.9	-342±2	244±1	263±1	0.93±0.02	10.64±0.16	61.6
	1.2	-340±2	241±2	259±3	0.61±0.02	7.02±0.22	74.7
	1.5	-337±2	239±1	256±2	0.44±0.03	5.02±0.35	81.9
40	Blank	-350±3	279±1	288±3	3.83±0.03	44.07±0.28	
	0.3	-347±1	283±1	292±2	2.08±0.02	23.88±0.15	45.8
	0.6	-343±2	274±2	284±1	1.72±0.01	19.75±0.11	55.2
	0.9	-340±3	271±2	281±1	1.35±0.03	15.53±0.28	64.8
	1.2	-336±3	268±1	278±3	0.85±0.03	9.72±0.34	78.3
	1.5	-333±3	266±3	276±2	0.57±0.03	6.50±0.29	85.3
45	Blank	-348±3	296±3	297±2	4.01±0.03	46.14±0.31	
	0.3	-345±3	292±3	295±1	2.03±0.03	23.35±0.29	49.4
	0.6	-340±1	288±1	287±1	1.65±0.03	18.98±0.26	58.9
	0.9	-335±2	283±1	284±1	1.26±0.03	14.51±0.31	68.6
	1.2	-332±1	279±3	281±1	0.73±0.04	8.36±0.38	81.9
	1.5	-329±1	276±3	279±3	0.43±0.03	4.96±0.26	89.3
50	Blank	-346±3	315±3	306±1	4.30±0.04	49.47±0.37	
	0.3	-343±3	319±2	302±1	2.03±0.03	23.39±0.31	52.7
	0.6	-341±3	311±3	298±2	1.62±0.01	18.66±0.10	62.3
	0.9	-339±3	308±3	293±3	1.20±0.03	13.82±0.31	72.1
	1.2	-335±3	305±2	289±3	0.62±0.02	7.16±0.17	85.5
	1.5	-332±1	303±1	286±2	0.30±0.02	3.47±0.15	93.4

Table 3.126: Results of potentiodynamic polarization studies for the corrosion of weld aged maraging steel in 1.0 M sulphuric acid containing different concentrations of DDPM.

Temperature (°C)	Conc. of inhibitor (mM)	E_{corr} (mV /SCE)	b_a (mV dec ⁻¹)	$-b_c$ (mV dec ⁻¹)	i_{corr} (mA cm ⁻²)	v_{corr} (mm y ⁻¹)	η (%)
30	Blank	-323±1	247±1	301±2	8.56±0.26	98.49±2.58	
	0.4	-326±3	247±1	295±1	4.22±0.32	48.60±3.23	50.7
	0.8	-316±2	240±2	291±3	3.43±0.33	39.46±3.33	59.9
	1.2	-312±3	237±2	287±2	2.67±0.34	30.72±3.41	68.8
	1.6	-308±1	234±2	279±2	1.90±0.26	21.87±2.62	77.8
	2.0	-307±1	232±2	278±2	1.42±0.28	16.35±2.80	83.4
35	Blank	-318±2	276±2	305±2	12.83±0.26	147.27±2.58	
	0.4	-311±1	270±3	300±3	5.87±0.30	67.54±3.97	54.1
	0.8	-308±3	266±3	293±2	4.69±0.29	54.00±2.90	63.3
	1.2	-314±3	262±1	290±3	3.57±0.32	41.06±3.24	72.1
	1.6	-307±3	254±3	287±1	2.43±0.36	27.97±3.62	81.0
	2.0	-298±1	253±2	285±2	1.72±0.17	19.78±1.73	86.6
40	Blank	-309±3	292±1	307±1	16.92±0.32	194.44±3.23	
	0.4	-308±1	293±3	308±2	7.25±0.35	83.42±3.48	57.1
	0.8	-302±3	286±1	301±3	5.71±0.33	65.72±3.29	66.2
	1.2	-301±2	283±2	298±2	4.24±0.25	48.81±2.54	74.9
	1.6	-297±1	280±3	295±3	2.76±0.22	31.69±2.23	83.7
	2.0	-291±1	278±2	293±2	1.83±0.27	21.00±2.72	89.2
45	Blank	-307±1	298±1	303±3	19.46±0.27	223.21±2.69	
	0.4	-304±2	292±1	297±1	8.00±0.12	91.98±1.19	58.8
	0.8	-306±2	288±2	293±3	6.21±0.22	71.47±2.19	68.0
	1.2	-309±2	284±3	289±1	4.51±0.23	51.85±2.33	76.8
	1.6	-304±2	276±2	281±3	2.78±0.21	32.01±2.07	85.7
	2.0	-291±2	275±1	280±1	1.71±0.19	19.62±1.91	91.2
50	Blank	-305±2	312±2	311±3	22.15±0.40	254.27±3.99	
	0.4	-300±3	313±2	306±1	8.58±0.37	98.66±3.71	61.2
	0.8	-296±2	306±2	299±3	6.52±0.37	75.06±3.66	70.5
	1.2	-296±3	303±1	296±1	4.56±0.35	52.48±3.46	79.4
	1.6	-290±1	300±3	293±3	2.58±0.30	29.65±2.97	88.3
	2.0	-284±2	298±1	291±2	1.34±0.12	15.38±1.19	94.0

Table 3.127: Results of potentiodynamic polarization studies for the corrosion of weld aged maraging steel in 1.5 M sulphuric containing different concentrations of DDPM.

Temperature (°C)	Conc. of inhibitor (mM)	E_{corr} (mV /SCE)	b_a (mV dec ⁻¹)	$-b_c$ (mV dec ⁻¹)	i_{corr} (mA cm ⁻²)	v_{corr} (mm y ⁻¹)	η (%)
30	Blank	-295±2	252±3	260±2	17.06±0.43	195.51±4.32	
	0.5	-295±3	247±2	255±3	9.33±0.42	107.38±3.20	45.1
	1.0	-289±3	240±1	248±3	7.74±0.23	89.05±2.27	54.5
	1.5	-287±1	237±2	245±1	6.22±0.35	71.51±3.48	63.4
	2.0	-282±3	234±3	242±1	4.67±0.29	53.75±2.94	72.5
	2.5	-281±1	232±1	240±2	3.71±0.16	42.68±1.63	78.2
35	Blank	-291±1	253±2	272±2	23.65±0.28	271.53±2.81	
	0.5	-285±2	253±1	265±2	12.49±0.41	143.72±4.14	47.1
	1.0	-286±3	246±2	258±1	10.26±0.37	118.01±3.72	56.5
	1.5	-285±2	243±3	255±3	8.12±0.31	93.41±3.08	65.6
	2.0	-281±2	240±3	252±2	5.95±0.24	68.51±2.41	74.8
	2.5	-276±1	238±1	250±2	4.61±0.39	53.00±2.89	80.5
40	Blank	-288±2	254±2	276±2	28.07±0.36	332.15±3.61	
	0.5	-289±1	248±1	268±1	14.06±0.38	161.82±3.75	49.8
	1.0	290±2	244±3	264±1	11.39±0.47	131.02±4.66	59.3
	1.5	-283±1	240±3	260±2	8.83±0.24	101.54±2.40	68.5
	2.0	-278±3	232±3	252±3	6.23±0.35	71.68±3.51	77.8
	2.5	-277±3	231±1	251±3	4.61±0.24	53.09±2.43	83.5
45	Blank	-285±3	266±1	283±3	30.34±0.24	348.61±2.36	
	0.5	-278±3	261±1	281±2	14.30±0.22	164.55±2.15	52.8
	1.0	-279±1	254±3	273±2	11.38±0.57	130.91±2.74	62.5
	1.5	-278±1	251±2	270±2	8.58±0.39	98.66±3.93	71.7
	2.0	-275±1	248±1	267±3	5.74±0.20	66.03±2.03	81.1
	2.5	-269±2	246±3	265±2	3.97±0.20	45.70±2.97	86.9
50	Blank	-283±3	272±1	296±1	33.03±0.36	379.60±3.60	
	0.5	-279±2	266±2	289±2	14.40±0.37	165.69±3.68	56.4
	1.0	-274±2	262±2	285±2	11.18±0.23	128.67±2.35	66.1
	1.5	-277±1	258±1	281±1	8.10±0.25	93.21±2.48	75.5
	2.0	-271±2	250±1	273±1	4.98±0.28	57.29±2.80	84.9
	2.5	-272±1	249±3	272±1	3.04±0.22	34.93±2.15	90.8

Table 3.128: Results of potentiodynamic polarization studies for the corrosion of weld aged maraging steel in 2.0 M sulphuric containing different concentrations of CPOB.

Temperature (°C)	Conc. of inhibitor (mM)	E_{corr} (mV /SCE)	b_a (mV dec ⁻¹)	$-b_c$ (mV dec ⁻¹)	i_{corr} (mA cm ⁻²)	v_{corr} (mm y ⁻¹)	η (%)
30	Blank	-281±2	223±3	251±3	20.32±0.44	233.50±4.40	
	0.5	-278±2	222±1	244±2	12.49±0.37	143.69±3.66	38.5
	1.0	-277±1	215±2	240±1	10.57±0.35	121.57±3.53	48.0
	1.5	-274±2	212±2	236±2	8.73±0.31	100.41±3.05	57.1
	2.0	-268±3	209±2	228±1	6.87±0.22	78.99±2.17	66.2
	2.5	-273±2	207±2	227±1	5.70±0.25	65.63±2.53	71.9
35	Blank	-279±1	245±3	263±2	27.66±0.56	317.55±5.60	
	0.5	-277±2	239±1	258±3	16.46±0.37	189.33±3.72	40.4
	1.0	-276±2	235±1	251±3	13.81±0.47	158.94±4.75	50.2
	1.5	-276±2	231±4	248±2	11.29±0.28	129.88±2.85	59.1
	2.0	-272±1	223±3	245±3	8.73±0.22	100.47±2.16	68.4
	2.5	-268±2	222±3	243±2	7.14±0.29	82.12±2.88	74.1
40	Blank	-278±3	269±3	274±3	35.04±0.44	402.65±4.42	
	0.5	-275±1	269±1	268±2	19.98±0.43	229.90±4.27	42.9
	1.0	-277±3	262±2	264±1	16.60±0.41	190.96±4.14	52.6
	1.5	-272±3	259±2	260±3	13.36±0.31	153.75±3.12	61.8
	2.0	-267±3	256±1	252±3	10.09±0.24	116.10±2.36	71.2
	2.5	-265±2	254±3	251±2	8.05±0.29	92.58±2.93	77.3
45	Blank	-275±1	281±2	288±1	40.74±0.26	468.28±2.57	
	0.5	-269±2	275±1	283±3	21.83±0.48	251.14±4.78	46.4
	1.0	-266±3	271±1	276±1	17.85±0.31	205.39±3.11	56.1
	1.5	-266±2	267±1	273±2	14.05±0.20	161.70±2.02	65.5
	2.0	-262±1	259±2	270±2	10.21±0.51	117.44±5.14	74.9
	2.5	-257±3	258±1	268±1	7.81±0.25	89.82±2.48	80.8
50	Blank	-273±2	301±3	302±1	45.28±0.41	520.05±4.11	
	0.5	-274±3	296±2	296±2	23.07±0.32	265.43±3.18	49.1
	1.0	-267±2	289±2	292±3	18.61±0.47	214.11±4.67	58.8
	1.5	-265±3	286±1	288±1	14.35±0.46	165.12±4.56	68.3
	2.0	-259±2	283±1	280±3	10.03±0.22	115.45±2.17	77.8
	2.5	-258±2	281±3	279±2	7.34±0.21	84.46±2.11	83.8

Table 3.129: EIS data for the corrosion of weld aged maraging steel in 0.1 M sulphuric acid containing different concentrations of DDPM.

Temperature (°C)	Conc. of inhibitor (mM)	R_{ct} (ohm. cm ²)	C_{dl} (mF cm ⁻²)	R_{pf} (ohm. cm ²)	C_{pf} (mF cm ⁻²)	η (%)
30	Blank	74.66±3.81	21.01±3.23			
	0.3	131.51±2.90	13.50±2.14	10.01±1.18	3.83±0.26	43.2
	0.6	156.91±2.68	11.35±1.75	11.57±1.30	3.22±0.29	52.4
	0.9	195.55±2.39	9.15±1.72	13.95±1.23	2.60±0.41	61.8
	1.2	295.68±3.12	6.13±3.46	20.11±1.83	1.76±0.28	74.8
	1.5	412.94±4.31	4.45±2.47	27.33±2.73	1.29±0.47	81.9
35	Blank	51.17±1.85	26.57±3.17			
	0.3	93.17±2.85	17.78±1.57	7.65±1.17	5.03±0.42	45.1
	0.6	112.36±3.41	14.78±2.00	8.83±1.06	4.18±0.47	54.5
	0.9	142.34±3.42	11.72±3.41	10.68±0.89	3.33±0.50	64.1
	1.2	224.82±3.00	7.50±3.26	15.75±1.39	2.14±0.32	77.2
	1.5	331.63±2.84	5.16±1.65	22.32±3.91	1.48±0.45	84.6
40	Blank	35.45±2.14	32.14±3.66			
	0.3	67.14±2.29	18.97±1.52	6.05±1.23	5.36±0.40	47.2
	0.6	82.02±3.28	15.57±1.69	6.97±1.79	4.41±0.35	56.8
	0.9	106.01±3.77	12.10±3.31	8.44±1.45	3.43±0.23	66.6
	1.2	177.43±3.52	7.32±3.28	12.84±1.17	2.09±0.33	80.0
	1.5	283.15±2.40	4.67±1.23	19.34±2.20	1.35±0.47	87.5
45	Blank	33.36±3.33	36.48±2.77			
	0.3	67.54±1.97	19.99±3.37	6.07±1.28	5.65±0.27	50.6
	0.6	84.18±3.04	16.08±2.99	7.10±1.50	4.55±0.44	60.4
	0.9	112.51±3.22	12.09±3.05	8.84±1.61	3.43±0.21	70.4
	1.2	209.68±3.10	6.59±1.75	14.82±1.06	1.89±0.21	84.1
	1.5	402.41±3.76	3.54±1.35	26.68±3.51	1.03±0.27	91.7
50	Blank	30.19±3.45	41.49±3.45			
	0.3	64.45±3.69	21.67±2.86	5.88±1.95	6.12±0.36	53.2
	0.6	81.86±2.07	17.11±3.03	6.96±1.62	4.84±0.50	63.1
	0.9	113.11±3.74	12.44±2.76	8.88±1.09	3.53±0.49	73.3
	1.2	238.09±3.88	6.03±2.11	16.57±1.08	1.73±0.39	87.3
	1.5	616.12±2.54	2.47±1.11	39.83±2.87	0.73±0.28	95.1

Table 3.130: EIS data for the corrosion of weld aged maraging steel in 0.5 M sulphuric containing different concentrations of DDPM.

Temperature (°C)	Conc. of inhibitor (mM)	R_{ct} (ohm. cm ²)	C_{dl} (μ F cm ⁻²)	R_{pf} (ohm. cm ²)	C_{pf} (mF cm ⁻²)	η (%)
30	Blank	33.56±2.43	40.12±2.63			
	0.3	57.99±3.64	26.44±2.05	5.49±2.30	7.46±0.92	42.1
	0.6	69.07±2.92	22.23±1.79	6.17±2.37	6.28±0.87	51.4
	0.9	85.83±3.34	17.94±2.16	7.20±1.96	5.07±0.97	60.9
	1.2	128.88±2.93	12.02±2.86	9.85±2.21	3.41±1.05	74.2
	1.5	178.51±3.61	8.74±2.61	12.90±3.91	2.49±0.83	81.2
35	Blank	26.64±2.10	65.92±3.08			
	0.3	47.98±3.41	39.80±3.09	4.87±1.92	11.21±1.85	44.5
	0.6	57.74±2.39	33.11±2.71	5.47±1.86	9.33±0.56	53.9
	0.9	72.87±2.11	26.28±3.34	6.40±1.29	7.41±1.11	63.4
	1.2	114.04±3.55	16.88±3.20	8.94±1.72	4.77±0.66	76.6
	1.5	165.98±4.58	11.67±2.50	12.13±2.17	3.31±0.56	84.3
40	Blank	17.85±2.18	109.77±1.62			
	0.3	33.78±3.53	56.77±2.60	4.00±1.08	15.97±1.17	47.2
	0.6	41.16±3.50	46.63±3.28	4.45±1.57	13.12±0.89	56.6
	0.9	52.98±3.15	36.28±2.35	5.18±1.69	10.22±0.98	66.3
	1.2	87.67±2.02	22.01±2.68	7.31±0.87	6.21±1.12	79.6
	1.5	137.52±3.82	14.11±1.21	10.38±2.45	4.00±0.52	87.2
45	Blank	17.84±3.33	125.60±2.69			
	0.3	35.97±3.27	66.60±1.66	4.13±1.12	18.73±1.88	50.4
	0.6	44.57±3.08	53.80±1.91	4.66±2.29	15.14±0.80	60.1
	0.9	58.99±2.07	40.70±1.74	5.55±2.04	11.46±0.58	69.8
	1.2	106.25±2.09	22.70±2.37	8.46±1.13	6.41±1.18	83.2
	1.5	191.21±4.93	12.71±1.82	13.68±2.90	3.60±0.79	90.7
50	Blank	17.42±2.68	158.27±3.46			
	0.3	37.47±2.97	80.77±1.69	4.22±0.93	22.71±1.96	53.5
	0.6	47.29±1.79	64.04±2.03	4.83±2.33	18.01±0.53	63.2
	0.9	64.64±2.54	46.91±1.81	5.90±1.31	13.20±0.70	73.1
	1.2	130.49±3.63	23.35±2.90	9.95±1.80	6.59±1.18	86.7
	1.5	298.80±4.63	10.33±2.83	20.30±2.38	2.94±0.54	94.2

Table 3.131: EIS data of weld aged maraging steel in 1.0 M sulphuric acid containing different concentrations of DDPM.

Temperature (°C)	Conc. of inhibitor (mM)	R_{ct} (ohm. cm ²)	C_{dl} (mF cm ⁻²)	R_{pf} (ohm. cm ²)	C_{pf} (mF cm ⁻²)	η (%)
30	Blank	7.09±1.61	11.00±2.34			
	0.4	14.59±1.75	6.15±1.35	2.82±1.13	1.76±0.41	51.4
	0.8	18.08±1.58	5.01±1.41	3.03±1.00	1.44±0.25	60.8
	1.2	23.45±1.56	3.91±1.74	3.36±1.15	1.13±0.26	69.8
	1.6	33.49±1.70	2.81±1.00	3.98±1.47	0.82±0.29	78.8
	2.0	45.71±2.75	2.12±1.37	4.73±1.85	0.63±0.18	84.5
35	Blank	5.05±1.62	11.83±2.87			
	0.4	11.28±1.53	5.70±1.60	2.61±1.00	1.64±0.30	55.2
	0.8	14.24±1.72	4.56±1.93	2.80±1.31	1.32±0.82	64.5
	1.2	18.98±1.57	3.48±1.99	3.09±1.24	1.01±0.54	73.4
	1.6	28.66±1.74	2.38±1.98	3.68±1.46	0.70±0.22	82.4
	2.0	42.08±2.51	1.69±1.31	4.51±1.91	0.51±0.13	88.1
40	Blank	3.95±1.79	12.37±2.29			
	0.4	9.53±1.64	5.74±1.49	2.51±1.38	1.65±0.49	58.5
	0.8	12.24±1.65	4.52±1.93	2.67±1.22	1.30±0.18	67.7
	1.2	16.82±1.70	3.35±1.70	2.95±1.05	0.98±0.33	76.5
	1.6	27.05±1.57	2.17±1.53	3.58±1.24	0.65±0.29	85.4
	2.0	43.69±2.59	1.43±1.07	4.61±2.91	0.44±0.14	91.2
45	Blank	3.49±1.61	15.26±2.66			
	0.4	8.83±1.74	6.71±1.57	2.46±1.23	1.92±0.44	60.5
	0.8	11.55±1.64	5.19±1.52	2.63±0.83	1.49±0.37	69.8
	1.2	16.35±1.52	3.73±1.55	2.93±1.26	1.08±0.29	78.7
	1.6	28.24±1.67	2.25±1.78	3.66±0.92	0.67±0.10	87.6
	2.0	51.63±2.80	1.33±1.00	5.10±1.41	0.41±0.19	93.2
50	Blank	3.15±1.59	18.08±2.63			
	0.4	8.59±1.58	8.23±1.50	2.45±0.87	2.35±0.46	63.3
	0.8	11.54±1.60	6.18±1.25	2.63±0.98	1.77±0.35	72.7
	1.2	17.19±1.59	4.22±1.47	2.98±1.43	1.22±0.21	81.7
	1.6	34.05±1.72	2.24±1.45	4.01±1.15	0.66±0.15	90.8
	2.0	87.74±3.54	1.01±0.73	7.32±1.88	0.32±0.14	96.4

Table 3.132: EIS data for the corrosion of weld aged maraging steel in 1.5 M sulphuric acid containing different concentrations of DDPM.

Temperature (°C)	Conc. of inhibitor (mM)	R_{ct} (ohm. cm ²)	C_{dl} (mF cm ⁻²)	R_{pf} (ohm. cm ²)	C_{pf} (mF cm ⁻²)	η (%)
30	Blank	3.34±1.93	13.71±2.26			
	0.5	6.11±2.20	8.35±1.78	2.30±0.31	2.38±1.18	45.4
	1.0	7.38±1.52	6.95±2.28	2.37±0.85	1.99±0.60	54.7
	1.5	9.20±2.03	5.62±1.98	2.49±0.77	1.61±0.82	63.7
	2.0	12.27±1.61	4.27±1.88	2.67±1.14	1.23±1.10	72.8
	2.5	15.48±1.85	3.43±0.62	2.87±1.17	1.00±0.50	78.4
35	Blank	2.46±0.42	14.52±2.73			
	0.5	4.74±1.50	8.52±2.94	2.21±0.88	2.43±0.47	48.1
	1.0	5.81±2.24	6.99±2.51	2.28±1.38	2.00±0.59	57.7
	1.5	7.41±2.15	5.53±2.49	2.38±1.20	1.59±0.65	66.8
	2.0	10.28±2.38	4.05±2.79	2.55±1.44	1.17±0.86	76.1
	2.5	13.55±1.70	3.13±0.95	2.75±1.13	0.91±0.10	81.9
40	Blank	2.09±0.58	16.09±2.71			
	0.5	4.27±2.38	8.65±2.16	2.18±1.37	2.46±0.47	51.0
	1.0	5.32±2.12	6.98±2.18	2.25±0.80	2.00±1.00	60.7
	1.5	6.95±2.45	5.40±2.71	2.35±0.77	1.55±0.92	69.9
	2.0	10.09±2.14	3.79±1.14	2.54±0.86	1.10±0.36	79.3
	2.5	14.05±2.06	2.78±0.61	2.78±1.23	0.82±0.28	85.1
45	Blank	2.01±1.00	18.30±1.83			
	0.5	4.41±2.17	9.40±2.94	2.19±1.41	2.67±0.83	54.4
	1.0	5.61±1.83	7.43±1.80	2.26±0.83	2.12±0.64	64.2
	1.5	7.60±1.63	5.55±2.77	2.39±1.06	1.59±0.45	73.5
	2.0	11.82±1.73	3.65±1.80	2.65±1.25	1.06±0.36	83.1
	2.5	18.08±2.44	2.46±0.15	3.03±0.84	0.73±0.27	88.9
50	Blank	1.90±0.58	21.47±2.85			
	0.5	4.53±1.03	10.64±2.10	2.20±0.91	3.02±0.76	58.2
	1.0	5.92±1.91	8.20±2.69	2.28±1.43	2.34±1.20	67.9
	1.5	8.38±1.72	5.86±2.94	2.43±0.93	1.68±0.78	77.3
	2.0	14.48±1.93	3.48±1.87	2.81±1.08	1.01±0.54	86.9
	2.5	26.50±2.34	2.01±0.13	3.55±1.04	0.60±0.11	92.8

Table 3.133: EIS data for the corrosion of weld aged maraging steel in 2.0 M sulphuric acid containing different concentrations of DDPM.

Temperature (°C)	Conc. of inhibitor (mM)	R_{ct} (ohm. cm^2)	C_{dl} (mF cm^{-2})	R_{pf} (ohm. cm^2)	C_{pf} (mF cm^{-2})	η (%)
30	Blank	2.58±0.98	16.42±3.97			
	0.5	4.24±1.88	10.82±2.17	2.18±0.64	3.07±1.28	39.1
	1.0	5.02±1.54	9.18±2.82	2.23±1.29	2.61±1.70	48.7
	1.5	6.11±2.36	7.58±2.70	2.30±0.70	2.16±1.42	57.8
	2.0	7.83±2.19	5.96±2.37	2.40±1.07	1.71±0.94	67.1
	2.5	9.50±2.00	4.96±2.21	2.50±1.33	1.43±0.19	72.8
35	Blank	2.04±1.16	17.25±3.10			
	0.5	3.47±1.08	11.23±2.30	2.13±1.29	3.19±1.26	41.1
	1.0	4.15±2.32	9.43±2.69	2.17±0.70	2.68±0.97	50.8
	1.5	5.11±1.77	7.70±2.63	2.23±0.76	2.20±1.32	60.1
	2.0	6.67±2.22	5.95±2.43	2.33±0.61	1.71±0.84	69.4
	2.5	8.24±1.74	4.86±1.41	2.43±0.50	1.40±0.29	75.2
40	Blank	1.72±0.26	19.51±2.92			
	0.5	3.07±1.84	12.05±2.79	2.11±0.28	3.42±1.29	44.0
	1.0	3.72±1.90	9.98±1.82	2.15±1.44	2.84±1.13	53.8
	1.5	4.66±1.95	8.01±2.50	2.21±1.33	2.28±1.14	63.1
	2.0	6.27±2.11	6.01±2.64	2.30±0.89	1.72±0.93	72.6
	2.5	7.98±1.93	4.77±2.98	2.41±0.97	1.38±0.56	78.4
45	Blank	1.55±0.85	23.80±3.72			
	0.5	2.97±1.71	13.28±1.85	2.10±1.32	3.76±0.88	47.8
	1.0	3.66±1.74	10.82±2.17	2.14±1.24	3.07±0.83	57.7
	1.5	4.71±2.47	8.45±2.11	2.21±1.22	2.41±1.55	67.1
	2.0	6.64±1.82	6.06±2.14	2.33±1.21	1.74±0.49	76.7
	2.5	8.92±2.02	4.57±1.16	2.47±0.16	1.32±0.58	82.6
50	Blank	1.48±0.46	26.05±2.76			
	0.5	3.00±1.21	13.86±2.84	2.10±1.43	3.93±0.77	50.7
	1.0	3.76±2.33	11.10±1.83	2.15±0.67	3.15±1.36	60.6
	1.5	4.96±1.55	8.47±2.73	2.22±1.33	2.41±0.46	70.2
	2.0	7.33±1.62	5.80±2.98	2.37±0.55	1.66±0.32	79.8
	2.5	10.44±2.87	4.14±0.77	2.56±0.57	1.20±0.25	85.8

Table 3.134: Comparison of maximum attainable inhibition efficiencies by the Tafel method and EIS method for the corrosion of weld aged maraging steel in sulphuric acid solutions of different concentrations in the presence of DDPM at 30 °C.

Molarity of sulphuric acid (M)	Conc. of DDPM (mM)	η (%)	
		Tafel	EIS
0.1	1.5	81.9	80.8
0.5	1.5	79.2	81.2
1.0	2.0	83.4	84.0
1.5	2.5	78.1	78.4
2.0	2.5	71.9	72.8

Table 3.135: Activation parameters for the corrosion of weld aged maraging steel in sulphuric acid containing different concentrations of DDPM.

Molarity of sulphuric acid (M)	Conc. of inhibitor (mM)	E_a ($\text{kJ}^{-1} \text{mol}^{-1}$)	ΔH^\ddagger ($\text{kJ}^{-1} \text{mol}^{-1}$)	ΔS^\ddagger ($\text{J mol}^{-1} \text{K}^{-1}$)
0.1	0.0	44.31	43.16	-88.32
	0.3	48.83	47.56	-80.21
	0.6	51.54	50.21	-63.85
	0.9	53.35	51.97	-43.89
	1.2	74.60	72.67	-20.73
	1.5	80.48	78.39	-13.52
0.5	0.0	35.50	37.48	-111.52
	0.3	39.12	47.56	-101.28
	0.6	41.30	50.21	-80.62
	0.9	42.74	51.97	-55.42
	1.2	59.77	72.67	-26.17
	1.5	64.48	78.39	-17.07
1.0	0.0	32.79	28.11	-144.08
	0.4	36.14	30.98	-130.85
	0.8	38.14	32.70	-104.16
	1.2	39.48	33.85	-71.60
	1.6	55.21	47.33	-33.81
	2.0	59.56	51.06	-22.05
1.5	0.0	25.24	23.69	-141.93
	0.5	27.82	26.11	-128.90
	1.0	29.36	27.56	-102.61
	1.5	30.39	28.52	-70.53
	2.0	42.50	39.89	-33.31
	2.5	45.84	43.03	-21.72
2.0	0.0	21.20	22.58	-142.28
	0.5	23.36	24.88	-129.21
	1.0	24.66	26.27	-102.86
	1.5	25.53	27.19	-70.70
	2.0	35.69	38.02	-33.39
	2.5	38.51	41.01	-21.78

Table 3.136: Thermodynamic parameters for the adsorption of DDPM on weld aged maraging steel surface in sulphuric acid at different temperatures.

Molarity of sulphuric acid (M)	Temperature (°C)	$-\Delta G^{\circ}_{\text{ads}}$ (kJ mol ⁻¹)	$\Delta H^{\circ}_{\text{ads}}$ (kJ mol ⁻¹)	$\Delta S^{\circ}_{\text{ads}}$ (J mol ⁻¹ K ⁻¹)
0.1	30	36.38	-26.54	176.87
	35	45.24		
	40	45.06		
	45	44.88		
	50	44.71		
0.5	30	45.44	-33.55	166.72
	35	45.33		
	40	45.12		
	45	44.94		
	50	44.77		
1.0	30	43.49	-45.76	277.04
	35	43.35		
	40	43.19		
	45	43.02		
	50	42.85		
1.5	30	42.16	-58.27	300.47
	35	42.02		
	40	41.86		
	45	41.70		
	50	41.54		
2.0	30	40.18	-63.70	313.57
	35	40.05		
	40	39.95		
	45	39.75		
	50	39.69		

CHAPTER 4

SUMMARY AND CONCLUSIONS

4.1 SUMMARY

The corrosion behaviour of M250 grade maraging steel was studied under weld aged conditions, in two different acid media, namely, hydrochloric acid and sulphuric acid in different concentration levels at different temperatures. The study was carried out by two methods, namely, Tafel polarisation and impedance spectroscopy methods. The effects of acid concentration and temperature on the corrosion rate were investigated. The inhibition effect of five inhibitors (ATPI, CPOB, CPOM, DNPH and DDPM), on the corrosion of weld aged maraging steel was investigated in the two acid media of hydrochloric acid and sulphuric acid in different concentrations and at different temperatures. The effects of acid concentration, temperature and inhibitor concentration on the inhibition efficiency were investigated in detail. The variation in the inhibition efficiency with the change in the structure of the inhibitor was analysed. The activation parameters and thermodynamic parameters were calculated for the corrosion of alloy both in the presence and absence of the inhibitors. Both the activation and thermodynamic parameters were analysed to determine the types of adsorption of inhibitor molecules on alloy surfaces. The probable mechanisms for the adsorption of the inhibitor molecules were proposed.

4.2 CONCLUSIONS

Based on the results of the present investigation, the following conclusions are drawn:

1. The corrosion rates of weld aged maraging steel in both hydrochloric acid sulphuric acid medium are substantial.
2. The potentiodynamic polarization and impedance studies showed that the corrosion rate of the alloy increases with the increase in the concentration of hydrochloric acid and the solution temperature.
3. The inhibitors, ATPI, CPOB, CPOM, DNPH and DDPM act as mixed inhibitors, with slightly predominant anodic control as indicated by the small shift in E_{corr} values towards the less negative side (anodic shift) in both the acids.

4. The inhibitors, ATPI, CPOB, CPOM, DNPH and DDPM affect both the anodic dissolution of weld aged maraging steel and cathodic hydrogen evolution reactions.
5. The inhibition efficiencies of ATPI, CPOB, CPOM and DNPH decrease with the increase in temperature, on both the alloy surface, in both the acid media.
6. The adsorption of ATPI, CPOB, CPOM and DNPH on the alloy is through both physisorption and chemisorption, with predominant physisorption.
7. The inhibition efficiency of DDPM increases with the increase in temperatures in both the acid media.
8. The adsorption of DDPM on the alloy surface is predominantly through chemisorption.
9. The adsorption of all the five inhibitors on alloy surfaces follows Langmuir adsorption isotherm.
10. The inhibition efficiencies of the five inhibitors vary in the following order $DNPH < DDPM < CPOB < ATPI < CPOM$ in the hydrochloric acid medium at all the temperatures, whereas for sulphuric acid medium it is in the order of $DDPM < CPOM < DNPH < ATPI < CPOB$.
11. Among the five inhibitors studied, CPOM is the most effective inhibitor in the hydrochloric acid medium and CPOB is the most efficient inhibitor in the sulphuric acid medium.

4.3 SCOPE FOR FUTURE WORK

The following extensions are recommended to the work presented in this thesis,

- Above study can be extended to other structurally related inhibitors to understand the effect of structure of inhibitor on corrosion inhibition.
- Study of corrosion behaviour and inhibition on the maraging steel welds.
- Comparative study of corrosion behaviour of 18 % Ni M250 grade maraging steel with other grades of maraging steel.

REFERENCES

- Abd EI Rehim, S. S., Hassan, H. H. and Amin, M. A. (2003). "The corrosion inhibition study of sodium dodecyl benzene sulphonate to aluminium and its alloys in 1.0 M HCl solution." *Mater. Chem. Phys.*, 78, 337–348.
- Abd Ei-Rehim, S. S., Ibrahim, M. A. M. and Khaled, K. F. (1999). "4-Aminoantipyrine as an inhibitor of mild steel corrosion in HCl solution." *J. Appl. Electrochem.*, 29, 593-599.
- Ahamad Ishtiaque, Rajendra Prasad, Quraishi, M. A. (2010). "Adsorption and inhibitive properties of some new mannich bases of isatin derivatives on corrosion of mild steel in acidic media." *Corros. Sci.*, 52, 1472-1481.
- Amin M. A., Abd El-Rehim S. S., El- Sherbini E. E. F. and Bayyomi R. S. (2007). "The inhibition of low carbon steel corrosion in hydrochloric acid solutions by succinic acid: Part I. Weight loss, polarization, EIS, PZC, EDX and SEM studies." *Electrochim. Acta.*, 52, 3588-3600.
- Arab S. T. and Emran, K. M. (2008). "Structure effect of thiosemicarbazone derivatives on corrosion of mild steel in hydrochloric acid." *Corros. Sci.*, 52, 1529-1539.
- Ashish Kumar, S. and Quraishi, M. A. (2010). "Effect of cefazolin on the corrosion of mild steel in HCl solution." *Corros. Sci.*, 52 152–160.
- Atta, N. F., Fekry, A. M. and Hassaneen, H. M. (2011). "Corrosion inhibition, hydrogen evolution and antibacterial properties of newly synthesized organic inhibitors on 316L stainless steel alloy in acid medium." *Int. J. Hydrogen Energy.*, 36, 6462-6471.
- Avadhani, G. S. (2001). "Hot deformation mechanisms and microstructural evolution during upset forging of gamma-Fe, Fe-5Ni, Fe-5Co and Fe-5Mo alloys and maraging steel." Doctoral dissertation, Indian Institute of science, Bangalore.

Balaram Gupta, Gopalakrishna, V., Ashok Kumar, J. S., Yadav, B. and Saha (1996). “*Aerospace materials.*” Vol.II, SCC Ltd, New Delhi.

Banerjee, S. N. (1985). *An introduction to science of corrosion and its inhibition*, Oxonian Press, New Delhi.

Bardal, E. (2004). *Corrosion and Protection*, Springer, London.

Barouni , K., Bazzi,L., Salghi, R., Mihit, M., Hammouti, B., Albourine, A. and El Issami, S. (2008). “Some amino acids as corrosion inhibitors for copper in nitric acid solution.” *Mater. Lett.*, 62, 3325-3327.

Barsoukov, E. and Macdonald, J. R. (2005). *Impedance spectroscopy theory, experiment and applications*. 2nd edition, John Wiley & Sons, New Jersey.

Bellanger, G. (1994). “Effect of carbonate in slightly alkaline medium on the corrosion of maraging steel.” *J. Nucl. Mater.*, 217, 187 - 192.

Bellanger, G. and Rameau, J. J. (1996). “Effect of slightly acid pH with or without chloride in radioactive water on the corrosion of maraging steel.” *J. Nucl. Mater.*, 228, 24 -29.

Benali, O. Larabi, L. and Harek, Y. (2009). “Adsorption and inhibitive corrosion properties of thiourea derivatives on cold rolled steel in 1 M HClO₄ solutions.” *J. Appl. Electrochem.*, 39, 769–778.

Bentiss, F., Lebrini, M. and Lagrenee, M. (2005). “Thermodynamic characterization of metal dissolution and inhibitor adsorption processes in mild steel 2,5-bis(n-thienyl)-1,3,4- thiadiazoles hydrochloric acid system”, *Corros. Sci.*, 47, 2915-2931.

Bockris, J. O. M and Amulya, K. N. Reddy (2000). “Modern electrochemistry”, volume 2B, second edition, Kluwer Academic/Plenum Publishers, New York.

Boonlerd Nilwanna, Suchada Chantrapomma, Patcharaporn Jansrisewangwong and Hoong-Kun Fun (2011). “(E)-1-(2,4-dinitrophenyl)-2-[1-(2-nitrophenyl) ethylidene] hydrazine.” *Acta Crystallogr. E*: 67, 3084–3085.

- Dautovich, D. P. (1976). "Corrosion resistance of maraging steels." *Corrosion.*, vol. 1, Shreir, L. L. (Ed.) second ed., Newnes–Butterworths, London, 3, 69.
- Davis, J.R., Davis and associates (Ed.by) (2003). *Corrosion understanding the basics*, ASM international, Ohio.
- De Souza, F. S and Spinelli, A. (2009). "Caffeic acid as a green corrosion inhibitor for mild steel." *Corros. Sci.*, 51, 642–649.
- Dean, S. W. (1999). Standard practice for calculation of corrosion rates and related information from electrochemical measurements. Norm ASTM G102, 2-3.
- Dean, S. W. and Copson, H. R. (1965). "Stress corrosion behavior of maraging nickel steels in natural environments," *Corrosion*, 21, 95-103.
- Deepika Rajamani (2003). "Processing and properties of environmentally-friendly corrosion resistant hybrid nanocomposite coatings for aluminum alloy AA2024." University of Cincinnati.
- Dehri, I. and Erbil, M. (2000). "The effect of relative humidity on the atmospheric corrosion of defective organic coating materials: an EIS study with a new approach." *Corros. Sci.*, 42, 969-978.
- Dehri, I. and Ozcan, M. (2006)., "The inhibitive effect of 6-amino-m-cresol and its Schiff base on the corrosion of mild steel in 0.5 M HCl medium." *Mater. Chem. Phys.*, 98(1), 316-323.
- Denny Jones, A. (1996). *Principles and prevention of corrosion*, II edition, Prentice Hall, Inc, NJ, Michigan.
- Eddy, N. O., Odoemelam, S. A. and Odiongenyi, A. O. (2009). "Joint effect of halides and ethanol extract of *Lasianthera Africana* on inhibition of corrosion of mild steel in H₂SO₄." *J. Appl. Electrochem.*, 39, 849–857.
- Einar Bardal (2004). *Corrosion and protection*, Springer -Verlag London Limited.

Ekpe, U. J., Ibok, U. J., Ita, B. I., Offiong, O. E. and Ebenso, E. E. (1995). "Inhibitory action of methyl and phenylthiosemicarbazone derivatives on the corrosion of mild steel in hydrochloric acid." *Mater. Chem. Phys.*, 40, 87-93.

El- Azhar, M., Mernari, B., Traisnel, M., Bentiss, F. and Lagrenee, M. (2001). "Corrosion inhibition of mild steel by the new class of inhibitors [2,5-bis(n-pyridyl)-1,3,4- thiadiazoles] in acidic media." *Corros. Sci.*, 43, 2229-2238.

El- Azhar, M., Mernari, B., Traisnel, M., Bentiss, F., Lagrenee, M. (2001). "Corrosion inhibition of mild steel by the new class of inhibitors [2,5-bis(n-pyridyl)-1,3,4- thiadiazoles] in acidic media." *Corros. Sci.*, 43, 2229-2238.

Elewady, G. Y. (2008). "Pyrimidine derivatives as corrosion inhibitors for carbon-steel in 2 M hydrochloric acid solution." *Int. J. Electrochem. Sci.*, 3, 1149 - 1161.

El-Sayed, A. (1997). "Phenothiazine as inhibitor of the corrosion of cadmium in acidic solutions." *J. Appl. Electrochem.*, 27, 193-200.

Fekry, A. M. and Ameer, M. A. (2010). "Corrosion inhibition of mild steel in acidic media using newly synthesized heterocyclic organic molecules." *Int. J. Hydrogen Energy*, 35, 7641 - 7651.

Fekry, A. M. and Ameer, M. A. (2011). "Electrochemical investigation on the corrosion and hydrogen evolution rate of mild steel in sulphuric acid solution." *Int. J. Hydrogen Energy*, 36, 11207 -11215.

Ferreira, E. S., Giacomelli, C., Giacomelli, F. C. and Spinelli, A. (2004). "Evaluation of the inhibitor effect of - ascorbic acid on the corrosion of mild steel." *Mater. Chem. Phys.*, 83, 129-134.

Fontana, M.G. (1987). *Corrosion engineering*, McGraw-Hill, Singapore.

Fouda, A. S., Heikal, F. E. and Radwan, M. S. (2009). "Role of some thiadiazole derivatives as inhibitors for the corrosion of C-steel in 1.0 M H₂SO₄." *J. Appl. Electrochem.*, 39, 391-402.

Fuchs-godec R. (2006). "The adsorption, CMC determination and corrosion inhibition of some", N-alkyl quaternary ammonium salts on carbon steel surface in 2 M H₂SO₄." *Colloid. Surface. A.*, 280, 130-139.

Gao, J., Weng, Y., Salitanat, Feng, Li and Yue, H. (2009). "Corrosion inhibition of α , β -unsaturated carbonyl compounds on steel in acid medium." *Pet.Sci.*, 6, 201-207.

Geetha, M. P., Nayak, J. and Shetty, A. N. (2011). "Corrosion inhibition of 6061Al-15vol.pct.SiC(p) composite and its base alloy in a mixture of sulphuric acid and hydrochloric acid by 4-(N,N-dimethylamino) benzaldehyde thiosemicarbazone." *Mater. Chem. Phys.*, 125, 628-640.

Ghanbari, A., Attar, M. M., Mahdavian, M. (2010). "Corrosion inhibition performance of three imidazole derivatives on mild steel in 1 M phosphoric acid." *Mater. Chem. Phys.*, 124 (2-3), 1205-1209.

Gomma, M. K and Wahdan, M. H. (1995). "Schiff bases as corrosion inhibitors for aluminium in hydrochloric acid solution." *Mater.Chem.Phys.*, 39, 209-213.

Gopi, D., Govindaraju, K. M., Collins, V., Arun Prakash, Manivannan, V. and Kavitha, L. (2009). "Inhibition of mild steel corrosion in ground water by pyrrole and thienylcarbonyl benzotriazoles." *J. Appl. Electrochem.*, 39, 269-276.

Grum, J. and Slabe, J. M. (2006). "Effect of Laser-Remelting of Surface Cracks on Microstructure and Residual Stresses in 12Ni Maraging Steel." *Appl. Surf. Sci.*, 252, 4486-4492.

Gunasekaran, G. and Chauhan, L. R. (2004). "Corrosion inhibition by beet root extract." *Portugaliae Electrochemica Acta.*, 49, 4387.

Hackerman, N., Snavely, E. S., J. S. and Payne, J. R. (1966). "Effects of anions on corrosion inhibition by organic compounds." *J. Electrochem. Soc.*, 113, 677-686.

Hoong-Kun Fun, Chin Sing Yeap, Garudachari, B., Arun Isloor, M. and Satyanarayan M. N. (2011). "2-(4-bromophenyl)-2-oxoethyl 4-chlorobenzoate." *Acta Crystallogr., Sect. E*: 67, 1723.

Hoong-Kun Fun, Tara Shahani, Garudachari, B., Arun Isloor, M. and Satyganarayan, M. N. (2011). “2-(4-Chlorophenyl)-2-oxoethyl benzoate.” *Acta Crystallogr., Sect. E:* 67, 1802 -1806.

Hoong-Kun, F., Thawanrat, K. and Suchada, C. (2009) “(2E)-1-(4- Aminophenyl)-3-(2-thienyl)prop-2-en-1-one Ethanol Hemisolvate.” *Acta Crystallogr. E:* 65 2532–2533.

Hosseini Nedjad, S., Teimouri, J., Tahmasebifar, A., Shirazib, H. and Nili Ahmadabadi, M. (2009). “A new concept in further alloying of Fe-Ni-Mn maraging steels.” *Scr. Mater.*, 60, 528–531.

Hosseini, M., Mertens S. F. L. and Arshadi, M. R. (2003). “Synergism and antagonism in mild steel corrosion inhibition by sodium dodecylbenzenesulphonate and hexamethylenetetramine.” *Corros. Sci.*, 45, 1473-1489.

Jagannath Nayak, (2004). “Corrosion behaviour of maraging steels in aqueous media” Doctoral dissertation, NITK Surathkal, India.

Kenyon, N., Kirk, W. W., and Van Rooyen, D. (1971). “Corrosion of 18 Ni 180 and 18 Ni 200 maraging steels in aqueous chlorides.” *Corrosion*, 27 (9), 390-400.

Kenyon, N., Kirk, W. W., and Van Rooyen, D., (1971). “Corrosion of 18 Ni 180 and 18 Ni 200 maraging steels in aqueous chlorides”, *Corrosion*, 27 (9), 390-400.

Khaled, K.F., Babic-Samardzija, K. and Hackerman, N. (2004). “Piperidines as corrosion inhibitors for iron in HCl.” *J. Appl. Electrochem.*, 34, 697-704.

Klobcar, D., Tusek, J., Taljat, B., Kosec, L. and Pleterški, M. (2008). “Aging of maraging steel welds during aluminum alloy die casting.” *Mater. Sci.*, 44, 515–522.

Kriaa, A., Hamdi, N., Jbali, K. and Tzinmann, M. (2009). “Corrosion of iron in highly acidic hydro-organic solutions.” *Corros. Sci.*, 51, 668–676.

- Lagrene, M., Mernari, B., Bouanis, M., Traisnel, M. and Bentiss, F. (2002). "Study of the mechanism and inhibiting efficiency of 3,5-bis(4-methylthiophenyl)-4H-1,2,4-triazole on mild steel corrosion in acidic media." *Corros. Sci.*, 44, 573-588.
- Larabi, L., Harek, Y., Benali, O. and Ghalem, S. (2005). "Hydrazide derivatives as corrosion inhibitors for mild steel in 1M HCl." *Prog. Org. Coat.*, 54, 256-262.
- Li, W. H., He, Q., Pei, C. L. and Hou, B. R. (2007). "Experimental and theoretical investigation of the adsorption behavior of new triazole derivatives as inhibitors for mild steel corrosion in acid media." *Electrochim. Acta.*, 52, 6386-6394.
- Li, W. H., He, Q., Pei, C. L., Hou and B. R. H. (2008). "Some new triazole derivatives as inhibitors for mild steel corrosion in acidic medium." *J Appl Electrochem.*, 38, 289-295.
- Lin-xiu Zhao and Gang-shen Li (2010). "5-diethylamino-2- {[2-(2,4-dinitrophenyl) hydrazin-1-ylidene]methyl}- phenol." *Acta Crystallogr. E*: 66, 3108.
- Maayta, A. K. and Al-Rawashdeh N. A. F. (2004). "Inhibition of acidic corrosion of pure aluminum by some organic compounds." *Corros. Sci.*, 46, 1129-1140.
- Machnikova, E., Kenton Whitmire, H. and Hackerman, N. (2008). "Corrosion inhibition of carbon steel in hydrochloric acid by furan derivatives." *Electrochim. Acta.*, 53, 6024-6032.
- Marsh, J. (1988). *Advanced organic chemistry*, 3rd edn. Wiley Eastern, New Delhi.
- Martinez, S. and Stern, I. (2002). "Thermodynamic characterization of metal dissolution and inhibitor adsorption processes in the low carbon steel/mimosa tannin/sulphuric acid system." *Appl. Surf. Sci.*, 199, 83-89.
- Menapace, C., Lonardelli, I. and Molinari, A. (2010). "Phase transformation in a nanostructured M300 maraging steel obtained by SPS of mechanically alloyed powders." *J. Therm. Anal. Calorim.*, 101, 815-822.

- Morad, M. S. (2007). "Effect of sulfur-containing amino acids on the corrosion of mild steel in sulfide-polluted sulfuric acid solutions." *J. Appl. Electrochem.*, 37, 1191-1200.
- Morad, M. S. and Kamal El-Dean, A. M. (2006). "2, 2'-Dithiobis (3-cyano-4, 6-dimethylpyridine): a new class of acid corrosion inhibitors for mild steel." *Corros. Sci.*, 48, 3398–3412.
- Mu, G. N., Zhao, T. P., Liu, M. and Gu, T. (1996). "Effect of metallic cations on corrosion inhibition of an anionic surfactant for mild steel." *Corrosion.*, 52, 853.
- Muralidharan, V. S. and Rajagopalan, K. S. (1979). "Kinetics and mechanism of corrosion of iron in phosphoric acid." *Corros. Sci.*, 19, 199-207.
- Muzaffer Ozcan, Ramazan Solmaz, Gulfeza Kardas and Ilyas Dehri, (2008). "Adsorption properties of barbiturates as green corrosion inhibitors on mild steel in phosphoric acid." *Colloid. Surface.*, 325, 57-63.
- Nageswara Rao, M., Mohan, M. K. and Uma Maheswara Reddy, P. (2009). "Environmentally assisted cracking of 18%Ni maraging steel." *Corros. Sci.*, 51, 1645 - 1650.
- Nestor, P. (2004). *Electrochemistry and corrosion science*, Kluwer academic publishers, New York.
- Obot, I. B. and Obi-Egbedi N. O. (2010). "2, 3-Diphenylbenzoquinoxaline: A new corrosion inhibitor for mild steel in sulphuric acid ." *Corros. Sci.*, 52, 282–285.
- Obot. I. B., Obi-Egbedi, N. O. and Odozi, N. W. (2010) "Acenaphtho [1,2-b] quinoxaline as a novel corrosion inhibitor for mild steel in 0.5 M H₂SO₄." *Corros. Sci.*, 52, 923-926.
- Oguzie, E. E., Li, Y. and Wang, F. H. (2007). "Corrosion inhibition and adsorption behavior of methionine on mild steel in sulfuric acid and synergistic effect of iodide ion." *J. Colloid Interface Sci.*, 310, 1, 90-98.

- Oguzie, E. E., Njoku, V. O., Enenebeaku, C. K., Akalezi, C. O. and Obi, C. (2008). "Effect of hexamethylpararosaniline chloride (crystal violet) on mild steel corrosion in acidic media." *Corros. Sci.*, 50, 3480-3486.
- Ohue, Y. and Matsumoto, K. (2007). "Sliding–rolling contact fatigue and wear of maraging steel roller with ion-nitriding and fine particle shot-peening." *Wear*, 263 782–789.
- Ousslim, A., Bekkouch, K., Hammouti B., Elidrissi, A. and Aouniti, A. (2009). "Piperazine derivatives as inhibitors of the corrosion of mild steel in 3.9 M HCl." *J. Appl. Electrochem.*, 39, 1075–1079.
- Ozacan, M. and Dehri, I. (2004). *Progress in organic coatings*, 51, 181-187.
- Ozcan, M., Dehri, I. and Erbil, M. (2004). "Organic sulphur-containing compounds as corrosion inhibitors for mild steel in acidic media: correlation between inhibition efficiency and chemical structure." *Appl. Surf. Sci.*, 236, 155-164.
- Papavinas, S. (2000). *Uhlig's Corrosion Handbook*, second edition, Electrochemical society series, Edited by Winston Revie, John Wiley and sons. Inc, 1089.
- Pereloma, E.V., Shekhter, A., Miller, M. K. and Ringer, S. P. (2004). "Ageing Behaviour of Fe-20Ni-1.8Mn-1.6Ti-0.59Al(wt%) Maraging Steel." *Acta Mater.*, 52, 5589 - 5602.
- Philip, A. S. (1996). *Corrosion engineering handbook*, Marcel Dekker, Inc. New York.
- Philip, A. S. (2007). *Fundamentals of metallic corrosion*, CRC press, Taylor and Francis group, New York.
- Pierre R. R. (2008). *Corrosion engineering principles and practice*, McGrawHill, New York.
- Pierre, R. R. (1999). *Handbook of corrosion engineering*, McGraw-Hill, New York.

Poornima, T. Nayak, J. and Shetty, A. N. (2010). “Studies on corrosion of annealed and aged 18 ni 250 grade maraging steel in sulphuric acid medium.” *Port. Electrochim. Acta*, 28 (3), 173-188.

Poornima, T. Nayak, J. and Shetty. A. N. (2011). “Effect of 4-(N, N-diethylamino) benzaldehyde thiosemicarbazone on the corrosion of aged 18 Ni 250 grade maraging steel in phosphoric acid solution.” *Corros. Sci.*, 53, 3688 - 3696.

Poornima, T., Nayak, J. and Shetty, A. N. (2010). “Corrosion of aged and annealed 18 Ni 250 grade maraging steel in phosphoric acid medium.” *Int. J. Electrochem. Sci.*, 5, 56 – 71.

Poornima, T., Nayak, J and Shetty, A. N. (2011). “3, 4-Dimethoxy benzaldehyde thiosemicarbazone as corrosion inhibitor for aged 18Ni 250 grade maraging steel in 0.5 M sulfuric acid.” *J. Appl. Electrochem.*, 41, 223-233.

Popova, A., Christov, M., Raicheva, S. and Sokolova, E. (2004). “Adsorption and inhibitive properties of benzimidazole derivatives in acid mild steel corrosion.” *Corros. Sci.*, 46, 1333–1350.

Prabhu, R. A., Venkatesha, T. V., Shanbhag, A. V., Kulkarni, G. M. and Kalkhambkar, R. G. (2008). “Inhibition effects of some schiff’s bases on the corrosion of mild steel in hydrochloric acid solution.” *Corros. Sci.*, 50, 3356–3362.

Quraishi, M. A. and Jamal, D. (2002). “Inhibition of mild steel corrosion in the presence of fatty acid triazoles.” *J. Appl. Electrochem.*, 32, 425-430.

Quraishi, M. A. and Sardar, R. (2003). “Hector bases – a new class of heterocyclic corrosion inhibitors for mild steel in acid solutions.” *J. Appl. Electrochem.*, 33, 1163–1168.

Quraishi, M.A. and Sardar, R. (2003). “Hector bases - a new class of heterocyclic corrosion inhibitors for mild steel in acid solutions.” *J. Appl. Electrochem.*, 33, 1163–1168.

Razek, J., Klein, I. E. and Yahalom, J. (1997). “Structure and corrosion resistance of oxides grown on maraging steel in steam at elevated temperatures.” *Appl. Surf. Sci.*, 108 159-167.

Rezek J., Klein I. E. and Yhalom, J. (1997). “Electrochemical properties of protective coatings on maraging steel.” *Corros Sci.*, 39, 2, 385 - 386.

Robert, G. K., John R. S., David, W. S. and Rudolph, G. B. (2003). *Electrochemical techniques in corrosion science and engineering*, Marcel Dekker, Inc. New York.

Rohrbach Kurt and Schmidt Michael (revised by), (1990). *Maraging steels*, ASM handbook, 10th ed., vol.1, 796.

Ronald Schnitzer, Michael Schober, Silvia Zinner and Harald Leitner (2010). “Effect of Cu on the evolution of precipitation in an Fe–Cr–Ni–Al–Ti maraging steel.” *Acta Mater.*, 58, 3733–3741.

Sastri, V.S., Edward Ghali and Mimoun Elboujdaini (2007). *Corrosion prevention and protection practical solutions*. John Wiley & Sons Ltd, England.

Satpati, A. K. and Ravindran, P.V. (2008). “Electrochemical study of the inhibition of corrosion of stainless steel by 1, 2, 3-benzotriazole in acidic media.” *Mater. Chem. Phys.*, 109, 352-359.

Selim, I. Z., Khedr, A. A. and El-Shobki, K. M. (1996). “Efficiency of chalcone compounds inhibitors for acid corrosion of Al and Al-3.5 Mg Alloy.” *J. Mater.Sci. Technol.*, 12, 267-272.

Shanbhag, A. V., Venkatesha, T. V., Prabhu, R. A., Kalkhambkar, R. G. and Kulkarni, G. M. (2008). “Corrosion inhibition of mild steel in acidic medium using hydrazide derivatives.” *J Appl Electrochem.*, 38, 279–287.

Singh, A. K. and Quraishi, M. A., (2010). “Inhibitive effect of diethylcarbazine on the corrosion of mild steel in hydrochloric acid.” *Corros. Sci.*, 52, 1529-1539.

Solmaz, R. Kardas, G. Culha, M., Yazıcı, B. and Erbil, M. (2008). “Investigation of adsorption and inhibitive effect of 2-mercaptothiazoline on corrosion of mild steel in hydrochloric acid media.” *Electrochim. Acta*, 53, 5941-5952.

Speller, N. F. (1951). *Corrosion, causes and prevention*, McGraw-Hill, Michigan.

Stanly Jacob. K and Parameswaran (2010). “Corrosion inhibition of mild steel in hydrochloric acid solution by schiff base furoin thiosemicarbazone.” *Corros. Sci.*, 52, 224–228.

Stansbury, E. E. (2000). *Fundamentals of electrochemical corrosion*, ASM International, Materials Park.

Stiller, K., Danoix, F. and Bostel, A. “Investigation of precipitation in a new maraging stainless steel.” *Appl Surf Sci*, 1996, 94, 326.

Szauer, T and Brand, A. (1981). “On the role of fatty acid in adsorption and corrosion inhibition of iron by amine-fatty acid salts in acidic solution.” *Electrochim. Acta.*, 26, 1257-1260.

Taner Arslan, Fatma Kandemirli, Eno, Ebenso, E., Ian Love and Hailemichael Alemu. (2009). “Quantum chemical studies on the corrosion inhibition of some sulphonamides on mild steel in acidic medium.” *Corros. Sci.*, 51, 35 – 47.

Tao, Z. Zhang, S. Li, W. and Hou, B. (2010) “Adsorption and corrosion inhibition behavior of mild steel by one derivative of benzoic-triazole in acidic solution.” *Ind. Eng. Chem. Res.*, 49, 2593-2599.

Touhamia, F., Aounitia., A., Abeda, Y., Hammoutia, B., Kertitb, S., Ramdanic, A. and Elkacemid, K. (2000). “Corrosion inhibition of armco iron in 1.0 M HCl media by new bipyrazolic derivatives.” *Corros. Sci.*, 42, 929-940.

Uhlig, H. H. (1948). *Corrosion Handbook*, Wiley-Interscience.

Umoren, S. A., Li Y. and Wang, F. H. (2010). “Electrochemical study of corrosion inhibition and adsorption behaviour for pure iron by polyacrylamide in H₂SO₄: Synergistic effect of iodide ions.” *Corros. Sci.*, 52, 1777- 1786.

Venkatasubramaniyan Sridharan (2009). “Measurement of carbon dioxide corrosion on carbon steel using electrochemical frequency modulation.” University of Saskatchewan, Canada.

Vracar, Lj. M. and Drazic, D. M, (2002), “Adsorption and corrosion inhibitive properties of some organic molecules on iron electrode in sulphuric acid.” *Corros. Sci.*, 44, 1669 – 1680.

Wang, Lin (2001). “Evaluation of 2-mercaptoimidazole as corrosion inhibitor for mild steel in phosphoric acid”, *Corros. Sci.*, 43, 2281-2289.

Wang, Lin. (2006). “Inhibition of mild steel corrosion in phosphoric acid solution by triazole derivatives”, *Corros. Sci.*, 48 (3), 608-616.

Wang, W., Yan, W., Duan, Q., Shan, Y., Zhang, Z. and Yang, K. (2010) “Study on fatigue property of a new 2.8 GPa grade maraging Steel.” *Mater. Sci. Eng. A*, 527 3057–3063.

Wang, X., Yang, H. and Wang, F. (2010). “A cationic gemini-surfactant as effective inhibitor for mild steel in HCl solutions.” *Corros. Sci.*, 52, 1268-1276.

Wei Sha and Zhanli Guo (2009). *Maraging steels: Modelling of microstructure, properties and applications*, Woodhead publishing limited, Cambridge.

Wei-hua Li, Qiao He , Sheng-tao Zhang ,Chang-ling Pei and Bao-rong Hou (2008). “Some new triazole derivatives as inhibitors for mild steel corrosion in acidic medium.” *J. Appl. Electrochem.*, 38, 289–295.

Winston R. R. and Uhlig, H. H. (2008). *Corrosion and corrosion control*, John Wiley & Sons, Inc. New Jersey.

Winston Revie, R. (2000). *Uhlig's corrosion handbook, Second edition*, Wiley-Interscience publication, New York.

Xianghong Li, Shuduan Deng, Hui Fu. (2009). “Synergistic inhibition effect of red tetrazolium and uracil on the corrosion of cold rolled steel in H₃PO₄ solution: Weight loss, electrochemical, and AFM approaches.” *Mater. Chem Phys.*, 115, 815–824.

LIST OF PUBLICATIONS

In Journals:

1. Sanatkumar, B. S., Nayak, J. and Shetty. A. N. (2011). "Corrosion behaviour of 18% Ni M 250 grade maraging steel under weld aged condition in hydrochloric acid medium." *Chemical Sciences Journal*, Volume 2011, CSJ-37.
2. Sanatkumar, B. S., Nayak, J. and Shetty. A. N. (2012). "Investigation of adsorption and corrosion inhibitive effect of 1(2E)-1-(4 amino phenyl)-3-(2-thienyl) prop-2-en-1-one on corrosion of weld aged maraging steel in 0.5 M sulphuric acid media." *J. Electrochem Soc. India*, 60, 4, 153-161.
3. Sanatkumar, B. S., Nayak, J. and Shetty. A. N. (2012). "Corrosion behaviour of 18% Ni M 250 grade maraging steel under weld aged condition in sulphuric acid medium." *Chem. Eng. Commun.*, GCEC - 2011-0180. R1
4. Sanatkumar, B. S., Nayak, J. and Shetty. A. N. (2012). "The corrosion inhibition of maraging steel under weld aged condition by 1(2E)-1-(4 - aminophenyl)-3-(2-thienyl) prop-2-en-1-one in 1.5 M hydrochloric acid medium." *J. Coat. Technol. Res.*, 9, 4, 483-493.
5. Sanatkumar, B. S., Nayak, J. and Shetty. A. N. (2012). "Influence of 2-(4-chlorophenyl)-2-oxoethyl benzoate on the hydrogen evolution and corrosion inhibition of 18 Ni 250grade weld aged maraging steel in 1.0 M sulphuric acid medium." *Int. J. Hydrogen Energy.*, 37, 9431 - 9442.

In Conferences:

1. Sanatkumar, B. S., Nayak, J. and Shetty. A. N. (2010). "Corrosion behaviour of weld aged maraging steel in hydrochloric acid medium." for CORCON 2010, September 23-26, 2010, The Hotel Lalit International Goa.
2. Sanatkumar, B. S., Nayak, J. and Shetty. A. N. (2011). "Corrosion behaviour of weld aged maraging steel in sulphuric acid medium." for SRCS -2011, March 26 - 27, Kuvempu university, Shankaraghatta.

3. Sanatkumar, B. S., Nayak, J. and Shetty. A. N. (2011). “The corrosion inhibition of maraging steel under weld aged condition by 1(2E)-1-(4-aminophenyl)-3-(2-thienyl) prop-2-en-1-one in 1.0 M hydrochloric acid medium.” for National symposium on chemistry and humanity – NHCH 2011, July 11-12, 2011, MIT Manipal.
4. Sanatkumar, B. S., Nayak, J. and Shetty. A. N. (2011). “Investigation of adsorption and inhibitive effect of 1(2E)-1-(4-aminophenyl)-3-(2-thienyl) prop-2-en-1-one on corrosion of weld aged maraging steel in 1.0 M sulphuric acid media.” for National symposium on electrochemical science and technology, NSEST- 2011, August 19-20, I.I.Sc. Campus Bangalore.
5. Sanatkumar, B. S., Nayak, J. and Shetty. A. N. (2011). “Investigation of adsorption and corrosion inhibitive effect of 1(2E)-1-(4 amino phenyl)-3-(2-thienyl) prop-2-en-1-one on corrosion of weld aged maraging steel in 2.0 M sulphuric acid media” for the national conference on Modern trends in science and technology (MTST -2011), held in Dr. M. V. Shetty institute of technology Moodbidri, Mangalore, during 14th - 15th October.
6. Sanatkumar, B. S., Nayak, J. and Shetty. A. N. (2011). “The corrosion inhibition of maraging steel under weld aged condition by CPOB (2- (4-Chlorophenyl) -2- oxoethyl benzoate) in 0.5 M sulphuric acid medium” for the Sixteenth national convention of electrochemists (NCE -16), held in P. S. G. R. Krishnammal College for women, Coimbatore, Tamil Nadu, during 15 – 16th December.
7. Sanatkumar, B. S., Nayak, J. and Shetty. A. N. (2012). “The corrosion inhibition of maraging steel under weld aged condition by CPOB (2- (4-Chlorophenyl) -2- oxoethyl benzoate) in 1.5 M sulphuric acid medium” For the 14th national symposium in chemistry (NSC -14), held at national institute of interdisciplinary science and technology (CSIR-NIIST), Triruvanthapuram, Kerala, during 3 - 5th February.

BIO DATA

Mr. SANATKUMAR B.S.

S/o: Sundar B.

No 37, Happy Home, Gajanana Street,

Bhatkal - 581 320,

State: Karnataka

Phone: +91- 9449424605 (M)

E-mail: sanatkumarbs@gmail.com

Date of Birth: 31/01/1985

Academic Details

Degree/Course	Institution	Year	Class
M. Sc - Chemistry	Kuvempu University, Shimoga	2008	I
B. Sc - Maths,Physics,Chemistry	Anjuman Arts, Science and Commerce college, Bhatkal	2006	I
Pre-University Course	Shree Guru Vidyadhiraj Pre - University College, Bhatkal	2002	II
S.S.L.C	The New English school, Bhatkal.	2000	I

Professional Experience

		Position	Year
Industry	Intermed pharma, Bangalore	Research associate	June 2008 - July 2009
Institution	Agnel Institute of Technology and Design Assagao, Bardez, Goa	Asst. Professor	July 2012 - Till date